# Transcriptional control of phenotype in melanoma




Laura Mosteo López

Oriel College

University of Oxford

Supervised by Prof. Colin Goding

Ludwig Institute for Cancer Research

Nuffield Department of Medicine

A thesis submitted for the degree of

*Doctor of Philosophy*

Trinity 2019

# Disclaimer

I declare that this submission is my own written work. To the best of my knowledge, it contains no material that has been written by another or previously submitted in the same or a different form as academic work, to this or any other university.

The results presented herein derive from my own experiments, with the exception of Figure 3.3 (work performed by Alex Schepsky), Figures 3.4 and 3.5 (work performed by Luis Sánchez del Campo) and Figures 4.2 and 4.3 and Supplementary Tables S.1 and S.2.A and B (work performed by Pakavarin Louphrasitthiphol).

Laura Mosteo López

Trinity Term 2019

## Acknowledgements

I am hugely grateful to Professor Colin Goding for giving me the opportunity to conduct my DPhil in his laboratory and for all his invaluable support, encouragement and guidance over the last four years. I would further like to thank past and present members of the Goding group for being such great colleagues and friends and for making my time at the laboratory much more enjoyable. Especially, I would like to thank Yurena Vivas for all the scientific discussions, for always being happy to hear about my work and for all her support at difficult times at lab. I am also grateful for the assistance rendered by the support staff in the Ludwig Institute, especially Mark Shipman and Richard Lisle for their help with the microscopes. Thanks go to the Computational Biology Research Group (WIMM, Oxford) as well for the training provided in bioinformatics. Furthermore, I would like to thank the "la Caixa Foundation" (Spain) and the Masonic Samaritan Fund (United Kingdom) for funding my DPhil studies.

Finally, my biggest thanks goes to my parents, for their unconditional trust in me and their unwavering support throughout these years for which I am immensely grateful; and to Derek, whom I feel incredibly fortunate to have shared this journey with, for all the help inside and outside lab and for being part of the best memories I take from Oxford.

# Abstract


## Transcriptional control of phenotype in melanoma

Laura Mosteo López, Oriel College

D.Phil. Clinical Medicine, Trinity Term 2019

Melanoma is the most aggressive and deadly type of skin cancer, mainly as a consequence of its high metastatic capacity and refractoriness to treatment. Over recent years increasing evidence suggests that the intra-tumour microenvironment can drive cells to adopt invasive and drug-resistant phenotypes that play a key role in disease progression. Understanding how phenotypic heterogeneity is generated, and the molecular mechanisms underpinning the acquisition of invasive or drug-resistant states is key to the development of more effective therapies. Current evidence suggests an important role for the microphthalmia-associated transcription factor MITF in the development of phenotypic heterogeneity in melanoma. Yet how MITF is regulated and how it controls melanoma biology remains poorly characterised.

Here we show that activating transcription factor 4 (ATF4), whose expression is induced via a translational switch that occurs under microenvironment stresses frequently found in tumours such as nutrient deprivation or hypoxia, has the potential to directly supress *MITF* expression and also directly target a repertoire of well-characterised and novel MITF target genes. In addition, ATF4 also directly binds and has the potential to activate expression of novel target genes linked to invasiveness/metastasis or with a cytoprotective role. Our results therefore suggest that in response to a stressful intra-tumour microenvironment the induction of ATF4 provides a potentially reversible mechanism for the generation of phenotype heterogeneity in melanoma leading to the acquisition of metastatic and/or drug-resistant capacities in specific subpopulations of cells.

# Table of Contents

**Chapter 1.- Introduction ..... 1**
1.1.- Cancer ..... 1
1.2.- Melanoma ..... 3
1.2.1.- Melanoma epidemiology ..... 3
1.2.2.- Melanoma histopathology ..... 4
1.2.3.- Molecular biology of melanoma ..... 6
1.2.3.1.- Genetic drivers of melanoma ..... 6
1.2.3.2.- Targeted anti-melanoma therapy ..... 10
1.2.3.3.- Melanoma heterogeneity ..... 11
1.2.3.4.- Phenotype-switching in melanoma ..... 12
1.3.- MITF in melanocyte development and melanoma ..... 16
1.3.1.- MITF target genes and role in development and melanoma biology ..... 18
1.3.2.- Regulation of MITF ..... 22
1.4.- ATF4 in the integrated stress response and melanoma ..... 30
1.5.- Gene regulation ..... 35
1.5.1.- Transcriptional regulation of gene expression ..... 35
1.5.2.- Post-transcriptional regulation of gene expression ..... 48
1.5.3.- Translational regulation of gene expression ..... 49
1.5.4.- Post-translational regulation of gene expression ..... 54
1.6.- Aims of the study ..... 54

**Chapter 2.- Materials and Methods ..... 57**
2.1.- Materials ..... 57
2.1.1.- Chemicals and reagents ..... 57
2.1.2.- Plasmids ..... 57
2.1.3.- Cell lines ..... 58
2.1.4.- Antibodies ..... 60
2.1.5.- qPCR primers ..... 61
2.1.6.- Small interfering RNAs (siRNAs) ..... 63
2.2.- Bacterial methods ..... 64
2.2.1.- Cultivation of bacteria ..... 64
2.2.2.- Transformation of competent bacteria ..... 64
2.3.- Mammalian cell methods ..... 65
2.3.1.- Cultivation of mammalian cell lines ..... 65
2.3.2.- Cryoconservation of mammalian cell lines ..... 65
2.3.3.- Transient expression of proteins of interest ..... 65
2.3.4.- Non-inducible stable expression of proteins of interest ..... 66

2.3.5.- Inducible stable expression of proteins of interest ..... 66
2.3.6.- Transient knock-down of endogenous proteins of interest ..... 67
2.4.- Nucleic acid methods ..... 67
2.4.1.- Extraction of nucleic acids ..... 67
2.4.2.- Quantification of nucleic acids ..... 68
2.4.3.- Polymerase chain reaction ..... 68
2.4.4.- Restriction enzyme digestion ..... 69
2.4.5.- DNA dephosphorylation ..... 69
2.4.6.- Ligation ..... 69
2.4.7.- Agarose gel electrophoresis ..... 70
2.4.8.- Quantitative reverse transcription polymerase chain reaction (qRT-PCR) ..... 70
2.4.9.- DNA sequencing ..... 71
2.4.10.- RNA sequencing (RNA-seq) ..... 71
2.5.- Protein methods ..... 72
2.5.1.- Whole cell extract ..... 72
2.5.2.- SDS – polyacrylamide gel electrophoresis ..... 72
2.5.3.- Western blot ..... 73
2.5.4.- Chromatin immunoprecipitation – sequencing (ChIP-seq) ..... 74
2.5.5.- Protein synthesis assays ..... 76
2.5.5.1.- Click-iT® plus OPP protein synthesis assay ..... 76
2.5.5.2.- Metabolic labelling ..... 77
2.6.- Cell biology methods ..... 77
2.6.1.- Immunofluorescence ..... 77
2.6.2.- Scratch-wound healing assay ..... 78
2.6.3.- Cell cycle analysis ..... 78
2.7.- Bioinformatics ..... 79
2.7.1.- Quality control of high-throughput sequencing data ..... 79
2.7.2.- 3’ RNA-sequencing ..... 79
2.7.3.- ChIP-sequencing ..... 80
2.7.4.- Intersection of RNA-sequencing and ChIP-sequencing data ..... 81
2.8.- Statistics ..... 81

**Chapter 3.- Potential ZMYND8 and NuRD regulation of MITF ..... 82**
3.1.- Introduction ..... 82
3.2.- Preliminary data ..... 84
3.2.1.- The NuRD complex interacts with MITF ..... 84
3.2.2.- The NuRD complex is required for MITF expression ..... 84

3.2.3.- ZMYND8 is highly expressed in metastatic melanoma cell lines ..... 86
3.3.- Investigating the potential role of ZMYND8 in the regulation of MITF ..... 86
3.3.1.- Overexpression of ZMYND8 leads to repression of MITF ..... 86
3.3.2.- Generation of human melanoma cell lines with stable inducible expression of HA-tagged ZMYND8 ..... 87
3.3.3.- ZMYND8 repression of MITF is specific and is reflected in the subsequent downregulation of MITF downstream targets ..... 89
3.3.4.- The effect of ZMYND8 on MITF expression involves regulation of transcription ..... 90
3.3.5.- Silencing of ZMYND8 does not change MITF protein levels ..... 91
3.3.6.- ZMYND8 overexpression leads to upregulation of N-Cadherin, a feature of invasiveness, but reduces cell migration ..... 92
3.3.7.- Mutant ZMYND8 constructs maintain the ability to repress MITF ..... 95
3.4.- Investigating the potential role of the NuRD complex in the regulation of MITF .... 98
3.4.1.- p66β seems to be essential for MITF expression ..... 98
3.4.2.- p66α seems to be essential for MITF expression ..... 102
3.4.3.- CHD4 is not required for MITF expression ..... 104
3.4.4.- Exogenous p66β does not rescue MITF expression upon silencing endogenous p66β ..... 107
3.4.5.- p66β is not required for MITF expression ..... 109
3.4.6.- p66α is not required for MITF expression ..... 111
3.5.- Discussion ..... 113

**Chapter 4.- Potential MITF regulation of translation ..... 118**
4.1.- Introduction ..... 118
4.2.- Preliminary data ..... 120
4.3.- MITF represses PTEN and DEPTOR ..... 123
4.4.- MITF can regulate PI3K/AKT and mTOR signalling ..... 125
4.5.- MITF may regulate protein translation ..... 128
4.6.- MITF might regulate translation through the upregulation of PTEN ..... 131
4.7.- MITF does not have a clear effect on translation ..... 132
4.8.- Discussion ..... 135

**Chapter 5.- Regulation of gene expression by ATF4 ..... 139**
5.1.- Introduction ..... 139
5.2.- Genome-wide analysis of ATF4 binding in melanoma cells ..... 140
5.2.1.- ATF4 binding peaks are associated with known ATF4 target genes ..... 143

5.3.- Genome-wide analysis of ATF4 gene regulation in melanoma cells ..... 149
5.3.1.- Generation of a human melanoma cell line with inducible stable expression of HA-tagged ATF4 and the effect of the induction of ectopic ATF4 on MITF levels ..... 149
5.3.2.- Induction of ATF4 produces extensive changes in genome-wide gene expression ..... 152
5.3.3.- Induction of ATF4 leads to upregulation of known ATF4 target genes ..... 155
5.3.4.- ATF4 mainly regulates processes involved in the integrated stress response 156
5.3.5.- ATF4 does not seem to regulate *AXL* at the transcriptional level..... 161
5.4.- Genome-wide analysis of gene regulation in glucose-starved cells ..... 164
5.4.1.- Glucose starvation leads to upregulation of known ATF4 target genes..... 166
5.4.2.- ATF4 is a major effector in the cellular response to glucose starvation..... 167
5.4.3.- ATF4 binds and regulates genes mainly involved in the integrated stress response under glucose starvation conditions ..... 169
5.4.4.- Identification of ATF4 target genes in melanoma..... 173
5.4.4.1.- ATF4 binds and regulates *HOXB9* under glucose starvation conditions 173
5.4.4.2.- ATF4 binds and regulates *HERPUD1* under glucose starvation conditions ..... 175
5.4.4.3.- ATF4 binds and regulates *S100P* under glucose starvation conditions . 178
5.4.4.4.- ATF4 binds and regulates *CLIC4* under glucose starvation conditions .. 180
5.4.4.5.- ATF4 binds and regulates *SERPINE2* under glucose starvation conditions ..... 182
5.4.4.6.- ATF4 binds and regulates *MITF* under glucose starvation conditions ... 183
5.4.4.7.- ATF4 binds and regulates *GLI2* under glucose starvation conditions .... 187
5.5.- Genome-wide analysis of gene regulation by both MITF and ATF4 ..... 188
5.6.- Discussion ..... 201

**Chapter 6.- Concluding discussion and future perspectives ..... 205**
6.1.- Potential limitations of the molecular and cell biology techniques used ..... 205
6.2.- Potential role of ATF4 in phenotype-switching as a regulator of the expression of MITF and other genes ..... 212

**References ..... 220**
**Appendix A – Supplementary Figures ..... 256**
**Appendix B – Supplementary Tables ..... 263**

# List of Figures

1.1.- Melanoma incidence rates in the UK 1993-2015 ..... 4
1.2.- Clark model of melanoma progression ..... 5
1.3.- MAPK and PI3K/AKT signalling pathways are frequently aberrantly activated in melanoma ..... 7
1.4.- Vemurafenib-induced tumour regression and subsequent relapse ..... 10
1.5.- Phenotype-switching vs genetic model of metastasis ..... 14
1.6.- MITF rheostat model ..... 17
1.7.- MITF target cellular processes and genes ..... 18
1.8.- Transcriptional regulation of MITF expression ..... 23
1.9.- Post-translational regulation of MITF ..... 27
1.10.- Integrated stress response signalling ..... 31
1.11.- Formation of the transcriptional preinitiation complex ..... 41
1.12.- Cap-dependent translation initiation ..... 51

3.1.- Core components of the NuRD complex ..... 82
3.2.- The domain structure of ZMYND8 ..... 83
3.3.- MITF interacts with p66α and p66β ..... 84
3.4.- Silencing of p66β, p66α or CHD4 (Mi-2) abolishes MITF expression ..... 85
3.5.- p66β binds the *MITF* promoter ..... 85
3.6.- ZMYND8 average transcript intensities (Z scores) for different cancer cell lines ..... 86
3.7.- ZMYND8 overexpression leads to repression of MITF in 501mel, SKmel28 and IGR37 cells ..... 87
3.8.- ZMYND8 overexpression leads to repression of MITF in 501mel cells ..... 88
3.9.- ZMYND8 overexpression does not change TFEB levels in 501mel cells ..... 89
3.10.- ZMYND8 overexpression leads to downregulation of Tyrosinase and MelanA levels in 501mel cells ..... 90
3.11.- MITF mRNA levels decrease upon ZMYND8 overexpression in 501mel cells ..... 91
3.12.- MITF levels do not change upon silencing of ZMYND8 in 501mel cells ..... 91
3.13.- ZMYND8 overexpression leads to upregulation of N-Cadherin in 501mel cells ..... 92
3.14.- ZMYND8 overexpression reduces cell migration in 501mel cells ..... 93
3.15.- ZMYND8 overexpression induces G1 cell cycle arrest in 501mel cells ..... 94
3.16.- ZMYND8 overexpression reduces proliferation rates in 501mel cells ..... 95
3.17.- ZMYND8 constructs used in this study ..... 95
3.18.- Overexpression of mutant ZMYND8 constructs can repress MITF in 501mel cells ..... 97
3.19.- p66β silencing (using sip66β(I)) leads to strong downregulation of MITF protein levels in 501mel cells ..... 99

3.20.- MITF mRNA levels decrease upon p66β silencing (using sip66β(I)) in 501mel cells . 100
3.21.- p66β silencing (using sip66β(I)) leads to strong downregulation of MITF protein levels in SKmel28 cells ..... 101
3.22.- MITF mRNA levels decrease upon p66β silencing (using sip66β(I)) in SKmel28 cells 102
3.23.- p66α silencing (using sip66α(I)) leads to strong downregulation of MITF protein levels in 501mel cells ..... 103
3.24.- MITF mRNA levels decrease upon p66α silencing (using sip66α(I)) in 501mel cells 104
3.25.- CHD4 silencing does not affect MITF protein levels in 501mel cells ..... 105
3.26.- CHD4 silencing does not affect MITF protein levels in SKmel28 cells ..... 106
3.27.- Introduction of silent mutations in p66β nucleotide sequence ..... 107
3.28.- Exogenous N-terminus HA-tagged p66β does not rescue MITF expression in 501mel cells ..... 108
3.29.- Exogenous C-terminus HA-tagged p66β does not rescue MITF expression in 501mel cells ..... 109
3.30.- p66β silencing (using sip66β(II) or sip66β(III)) does not affect MITF protein levels in 501mel cells ..... 110
3.31.- p66α silencing (using sip66α(II) or sip66α(III)) does not affect MITF protein levels in 501mel cells ..... 112

4.1.- Regulation of 5' cap-dependent translation by PI3K/AKT and mTOR signalling pathways ..... 119
4.2.- MITF silencing leads to upregulation of *PTEN* and *DEPTOR* ..... 121
4.3.- MITF ChIP-seq peaks associate with *PTEN* and *DEPTOR* genes in 501mel cells ..... 122
4.4.- PTEN and DEPTOR mRNA levels increase upon MITF silencing (using siMITF(I)) in IGR37 cells ..... 123
4.5.- PTEN and DEPTOR mRNA levels increase upon MITF silencing (using siMITF(I), siMITF(II) or siMITF(III)) in SKmel30 cells ..... 124
4.6.- PTEN and DEPTOR protein levels increase upon MITF silencing (using siMITF(I)) in IGR37 cells ..... 125
4.7.- Phosphorylation of Akt, S6K1, S6 and 4E-BP1, indicative of activity through the PI3K/AKT and mTOR signalling pathways, is overall decreased upon MITF silencing (using siMITF(I)) in IGR37 and SKmel30 cells ..... 127
4.8.- OPP incorporation (indicative of protein synthesis) is reduced upon silencing of MITF (using siMITF(I)) in IGR37 and SKmel30 cells ..... 129
4.9.- $^{35}$S incorporation (indicative of protein synthesis) is reduced upon silencing of MITF (using siMITF(I)) in SKmel30 cells ..... 130

4.10.- $^{35}$S incorporation (indicative of protein synthesis) is reduced upon silencing of MITF (using siMITF(I)), increased following silencing of PTEN, and not altered after combined silencing of MITF (using (siMITF(I)) and PTEN in SKmel30 cells ..... 132
4.11.- $^{35}$S incorporation (indicative of protein synthesis) is reduced upon silencing of MITF (using siMITF(I)) but increased following silencing of MITF using siMITF(II) or siMITF(III) in SKmel30 cells ..... 133
4.12.- $^{35}$S incorporation (indicative of protein synthesis) is slightly increased upon silencing of MITF using siMITF(IV) or siMITF (V) in SKmel30 cells ..... 134

5.1.- ATF4 protein levels increase upon glucose starvation in 501mel cells ..... 140
5.2.- Distribution of peaks over the genome in ATF4 ChIP-seq experiment performed in glucose-starved 501mel cells ..... 141
5.3.- Consensus ATF4 binding motif ..... 143
5.4.- ATF4 binds the *DDIT3* promoter upon glucose starvation in 501mel cells ..... 145
5.5.- ATF4 binds upstream of *DDIT4* upon glucose starvation in 501mel cells ..... 146
5.6.- ATF4 binds the *ASNS* promoter upon glucose starvation in 501mel cells ..... 147
5.7.- ATF4 binds upstream of *CHAC1* upon glucose starvation in 501mel cells ..... 148
5.8.- ATF4 overexpression leads to repression of MITF in 501mel cells ..... 150
5.9.- MITF mRNA levels decrease upon ATF4 overexpression in 501mel cells ..... 151
5.10.- MITF protein levels decrease upon ATF4 overexpression in 501mel cells ..... 151
5.11.- Heatmaps showing differential gene expression following ATF4 induction in 501mel cells ..... 154
5.12.- Only small ATF4 ChIP-seq peaks are associated with *AXL* upon glucose starvation in 501mel cells ..... 163
5.13.- Heatmaps showing differential gene expression following glucose starvation in 501mel cells ..... 165
5.14.- ATF4 binds the *HOXB9* promoter upon glucose starvation in 501mel cells ..... 174
5.15.- ATF4 binds the *HERPUD1* promoter upon glucose starvation in 501mel cells ..... 177
5.16.- ATF4 binds the *S100P 3' region* upon glucose starvation in 501mel cells ..... 179
5.17.- ATF4 binds *CLIC4* intron 1 upon glucose starvation in 501mel cells ..... 181
5.18.- ATF4 binds *SERPINE2* 5' region upon glucose starvation in 501mel cells ..... 183
5.19.- ATF4 binds *MITF* exon 4 upon glucose starvation in 501mel cells ..... 186
5.20.- ATF4 binds *GLI2* 5' region upon glucose starvation in 501mel cells ..... 188
5.21.- ATF4 binds *MET* TTS upon glucose starvation in 501mel cells ..... 191
5.22.- ATF4 binds *PPARGC1A* 5' region upon glucose starvation in 501mel cells ..... 192
5.23.- ATF4 binds *RAB27A* gene body upon glucose starvation in 501mel cells ..... 192

5.24.- ATF4 binds *DCT* 5' region upon glucose starvation in 501mel cells ..... 193
5.25.- ATF4 binds *MLANA* 5' region upon glucose starvation in 501mel cells ..... 194
5.26.- ATF4 binds *KIT* gene body upon glucose starvation in 501mel cells ..... 195
5.27.- ATF4 binds *TRPM1* gene body upon glucose starvation in 501mel cells ..... 196
5.28.- ATF4 binds *PTEN* gene body upon glucose starvation in 501mel cells ..... 198
5.29.- ATF4 binds *DEPTOR* gene body upon glucose starvation in 501mel cells ..... 199

A.1.- ZMYND8 overexpression leads to repression of MITF in 501mel cells ..... 256
A.2.- Doxycycline treatment does not affect ZMYND8 and MITF mRNA levels in 501mel cells ..... 256
A.3.- Doxycycline treatment does not change cell migration in 501mel cells ..... 257
A.4.- Doxycycline treatment does not change the cell cycle profile of 501mel cells ..... 257
A.5.- Doxycycline treatment does not change proliferation rates in 501mel cells ..... 258
A.6.- MITF knock-down using different siRNAs against MITF leads to distinct cell morphologies ..... 258
A.7.- OPP incorporation (indicative of protein synthesis) does not change upon DEPTOR overexpression in 501mel cells ..... 259
A.8.- Expression of ATF4 following induction with doxycycline in 501mel-i-ATF4-HA cells 260
A.9.- Doxycycline treatment generally does not affect ATF4 and MITF mRNA levels in 501mel cells ..... 260
A.10.- Heatmaps showing differential gene expression following doxycycline treatment in 501mel cells ..... 261
A.11.- Confirmation of ATF4 binding to *MITF* exon 4 upon glucose starvation in 501mel cells ..... 262

# List of Tables

2.1.- Description and source of plasmids used ..... 57
2.2.- Description and source of cell lines used ..... 59
2.3.- List of primary antibodies used ..... 60
2.4.- List of secondary antibodies used ..... 61
2.5.- List of qPCR primers used ..... 61
2.6.- List of RNA oligonucleotides used ..... 63

5.1.- Major ATF4 binding peaks associated with known ATF4 target genes ..... 144
5.2.- Known ATF4 target genes and ATF4 itself are upregulated following induction of ectopic ATF4 in 501mel cells ..... 156
5.3.- Top correlated TF-driven networks for the sets of ATF4-bound genes upregulated following induction of ectopic ATF4 in 501mel cells ..... 158
5.4.- Top biological processes correlated with the sets of ATF4-bound genes upregulated following induction of ectopic ATF4 in 501mel cells ..... 159
5.5.- Top signalling pathways correlated with the sets of ATF4-bound genes upregulated following induction of ectopic ATF4 in 501mel cells ..... 161
5.6.- Known ATF4 target genes and ATF4 itself are upregulated under glucose starvation conditions in 501mel cells ..... 166
5.7.- Top correlated TF-driven networks for the sets of upregulated genes upon glucose deprivation in 501mel cells ..... 167
5.8.- Top biological processes correlated with the sets of upregulated genes upon glucose deprivation in 501mel cells ..... 168
5.9.- Top biological processes correlated with the set of genes downregulated upon glucose deprivation in 501mel cells ..... 169
5.10.- Top correlated TF-driven networks for the set of ATF4-bound genes upregulated following induction of ectopic ATF4 and upon glucose deprivation in 501mel cells 171
5.11.- Top biological processes correlated with the set of ATF4-bound genes upregulated following induction of ectopic ATF4 and upon glucose deprivation in 501mel cells 172
5.12.- Top signalling pathways correlated with the set of ATF4-bound genes upregulated following induction of ectopic ATF4 and upon glucose deprivation in 501mel cells 172
5.13.- Well-known MITF target genes differentially expressed upon ATF4 overexpression in 501mel cells ..... 189

B.1.- Top 125 MITF-bound upregulated genes following MITF silencing in 501mel cells ... 263
B.2.- ATF4-bound differentially expressed genes following induction of ectopic ATF4 and upon glucose starvation in 501mel cells ..... 265

B.3.- MITF and ATF4-bound genes differentially expressed upon both MITF silencing and induction of ectopic ATF4 expression in 501mel cells ..... 271

S.1.- Differentially expressed genes upon MITF silencing in 501mel cells ..... DATA CD
S.2.A.- Annotated MITF ChIP-seq called peaks (Replicate 1) ..... DATA CD
S.2.B.- Annotated MITF ChIP-seq called peaks (Replicate 2) ..... DATA CD
S.3.- MITF-bound differentially expressed genes upon MITF silencing in 501mel cells ..... DATA CD
S.4.A.- Annotated ATF4 ChIP-seq called peaks (Replicate 1) ..... DATA CD
S.4.B.- Annotated ATF4 ChIP-seq called peaks (Replicate 2) ..... DATA CD
S.5.A.- Differentially expressed genes following 8 h induction of ectopic ATF4 expression in 501mel cells ..... DATA CD
S.5.B.- Differentially expressed genes following 24 h induction of ectopic ATF4 expression in 501mel cells ..... DATA CD
S.5.C.- Differentially expressed genes following 8 h doxycycline treatment in 501mel cells ..... DATA CD
S.5.D.- Differentially expressed genes following 24 h doxycycline treatment in 501mel cells ..... DATA CD
S.6.A.- ATF4-bound differentially expressed genes following 8 h induction of ectopic ATF4 expression in 501mel cells ..... DATA CD
S.6.B.- ATF4-bound differentially expressed genes following 24 h induction of ectopic ATF4 expression in 501mel cells ..... DATA CD
S.7.A.- Differentially expressed genes following 8 h glucose starvation in 501mel cells ..... DATA CD
S.7.B.- Differentially expressed genes following 24 h glucose starvation in 501mel cells ..... DATA CD

# List of Abbreviations

| | |
|---|---|
| α-MSH | α-melanocyte stimulating hormone |
| 3C | Chromosome conformation capture |
| 4E-BP1/2 | 4E(eIF4E)-binding protein 1/2 |
| ASNS | Asparagine synthetase |
| ATF4 | Activating transcription factor 4 |
| ATG7 | Autophagy related 7 |
| ATP | Adenosine triphosphate |
| AP-1 | Activator protein-1 |
| APS | Ammonium persulphate |
| BAM | Binary alignment map |
| BBC3 | BCL2 binding component 3 |
| BCL2 | B-cell lymphoma 2 |
| bHLH | Basic helix-loop-helix |
| BIRC7 | Baculoviral IAP repeat containing 7 |
| BRCA1 | Breast cancer type 1 susceptibility protein |
| BRD | Bromodomain |
| Brn-2 | Brain-2 |
| BSA | Bovine serum albumin |
| BTG1 | B-cell translocation gene 1 |
| bZIP | Basic leucine zipper |
| C/EBPβ | CCAAT/enhancer-binding protein β |
| C/EBPγ | CCAAT/enhancer-binding protein γ |
| cAMP | Cyclic adenosine monophosphate |
| CBP | CREB-binding protein |
| CDK2 | Cyclin-dependent kinase 2 |
| CDK4 | Cyclin-dependent kinase 4 |
| CDKN1A | Cyclin-dependent kinase inhibitor 1A |
| CDKN1B | Cyclin-dependent kinase inhibitor 1B |
| CDKN2A | Cyclin-dependent kinase inhibitor 2A |
| CDS | Coding sequence |
| CEACAM1 | Carcinoembryonic antigen-related cell adhesion molecule 1 |
| ChIP-seq | Chromatin immunoprecipitation – sequencing |

| | |
|---|---|
| CHD3 | Chromodomain-helicase-DNA-binding 3 |
| CHD4 | Chromodomain-helicase-DNA-binding 4 |
| CHOP | C/EBP-homologous protein |
| CIP | Calf intestinal alkaline phosphatase |
| CK2 | Casein kinase 2 |
| CLIC4 | Chloride intracellular channel 4 |
| CNS | Central nervous system |
| CRE | cAMP response element |
| CREB | cAMP response element binding protein |
| CTCF | CCCTC-binding factor |
| CTD | Carboxy-terminal domain |
| DCT | Dopachrome tautomerase |
| DDIT3 | DNA damage inducible transcript 3 |
| DDIT4 | DNA damage inducible transcript 4 |
| DEC1 | Differentially expressed in chondrocytes protein 1 |
| DEG | Differentially expressed gene |
| DEPTOR | DEP-domain containing mTOR-interacting protein |
| DIAPH1 | Diaphanous-related formin-1 / Dia1 |
| DMSO | Dimethyl sulfoxide |
| DNA | Deoxyribonucleic acid |
| Dox | Doxycycline |
| DSIF | DRB sensitivity-inducing factor |
| dsRNA | Double-stranded DNA |
| DUF3544 | Domain of unknown function 3544 |
| ECL | Enhanced chemiluminescence |
| EDTA | Ethylenediamine tetraacetic acid |
| eIF2 | Eukaryotic translation initiation factor 2 |
| eIF2α | Eukaryotic translation initiation factor 2 subunit alpha |
| eIF2B | Eukaryotic translation initiation factor 2B |
| eIF4A | Eukaryotic translation initiation factor 4A |
| eIF4B | Eukaryotic translation initiation factor 4B |
| eIF4E | Eukaryotic translation initiation factor 4E |

| | |
|---|---|
| eIF4F | Eukaryotic translation initiation factor 4F |
| eIF4G | Eukaryotic translation initiation factor 4G |
| eIF5B | Eukaryotic translation initiation factor 5B |
| EGFR | Epidermal growth factor receptor |
| EMT | Epithelial mesenchymal transition |
| ER | Endoplasmic reticulum |
| eRNA | Enhancer RNA |
| ERK | Extracellular signal-regulated kinase |
| ERK2 | Extracellular signal-regulated kinase 2 |
| FDA | Food and drug administration |
| FDR | False discovery rate |
| FL | Full length |
| FOXD3 | Forkhead box protein D3 |
| FOXO3 | Forkhead box protein O3 |
| GADD45A | Growth arrest and DNA damage inducible 45 alpha |
| GCN2 | General control non-derepressible 2 |
| GDP | Guanosine diphosphate |
| GEF | Guanine nucleotide exchange factor |
| GLI2 | Glioma associated oncogene family zinc finger 2 |
| GMPR | Guanosine monophosphate reductase |
| GO | Gene ontology |
| GRCh37 | Genome reference consortium human build 37 |
| GSK3 | Glycogen synthase kinase 3 |
| GTF | General transcription factor or gene transfer format |
| GTP | Guanosine triphosphate |
| h | Hour/s |
| HAT | Histone acetyltransferase |
| HDAC | Histone deacetylase |
| HDAC1 | Histone deacetylase 1 |
| HDAC2 | Histone deacetylase 2 |
| HERPUD1 | Homocysteine-inducible ER protein with ubiquitin-like domain 1 |
| HKMT | Histone lysine methyltransferase |

| | |
|---|---|
| HOXB7 | Homeobox B7 |
| HOXB9 | Homeobox B9 |
| HRI | Heme-regulated inhibitor |
| IRES | Internal ribosomal entry site |
| ISR | Integrated stress response |
| kDa | Kilodalton |
| KEGG | Kyoto encyclopedia of genes and genomes |
| LB | Luria-Bertani |
| LEF1 | Lymphoid enhancer-binding factor 1 |
| LIG1 | DNA ligase 1 |
| Lys | Lysine |
| $m^7G$ | 7-methylguanosine |
| MACS | Model-based analysis of ChIP-seq |
| MAPK | Mitogen-activated protein kinase |
| MBD | Methyl-CpG binding domain |
| MBD2 | Methyl-CpG binding domain protein 2 |
| MBD3 | Methyl-CpG binding domain protein 3 |
| MC1R | Melanocortin 1 receptor |
| MEK | MAPK/ERK kinase |
| MEK1 | MAPK/ERK kinase 1 |
| MEME | Multiple em for motif elicitation |
| Min | Minute/s |
| miRISC | miRNA-induced silencing complex |
| miRNA | microRNA |
| MiT | Microphthalmia |
| MITF | Microphthalmia-associated transcription factor |
| mLST8 | Mammalian lethal with Sec13 protein 8 |
| MRD | Minimal residual disease |
| mRNA | Messenger RNA |
| MTA | Metastasis associated |
| MTA1 | Metastasis associated 1 |
| MTA2 | Metastasis associated 2 |

| | |
|---|---|
| MTA3 | Metastasis associated 3 |
| mTOR | Mechanistic target of rapamycin |
| mTORC1 | Mechanistic target of rapamycin complex 1 |
| MYND | Myeloid, nervi and DEAF-1 |
| MYO5A | Myosin-5a |
| NELF | Negative elongation factor |
| NLS | Nuclear localization signal |
| NoRC | Nucleolar remodelling complex |
| NuRD | Nucleosome remodelling and histone deacetylase |
| NURF | Nucleosome remodelling factor |
| OC-2 | Onecut-2 |
| OPP | O-propargyl-puromycin |
| P-TEBb | Positive transcription elongation factor b |
| P4HB | Prolyl 4-hydroxylase subunit beta |
| p70S6K | 70kDa ribosomal S6 kinase |
| PABP | Poly(A)-binding protein |
| PADI4 | Protein arginine deiminase type 4 |
| PAX3 | Paired box gene 3 |
| PB | PiggyBac |
| PBS | Phosphate-buffered saline |
| PCR | Polymerase chain reaction |
| PDCD4 | Programmed cell death 4 |
| PDK1 | Phosphoinositide dependent kinase 1 |
| PERK | Protein kinase R (PKR)-like endoplasmic reticulum kinase |
| PFA | Paraformaldehyde |
| PGC-1α | Peroxisome proliferator-activated receptor gamma coactivator 1-alpha |
| PHD | Plant homeodomain |
| PI | Propidium iodide |
| PI3K | Phosphatidylinositol-3-kinase |
| PIAS3 | Protein inhibitor of activated STAT3 |
| PIC | Protease inhibitor cocktail or preinitiation complex |
| PIP2 | Phosphatidylinositol (4,5)-bisphosphate |

| | |
|---|---|
| PIP3 | Phosphatidylinositol (3,4,5)-triphosphate |
| PKA | Protein kinase A |
| PKB | Protein kinase B |
| PKR | Protein kinase R |
| PMAIP1 | Phorbol-12-myristate-13-acetate-induced protein 1 |
| PMEL | Pre-melanosome protein |
| PMI | Personal molecular imager |
| PMSF | Phenylmethylsulfonyl fluoride |
| Pol II | RNA polymerase II |
| POMC | Proopiomelanocortin |
| PPARGC1A | Peroxisome proliferator-activated receptor gamma coactivator 1-alpha |
| PPP1R15A | Protein phosphatase 1 regulatory subunit 15A |
| PRAS40 | Proline-rich Akt substrate of 40 kDa |
| pri-miRNA | Primary precursor miRNA |
| pre-miRNA | Precursor miRNA |
| pre-mRNA | Precursor mRNA |
| PRMT1 | Protein arginine N-methyltransferase 1 |
| PTEN | Phosphatase and tensin homolog |
| PTM | Post-translational modification |
| PWWP | Proline-tryptophan-tryptophan-proline |
| QC | Quality control |
| qRT-PCR | Quantitative reverse transcription polymerase chain reaction |
| RAB27A | Ras-related protein Rab-27A |
| RAC1 | Rac family small GTPase 1 |
| RAD51L3 | RAD51-like protein 3 |
| RAPTOR | Regulatory-associated protein of mTOR |
| Rb1 | Retinoblastoma 1 |
| RBBP4 | Retinoblastoma-binding protein 4 |
| RBBP7 | Retinoblastoma-binding protein 7 |
| RefSeq | Reference sequence |
| RHO-A | Ras homolog family member A |
| RHO-C | Ras homolog family member C |

| | |
|---|---|
| RNA | Ribonucleic acid |
| RNA-seq | RNA sequencing |
| RNAi | RNA interference |
| RPMI | Roswell Park Memorial Institute |
| RT | Room temperature |
| rtTA | Reverse tetracycline transactivator |
| S100P | S100 calcium binding protein P |
| S6K1 | p70S6 kinase 1 |
| SAGA | Spt-Ada-Gcn5 acetyltransferase |
| SAM | S-adenosylmethionine or sequence alignment map |
| SDS-PAGE | Sodium dodecyl sulphate polyacrylamide gel electrophoresis |
| sec / SEC | Second/s / Super elongation complex |
| SEM | Standard error of the mean |
| Ser | Serine |
| SERPINE2 | Serpin clade E member 2 |
| SESN2 | Sestrin 2 |
| shRNA | Short hairpin RNA |
| siRISC | siRNA-induced silencing complex |
| SIRT1 | Sirtuin 1 |
| siRNA | Small interfering RNA |
| SLC7A5 | Solute carrier family 7 member 5 |
| SOX10 | SRY-related high mobility group-box 10 |
| STAR | Spliced transcripts alignment to a reference |
| STAT3 | Signal transducer and activator of transcription 3 |
| STR | Short tandem repeat |
| SWI/SNF | Switch/sucrose non-fermentable |
| TAD | Topologically associating domain |
| TBP | TATA-binding protein |
| TC | Ternary complex |
| TEMED | Tetramethylethylenediamine |
| TERT | Telomerase reverse transcriptase |
| TF | Transcription factor |

| | |
|---|---|
| TFIIA | Transcription factor IIA |
| TFIIB | Transcription factor IIB |
| TFIID | Transcription factor IID |
| TFIIE | Transcription factor IIE |
| TFIIF | Transcription factor IIF |
| TFIIH | Transcription factor IIH |
| TFIIS | Transcription factor IIS |
| TFEB | Transcription factor EB |
| TFEC | Transcription factor EC |
| TFE3 | Transcription factor E3 |
| TGF-β | Transforming growth factor beta |
| TLR | Toll-like receptor |
| TNF-α | Tumour necrosis factor alpha |
| tRNA | Transfer RNA |
| TRRUST | Transcriptional regulatory relationships unraveled by sentence-based text |
| TSS | Transcription start site |
| TTS | Transcription termination site |
| TYR | Tyrosinase |
| TYRP-1 | Tyrosinase-related protein 1 |
| UCSC | University of California Santa Cruz |
| UK | United Kingdom |
| uORF | Upstream open reading frame |
| UV | Ultraviolet light |
| USP13 | Ubiquitin-specific protease 13 |
| UTR | Untranslated region |
| VEGFA | Vascular endothelial growth factor A |
| vs | Versus |
| Wnt | Wingless-type |
| XBP1 | X-box binding protein 1 |
| YAP | Yes-associated protein |
| ZMYND8 | Zinc finger MYND-type containing 8 |
| ZnF or ZF | Zinc finger |

# Chapter 1 - Introduction

## 1.1. – Cancer

The generation of cancer is a multi-step process where accumulation of genetic and epigenetic modifications drives senescence bypass and deregulated proliferation. Notably cancer initiation usually requires a combination of complementary events. These normally include activation of oncogenes that provide a constitutive pro-proliferation signal including activating mutations in receptor tyrosine kinases (e.g. epidermal growth factor receptor, EGFR) or downstream effectors of MAPK signalling (such as the Ras family members or BRAF) combined with inactivation of tumour suppressors (e.g. p53, Rb1, CDKN1A, CDKN2A) that can impose senescence in response to oncogene activation to limit cancer progression (Sigal and Rotter 2000; Sharpless 2005; Pedraza-Fariña 2006; Dhillon et al. 2007; Zandi et al. 2007; Abbas and Dutta 2009; Solomon et al. 2010; Oikonomou et al. 2014; Dyson 2016). The biological capabilities arising as a consequence of these initiation events have been reviewed by Hanahan and Weinberg (Hanahan and Weinberg 2011), who outline the following characteristics associated with cancer initiation and progression: 1) self-sufficient proliferation, 2) refractoriness to growth suppressors, 3) resistance to cell death, 4) limitless replicative potential, 5) sustained angiogenesis, 6) capacity to invade surrounding tissue and metastasise, 7) reprogramming of energy metabolism, and 8) evasion of the immune system.

Underlying these so-called “hallmarks of cancer” are genome instability, that can contribute to the genetic diversity that may facilitate cancer progression, and inflammation, which promotes several hallmark functions (Hanahan and Weinberg 2011). However, how genetic lesions lead cells to invade surrounding tissue and metastasise is still not fully understood. Since metastases cause the vast majority of cancer-associated deaths, increasing our understanding of this process is crucial.

The acquisition of an invasive phenotype is a prerequisite for metastasis, a process by which cells detach from the primary tumour and penetrate into surrounding tissues to travel through blood or lymphatic vessels and finally colonise and establish secondary tumours in new locations (Lambert et al. 2017). Both genetic mutations and microenvironmental events most likely work together to induce the initially invasive phenotype required for the process of metastasis. Regarding the genetic component, while it has been suggested that activation of oncogenes and loss of tumour suppressors early in carcinogenesis predispose to metastasis (Bernards and Weinberg 2002), acquisition of additional genetic alterations usually characterises the transition from non-metastasising "benign" tumours to potentially metastasising "malignant" tumours, indicating that these additional lesions may increase the capacity of cells to adopt an invasive phenotype (Klein 2013). For example, while only benign non-metastatic lesions appear in mouse models of melanoma harbouring the $BRAF^{V600E}$ mutation alone, the combination of $BRAF^{V600E}$ mutation with *PTEN* loss in these animal models allows for the transition to malignant melanoma where lung and lymph node metastases are frequently observed (Dankort et al. 2009). However, it must be noted that only an extremely small fraction of cells from the primary tumour migrate and eventually give rise to metastasis. Therefore, while *PTEN* loss (when combined with $BRAF^{V600E}$ mutation) increases the probability for metastatic spread, it does not impose an unavoidable transition into an invasive phenotype. Metastasis could therefore constitute a stochastic process where combinations of certain genetic alterations are predisposing factors but microenvironmental signals modulate the likelihood of phenotype transitions (Hoek and Goding 2010; Vogelstein et al. 2013).

Among the best models for the study of invasion and metastasis is melanoma, a cancer that originates in the skin and therefore offers the opportunity to easily follow cancer progression from the initial stages to metastatic disease.

## 1.2. – Melanoma

Melanoma is a cancer that arises in melanocytes, neural crest-derived melanin-producing cells located predominantly in the epidermis. Although melanoma accounts for only around 1% of all dermatological cancers, it is responsible for the vast majority of deaths from skin cancer (American Cancer Society). The main underlying reasons for the aggressiveness of melanoma are the early progression to metastatic cancer and the refractoriness to treatment. Thus, in the UK, when melanoma is diagnosed at early stages, 5-year survival rates are above 90% but plummet to around 16% if diagnosed at advanced stages when it has already metastasised (Cancer Research UK).

### 1.2.1. – Melanoma epidemiology

Melanoma is especially common in Europe, Australia, New Zealand and North America (Ferlay et al. 2015), reflecting the higher susceptibility of populations with fair skin to develop this type of cancer as well as the crucial influence of the exposure to UV radiation. Indeed, 86% of all cases diagnosed in the UK in 2015 were attributed to overexposure to UV radiation (and therefore considered preventable) (Cancer Research UK). Especially, intense and intermittent sun exposure has been associated with a higher risk of developing melanoma compared to a chronic and continuous pattern of exposure (Gandini et al. 2005). Furthermore, a history of sunburn in childhood or adolescence has been linked to the highest risk, with individuals having experienced more than 5 episodes of severe sunburn being at double risk of developing melanoma (Leonardi et al. 2018).

Apart from polymorphisms in genes that confer distinct human skin colour phenotypes determining the elevated sensitivity to sun exposure of individuals with low pigmented skin, germline inactivating mutations in the *CDKN2A* gene or mutations in *CDK4* that render it insensitive to inhibition are known high risk factors for melanoma (Zuo et al. 1996; Soufir et

al. 1998; Hayward 2000), where around 10% of cases occur in a familial context (Potrony et al. 2015).

Finally, although the risk for developing melanoma increases with age, with around half of the people diagnosed in the UK aged 65 and over, it is also the second most common type of cancer in adults aged under 50 (Cancer Research UK).

Overall, melanoma is the 5$^{th}$ most common type of cancer in the UK (Cancer Research UK), with an incidence that has been rising (**Figure 1.1**), faster than for any other type of malignancy. Despite numerous skin cancer prevention campaigns, poor sun-related practice has been observed at a much higher frequency over the last few decades. It is therefore of vital importance to raise melanoma awareness and promote healthier sun-related behaviour in our society. With currently around 2,400 deaths per year from melanoma in the UK alone (Cancer Research UK), the development of therapies that improve survival of melanoma patients is also urgently required.

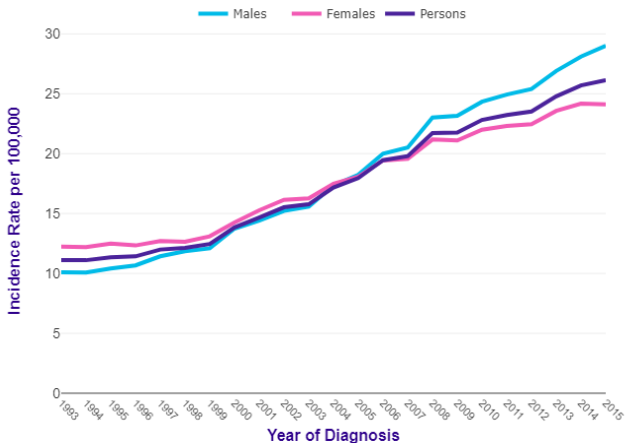


**Figure 1.1.- Melanoma incidence rates in the UK 1993-2015.** *Reproduced from "Cancer Research UK Melanoma Statistics" (Cancer Research UK).*

### 1.2.2. – Melanoma histopathology

The pathological changes associated with a stepwise progression to malignant melanoma from normal melanocytes are described in the Clark model of melanoma progression (**Figure 1.2**) (Clark et al. 1984; Miller and Mihm 2006).

The first step involves the development of benign nevi, as a consequence of deregulated proliferation of melanocytes due to the disruption of growth control in these cells usually resulting from the genetic activation of a pro-proliferative oncogene such as NRAS or BRAF. In most cases such lesions are confined due to the activation of oncogene-induced senescence (irreversible arrest of proliferation), which limits the growth stimulated by activation of oncogenic pathways (Bennett 2016).

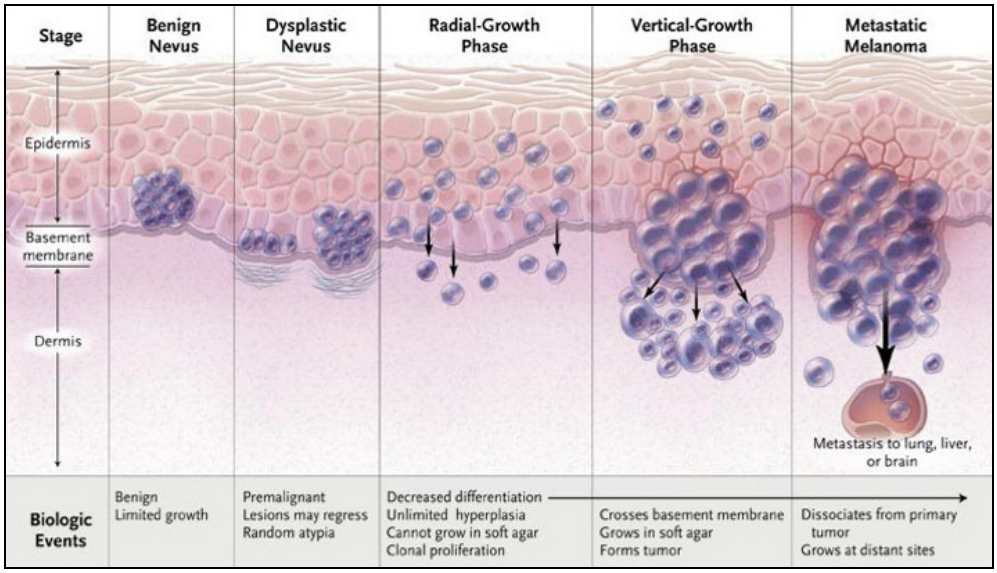


**Figure 1.2.- Clark model of melanoma progression.** The Clark model of melanoma describes the series of histopathological changes associated with the progression from normal melanocytes to metastatic melanoma. *Adapted from "Melanoma" (Miller and Mihm 2006).*

However, in a few cases benign nevi progress to dysplastic nevi, which can also arise as new lesions. Dysplastic nevi present higher proliferation activity as a consequence of the accumulation of further molecular abnormalities affecting cell growth, DNA repair and susceptibility to cell death (Miller and Mihm 2006). While these nevi are considered pre-malignant lesions, they might still regress through differentiation or via the effects of the immune system.

Decreased differentiation is associated with the radial-growth phase in the Clark model, where cells start proliferating intra-epidermally. These cells however still fail to form colonies in soft agar (Miller and Mihm 2006).

The Clark model places the appearance of invasive characteristics in the vertical-growth phase, when melanoma cells acquire the ability to grow intra-dermally forming an expanding nodule. In this step melanoma cells can also reach the subcutaneous layer of fat, are able to grow in soft agar and have the ability to form tumours when implanted in mice (Miller and Mihm 2006).

Finally, metastatic melanoma develops when cancer cells dissociate from the primary tumour and migrate through the surrounding stroma, lymphatic system and blood vessels to other areas of the skin and distant organs where they can successfully establish metastasis. These invasive cells can grow in soft agar and have the capacity to form tumours that may metastasise when implanted in mice (Miller and Mihm 2006).

While the Clark model has been clinically used for the staging of melanomas for many years, it is currently in disuse due to the diagnostic and prognostic difficulty of intermediate lesions, which in practise often fail to clearly fall into one of the described stages. Moreover, it has become clear that a linear progression model is inadequate to describe the molecular features of the disease where, for example, expression of E-cadherin (a key adhesion molecule) in the primary tumour may be lost in invasive cells, but re-established in metastases (Danen et al. 1996).

### 1.2.3.- Molecular biology of melanoma

#### 1.2.3.1. – Genetic drivers of melanoma

Melanoma is associated with one of the highest somatic mutational burdens of all types of human cancers, primarily in the form of C>T lesions that reflect UV-mediated DNA damage (Vogelstein et al. 2013; Cancer Genome Atlas Network 2015). Among the signalling pathways most commonly activated in melanoma as a consequence of somatic mutations

are the mitogen-activated protein kinase (MAPK) and phosphatidylinositol 3-kinase/protein kinase B (PI3K/AKT) pathways (**Figure 1.3**).

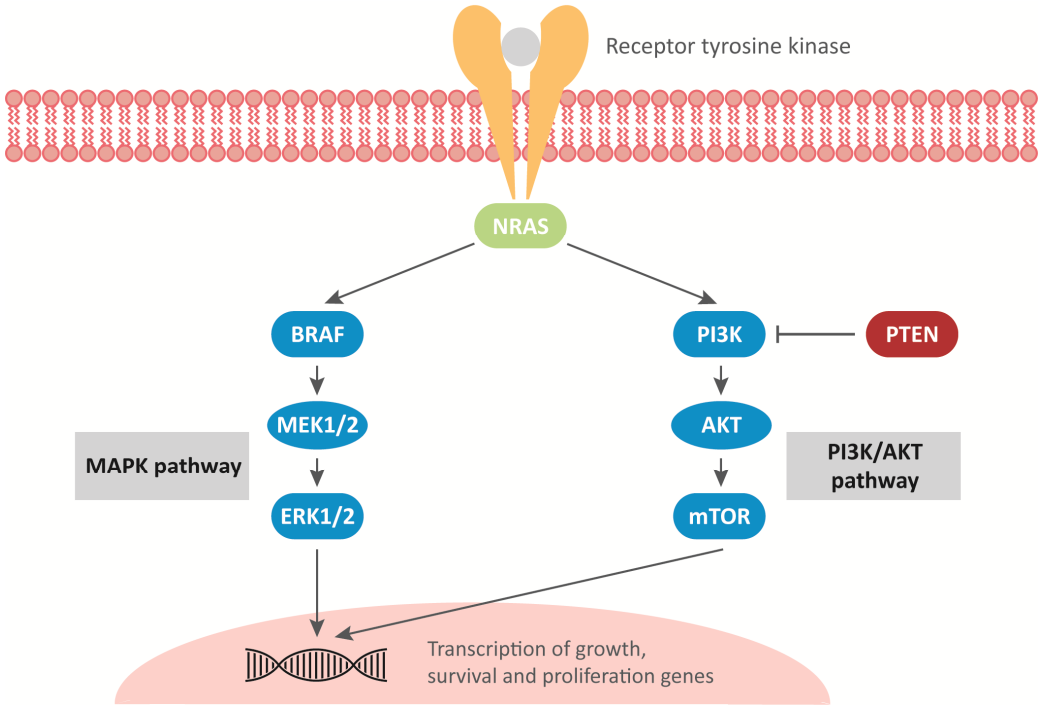


**Figure 1.3.- MAPK and PI3K/AKT signalling pathways are frequently aberrantly activated in melanoma.** Somatic mutations activating genes involved in the mitogen-activated protein kinase (MAPK) and phosphatidylinositol 3-kinase/protein kinase B (PI3K/AKT) pathways are well known drivers of melanoma, with inactivating mutations in PTEN also driving activation of PI3K signalling. BRAF: B-Raf proto-oncogene serine/threonine kinase; ERK1/2: extracellular signal-regulated kinases 1 and 2; MEK1/2: MAP kinase kinases 1 and 2; mTOR: mechanistic target of rapamycin; NRAS: neuroblastoma rat sarcoma viral oncogene homologue; PTEN: phosphatase and tensin homologue.

The MAPK signalling pathway in melanoma

The MAPK signalling pathway is normally involved in the transduction of extracellular signals, including growth factors via their cell surface receptors, to the nucleus, where it leads to activation of genes mainly driving cell proliferation, growth, and survival (Lim et al. 2017). Aberrant activation of the MAPK signalling pathway is observed in the vast majority of melanomas, constituting a central step in the development of this type of cancer (Shain et al. 2015). Among the mechanisms underlying aberrant activation of the MAPK pathway, the most frequent genetic alterations are activating mutations in the *BRAF* gene which are

present in around 50% of melanomas (Davies et al. 2002). *BRAF* encodes the serine/threonine protein kinase B-Raf, a component and critical regulator of the MAPK signalling pathway. Over 90% of the *BRAF* mutations observed in melanoma occur in codon 600, and among these, more than 90% are a single nucleotide change that results in the substitution from valine to glutamic acid ($BRAF^{V600E}$) (Ascierto et al. 2012). This amino acid modification, which affects the activation segment of B-Raf's kinase domain, produces a constitutively active form of the protein.

Despite the key role of *BRAF* mutations in the initiation and maintenance of melanoma, oncogenic B-Raf alone is not sufficient and needs to be combined with inactivation of tumour suppressors such as p53 or PTEN for the progression to this malignancy (Patton et al. 2005; Dankort et al. 2009). Thus, melanocyte-specific expression of mutated B-Raf in zebrafish models leads to patches of ectopic proliferation of melanocytes similar to human benign nevi but only produces melanoma when the expression of mutated B-Raf is combined with inactivation of *p53* (Patton et al. 2005).

The second most common mutations aberrantly activating MAPK signalling in melanoma are *NRAS* mutations. *NRAS* encodes the GTPase protein N-Ras, which, when active, binds to and activates B-Raf (**Figure 1.3**). *NRAS* mutations are present in 15-30% of melanomas, and in most cases are missense mutations in codons 12, 13 or 61 which compromise the GTPase activity of N-Ras leading to an abnormal prolongation of the GTP-bound N-Ras active state (Leonardi et al. 2018).

Interestingly, *NRAS* mutations are almost exclusively detected in melanomas not harbouring *BRAF* mutations, likely due to the large degree of functional redundancy of these genomic alterations (both leading to aberrant activation of the MAPK signalling pathway).

The PI3K/AKT pathway in melanoma

As represented in **Figure 1.3**, N-Ras, when active, can also interact with and activate phosphatidylinositol 3-kinase (PI3K), leading to activation of the PI3K/AKT pathway which is primarily involved in the regulation of survival but also controls many other processes such as metabolism, cell growth and proliferation (Janku et al. 2018). In contrast to activation of *BRAF*, which drives MAPK activation alone, activating *NRAS* mutations in melanoma therefore result in aberrant activation of the PI3K/AKT signalling pathway as well (Leonardi et al. 2018).

In addition, genetic alterations in *PTEN* are common in melanoma, with mutations or deletions affecting this gene observed in around 20% of melanomas (Cancer Genome Atlas Network 2015). *PTEN* encodes the tumour suppressor phosphatase and tensin homologue (PTEN), which degrades the product of the enzymatic activity of PI3K and as a consequence negatively regulates the PI3K/AKT signalling pathway (Chalhoub and Baker 2009). *PTEN* loss-of-function mutations or deletions therefore lead to amplification of PI3K/AKT pathway promoting tumorigenesis.

Genomic alterations in *PTEN* and *NRAS* are usually mutually exclusive, again likely due to their partial functional redundancy (both leading to aberrant PI3K/AKT pathway activation), analogous to that of *BRAF* and *NRAS* mutations. However, *PTEN* loss-of-function mutations frequently co-occur with activating *BRAF* mutations in melanoma, with the biological meaning underlying this observation likely being the cooperativity between these genomic alterations to aberrantly activate both MAPK and PI3K/AKT signalling pathways together (a result ultimately equivalent to that of *NRAS* activating mutations alone). The complementarity between these signalling pathways is likely to reflect the ability of the PI3K pathway to promote the increased protein synthesis, survival and glucose uptake required to support proliferation driven by activation of the MAPK pathway (Mendoza et al. 2011).

1.2.3.2. – Targeted anti-melanoma therapy

The improvement in our understanding of melanoma biology has led to the generation of several forms of targeted therapy for melanoma over the last years. However, while these approaches initially showed very promising results, an inevitable wave of disappointment followed due to the development of resistance to these drugs by a large proportion of the patients treated.

The most prominent example is characterised by the B-Raf inhibitors vemurafenib and dabrafenib. As described in the previous section, $BRAF^{V600E}$ mutations are highly prevalent in melanoma patients and lead to aberrant activation of the MAPK pathway, a central step in the development of this malignancy. Vemurafenib and debrafenib were designed to specifically bind and inactivate the mutant, constitutively active form of B-Raf (Tsai et al. 2008; Bollag et al. 2010; Menzies et al. 2012; Rheault et al. 2013). The initial results obtained from the use of both inhibitors were remarkable, leading to partial or even complete tumour regression in most of the patients treated. However, early relapses featuring even more aggressive tumours unfortunately followed in the majority of the cases. Strikingly, recurrent tumours usually reappear at the same locations as the original primary lesions, pointing to the underlying resistance of a few cancer cells from the primary tumour nodules subsequently able to repopulate the lesions after therapy (**Figure 1.4**) (Wagle et al. 2011).

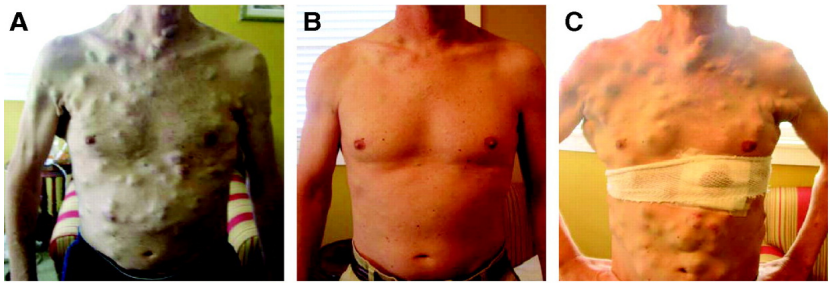


**Figure 1.4.- Vemurafenib-induced tumour regression and subsequent relapse.** BRAF-mutant metastatic melanoma patient before treatment (A), after 15 weeks of vemurafenib therapy (B) and upon relapse, following 23 weeks of therapy (C). *Adapted from "Dissecting therapeutic resistance to RAF inhibition in melanoma by tumour genomic profiling" (Wagle et al. 2011).*

Several mechanisms of resistance have been described to date, most of them leading to the reactivation of the MAPK pathway. For example, upstream of B-Raf, overexpression or activating mutations in *NRAS*, normally mutually exclusive with *BRAF* mutations, or aberrant activation of receptor tyrosine kinases such as EGFR can drive resistance to B-Raf inhibitors (Nazarian et al. 2010; Girotti et al. 2013; Sun et al. 2014). Moreover, increased activity of MEK, downstream of B-Raf (**Figure 1.3**), as a consequence of overexpression or mutation of *MEK* itself or its activators has been described as a mechanism of resistance (Emery et al. 2009; Johannessen et al. 2010; Nazarian et al. 2010).

At the level of RAF kinases, overexpression of c-Raf, amplification of the *BRAF* gene and B-Raf truncations resulting from alternative splicing can maintain activation of ERK, a downstream effector of the MAPK pathway (**Figure 1.3**) (Poulikakos et al. 2011; Shi et al. 2012).

In addition to these primarily genetic mechanisms of resistance, it has recently become evident, both from studies in cell lines and tumour models, that resistance can also be conferred by specific phenotypic states. For example, recent evidence from single cell melanoma sequencing of xenograft tumours before, during, and after RAF/MEK-inhibition revealed four distinct resistant phenotypes at the minimal residual disease state (Rambow et al. 2018). As such, the development of B-Raf inhibitors in melanoma evidences both the promise and challenges of targeted therapy and highlights the importance of the high heterogeneity and plasticity of melanoma cells within tumours as a barrier to successful therapy.

1.2.3.3. – Melanoma heterogeneity

Melanoma is associated with genetic and epigenetic as well as transcriptome/proteome intra-tumoural heterogeneity which is observed in virtually all

melanoma tumours (Grzywa et al. 2017). While some of the heterogeneity observed at the gene expression level is a consequence of the genomic and epigenetic alterations, the tumour microenvironment can also contribute to the generation of so-called phenotypic heterogeneity, which at the same time would also contribute to the modification of the epigenome (Hoek and Goding 2010; Fane et al. 2019). Understanding how phenotypic heterogeneity is generated in melanoma is crucial as it has been reported to play a key role in metastasis, drug response and resistance to therapy (Li et al. 2015; Ahmed and Haass 2018; Rambow et al. 2018; Tsoi et al. 2018).

1.2.3.4. – Phenotype-switching in melanoma

While the study of the genetic alterations frequently found in melanoma has led to a substantial improvement in our understanding of the biology of the development of this disease, it has resulted in a very limited progress regarding our understanding of the process of melanoma metastasis. Thus, although a few mutations have been associated with the metastatic behaviour of melanoma (Turner et al. 2018), a genetic signature of metastasis has not been identified. In fact, in some studies, melanoma metastases have been found to be genetically almost identical to the primary tumour (Turajlic et al. 2012; Reiter et al. 2018; Shain et al. 2018). One explanation for this observation is that genetic alterations, although required for the process of melanoma metastasis, are not the main drivers of this aspect of progression, a role that could however be played by changes in gene expression programmes induced by microenvironment imposed phenotype-switches.

Genetic and epigenetic lesions acquired during cancer development lead to a widespread rewiring of the signalling networks responding to microenvironmental signals. Cooperation between several of these genetic modifications might sensitise cancer cells to microenvironment cues that in normal cells would not be enough to trigger a phenotype-

switch. This way, genetic alterations might predispose to invasiveness, but the likelihood of metastasis would be determined by microenvironmental signals which may greatly vary with location within the tumour. But what signals in the microenvironment could trigger cells to become invasive?

Deregulated proliferation in cancer increases the demand for nutrients (Keibler et al. 2016), leading to regions of nutrient starvation in solid tumours. Just as invasiveness in bacteria is linked to nutrient limitation (Serra and Hengge 2014), recent evidence suggests that starvation may also promote invasion in cancer. For example, glutamine starvation can induce an invasive and drug-resistant phenotype in melanoma cell lines (Falletta et al. 2017). Furthermore, a single-cell RNA-seq study of the gene expression profiles of melanoma cells from patient-derived xenografts recently showed the presence of a subpopulation of cells emerged through non-mutational events that had a gene expression signature characteristic of "starvation" (Rambow et al. 2018). This subpopulation was resistant to therapy and appeared to be a transition state to other phenotypic subpopulations detected in minimal residual disease, including one characterised by an "invasive" gene expression signature (Rambow et al. 2018).

Furthermore, many other factors within the microenvironment have been associated with melanoma invasion including hypoxia and TGF-β (Pinner et al. 2009; Cheli et al. 2012; Widmer et al. 2013; Loftus et al. 2017). Collectively, these observations suggest that the microenvironment can play a major role in inducing specific adaptive gene expression programs, in which a switch from proliferation to invasion may represent a key adaptive survival strategy (Hoek and Goding 2010). A phenotype-switching model underlying the process of metastasis, as opposed to a genetic model (**Figure 1.5**), may therefore better explain the early metastases observed in melanoma and the absence of any genetic metastasis signature (Chin et al. 2006).

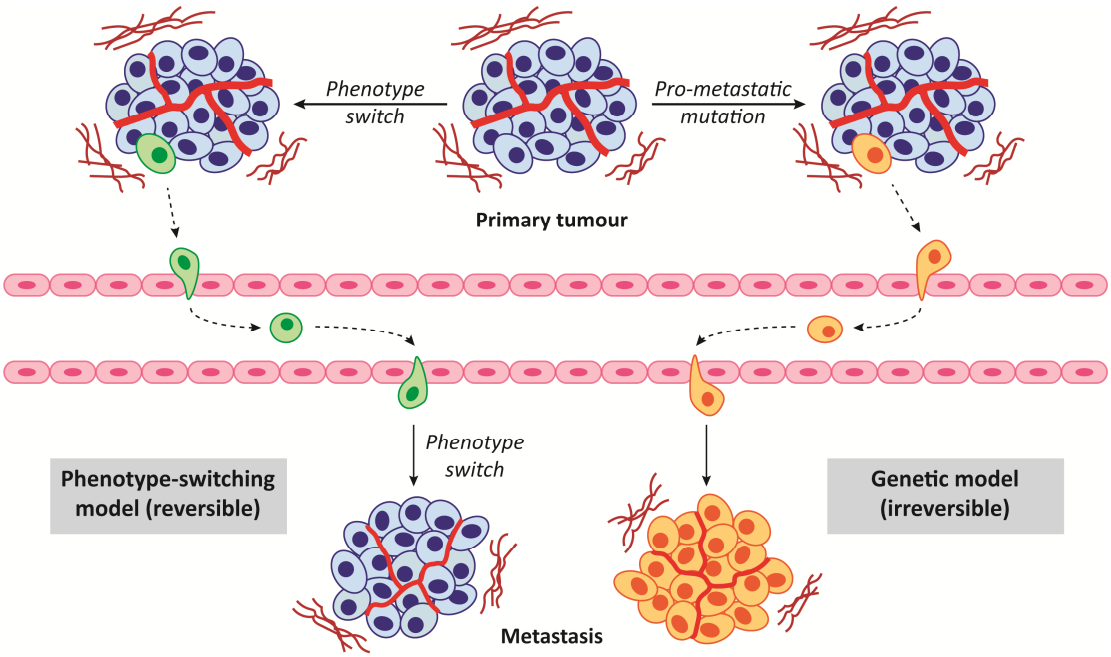


**Figure 1.5.- Phenotype-switching vs genetic model of metastasis.** In the phenotype-switching model (left), the microenvironment induces changes in the gene expression programme of a cell (represented in green) allowing it to acquire an invasive phenotype for its migration out of the tumour that is then reverted by further changes in gene expression induced by the microenvironment allowing it to regain a proliferative phenotype for the establishment of the metastasis. In the genetic model (right), the acquisition of an irreversible pro-metastatic mutation by a cell (represented in orange) allows it to become invasive and give rise to a metastasis that is genetically different to the primary tumour (Hoek and Goding 2010).

As the process of metastasis involves cells going through a series of steps where different cell properties or phenotypes (invasive, quiescent, proliferative) are required depending on the stage (Gómez-Cuadrado et al. 2017; Lambert et al. 2017), the irreversibility of mutations fails to properly explain this process. By contrast, the flexibility of the phenotype-switching model fits well with the dynamics of the metastatic cascade.

Numerous studies have reported the implication of EMT-related genes in the progression to metastatic disease in melanoma (Alonso et al. 2007; Caramel et al. 2013; Li et al. 2015). The trans-differentiation of epithelial cells into motile mesenchymal cells (EMT or epithelial-mesenchymal transition) is a biological process integral to the generation of many tissues and organs during development that can confer metastatic capacity to tumour cells

in many carcinomas (Thiery et al. 2009; Heerboth et al. 2015). Through this reversible switch in phenotypes, epithelial cells lose their polarity and cell-to-cell adhesion and gain migratory ability by the control of a gene expression program involving the upregulation of Snail, Twist and N-Cadherin and the downregulation of E-Cadherin, among others (Chae et al. 2018). While melanoma is not an epithelial cell-derived malignancy and therefore does not undergo traditional EMT, the detection of a number of EMT markers in metastatic melanoma suggests a potential EMT-like process of phenotype-switching leading to the acquisition of invasive properties in this malignancy (Alonso et al. 2007; Caramel et al. 2013; Li et al. 2015).

Since the modulation of the migratory capacity of melanoblasts (the precursors of melanocytes) in development is achieved by extracellular cues, without the need of any genetic changes (Thomas and Erickson 2008), an analogous activation of invasive properties in melanoma cells induced by the microenvironment would therefore seem feasible. Indeed, an experimental metastatic melanoma matrix can reprogram normal melanocytes to a reversible invasive phenotype (Seftor et al. 2005), supporting the sufficiency of the tumour microenvironment to induce phenotype-switches in melanocytes.

Finally, experiments transforming primary human melanocytes, human fibroblasts and epithelial cells using an identical set of genes give rise to tumours that metastasise to multiple secondary sites in the case of the melanocytes but that rarely do so when originated from fibroblasts or epithelial cells (Gupta et al. 2005).

Together, these observations suggest that part of the high metastatic proclivity of melanoma could be attributable to dynamic changes in the expression of melanocyte-specific factors induced by microenvironmental signals such as tumour starvation or inflammatory signalling, which could also be playing a role in drug resistance and relapse.

## 1.3. – MITF in melanocyte development and melanoma

During lineage development, a number of transcription factors play crucial roles in the process of specification of cell types. The microphthalmia-associated transcription factor (MITF) is known as the master transcriptional regulator of the melanocyte lineage. MITF governs the differentiation of melanocytes (which involves activation of pigmentation genes) and controls cell-cycle progression, metabolism and survival (Kawakami and Fisher 2017). Additionally, different isoforms of MITF driven by alternative promoters play a role in the development of retinal pigment epithelial cells, osteoclasts and mast cells (Kawakami and Fisher 2017). As a consequence, *MITF*-null mice exhibit absence of coat pigmentation, deafness, microphthalmia (small eyes), osteopetrosis and mast cell defects resulting from loss of melanocytes in the skin and inner ear and disruption of the development of retinal pigment epithelial cells, osteoclasts and mast cells, respectively (Moore 1995). Moreover, *MITF* heterozygous loss-of-function mutations in humans cause Waardenburg syndrome type IIA, characterised by hypopigmentation of eyes, hair and skin, varying degrees of deafness and microphthalmia (Tassabehji et al. 1994).

From the use of alternative promoters the *MITF* gene produces at least 9 isoforms that differ in their amino-termini encoded by their first exon and which show tissue-specific expression patterns: MITF-A (Amae et al. 1998), MITF-B (Udono et al. 2000), MITF-C (Fuse et al. 1999), MITF-D (Takeda et al. 2002), MITF-E (Oboki et al. 2002), MITF-H (Steingrímsson et al. 1994), MITF-J (Hershey and Fisher 2005), MITF-Mc (Takemoto et al. 2002), and MITF-M (Hodgkinson et al. 1993; Tassabehji et al. 1994). Since the MITF-M isoform is the one selectively expressed in melanocytes and melanoma cells (Tassabehji et al. 1994), all references to MITF henceforth will be in regard to this isoform unless otherwise stated.

A number of *MITF* mutations and *MITF* amplification have been associated with increased susceptibility to the development of melanoma, leading MITF to be designated a lineage-addition oncogene (Garraway et al. 2005; Bertolotto et al. 2011; Yokoyama et al. 2011; Kawakami and Fisher 2017). Significantly, different levels of MITF expression and activity have been associated with distinct phenotypes in melanoma cells (Hoek and Goding 2010; Goding 2011). To explain the observation that MITF can play both a pro- and anti-proliferative role (Carreira et al. 2005; Loercher et al. 2005; Carreira et al. 2006), a rheostat model (**Figure 1.6**) has been proposed in which high MITF levels and activity (as found in melanocytes) confer a differentiated, cell cycle arrested phenotype; elevated/medium levels of MITF activity (characteristic of melanoblasts and the proliferating cells in melanoma tumours) drive a proliferative phenotype; and low levels of MITF associate with stem cell-like invasive cells (Carreira et al. 2006). Finally, long-term MITF suppression has been shown to lead to senescence (Giuliano et al. 2010; Goding 2011).

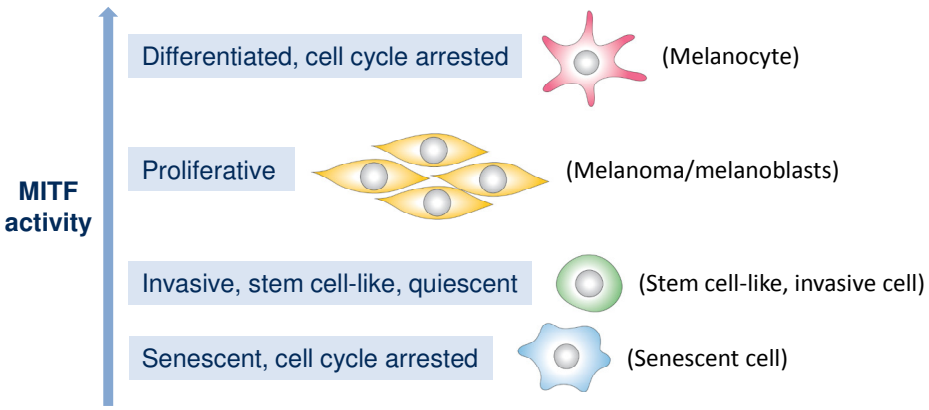


**Figure 1.6.- MITF rheostat model.** High levels of MITF activity confer a differentiated, cell cycle arrested phenotype characteristic of melanocytes, elevated/medium levels of MITF activity drive a proliferative phenotype attributable to melanoblasts and most cells in melanoma tumours, and low MITF levels associate with undifferentiated stem cell-like invasive cells. Finally, long-term depletion of MITF leads to senescence (Goding 2011).

The association of MITF expression and activity with different cell phenotypes varying from proliferative to invasive and quiescent suggests that it may have a key role in the phenotype-switching process underlying metastasis, drug-resistance and relapse in

melanoma. It is therefore essential to understand how MITF is regulated and what cellular processes and target genes MITF modulates to contribute to the establishment of different phenotypes in cells.

### 1.3.1. – MITF target genes and role in development and melanoma biology

MITF belongs to the basic helix-loop-helix leucine-zipper microphthalmia-related family of transcription factors (MiT), which also includes transcription factor EB (TFEB), transcription factor EC (TFEC) and transcription factor E3 (TFE3) (Martina et al. 2014). Through the formation of homodimers or heterodimers with another member of the family, these transcription factors bind DNA motifs with the core consensus sequence CA[T/C]GTG, also called E-boxes (Hartman and Czyz 2015). However, for MITF to bind effectively the core E-box motif is extended to include a 5' T residue (Aksan and Goding 1998). Thus, MITF may bind TCATGTG or TCATGTGA motifs (termed M-boxes) or TCACGTG or TCACGTGA elements (CLEAR boxes) related to TFEB binding sites (Hartman and Czyz 2015).

MITF functions to coordinate a wide range of cellular processes (**Figure 1.7**), which include the following:

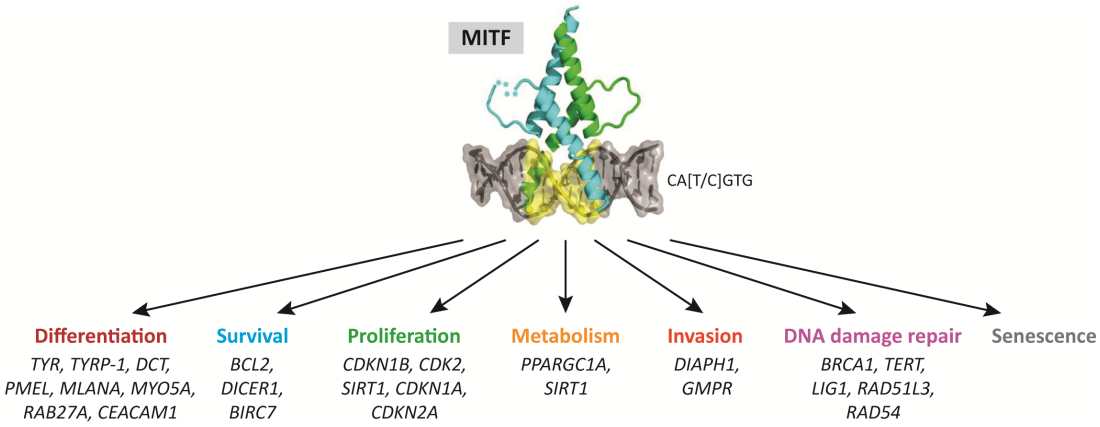


**Figure 1.7.- MITF target cellular processes and genes.** MITF regulates gene transcription by binding as a dimer to the core consensus sequence CA[T/C]GTG. MITF plays a role in the control of cell differentiation, survival, proliferation, metabolism, invasion and senesce, as well as in DNA damage repair. Cellular processes modulated by MITF are shown with examples of associated MITF target genes.

Differentiation: MITF promotes differentiation, including the activation of pigmentation genes encoding enzymes required for the synthesis of melanin such as tyrosinase (*TYR*), tyrosinase-related protein 1 (*TYRP-1*) and dopachrome tautomerase (*DCT*), as well as proteins required for the biogenesis and function of melanosomes (the melanin-producing organelles in melanocytes) including pre-melanosome protein (*PMEL*) and melanA (*MLANA*) (Kawakami and Fisher 2017). Furthermore, MITF modulates the expression of genes involved in melanosome transport such as myosin-5a (*MYO5A*) and Ras-related protein Rab-27A (*RAB27A)* (Chiaverini et al. 2008; Alves et al. 2017). Finally, MITF positively regulates the expression of the cell adhesion glycoprotein carcinoembryonic antigen-related cell adhesion molecule 1 (*CEACAM1*) (Ullrich et al. 2015).

Survival: In melanocyte development, MITF is essential for the survival of melanoblasts (Hodgkinson et al. 1993). Thus, in mutant mouse embryos lacking functional MITF, melanoblasts die, presumably by apoptosis, within 2 days following their migration out of the neural crest (Opdecamp et al. 1997; Nakayama et al. 1998). Since MITF positively regulates the expression of the anti-apoptotic gene B-cell lymphoma 2 (*BCL2*) (McGill et al. 2002; Kalkavan and Green 2018), it is likely that the absence of functional MITF sensitises melanoblasts to pro-apoptotic signals.

While the nature of these apoptotic triggers is unknown, one hypothesis could be related to the key mediator of the integrated stress response activating transcription factor 4 (ATF4), which is expressed in the neural crest (Suzuki et al. 2010). As it will be later described, ATF4 can upregulate *CHOP*/*DDIT3* which then represses *BCL2* and activates the expression of the pro-apoptotic factor *BIM* (O'Connor et al. 1998; McCullough et al. 2001; Puthalakath et al. 2007; Rozpedek et al. 2016). It is possible that in a setting where the combined effect of ATF4 expression and MITF absence reduces BCL2 to a minimum level, the activation of BIM by ATF4 could trigger the apoptotic cascade. Interestingly, deletion of

BIM in mouse models has been shown to rescue melanocyte loss consequence of BCL2 deletion, restoring pigmentation and thus establishing a key role of BIM in the modulation of melanocyte survival (Bouillet et al. 2001).

Additionally, the expression of DICER, a regulator of micro-RNA processing, is positively regulated by MITF, and deletion of DICER is lethal to melanocytes (Levy et al. 2010). Intriguingly, the effect of DICER promoting melanocyte survival appears to be at least partly mediated by downregulation of BIM through miR-17 (Levy et al. 2010), which again suggests BIM is a potential inducer of melanocyte apoptosis following MITF loss.

MITF seems to also modulate apoptosis by positively regulating the expression of the anti-apoptotic protein BIRC7, which is found at extremely low levels of expression in normal tissues but is highly expressed in melanoma and other cancers (Dynek et al. 2008).

Proliferation: The first reports on the role of MITF in proliferation seemed to contradictorily point to a function as both activator and repressor of cell cycle progression (Widlund et al. 2002; Carreira et al. 2005; Garraway et al. 2005). However, underlying this apparent paradox was the fact that among MITF targets are both activators and inhibitors of cell cycle progression, and the levels of MITF expression and activity are determinants of the overall effect on cell proliferation. As indicated in the rheostat model (**Figure 1.6**), low levels of MITF associate with a quiescent state where very low proliferation appears to be at least partly due to the presence of high levels of the cyclin-dependent kinase inhibitor p27 (CDKN1B), whose protein stability is indirectly regulated by MITF (Carreira et al. 2006). The effect of MITF on reducing p27 protein stability allows for a transition to a proliferative phenotype when there is an increase in MITF activity to intermediate levels, such as those found in melanoblasts and in proliferating melanoma cells in tumours (**Figure 1.6**). Furthermore, MITF upregulates the expression of the activator of cell cycle progression cyclin-dependent kinase 2 (CDK2) and the NAD-dependent protein deacetylase sirtuin 1

(SIRT1), both of which promote proliferation in melanoma (Du et al. 2004; Ohanna et al. 2014). Finally, MITF transcriptionally activates the cell cycle inhibitors p21 (CDKN1A) and p16 (CDKN2A), which lead to cell cycle arrest when MITF activity levels are very high (such as in differentiated melanocytes, **Figure 1.6**) (Carreira et al. 2005; Loercher et al. 2005).

The pro-proliferative role of MITF in melanoma cells has however been recently challenged in studies performed in melanoma cell lines where MITF depletion using shRNA, while reducing differentiation, did not show the expected dependence on MITF for cell proliferation (Vlčková et al. 2018). Whether other factors, for example TFEB/TFE3, are able to compensate the lack of MITF expression by promoting proliferation remains unclear.

Metabolism: MITF controls metabolism by positively regulating *PPARGC1A*, which encodes peroxisome proliferator-activated receptor gamma coactivator 1-alpha (PGC-1α), a regulator of energy homeostasis which particularly promotes mitochondrial oxidative phosphorylation (Vazquez et al. 2013).

As mentioned above, MITF has also been reported to regulate the expression of the NAD-dependent protein deacetylase SIRT1, which plays a key role as a metabolic sensor (Li 2013; Ohanna et al. 2014).

Invasion: As indicated in the rheostat model (**Figure 1.6**), low levels of MITF activity usually associate with an invasive phenotype (Goding 2011), and MITF depletion using siRNA increases invasiveness in melanoma cell lines (Carreira et al. 2006). While the mechanisms underlying this change in phenotype when reducing MITF levels are not completely understood, regulation of the actin cytoskeleton may be important as MITF can upregulate the diaphanous-related formin Dia1 (*DIAPH1*), which promotes actin polymerisation (Carreira et al. 2006).

In addition, MITF can positively regulate the expression of guanosine monophosphate reductase (GMPR), and consequently, MITF depletion leads to elevated levels of intracellular

GTP, leading to increased levels of the GTP-bound (active) form of the modulators of actin cytoskeleton: RAC1, RHO-A and RHO-C (Bianchi-Smiraglia et al. 2017).

However, the potential role of MITF as a suppressor of invasion was recently challenged in a study where repression of MITF using a physiological regulator instead of siRNA did not lead to the expected invasive phenotype (Falletta et al. 2017). It is therefore possible that low MITF is necessary but not sufficient for invasiveness.

DNA damage repair: Depletion of MITF can lead to accumulation of DNA damage and activation of the DNA damage response (Giuliano et al. 2010). Among the underlying mechanisms appears to be the transcriptional upregulation of several factors with an important role in DNA repair by MITF, including *BRCA1*, *TERT*, *LIG1*, *RAD51L3* and *RAD54* (Beuret et al. 2011; Strub et al. 2011).

Senescence: While short-term suppression of MITF using siRNA leads to invasiveness, prolonged siRNA-mediated MITF depletion results in senescence (Giuliano et al. 2010). In this context, it seems that the underlying mechanism at least partly involves the accumulation of DNA damage following MITF depletion, which triggers the DNA damage response signalling cascade leading to upregulation of the tumour suppressor p53, a key player in cellular senescence (Giuliano et al. 2010).

### 1.3.2. – Regulation of MITF

The regulation of MITF expression and activity is complex, involving several levels of regulation and many factors and signalling pathways.

#### Transcriptional regulation of MITF

There are three key genomic regions that have been reported to play a role in the regulation of the expression of MITF-M. First, MITF-M is not expressed in the black-eyed white (*Mitf*$^{mi\text{-}bw}$) mouse, which has an L1 retrotransposable element inserted into intron 3

(Yajima et al. 1999), though expression of other MITF isoforms is unaffected. It is however currently unknown whether an enhancer is located in this region of the gene or a different mechanism underlies its involvement, for example the interruption of regulatory looping from an *MITF* enhancer to the *MITF-M* promoter by the line element. Second, around 92 kb upstream of *MITF*'s transcription start site there is an enhancer regulated by the Med23 subunit of the Mediator complex, a key factor in the transcriptional machinery (Xia et al. 2017). Finally, the *MITF* promoter sitting immediately upstream of *MITF-M*'s transcription start site, which has been widely studied, is controlled by many transcription factors and signalling pathways (**Figure 1.8**).

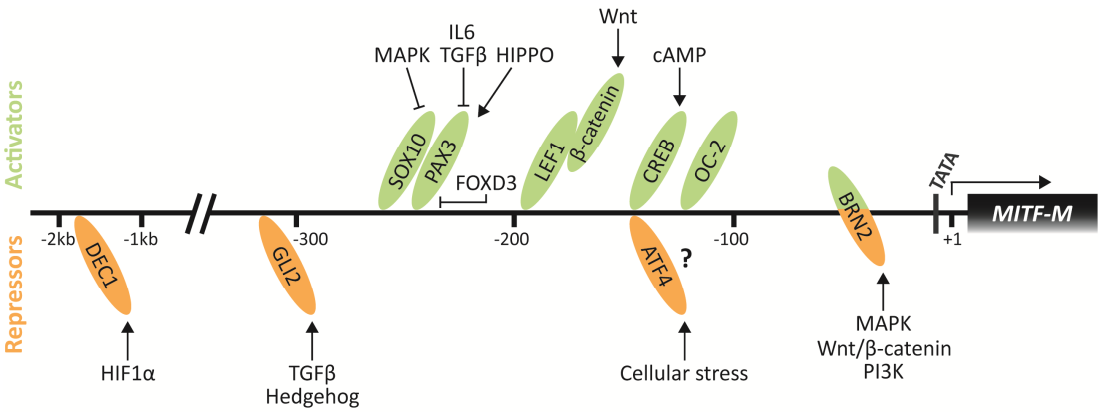


**Figure 1.8.- Transcriptional regulation of MITF expression.** Schematic diagram showing the regulation of the *MITF-M* promoter by transcription factors and signalling pathways. Positive regulators are shown in green. Negative regulators are shown in orange. ATF4 may compete with CREB for direct binding and regulation of the *MITF-M* promoter (Ferguson et al. 2017).

Among the main transcription factors regulating *MITF-M* expression are the following:

**CREB** (cAMP response element binding protein) is a bZIP transcription factor that enables MITF expression to be responsive to intracellular cyclic adenosine monophosphate (cAMP) levels. Significantly, elevated cAMP arises as a consequence of UV irradiation that leads to MITF-dependent activation of pigmentation gene expression as part of the tanning response. Thus, the absorption of UV light by keratinocytes in the skin turns on a cellular damage response involving the activation of the tumour suppressor p53, which upregulates

the transcription of proopiomelanocortin (POMC) (Cui et al. 2007). Enzymatic cleavage of POMC then produces α-melanocyte stimulating hormone (α-MSH), which binds to the melanocortin 1 receptor (MC1R) in melanocytes. This signal is transmitted intracellularly through activation of adenylyl cyclase, which produces cAMP that activates protein kinase A (PKA), ultimately resulting in the phosphorylation of CREB. Phosphorylated CREB finally activates MITF transcription through binding to a cAMP response element (CRE) site in its promoter (TGACGTCA) (Bertolotto et al. 1998a; Price et al. 1998b).

**PAX3** (Paired Box 3) is mainly expressed in undifferentiated (but committed) melanoblasts and has a role in both initiating melanogenesis (through activation of MITF) and preventing terminal differentiation (through competition with MITF for the occupancy of the *DCT* enhancer) (Watanabe et al. 1998; Lang et al. 2005a). As a consequence of its role as activator of MITF expression, inactivating mutations in *PAX3* cause variations of Waardenburg syndrome, characterised by pigmentation defects (Watanabe et al. 1998).

Pax3 is downregulated by both TGF-β and interleukin-6 receptor signalling (Kamaraju et al. 2002; Yang et al. 2008). Furthermore, the Hippo pathway regulates the expression of Pax3, and its effectors YAP and TAZ act as cofactors of Pax3 (Manderfield et al. 2014; Meng et al. 2016). The transcription factor forkhead box protein D3 (FOXD3) can prevent binding of Pax3 to the *MITF* promoter, therefore leading to *MITF* repression (Thomas and Erickson 2009). Since both neural/glial cells and melanocytes originate from neural crest cell progenitors, FOXD3 regulates the lineage switch between neural/glial and pigment cells through its ability to repress MITF expression. Consequently, only FOXD3 is expressed in neural/glial precursors and only melanoblasts express MITF (Curran et al. 2009; Thomas and Erickson 2009).

**SOX10** (SRY-related high mobility group-box 10) is another transcription factor with a major role in the development of melanocytes from the neural crest, being a strong

activator of the *MITF* promoter (Verastegui et al. 2000). As a consequence of its role as an activator of *MITF* expression, SOX10 mutations can also cause Waardenburg syndrome (Pingault et al. 1998; Verastegui et al. 2000). SOX10 plays an essential role in melanocyte biology, cooperating with CREB to promote the expression of *MITF* in response to cAMP (Huber et al. 2003).

The transcriptional activity of SOX10 is tightly regulated at the post-translational level, with sumoylation being normally required for its function and ERK-mediated phosphorylation inhibiting its activity by preventing sumoylation (Han et al. 2018b). It is therefore possible that high ERK activity in $BRAF^{V600E}$ melanomas can modulate *MITF* expression through reduction of SOX10 transcriptional activity.

**LEF1** (lymphoid enhancer-binding factor 1) is a transcription factor that binds to and activates the *MITF* promoter when forming a complex with β-catenin. As a consequence, Wnt signalling, which stabilises β-catenin protein, can control the specification of the melanocyte lineage from the neural crest and promote MITF-dependent melanoma proliferation (Dorsky et al. 2000; Takeda et al. 2000b; Widlund et al. 2002).

**ATF4** (activating transcription factor 4) is a bZIP transcription factor which is an effector of a signalling cascade responsive to different types of cellular stresses including nutrient limitation and endoplasmic reticulum (ER) stress (Harding et al. 2003). ATF4 can repress *MITF* expression, reportedly through binding to a CRE site located in the *MITF* promoter and displacing CREB (Falletta et al. 2017; Ferguson et al. 2017), an important previously described activator of *MITF* expression (Bertolotto et al. 1998a; Price et al. 1998b).

**Jun** is a bZIP transcription factor that is also activated in response to some types of cellular stress (Leppä and Bohmann 1999). In melanoma, Jun and MITF transcriptionally repress each other creating a feed-forward loop that leads to dedifferentiation consequence

of MITF loss in response to inflammatory signalling (Riesenberg et al. 2015). However, direct binding of Jun to *MITF* regulatory elements has not yet been confirmed.

**BRN2** is a POU domain transcription factor which is not expressed in melanocytes or their precursors but is widely expressed in melanoma, where it promotes melanoma invasion (Goodall et al. 2008; Arozarena et al. 2011; Thurber et al. 2011; Zeng et al. 2018; Fane et al. 2019). BRN2 can repress *MITF*, and the expression of *BRN2* and *MITF* is mutually exclusive in tumours and melanomaspheres (Goodall et al. 2008; Thurber et al. 2011). However, one report also suggests that BRN2 can activate *MITF* expression in cultured melanoma cells (Wellbrock et al. 2008). How BRN2 might switch from activator to repressor is not well understood, but recent evidence obtained by examining the BRN2 interactome suggests that BRN2, while clearly able to bind DNA and regulate transcription, does not interact with transcription cofactors (Herbert et al. 2019). This observation raises the possibility that BRN2 may regulate *MITF* expression by facilitating recruitment of other DNA-binding transcription factors. *BRN2* expression in melanoma is controlled by BRAF/MAPK, Wnt/β-catenin, and PI3K signalling (Goodall et al. 2004a; Goodall et al. 2004b; Bonvin et al. 2012).

**DEC1** (differentially expressed in chondrocytes protein 1) (also known as BHLHB2 and BHLHE40) is a bHLH transcription factor that can repress *MITF* in hypoxic conditions (Feige et al. 2011; Cheli et al. 2012). DEC1 is positively regulated by HIF1α (hypoxia-inducible factor 1) under low oxygen conditions (Feige et al. 2011; Cheli et al. 2012).

**OC-2** (cut homeodomain transcription factor Onecut-2) is expressed in melanocytes and can bind and stimulate the *MITF* promoter (Jacquemin et al. 2001). It is however currently not known how the expression and transcriptional activity of OC-2 are regulated.

**GLI2** is a transcription factor that represses *MITF e*xpression and promotes invasion in melanoma (Alexaki et al. 2010; Javelaud et al. 2011; Pierrat et al. 2012). GLI2 is a mediator

of the hedgehog signalling pathway and is upregulated by the TGF-β pathway (Alexaki et al. 2010; Javelaud et al. 2011).

Note that although the evidence suggests that the repertoire of TFs listed above can regulate MITF-M mRNA expression, most of the experimental observations are obtained through *in vitro* studies in which transfection of *MITF-M* promoter reporters and *in vitro* DNA binding assays are used to determine whether the *MITF* promoter is a target. To date, only SOX10 chromatin immunoprecipitation-high throughput sequencing (ChIP-seq) has been used to confirm *in vivo* direct binding at the *MITF-M* promoter. Additionally, it is possible that complementary techniques to map transcription factor binding sites, such as ChIP-seq, reveal occupancy of other regulatory elements outside the *MITF-M* promoter.

Finally, *MITF* expression is also subject to regulation at the post-transcriptional level, and many microRNAs (miRNAs) inhibit *MITF* expression and thereby play an important role in melanoma biology. These include miR-26a, miR-101, miR-137, miR-148, miR-155, miR-182 and miR-218 (Bemis et al. 2008; Segura et al. 2009; Haflidadóttir et al. 2010; Kunz 2013; Luo et al. 2013; Guo et al. 2014; Arts et al. 2015; Qian et al. 2017).

Post-translational regulation of MITF

Given the importance of MITF in melanocyte and melanoma biology it is not surprising that MITF protein stability and transcriptional activity are regulated by post-translational modifications (**Figure 1.9**).

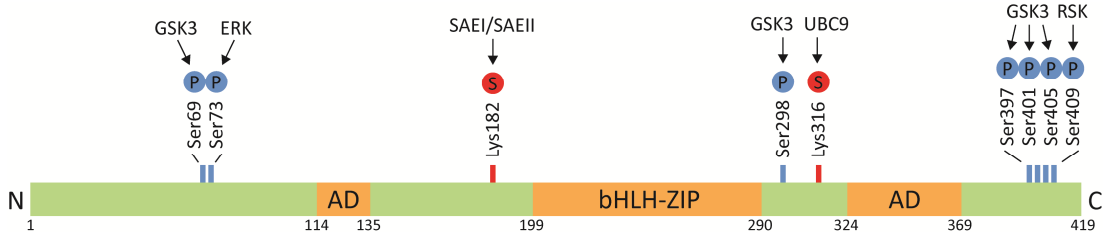


**Figure 1.9.- Post-translational regulation of MITF.** Schematic representation of MITF-M protein showing the post-translational modifications to which MITF-M is subjected and how these are established. AD: transcription activation domain; bHLH-ZIP: basic helix-loop-helix leucine-zipper. Numbers refer to amino acids in the MITF-M protein.

Those that have been characterised to date include the following:

**Phosphorylation** – MITF phosphorylated at Ser73 and Ser409 by ERK and RSK, respectively, which are both activated by the NRAS/BRAF/MAPK pathway (Hemesath et al. 1998). Phosphorylation of MITF at Ser73 reportedly promotes its interaction with p300/CBP, an MITF coactivator (Sato et al. 1997; Price et al. 1998a). On the other hand, this modification enhances the interaction between MITF and PIAS3 (protein inhibitor of activated STAT3), which attenuates MITF transcriptional activity (Levy et al. 2003; Levy et al. 2006). Phosphorylation at Ser409 can however prevent the effect of PIAS3 inhibiting MITF function (Levy et al. 2003). Additionally, phosphorylation of MITF at Ser73 has been recently shown to prime for phosphorylation by GSK3 at Ser69, with the resulting dual phosphorylation activating a nuclear export signal (Ngeow et al. 2018). Moreover, phosphorylation at Ser409 appears to prime MITF for further phosphorylation by GSK3 at Ser397, Ser401 and Ser405, which reduces MITF protein stability (Ploper et al. 2015). Interestingly, phosphorylation of these sites is inhibited by Wnt signalling, which has a key role in the development of melanocytes (Dorsky et al. 2000; Takeda et al. 2000b; Ploper et al. 2015).

GSK3 has also been reported to phosphorylate MITF at Ser298, and mutation of this site has been associated with Waardenburg syndrome type IIA (Takeda et al. 2000a). However, while it was first shown that mutation of Ser298 to proline significantly impaired binding of MITF to the tyrosinase promoter (Takeda et al. 2000a), this observation was later challenged by a different study where the same mutation did not affect MITF DNA binding (Grill et al. 2013), and no evidence for Ser298 phosphorylation has been observed by others (Ngeow et al. 2018).

Finally, MITF is phosphorylated by p38, a stress activated kinase, at Ser307 in osteoclasts, enhancing its transcriptional activity in these cells (Mansky et al. 2002).

However, to date the role of Ser307 phosphorylation in melanocyte/melanoma biology has yet to be described.

**Sumoylation** – MITF is sumoylated at Lys182 and Lys316 by SAEI/SAEII (an E1 sumo-activating enzyme) and UBC9 (an E2 sumo-conjugating enzyme), respectively (Miller et al. 2005; Murakami and Arnheiter 2005). MITF sumoylation can modulate MITF transcriptional activity in regard to the activation of specific targets (Miller et al. 2005; Murakami and Arnheiter 2005). Thus, mutated non-sumoylatable forms of MITF exhibit enhanced transcription of a subset of target genes and patients bearing a mutation in K318 that prevents sumoylation on K316 exhibit a significantly increased predisposition to melanoma (Murakami and Arnheiter 2005; Bertolotto et al. 2011; Yokoyama et al. 2011).

**Ubiquitination** – While specific ubiquitination sites in MITF have not yet been clearly defined, the deubiquitinating enzyme USP13 (ubiquitin-specific protease 13) prevents proteasomal degradation of MITF in melanoma cells (Zhao et al. 2011a). Consequently, USP13 knock-down in melanoma cells reduces MITF protein levels (without affecting MITF mRNA) and decreases cell proliferation (Zhao et al. 2011a).

MITF cofactors

The transcriptional activity of MITF is also mediated by its interaction with cofactors, among which are the following:

**p300/CBP** – p300 and its homologue CREB-binding protein (CBP) are lysine acetyl transferases that act as transcriptional coactivators and which bind MITF through an interaction facilitated by phosphorylation of Ser73 (Sato et al. 1997; Price et al. 1998a). p300 and CBP enhance transcription of genes by linking transcription factors with the basal transcriptional machinery, by acting as a platform for the recruitment of additional coactivators, and via chromatin modification through their histone acetyltransferase activity

(Chan and La Thangue 2001; Wang et al. 2013a; Dancy and Cole 2015). While p300/CBP can modulate transcription by acetylation of transcription factors (Dancy and Cole 2015), acetylation of MITF has not yet been reported.

**SWI/SNF** – The SWI/SNF (switch/sucrose non-fermentable) chromatin remodelling complex plays an important role in cooperating with MITF to control the expression of its target genes (de la Serna et al. 2006). The subunit composition of SWI/SNF is variable and appears to confer specificity to the set of MITF target genes activated (Keenen et al. 2010). Interestingly, SWI/SNF is also required for *MITF* expression (Vachtenheim et al. 2010).

**β-catenin** – As described above, β-catenin (downstream from Wnt signalling) is an important regulator of MITF expression during melanocyte development (Dorsky et al. 2000; Widlund et al. 2002). However, β-catenin is also an MITF cofactor, promoting transcription of differentiation-associated MITF target genes (Schepsky et al. 2006).

## 1.4. – ATF4 in the integrated stress response and melanoma

Activating transcription factor 4 (ATF4) is a key mediator of the integrated stress response (ISR) (**Figure 1.10**), a signalling pathway present in all eukaryotic cells (Pakos-Zebrucka et al. 2016). The physiological stresses that upregulate ATF4 activating the ISR are sensed by four different kinases (**Figure 1.10**): general control non-derepressible 2 (GCN2) is mainly activated under glucose and/or amino acid deficiency (Ye et al. 2010); protein kinase R (PKR)-like endoplasmic reticulum kinase (PERK) signals the accumulation of misfolded proteins and can also be activated by low glucose and/or oxygen (Harding et al. 1999; Koumenis et al. 2002; Moore et al. 2011); heme deficiency activates heme-regulated inhibitor (HRI) (Chen 2007); and protein kinase RNA-activated, also called protein kinase R (PKR), senses the presence of dsRNA, typically found during viral infections, and can also be activated in response to interferon (García et al. 2007; Pindel and Sadler 2011).

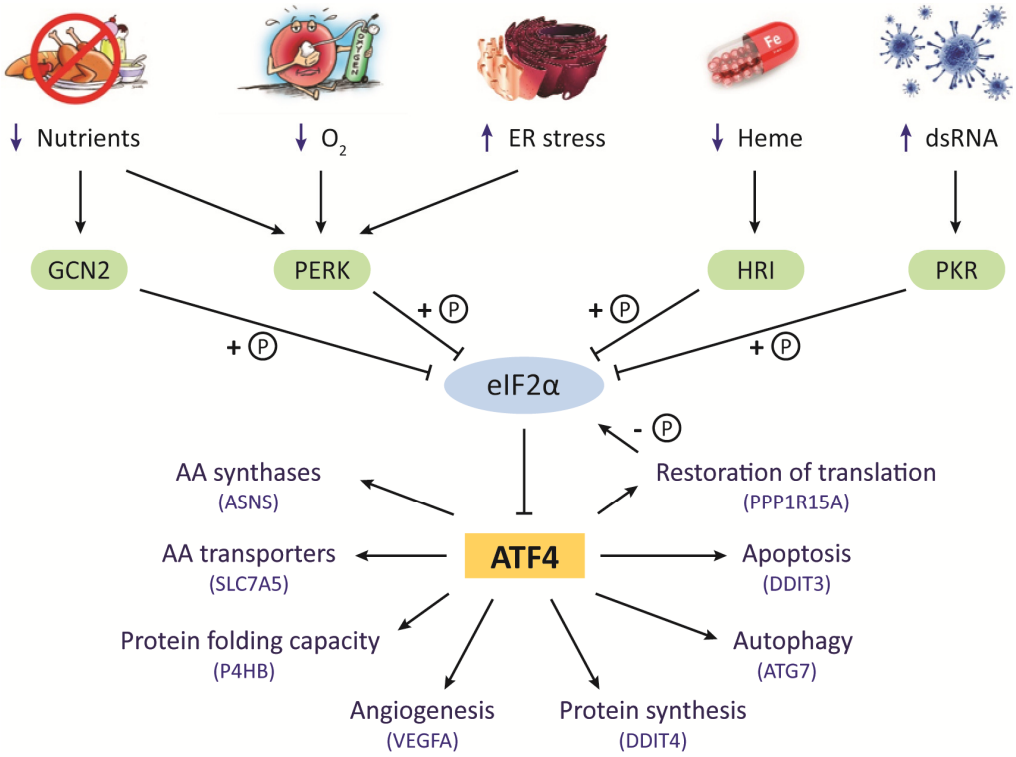


**Figure 1.10.- Integrated stress response signalling.** Under stress conditions including nutrient deprivation, hypoxia, accumulation of misfolded proteins (ER stress), heme deficiency or presence of double-stranded RNA (dsRNA), the α-subunit of eukaryotic initiation factor 2 (eIF2α) is phosphorylated by one of the protein kinases represented (GCN2: general control non-derepressible 2, PERK: protein kinase R (PKR)-like endoplasmic reticulum kinase, HRI: heme-regulated inhibitor, PKR: protein kinase R). Phosphorylation of eIF2α leads to global protein synthesis repression and increased translation of ATF4, which then promotes an adaptive response regulating genes involved in amino acid transport and metabolism, such as asparagine synthetase (ASNS) or solute carrier family 7 member 5 (SLC7A5), autophagy, for example autophagy related 7 (ATG7), angiogenesis, such as vascular endothelial growth factor A (VEGFA), protein synthesis, including DNA damage inducible transcript 4 (DDIT4) and protein folding capacity, such as prolyl 4-hydroxylase subunit beta (P4HB), or an anti-survival response regulating pro-apoptotic genes including DNA damage inducible transcript 3 (DDIT3). Finally, ATF4 upregulates protein phosphatase 1 regulatory subunit 15A (PPP1R15A), which restores translation upon stress mitigation. (Singleton and Harris 2012; Wortel et al. 2017).

Activation of these kinases converges on the phosphorylation of the α-subunit of eukaryotic initiation factor 2 (eIF2α), which leads to suppression of general translation initiation (Harding et al. 2000; Sonenberg and Hinnebusch 2009). While this results in global protein synthesis repression, paradoxically, the translation of a small subset of mRNAs containing upstream open reading frames (uORFs), including that of ATF4 mRNA, is enhanced (Harding et al. 2000). Thus, different types of cellular stresses such us nutrient

limitation, hypoxia and accumulation of misfolded proteins all ultimately lead to phosphorylation of eIF2α and consequent upregulation of ATF4.

Following activation of the ISR, ATF4 coordinates an adaptive response through the regulation of genes involved in amino acid transport and metabolism, autophagy, angiogenesis, protein folding and homeostasis, and redox balance, thus promoting survival (**Figure 1.10**) (Singleton and Harris 2012; Wortel et al. 2017). However, under conditions of severe or prolonged stress, ATF4 adopts an anti-survival role, promoting genes involved in the induction of apoptosis (**Figure 1.10**) (Singleton and Harris 2012; Wortel et al. 2017).

Cancer cells inevitably encounter different types of stress during tumour development. High rates of proliferation increase the demand for protein synthesis that can lead to the saturation of the protein folding capacity of the ER and the accumulation of misfolded proteins that results in ER stress (Wang et al. 2010). Furthermore, as tumours grow, cells in the tumour core are challenged by hypoxia and nutrient limitation, which constitute further triggers of ER stress and activate the ISR (Wang et al. 2010; Pakos-Zebrucka et al. 2016). As a consequence, it is not surprising that ATF4 expression is upregulated in tumours compared to matched normal tissue (Ameri et al. 2004). Immunohistochemical analysis has shown how ATF4 expression is confined to hypoxic, peri-necrotic regions distant from the tumour vasculature, in accordance with a mechanism of translational reprogramming induced by nutrient and oxygen deprived microenvironment conditions (Ameri et al. 2004; Bi et al. 2005).

Especially important for melanoma, as mentioned above, ATF4 can negatively regulate *MITF* expression (Falletta et al. 2017; Ferguson et al. 2017). Since ATF4 expression is modulated by microenvironmental conditions frequently found in tumours, it constitutes a potential candidate for a role in the regulation of MITF in response to the environment leading to phenotype-switches in melanoma. Consistent with this, both nutrient starvation

and hypoxia can modulate *MITF* expression in melanoma cells (Feige et al. 2011; Cheli et al. 2012; Falletta et al. 2017; Ferguson et al. 2017).

Transcriptional regulation of target genes by ATF4

ATF4 belongs to the basic leucine zipper (bZIP) family of transcription factors, which form homodimers and/or heterodimers with other family members. ATF4 frequently heterodimerises with members of the AP-1 and C/EBP subfamilies, including Fos and Jun (Hai and Curran 1991) and different C/EBP proteins (Vallejo et al. 1993). These dimerisation partners contribute both to DNA binding and the target specificity of ATF4. Thus, while ATF4 normally binds to the consensus ATF/CRE binding site 'TGACGTCA' (Deutsch et al. 1988; Hai and Hartman 2001), heterodimers have been reported to bind to variations of this sequence (Hai and Curran 1991; Vallejo et al. 1993; Fawcett et al. 1999; Kilberg et al. 2009; Han et al. 2013). Finally, as an example of the contribution to target specificity, ATF4 binding partners CCAAT/enhancer-binding protein β (C/EBPβ) and CCAAT/enhancer-binding protein γ (C/EBPγ) have been associated with the regulation of adaptive response genes, and C/EBP homologous protein (CHOP), also known as DNA damage inducible transcript 3 (DDIT3), has been related to the pro-apoptotic response (Halterman et al. 2008; Matsumoto et al. 2013; Huggins et al. 2015).

The transcriptional activity and specificity of ATF4 is also influenced by its interaction with cofactors. For example, p300/CBP is a coactivator of ATF4, stimulating ATF4-driven transcription through its histone acetyltransferase activity and enhancing the transcription of specific targets including CHOP in response to amino acid limitation (Chérasse et al. 2007).

Additionally, some post-translational modifications can also modulate the target and DNA binding specificity of ATF4. For example, methylation of ATF4 at Arg239 by protein

arginine N-methyltransferase 1 (PRMT1) enhances transcription of a specific set of ATF4 target genes related to the induction of apoptosis in conditions of nutrient starvation, as does loss of BTG1, which mediates the interaction between ATF4 and PRMT1 promoting repression of this particular subset of targets in this setting (Yuniati et al. 2016). Similarly, phosphorylation of ATF4 at the threonine residues 107, 114, 115 and 119 by RET, a receptor tyrosine kinase with a recently identified dual (tyrosine/threonine) specificity which is frequently hyperactivated in cancer, can decrease the occupancy and transcriptional activation at the promoters of the pro-apoptotic genes *NOXA* and *PUMA* (Bagheri-Yarmand et al. 2015). Finally, phosphorylation of ATF4 at Ser215 by casein kinase 2 (CK2) may stimulate transcriptional activation at the promoters of the target genes *ATF3* and *CHOP* (Ampofo et al. 2013). Interestingly, CK2 also phosphorylates ATF4 dimerisation partners such as C/EBPδ, enhancing its transcriptional activity (Schwind et al. 2015), and CHOP, in this case with an inhibitory effect (Ubeda and Habener 2003). It is therefore possible that through ATF4 phosphorylation, CK2 is able to contribute to determining the specific subset of target genes transcribed, as suggested by Wortel *et al.* (Wortel et al. 2017). Indeed, overexpression of CK2 in cancer cells has already been observed to protect against apoptosis and inhibition of CK2 can lead to apoptosis via CHOP (Intemann et al. 2014).

Finally, epigenetic marks can contribute to the target and DNA binding specificity of ATF4. For example, acetylation of histones H2B and H4 induced by prior DNA-binding of phosphorylated ATF2 is necessary for ATF4-mediated activation of transcription of *CHOP* and *ATF3* but not *ASNS* (Bruhat et al. 2007). Moreover, DNA methylation can modulate the binding affinity of ATF4 dimers to different binding sites. For example, the ATF4-C/EBPβ dimer strongly increases its affinity for the non-canonical site 'CGATGCAA' following methylation of the first cytosine (Mann et al. 2013).

## 1.5. – Gene regulation

In multicellular mechanisms, virtually all cells contain the same DNA yet striking differences exist among different cell types which carry out very diverse functions. Cell specialisation or differentiation is achieved through the induction of distinct gene expression programs. Furthermore, gene regulation is fundamental for the adaptation of cells to environmental changes.

In line with its importance to cell function and survival, gene expression is finely regulated by multiple complex mechanisms, which can be classified into the following layers: transcriptional regulation (which modulates the amount of mRNA that is transcribed from a particular gene), post-transcriptional regulation (which further tunes the amount of specific mRNAs available), translational regulation (which determines how much of each mRNA is translated into protein), and post-translational regulation (which controls the stability and activity of the synthesised proteins).

### 1.5.1. – Transcriptional regulation of gene expression

#### Transcription factors, genomic regulatory elements and the transcription machinery

Protein-coding genes in eukaryotes are transcribed by the multiprotein complex RNA polymerase II (Pol II) in a highly regulated process that requires the concerted activity of sequence-specific transcription factors (TFs), general transcription factors (GTFs) and cofactors (Soutourina 2018).

Regulatory elements in the genome provide a code that contains information on the regulation of the expression of specific genes. TFs have a leading role in the regulation of the activation of transcription, interpreting and integrating the output from signalling pathways and genomic regulatory elements to activate or repress transcription of specific genes.

TFs are able to induce transcriptional activation by facilitating the recruitment of the basal transcription machinery, including Pol II, to core promoters. Following the assembly of the preinitiation complex (PIC), which signals the unwinding of the DNA, transcription is initiated but pauses when around 20-50 nucleotides have been transcribed. Further activating signals are needed to allow for Pol II escape from the promoter-proximal pause region and switch to productive elongation. Once the entire gene has been transcribed, Pol II undergoes termination and is able to restart the process of transcription. Finally, precursor mRNAs (pre-mRNAs) are processed into mature mRNAs and exported from the nucleus.

For the process of transcription to take place, chromatin decompaction is required. If stretched end-to-end, the DNA contained in each of our cells measures around 2 meters, yet it is contained in a cell nucleus of approximately 6 μm diameter. To fit in this space, DNA is tightly wrapped around histones and further condensed into chromatin. This highly compacted structure acts as a barrier to recruitment of TFs and the basal transcription machinery to DNA and needs to be overcome for successful transcription to occur.

The basic structural (and functional) unit of chromatin is the nucleosome, which limits the accessibility of TFs to regulatory elements in the genome. Underlying DNA sequences can play an important role determining nucleosome positioning to allow exposure of specific regulatory elements for binding of TFs (Segal and Widom 2009b; Bai and Morozov 2010). However, this is still controversial (Kaplan et al. 2010; Zhang et al. 2010), but may be relevant to a specific subset of genes. Additionally, a specific class of TFs, termed pioneer factors, are able to bind their target sequences within nucleosomal DNA and induce the local opening of the chromatin through the recruitment of chromatin remodelling complexes (Magnani et al. 2011; Zaret and Carroll 2011; Iwafuchi-Doi 2019). According with their priming function, pioneer TFs often drive gene expression programs acting at the top of gene regulatory networks (Zaret and Carroll 2011; Drouin 2014; Iwafuchi-Doi and Zaret

2014; Iwafuchi-Doi et al. 2016). Examples of pioneer factors include MYOD, AP1, FOXA, PU.1 and C/EBPβ (de la Serna et al. 2005; Ghisletti et al. 2010; Heinz et al. 2010; Biddie et al. 2011; Siersbæk et al. 2011; Iwafuchi-Doi et al. 2016).

Following their binding to regulatory sequences in the DNA, TFs coordinate the regulation of expression of target genes by modulating the assembly and activity of the transcription machinery and the structure of chromatin, usually through the action of cofactors.

TFs can be divided into different types according to the structure of their DNA-binding domains, with the zinc finger (ZF), basic helix-loop-helix (bHLH) and basic leucine zipper (bZIP) families of TFs being among the largest in eukaryotes (Lambert et al. 2018). TFs have also been traditionally classified as activators or repressors. However, studies have shown how many TFs can act as both activators and repressors depending on the cofactors they interact with or their binding sequence context (Lambert et al. 2018).

TFs recognise specific sequences located in promoter regions or at greater distances from transcription start sites, in regulatory regions referred to as enhancers or silencers depending on whether they are involved in transcriptional activation or repression, respectively (Ayer and Benyajati 1990; Petrykowska et al. 2008; Vokes et al. 2008; Spitz and Furlong 2012). Additionally, insulators have been defined as DNA sequences which act as barriers that limit the spatial influence of enhancers, silencers, or repressive chromatin following binding of TFs such as CTCF (Gaszner and Felsenfeld 2006).

Apart from the long-recognised role in transcriptional regulation of TFs bound to promoter regions, over the last few decades the interplay between enhancers and TFs has been shown to have a prevalent role in gene regulation, particularly in the establishment of gene expression patterns throughout development and cell specialisation (Ong and Corces 2011; Spitz and Furlong 2012). Enhancers are clusters of DNA sequences normally a few

hundred base pairs long that frequently contain binding motifs for multiple TFs, and therefore can function as operational platforms allowing for the coordinated action of combinations of TFs.

Enhancer binding and activation by TFs normally regulates transcription through the recruitment of cofactors and Pol II to the core promoter of target genes (Ong and Corces 2011; Spitz and Furlong 2012). Looping of the DNA allows enhancers to come into close proximity to core promoters of distant genes and physically interact with components of the transcription machinery (**Figure 1.11**) (Krivega and Dean 2012; Sanyal et al. 2012; Kieffer-Kwon et al. 2013).

While a few proteins have been implicated in DNA looping, the underlying mechanisms of this process remain mostly unknown. Cohesin has been shown to play a role in the stabilisation of these DNA loops, recruited by NIPBL (also known as cohesin loading factor) which associates with Mediator, a multi-subunit protein complex generally required for the transcription by Pol II that will be described later (Kagey et al. 2010). The circular structure of the cohesin complex allows for the formation of a ring connecting two DNA regions, in this case that of enhancer and distal promoter regions (**Figure 1.11**). Thus, through its indirect recruitment by Mediator, cohesin can stabilise gene loops involving active promoters. Interestingly, cohesin can associate with CTCF, enabling the insulation of promoters from distant enhancers (Wendt et al. 2008).

However, the potential requirement for cohesin and Mediator for the establishment of enhancer-promoter loops allowing transcription activation has been recently challenged by a study showing enhancer looping that is independent of cohesin and Mediator (Krivega and Dean 2017).

Enhancer RNAs (eRNAs), which are transcribed from enhancer sequences and have been established as indicators of enhancer activity (De Santa et al. 2010; Kim et al. 2010;

Melgar et al. 2011), may also play a role in enhancer-promoter looping, and eRNA knock-down can result in impaired looping in specific cases (Sanyal et al. 2012; Li et al. 2013; Hsieh et al. 2014). However, there are also studies that have questioned the necessity of eRNAs for this process (Hah et al. 2013; Schaukowitch et al. 2014). Thus, the precise details of how transcription-associated loops are established remains unclear.

How enhancers find the promoters of their target genes via looping is currently not fully understood. A role for some regulatory sequences (referred to as tethering elements) present in promoter-proximal regions that contribute to guiding enhancers to specific genes has been reported (Calhoun et al. 2002). Additionally, insulator elements are able to limit the spatial influence of enhancers (Gaszner and Felsenfeld 2006), and chromatin structure can also facilitate or restrict certain interactions (Andrey and Mundlos 2017; Hansen et al. 2018).

A facilitated diffusion model involving a combination of 3D nucleoplasm diffusion and 1D sliding of TFs along the DNA interacting non-specifically is currently the most accepted model to explain how TFs find their binding sites throughout the genome. Originally proposed around three decades ago, supporting evidence has been produced both *in vivo* and *in vitro* (Berg et al. 1981; von Hippel and Berg 1989; Blainey et al. 2006; Wang et al. 2006; Elf et al. 2007; Bonnet et al. 2008; van den Broek et al. 2008; Hammar et al. 2012; Leith et al. 2012). However, the details of this apparently highly inefficient process are still far from understood. Recent evidence has shown how the environment of the binding motifs could play an important role attracting TFs to their functional sites and therefore facilitating their search (Dror et al. 2016).

Finally, binding of TFs to their regulatory sequences in the genome appears to be highly dynamic, and measurement of TF residence time is a much better indicator of functional binding than occupancy measured by ChIP-seq, which by averaging binding in many cells

does not distinguish between frequent short-term binding events and few long-term residence times (Lickwar et al. 2012; Liu and Tjian 2018). TF residence time can be dependent on a competition between TFs and nucleosomes as well as the affinity of TFs for their binding sites, and correlates with enhanced transcription of the corresponding genes presumably by increasing the likelihood of recruitment of additional cofactors required for transcriptional activation (Segal and Widom 2009a; Lickwar et al. 2012). For example, using single-molecule imaging techniques, the residence time of p53 at putative specific-binding sites has been shown to almost double following activation by genotoxic stress, resulting from an increase in its binding affinity induced by acetylation of its carboxy-terminal domain (CTD) and correlating with enhanced transcription of target genes (Loffreda et al. 2017).

Cofactors

Cofactors associate with TFs to mediate their effect on transcription mainly through their interaction with the transcription machinery or alteration of chromatin structure through histone modifications or chromatin remodelling. Cofactors generally lack DNA-binding properties, and are usually referred to as coactivators or corepressors depending on how they affect transcription. However, DNA-binding cofactors also exist and may modulate the binding affinity of specific TFs to regulatory DNA, and some TFs can also act as cofactors.

Over the last two decades, a key role has been described for Mediator, a coactivator involved in the regulated transcription of nearly all RNA polymerase II-dependent genes. Mediator is a large multiprotein complex that acts as a functional bridge between transcription factors bound to promoter-proximal regions or enhancers and the basal transcription machinery, including Pol II and GTFs, promoting the assembly of the PIC at core promoters (**Figure 1.11**) (Soutourina 2018). Specifically, Mediator physically interacts with Pol II and the transcription factor IID (TFIID) (facilitating its recruitment to TATA-boxes

in core promoters, which are recognised by TFIID's TATA-binding protein (TBP) subunit), TFIIB, TFIIE, TFIIF, TFIIH and TFIIS (Johnson et al. 2002; Plaschka et al. 2015; Robinson et al. 2016; Nozawa et al. 2017; Tsai et al. 2017).

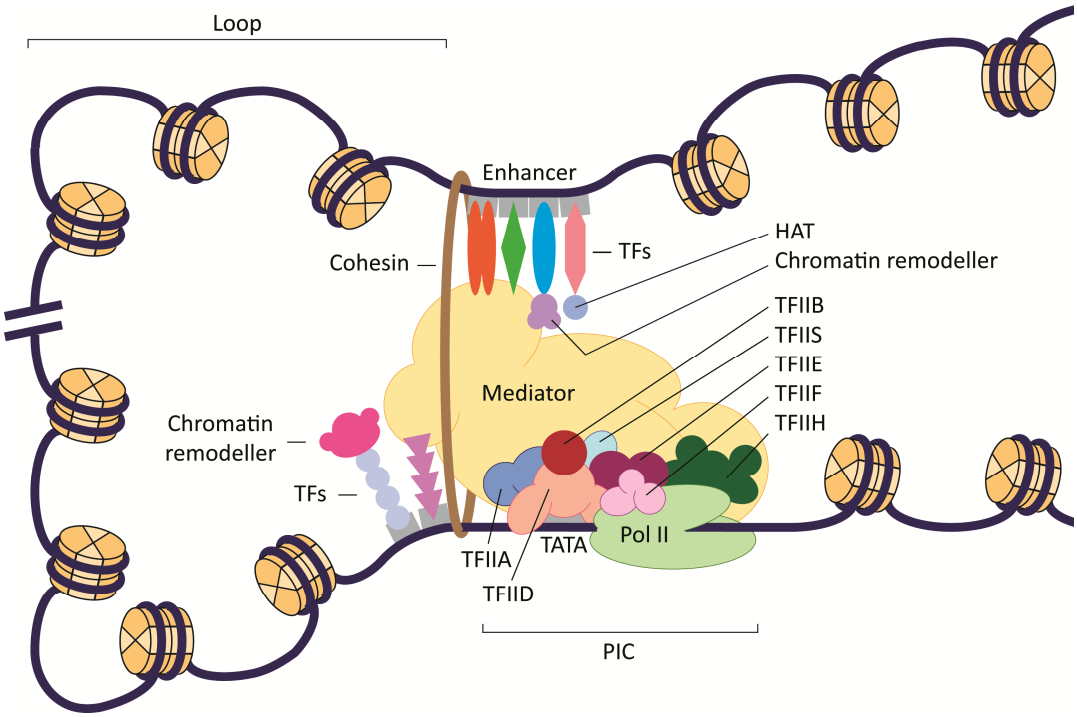


**Figure 1.11.- Formation of the transcriptional preinitiation complex.** Schematic representation of the assembly of the preinitiation complex (PIC) in the core promoter of a gene. Mediator functions as a bridge between sequence-specific transcription factors (TFs) bound to enhancer and promoter-proximal regions and the basal transcription machinery, facilitating the recruitment and/or stabilisation of PIC components in the core promoter. Chromatin looping brings TFs bound to enhancer regions into the vicinity of core promoters, a process potentially facilitated by cohesin rings. TFs also bind other cofactors such as chromatin remodelling complexes and histone modifiers (including histone acetyltransferases, HATs) that allow for chromatin decompaction.

Furthermore, Mediator is able to modify chromatin structure (specially nucleosome occupancy and positioning) around promoter regions through the recruitment of chromatin modulators to promote or in a few cases suppress transcription (Lorch et al. 2000; Zhu et al. 2011; Kremer et al. 2012; Liu and Myers 2012; Nock et al. 2012; Ansari et al. 2014). For example, Mediator interacts with the acetyltransferase p300 and the chromatin remodeller SWI/SNF for transcriptional activation, while its recruitment of G9a histone (H3K9) methyltransferase and the PRMT5 histone arginine methyltransferase has been associated

with transcriptional repression (Huang et al. 2003; Ding et al. 2008; Ansari et al. 2014; Aranda-Orgilles et al. 2016). Moreover, as previously mentioned, Mediator may play a role in the formation of enhancer-promoter loops (Kagey et al. 2010).

Mediator is also essential for the switch to productive transcription elongation, stimulating the phosphorylation of Pol II CTD by TFIIH, an event required for the release of Pol II from promoters (Kim et al. 1994). Moreover, Mediator contributes to the recruitment of the positive transcription elongation factor b (P-TEFb) or the P-TEFb-containing super elongation complex (SEC), which phosphorylate the pause-regulatory factors DSIF (DRB sensitivity-inducing factor) and NELF (negative elongation factor), required for Pol II pause release (Adelman and Lis 2012; Lu et al. 2016). P-TEFb further phosphorylates the Pol II CTD creating a binding platform for chromatin modulators and RNA-processing factors such as the 5' capping enzyme, which has also been reported to interact with the pause control factor DSIF (Mandal et al. 2004; Peterlin and Price 2006; Moore and Proudfoot 2009). This way, the regulation of pause release is coupled to the recruitment of factors required for productive RNA synthesis. Finally, Mediator has also been suggested to contribute to pause release through its ability to influence nucleosome positioning (Nock et al. 2012).

The multisubunit complex Spt-Ada-Gcn5 acetyltransferase (SAGA) may constitute another general cofactor for the transcription of genes by Pol II (Bonnet et al. 2014; Baptista et al. 2017). SAGA contributes to transcriptional activation mainly through its acetyltransferase and deubiquitinase histone modifying activities and by facilitating the recruitment of TBP to promoters (Koutelou et al. 2010). Interactions between SAGA and TFs as well as the recognition of acetylated histones through its bromodomain can guide this complex to specific gene loci (Koutelou et al. 2010). Recent studies have reported the requirement of SAGA for the recruitment of Pol II to the vast majority of active promoters,

and disruption of this complex results in a global decrease of transcription by Pol II, suggesting SAGA's role as a Pol II general cofactor (Bonnet et al. 2014; Baptista et al. 2017).

Apart from SAGA and Mediator, other cofactors such as p300/CBP or the SWI/SNF complex, which were previously introduced in the context of ATF4 and/or MITF cofactors, have a widespread role in the activation of transcription (Chan and La Thangue 2001; Clapier and Cairns 2009; Tang et al. 2010; Hargreaves and Crabtree 2011).

p300/CBP is also involved in the recruitment of the basal transcription machinery, and can interact with TFIIB, TFIIE, TFIIF and the TBP subunit of TFIID (Chan and La Thangue 2001). Additionally, it can modify chromatin structure through its histone acetyltransferase activity, as well as acting as a scaffold for the recruitment of chromatin remodelling complexes such as SWI/SNF (Chan and La Thangue 2001; Huang et al. 2003).

ATP-dependent nucleosome remodelling factors use the energy from ATP hydrolysis to loosen the wrapping of DNA around histones and relocate histone octamers to neighbouring DNA segments (Becker and Hörz 2002). The SWI/SNF complex is one of the most studied ATP-dependent chromatin remodellers, which plays a key role in activating gene expression through nucleosome remodelling and eviction at gene promoters (Imbalzano et al. 1994). TFs, cofactors such as p300 and Mediator, and histone modifications have all been reported to be involved in the recruitment of the SWI/SNF complex to gene promoters (Huang et al. 2003; de la Serna et al. 2006; Ansari et al. 2014; Swygert and Peterson 2014).

ISWI constitutes the ATPase subunit of another family of chromatin remodelling complexes (Mellor and Morillon 2004; Erdel et al. 2010). ISWI has the ability to remodel nucleosomes by itself *in vitro*, and can therefore be independently referred to as a chromatin remodelling factor (Corona et al. 1999; Havas et al. 2000; Längst and Becker 2001; Clapier and Cairns 2012). However, it is always found as part of multiprotein complexes *in vivo*, and this association with other subunits can considerably modulate its

activity quantitatively, as well as qualitatively through the modification of the directionality of nucleosome sliding (Ito et al. 1999; Eberharter et al. 2001). Specific ISWI-containing complexes with diverse compositions can exert opposing effects in transcription. For example, NoRC (nucleolar remodelling complex) is associated with transcriptional repression, through the alteration of nucleosome positioning and the formation of heterochromatin-like structure at gene promoters, while NURF (nucleosome remodelling factor) generally activates transcription mobilising nucleosomes away from promoter regions to facilitate binding of TFs and the transcription machinery (Badenhorst et al. 2002; Strohner et al. 2004; Eleuteri et al. 2018). Both complexes can be recruited to DNA through interactions with TFs or histone modifications or variations (Strohner et al. 2004; Wysocka et al. 2006; Alkhatib and Landry 2011; Eleuteri et al. 2018).

Finally, the nucleosome remodelling and histone deacetylase (NuRD) complex plays an important role in transcriptional gene repression, primarily increasing nucleosome density at promoters and enhancers through its ATP-dependent nucleosome remodelling activity, which resides in its Mi-2 subunit, and also through its linked histone deacetylase activity (Xue et al. 1998; Lai and Wade 2011; Bornelöv et al. 2018). However, transcriptional activation mediated by NuRD has been shown as well (Miccio and Blobel 2010; Basta and Rauchman 2015; Bornelöv et al. 2018). NuRD can be recruited to gene promoters by some TFs, other cofactors, or through interactions with methylated DNA (Kim et al. 1999; Cismasiu et al. 2005; Hong et al. 2005; Garnatz et al. 2014; Liu et al. 2015; Waldron et al. 2016). However, the details of NuRD genomic targeting in many cases remain unknown.

Histone modifications

Histones contained in nucleosomes are susceptible to many post-translational modifications (PTMs) (particularly in their protruding N-terminal tails) which can affect

chromatin structure directly or through the recruitment of chromatin remodelling complexes (Bannister and Kouzarides 2011).

**Acetylation** – Histone lysines are acetylated in a reaction catalysed by histone acetyltransferases (HATs), which transfer an acetyl group from acetyl-CoA to the ε-amino group of lysines in histone tails, neutralising its charge and therefore loosening the interaction between DNA and histones, generally contributing to transcription activation (Bannister and Kouzarides 2011). Acetylation of histones also leads to the recruitment of proteins containing a bromodomain, which recognises acetylated lysine residues. Frequently these bromodomain proteins are HATs or components of chromatin remodelling complexes which can further contribute to the opening of chromatin. Examples of bromodomain proteins are the histone acetyltransferase p300/CBP complex and the chromatin remodeller SWI/SNF, which, as previously described, are cofactors for a wide range of TFs that play an important role in the transcriptional regulation of many genes; and ZMYND8, that has been reported to act as a corepressor of genes through the recruitment of additional factors such as the NuRD complex (Hassan et al. 2002; Dancy and Cole 2015; Gong et al. 2015; Li et al. 2016) but also has recently been implicated in transcription activation by recruiting the P-TEFb complex that phosphorylates Pol II to promote transcription elongation (Ghosh et al. 2018).

Acetylation of histones is highly dynamic, with histone deacetylases (HDACs) catalysing the removal of the lysine acetyl groups, which restores their positive charge leading to a more compacted chromatin structure and generally contributing to transcriptional repression (Bannister and Kouzarides 2011). Deacetylation can also lead to modification of the deacetylated lysine by alternative post-translational modifications such as lysine methylation, ubiquitylation or sumoylation. HDACs are frequently part of large multi-subunit protein complexes, as it is the case for the NuRD complex for example (Lai and Wade 2011).

**Phosphorylation** – Histone serines, threonines and tyrosines (predominantly, but not only, located on histone tails) can be phosphorylated in a reaction catalysed by protein kinases, which transfer a phosphate group from ATP to the hydroxyl group of the target amino acid, adding negative charge and therefore in principle relaxing chromatin structure. The effects of histone phosphorylation, however, have been shown to be highly context-dependent, involving a complex cross-talk with other PTMs and the modulation of the recruitment of many diverse factors (Banerjee and Chakravarti 2011; Rossetto et al. 2012; Sawicka and Seiser 2014). Histone phosphorylation is also highly dynamic, with protein phosphatases reverting the phosphorylation reaction catalysed by kinases (Oki et al. 2007).

**Methylation** – Histone methylation mainly takes place on lysines (which can be mono-, di- or tri-methylated) and arginines (which can be mono- or di-methylated, symmetrically or asymmetrically in the latter case) within histone tails (Bannister and Kouzarides 2011). The effects of histone methylation in transcription are also highly context-dependent, but can modulate chromatin structure and the recruitment of specific and general transcription factors (Greer and Shi 2012).

Histone lysine methyltransferases (HKMTs) and protein arginine methyltransferases (PRMTs) catalyse the transfer of a methyl group from S-adenosylmethionine (SAM) to the ε-amino group of lysine residues or the ω-guanidino group of arginines, respectively (Copeland et al. 2009). While histone methylation was for long considered a stable modification, two families of histone lysine demethylases have been identified over the last two decades (Greer and Shi 2012; D'Oto et al. 2016). The reversibility of arginine methylation is however less clear. While a subset of histone lysine demethylases has been reported to catalyse the demethylation of arginine residues, this is still controversial (Chang et al. 2007; Webby et al. 2009; Greer and Shi 2012; Walport et al. 2016). Additionally, monomethylated arginines can be converted to citrulline in a reaction catalysed by protein

arginine deiminase type 4 (PADI4) that is not a direct reversal of arginine methylation but could be considered as a mechanism for elimination of methylated arginines (Cuthbert et al. 2004; Wang et al. 2004). However, *in vivo* evidence supporting this activity is still limited (Thompson and Fast 2006).

**Other modifications** – A *β-N*-acetylglucosamine group can be added to histone tails, or these can be ubiquitylated, sumoylated or removed through histone tail clipping (for review see (Bannister and Kouzarides 2011)).

Chromatin interactions in 3D

Over the last two decades, the development of chromosome conformation capture techniques and the advances in microscopy for the study of DNA/RNA subnuclear localisation have led to a dramatic increase in our understanding of the nuclear 3D organisation of the genome (Dekker et al. 2002; Osborne et al. 2004; Eskiw and Fraser 2011; de Wit and de Laat 2012; Dixon et al. 2012; Nora et al. 2012; Denker and de Laat 2016).

Chromosomes occupy discrete non-overlapping spaces in interphase nuclei, which have been defined as chromosome territories (Cremer and Cremer 2010). Rules determining the particular organisation of these territories remain elusive, and it seems that following cell divisions they are randomly re-arranged. However, a preference for radial positions has been observed, which could be related to potential interactions with the nuclear envelope (Cremer and Cremer 2010; Zuleger et al. 2011). Additionally, inactive genes are generally found in the interior of these chromosome territories, while active genes are normally located at the surface, and specifically, highly expressed genes have been suggested to cluster in specific foci termed transcription factories (Sutherland and Bickmore 2009; Razin et al. 2011). However, this concept is still controversial and many questions remain to be answered, such as whether RNA polymerases are recruited to transcription factories or

these gene clusters are the ones moving to locations where RNA polymerases are anchored, or whether these factories constitute a cause or a consequence of gene expression (Sutherland and Bickmore 2009).

Furthermore, recent studies have demonstrated that chromosomes are comprised of distinct chromatin domains referred to as topologically associating domains (TADs), which are stable through cell divisions and largely conserved among cell types and related species (Dixon et al. 2012; Nora et al. 2012; Dixon et al. 2016). TADs are not only structural units but also functional domains, characterised by high levels of internal interactions and separated by boundary elements where interactions are sharply depleted (Dixon et al. 2012; Nora et al. 2012; Dixon et al. 2016). Consequently, TADs have emerged as fundamental players in transcriptional regulation, facilitating and restraining specific enhancer-promoter interactions within chromosomes (Dixon et al. 2012; Nora et al. 2012; Shen et al. 2012; Andrey and Mundlos 2017). Further research will be required to understand the details and dynamics of TAD organisation and the process by which these domains are formed, where CTCF has been suggested to play a key role in line with its insulator activity (Dixon et al. 2012; Nora et al. 2017).

1.5.2. – Post-transcriptional regulation of gene expression

Following transcription, the generated precursor mRNAs are subjected to a series of regulated processing steps required to obtain mature mRNAs competent for translation. These steps include 5'-end capping (where a 7-methylguanosine ($m^7G$) is produced and appended to the 5'-end of mRNAs), splicing out of introns (which is mediated by the spliceosome and can contribute to the diversity of the proteasome through alternative splicing), and 3'-end cleavage/polyadenylation (which allows for the addition of a poly(A) tail to the 3'-end of mRNAs) (Ramanathan et al. 2016; Neve et al. 2017; Shi 2017; Corbett 2018).

Additionally, the process of mRNA export from the nucleus to the cytoplasm can play a role in the regulation of gene expression (Wickramasinghe and Laskey 2015).

Once mRNAs have reached the cytoplasm, mRNA decay pathways are important regulators of gene expression, and alteration of these pathways allows for a rapid control of protein synthesis in response to changing cellular needs (Yang et al. 2003; Garneau et al. 2007; Schoenberg and Maquat 2012).

Finally, miRNAs are key players in the post-transcriptional regulation of gene expression. miRNAs are short non-coding RNAs that associate with Argonaute proteins to form miRNA-induced silencing complexes (miRISCs) which are able to target and degrade mRNAs through sequence-specific base pairing with their 3' UTRs (untranslated regions) (Jonas and Izaurralde 2015; Gebert and MacRae 2019). Additionally, when miRNA and mRNA sequences are not fully complementary, miRISCs can still silence the expression of the corresponding genes through translational repression (Filipowicz et al. 2008; Meijer et al. 2013; Jonas and Izaurralde 2015; Gebert and MacRae 2019).

1.5.3. – Translational regulation of gene expression

The process of mRNA translation or protein synthesis involves three stages: initiation, elongation and termination, with most regulation being exerted at the initiation stage (**Figure 1.12**). Canonical (cap-dependent) translation begins with the recognition of the mRNA 5' $m^7G$ cap by the eukaryotic translation initiation factor 4E (eIF4E), a subunit of the multiprotein complex eIF4F which also contains eIF4A (an RNA helicase that unwinds inhibitory secondary structure in the 5'UTR of mRNAs) and eIF4G (which facilitates the assembly of the translation initiation complex acting as a scaffold and establishing interactions with other initiation factors) (Sonenberg and Hinnebusch 2009; Spriggs et al. 2010). This step is mainly regulated by the availability of eIF4E, which is controlled by a

family of repressors termed eIF4E-binding proteins (4E-BPs) (Sonenberg and Hinnebusch 2009; Saxton and Sabatini 2017).

Binding of 4E-BPs to eIF4E is modulated through their phosphorylation in multiple sites by mTORC1, which highly reduces the strength of the interactions, thereby increasing the levels of dissociated eIF4E available for translation initiation (Sonenberg and Hinnebusch 2009; Saxton and Sabatini 2017). Additionally, mTORC1 phosphorylates p70S6 kinase 1 (S6K1) at Thr389, which is then able to phosphorylate Ser422 of eIF4B, another translation initiation factor that following its activation by S6K1 stimulates the RNA helicase activity of eIF4A (Raught et al. 2004; Saxton and Sabatini 2017). Moreover, activated S6K1 phosphorylates PDCD4, an eIF4A inhibitor, inducing its degradation (Dorrello et al. 2006; Suzuki et al. 2008). mTORC1 is activated by growth signals and nutrients, among other stimuli, and is inhibited by different types of cellular stresses (Sengupta et al. 2010; Saxton and Sabatini 2017). The mTORC1 complex comprises the three core subunits: mTOR (mammalian target of rapamycin), Raptor (regulatory protein associated with mTOR), and mLST8 (mammalian lethal with Sec13 protein 8); as well as two inhibitory proteins: PRAS40 (proline-rich Akt substrate of 40 kDa), and DEPTOR (DEP domain containing mTOR interacting protein) (Saxton and Sabatini 2017). Activation of mTORC1 by PI3K/Akt signalling in response to growth factors has been shown to be at least partly mediated through phosphorylation of PRAS40 by Akt, which releases its inhibition (Sancak et al. 2007; Vander Haar et al. 2007; Wang et al. 2012a). While the regulation of DEPTOR is still not fully understood, it is responsive to different types of stress, including glucose starvation, at least partly through the upregulation of its expression by Che-1 (Desantis et al. 2015). Furthermore, it can be phosphorylated by the catalytic subunit of the mTORC1 complex following activation of mTORC1 signalling, which enhances its recognition by an E3 ligase, leading to its ubiquitination and ultimately proteosomal degradation (Duan et al. 2011; Gao

et al. 2011; Zhao et al. 2011b). The regulation of the activity of 4E-BPs and eIF4A by mTORC1 signalling therefore provides a means for cells to respond to growth signals and nutrient availability (among other conditions) through the regulation of protein synthesis.

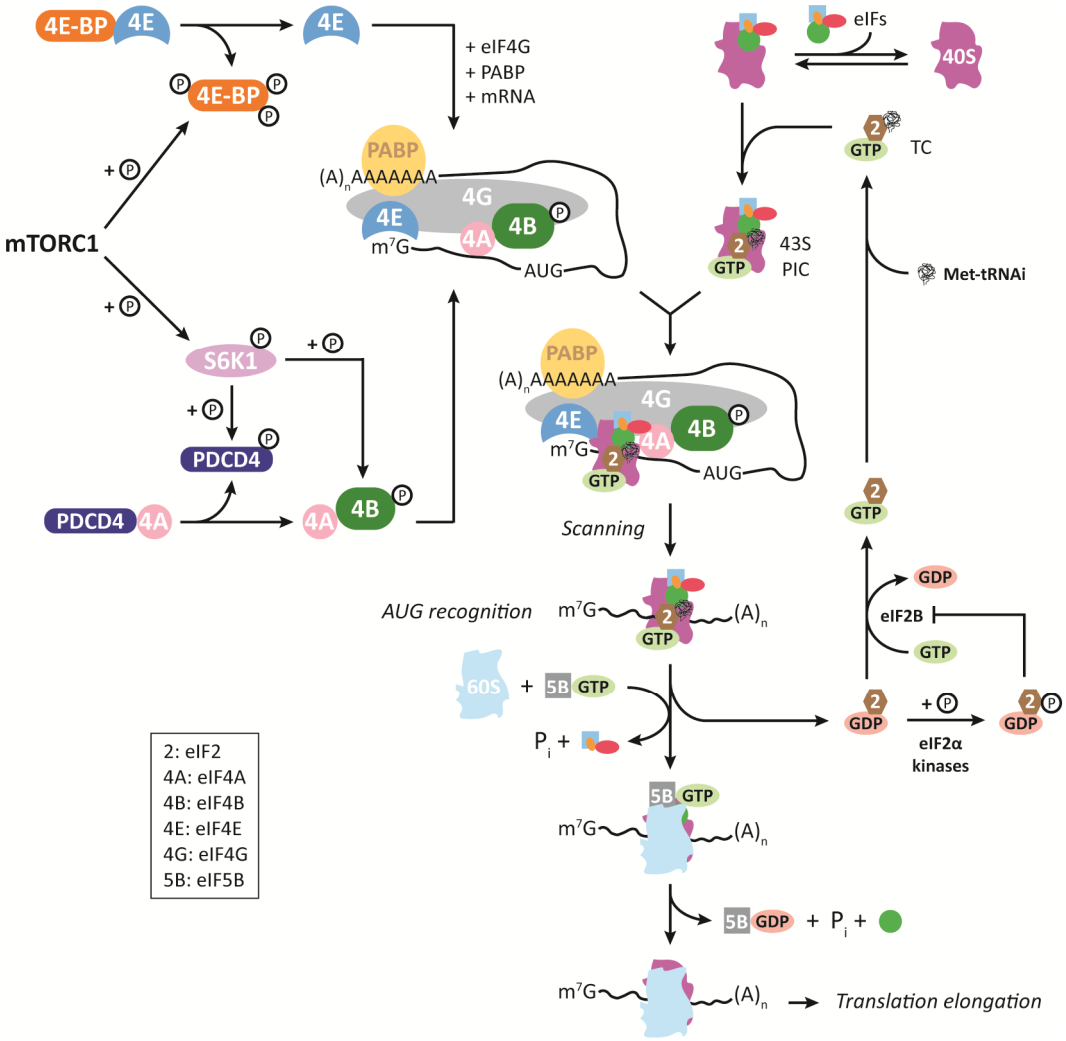


**Figure 1.12.- Cap-dependent translation initiation.** Schematic representation of the process of translation initiation and its regulation by mTORC1 and eIF2α kinases. Translation initiation starts with binding of the mRNA to the eIF4F complex (containing eIF4A, eIF4E and eIF4G) and the poly(A)-binding protein (PABP). A preassembled 43S preinitiation complex (PIC) containing the 40S ribosomal subunit, the ternary complex (TC) eIF2-GTP-Met-tRNAi, and several additional initiation factors is then recruited to the cap region facilitated by interactions with eIF4A, eIF4E and eIF4G. Following scanning of the 5'UTR, recognition of the start codon triggers the hydrolysis of eIF2-bound GTP, releasing eIF2-GDP, which is converted back to eIF2-GTP by eIF2B. Translation elongation proceeds following binding of the 60S ribosomal subunit, which is catalysed by eIF5B. Activation of mTORC1 signalling leads to phosphorylation of the inhibitory 4E-binding protein (4E-BP), which results in an increase in eIF4E available for translation. Activation of p70S6 kinase 1 (S6K1) by mTORC1 leads to phosphorylation and degradation of PDCD4, an eIF4A inhibitor, and phosphorylates eIF4B, which then stimulates eIF4A helicase activity. Phosphorylation of eIF2-GDP by eIF2α kinases leads to inactivation of eIF2B, reducing the amount of TC available for translation. (Sonenberg and Hinnebusch 2009).

mRNA activation is completed with the binding of poly(A)-binding protein (PABP) to the mRNA poly(A), which also interacts with eIF4G circularising the mRNA and stabilising the complex (Sonenberg and Hinnebusch 2009). Once the mRNA is activated, a preassembled 43S preinitiation complex (PIC) comprised of Met-tRNAi, eIF2-GTP and several additional initiation factors is recruited to its 5' cap region, facilitated by interactions with the eIF4E, eIF4A and eIF4G subunits of the eIF4F complex (Sonenberg and Hinnebusch 2009). The loaded small ribosomal subunit then scans the mRNA 5' UTR until it finds an AUG start codon, which triggers the hydrolysis of eIF2-GTP and uncouples tRNAi from eIF2, releasing an inactive eIF2-GDP binary complex and other eIFs (Sonenberg and Hinnebusch 2009). The large ribosomal subunit is then recruited in a reaction catalysed by eIF5B-GTP, allowing for the start of translation elongation (Jackson et al. 2010).

Following translation initiation, the guanine nucleotide exchange factor (GEF) eIF2B converts eIF2-GDP back into the GTP-bound active form, which allows eIF2 to participate in another round of translation initiation (Sonenberg and Hinnebusch 2009). Phosphorylation of the α subunit of eIF2 (eIF2α) however highly increases the strength of the interaction between this factor and the GEF, turning the p-eIF2-GDP complex into a competitive inhibitor of eIF2B (Sonenberg and Hinnebusch 2009). Phosphorylation of eIF2α therefore constitutes another key point of regulation of translation initiation, leading to an overall reduction in the available active eIF2 and consequently limiting the formation of the PIC. As described in section 1.4, eIF2α is phosphorylated by a series of kinases that are activated by a wide variety of cellular stresses including amino acid starvation, glucose limitation and endoplasmic reticulum stress, allowing for a reduction in global protein synthesis as part of an adaptive stress response (Harding et al. 2000).

A few alternative mechanisms can however mediate translation of specific mRNAs in conditions of cellular stress, allowing for the selective protein synthesis of effectors of the

stress response. One of these mechanisms, which is generally not fully understood but has been well characterised for some mRNAs, involves the presence of upstream open reading frames (uORFs) in the 5' UTR of the transcripts. For example, in the case of ATF4, which contains two major uORFs, the first one being located near the 5'-end and the second one overlapping with the protein coding sequence out-of-frame, ATF4 is only synthesised as a consequence of a delayed translation reinitiation mechanism following eIF2α phosphorylation in cellular stress conditions (Young and Wek 2016). In normal conditions, when ribosomes can quickly reload new eIF2-GTP-Met-tRNAi (ternary complex, TC) due to its high availability, following translation of the first uORF the 43S ribosome complex continues scanning along the mRNA until it reaches the uORF2 where it reinitiates translation ultimately preventing translation of ATF4 coding sequence. However, in stress conditions, when formation of the ternary complex is limited, reloading of the ribosome is delayed and consequently ribosomes bypass the inhibitory uORF2 and instead restart translation in the main ORF (protein coding sequence), producing ATF4 protein (Young and Wek 2016).

Additionally, in cellular stress conditions where cap-dependent translation is suppressed, for example as a consequence of decreased phosphorylation of 4E-BPs resulting from mTORC1 inhibition by amino acid limitation, a cap-independent mechanism of translation of specific mRNAs containing internal ribosomal entry sites (IRESs) in their 5'UTRs has been observed (Komar and Hatzoglou 2011). IRESs are highly structured elements that stimulated by a number of IRES *trans*-acting factors (ITAFs) are able to recruit 40S ribosomes in a cap-independent manner (Komar and Hatzoglou 2011). Interestingly, this alternative mechanism of translation is also promoted by and dependent on eIF2α phosphorylation in cellular stress conditions, meaning that IRES-dependent translation can effectively take place with low ternary complex levels in these conditions and therefore

suggesting a potential mechanistic independence of eIF2 as well (Komar and Hatzoglou 2011; Godet et al. 2019). Further research will be needed to elucidate the details of this potential eIF2-independent mechanism, where a role for the initiation factor eIF5B has already been proposed (Thakor and Holcik 2012; Holcik 2015).

1.5.4. – Post-translational regulation of gene expression

PTMs of proteins constitute the last layer of regulation of gene expression through the modulation of protein function and stability. PTMs commonly observed include phosphorylation, acetylation, ubiquitination, methylation, hydroxylation, carbonylation, glycosylation and glycation, nitration, palmitoylation, ADP-ribosylation, sumoylation and sulfation (Karve and Cheema 2011). While ubiquitination has been shown to have a main (but not exclusive) role in the targeting of proteins for degradation, the remaining modifications have been associated with a wide myriad of highly context-dependent roles, as it was previously introduced in the context of histone, MITF and ATF4 PTMs. Due to space limitations, the role of specific PTMs of proteins will not be described here, but they can influence protein-protein interactions, subcellular localisation, stability and conformation and therefore constitute a major molecular mechanism that controls gene expression (for review see (Karve and Cheema 2011)).

## 1.6. – Aims of the study

While strong evidence has been generated regarding the association of different levels of MITF expression and activity with distinct phenotypes in cells, our understanding of how these different levels of MITF determine the characteristics of the distinct phenotypes adopted is still incomplete. Likely, many additional MITF target genes and their role in influencing cell phenotype are yet to be discovered. Moreover, further research is needed

to understand how the target specificity of MITF is determined. For example, MITF regulates both proliferation and differentiation-associated genes, yet the proliferative and differentiated phenotypes are to a great extent mutually exclusive *in vivo*. While several post-translational modifications and cofactors have been identified to play a role in the selective promotion of transcription of specific sets of MITF downstream genes, our understanding of how MITF target specificity is achieved is still severely limited, as it is how MITF activates transcription of some genes and transcriptionally represses others.

Furthermore, while many transcriptional regulators of *MITF* expression have been identified, the underlying mechanisms of gene regulation are in many cases not clear. For example, in the absence of ChIP-seq data for most regulators, do they work only via the *MITF* promoter, or can they function to regulate *MITF* via enhancer or silencer elements? Additionally, our knowledge regarding how microenvironment conditions in tumours can modulate MITF activity potentially leading to switches in cell phenotype remains very limited.

The aim of this project is to broaden our knowledge of both the regulation of genes by MITF and the transcriptional regulation of *MITF* that may have implications for determining cell phenotype.

First, the potential role of the NuRD complex and the bromodomain protein ZMYND8 as MITF regulators will be explored. As previously described, the chromatin remodelling complex SNF/SWI is an MITF cofactor with an important role in the transcriptional activation of MITF targets. However, an MITF cofactor leading to transcriptional repression has not been identified yet. Following the detection of an interaction between a key NuRD subunit and MITF by previous members of the laboratory, the potential role of NuRD, a chromatin remodelling complex that can repress the expression of many genes (Fujita et al. 2004; Cismasiu et al. 2005; Hong et al. 2005; Lai and Wade 2011), as an MITF cofactor was

explored. Unexpectedly, these experiments uncovered a potential role for NuRD as an MITF regulator (see section 3.2), which will be further examined in this study. Additionally, the potential role of ZMYND8, which is involved in the recruitment of NuRD to DNA (Gong et al. 2015; Spruijt et al. 2016), in MITF regulation will be investigated.

Secondly, further analysis of genome-wide studies of MITF previously performed in the laboratory will be carried out with the aim of identifying new genes regulated by MITF with a potential role in the specification of cell phenotypes.

Finally, regarding the regulation of MITF by microenvironment conditions, this work will focus on the study of the modulation of *MITF* expression by ATF4, a transcription factor upregulated in response to different types of cellular stress frequently found in tumours, such as nutrient limitation. While an inverse correlation between *ATF4* and *MITF* expression has already been described, and ATF4 can repress *MITF* via its promoter in luciferase reporter assays (Falletta et al. 2017; Ferguson et al. 2017), this has not been validated by more robust methodologies to examine ATF4 DNA binding in cells. Whether ATF4 does indeed regulate *MITF* via promoter binding, or by targeting other regulatory elements in the *MITF* gene remains to be understood. This will be explored by identifying the genome-wide occupancy of ATF4 and the regulation of its full repertoire of target genes to identify not only how ATF4 regulates *MITF*, but also other genes potentially involved in the induction of phenotype-switches as a consequence of the inverse expression of *ATF4* and *MITF*. Such an analysis may also determine whether ATF4 has a potential role in globally antagonising the effects of MITF on gene expression.

In the long term, by expanding our knowledge of the regulation of MITF and its role in the induction of different cell phenotypes we may be able to target tumour phenotypic heterogeneity for therapy, driving therapy-resistant melanoma cells to acquire phenotypes sensitive to treatment.

# Chapter 2 – Materials and Methods

# 2.1. – Materials

### 2.1.1. – Chemicals and reagents

Autoclaved double-distilled 18 MΩ water was used throughout the study for nucleic acids solutions. Double-distilled 15 MΩ water was used to prepare all other solutions and buffers.

Unless otherwise stated, chemicals and reagents were purchased from Sigma-Aldrich.

### 2.1.2. – Plasmids

The following plasmids were used throughout the study:

**Table 2.1: Description and source of plasmids used**

| Construct | Source and notes |
|---|---|
| pcDNA5/FRT/TO-HA-ZMYND8 | Mammalian expression vector promoting constitutive expression of HA-tagged ZMYND8; kindly provided by Panagis Filippakopoulos laboratory (Ludwig Institute for Cancer Research, Oxford) |
| pcDNA5/FRT/TO-FLAG-ZMYND8 | Mammalian expression vector promoting constitutive expression of FLAG-tagged ZMYND8; kindly provided by Panagis Filippakopoulos laboratory (Ludwig Institute for Cancer Research, Oxford) |
| pPB-hCMV1-MCS | PiggyBac construct for doxycycline-inducible expression of cloned DNA inserts in mammalian cells; available in the laboratory |
| pPB-hCMV1-2xHA-MCS | PiggyBac construct for doxycycline-inducible expression of cloned DNA inserts with 2xHA-tag in mammalian cells; prepared by the candidate |
| pPB-hCMV1-3xHA-ZMYND8 | PiggyBac construct for doxycycline-inducible expression of 3xHA-tagged ZMYND8 in mammalian cells; prepared by the candidate |
| pCMV-3xFLAG | Mammalian expression vector promoting constitutive expression of cloned DNA inserts with 3xFLAG-tag; available in the laboratory |
| pCMV-ZMYND8$^{FL}$-3xFLAG | Mammalian expression vector promoting constitutive expression of 3xFLAG-tagged ZMYND8; prepared by the candidate |

| | |
|---|---|
| pCMV-ZMYND8$^{1-1005}$-3xFLAG | Mammalian expression vector promoting constitutive expression of 3xFLAG-tagged ZMYND8 (1 to 1005 aa); prepared by the candidate |
| pCMV-ZMYND8$^{1-925}$-3xFLAG | Mammalian expression vector promoting constitutive expression of 3xFLAG-tagged ZMYND8 (1 to 925 aa); prepared by the candidate |
| pCMV-ZMYND8$^{1-500}$-3xFLAG | Mammalian expression vector promoting constitutive expression of 3xFLAG-tagged ZMYND8 (1 to 500 aa); prepared by the candidate |
| pCMV-3xHA-ZMYND8$^{350-850}$ | Mammalian expression vector promoting constitutive expression of 3xHA-tagged ZMYND8 (350 to 850 aa); prepared by the candidate |
| pCMV-3xHA-ZMYND8$^{700-1186}$ | Mammalian expression vector promoting constitutive expression of 3xHA-tagged ZMYND8 (700 to 1186 aa); prepared by the candidate |
| pCMV-5'2N3T | Mammalian expression vector promoting constitutive expression of cloned DNA inserts with 3xHA-tag; contains an NLS; available in the laboratory |
| pCMV-3xHA-p66β | Mammalian expression vector promoting constitutive expression of 3xHA-tagged p66β; kindly provided by Luis Sanchez del Campo, a former member of the laboratory |
| pCMV-3xHA-(siRes)p66β | Mammalian expression vector promoting constitutive expression of an siRNA-resistant form of p66β 3xHA-tagged at the N-terminus; prepared by the candidate |
| pCMV-(siRes)p66β-3xHA | Mammalian expression vector promoting constitutive expression of an siRNA-resistant form of p66β 3xHA-tagged at the C-terminus; prepared by the candidate |
| pRK5-FLAG-DEPTOR | Mammalian expression vector promoting constitutive expression of FLAG-tagged DEPTOR; purchased from Addgene (Plasmid #21334) |
| pPB-hCMV-ATF4-3xHA | PiggyBac construct for doxycycline-inducible expression of 3xHA-tagged ATF4 in mammalian cells; prepared by the candidate |

### 2.1.3. – Cell lines

All parental cell lines were screened regularly for mycoplasma using our in house service and were authenticated using short tandem repeat (STR) analysis. The following cell lines were used throughout the study:

**Table 2.2: Description and source of cell lines used**

| | |
|---|---|
| 501mel | Human melanoma cell line derived from a metastasis (Zakut et al. 1993) $BRAF^{V600E}$, $NRAS^{WT}$, $PTEN^{WT}$, $p53^{C277W}$ ; *Doubling time: ~ 24 h |
| SKmel28 | Human melanoma cell line derived from a metastasis (Fogh et al. 1977) $BRAF^{V600E}$, $NRAS^{WT}$, $PTEN^{T167A}$, $p53^{L145R}$ ; *Doubling time: ~ 35 h |
| IGR37 | Human melanoma cell line derived from a metastasis (Aubert et al. 1980) $BRAF^{V600E}$, $NRAS^{WT}$, $PTEN^{WT}$, $p53^{C229fs}$ ; *Doubling time: ~ 48 h |
| SKmel30 | Human melanoma cell line derived from a metastasis (Carey et al. 1976) $BRAF^{WT}$, $NRAS^{Q61K}$, $PTEN^{WT}$, $p53^{R273H\ \&\ T284fs}$ ; *Doubling time: ~ 28 h |
| HEK293 | Adenovirus E1A-transformed human embryonic kidney cells of neuronal origin (Shaw et al. 2002) |
| 501mel-i-HA-ZMYND8 (p) | Stable 501mel polyclonal cell line with doxycycline-inducible expression of 3xHA-tagged ZMYND8; generated by the candidate using the pPB-hCMV1-3xHA-ZMYND8 vector described in Table 2.1 |
| 501mel-i-HA-ZMYND8 (m) | Stable 501mel monoclonal cell line with doxycycline-inducible expression of 3xHA-tagged ZMYND8; generated by the candidate from the 501mel-i-HA-ZMYND8 (p) cell line |
| 501mel-HA-(siRes)p66β | Stable 501mel polyclonal cell line constitutively expressing N-terminus 3xHA-tagged siRNA resistant p66β; generated by the candidate using the pCMV-3xHA-(siRes)p66β vector described in Table 2.1 |
| 501mel-(siRes)p66β-HA | Stable 501mel polyclonal cell line constitutively expressing C-terminus 3xHA-tagged siRNA resistant p66β; generated by the candidate using the pCMV-(siRes)p66β-3xHA vector described in Table 2.1 |
| 501mel-i-ATF4-HA | Stable 501mel polyclonal cell line with doxycycline-inducible expression of 3xHA-tagged ATF4; generated by the candidate using the pPB-hCMV-ATF4-3xHA vector described in Table 2.1 |

* Note that doubling times depend on nutrient availability and therefore tissue culture medium used. The doubling times shown here were derived from cells grown in RPMI.

### 2.1.4. – Antibodies

The following antibodies were used throughout the study:

**Table 2.3: List of primary antibodies used**

| Target | Host | Source | Dilution |
|---|---|---|---|
| α-HA | Mouse | Sigma Aldrich (H3663) | 1:100 (IF), 1:1000 (WB) |
| α-HA | Rabbit | Cell Signaling (3724) | 1:100 (IF), 1:1000 (WB) |
| α-FLAG M2 | Mouse | Sigma Aldrich (F1804) | 1:100 (IF), 1:1000 (WB) |
| α-FLAG | Rabbit | Sigma Aldrich (F7425) | 1:1000 (WB) |
| α-MITF | Rabbit | Sigma Aldrich (HPA003259) | 1:250 (IF), 1:1000 (WB) |
| α-PRKCBP1 (ZMYND8) | Rabbit | Bethyl Laboratories (A302-089A) | 1:100 (IF), 1:1000 (WB) |
| α-TFEB | Goat | Abcam (ab2636) | 1:100 (IF) |
| α-Tyrosinase | Mouse | Santa Cruz Biotechnology (SC-20035) | 1:100 (IF) |
| α-MelanA | Mouse | Abcam (ab140503) | 1:100 (IF) |
| α-ERK2(C-14) | Rabbit | Santa Cruz Biotechnology (SC-154) | 1:4000 (WB) |
| α-N-Cadherin | Mouse | BD Biosciences (610921) | 1:1000 (WB) |
| α-p66β | Rabbit | Novus (NB100-60645) | 1:1000 (WB) |
| α-p66β | Rabbit | Novus (NP1-87358) | 1:100 (IF) |
| α-p66α | Rabbit | Novus (NB100-56643) | 1:1000 (WB) |
| α-p66α | Rabbit | Novus (NP1-87360) | 1:100 (IF), 1:1000 (WB) |
| α-CHD4 | Mouse | Abcam (ab54604) | 1:100 (IF), 1:1000 (WB) |
| α-CHD4 | Mouse | Abcam (ab70469) | 1:100 (IF), 1:1000 (WB) |

| | | | |
|---|---|---|---|
| α-PTEN | Mouse | Pharmingen (559600) | 1:1000 (WB) |
| α-DEPTOR | Rabbit | Novus (NBP1-49674) | 1:1000 (WB) |
| α-p(Ser473)-Akt | Rabbit | Cell Signaling (4058) | 1:1000 (WB) |
| α-p(Thr389)-S6K1 | Rabbit | Cell Signaling (9205) | 1:1000 (WB) |
| α-p(Ser235/236)-S6 | Rabbit | Cell Signaling (2211) | 1:1000 (WB) |
| α-p(Thr37/46)-4E-BP1 | Rabbit | Cell Signaling (2855) | 1:1000 (WB) |
| α-ATF4 | Rabbit | Cell Signaling (11815) | 1:400 (ChIP); 1:1000 (WB) |

**Table 2.4: List of secondary antibodies used**

| Target | Host | Source | Dilution |
|---|---|---|---|
| α-Mouse IgG (H+L)-HRP conjugate | Goat | BIO-RAD (1706516) | 1:10000 (WB) |
| α-Rabbit IgG (H+L)-HRP conjugate | Goat | BIO-RAD (1706515) | 1:10000 (WB) |
| α-Mouse IgG(H+L)- Alexa-Fluor®488 conjugate | Donkey | Life Technologies (A21202) | 1:1000 (IF) |
| α-Rabbit IgG(H+L)- Alexa-Fluor®546 conjugate | Donkey | Life Technologies (A10040) | 1:1000 (IF) |
| α-Goat IgG(H+L)- Alexa-Fluor®488 conjugate | Donkey | Life Technologies (A11055) | 1:1000 (IF) |

### 2.1.5. – qPCR primers

The following qPCR primers were used throughout the study for gene expression analyses:

**Table 2.5: List of qPCR primers used**

| Oligonucleotide Sequence | Description |
|---|---|
| 5'-CATTTGGGCCTGGACTCTGAT-3' | ZMYND8 Gene Expression Forward Primer |

| | |
|---|---|
| 5’-GGAGATGGTTCTTTGGGTTCCT-3’ | ZMYND8 Gene Expression Reverse Primer |
| 5’-AGGTACTTTGATTCCCAAGTCA-3’ | MITF Gene Expression Forward Primer |
| 5’-AAGTTCTTTTGCGCGTTGCT-3’ | MITF Gene Expression Reverse Primer |
| 5’-ATTGACAGCCAAGGCAAAAG-3’ | p66β Gene Expression Forward Primer |
| 5’-TTCCAGTGAGGGGTGAAATC-3’ | p66β Gene Expression Reverse Primer |
| 5’-TTAGGCAACATTCCAGCACA-3’ | p66α Gene Expression Forward Primer |
| 5’-GGATGATCCTCTGTCCCTGA-3’ | p66α Gene Expression Reverse Primer |
| 5’-TGGCACTGTTGTTTCACAAGAT-3’ | PTEN Gene Expression Forward Primer |
| 5’-TAGCTGGCAGACCACAAACT-3’ | PTEN Gene Expression Reverse Primer |
| 5’-ACTCATGACAGTCCCTTCTGC-3’ | DEPTOR Gene Expression Forward Primer |
| 5’-GACACGATCTTGATCTCCTTGCT-3’ | DEPTOR Gene Expression Reverse Primer |
| 5’- TCAAACCTCATGGGTTCTCC-3’ | ATF4 Gene Expression Forward Primer |
| 5’- GTGTCATCCAACGTGGTCAG-3’ | ATF4 Gene Expression Reverse Primer |
| 5’-AGCCAGACTTTGTTGGATTTG-3’ | HPRT Gene Expression Reverse Primer |
| 5’-TTTACTGGCGATGTCAATAGG-3’ | HPRT Gene Expression Reverse Primer |

### 2.1.6. – Small interfering RNAs (siRNAs)

The following RNA oligonucleotides were used throughout the study:

**Table 2.6: List of RNA oligonucleotides used**

| Oligonucleotide Sequence | Target/Description | Source |
|---|---|---|
| 5'-GAGAUGGAGGUUUACGUGGAGAACA-3'<br>5'-UGUUCUCCACGUAAACCUCCAUCUC-3' | siZMYND8 Sense Primer<br>siZMYND8 Antisense Primer | Sigma Aldrich |
| 5'-UCAACCGCAGUCAAGUUCUUCUGUU-3'<br>5'-AACAGAAGAACUUGACUGCGGUUGA-3' | sip66β(I) Sense Primer<br>sip66β(I) Antisense Primer | Sigma Aldrich |
| 5'-GCGAGUUCAUCUACAUGGUAGGCUU-3'<br>5'-AAGCCUACCAUGUAGAUGAACUCGC-3' | sip66β(II) Sense Primer<br>sip66β(II) Antisense Primer | Sigma Aldrich |
| 5'-ACAUGUUGAUGUCUCAACGUGUUAU-3'<br>5'-AUAACACGUUGAGACAUCAACAUGU-3' | sip66β(III) Sense Primer<br>sip66β(III) Antisense Primer | Sigma Aldrich |
| Not available | sip66α(I) | Invitrogen (5175567, HSS147779) |
| 5'-GCCAGCGAGAGUACCUCCUGGACAU-3'<br>5'-AUGUCCAGGAGGUACUCUCGCUGGC-3' | sip66α(II) Sense Primer<br>sip66α(II) Antisense Primer | Sigma Aldrich |
| 5'-CAGCAUUAGGCAACAUUCCAGCACA-3'<br>5'-UGUGCUGGAAUGUUGCCUAAUGCUG-3' | sip66α(III) Sense Primer<br>sip66α(III) Antisense Primer | Sigma Aldrich |
| Not available | siCHD4 | Invitrogen (5204331, HSS101848) |
| 5'-AAAGCAGUACCUUUCUACCAC-3'<br>5'-GUGGUAGAAAGGUACUGCUUU-3' | siMITF(I) Sense Primer<br>siMITF(I) Antisense Primer | Sigma Aldrich |
| 5'-GGUGAAUCGGAUCAUCAAG-3'<br>5'-CUUGAUGAUCCGAUUCACC-3' | siMITF(II) Sense Primer<br>siMITF(II) Antisense Primer | Sigma Aldrich |
| 5'-GCUCAUGGACUUUCCCUUA-3'<br>5'-UAAGGGAAAGUCCAUGAGC-3' | siMITF(III) Sense Primer<br>siMITF(III) Antisense Primer | Sigma Aldrich |
| 5'-UGGCUAUGCUUACGCUUAA-3'<br>5'-UUAAGCGUAAGCAUAGCCA-3' | siMITF(IV) Sense Primer<br>siMITF(IV) Antisense Primer | Sigma Aldrich |

| | | |
|---|---|---|
| 5'-AGACGGAGCACACUUGUUA-3'<br>5'-UAACAAGUGUGCUCCGUCU-3' | siMITF(V) Sense Primer<br>siMITF(V) Antisense Primer | Sigma Aldrich |
| Not available | siPTEN | QIAGEN (FlexiTube Hs_PTEN_6, S100301504) |

## 2.2. – Bacterial methods

### 2.2.1. – Cultivation of bacteria

Bacteria were grown on LB/agar plates at 37°C to obtain clonal colonies. To prepare these plates, autoclaved Luria-Bertani broth (LB; 1% w/v bactotryptone, 0.5% w/v yeast extract, 1% w/v NaCl, pH 7.5) containing 1.5% agar was warmed up, supplemented with ampicillin (100 μg/ml), poured into Petri dishes (Sterilin) and left to solidify. Plates were stored at 4°C until use.

To amplify clones, bacteria were grown in liquid LB medium supplemented with ampicillin (100 μg/ml) at 37°C and shaking at 225 rpm.

### 2.2.2. – Transformation of competent bacteria

DH5α competent bacteria (ThermoFisher) were transformed for amplification of plasmid DNA of interest. An aliquot of 25 μl of competent bacteria was thawed and 0.2-2 μl of plasmid DNA added. The mix was then incubated on ice for 20 min and subsequently subjected to a heat shock at 42°C for 42 seconds before it was returned to ice for another 3 min. 250 μl of S.O.C. medium (2% w/v tryptone, 0.5% w/v yeast extract, 10 mM NaCl, 2.5 mM KCl, 10 mM $MgCl_2$, 10 mM $MgSO_4$, 20 mM glucose; Invitrogen) were added to the bacterial mix which was then incubated at 37°C for an hour shaking at 225 rpm. Finally, the bacteria were plated in LB/agar plates supplemented with ampicillin (selection antibiotic).

## 2.3. – Mammalian cell methods

### 2.3.1. – Cultivation of mammalian cell lines

All human cell lines used in this study (Table 2.2) were grown in a monolayer in Roswell Park Memorial Institute Medium 1640 (RPMI; Gibco) supplemented with 10% foetal bovine serum (FBS; Sigma Aldrich). Cells were kept at 37°C in a $CO_2$ incubator (Binder) providing a humidified atmosphere with 5% $CO_2$.

Cells were passaged routinely when reaching ~85% confluency. 0.25% Trypsin-EDTA (Gibco) was used to detach cells when passaging.

### 2.3.2. – Cryoconservation of mammalian cell lines

For storage of a vial of cells, around 4 x $10^6$ cells were detached, centrifuged (500 xg, 5 min) and resuspended in FBS suplemmented with 10% DMSO. Cells were then moved into a Mr. Frosty freezing container (Thermo Fisher Scientific) and stored at -80°C to allow progressive cooling.

### 2.3.3. – Transient expression of proteins of interest

Transfection of cells for transient expression of proteins was carried out using FuGENE® 6 Transfection Reagent (Promega) following the manufacturer's instructions. First, cells were seeded at ~60% confluency and incubated overnight. Then, FuGENE® 6 was incubated in Opti-MEM® (ThermoFisher) for 5 min before adding the DNA (vector of interest) using a 3 µl FuGENE® 6 : 1 µg DNA ratio and the mix was then incubated for another 15 min at RT. Finally, the FuGENE® 6 / DNA mix was added to the cells culture medium and analysis was performed after 48 h incubation.

**2.3.4. – Non-inducible stable expression of proteins of interest**

Stable expression of proteins of interest was achieved by simultaneous transfection (using FuGENE® 6 Transfection Reagent (Promega) as described above) of an expression vector containing an antibiotic resistance cassette and the expression vector containing the protein of interest and subsequent selection adding the appropriate antibiotic to the culture medium 48 h after transfection for 10 days.

Subcloning was in some cases performed to get a cell population with homogeneous expression of the protein of interest.

**2.3.5. – Inducible stable expression of proteins of interest**

The PiggyBac (PB) Transposon System was used for inducible and stable expression of proteins of interest.

First, terminal repeats recognised by the PB transposase were cloned into the expression vector of the protein of interest flanking the sequence codifying for such protein plus its promoter. Then, this construct was co-transfected into melanoma cells with an expression vector for the PB transposase (10:1 ratio) using FuGENE® 6 Transfection Reagent (Promega) as described above. Consequent to the expression of the transposase, the sequence codifying for the protein of interest is randomly integrated into the cell's genome, providing a stable expression.

In order to allow for inducible expression of the protein of interest, a reverse tetracycline transactivator (rtTA) controlled promoter (hCMV1), only active when bound by an rtTA/tetracycline complex, was used. Induction of expression was then achieved by addition of doxycycline (a tetracycline analogue) into the cell culture medium.

Subcloning was finally performed in some cases to get a cell population with homogeneous expression of the protein of interest.

### 2.3.6. – Transient knock-down of endogenous proteins of interest

To transiently knock-down the expression of a protein of interest, cells were transfected with small interfering RNA (siRNA) with sequence homology to the target protein (see Table 2.6 for specific siRNA sequences).

Lipofectamine® RNAiMAX Reagent (Invitrogen) was used to allow for the transfection following the manufacturer's instructions. First, cells were seeded at ~60% confluency and incubated overnight. Then, Lipofectamine® RNAiMAX Reagent and siRNA were separately incubated in Opti-MEM (ThermoFisher) for 2 min at RT and then mixed into one solution (2 µl Lipofectamine® RNAiMAX : 1.2 µl siRNA (20 µM) ratio) and further incubated for another 15 min. Finally, the Lipofectamine® RNAiMAX / siRNA mix was added to the cells culture medium and analysis was performed after 48 h-72 h incubation. AllStars Negative Control siRNA (QIAGEN) was used as negative control.

## 2.4. – Nucleic acid methods

### 2.4.1. – Extraction of nucleic acids

Plasmid DNA

"QIAprep Spin Miniprep Kit" and "QIAGEN Plasmid Maxi Kit" (QIAGEN) were used to isolate plasmid DNA from bacterial cultures of *E.coli* containing the construct of interest following the manufacturer's instructions.

RNA

"RNeasy Mini Kit" (QIAGEN) was used to isolate RNA from human melanoma cells following the manufacturer's instructions.

**2.4.2. – Quantification of nucleic acids**

NanoDrop™ 2000 (ThermoFisher) was used to quantify nucleic acids as well as to assess their purity. An $A_{260}/A_{280}$ ratio of ≃ 1.8 was considered to correspond to pure DNA and an $A_{260}/A_{280}$ ratio of ≃ 2.0 was considered to correspond to pure RNA. An $A_{260}/A_{230}$ ratio of ≃ 2.1 was considered to correspond to pure DNA or RNA.

**2.4.3. – Polymerase chain reaction**

To amplify DNA fragments for cloning purposes, High Fidelity AccuPrime™ Taq DNA polymerase (ThermoFisher) was used following the manufacturer's instructions. 5 µl 10x AccuPrime PCR buffer I, 0.1 µl forward primer (100 µM), 0.1 µl reverse primer (100 µM), 20 ng plasmid DNA (template) and 0.2 µl AccuPrime™ Taq DNA polymerase were used per reaction (water based solution, 50 µl total volume). A Veriti™ 96-Well Thermal Cycler (Applied Biosystems) was used to carry out the reactions using the following program: initial denaturation (45'' at 94°C); 25 cycles of denaturation (20'' at 94°C), annealing (20'' at 52-64°C depending on the primers Tm) and extension (1' per kb of PCR product at 68°C); and final elongation (8' at 68°C). PCR products were examined by agarose gel electrophoresis and purified using the QIAquick PCR Purification Kit (QIAGEN).

To amplify DNA fragments for screening purposes, MyTaq™ Red Mix (Bioline) was used following the manufacturer's instructions. 5 µl 2x MyTaq™ Red Mix, 0.03 µl forward primer (100 µM) and 0.03 µl reverse primer (100 µM) were used per reaction (water based solution, 10 µl total volume). A Veriti™ 96-Well Thermal Cycler (Applied Biosystems) was used to carry out the reactions using the following program: initial denaturation (2 min at 95°C); 30 cycles of denaturation (15 sec at 95°C), annealing (15 sec at 52-64°C depending on the primers Tm) and extension (15 sec at 72°C); and final elongation (2 min at 72°C). PCR products were examined by agarose gel electrophoresis.

**2.4.4. – Restriction enzyme digestion**

Restriction enzyme digestions were used for cloning and screening purposes. All restriction enzymes were purchased from New England Biolabs and used following the manufacturer's instructions. Briefly, 2 µg DNA were dissolved in 16 µl water and 2 µl of the recommended buffer provided by the supplier plus 1 µl of the restriction enzyme (1 µl each enzyme for double digestions) were added. The mix was then incubated at the temperature recommended by the supplier for 2 h. Finally, digestion products were purified using the QIAquick PCR Purification Kit (QIAGEN).

**2.4.5. – DNA dephosphorylation**

Calf intestinal alkaline phosphatase (CIP) (New England Biolabs) was used to prevent re-ligation of vectors when performing restriction digest. For vector digestions carried out at 37°C, 1 unit of CIP was added to the digestion mix 30 min before the end of the 2 h incubation. For vector digestions performed at a different temperature, 1 unit of CIP was added at the end of the 2 h incubation and the mix was incubated for another 30 min at 37°C. Digestion products were then purified using the QIAquick PCR Purification Kit (QIAGEN) (as detailed in the previous section).

**2.4.6. – Ligation**

T4 DNA Ligase (New England Biolabs) was used to ligate the digested DNA fragments following the manufacturer's instructions. Briefly, mixtures of DNA fragments in a 1:3 and/or 1:10 vector:insert ratio were prepared in 9 µl water. 1 µl of 10x T4 DNA Ligase buffer and 1 µl of T4 DNA Ligase were then added to the mixtures and the ligation reaction was incubated at room temperature for 1 h.

2 µl of ligation reaction were finally transformed into competent bacteria and successful integration of the insert in the recipient vector was examined by colony PCR and confirmed by DNA sequencing.

**2.4.7. – Agarose gel electrophoresis**

Agarose gel electrophoresis was performed to study the size of DNA fragments. To prepare the gels, agarose (Web Scientific) was dissolved in TBE buffer (100 mM TRIS, 90 mM boric acid, 1 mM EDTA) from Invitrogen using a microwave to heat the solution to facilitate dissolving. The nucleic acid dye peqGREEN (PEQLAB) was then added in a concentration of 1:10000 and the mixture was poured into a gel tray with a comb to allow for the formation of wells and left it solidify at RT for around 15 min. Once the gels were ready they were submerged in TBE buffer and the samples were loaded after addition of 0.2 volumes of 6x Gel Loading Dye (New England Biolabs). Electrophoresis was carried out at 120 V and DNA fragments were finally visualised under UV light using a BioDoc-It$^{TM}$ Imaging System (UVP).

**2.4.8. – Quantitative reverse transcription polymerase chain reaction (qRT-PCR)**

To examine the abundance of specific mRNAs in different cell populations, reverse transcription from RNA extracted as previously described (see section 2.4.1) and subsequent qPCR were performed.

QuantiTect Reverse Transcription Kit (QIAGEN) was used for the generation of cDNA following the manufacturer's instructions. Briefly, solutions of 1 µg RNA in 12 µl water were prepared and incubated with 2 µl gDNA Wipeout Buffer for 2 min at 42°C to allow for elimination of contaminating genomic DNA. A mix of 4 µl Quantiscript RT Buffer, 1 µl Quantiscript Reverse Transcriptase and 1 µl Primer Mix was then added to the samples and these were incubated for another 15 min at 42°C to allow for the reverse transcription

reaction to take place. Finally, samples were incubated for 3 min at 95°C to inactivate the Quantiscript Reverse Transcriptase.

The resulting cDNA was then diluted in water (1:13) and used for qPCR. A total volume of 15 µl was used per qPCR reaction, including 6.5 µl diluted cDNA, 0.5 µl forward primer (100 µM), 0.5 µl reverse primer (100 µM) and 7.5 µl Brilliant III Ultra-Fast SYBR Green qPCR Master Mix (Agilent Technologies). Target specific primers were designed spanning exon-exon junctions to avoid amplification from genomic DNA in case of contamination. PCR reactions were carried out in a Rotor-Gene 6000 (Corbett Research), where an initial step of denaturation (95°C, 10 min) was followed by 65 cycles of denaturation (96°C, 8 sec), annealing (62°C, 12 sec), and elongation (72°C, 12 sec). The final step involved a gradual increase of the temperature (72°C to 95°C at a rate of 1°C per 5 sec) to generate melting curves.

The comparative Ct method (Livak and Schmittgen 2001) was used to analyse the raw data, normalising the mRNA levels of target genes to a housekeeping gene and calculating fold changes in gene expression as follows:

$$\text{Relative fold change of target gene} = 2^{-\Delta\Delta CT}$$

$$\text{where } \Delta\Delta C_T = \Delta C_T[\text{experiment}] - \Delta C_T[\text{control}]$$

$$\text{and } \Delta C_T = C_T[\text{target gene}] - C_T[\text{housekeeping gene}]$$

**2.4.9. – DNA sequencing**

Sequencing of plasmid DNA was carried out by either Source BioScience or Eurofins.

**2.4.10. – RNA sequencing (RNA-seq)**

To analyse changes in gene expression genome-wide, RNA was extracted from cells grown in a 60 mm dish to around 75% confluency as indicated in section 2.4.1. and sequenced to assess relative abundance of mRNAs in different cell populations. Library

preparation (using the QuantSeq 3' mRNA-Seq Library Prep Kit FWD for Illumina (Lexogen) and 500 ng starting material), and 3' sequencing of RNA-seq samples (using an Illumina HiSeq4000 and generating above 3,200,000 reads per sample) were carried out by the Oxford Genomics Centre (Wellcome Trust Centre for Human Genetics, University of Oxford). Further analysis is detailed in section 2.7.2.

## 2.5. – Protein methods

### 2.5.1. – Whole cell extract

Whole cell extracts were prepared for the analysis of whole cell proteomes. Cells were washed in PBS and lysed in 1x Laemmli Sample Buffer (62.5 mM Tris-HCl - pH 6.8, 2% SDS, 10% glycerol, 5% β-mercaptoethanol, dash of bromophenol blue). Extracts were finally boiled at 95°C for 5-10 min to achieve protein denaturation and stored at -20°C until use.

### 2.5.2. – SDS – polyacrylamide gel electrophoresis

To resolve proteins contained in whole cell extracts or samples from immunoprecipitation or nuclear fractionation by size, sodium dodecyl sulphate polyacrylamide gel electrophoresis (SDS-PAGE) was performed. To prepare the resolving part of the gels, an appropriate amount of 45% acrylamide solution (200:1 acrylamide:bis-acrylamide) (Severn Biotech) was diluted in water and mixed with 4x resolving gel buffer (1.5 M Tris, 0.4% SDS, pH 8.9) to obtain a final solution containing 12.5% acrylamide, 375 mM Tris and 0.1% SDS (pH 8.9). Ammonium persulphate (APS) and tetramethylethylenediamine (TEMED) were then added at a 0.1% final concentration to catalyse the polymerisation of the acrylamide. The mix was then immediately poured into the moulds for gel casting, covered with water, and left to polymerise at RT for around 10 min. For the stacking part of the gels, an appropriate amount of 30% acrylamide solution

(37.5:1 acrylamide:bis-acrylamide) (Severn Biotech) was diluted in water and mixed with 4x stacking gel buffer (0.5 M Tris, 0.4% SDS, pH 6.8) to obtain a final solution containing 5% acrylamide, 125 mM Tris and 0.1% SDS (pH 6.8). APS and TEMED were then added at a 0.1% final concentration to catalyse the polymerisation of the acrylamide. The mix was then immediately poured on top of the resolving part of the gels after removing the water and left to polymerise at RT for around 10 min after introducing a comb to create the wells for sample loading.

Denatured samples as well as a protein ladder (Precision Plus Protein™ Dual Color Standards, BIO-RAD) were loaded into the gels and these were run at 180 V for 50-80 min (depending on the desired level of resolution of the proteins) in running buffer (53 mM Tris, 53 mM Glycine, 0.1% SDS) at RT.

**2.5.3. – Western blot**

To detect specific proteins contained in whole cell extracts or samples from immunoprecipitation, western blot was performed. First, proteins were separated according to size by SDS-PAGE and then electro-transferred to Amersham™ Protran™ 0.45 µm nitrocellulose blotting membranes (GE Healthcare Life Sciences) in transfer buffer (31 mM Tris, 192 mM Glycine, 20% isopropanol) at 150 mA for 90 min. In order to check that the proteins were successfully transferred, the resulting nitrocellulose membranes were incubated at RT for 1 min with Ponceau solution (0.1% Ponceau S, 5% acetic acid) which stains all protein bands. The staining solution was then removed by washing with PBS supplemented with 0.1% Tween-20 (PBS-T). In order to block non-specific binding, the membranes were incubated with blocking solution (5% skimmed milk in PBS-T) at RT for 1 h before incubating with the primary antibody diluted in blocking solution as specified in Table 2.3 at 4°C overnight. All incubations were carried out in a rocking platform providing even

and gentle agitation. The following day membranes were washed with PBS-T (3 times, 5 min each) and then incubated with the corresponding horseradish peroxidase-conjugated secondary antibody diluted in blocking solution as detailed in Table 2.4 at RT for 2 h. Following another 3 rounds of washes (5 min each) with PBS-T, enhanced chemiluminescence (ECL) reagent (Amersham) was added and the signal detected using Super RX X-Ray films (Fujifilm) and an SRX-101A film processor.

**2.5.4. – Chromatin immunoprecipitation – sequencing (ChIP-seq)**

To investigate the specific DNA binding sites of a protein of interest genome-wide, chromatin immunoprecipitation followed by high throughput sequencing (ChIP-seq) was performed. Cells were grown in thirty 150 mm dishes to around 80% confluency and then harvested using 0.25% Trypsin-EDTA (Gibco) and centrifuged at 500xg for 5 min. Following removal of the supernatant, cells were fixed in 300 ml ice-cold PBS containing 0.4% paraformaldehyde in a 10 min incubation at 4°C with gentle rotation. To quench crosslinking, glycine was added to a final concentration of 200 mM and rotation at 4°C was kept for another 10 min. Crosslinked cells were then centrifuged (500xg, 5 min), washed in PBS, centrifuged again (500xg, 5 min), resuspended in 10 ml ChIP lysis buffer (50 mM Tris-HCl (pH 8), 10 mM EDTA, 10 mM sodium butyrate, 1% SDS, 0.5 mM phenylmethylsulfonyl fluoride (PMSF), 4x PIC) and incubated in ice for 20 min. The lysed cell suspension was passed through a 25g needle (Terumo) before proceeding to sonication in a Covaris S220 (160 W peak incident power, 5% duty cycle, 200 cycles per burst, 4°C) until 150-300 bp fragments were obtained. For assessment of fragments size, crosslinking was reversed for an aliquot of chromatin as described below and examined in a 2100 Bioanalyzer (Agilent). This aliquot was kept as input fraction.

Before proceeding to the immunoprecipitation, the sonicated chromatin was centrifuged at 13,000xg for 10 min for clearing, and the supernatant was diluted in 70 ml of ChIP dilution buffer (16.7 mM Tris-HCl (pH 8), 167 mM NaCl, 1.2 mM EDTA, 1% Triton X-100, 0.01% SDS). The antibody was then added to the fragmented chromatin solution to reach the final dilution specified in Table 2.3 and the solution was incubated with gentle rotation at 4°C overnight. At the same time, 400 µl Dynabeads$^{TM}$ Protein G (Invitrogen) were washed in ChIP dilution buffer and blocked in ChIP dilution buffer containing 0.5 mg/ml BSA with gentle rotation at 4°C overnight. All steps requiring separation of the beads from supernatant were performed using a DynaMag$^{TM}$-2 magnet (Life Technologies). The following day the blocked beads were added to the fragmented chromatin suspension incubated with the primary antibody and the incubation with rotation at 4°C was kept for another 90 min to allow binding of the antibody (together with its bound protein-DNA complexes) to the magnetic beads. These beads were then transferred to a 2 ml Eppendorf tube (by subsequent additions of the containing solution and supernatant discarding) where they were washed twice in 2 ml ChIP low salt wash buffer (20mM Tris-HCl (pH 8), 150 mM NaCl, 2 mM EDTA, 1% Triton X-100, 0.1% SDS) before transferring to a fresh 2 ml Eppendorf tube. The following further washes were carried out in this tube: 1x ChIP low salt wash buffer, 3x ChIP high salt wash buffer (20 mM Tris-HCl (pH 8), 500 mM NaCl, 2 mM EDTA, 1% Triton X-100, 0.1% SDS) and 3x LiCl wash buffer (10 mM Tris-HCl (pH 8), 250 mM LiCl, 1 mM EDTA, 10 mM sodium deoxycholate, 1% NP-40). Protein-DNA complexes were finally eluted from the beads in 1.2 ml elution buffer (100 mM $NaHCO_3$, 1% SDS) in a 30 min incubation at RT with gentle rotation.

To reverse crosslinks, the eluted protein-DNA complexes were incubated at 55°C overnight after adding 300 mM NaCl (final concentration) and also 20 µg RNase A (Invitrogen) to remove potential RNA contamination and 20 µg Proteinase K (Thermo

Scientific) to degrade the protein content. The DNA was subsequently extracted using the QIAquick PCR Purification Kit (QIAGEN) in a final volume of 30 µl water.

Samples were finally subjected to pair-end sequencing using an Illumina HiSeq4000 and generating a minimum of 32,000,000 reads per sample. Library preparation, sequencing, base-calling and demultiplexing were carried out by the Oxford Genomics Centre (Wellcome Trust Centre for Human Genetics, University of Oxford). Details of subsequent bioinformatic analysis can be found in section 2.7.3.

**2.5.5. – Protein synthesis assays**

To determine protein synthesis rates in cells, two different methods were used:

2.5.5.1- Click-iT® plus OPP protein synthesis assay

Protein synthesis was in this case estimated by measuring incorporation of a puromycin analogue to newly synthesised proteins using the Click-iT® Plus OPP Alexa Fluor® 647 protein synthesis assay kit (Life Technologies) following the manufacturer's instructions.

Upon any desired treatment, cells were subjected to a 30 min pulse with O-propargyl-puromycin (OPP), which was directly added to their culture medium with maintenance of the culture conditions. OPP inhibits protein synthesis through disruption of peptide transfer on ribosomes, which causes premature chain termination during translation. Since this puromycin analogue contains an alkyne moiety, subsequent addition of Alexa Fluor® 647 picolyl azide and the Click reaction agents leads to a chemoselective ligation or "click" reaction between the picolyl azide dye and the alkyne OPP, allowing the detection of the modified proteins by fluorescence. For those cases where the presence of a specific additional protein was to be imaged, immunofluorescence staining was carried out following the Click-iT reaction as detailed in section 2.6.1 (directly from primary antibody incubation). DNA staining was in these cases performed together with secondary antibody

incubation. Finally, cells were mounted with Vectashield (Vector Laboratories) on Polysine® slides (Thermo Scientific) and imaged using a LSM710 confocal microscope (Zeiss). The images obtained were processed using ImageJ software.

2.5.5.2- Metabolic labelling

Alternatively, protein synthesis was estimated by measuring incorporation of radiolabelled amino acids to newly synthesised proteins.

Following any desired treatment, cells were subjected to a 30 min pulse with EasyTag™ Express [$^{35}$S]-methionine/cysteine protein labelling mix (Perkin Elmer), which was added in fresh culture medium at 110 µCi/ml, with maintenance of the culture conditions. Upon this incubation, cells were washed in PBS twice and lysed in 1x Laemmli Sample Buffer (see section 2.5.1). The lysates were then analysed by SDS-PAGE (see section 2.5.2) and their total protein content visualised by incubation with Coomassie blue staining solution (0.03% Coomassie Brilliant Blue R-250 (w/v), 50% methanol, 10% glacial acetic acid) for 30 min followed by 1 h wash with water, both in a rocking platform providing gentle agitation. The gel was then dried into Whatman® filter paper (Fisher Scientific) at 65°C for 1 h using an MGD-4534 gel dryer (VWR) connected to a vacuum pump. Finally, quantification of the labelled proteins was carried out by exposure of the dried gel to imaging screens (BIO-RAD) and signal detection using a Personal Molecular Imager™ (PMI™) System (BIO-RAD).

## 2.6. – Cell biology methods

### 2.6.1. – Immunofluorescence

Immunofluorescence was performed to study localisation and relative intracellular abundance of proteins of interest. Cells were grown on glass coverslips for cell culture (VWR), subjected to any desired treatment and then fixed in PBS containing 2% PFA at RT

for 15 min. After washing 3 times with PBS, cells were permeabilised in PBS containing 0.2% Triton X-100 at RT for 7 min and blocked in blocking buffer (PBS containing 5% BSA and 0.1% Tween) at RT for 30 min. Subsequently, cells were incubated with the primary antibody diluted in blocking buffer as detailed in Table 2.3 in a humidified chamber at RT for 1 h. Following another round of washes (3x) with PBS, cells were incubated with the corresponding Alexa Fluor conjugated secondary antibody (Life Technologies) diluted in blocking buffer as detailed in Table 2.4 plus DAPI diluted 1:10000 in the same blocking solution in a humidified chamber at RT for 1 h. Finally, cells were washed in PBS (3x), mounted with Vectashield (Vector Laboratories) on Polysine® slides (Thermo Scientific) and imaged using a LSM710 confocal microscope (Zeiss). The images obtained were processed using ImageJ software.

**2.6.2. – Scratch-wound healing assay**

To study cell migration, a scratch-wound healing assay was performed. Cells were grown to ~100% confluency while being subjected to any desired treatment and then a scratch was produced using a P200 pipette tip. To assess the amount of time required for closing of the introduced wound, time-lapse microscopy was used. A brightfield image was taken every 10 min for 72 h and the data produced was analysed in ImageJ using macros created by Mark Shipman (Ludwig Institute for Cancer Research, University of Oxford).

**2.6.3. – Cell cycle analysis**

To study the cell cycle profile of cell populations, cell cycle analysis was performed using flow cytometry. After subjecting cells to any desired treatment, they were harvested using 0.25% Trysin-EDTA (Gibco), washed in PBS, transferred to an Eppendorf tube, centrifuged at 4,000 rpm for 2 min in a Centrifuge 5424 R (Eppendorf) and resuspended in 300 µl PBS. 750 µl 100% ethanol were then added to the cell suspension and this was

incubated on ice for 1 h to allow for cell fixation. Cells were then centrifuged again at 4,000 rpm for 2 min and this time resuspended in 250 µl propidium iodide (PI) solution (50 µg/ml PI, 0.1 mg/ml RNase A, 0.05% Triton X-100) and incubated at 37°C for 40 min to allow for DNA staining. Following addition of 750 µl PBS, cells were centrifuged at 4,000 rpm for 2 min and resuspended in 250 µl staining solution (PBS containing 5% FBS and 2 mM EDTA). Finally, PI fluorescence was measured in a BD FACSCanto$^{TM}$ (BD Biosciences) and the data analysed using FlowJo software.

## 2.7. – Bioinformatics

### 2.7.1. – Quality control of high-throughput sequencing data

A quality control check was initially carried out on the raw sequencing data produced by the Oxford Genomics Centre (Wellcome Trust Centre for Human Genetics, University of Oxford) corresponding to the RNA-seq and ChIP-seq experiments performed using the FastQC tool (http://www.bioinformatics.babraham.ac.uk/projects/fastqc/) to ensure high sequencing quality and assess whether pre-processing of the files was necessary. As FastQC reported high quality of the sequencing reads, no overrepresented sequences, and low level of sequence duplication for all samples, the raw data was directly subjected to the analysis described below.

### 2.7.2. – 3' RNA-sequencing

Following the quality control check, single-end reads were aligned to the human genome build hg19 (GRCh37, February 2009) using STAR (Dobin et al. 2013) (default parameters). In order to visualise the mapped data, the generated BAM files were used to produce BigWig files which were uploaded into the University of California at Santa Cruz (UCSC) Genome Browser.

For transcript quantification, the number of reads mapping to each genomic feature or gene was measured using *featureCounts* (Liao et al. 2014) and the GTF annotation file corresponding to the human genome build hg19 from UCSC. Differential gene expression analysis was then performed using the R package "edgeR" (Robinson et al. 2010), including the use of the exactTest and decideTestsDGE functions (with Benjamini-Hochberg correction for the decideTestsDGE function). During the analysis, lowly expressed genes (not reaching 1 count per million in at least 3 samples) were filtered out. Also, a normalisation step was performed to adjust for differences in RNA composition between samples using the function calcNormFactors (normalisation for sequencing depth is automatically performed within the *edgeR* algorithm). Finally, only differentially expressed genes with adjusted p-value (FDR) smaller than 0.05 were extracted in the final output from the analysis.

Heatmaps representing differential gene expression were generated using the heatmap.2 function of the R package "gplots", and ontology analysis of the data on differential gene expression was performed using EnrichR (Chen et al. 2013a; Kuleshov et al. 2016).

**2.7.3. – ChIP-sequencing**

Following the quality control check, pair-end reads were aligned to the human genome build hg19 (GRCh37, February 2009) using Bowtie2 (Langmead and Salzberg 2012) with a maximum of 1 mismatch allowed (default for all other parameters). In order to visualise the mapped data, the generated SAM files were used to produce BigWig files which were uploaded into the UCSC Genome Browser following normalisation to 32 million reads (which is just below the smallest sample size) using the bamtoscaledbigwig.pl function.

Significant peaks above background were then detected using the *callpeak* function of MACS2 (Zhang et al. 2008), which automatically normalises for sequencing depth and

removes duplicate alignments. Chromatin input corresponding to each ChIP sample before IP was used as control establishing background levels. 1 x $10^{-6}$ *Q* value was established as cutoff (minimum FDR) to call significant regions. Finally, annotation of peaks to nearby genes in the RefSeq database corresponding to the human genome build hg19 (GRCh37, February 2009) was carried out using the program annotatePeaks.pl from Homer (Heinz et al. 2010), which defines promoter-TSS (transcription start site) regions as ± 1 kb from the TSS and TTS (transcription termination site) regions as ± 1 kb from the TTS.

Additionally, sequences under the peaks called were extracted and used for *de novo* prediction of DNA binding motifs (relative to random background control genomic sequences matched for GC-content) using MEME-ChIP (Machanick and Bailey 2011) in the differential enrichment mode.

#### 2.7.4. – Intersection of RNA-sequencing and ChIP-sequencing data

To extract genes identified as differentially expressed through RNA-sequencing analysis that present associated binding peaks in a related ChIP-sequencing analysis, the corresponding lists of genes were intersected using the inner_join and merge functions of the R package "dplyr".

## 2.8. – Statistics

All statistical analyses shown in this study correspond to unpaired t tests comparing one experimental condition versus the corresponding control.

In each case, mean values for 3 biological replicates were generated from 3 technical replicates each and the mean of these values was represented together with the standard error of the mean (SEM) referring to the variation in the mean over the set of 3 biological replicates analysed.

# Chapter 3 – Study of the potential role of ZMNYD8 and the NuRD complex in the regulation of MITF

## 3.1. – Introduction

Epigenetic dysregulation is currently accepted to play a crucial role in cancer development. In particular, several chromatin remodelling complexes regulate transcriptional events integral to oncogenesis and cancer progression, including the nucleosome remodelling and histone deacetylase (NuRD) complex (Lai and Wade 2011; Mayes et al. 2014; Lu and Allis 2017).

The NuRD complex links at least two enzymatic activities that are essential to epigenetic regulation: histone deacetylation and ATP-dependent nucleosome mobilization, regulating a high number of genes mainly involved in cancer and development (Xue et al. 1998; Lai and Wade 2011; Zhang et al. 2011; Basta and Rauchman 2015). While NuRD is most frequently found to exert transcriptional repression, it can also lead to enhanced transcription of genes, and both function and genomic targeting of the complex are at least partly determined by its composition, which is not fixed but context-dependent (**Figure 3.1**) (Bowen et al. 2004; Fujita et al. 2004; Le Guezennec et al. 2006; Miccio and Blobel 2010).

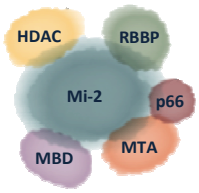


- **Mi2** – ATP dependent nucleosome mobilization activity (CHD3/CHD4)
- **HDAC** – Histone deacetylase activity (HDAC1/HDAC2)
- **MBD** – Genomic targeting (MBD2/MBD3)
- **MTA** – Genomic targeting (MTA1/MTA2/MTA3)
- **p66** – Structural component, genomic targeting (GATAD2A/GATAD2B)
- **RBBP** – Structural component (RBBP4/RBBP7)

**Figure 3.1.- Core components of the NuRD complex.** The Mi-2 subunit of NuRD, chromodomain-helicase-DNA-binding 3 or 4 (CHD3 or CHD4), harbours the ATP dependent nucleosome mobilization activity of the complex (Becker and Hörz 2002; Bouazoune et al. 2002). Histone deacetylases 1 and 2 (HDAC1 and HDAC2) constitute the other enzymatic subunit of the complex (Thiagalingam et al. 2003). The MBD subunit is involved in genomic targeting, with both MBD2 and MBD3 containing a methyl-CpG binding domain (MBD) but only MBD2 found to bind methylated DNA (Saito and Ishikawa 2002; Hendrich and Tweedie 2003). The metastasis associated (MTA) subunits (MTA1/MTA2/MTA3) and p66 subunits (p66α/p66β) have been involved in genomic targeting as well, with the latter also described to play a fundamental structural role (Feng et al. 2002; Fujita et al. 2004; Brackertz et al. 2006). Finally, the retinoblastoma-binding proteins 4 and 7 (RBBP4 and RBBP7) are considered structural subunits of the NuRD complex with the ability to interact with histones (Loyola and Almouzni 2004).

The NuRD complex can be recruited to specific genomic regions through protein interactions with TFs and cofactors (Cismasiu et al. 2005; Hong et al. 2005; Bhattacharyya et al. 2009; Garnatz et al. 2014; Waldron et al. 2016). Recently, an interaction between NuRD and the bromodomain protein ZMYND8 was identified and associated with NuRD genomic targeting (Gong et al. 2015; Spruijt et al. 2016).

ZMYND8 (zinc finger MYND-type containing 8) is a multi-domain protein that contains a bromodomain (BRD) (reader of acetylated chromatin) and other reader domains in its N-terminus and a MYND domain (likely implied in protein-protein interactions) in its C-terminus (**Figure 3.2**) (Gong et al. 2015).




**Figure 3.2.- The domain structure of ZMYND8.** PHD: plant homeodomain; BRD: bromodomain; ZnF: zinc finger; PWWP: Proline-Tryptophan-Tryptophan-Proline; DUF3544: domain of unknown function 3544; MYND: myeloid, nervi, and DEAF-1. Numbers refer to amino acids in the ZMYND8 protein.

Although the precise function of this bromodomain protein is not currently known, it has a role in neural development in Xenopus (Zeng et al. 2010). ZMYND8 has also been linked to the DNA damage response as a recruiter of the NuRD complex to damaged chromatin (Gong et al. 2015; Spruijt et al. 2016), and has been associated with cancer progression by promoting angiogenesis through the induction of vascular endothelial growth factor A (VEGFA) expression in prostate cancer (Kuroyanagi et al. 2014). As previously introduced, ZMYND8 is a transcriptional corepressor of several genes (Hassan et al. 2002; Dancy and Cole 2015; Gong et al. 2015; Li et al. 2016), but has also been recently suggested to have a role in positive regulation of transcription through the recruitment of the P-TEFb complex (Ghosh et al. 2018).

## 3.2. – Preliminary data

### 3.2.1. – The NuRD complex interacts with MITF

In an attempt to identify MITF cofactors implicated in transcription regulation, a yeast two-hybrid screen was performed by Alex Schepsky (former member of the laboratory) using the MITF bHLH-LZ domain as bait. The result (not shown) indicated that MITF could interact with the p66α subunit (GATAD2A) of the NuRD complex. The interaction between MITF and the highly related p66α and p66β (GATAD2B), encoded by different genes, was then validated by co-immunoprecipitation (**Figure 3.3**) and by immunofluorescence performed by Suzanne Carreira (former member of the laboratory) (not shown) that revealed p66 and MITF subcellular co-localisation within sub-nuclear foci.

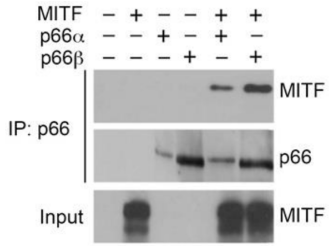


**Figure 3.3.- MITF interacts with p66α and p66β.** HEK293 cells were co-transfected with expression vectors for MYC epitope-tagged MITF and either p66α or p66β and 48 h later whole cell extracts were used for a co-IP experiment pulling down p66α/β with an α-p66 antibody. Western blot analysis of the inputs and IP extracts shows that MITF was co-immunoprecipitated with both p66α and p66β. (*Performed by Alex Schepsky*)

### 3.2.2. – The NuRD complex is required for MITF expression

The ability of p66α/β to interact with MITF further suggested a potential role of p66/NuRD complex as a cofactor cooperating with MITF in the regulation of expression of downstream genes. To investigate this hypothesis, an experiment silencing p66β was performed by Luis Sánchez del Campo (former member of the laboratory) with the outcome expected to reveal that known MITF-repressed genes would be activated on p66 depletion. Surprisingly, MITF itself turned out to be regulated by p66β/NuRD, since silencing p66β abolished MITF expression (**Figure 3.4.A**).

Subsequently, the role of NuRD in the regulation of MITF was confirmed by similar experiments where silencing of p66α or CHD4 (Mi-2) subunits of the complex also abolished or decreased, respectively, the expression of MITF (**Figure 3.4.B** and **C**).

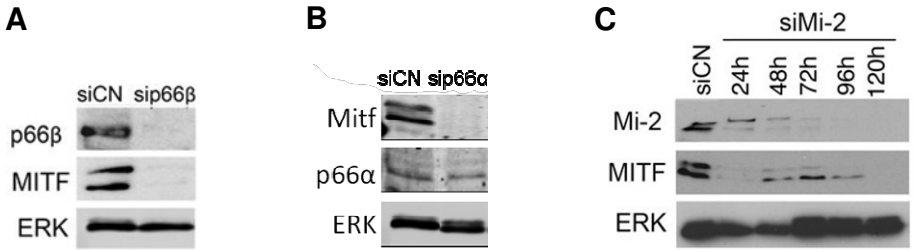


**Figure 3.4.- Silencing of p66β, p66α or CHD4 (Mi-2) abolishes MITF expression. (A)** Western blot analysis of p66β and MITF levels upon silencing of p66β for 72 h in 501mel cells. **(B)** Western blot analysis of p66α and MITF levels upon silencing of p66α for 72 h in 501mel cells. **(C)** Western blot analysis of CHD4 (Mi-2) and MITF levels upon silencing of CHD4 for 24, 48, 72, 96 and 120 h in 501mel cells. (Antibodies: α-p66β, α-p66α, α-Mi-2, α-MITF and α-ERK). ERK was used as a loading control in all cases. (*Performed by Luis Sánchez del Campo*)

Finally, to investigate whether the regulation of MITF by the NuRD complex is direct, a 501mel cell line stably overexpressing HA-tagged p66β was generated by Luis Sánchez del Campo and a ChIP-seq analysis performed using an α-HA antibody. The results showed the binding of the NuRD complex subunit to the promoter of the melanocyte-specific MITF isoform (MITF-M) (**Figure 3.5**).

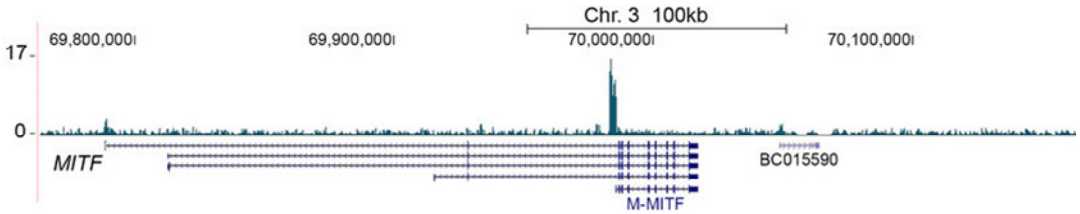


**Figure 3.5.- p66β binds the *MITF* promoter.** ChIP-seq analysis in 501mel cells expressing doxycycline-inducible HA-p66β. Cells were induced using 20 ng doxycycline for 12 h prior to processing for ChIP-seq. The image shows a UCSC browser screenshot of the *MITF* gene with a p66β binding peak in the *MITF-M* promoter. (*Performed by Luis Sánchez del Campo*)

Although the ChIP-seq experiment was only performed once, collectively, the preliminary data suggested an unexpected role for the NuRD complex in maintaining expression of MITF.

### 3.2.3. – ZMYND8 is highly expressed in metastatic melanoma cell lines

Examination of ZMYND8 transcript levels in different cancer cell lines using the CellMiner™ Database revealed that ZMYND8 is highly expressed (at least at the mRNA level) in metastatic melanoma cell lines compared to other cancer cell lines, suggesting a potential role of this protein in melanoma progression (**Figure 3.6**) (National Cancer Institute).

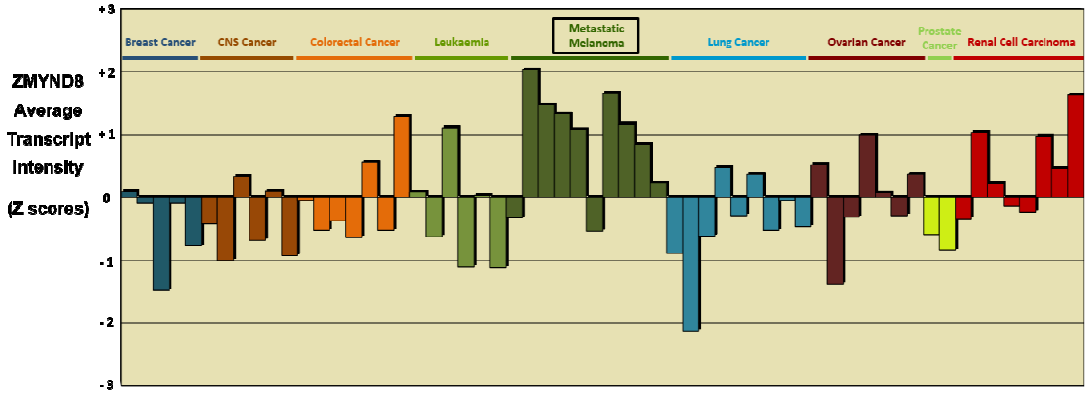


**Figure 3.6.- ZMYND8 average transcript intensities (Z scores) for different cancer cell lines.** Each column represents a specific cell line. CNS: central nervous system. (CellMiner™ Database, National Cancer Institute).

## 3.3. – Investigating the potential role of ZMYND8 in the regulation of MITF

The identification of an interaction between several subunits of the NuRD complex and ZMNYD8 associated with NuRD genomic targeting (Gong et al. 2015; Spruijt et al. 2016) and the apparent requirement of NuRD for *MITF* expression led us to study a potential role of ZMYND8 in the regulation of MITF expression, where we hypothesised that ZMYND8 could act as a cofactor to guide the NuRD complex to the MITF promoter.

### 3.3.1. – Overexpression of ZMYND8 leads to repression of MITF

To study the effect of ZMYND8 levels on MITF in different melanoma cell lines, FLAG-tagged ZMYND8 was transiently overexpressed in 501mel, SKmel28 and IGR37 cells for 48 hours. Subsequent analysis of FLAG-tagged ZMYND8 and endogenous MITF by immunofluorescence showed a dramatic reduction of MITF expression in those cells

successfully transfected for all cell lines tested (**Figure 3.7**), suggesting a role of ZMYND8 as a repressor of MITF.

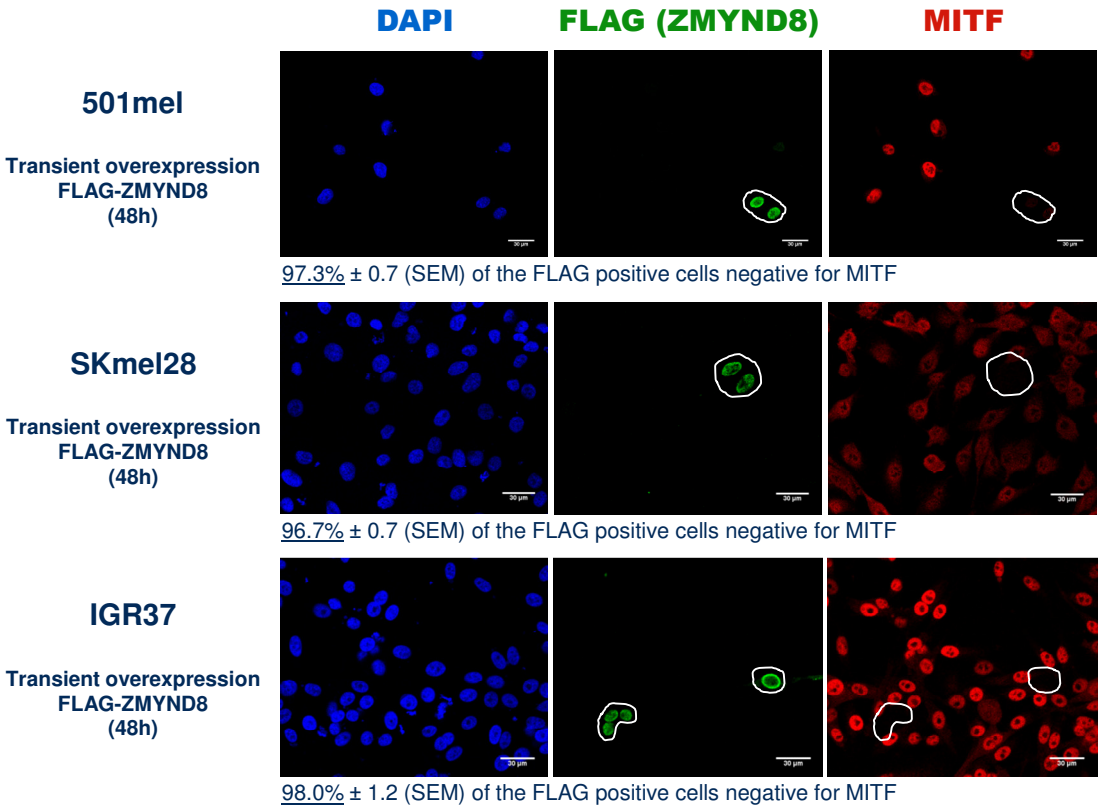


**Figure 3.7.- ZMYND8 overexpression leads to repression of MITF in 501mel, SKmel28 and IGR37 cells.** Immunofluorescence analysis of ZMYND8 and MITF in 501mel, SKmel28 and IGR37 cells after transient expression of FLAG-ZMYND8 for 48 h. 97.3 % ± 0.7 (SEM), 96.7 % ± 0.7 (SEM) and 98.0 % ± 1.2 (SEM) of the FLAG-positive cells were negative for MITF in 501mel, SKmel28 and IGR37 cells, respectively. (n=3, 50 FLAG-positive cells counted per experiment). (Antibodies: α-FLAG and α-MITF). FLAG-positive cells are outlined in white. Scale bars: 30 µm.

### 3.3.2. – Generation of human melanoma cell lines with stable inducible expression of HA-tagged ZMYND8

To further characterise the role of ZMYND8 in the regulation of MITF, a 501mel polyclonal cell line stably expressing 3xHA-tagged ZMYND8 upon induction with doxycycline (501mel-i-HA-ZMYND8 (p)) was generated using the PiggyBac (PB) Transposon System described in section 2.3.5 and sub-cloned to obtain a monoclonal cell line (501mel-i-HA-ZMYND8 (m)) with homogeneous expression of the bromodomain protein.

The analysis of ZMYND8 and MITF levels in doxycycline-induced 501mel-i-HA-ZMYND8 (p) cells by immunofluorescence (**Figure 3.8.A**) further suggested a role of ZMYND8 as a repressor of MITF, with MITF expression being substantially reduced in cells expressing ZMYND8. The ability of ZMYND8 to repress MITF was confirmed by western blotting in doxycycline-induced 501mel-i-HA-ZMYND8 (m) cells where induction of ZMYND8 over time led to a decrease in MITF expression (**Figure 3.8.B** and **C** and **Supplementary Figure A.1**).

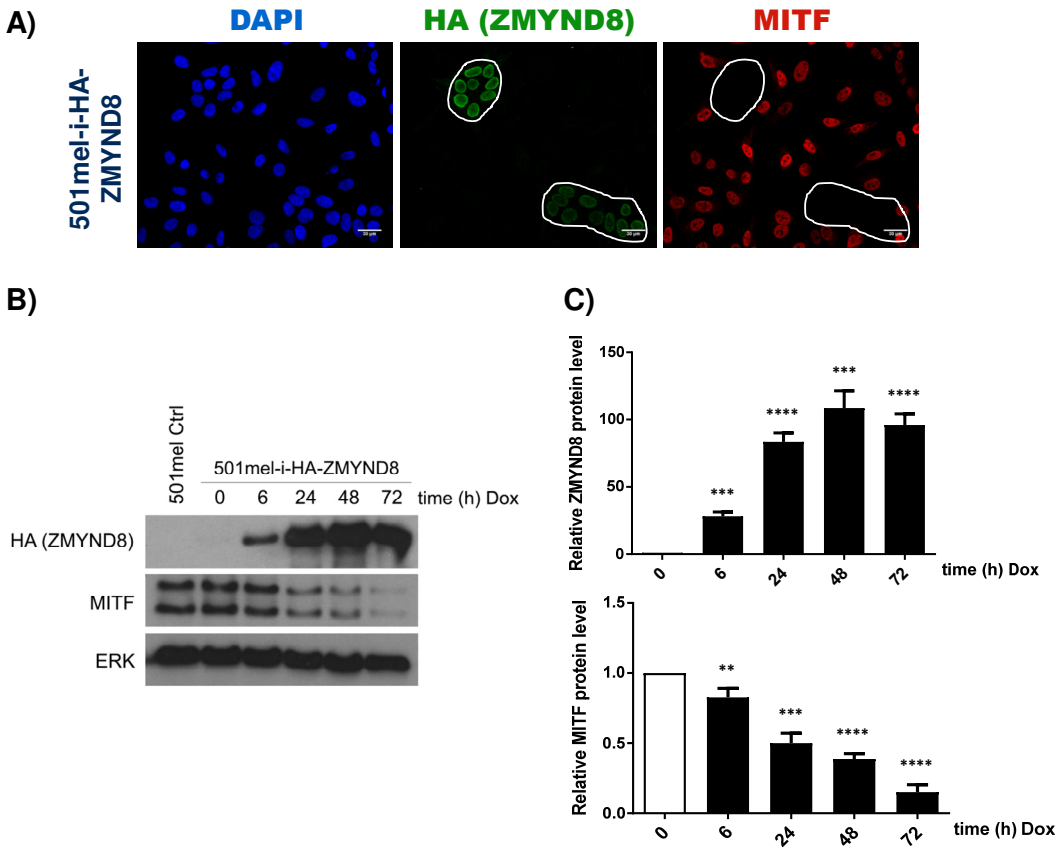


**Figure 3.8.- ZMYND8 overexpression leads to repression of MITF in 501mel cells. (A)** Immunofluorescence analysis of ZMYND8 and MITF in 501mel-i-HA-ZMYND8 (p) cells after 72 h induction with 200 ng/ml doxycycline. 99.0 % ± 0.6 (SEM) of the HA-positive cells were negative for MITF. (n=3, 100 HA-positive cells counted per experiment). (Antibodies: α-HA and α-MITF). HA-positive cells are outlined in white. Scale bars: 30 µm. **(B)** Western blot analysis of whole cell protein extracts from 501mel control and 501mel-i-HA-ZMYND8 (m) cells induced with 200 ng/ml doxycycline for 0, 6, 24, 48 and 72 h. (Antibodies: α-HA, α-MITF and α-ERK). ERK was used as a loading control. **(C)** Quantification of ZMYND8 and MITF protein levels detected in doxycycline-induced and non-induced 501mel-i-HA-ZMYND8 cells in the western blot analysis shown in (B). (**** $P \leq 0.0001$, *** $P \leq 0.001$, ** $P \leq 0.01$, n=3, data represent mean ± SEM).

The repression of MITF by ZMYND8 does not support the hypothesis that ZMYND8 potentially recruits NuRD to mediate transcriptional activation of *MITF.* Instead, the results may mean that ZMYND8 and NuRD regulate MITF expression through independent mechanisms. However, it is also possible that the interaction with ZMYND8 or its recruitment of additional factors might affect NuRD composition and/or function to alter the regulation of MITF by NuRD.

### 3.3.3. – ZMYND8 repression of MITF is specific and is reflected in the subsequent downregulation of MITF downstream targets

The effect of ZMYND8 on MITF could either be specific, or reflect a generalised repression of gene expression. To verify the specificity of the repression of MITF by ZMYND8, the levels of TFEB, an MITF-related transcription factor, were also studied by immunofluorescence in doxycycline-induced 501mel-i-HA-ZMYND8 (p) cells. In contrast to the repression observed on MITF (see above), no changes were observed in TFEB levels in those cells overexpressing ZMYND8 (**Figure 3.9**), indicating that the repressive effect of ZMYND8 on MITF does not reflect a generalised effect on gene regulation.




**Figure 3.9.- ZMYND8 overexpression does not change TFEB levels in 501mel cells.** Immunofluorescence analysis of ZMYND8 and TFEB in 501mel-i-HA-ZMYND8 (p) cells after 72 h induction with 200 ng/ml doxycycline. (Antibodies: α-HA and α-TFEB). HA-positive cells are outlined in white. Scale bars: 30 µm.

To confirm that the repression of MITF by ZMYND8 results in alteration of the expression of MITF target genes, the levels of Tyrosinase and MelanA, two MITF

downstream targets, were studied by immunofluorescence in doxycycline-induced 501mel-i-HA-ZMYND8 (p) cells. No expression of Tyrosinase or MelanA was detected in ZMYND8-overexpressing cells (**Figure 3.10**), confirming that the repression of MITF by ZMYND8 is reflected in the subsequent downregulation of its downstream targets.

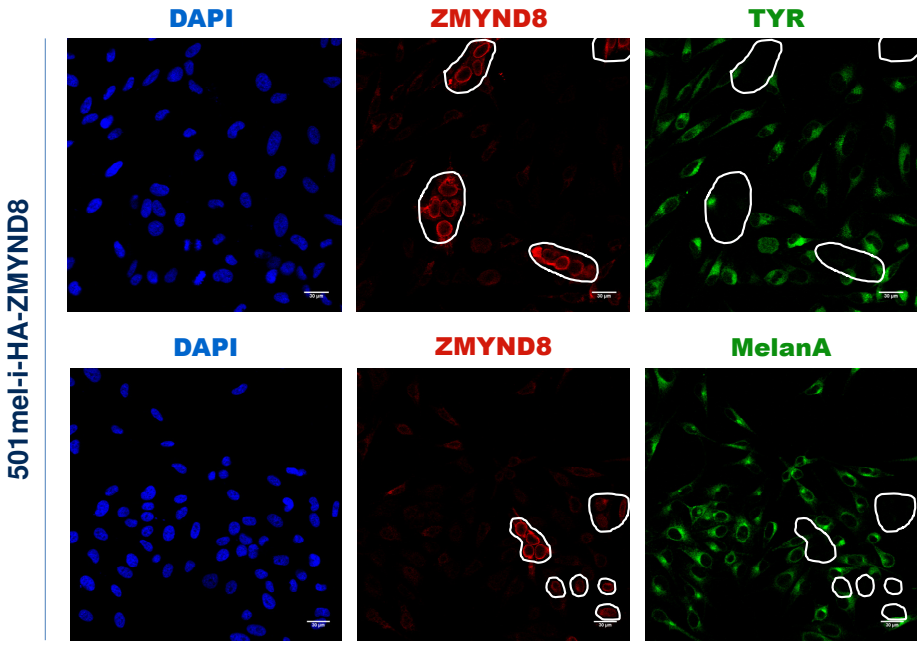


**Figure 3.10.- ZMYND8 overexpression leads to downregulation of Tyrosinase and MelanA levels in 501mel cells.** Immunofluorescence analysis of ZMYND8, Tyrosinase (TYR) and MelanA in 501mel-i-HA-ZMYND8 (p) cells after 72 h induction with 200 ng/ml doxycycline. (Antibodies: α-ZMYND8, α-Tyrosinase and α-MelanA). ZMYND8-positive cells are outlined in white. Scale bars: 30 µm.

### 3.3.4. – The effect of ZMYND8 on MITF expression involves regulation of transcription

Since the experiments outlined above rely on the detection of MITF protein, it was possible that ZMYND8 was operating either to regulate MITF mRNA expression or MITF protein levels in a transcription-independent fashion. The effect of ZMYND8 on MITF mRNA expression was therefore examined.

Following treatment of 501mel-i-HA-ZMYND8 (m) cells with 100 ng/ml doxycycline for 0, 6, 12, 24, 48 and 72 h, a qRT-PCR analysis was carried out. While ZMYND8 mRNA levels increased upon induction with doxycycline, MITF mRNA levels were decreased around 4-fold

after 72 h induction of ZMYND8 (**Figure 3.11**). Since no effect was observed for doxycycline-treated 501mel compared to 501mel control cells in an equivalent experiment (**Supplementary Figure A.2**), we can conclude that the repression of MITF mRNA observed can be attributed to ZMYND8.

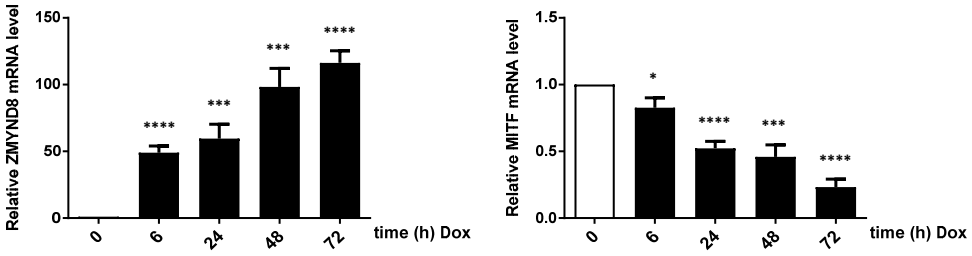


**Figure 3.11.- MITF mRNA levels decrease upon ZMYND8 overexpression in 501mel cells.** qRT-PCR analysis results for ZMYND8 and MITF mRNA levels in 501mel-i-HA-ZMYND8 (m) cells induced with 100 ng/ml doxycycline for 0, 6, 12, 24, 48 and 72 h. (**** $P \leq 0.0001$, *** $P \leq 0.001$, * $P \leq 0.05$, n=3, data represent mean ± SEM).

### 3.3.5. – Silencing of ZMYND8 does not change MITF protein levels

To study the potential effect of endogenous ZMYND8 in the regulation of MITF, a small interfering RNA (siRNA) was used to silence ZMYND8 in 501mel cells. Subsequent western blot analysis showed no changes in MITF protein levels upon silencing of ZMYND8 (**Figure 3.12**).

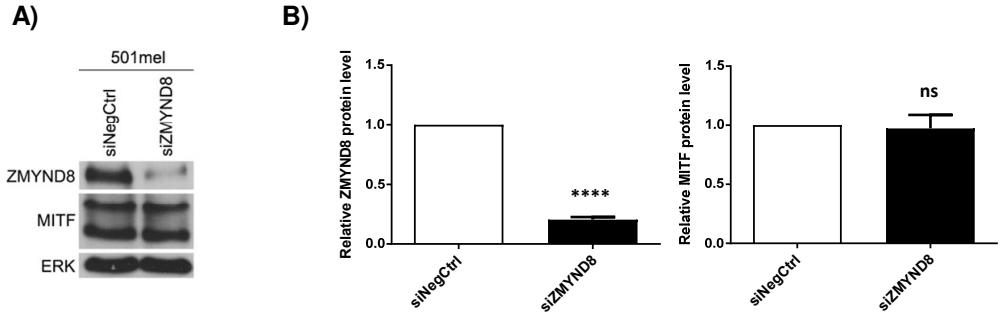


**Figure 3.12.- MITF levels do not change upon silencing of ZMYND8 in 501mel cells. (A)** Western blot analysis of whole cell protein extracts from 501mel cells upon 48 h silencing of ZMYND8. (Antibodies: α-ZMYND8, α-MITF and α-ERK). ERK was used as a loading control. **(B)** Quantification of ZMYND8 and MITF protein levels detected in the western blot analysis shown in (A). (**** $P \leq 0.0001$, ns $P > 0.05$, n=3, data represent mean ± SEM).

The strong repression of MITF upon ZMYND8 overexpression, but absence of effect on MITF upon silencing of ZMYND8, may suggest a role of the bromodomain protein as a repressor of MITF that exerts its function only when levels are increased in response to a stimulus.

However, the lack of an effect of silencing ZMYND8 on MITF expression presumably rules out the possibility of ZMYND8 being a cofactor of NuRD targeting the complex to the *MITF* promoter for the activation of *MITF* expression, unless the extremely low expression of ZMYND8 that remains following siRNA treatment is enough to exert this function.

### 3.3.6. – ZMYND8 overexpression leads to upregulation of N-Cadherin, a feature of invasiveness, but reduces cell migration

Since ZMYND8 overexpression results in downregulation of MITF and low MITF levels associate with an invasive phenotype, levels of N-Cadherin (a marker of invasiveness) upon induction of ZMYND8 expression in 501mel-i-HA-ZMYND8 (m) cells were determined.

An increase in the levels of N-Cadherin was observed when treating 501mel-i-HA-ZMYND8 (m) cells with 200 ng/ml doxycycline for 48 or 72 h (**Figure 3.13**), suggesting that ZMYND8 overexpression may produce an invasive phenotype in 501mel cells.

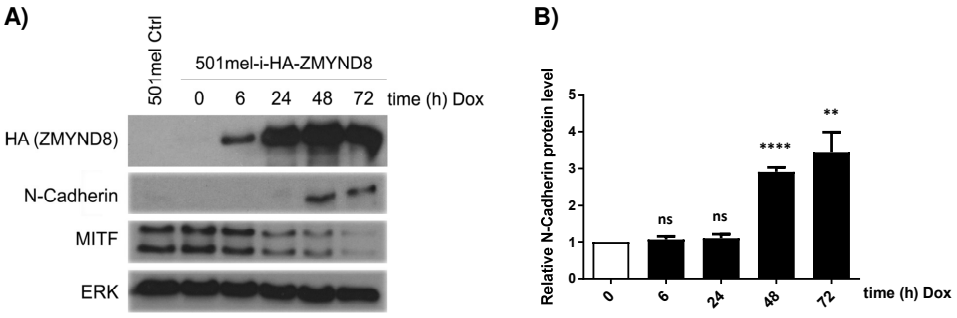


**Figure 3.13.- ZMNYD8 overexpression leads to upregulation of N-Cadherin in 501mel cells. (A)** Western blot analysis of whole cell protein extracts from 501mel control and 501mel-i-HA-ZMYND8 (m) cells upon 0, 6, 24, 48 and 72 h induction of ZMYND8 expression with 200 ng/ml doxycycline. (Antibodies: α-HA, α-N-Cadherin, α-MITF and α-ERK). ERK was used as a loading control. **(B)** Quantification of N-Cadherin levels detected in doxycycline-induced 501mel-i-HA-ZMYND8 (m) cells in the western blot analysis shown in (A). (**** $P \leq 0.0001$, ** $P \leq 0.01$, ns $P > 0.05$, n=3, data represent mean ± SEM).

However, a scratch-wound healing assay performed in non-induced and doxycycline-induced 501mel-i-HA-ZMYND8 (m) cells did not show an increase in cell migration resulting from ZMYND8 overexpression (**Figure 3.14**). No effect on cell migration was observed for doxycycline-treated 501mel compared to 501mel control cells in an equivalent experiment (**Supplementary Figure A.3**), indicating that the effect is dependent on ZMYND8 expression.

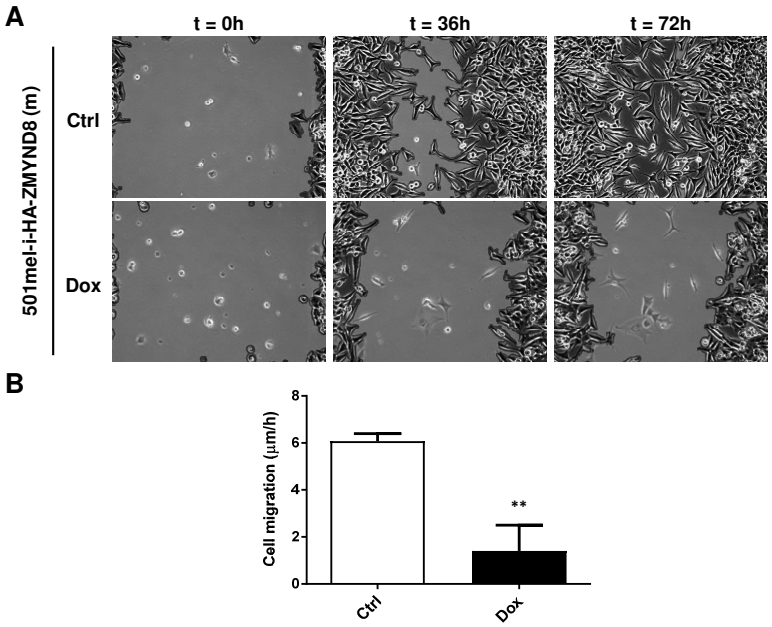


**Figure 3.14.- ZMNYD8 overexpression reduces cell migration in 501mel cells. (A)** Brightfield microscopy images showing the 0, 36 and 72 h time points of a scratch-wound healing assay performed in 501mel-i-HA-ZMYND8 (m) cells non-induced and induced with 100 ng/ml doxycycline. **(B)** Quantification of cell migration corresponding to the experiment showed in (A). (** $P \leq 0.01$, n=3, data represent mean ± SEM).

Would healing in the scratch wound assay depends on a contribution of cell proliferation and cell migration. The fact that ZMYND8-overexpressing 501mel cells actually showed less wound healing than the control cells could arise either from a change on cell migration, or perhaps more likely from a strong effect on proliferation in this experiment. Since low MITF is associated with cell cycle arrest, a reduction in the proliferation of doxycycline-induced 501mel-i-HA-ZMYND8 (m) cells likely underlies the reduction in their wound healing capacity.

To examine the effect of ZMYND8 overexpression in cell cycle, 501mel-i-HA-ZMYND8 (m) cells were treated with 100 ng/ml doxycycline for induction of ZMYND8 and a subsequent analysis of the cell cycle profile was performed by flow cytometry following staining with propidium iodide.

The results showed an increase in the percentage of cells in G1-phase and a decrease in S-phase upon induction with doxycycline (**Figure 3.15**), indicating that ZMYND8 induces cell cycle arrest in 501mel cells. No effect on the cell cycle profile was observed for doxycycline-treated 501mel compared to 501mel control cells in an equivalent experiment (**Supplementary Figure A.4**).

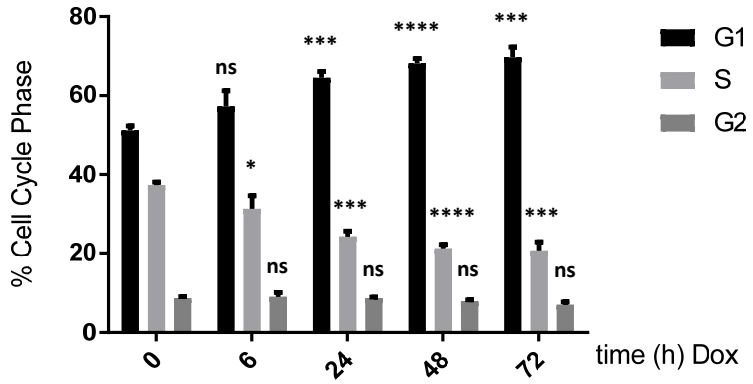


**Figure 3.15.- ZMNYD8 overexpression induces G1 cell cycle arrest in 501mel cells.** Cell cycle profiles of 501mel-i-HA-ZMYND8 (m) cells induced with 100 ng/ml doxycycline for 0, 6, 24, 48 and 72 h. (**** $P \leq 0.0001$, *** $P \leq 0.001$, * $P \leq 0.05$, ns $P > 0.05$, n=3, data represent mean ± SEM).

Finally, to confirm the reduction in proliferation of ZMYND8-overexpressing cells, 501mel-i-HA-ZMYND8 cells were plated in triplicate at the same cell density and treated with 100 ng/ml doxycycline or kept as controls. Cell numbers were then counted at 24, 48 and 72 h.

As expected, a statistically significant reduction in the proliferation rate of ZMYND8-overexpressing cells was detected at 72 h of induction (**Figure 3.16**). No effect on proliferation was observed in doxycycline-treated 501mel compared to 501mel control cells in an equivalent experiment (**Supplementary Figure A.5**).

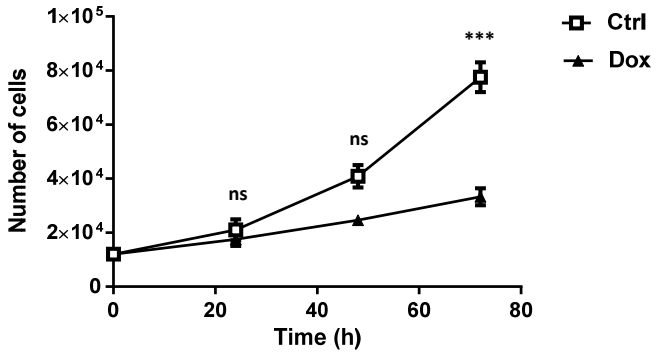


**Figure 3.16.- ZMNYD8 overexpression reduces proliferation rates in 501mel cells.** Proliferation curves for non-induced and 100 ng/ml doxycycline-induced 501mel-i-HA-ZMYND8 (m) cells. (** $P \leq 0.01$, n=3, data represent mean ± SEM).

We therefore concluded that the reduction in wound healing observed when overexpressing ZMYND8 in 501mel cells is most likely due to the concomitant reduction in cell proliferation. Consequently, further research will be needed to uncover if ZMYND8 overexpression, which we show here leads to upregulation of N-Cadherin, a marker of invasiveness, actually has an effect on cell migration / invasion.

### 3.3.7. – Mutant ZMYND8 constructs maintain the ability to repress MITF

To investigate the requirement of different protein domains for ZMYND8 repression of MITF, several truncation mutants of the bromodomain protein were generated (**Figure 3.17**).

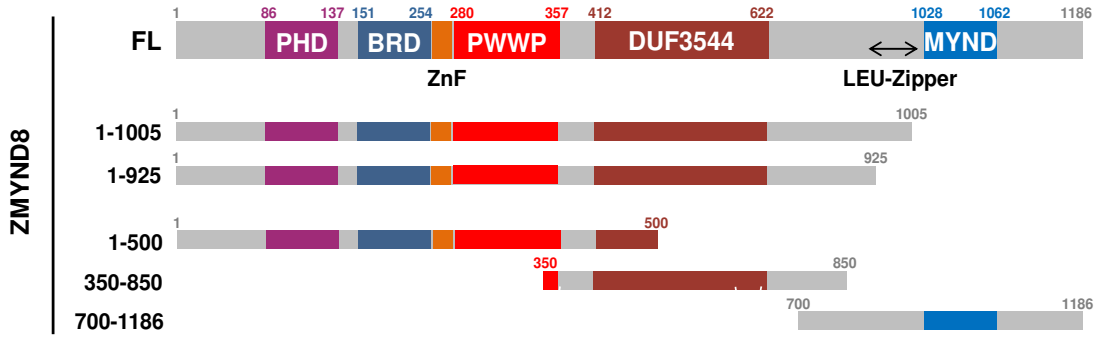


**Figure 3.17.- ZMYND8 constructs used in this study.** Full length (FL) ZMYND8 and mutant ZMYND8 constructs generated for this study. Numbers indicate amino acid positions.

The new full length (FL) and mutant ZMYND8 constructs were first cloned into a mammalian expression vector and transfected into 501mel cells to confirm their expression and determine their effects on MITF expression.

Immunofluorescence analysis performed 48 h after transfection confirmed the expression of all constructs and showed the expected suppression of MITF expression in most cells successfully transfected with $ZMYND8^{FL}$ (**Figure 3.18**). However, a notable reduction in the percentage of $ZMYND8^{FL}$-positive cells with associated MITF negative staining was observed compared to previous analogous experiments (see section 3.3.1). This might be due to the use of a different mammalian expression vector, which might result in a distinct level of expression of the constructs consequently leading to slightly different results. Alternatively, it could reveal a previously unsuspected cell cycle-dependent effect of ZMYND8 overexpression on MITF, in which repression might occur only at a specific phase in the cell cycle.

Even more strikingly, this analysis unexpectedly showed repression of MITF for most cells successfully transfected with $ZMYND8^{1-1005}$ or $ZMYND8^{1-925}$, and above half of the cells successfully transfected with $ZMYND8^{1-500}$, $ZMYND8^{350-850}$ or $ZMYND8^{700-1186}$ (**Figure 3.18**).

The repression of MITF observed after transfection with $ZMYND8^{1-1005}$, which lacks the protein's MYND domain, and the repression observed following transient expression of $ZMYND8^{1-925}$, which lacks both the MYND and LEU-Zipper domains, led us to think that both the DNA binding domain and MYND domain (considered to mediate protein-protein interactions) of ZMNYD8 are dispensable for its ability to repress MITF.

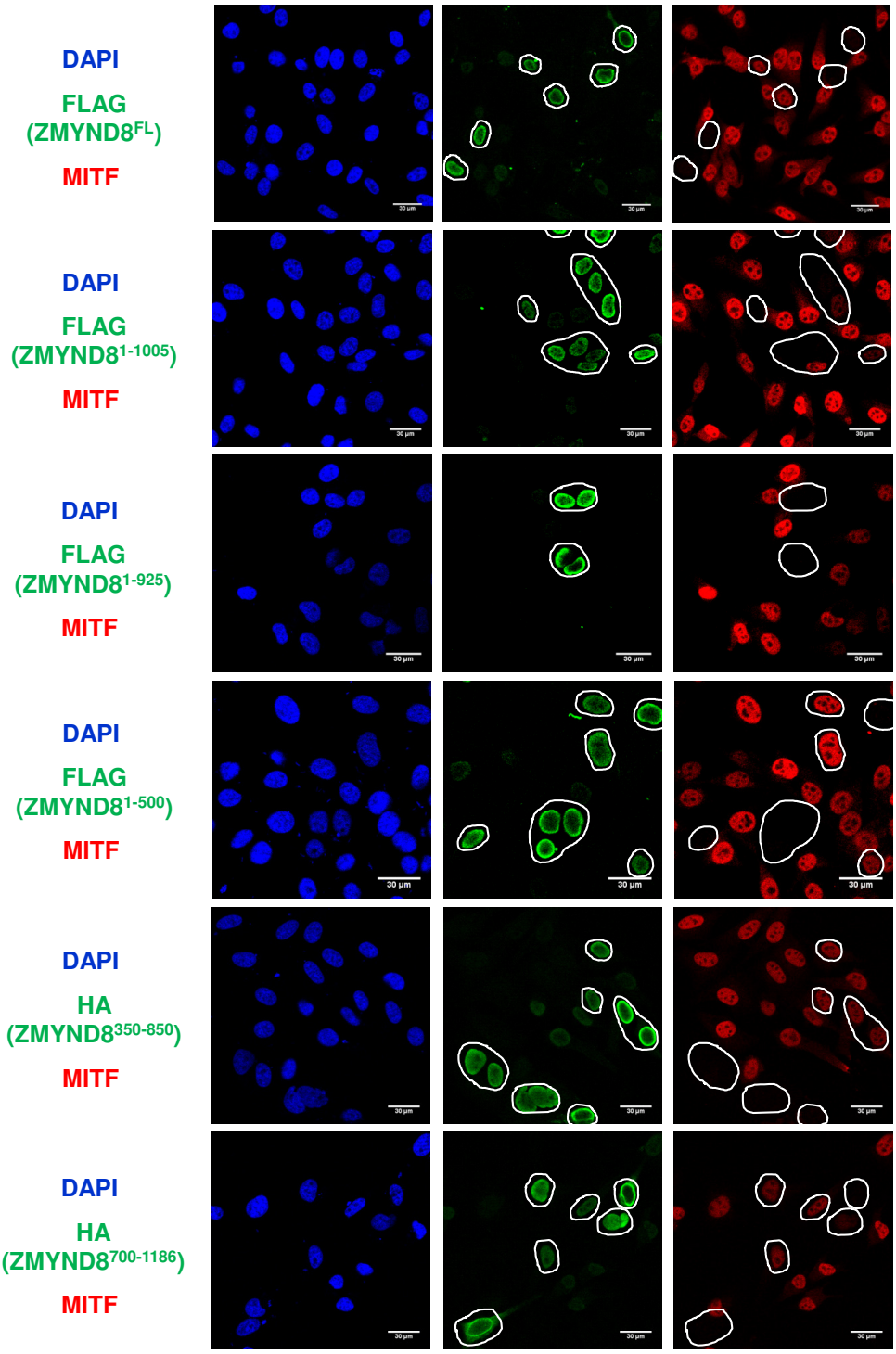


**Figure 3.18.- Overexpression of mutant ZMYND8 constructs can repress MITF in 501mel cells.** Immunofluorescence analysis of ZMYND8 and MITF after 48 h transient expression of ZMYND8$^{FL}$, ZMYND8$^{1-1005}$, ZMYND8$^{1-925}$, ZMYND8$^{1-500}$, ZMYND8$^{350-850}$ and ZMYND8$^{700-1186}$ in 501mel cells. 75.2% ± 3.4 (SEM), 71.4% ± 7.9 (SEM), 77.1% ± 4.6 (SEM), 64.3% ± 6.2 (SEM), 52.9% ± 8.9 (SEM) and 58.6% ± 8.7(SEM) of the FLAG/HA-positive cells were negative for MITF in the transfections with ZMYND8$^{FL}$, ZMYND8$^{1-1005}$, ZMYND8$^{1-925}$, ZMYND8$^{1-500}$, ZMYND8$^{350-850}$ and ZMYND8$^{700-1186}$, respectively. (n=3, 70 FLAG/HA-positive cells counted per experiment). (Antibodies: α-FLAG, α-HA and α-MITF). FLAG/HA-positive cells are outlined in white. Scale bars: 30 µm.

However, the repression of MITF observed when overexpressing the ZMYND8$^{1-500}$, ZMYND8$^{350-850}$ and ZMYND8$^{700-1186}$ fragments, which account for relatively small portions of the protein with little overlap among them, led us to suspect a non-specific stress response triggered by the overexpression of the constructs underlying the mechanism of repression of MITF.

While no confirmation was obtained for this potential non-specific stress response following full length or mutant ZMYND8 overexpression, the absence of a specific domain of ZMYND8 required for repression of MITF expression would fit with the lack of an effect on MITF expression observed when silencing ZMYND8 (section 3.3.5). Further research will therefore be needed to definitively dismiss, or establish a specific role of ZMYND8 in the regulation of MITF.

## 3.4. – Investigating the potential role of the NuRD complex in the regulation of MITF

The identification of the requirement of the CHD4, p66α and p66β subunits of the NuRD complex for the expression of MITF, and the presence of a p66β peak in the MITF promoter identified in a p66β ChIP-seq analysis (preliminary data, section 3.2.2), led us to study further the potential role of the NuRD complex in the regulation of MITF expression.

To verify the robustness of the preliminary data, a series of experiments were first performed to confirm the conclusions reached from the previous investigation.

### 3.4.1. – p66β seems to be essential for MITF expression

To confirm the requirement of the p66β subunit of the NuRD complex for MITF expression, p66β was knocked-down in 501mel cells using the same siRNA against p66β used for the generation of the preliminary data (sip66β(I)).

Analysis of p66β and MITF levels in 501mel cells 72 h after transfection with sip66β(I) or siRNA negative control showed highly efficient silencing of p66β and consequently almost complete abolishment of MITF expression in sip66β(I) transfected cells, as determined by immunofluorescence (**Figure 3.19.A** and **B**) and western blot (**Figure 3.19.C** and **D**).

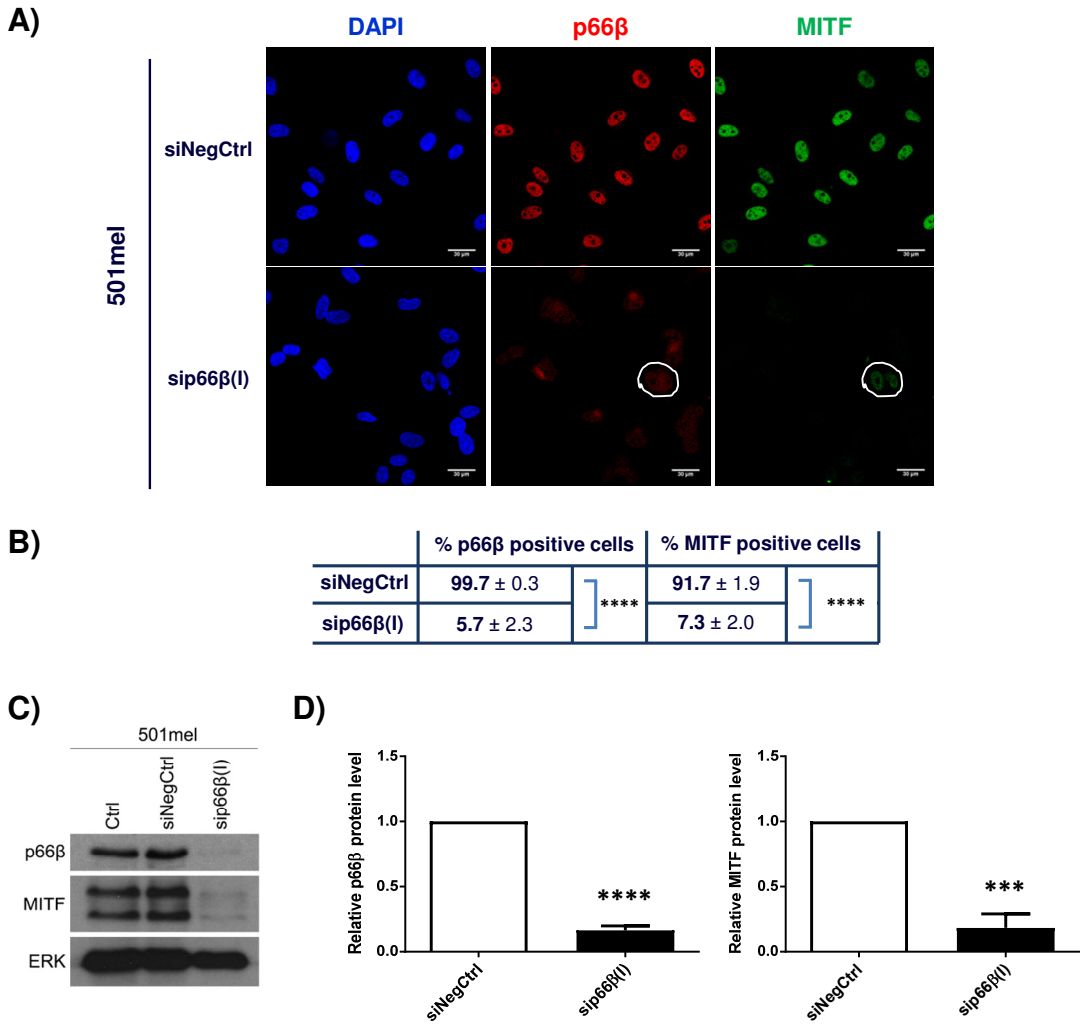


**Figure 3.19.- p66β silencing (using sip66β(I)) leads to strong downregulation of MITF protein levels in 501mel cells. (A)** Immunofluorescence analysis of p66β and MITF in 501mel cells 72 h after transfection with sip66β(I) or siRNA negative control. (Antibodies: α-p66β and α-MITF). For the sip66β condition, the few cells that maintain p66β expression are outlined in white. Scale bars: 30 µm. **(B)** Quantification of p66β-positive and MITF-positive cells in the immunofluorescence analysis shown in (A). (**** $P \leq 0.0001$, n=3, 200 cells counted per experiment, data represent mean ± SEM). **(C)** Western blot analysis of whole cell protein extracts from 501mel control cells and 501mel cells 72 h after transfection with sip66β(I) or siRNA negative control. (Antibodies: α-p66β, α-MITF and α-ERK). ERK was used as a loading control. **(D)** Quantification of p66β and MITF levels in 501mel cells 72 h after transfection with sip66β(I) or siRNA negative control detected in the western blot analysis shown in (C). (**** $P \leq 0.0001$, *** $P \leq 0.001$, n=3, data represent mean ± SEM).

The analysis of p66β and MITF mRNA levels in 501mel cells 72 h after transfection with sip66β(I) or siRNA negative control by qRT-PCR further demonstrated the efficient silencing of p66β and strong downregulation of MITF mRNA expression resulting from transfection of the p66β siRNA, indicating that the underlying mechanism at least partly involves transcriptional regulation (**Figure 3.20**).

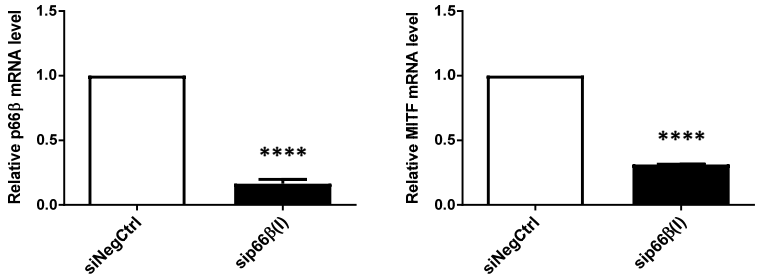


**Figure 3.20.- MITF mRNA levels decrease upon p66β silencing (using sip66β(I)) in 501mel cells.** qRT-PCR analysis results for p66β and MITF mRNA levels in 501mel cells 72 h after transfection with sip66β(I) or siRNA negative control. (**** $P \leq 0.0001$, n=3, data represent mean ± SEM).

To rule out a dependency on the melanoma cell line used for the effect on MITF expression when silencing p66β, the same experiments were also performed in SKmel28 cells.

Analysis of p66β and MITF levels in SKmel28 cells 72 h after transfection with sip66β(I) or siRNA negative control also showed highly efficient silencing of p66β and consequently a strong reduction in MITF expression in sip66β(I) transfected cells, as determined by immunofluorescence (**Figure 3.21.A** and **B**) and western blot (**Figure 3.21.C** and **D**).

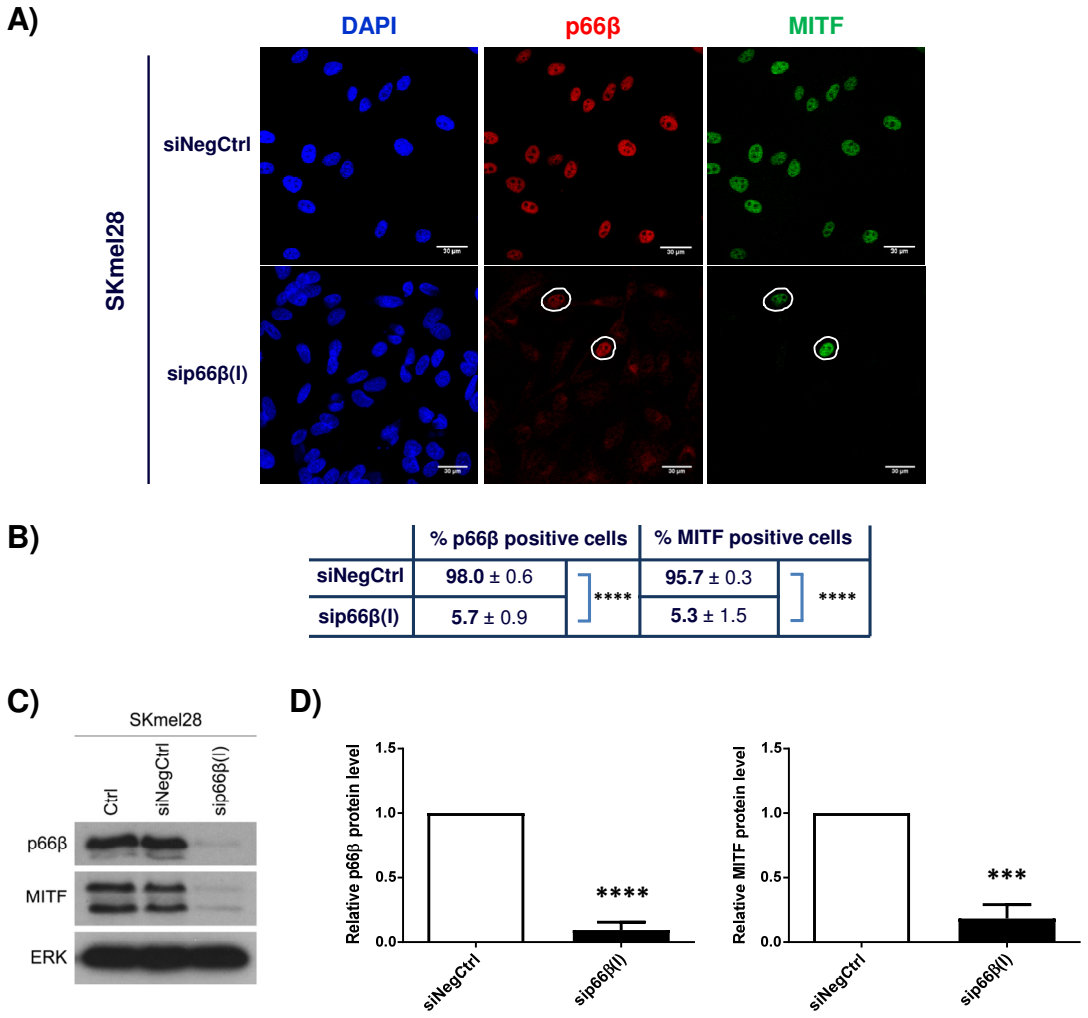


**Figure 3.21.- p66β silencing (using sip66β(I)) leads to strong downregulation of MITF protein levels in SKmel28 cells. (A)** Immunofluorescence analysis of p66β and MITF in SKmel28 cells 72 h after transfection with sip66β(I) or siRNA negative control. (Antibodies: α-p66β and α-MITF). For the sip66β condition, the few cells that maintain p66β expression are outlined in white. Scale bars: 30 µm. **(B)** Quantification of p66β-positive and MITF-positive cells in the immunofluorescence analysis shown in (A). (**** $P \leq 0.0001$, n=3, 200 cells counted per experiment, data represent mean ± SEM). **(C)** Western blot analysis of whole cell protein extracts from SKmel28 control cells and SKmel28 cells 72 h after transfection with sip66β(I) or siRNA negative control. (Antibodies: α-p66β, α-MITF and α-ERK). ERK was used as a loading control. **(D)** Quantification of p66β and MITF levels in SKmel28 cells 72 h after transfection with sip66β(I) or siRNA negative control detected in the western blot analysis shown in (C). (**** $P \leq 0.0001$, *** $P \leq 0.001$, n=3, data represent mean ± SEM).

Finally, the analysis of p66β and MITF mRNA levels in SKmel28 cells 72 h after transfection with sip66β(I) or siRNA negative control by qRT-PCR also showed efficient silencing of p66β and strong downregulation of MITF resulting from p66β knock-down (**Figure 3.22**).

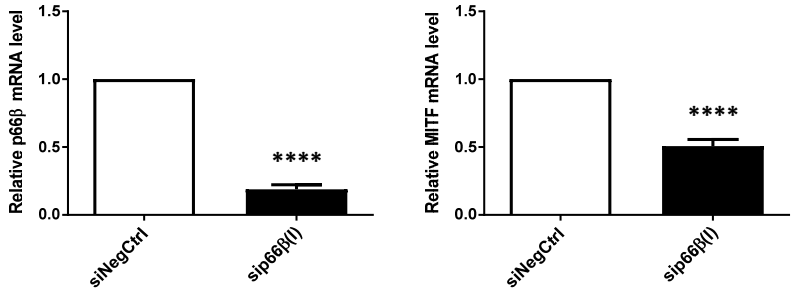


**Figure 3.22.- MITF mRNA levels decrease upon p66β silencing (using sip66β(I)) in SKmel28 cells.** qRT-PCR analysis results for p66β and MITF mRNA levels in SKmel28 cells 72 h after transfection with sip66β(I) or siRNA negative control. (**** $P \leq 0.0001$, n=3, data represent mean ± SEM).

### 3.4.2. – p66α seems to be essential for MITF expression

To confirm that the p66α subunit of the NuRD complex was also implicated in controlling MITF expression, p66α was knocked-down in 501mel cells using the same siRNA against p66α used for the generation of the preliminary data (sip66α(I)).

Analysis of p66α and MITF levels in 501mel cells 72 h after transfection with sip66α(I) or siRNA negative control showed highly efficient silencing of p66α and consequently a significant reduction in MITF expression in sip66α(I) transfected cells, as determined by immunofluorescence (**Figures 3.23.A** and **B**) and western blot (**Figures 3.23.C** and **D**).

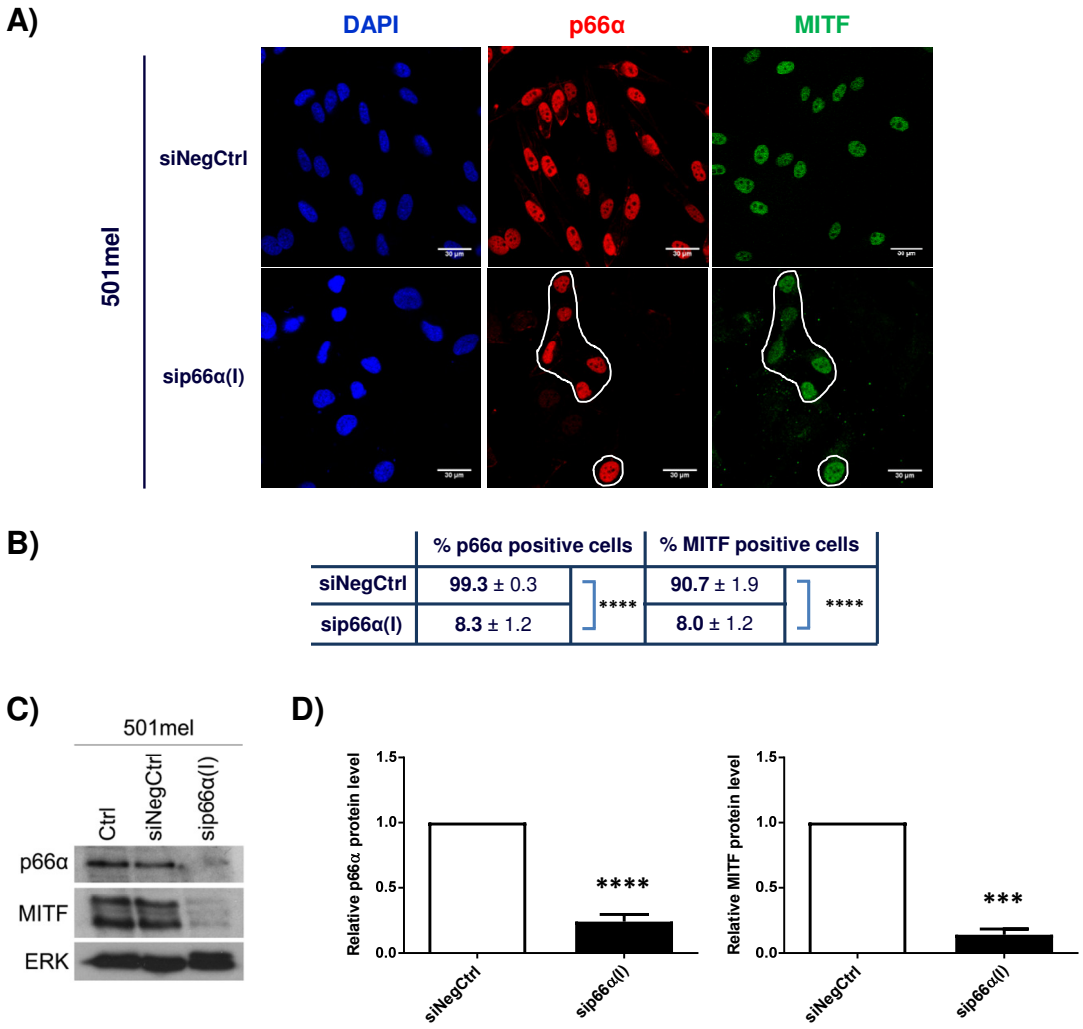


**Figure 3.23.- p66α silencing (using sip66α(I)) leads to strong downregulation of MITF protein levels in 501mel cells. (A)** Immunofluorescence analysis of p66α and MITF in 501mel cells 72 h after transfection with sip66α(I) or siRNA negative control. (Antibodies: α-p66α and α-MITF). For the sip66α condition, the few cells that maintain p66α expression are outlined in white. Scale bars: 30 µm. **(B)** Quantification of p66α-positive and MITF-positive cells in the immunofluorescence analysis shown in (A). (**** $P \leq 0.0001$, n=3, 200 cells counted per experiment, data represent mean ± SEM). **(C)** Western blot analysis of whole cell protein extracts from 501mel control cells and 501mel cells 72 h after transfection with sip66α(I) or siRNA negative control. (Antibodies: α-p66α, α-MITF and α-ERK). ERK was used as a loading control. **(D)** Quantification of p66α and MITF levels in 501mel cells 72 h after transfection with sip66α(I) or siRNA negative control detected in the western blot analysis shown in (C). (**** $P \leq 0.0001$, *** $P \leq 0.001$, n=3, data represent mean ± SEM).

The analysis of p66α and MITF mRNA levels in 501mel cells 72 h after transfection with sip66α(I) or siRNA negative control by qRT-PCR further demonstrated the efficient silencing of p66α and strong downregulation of MITF resulting from p66α knock-down and indicated

that the underlying mechanism at least partly involves transcriptional regulation (**Figure 3.24**).

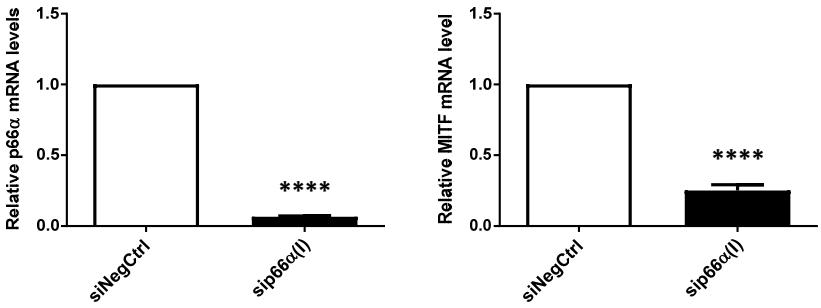


**Figure 3.24.- MITF mRNA levels decrease upon p66α silencing (using sip66α(I)) in 501mel cells.** qRT-PCR analysis results for p66α and MITF mRNA levels in 501mel cells 72 h after transfection with sip66α(I) or siRNA negative control. (**** $P \leq 0.0001$, n=3, data represent mean ± SEM).

### 3.4.3. – CHD4 is not required for MITF expression

To confirm the requirement for the CHD4 subunit of the NuRD complex for MITF expression, CHD4 was knocked-down in 501mel cells using the same siRNA against CHD4 used for the generation of the preliminary data (siCHD4).

Analysis of CHD4 and MITF levels in 501mel cells 72 h after transfection with siCHD4 or siRNA negative control showed highly efficient silencing of CHD4 but, unexpectedly, no changes in MITF protein levels, as determined by immunofluorescence (**Figure 3.25.A** and **B**) and western blot (**Figure 3.25.C** and **D**).

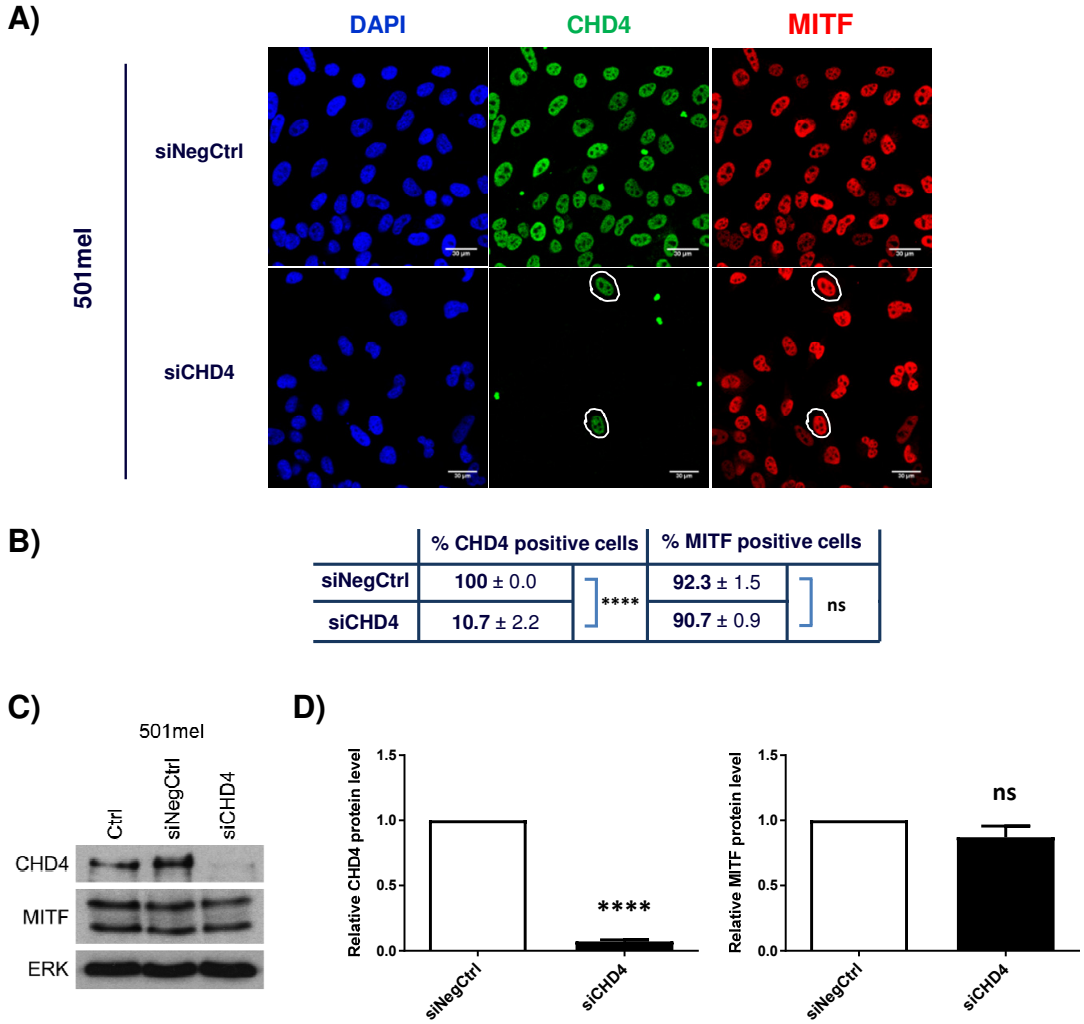


**Figure 3.25.- CHD4 silencing does not affect MITF protein levels in 501mel cells. (A)** Immunofluorescence analysis of CHD4 and MITF in 501mel cells 72 h after transfection with siCHD4 or siRNA negative control. (Antibodies: α-CHD4 and α-MITF). For the siCHD4 condition, the few cells that maintain CHD4 expression are outlined in white. Scale bars: 30 µm. **(B)** Quantification of CHD4-positive and MITF-positive cells in the immunofluorescence analysis shown in (A). (**** $P \leq 0.0001$, ns $P > 0.05$, n=3, 200 cells counted per experiment, data represent mean ± SEM). **(C)** Western blot analysis of whole cell protein extracts from 501mel control cells and 501mel cells 72 h after transfection with CHD4 or siRNA negative control. (Antibodies: α-CHD4, α-MITF and α-ERK). ERK was used as a loading control. **(D)** Quantification of CHD4 and MITF levels in 501mel cells 72 h after transfection with siCHD4 or siRNA negative control detected in the western blot analysis shown in (C). (**** $P \leq 0.0001$, ns $P > 0.05$, n=3, data represent mean ± SEM).

To rule out that the failure of CHD4 silencing to affect MITF expression arose because of a cell line-specific effect, the experiments and analyses just described for 501mel cells were also performed in the SKmel28 cell line.

Analysis of CHD4 and MITF levels in SKmel28 cells 72 h after transfection with siCHD4 or siRNA negative control also confirmed highly efficient silencing of CHD4 in those cells

transfected with siCHD4 but, as observed for 501mel, no changes in MITF protein levels were detected as determined by immunofluorescence (**Figure 3.26.A** and **B**) and western blot (**Figure 3.26.C** and **D**). We therefore concluded that the CHD4 subunit of the NuRD complex is not required for MITF expression.

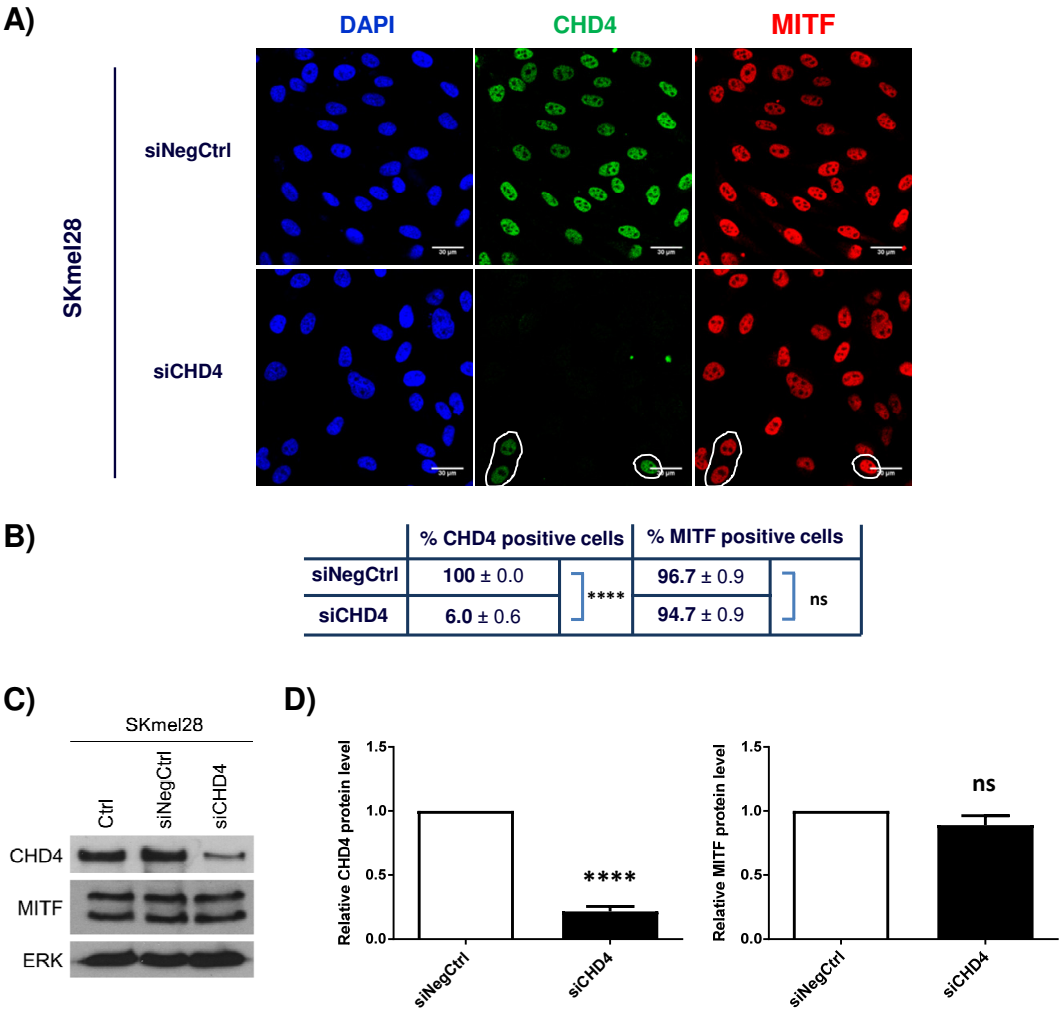


**Figure 3.26.- CHD4 silencing does not affect MITF protein levels in SKmel28 cells. (A)** Immunofluorescence analysis of CHD4 and MITF in SKmel28 cells 72 h after transfection with siCHD4 or siRNA negative control. (Antibodies: α-CHD4 and α-MITF). For the siCHD4 condition, the few cells that maintain CHD4 expression are outlined in white. Scale bars: 30 µm. **(B)** Quantification of CHD4-positive and MITF-positive cells in the immunofluorescence analysis shown in (A). (**** $P \leq 0.0001$, ns $P > 0.05$, n=3, 200 cells counted per experiment, data represent mean ± SEM). **(C)** Western blot analysis of whole cell protein extracts from SKmel28 control cells and SKmel28 cells 72 h after transfection with CHD4 or siRNA negative control. (Antibodies: α-CHD4, α-MITF and α-ERK). ERK was used as a loading control. **(D)** Quantification of CHD4 and MITF levels in SKmel28 cells 72 h after transfection with siCHD4 or siRNA negative control detected in the western blot analysis shown in (C). (**** $P \leq 0.0001$, ns $P > 0.05$, n=3, data represent mean ± SEM).

### 3.4.4. – Exogenous p66β does not rescue MITF expression upon silencing endogenous p66β

The unexpected result showing the absence of an effect of silencing CHD4 on MITF expression led us to question if the requirement of p66β/α is dependent or independent of the NuRD complex.

Before addressing this question, a set of experiments was carried out to further confirm the requirement of p66β for MITF expression.

First, an expression vector encoding an siRNA-resistant form of p66β HA-tagged at the N-terminus was generated. Prevention of knock-down of exogenous p66β was achieved by introducing several silent mutations in the p66β nucleotide sequence targeted by the siRNA against p66β previously used in this study (sip66β(I)) (**Figure 3.27**).

| | |
|---|---|
| **... TATCAACCGCAGTCAAGTTCTTCTGTTCCA ...** | **(p66β original nucleotide sequence)** |
| **... TACCAGCCTCAAAGCTCCAGCAGCGTGCCA ...** | **(Mutated p66β nucleotide sequence)** |
| **... YQPQSSSSVP ...** | **(p66β protein sequence)** |

**Figure 3.27.- Introduction of silent mutations in p66β nucleotide sequence.** Mutated nucleotides are marked in red.

A melanoma cell line derived from 501mel cells was subsequently generated with constitutive stable expression of the N-terminus HA-tagged and mutated p66β (501mel-HA-(siRes)p66β). This polyclonal cell line was then used in a p66β silencing experiment equivalent to those previously performed.

72 h after transfection with sip66β(I) or siRNA negative control, exogenous p66β and MITF levels in 501mel-HA-(siRes)p66β cells were analysed by immunofluorescence (**Figure 3.28**). Regardless of levels of endogenous p66β (which were not determined but assumed to be extremely low in virtually all cells in accordance with the high efficiency of the silencing with sip66β(I) consistently observed in previous experiments), all cells expressing exogenous siRNA-resistant p66β were expected to maintain MITF expression. However, none of the

cells positive for HA-p66β showed MITF staining, indicating that exogenous p66β was not able to rescue MITF expression when silencing endogenous p66β. The very few cells that were positive for MITF were assumed to constitute the small percentage of cells for which the transfection with sip66β(I) was unsuccessful.

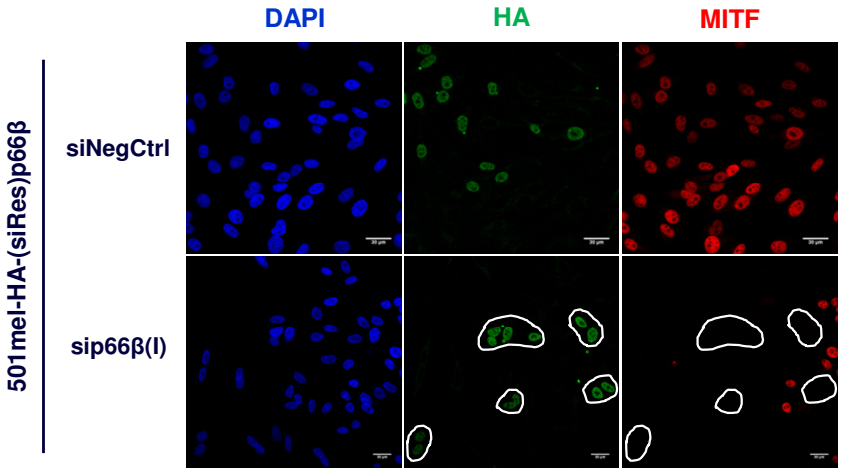


**Figure 3.28.- Exogenous N-terminus HA-tagged p66β does not rescue MITF expression in 501mel cells.** Immunofluorescence analysis of exogenous HA-tagged p66β and MITF in 501mel-HA-(siRes)p66β cells 72 h after transfection with sip66β(I) or siRNA negative control. 100 ± 0.0 (SEM) of the HA-positive cells were negative for MITF. (n=3, 100 HA-positive cells counted per experiment). (Antibodies: α-HA and α-MITF). For the sip66β condition, HA-positive cells are outlined in white. Scale bars: 30 µm.

To rule out a potential impairment of the exogenous p66β function by the N-terminal HA tag, a second melanoma cell line was generated using an equivalent construct for the stable expression of siRNA resistant p66β but harbouring the HA tag at the C-terminus instead. The resulting polyclonal cell line (501mel-(siRes)p66β-HA) was then used for an equivalent experiment to the one described above.

72 h after transfection with sip66β(I) or siRNA negative control, exogenous p66β and MITF levels in 501mel-(siRes)p66β-HA cells were analysed by immunofluorescence (**Figure 3.29**). Similarly to what was observed for 501mel-HA-(siRes)p66β cells, almost all of the HA-positive cells were negative for MITF, meaning that the new exogenous p66β was not able to recue MITF expression either.

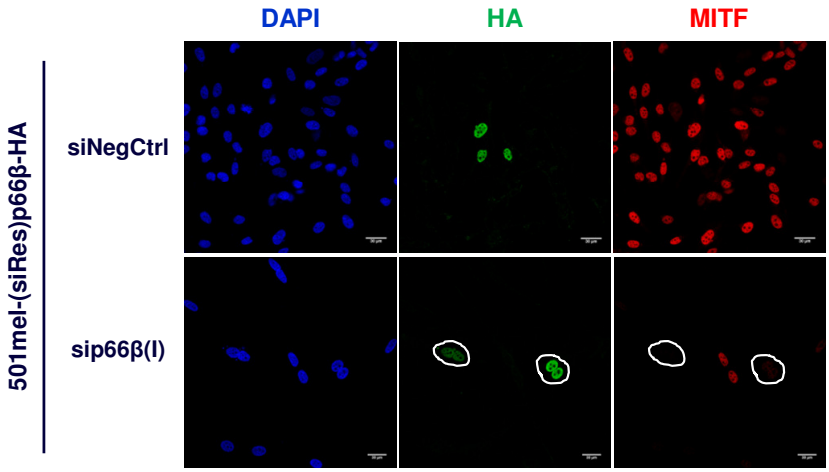


**Figure 3.29.- Exogenous C-terminus HA-tagged p66β does not rescue MITF expression in 501mel cells.** Immunofluorescence analysis of exogenous HA-tagged p66β and MITF in 501mel-(siRes)p66β-HA cells 72 h after transfection with sip66β(I) or siRNA negative control. 98.6 ± 0.8 (SEM) of the HA-positive cells were negative for MITF. (n=3, 100 HA-positive cells counted per experiment). (Antibodies: α-HA and α-MITF). For the sip66β condition, HA-positive cells are outlined in white. Scale bars: 30 μm.

### 3.4.5. – p66β is not required for MITF expression

The inability of exogenous p66β to prevent repression of MITF when silencing endogenous p66β led us to suspect the potential presence of off-target effects in the system used for the silencing of endogenous p66β leading to repression of MITF. This possibility seemed unlikely due to the fact that silencing p66α, encoded by a different gene, using a completely unrelated siRNA also resulted in the shutdown of MITF expression. Nevertheless, two additional siRNAs against p66β (sip66β(II) and sip66β(III)) were obtained and used in a silencing experiment equivalent to those previously performed.

Analysis of p66β and MITF levels in 501mel cells 72 h after transfection with sip66β(II), sip66β(III) or siRNA negative control showed highly efficient silencing of p66β in those cells transfected with sip66β(II) or sip66β(III) but no changes in MITF protein levels, as determined by immunofluorescence (**Figure 3.30.A** and **B**) and western blot (**Figure 3.30.C** and **D**).

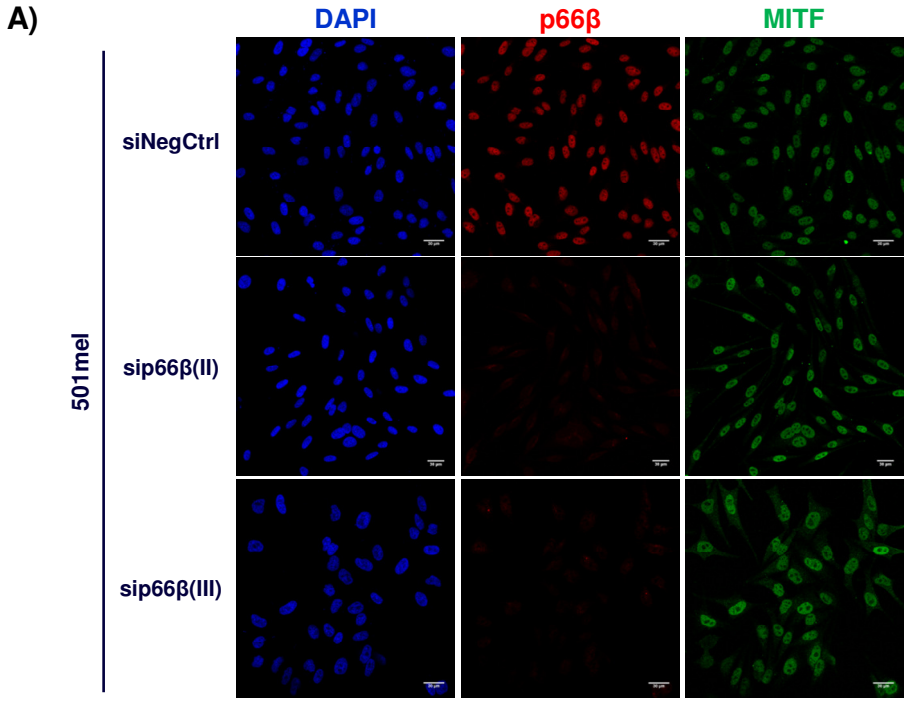


B)

| | % p66β positive cells | % MITF positive cells |
|---|---|---|
| siNegCtrl | **99.3** ± 0.3 | **92.7** ± 0.9 |
| sip66β(II) | **0.0** ± 0.0 **** | **95.3** ± 0.9 ns |
| sip66β(III) | **0.3** ± 0.3 **** | **92.7** ± 1.2 ns |

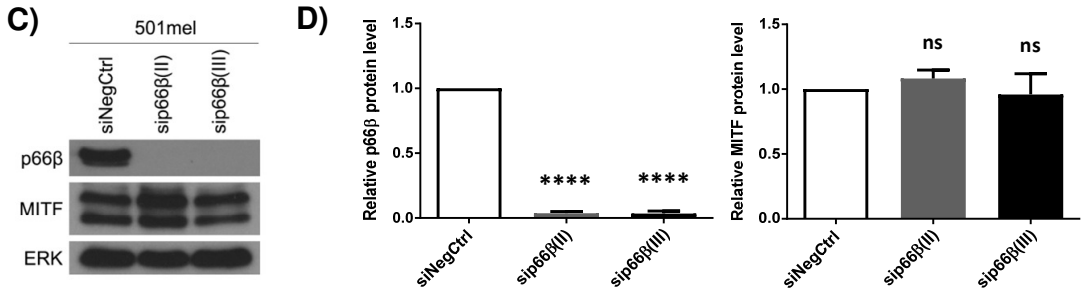


**Figure 3.30.- p66β silencing (using sip66β(II) or sip66β(III)) does not affect MITF protein levels in 501mel cells. (A)** Immunofluorescence analysis of p66β and MITF in 501mel cells 72 h after transfection with sip66β(II), sip66β(III) or siRNA negative control. (Antibodies: α-p66β and α-MITF). Scale bars: 30 µm. **(B)** Quantification of p66β-positive and MITF-positive cells in the immunofluorescence analysis shown in (A). (**** $P \leq 0.0001$, ns $P > 0.05$, n=3, 200 cells counted per experiment, data represent mean ± SEM). **(C)** Western blot analysis of whole cell protein extracts from 501mel control cells and 501mel cells 72 h after transfection with sip66β(II), sip66β(III) or siRNA negative control. (Antibodies: α-p66β, α-MITF and α-ERK). ERK was used as a loading control. **(D)** Quantification of sip66β and MITF levels in 501mel cells 72 h after transfection with sip66β(II), sip66β(III) or siRNA negative control detected in the western blot analysis shown in (C). (**** $P \leq 0.0001$, ns $P > 0.05$, n=3, data represent mean ± SEM).

The absence of an effect on MITF expression upon p66β silencing using sip66β(II) or sip66β(III) together with the inability of exogenous p66β to rescue MITF expression when silencing p66β using sip66β(I) (section 3.4.4), led us to conclude that p66β does not regulate MITF and that the silencing of MITF expression resulting from sip66β depletion using sip66β(I) is due to the presence of associated off-target effects affecting MITF expression.

### 3.4.6. – p66α is not required for MITF expression

The uncovering of the presence of off-target effects leading to silencing of MITF expression on depletion of p66β using sip66β(I), led us to suspect the possibility of the repression of MITF observed upon p66α silencing using sip66α(I) being caused by associated off-target effects influencing MITF expression as well.

To check this, two additional siRNAs against p66α (sip66α(II) and sip66α(III)) were obtained and used in a silencing experiment equivalent to those previously performed.

Analysis of p66α and MITF levels in 501mel cells 72 h after transfection with sip66α(II), sip66α(III) or siRNA negative control showed highly efficient silencing of p66α in those cells transfected with sip66α(II) or sip66α(III) but no changes in MITF protein levels, as determined by immunofluorescence (**Figure 3.31.A** and **B**) and western blot (**Figure 3.31.C** and **D**).

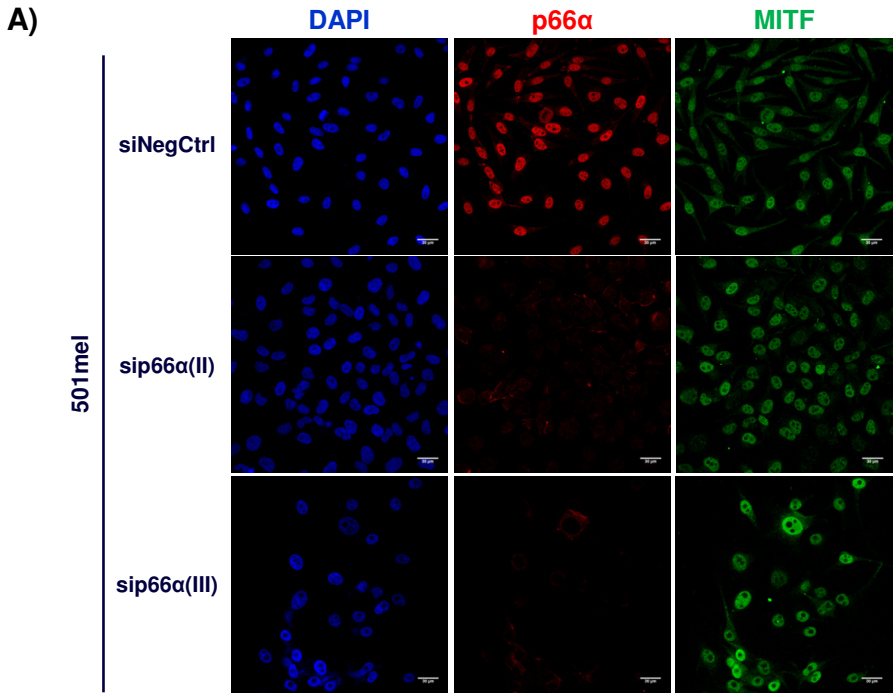


B)

| | % p66α positive cells | % MITF positive cells |
|---|---|---|
| siNegCtrl | **100** ± 0.0 | **92.3** ± 1.5 |
| sip66α(II) | **0.3** ± 0.3 **** | **94.7** ± 1.2 |
| sip66α(III) | **0.0** ± 0.0 **** | **96.3** ± 1.2 |

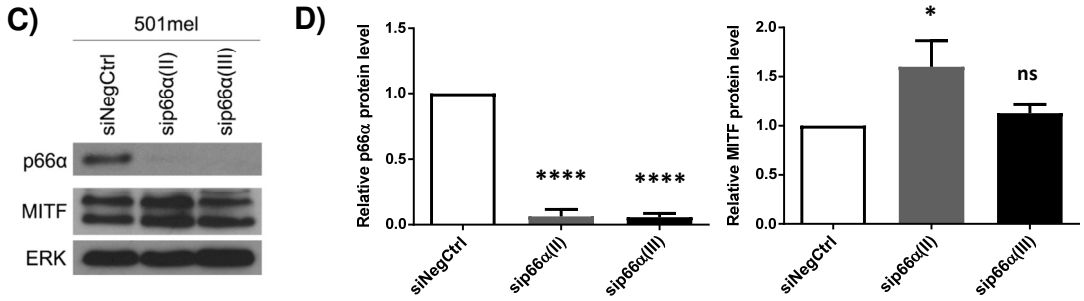


**Figure 3.31.- p66α silencing (using sip66α(II) or sip66α(III)) does not affect MITF protein levels in 501mel cells. (A)** Immunofluorescence analysis of p66α and MITF in 501mel cells 72 h after transfection with sip66α(II), sip66α(III) or siRNA negative control. (Antibodies: α-p66α and α-MITF). Scale bars: 30 µm. **(B)** Quantification of p66α-positive and MITF-positive cells in the immunofluorescence analysis shown in (A). (**** $P \leq 0.0001$, ns $P > 0.05$, n=3, 200 cells counted per experiment, data represent mean ± SEM). **(C)** Western blot analysis of whole cell protein extracts from 501mel control cells and 501mel cells 72 h after transfection with sip66α(II), sip66α(III) or siRNA negative control. (Antibodies: α-p66α, α-MITF and α-ERK). ERK was used as a loading control. **(D)** Quantification of sip66α and MITF levels in 501mel cells 72 h after transfection with sip66α(II), sip66α(III) or siRNA negative control detected in the western blot analysis shown in (C). (**** $P \leq 0.0001$, ns $P > 0.05$, n=3, data represent mean ± SEM).

The absence of an effect on MITF expression upon p66α silencing using sip66α(II) or sip66α(III) led us to conclude that p66α does not regulate MITF and the abolishment of MITF expression resulting from sip66α silencing using sip66α(I) is due to the presence of associated off-target effects affecting MITF expression.

## 3.5. – Discussion

In this chapter, the study of a potential role of the bromodomain protein ZMYND8 in the regulation of MITF was first addressed.

The results obtained from the initial ZMYND8 overexpression experiments seemed to indicate a role of ZMYND8 as a repressor of MITF expression. Moreover, the phenotype of ZMYND8-overexpressing cells appeared to correlate well with that characteristic of MITF low-expressing cells. Silencing of ZMYND8 however did not lead to any change in MITF levels. While this was unexpected, potential explanations would be that ZMYND8 only exerts its function when upregulated in response to a stimulus or that the very low levels of ZMYND8 remaining following siRNA treatment are preventing us from seeing an effect resulting from its knock-down. Alternatively, other proteins of the ZMYND family could be able to compensate for the lack of ZMYND8 when depleted.

However, the observation that overexpression of fragments of ZMYND8 lacking several domains considered key for its function was able to exert a similar effect on MITF expression suggested a potential non-specific response underlying the effect observed on MITF when overexpressing ZMYND8 or its truncation mutants. This would be in agreement with the absence of an effect of ZMYND8 knock-down on MITF expression. However, these observations do not rule out a potential specific role of ZMYND8 in the regulation of MITF under some conditions, especially since no effect of ZMYND8 overexpression on TFEB was

observed. We therefore conclude that with the data generated to date, a specific role of ZMYND8 on the regulation of MITF cannot yet be definitely established.

While exogenous overexpression of proteins is a useful strategy for the study of protein function, it is known that a potential risk of non-specific cellular effects exists. Protein overexpression can affect cellular fitness and prevent cell growth in many ways, including the exhaustion of cellular resources for protein synthesis, folding and transport (Stoebel et al. 2008; Moriya 2015; Kintaka et al. 2016). Specifically, the saturation of the folding capacity of the ER and accumulation of unfolded proteins triggers the ISR (section 1.4), activated by PERK (Harding et al. 2003). As previously seen, the ISR results in the upregulation of ATF4, a negative regulator of *MITF* expression (sections 1.4 and 1.3.2) (Harding et al. 2003; Falletta et al. 2017; Ferguson et al. 2017). Therefore, it is possible that overexpression of ZMYND8 in the experiments presented might have triggered the ISR leading to *MITF* suppression mediated by ATF4, with the low levels of MITF arising as a consequence leading to the observed reduced cell cycle progression.

The potential role of the NuRD complex in the regulation of MITF was also examined. While the preliminary data generated by others, and the first confirmatory experiments performed in this part of the Chapter seemed to indicate a requirement of the p66β and p66α subunits of the NuRD complex for the expression of MITF, further investigation uncovered the presence of off-target effects associated to the siRNAs used underlying the repression of MITF observed in these experiments. Since silencing of p66β and p66α using alternative siRNAs did not affect MITF expression, and neither did silencing of CHD4, another key subunit of NuRD, we conclude that the NuRD complex does not seem to have a role in the regulation of MITF.

The use of siRNAs for the study of gene function is based on the RNA interference (RNAi) gene silencing system, in which the main players are the short non-coding RNAs miRNAs and siRNAs.

As previously introduced, miRNAs are endogenous non-coding RNAs that play a key role in the post-transcriptional regulation of the expression of specific genes (section 1.5.2). miRNAs are generated from the genome as long primary precursors (pri-miRNAs) which are processed in the nucleus to pre-miRNAs of around 70 nucleotides and then exported and further processed by Dicer in the cytoplasm to mature miRNAs of around 22 nucleotides (Shukla et al. 2011). The guide strand of the miRNAs is then incorporated into the miRISC complexes and guides them to the 3' UTRs of target mRNAs for their cleavage (when sequences are fully or almost fully complementary) or to induce translation arrest (when sequences are only partially complementary) (Filipowicz et al. 2008; Meijer et al. 2013; Jonas and Izaurralde 2015; Gebert and MacRae 2019). Targeting to the 3' UTRs is mainly driven by the seed region in the guide strand of the miRNAs, which normally encompasses nucleotides 2 to 8 (counting from the 5' end) (Gebert and MacRae 2019). Consequently, individual mRNAs may have the ability to regulate hundreds of target mRNAs through sequence complementarity with their 3' UTRs partly or largely limited to the 5' region of the guide strand of miRNAs (Bartel 2009; Gebert and MacRae 2019).

siRNAs in mammalian cells are primarily exogenous, frequently introduced by viruses. Viral dsRNAs are also processed by Dicer into siRNAs of 21 to 25 nucleotides (Hammond et al. 2000; Carthew and Sontheimer 2009). Following binding to an siRNA-induced silencing complex (siRISC), the guide strand of the siRNA can guide the complex to the fully complementary target mRNA and induce its degradation through the activation of Argonaute, the catalytic subunit of the silencing complex (Hammond et al. 2000; Carthew and Sontheimer 2009).

Synthetic siRNAs are widely used for the study of gene function. siRNAs share complete sequence complementarity with their intended mRNA targets and early studies described them as highly specific (Tuschl et al. 1999; Caplen et al. 2001; Elbashir et al. 2001). However, as more data was generated, reports revealing the presence of off-target effects started to emerge. The first one of these studies showed how the use of distinct siRNAs targeting the same gene produced different gene expression signatures (Jackson et al. 2003). Analysis of the regulated off-target transcripts detected complementarity between the 5' region of the siRNA guide strand and the 3' UTR of the transcripts, which in some cases involved only as little as 8 nucleotides (Jackson et al. 2003). Further studies confirmed the enrichment of transcripts presenting some degree of complementarity between their 3' UTRs and the 5' region of the siRNA guide strand among those regulated as off-targets (Birmingham et al. 2006; Jackson et al. 2006b). Following more than a decade of further investigation, it is now widely accepted that as well as inducing the degradation of their target fully complementary mRNAs, siRNAs can regulate off-target transcripts enriched for seed-region motifs similarly to how miRNAs are able to regulate large numbers of seed-matched mRNAs. It is therefore possible that the 5' region of the two siRNAs used in this study for the depletion of p66β and p66α that led to *MITF* repression might have presented complementarity with the 3' UTR of the MITF transcript or that of an MITF regulator, leading to *MITF* repression through miRNA-like off-target effects.

While it is disappointing that the clear regulation of MITF expression by two independent siRNAs targeting two different components of the NuRD complex, p66α and p66β, was not recapitulated using different siRNAs, there are nevertheless important lessons to be learned. Most notably that any robust conclusion based on the use of siRNA-mediated depletion of any gene should be backed up by the use of other independent siRNAs. Examination of the published literature reveals that even in so-called high impact

journals, many studies rely on the use of a single siRNA to deplete a gene (Iwabu et al. 2010; Hao et al. 2012; Kaidi and Jackson 2013; Gao et al. 2014; Murthy et al. 2014; Coquel et al. 2018). As such, and given the experience reported here, the conclusions generated should be treated with some scepticism.

The improvement in our understanding of the mechanisms underlying siRNA off-target silencing is however leading to the development of strategies for their mitigation. For example, the introduction of a 2'-*O*-methyl chemical modification at position 2 of the siRNA guide strand has been shown to minimise miRNA-like off-target effects (Jackson et al. 2006a). Additionally, the introduction of a circular structure in the sense strand of siRNAs was recently suggested as another strategy with the potential to circumvent off-target silencing (Zhang et al. 2018).

Finally, the use of siRNAs is currently being replaced to some extent by the use of vector-based short hairpin RNAs (shRNAs), which can lead to a more efficient, as well as stable and inducible knock-down of genes of interest (Gupta et al. 2004; Siolas et al. 2005). However, since shRNAs are processed intracellularly into siRNAs (also by Dicer) and following their loading into RISC complexes share an equivalent mechanism of targeting and degradation of mRNAs, similar miRNA-like off-target effects are observed (Rao et al. 2009). Moreover, shRNAs are associated with additional potential sources of off-target effects, such as those derived from the genomic integration of shRNAs or the Dicer-mediated hairpin processing, which can generate multiple sequences (Gu et al. 2012; Bhinder and Djaballah 2013). Different strategies are therefore also being studied for the reduction of off-target effects associated to the use of shRNAs (Gu et al. 2012; Gu et al. 2014; Mockenhaupt et al. 2015).

# Chapter 4 – Study of the potential role of MITF in the regulation of translation

## 4.1. – Introduction

Protein synthesis, or the process of mRNA translation, is tightly controlled in cells, playing a major role in the regulation of gene expression. Dysregulation of translation is however a feature of cancer, having been linked to aberrant proliferation, metabolism, survival, angiogenesis, altered immune response, and metastasis (Johnson et al. 1976; Kevil et al. 1996; Polunovsky et al. 1996; Larsson et al. 2006; Larsson et al. 2007; Colina et al. 2008; Topisirovic and Sonenberg 2011; Nasr et al. 2013; Robichaud et al. 2015; Xu et al. 2019).

Translational control allows for a faster adaptive response to environmental cues than any other upstream level of regulation of gene expression. As such, translation is influenced by stress conditions frequently found in the tumour microenvironment, such as hypoxia or nutrient deprivation (van den Beucken et al. 2011; Falletta et al. 2017; Robichaud and Sonenberg 2017). Under these stress conditions, cells respond by reducing global protein synthesis, with two key mechanisms operating. First, phosphorylation of eIF2α by different kinases, including PERK and GCN2 that are activated by ER stress and amino acid limitation, respectively, acts as a major suppressor of global translation as introduced in sections 1.4 and 1.5.3 (Harding et al. 2000; Sonenberg and Hinnebusch 2009). Second, mTORC1 signalling, which is activated by growth factors and high levels of amino acids, oxygen and energy, and is inhibited by different types of cellular stress including amino acid limitation, plays a key role in the control of protein synthesis via its ability to activate S6K1 or inhibit 4E-BP1 (**Figure 4.1**) (section 1.5.3) (Guertin and Sabatini 2007; Roux and Topisirovic 2012; Saxton and Sabatini 2017). Recently it was reported that modulation of mTORC1 activity is partly exerted through regulation of DEPTOR, a component of the mTORC1 complex and

inhibitor of its catalytic activity (section 1.5.3) (Peterson et al. 2009; Saxton and Sabatini 2017).

As it was introduced in section 1.2.3.1, aberrant activation of the PI3K/AKT signalling pathway is frequently observed in melanoma, either through activating mutations in PI3K itself, or via loss of function or expression of the tumour suppressor PTEN, that normally counteracts PI3K activity by degradation of PIP3, the enzymatic product of PI3K (**Figure 4.1**) (Chalhoub and Baker 2009). The kinase AKT lies downstream from PI3K and, as an activator of mTORC1, modulation of AKT activity through the PI3K pathway results in the regulation of mTORC1 signalling, ultimately exerting a controlling influence on protein synthesis (Porta et al. 2014). Thus, hyperactivation of the PI3K/AKT and/or mTORC1 signalling pathways results in enhanced protein synthesis and their negative regulation reduces translation.

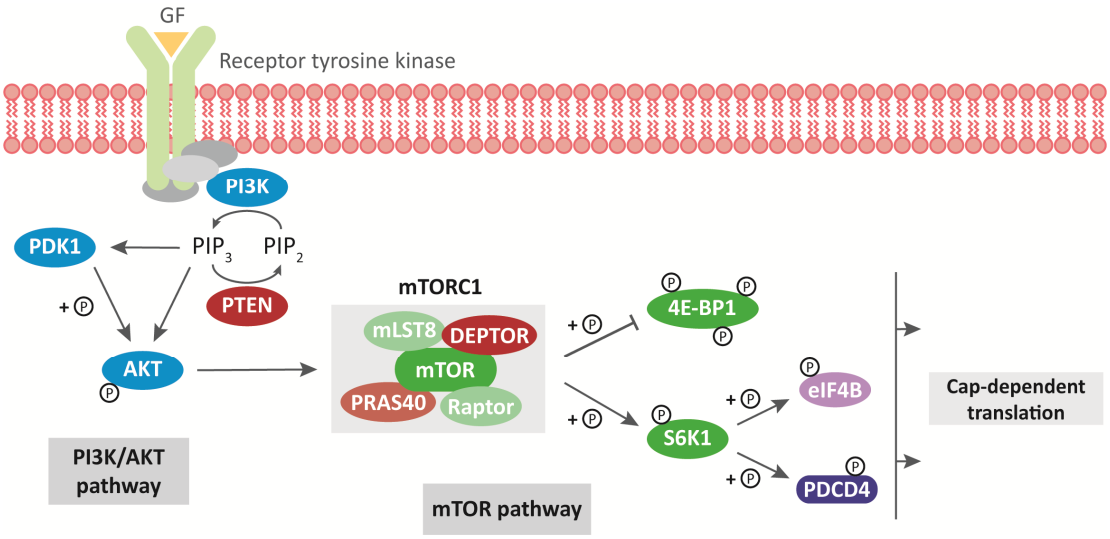


**Figure 4.1.- Regulation of cap-dependent translation by PI3K/AKT and mTOR signalling pathways. Activation of growth factor receptors leads to PI3K signalling and activation of AKT which subsequently activates the mTORC1 complex to promote protein synthesis via activation of S6K1 and inactivation of 4E-BP1. PTEN is a negative regulator of PI3K signalling and DEPTOR inhibits mTORC1 activity. GF: growth factor;** PI3K: phosphatidylinositol 3-kinase; PIP3: phosphatidylinositol (3,4,5)-triphosphate; PIP2: phosphatidylinositol (4,5)-bisphosphate; PTEN: phosphatase and tensin homolog; PDK1: phosphoinoisitide dependent kinase 1; AKT: protein kinase B; mTORC1: mechanistic target of rapamycin complex 1; mTOR: mechanistic target of rapamycin; mLST8: mammalian lethal with Sec13 protein 8; Raptor: regulatory-associated protein of mTOR; DEPTOR: DEP domain-containing mTOR-interacting protein; PRAS40: proline-rich Akt substrate of 40 kDa; 4E-BP1: 4E (eIF4E)-binding protein 1; S6K1: 70kDa ribosomal S6 kinase; eIF4B: eukaryotic translation initiation factor 4B; PDCD4: programmed cell death protein 4. (Guertin and Sabatini 2007)

## 4.2. – Preliminary data

To identify genes regulated by MITF, a 3' RNA-seq analysis following 48 h of knock-down of MITF (using siMITF(I)) in 501mel cells was performed by Pakavarin Louphrasitthiphol, a member of the laboratory. Of the differentially expressed genes (FDR < 0.05; fold-change ≥ 2), a total of 791 genes was detected as being significantly upregulated while 1,008 genes exhibited reduced gene expression (**Supplementary Table S.1** on Data CD). However, many of the genes whose expression is deregulated on MITF depletion could be affected indirectly. To filter for those genes with the potential for a direct mechanism of regulation by MITF, an MITF ChIP-seq dataset also generated by Pakavarin Louphrasitthiphol using a 501mel cell line stably expressing HA-tagged MITF and an α-HA antibody (**Supplementary Tables S.2.A** and **B** on Data CD) was examined. Selection of only those differentially expressed genes with associated MITF binding peaks in both replicates of the ChIP-seq experiment returned a total of 592 and 720 MITF-bound genes upregulated and downregulated (FDR < 0.05; fold-change ≥ 2), respectively, following MITF depletion (**Supplementary Table S.3** on Data CD).

Since most laboratories have focussed on genes that are positively-regulated by MITF, we were especially interested in those that were MITF-repressed. Examining the list of MITF-bound and repressed genes, that is, those upregulated on MITF silencing with associated MITF ChIP-seq binding peaks, revealed two that were of particular interest among the top 125 MITF-bound genes upregulated upon MITF depletion, namely *PTEN* and *DEPTOR*, whose expression increased by 4.4-fold and 7.1-fold, respectively (**Figure 4.2** and **Supplementary Table B.1**). MITF ChIP-seq analysis showed several peaks of MITF binding at the *PTEN* gene, notably a few small peaks in the gene body, a major peak lying around 35 kb downstream and some other peaks further downstream (**Figure 4.3.A**). For *DEPTOR*, several

MITF binding sites were detected within the gene body and the 5' and 3' flanking regions (**Figure 4.3.B**).

**A)**

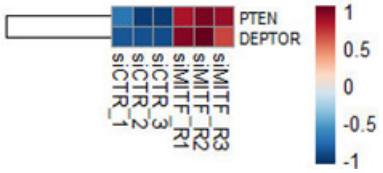


**B)**

| | Fold Change | P value |
|---|---|---|
| PTEN | 4.4 | $7.1 \times 10^{-16}$ |
| DEPTOR | 7.1 | $3.2 \times 10^{-10}$ |

**Figure 4.2.- MITF silencing leads to upregulation of *PTEN* and *DEPTOR*. (A)** Heatmap representing the differential expression of *PTEN* and *DEPTOR* in 501mel cells 48 h after transfection with siMITF(I) or siRNA negative control, analysed by RNA-seq. **(B)** Fold change of *PTEN* and *DEPTOR* expression 48 h after transfection with siMITF(I) (relative to siRNA negative control) in 501mel cells and associated *P* values. Data obtained from the same RNA-seq analysis referred in (A). (*Performed by Pakavarin Louphrasitthiphol*)

These observations raised the possibility that MITF directly represses both *PTEN* and *DEPTOR* expression.

The roles of PTEN and DEPTOR as negative regulators of PI3K/AKT and mTOR signalling pathways, respectively (Chalhoub and Baker 2009; Peterson et al. 2009), and their potential regulation by MITF, led us to consider the possibility of a role of MITF regulating protein translation through the modulation of PTEN and DEPTOR expression. Since high MITF levels associate with a proliferative/differentiated phenotype with an elevated requirement of protein synthesis for proliferation/pigmentation, and MITF low levels associate with a quiescent phenotype with low demand of protein synthesis, a potential role of MITF in activating protein synthesis to ensure translation of transcriptionally activated genes only when needed would fit well. As such, determining whether MITF could promote protein translation will be the main focus of the study presented in this chapter.

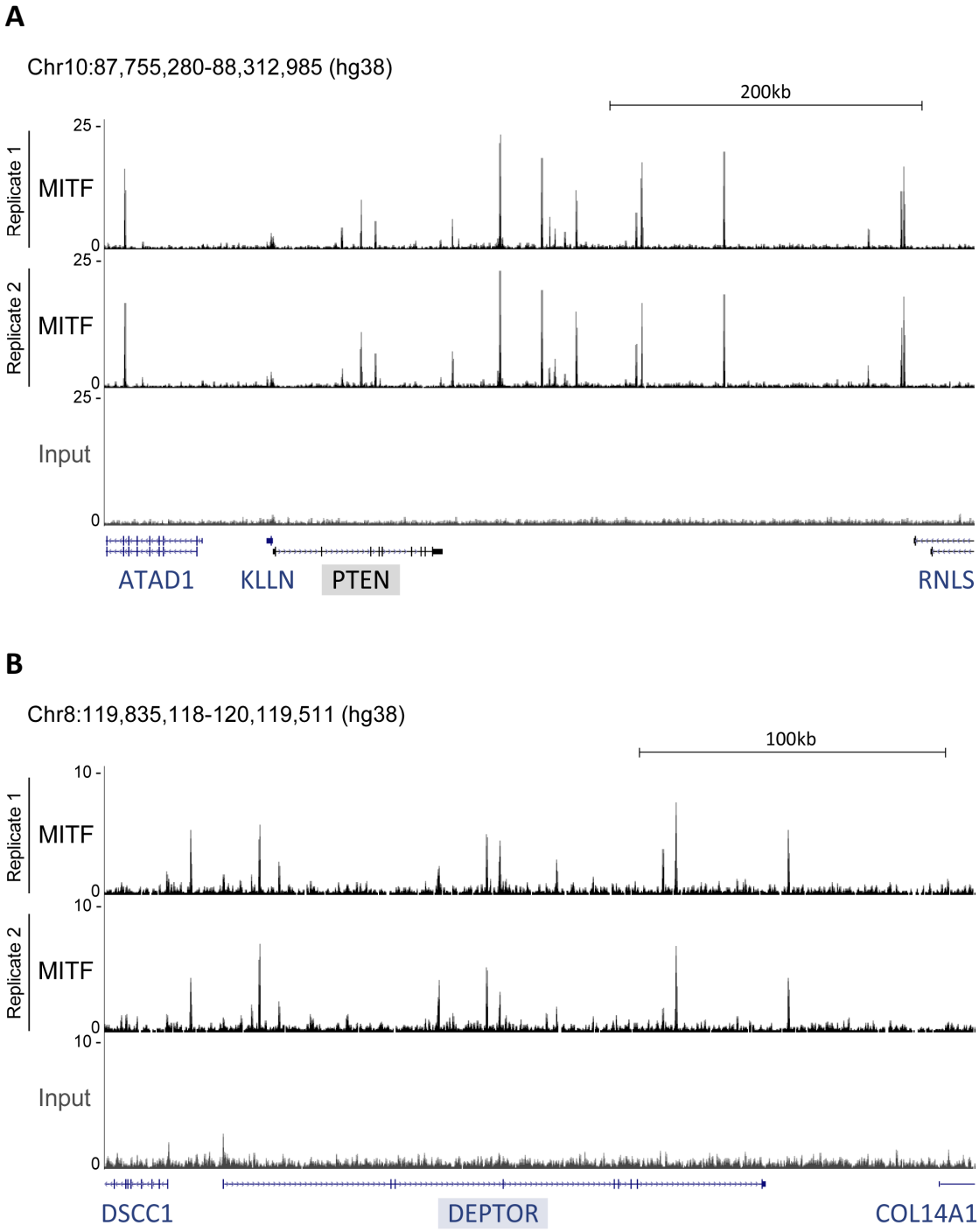


**Figure 4.3.- MITF ChIP-seq peaks associate with *PTEN* and *DEPTOR* genes in 501mel cells.** ChIP-seq analysis in 501mel cells expressing doxycycline-inducible HA-MITF. Cells were induced using 20 ng doxycycline for 16 h prior to processing for ChIP-seq. The images show UCSC browser screenshots of the *PTEN* (A) and *DEPTOR* (B) genes with binding peaks in their gene bodies and flanking genomic regions. (*Performed by Pakavarin Louphrasitthiphol*)

## 4.3. – MITF represses PTEN and DEPTOR

To validate the preliminary results obtained in the RNA-seq analysis, MITF, PTEN and DEPTOR mRNA levels were determined by qRT-PCR following MITF knock-down (using siMITF(I)) for 72 h in IGR37 cells.

An increase of around 4-6 fold was observed in PTEN and DEPTOR mRNA levels following MITF silencing (relative to transfection with siRNA negative control) (**Figure 4.4**). These data therefore correlated well with the results from the preliminary RNA-seq analysis.

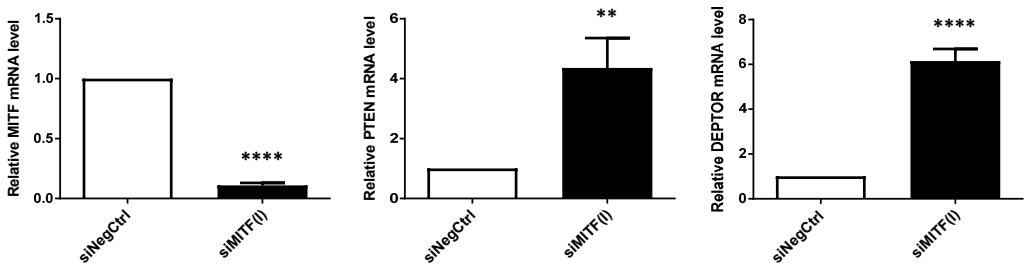


**Figure 4.4.- PTEN and DEPTOR mRNA levels increase upon MITF silencing (using siMITF(I)) in IGR37 cells.** qRT-PCR analysis results for MITF, PTEN and DEPTOR mRNA levels in IGR37 cells 72 h after transfection with siMITF(I) or siRNA negative control. (**** $P \leq 0.0001$, ** $P \leq 0.01$, n=3, data represent mean ± SEM).

To verify that the effect observed on PTEN and DEPTOR expression following MITF silencing was not dependent on the cell line or the siRNA against MITF used (siMITF(I)), an equivalent experiment was then performed in the human SKmel30 melanoma cell line using three different siRNAs (siMITF(I), siMITF(II) and siMITF(III)).

A significant increase in PTEN and DEPTOR mRNA was detected for all siRNAs against MITF used in SKmel30 cells (**Figure 4.5**), ruling out a dependency of a specific siRNA or cell line for the effects observed on the expression of PTEN and DEPTOR following MITF silencing.

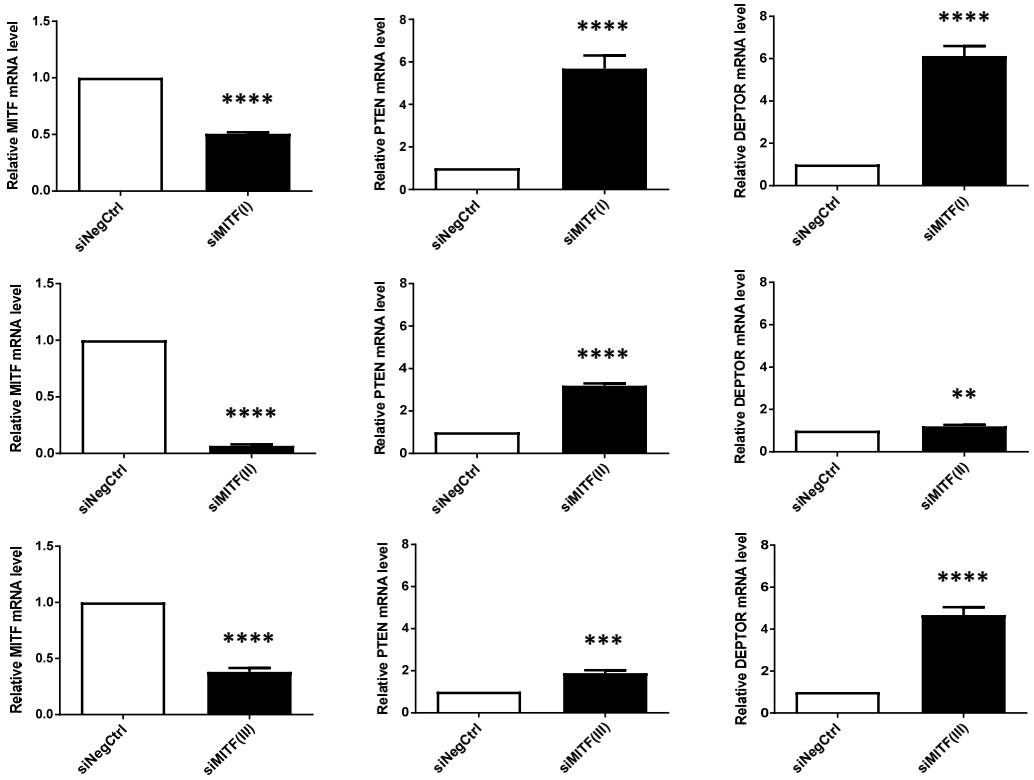


**Figure 4.5.- PTEN and DEPTOR mRNA levels increase upon MITF silencing (using siMITF(I), siMITF(II) or siMITF(III)) in SKmel30 cells.** qRT-PCR analysis results for MITF, PTEN and DEPTOR mRNA levels in SKmel30 cells 72 h after transfection with siMITF(I), siMITF(II), siMITF(III) or siRNA negative control. (**** $P \leq 0.0001$, *** $P \leq 0.001$, ** $P \leq 0.01$, n=3, data represent mean ± SEM).

Finally, a western blot analysis performed 72 h after transfection with siMITF(I) or siRNA negative control in IGR37 cells confirmed that the increase in PTEN and DEPTOR mRNA levels following MITF knock-down is also reflected in an increase in PTEN and DEPTOR protein levels (**Figure 4.6**).

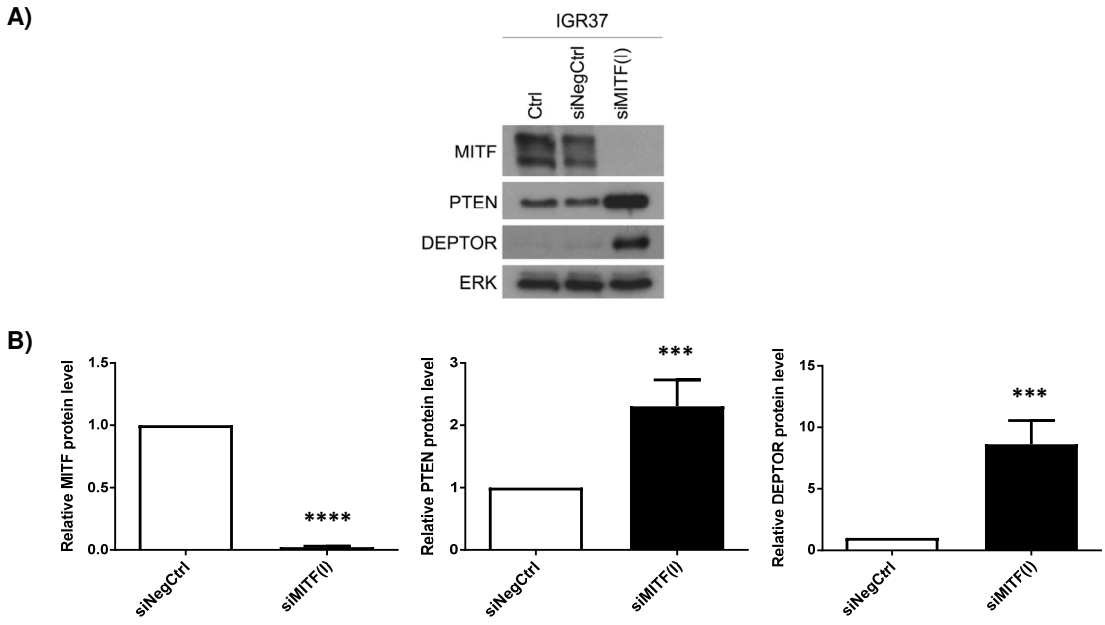


**Figure 4.6.- PTEN and DEPTOR protein levels increase upon MITF silencing (using siMITF(I)) in IGR37 cells. (A)** Western blot analysis of whole cell protein extracts from IGR37 control cells and IGR37 cells 72 h after transfection with siMITF(I) or siRNA negative control. (Antibodies: α-MITF, α-PTEN, α-DEPTOR and α-ERK). ERK was used as a loading control. **(B)** Quantification of MITF, PTEN and DEPTOR protein levels detected in the western blot analysis shown in (A). (**** $P \leq 0.0001$, *** $P \leq 0.001$, ns $P > 0.05$, n=3, data represent mean ± SEM).

We therefore concluded that MITF represses PTEN and DEPTOR through a mechanism at least partly mediated by transcriptional regulation via a reduction in their mRNA levels, either as a result of decreased mRNA stability or more likely, via regulation of their transcription given the binding at the loci by MITF detected by ChIP-seq (Figure 4.3).

## 4.4. – MITF can regulate PI3K/AKT and mTOR signalling

To confirm that the regulation of PTEN and DEPTOR by MITF is reflected in the modulation of the activity through PI3K/AKT and mTOR signalling, phosphorylation of AKT, S6K1 and 4E-BP1, components of these pathways and involved in the regulation of cap-dependent translation (Figure 4.1) was studied. Additionally, phosphorylation of ribosomal protein S6, a direct target of S6K1 whose potential role in the regulation of translation remains controversial (Tang et al. 2001; Stolovich et al. 2002; Mamane et al. 2004; Ruvinsky

et al. 2005; Ruvinsky and Meyuhas 2006; Roux et al. 2007; Puighermanal et al. 2017), was determined as an extra readout for S6K1 activity.

Western blot analysis was performed 72 h after transfection with siMITF(I) or siRNA negative control in IGR37 and SKmel30 cells in three independent experiments (A-C) (**Figure 4.7**).

In IGR37 cells in experiment A, DEPTOR and PTEN are increased on MITF depletion (reproduced for Figure 4.6) with a marked decrease in phosphorylation of AKT, S6K1 and S6 being observed. For 4E-BP1, decreased phosphorylation is characterised by a shift down in mobility. This result strongly suggests that elevated PTEN and/or DEPTOR affect PI3K signalling through AKT and mTORC1 to its downstream effectors S6K1, S6 and 4E-BP1. In the same cells in experiments B and C, the effects of MITF depletion on PTEN and DEPTOR are similar. In experiment B, p-AKT and p-S6K1 are also nicely reduced and there is a slight reduction in p-S6, with a small but detectable downward shift in 4E-BP1. Experiment C also shows a reduction of p-S6 and a shift in mobility of 4E-BP1 consistent with decreased mTORC1 signalling, but only a moderate effect of MITF depletion on p-AKT was observed.

In SKmel30 cells a similar trend was observed though the effects were less clear despite the fact that the induction of PTEN and DEPTOR by MITF-depletion was reproducible in all three experiments. In experiment A, p-S6 was clearly strongly reduced by MITF depletion, but only a moderate decrease in p-AKT and p-S6K1 was detected that in part may have arisen owing to a slight decrease in loading. In experiment B, compared to the control siRNA, transfection with the siRNA for MITF led to reduced p-AKT and p-S6K1, a moderate reduction in p-S6, and the mobility shift in 4E-BP1 characteristic of its dephosphorylation. In experiment C, compared to the control siRNA, depletion of MITF reduced p-AKT and led to a minor reduction in p-S6, though no obvious effect was observed on 4E-BP1.

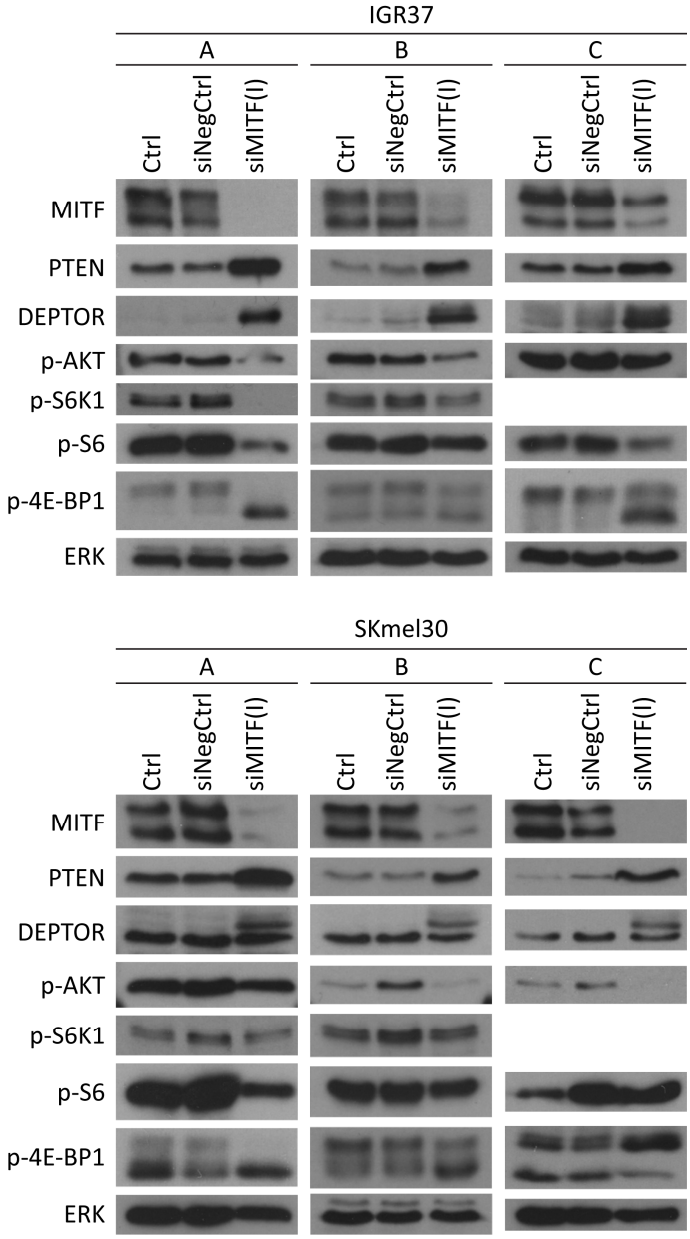


**Figure 4.7.- Phosphorylation of AKT, S6K1, S6 and 4E-BP1, indicative of activity through the PI3K/AKT and mTOR signalling pathways, is overall decreased upon MITF silencing (using siMITF(I)) in IGR37 and SKmel30 cells.** Western blot analyses of whole cell protein extracts from IGR37 and SKmel30 control cells and IGR37 and SKmel30 cells 72 h after transfection with siMITF(I) or siRNA negative control in three independent experiments (A, B and C). (Antibodies: α-MITF, α-PTEN, α-DEPTOR, α-p(Ser473)-Akt, α-p(Thr389)-S6K1, α-p(Ser235/236)-S6, α-p(Thr37/46)-4E-BP1 and α-ERK). ERK was used as a loading control.

Taken together, and against the background of some variability between the different experiments, the impression gained is that depletion of MITF can lead to decreased mTORC1 signalling. The variability may possibly be attributable to slightly different cell

confluency prior to transfection or different efficiencies of transfection of the siRNAs between experiments leading to temporal changes in PI3K signalling. Nevertheless, while the trend is clear, with MITF promoting mTORC1 activity, additional experiments in other melanoma cell lines may be required to validate the conclusions.

## 4.5. – MITF may regulate protein translation

The regulation of PTEN and DEPTOR and consequent modulation of the activity of the PI3K/AKT and mTOR signalling pathways by MITF led us to ask whether MITF could also potentially control protein translation.

To test this hypothesis, a Click-iT™ Plus OPP Alexa Fluor™ 647 Protein Synthesis Assay Kit (Thermo Fisher Scientific) was used to measure translation via analysis of the incorporation of fluorescently labelled O-propargyl-puromycin (OPP) into newly synthesised proteins.

72 h after transfection with siMITF(I) or siRNA negative control in IGR37 and SKmel30 cells and 30 min after addition of OPP to the culture medium, immunofluorescence analysis showed a dramatic reduction in the incorporation of OPP in those cells where MITF was successfully knocked-down, with cells retaining MITF expression, most likely because they were not transfected with the siRNA, acting as an internal control (**Figure 4.8**). Protein synthesis was also measured in IGR37 and SKmel30 cells following 4 h treatment with cycloheximide, an inhibitor of protein synthesis, as an additional control. As expected, cells treated with cycloheximide did not show any OPP incorporation (**Figure 4.8**).

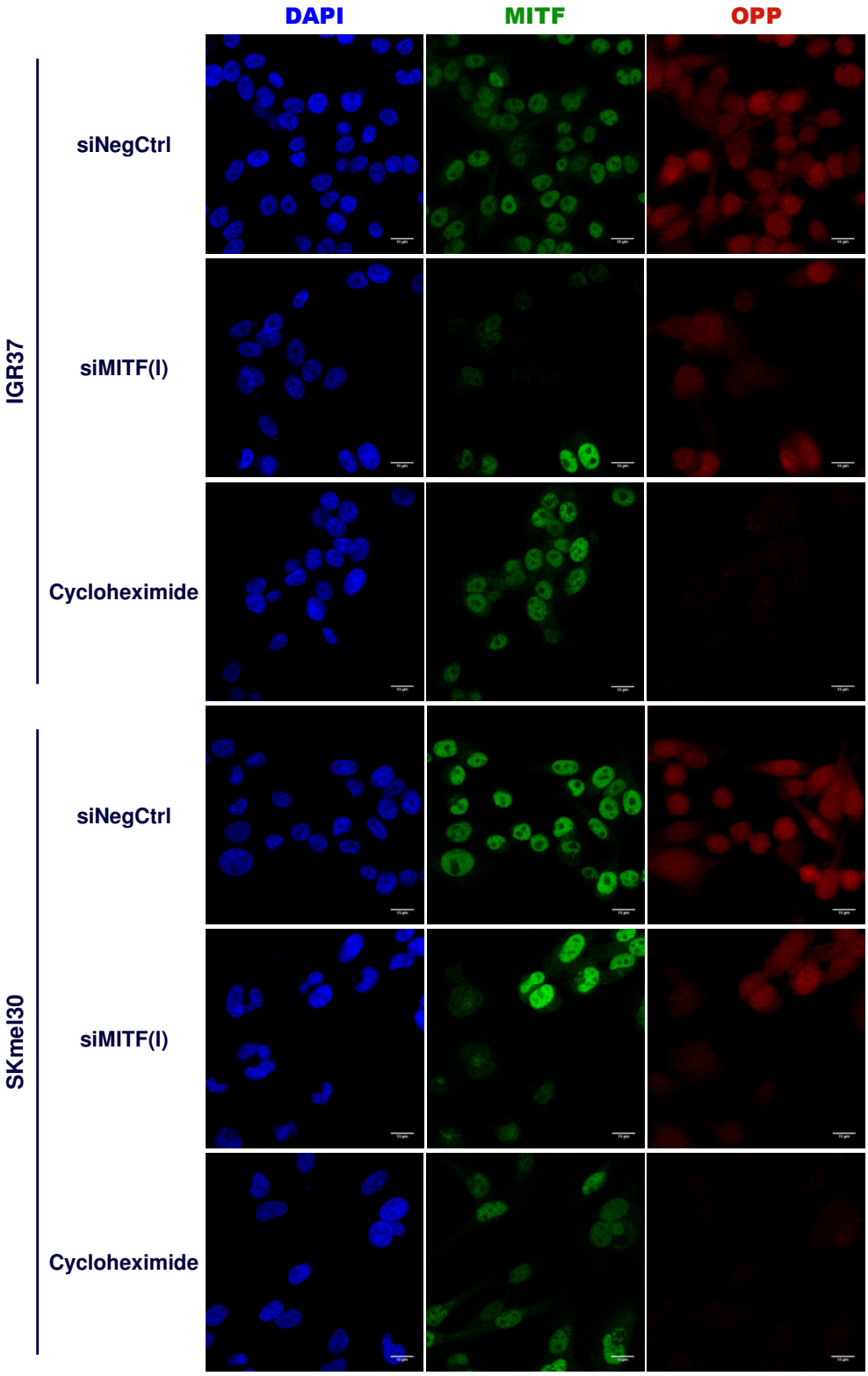


**Figure 4.8.- OPP incorporation (indicative of protein synthesis) is reduced upon silencing of MITF (using siMITF(I)) in IGR37 and SKmel30 cells.** Immunofluorescence analysis of MITF and fluorescently labelled O-propargyl-puromycin in IGR37 and SKmel30 cells 72 h after transfection with siMITF(I) or siRNA negative control or following 4 h treatment with 10 µg/ml cyclohemixide. (Antibody: α-MITF). Scale bars: 15 µm.

To confirm the observed effect on translation following silencing of MITF, an equivalent experiment was performed where protein synthesis was measured by metabolic radiolabelling instead.

72 h after transfection with siMITF(I) or siRNA negative control in SKmel30 cells, a mix of $^{35}$S-methionine and $^{35}$S-cysteine was added to the culture medium and 30 min later incorporation of the radiolabelled amino acids to newly synthesised proteins was quantified by phosphorimaging following SDS-page for protein separation. A reduction in translation ($^{35}$S-methionine and $^{35}$S-cysteine incorporation) upon MITF silencing (relative to transfection with siRNA negative control) in SKmel30 cells was also observed with this method (**Figure 4.9**).

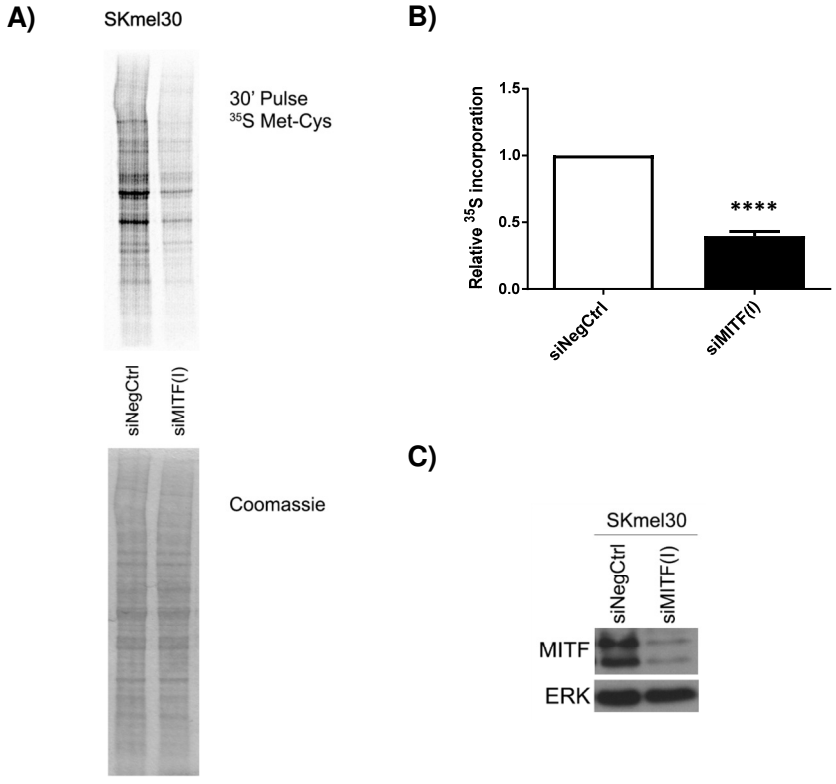


**Figure 4.9.- $^{35}$S incorporation (indicative of protein synthesis) is reduced upon silencing of MITF (using siMITF(I)) in SKmel30 cells. (A)** Autoradiograph showing $^{35}$S incorporation in SKmel30 cells 72 h after transfection with siMITF(I) or siRNA negative control and corresponding coomassie-stained gel (below) showing comparable levels of total protein in these samples. **(B)** Quantification of $^{35}$S incorporation in the analysis shown in (A). (**** $P \leq 0.0001$, n=3, data represent mean ± SEM). **(C)** Western blot analysis of whole cell protein extracts 72 h after transfection with siMITF(I) or siRNA negative control (replicate from the experiment shown in (A)) showing efficient silencing of MITF. (Antibodies: α-MITF and α-ERK). ERK was used as a loading control.

We therefore concluded that, consistent with its ability to promote mTORC1 signalling, MITF appears to have a role in promoting protein translation.

## 4.6. – MITF might regulate translation through the regulation of PTEN

We next aimed to address whether the mechanism underlying the observed change in protein synthesis when silencing MITF is dependent on upregulation of PTEN.

To do so, protein synthesis was measured after silencing MITF and PTEN either independently or both MITF and PTEN together. If MITF were to promote translation by supressing PTEN expression, the double knock-down would be expected to reverse the decrease in translation seen after independent MITF knock-down.

72 h after transfection with siMITF(I), siPTEN, siMITF(I) + siPTEN or siRNA negative control in SKmel30 cells, $^{35}$S-methionine and $^{35}$S-cysteine metabolic labelling showed an expected decrease in protein synthesis when MITF was knocked-down alone, but no change for the double MITF + PTEN knock-down (relative to siRNA negative control) (**Figure 4.10**). These results pointed to a potential role of PTEN underlying the mechanism of MITF regulation of translation. However, the fact that PTEN knock-down alone led to an increase in protein synthesis (**Figure 4.10**) introduced an alternative possible explanation in which opposing effects on translation (inactivating for MITF knock-down and activating for PTEN knock-down) compensate each other without the need of a direct mechanistic link.

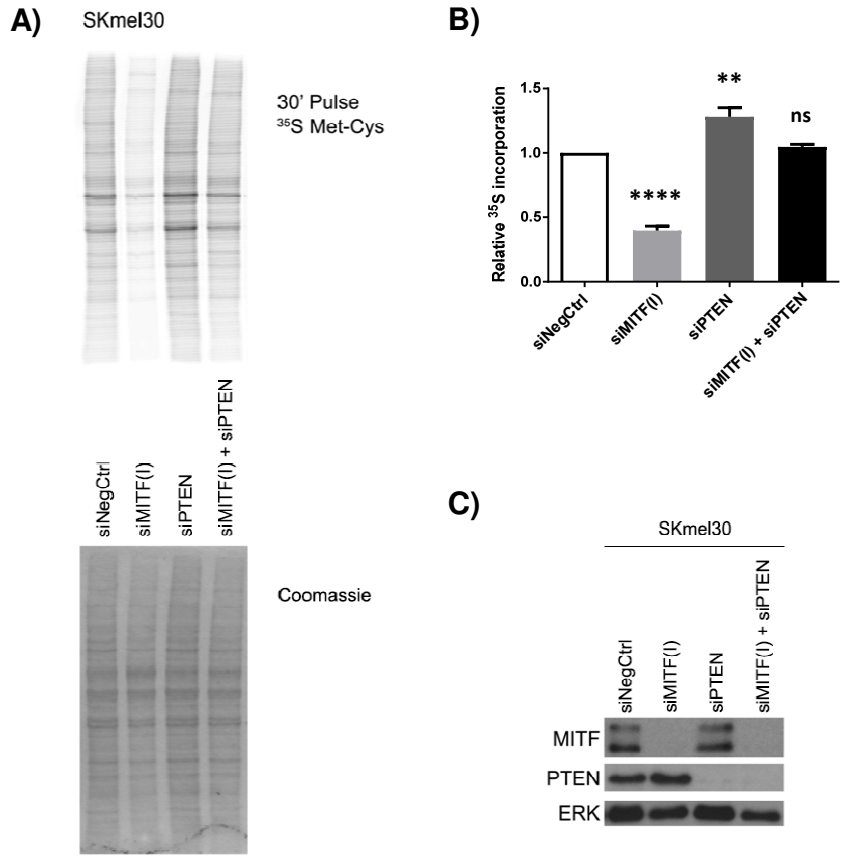


**Figure 4.10.- $^{35}$S incorporation (indicative of protein synthesis) is reduced upon silencing of MITF (using siMITF(I)), increased following silencing of PTEN, and not altered after combined silencing of MITF (using siMITF(I)) and PTEN in SKmel30 cells. (A)** Autoradiograph showing $^{35}$S incorporation in SKmel30 cells 72 h after transfection with siMITF(I), siPTEN, siMITF(I) + siPTEN, or siRNA negative control and corresponding coomassie-stained gel (below) showing comparable levels of total protein in these samples. **(B)** Quantification of $^{35}$S incorporation in the analysis shown in (A). (**** $P \leq$ 0.0001, ** $P \leq 0.01$, ns $p > 0.05$, n=3, data represent mean ± SEM). **(C)** Western blot analysis of whole cell protein extracts 72 h after transfection with siMITF(I), siPTEN, siMITF(I) + siPTEN, or siRNA negative control (replicate from the experiment shown in (A)) showing efficient silencing of MITF and PTEN. (Antibodies: α-MITF, α-PTEN and α-ERK). ERK was used as a loading control.

Further research will therefore be needed to definitively establish whether the mechanism underlying the effect observed in translation when knocking down MITF (using siMITF(I)) is dependent on PTEN or not.

## 4.7. – MITF does not have a clear effect on translation

To verify that the effect observed in translation when knocking down MITF is not dependent on the siRNA against MITF used so far (siMITF(I)), an experiment knocking-down

MITF using different siRNAs followed by $^{35}$S-methionine and $^{35}$S-cysteine metabolic labelling to measure protein synthesis was performed.

72 h after transfection with siMITF(I), siMITF(II), siMITF(III) or siRNA negative control in SKmel30 cells, metabolic labelling showed an expected decrease in protein synthesis for the silencing corresponding to siMITF(I) (relative to siRNA negative control), but unexpectedly, an increase in translation for the silencing corresponding to siMITF(II) and siMITF(III), in spite of the upregulation of PTEN protein levels (**Figure 4.11**).

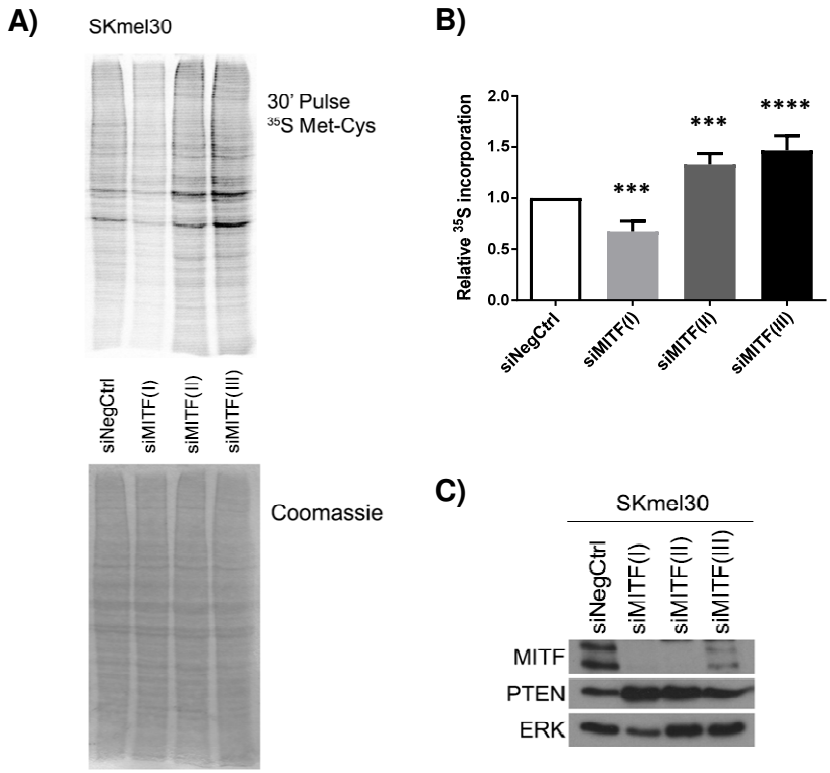


**Figure 4.11.- $^{35}$S incorporation (indicative of protein synthesis) is reduced upon silencing of MITF using siMITF(I) but increased following silencing of MITF using siMITF(II) or siMITF(III) in SKmel30 cells. (A)** Autoradiograph showing $^{35}$S incorporation in SKmel30 cells 72 h after transfection with siMITF(I), siMITF(II), siMITF(III) or siRNA negative control and corresponding coomassie-stained gel (below) showing comparable levels of total protein in these samples. **(B)** Quantification of $^{35}$S incorporation in the analysis shown in (A). (**** $P \leq 0.0001$, *** $P \leq 0.001$, ns $P > 0.05$, n=3, data represent mean ± SEM). **(C)** Western blot analysis of whole cell protein extracts 72 h after transfection with siMITF(I), siMITF(II), siMITF(III) or siRNA negative control (replicate from the experiment shown in (A)) showing efficient silencing of MITF and increase in PTEN protein levels for all siRNAs against MITF used (relative to siRNA negative control). (Antibodies: α-MITF, α-PTEN and α-ERK). ERK was used as a loading control.

The observation of different effects on translation following MITF knock-down with siMITF(I), siMITF(II) or siMITF (III) led us to question what the real impact of silencing MITF in translation is and what should be attributed to off-target effects.

To address this issue, two additional siRNAs against MITF (siMITF(IV) and siMITF(V)) were obtained and used in an equivalent experiment to the one just described.

72 h after transfection with siMITF(IV), siMITF(V) or siRNA negative control in SKmel30 cells, $^{35}$S-methionine and $^{35}$S-cysteine metabolic labelling showed a very slight but significant increase in protein synthesis for the silencing corresponding to both siMITF(IV) and siMITF(V) (relative to siRNA negative control) (**Figure 4.12**).

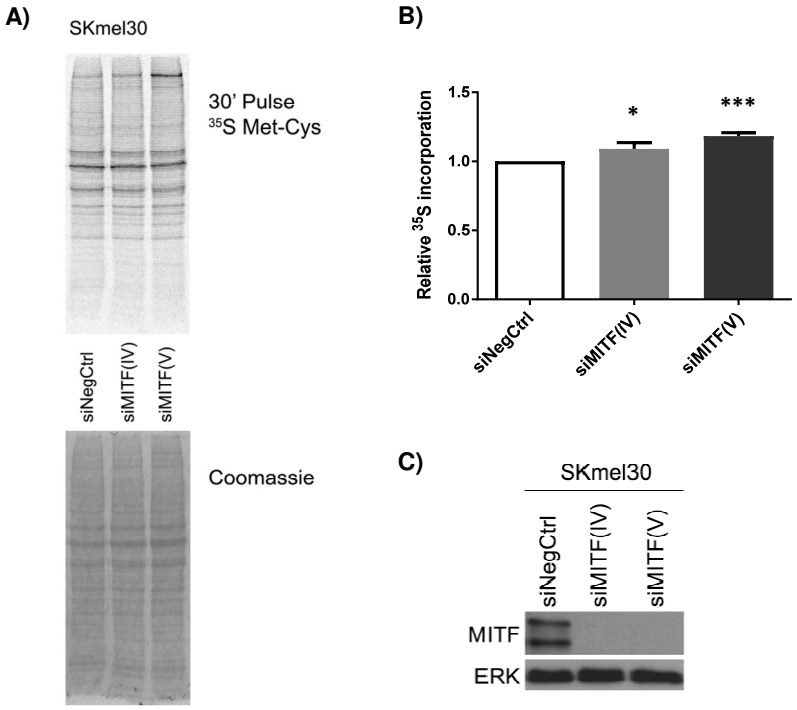


**Figure 4.12.- $^{35}$S incorporation (indicative of protein synthesis) is slightly increased upon silencing of MITF using siMITF(IV) or siMITF(V) in SKmel30 cells. (A)** Autoradiograph showing $^{35}$S incorporation in SKmel30 cells 72 h after transfection with siMITF(IV), siMITF(V) or siRNA negative control and corresponding coomassie-stained gel (below) showing comparable levels of total protein in these samples. **(B)** Quantification of $^{35}$S incorporation in the analysis shown in (A). (*** $P \leq 0.001$, * $P \leq 0.05$, n=3, data represent mean ± SEM). **(C)** Western blot analysis of whole cell protein extracts 72 h after transfection with siMITF(IV), siMITF(V) or siRNA negative control (replicate from the experiment shown in (A)) showing efficient silencing of MITF for both siRNAs against MITF used. (Antibodies: α-MITF and α-ERK). ERK was used as a loading control.

The fact that the effects observed in translation when knocking-down MITF using siMITF(II)-(V) all went in the same direction made us more inclined to consider that the reduction in translation following MITF silencing using siMITF(I) was most likely due to off-target effects associated to this siRNA.

However, the variability of the effect observed on translation still present depending on the use of siMITF(II)-(V) together with the fact that this effect was overall very small, led us to just conclude that MITF does not have a clear effect on translation.

## 4.8. – Discussion

In this chapter, the study of a potential role of MITF in the regulation of translation was addressed.

The preliminary data together with the first experiments performed uncovered the repression of PTEN and DEPTOR (negative regulators of the PI3K/AKT and mTOR signalling pathways, respectively) by MITF through a mechanism at least partly mediated by transcription. Whether MITF directly regulates PTEN and DEPTOR remains to be confirmed. Although depletion of MITF decreases PTEN and DEPTOR mRNA levels and binding to these loci is detected using ChIP-seq, formal proof of direct regulation awaits the genetic modification of these binding sites to impair MITF binding and confirm if the regulation of PTEN and DEPTOR levels is a direct consequence of MITF.

The effect of MITF depletion on PTEN and DEPTOR expression was verified in two cell lines and using three different MITF siRNAs. Importantly, although there was some variability on the outcome, the regulation of the activity of the PI3K/AKT and mTORC1 signalling pathways by MITF (likely through modulation of PTEN and DEPTOR levels) was then confirmed. Although further experiments are needed to provide more robust data, the

results obtained were indicative of a previously unsuspected role for MITF in the control of PI3K and mTORC1 signalling.

This is likely important, as PI3K signalling is known to promote survival as well as nutrient uptake (Porta et al. 2014), two biological processes aligned with MITF's role in promoting survival via upregulation of the anti-apoptotic factor BCL2 (McGill et al. 2002), as well as its capacity to promote proliferation via regulation of CDK2 (Du et al. 2004). Moreover, suppression of PTEN by MITF may establish a positive feedback loop, since PI3K signalling has been shown to promote expression of PAX3, a key melanocyte transcription factor that is a positive regulator of the MITF promoter (Potterf et al. 2000; Medic et al. 2011; Bonvin et al. 2012). In this scenario, PAX3 mediated activation of MITF would then suppress PTEN leading to elevated PI3K and more PAX3 expression. Such positive feedback loops are frequently used to establish stable cell states and in this case, the ability of MITF to supress PTEN could potentially play a role in driving melanocyte differentiation or specification of the melanocyte lineage during development.

mTORC1, downstream of PI3K, promotes cell growth partly through the phosphorylation of the protein synthesis regulators S6K1 and 4E-BP1 (Guertin and Sabatini 2007). Regulation of mTORC1 activity fits well with MITF's role in promoting proliferation and pigmentation which requires significant levels of protein synthesis.

However, although it seems likely that MITF can regulate PI3K and mTORC1 signalling, whether it regulates protein synthesis downstream remains unclear given the variability in the outcomes of the $^{35}$S-labelling experiments following depletion of MITF. Using siMITF(I), both an immunofluorescence approach estimating the incorporation of a fluorescently labelled puromycin analogue to newly synthesised proteins, as well as metabolic labelling, measuring translation through the quantification of incorporation of radiolabelled amino acids, indicated that translation was diminished on MITF depletion. However, this result was

not reproduced following MITF knock-down using four alternative siRNAs against MITF. These results tend to point to off-target effects of the siRNAs yielding variable results. Indeed, different MITF siRNAs also generated distinct cell morphologies, clearly distinguishable under the microscope (**Supplementary Figure A.6**). It seems that a (probably large) number of intracellular processes may be differentially affected by these siRNAs beyond the direct effects on MITF depletion and its consequences.

As discussed in section 3.5, the uncovering of the variability in the effects of different anti-MITF siRNAs underscores the importance of using several independent siRNAs to confirm any result obtained from gene-silencing experiments.

The said, we cannot rule out a role for MITF in promoting protein translation, a function that would be compatible with its known ability to drive proliferation determined by several laboratories using independent siRNAs. For example, it is possible that siMITF(I) has the fewest off-target effects and that the results obtained with the other anti-MITF siRNAs arise because of their off-target effects. Alternatively, some siRNAs mediating depletion of MITF may promote nuclear localisation of the MITF-related factors TFEB and TFE3 (Raben and Puertollano 2016) leading to some degree of compensation. Although this has been observed by other members of the laboratory (not shown), it seems unlikely given that three independent anti-MITF siRNAs all led to reproducible induction of PTEN and DEPTOR. Nevertheless, more reproducible results may be obtained in cells in which MITF, TFEB and TFE3 are knocked-out or knocked-down and complemented with an inducible MITF in which titration of MITF expression may be used to determine its effects on protein translation.

It is also possible that the nutrient rich culture conditions used in the experiments performed may prevent a potential effect on translation resulting from the increase in PTEN and DEPTOR on MITF knock-down from being evident.

Supporting this hypothesis, overexpression of DEPTOR in 501mel cells in the culture conditions used for previous experiments did not affect protein synthesis, as determined by immunofluorescence analysis of the incorporation of fluorescently labelled O-propargyl-puromycin (OPP) (**Supplementary Figure A.7**). Thus, although DEPTOR has been reported as a negative regulator of mTORC1 activity (Peterson et al. 2009), and by implication protein synthesis, we have not yet been able to confirm this in melanoma cells. Why overexpression of DEPTOR had no effect on translation in melanoma cells is not clear, but will require additional work to determine whether in fact it can regulate mTORC1 activity in the cells used.

In summary, while it is evident that MITF can regulate the expression of PTEN and DEPTOR, previously unsuspected targets of MITF, confirmation that downstream signalling pathways and cellular processes are also controlled by MITF awaits confirmation.

# Chapter 5 – Regulation of gene expression by ATF4

## 5.1. – Introduction

Activating transcription factor 4 (ATF4), a central player in the integrated stress response (ISR), is upregulated in response to nutrient deprivation (among other cellular stresses including inflammatory signalling and ER stress) (section 1.4), leading to downregulation of MITF (Pakos-Zebrucka et al. 2016; Falletta et al. 2017; Ferguson et al. 2017).

Both the sufficiency of ATF4 upregulation for transcriptional repression of MITF and the requirement of ATF4 for downregulation of MITF under glutamine or glucose starvation have been previously demonstrated (Falletta et al. 2017; Ferguson et al. 2017). However, whether the regulation of MITF by ATF4 is direct or not has yet to be established.

The correlation between low MITF and an invasive phenotype makes the elucidation of the mechanisms repressing its expression highly relevant and potentially targetable. So far, evidence points to a direct regulation of MITF by ATF4 through binding to the *MITF* promoter, as both glucose starvation and overexpression of ectopic ATF4 lead to a decrease in the activity of an *MITF* promoter-luciferase reporter (Falletta et al. 2017; Ferguson et al. 2017). However, overexpression assays can give artefactual results and although ATF4 can suppress the activity of the MITF promoter in co-transfection reporter assays, whether it does so in reality has not been established. Similarly, artificial upregulation of ATF4 under nutrient-rich non-stress conditions can also greatly increase the expression of the receptor tyrosine kinase AXL (Falletta et al. 2017). Since an MITF-low/AXL-high phenotype is a hallmark of drug-resistance in melanoma (Konieczkowski et al. 2014; Müller et al. 2014; Dugo et al. 2015), elucidating the mechanism of AXL regulation by ATF4 is also of crucial importance. Yet again, whether the regulation of AXL by ATF4 is direct or not, is yet to be established.

Finally, the inverse correlation between the expression of ATF4 and MITF in cells and the association of MITF low-expressing cells with an invasive phenotype led us to hypothesise a potential role of ATF4 in the repression of genes normally activated by MITF and possibly in the regulation of additional genes associated with invasiveness and melanoma de-differentiation.

## 5.2. – Genome-wide analysis of ATF4 binding in melanoma cells

To address the open questions related to the role of ATF4 in melanoma gene expression in response to stress, a chromatin immunoprecipitation followed by high throughput sequencing (ChIP-seq) analysis of endogenous ATF4 was performed in melanoma cells to determine the repertoire of ATF4 DNA-binding sites genome-wide.

501mel cells were first subjected to 4 h glucose starvation, which leads to upregulation of ATF4 expression as shown in **Figure 5.1**. Treatment with tunicamycin, an inducer of ER stress, was used as a positive control for the induction of ATF4 expression (**Figure 5.1**).

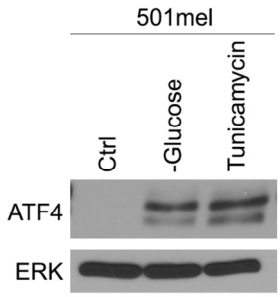


**Figure 5.1.- ATF4 protein levels increase upon glucose starvation in 501mel cells.** Western blot analysis of whole cell protein extracts from 501mel cells upon 4 h glucose starvation or 4 h treatment with 2.5 μg/ml tunicamycin. (Antibodies: α-ATF4 and α-ERK). ERK was used as a loading control.

Following glucose starvation, samples for ChIP-seq were generated in biological duplicates as described in section 2.5.4, using an antibody against endogenous ATF4 for the immunoprecipitation step. Finally, sequencing of the immunoprecipitated DNA was carried

out by the Oxford Genomics Centre (Wellcome Trust Centre for Human Genetics, University of Oxford).

Bioinformatic analysis of the raw data generated in this ChIP-seq experiment identified 76,163 ATF4 binding peaks (1 x $10^{-6}$ *Q* value cutoff) that were associated with 17,563 different genes for the first biological replicate (**Supplementary Table S.4.A** on Data CD), and 60,737 ATF4 binding peaks (1 x $10^{-6}$ *Q* value cutoff) assigned to 16,149 genes for the second biological replicate (**Supplementary Table S.4.B** on Data CD). The distribution of annotated peaks over the genome is shown in **Figures 5.2.A** and **B** for the first and second replicates of the experiment, respectively.

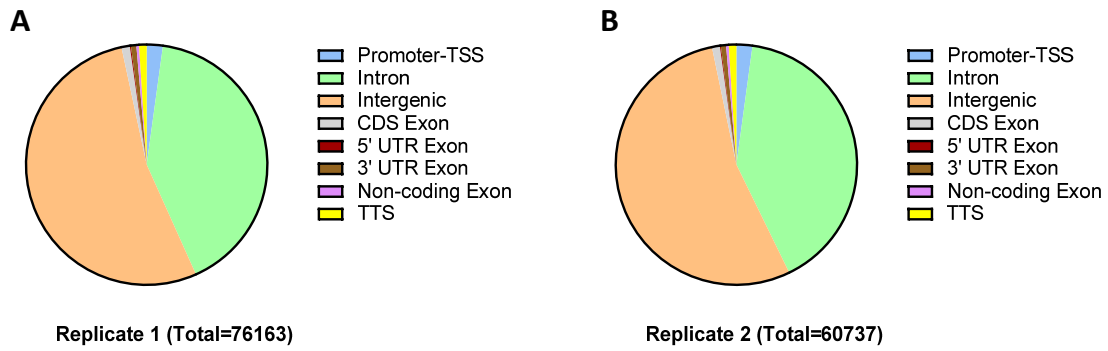


**Figure 5.2.- Distribution of peaks over the genome in ATF4 ChIP-seq experiment performed in glucose-starved 501mel cells.** The proportion of peaks annotated using HOMER to promoter-TSS (transcription start site) regions (defined as ±1kb from the TSS), introns, intergenic regions, CDS (coding sequence) exons, 5' UTR (untranslated region) exons, 3' UTR exons, non-coding exons, and TTS (transcription termination site) regions (defined as ±1kb from the TTS). **A)** In the first replicate of the experiment, 2.2% of the peaks were annotated to promoter-TSS regions, 41.1% to introns, 53.3% to intergenic regions, 1.1% to CDS exons, 0.1% to 5' UTR exons, 0.7% to 3' UTR exons, 0.4% to non-coding exons, and 1.0% to TTS regions. **B)** In the second replicate of the experiment, 2.1% of the peaks were annotated to promoter-TSS regions, 40.7% to introns, 53.9% to intergenic regions, 1.0% to CDS exons, 0.1% to 5' UTR exons, 0.7% to 3' UTR exons, 0.4% to non-coding exons, and 1.0% to TTS regions.

Annotated peaks in Supplementary Tables S.4.A and B are ranked by "peak score", which is defined as –log10(qvalue). For the first biological replicate, peak score was ≥ 100 for 19,291 peaks, between 100 and 50 (not inclusive) for 15,292 peaks, and ≤ 50 for 41,580 peaks. For the second biological replicate, peak score was ≥ 100 for 13,403 peaks, between

100 and 50 (not inclusive) for 12,310 peaks, and ≤ 50 for 35,024 peaks. It is highly unlikely that all the peaks detected will be productive in terms of transcriptional regulation. Work from Pakavarin Louphrasitthiphol in our laboratory has established that, at least for some transcription factors, such as MITF, a ChIP-seq peak score largely reflects its *in vitro* affinity for DNA (determined using fluorescence anisotropy), implying that in general, higher peak scores will reflect more stable binding and therefore will be more likely to be productive in terms of transcription output. However, while a high peak score suggests functionality, a proportion of these peaks may be non-productive. Indeed, it has been shown that DNA occupancy determined by conventional ChIP experiments, which presents a static picture without information regarding factor exchange, constitutes a poor estimation of functional regulation compared to analysis of DNA-binding dynamics (Lickwar et al. 2012). In this respect, two ChIP-seq peaks of the same height may reflect binding by the same factor with fundamentally different exchange rates (Lickwar et al. 2012). Thus, ChIP-seq peaks do not distinguish between long residence and fast binding turnover, associated with high and low transcriptional output, respectively (Lickwar et al. 2012). Therefore, to avoid using thresholds on the ChIP-seq dataset generated that cannot necessarily be justified, all peaks called were considered for further analysis in this study.

Analysis of the enrichment of motifs in the sequences underlying all called peaks (relative to random background control genomic sequences matched for GC-content) was performed using MEME-ChIP for *de novo* prediction of the ATF4 consensus binding site (Machanick and Bailey 2011). The resulting most significantly enriched consensus motif found is shown in **Figure 5.3**, which matches well previously described ATF4 binding motifs (Vinson et al. 1993; Hai and Hartman 2001; Gjymishka et al. 2008), and consequently was matched to ATF4 by MEME-ChIP.

| Motif | E-value | Best Match |
|---|---|---|
| 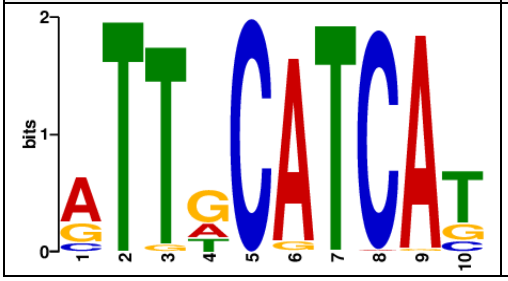 | $4 \times 10^{-11,812}$ | ATF4 |

**Figure 5.3.- Consensus ATF4 binding motif.** Top consensus binding motif discovered *de novo* through the analysis of the enrichment of motifs in the sequences underlying ATF4 peaks in the full ATF4 ChIP-seq dataset using MEME-ChIP (Machanick and Bailey 2011).

### 5.2.1. – ATF4 binding peaks are associated with known ATF4 target genes

To confirm that the ATF4 ChIP-seq experiment performed worked well and that solid hypotheses can therefore be generated from the data obtained, the presence of peaks associated with known ATF4 target genes was first examined as a positive control for the ChIP-quality. Prominent peaks were found associated with all known ATF4 target genes examined (Lin et al. 2010; Teske et al. 2011; Singleton and Harris 2012; B'chir et al. 2013; Brüning et al. 2013; Han et al. 2013; Crawford et al. 2015; Fusakio et al. 2016; Pakos-Zebrucka et al. 2016; Quirós et al. 2017; Wortel et al. 2017), as it is shown in **Table 5.1** (only details corresponding to the main peak associated with each gene and the first replicate of the experiment are included). **Figures 5.4**, **5.5**, **5.6** and **5.7** show UCSC screenshots of the peaks corresponding to the ATF4 target genes *DDIT3*, *DDIT4*, *ASNS*, and *CHAC1*, respectively, as examples. The ATF4 consensus binding site obtained in the MEME-ChIP analysis described above (Figure 5.3) was found under all major peaks associated with these ATF4 target genes and is represented for the peaks shown in Figures 5.4 to 5.7.

| Gene Name | Chromosome | Start | End | Peak Score | Annotation | Distance to TSS |
|---|---|---|---|---|---|---|
| SLC7A5 | chr16 | 87886990 | 87887784 | 733.14 | Intron | 15749 |
| WARS | chr14 | 100841637 | 100842335 | 693.25 | Promoter-TSS | -22 |
| DDIT3 | chr12 | 57914261 | 57914922 | 690.75 | Promoter-TSS | -297 |
| TARS | chr5 | 33440762 | 33441502 | 686.40 | Non-coding | 196 |
| DDIT4 | chr10 | 74032168 | 74033091 | 683.96 | Promoter-TSS | -980 |
| ASNS | chr7 | 97501400 | 97502108 | 680.06 | Promoter-TSS | 74 |
| CHAC1 | chr15 | 41245020 | 41245818 | 630.86 | Promoter-TSS | -209 |
| MARS | chr12 | 57881577 | 57882241 | 616.76 | 5’ UTR | 112 |
| SARS | chr1 | 109757198 | 109757969 | 607.76 | Non-coding | 1106 |
| TRIB3 | chr20 | 361311 | 361841 | 607.33 | Promoter-TSS | 300 |
| LARS | chr5 | 145572057 | 145572652 | 582.91 | Intergenic | -10093 |
| ATF6 | chr1 | 161734753 | 161735430 | 573.54 | Promoter-TSS | -893 |
| SESN2 | chr1 | 28575804 | 28576400 | 571.67 | Intergenic | -9859 |
| IARS | chr9 | 95055698 | 95056333 | 568.99 | Promoter-TSS | 50 |
| ATF3 | chr1 | 212781655 | 212782396 | 568.97 | Promoter-TSS | 66 |
| GARS | chr7 | 30634194 | 30634798 | 565.02 | 5’ UTR | 289 |
| PCK2 | chr14 | 24562899 | 24563555 | 551.02 | Promoter-TSS | -86 |
| CTH | chr1 | 70877686 | 70878316 | 542.06 | Intron | 1069 |
| XPOT | chr12 | 64798523 | 64799098 | 504.92 | Intron | 666 |
| PPP1R15A | chr19 | 49378338 | 49378849 | 441.01 | Intron | 2932 |
| ATG7 | chr3 | 11313822 | 11314341 | 414.12 | Promoter-TSS | 51 |
| ATF5 | chr19 | 50427444 | 50427987 | 380.20 | Intron | -4226 |
| VEGFA | chr6 | 43739452 | 43740024 | 258.28 | Promoter-TSS | 50 |
| P4HB | chr17 | 79818738 | 79819222 | 243.49 | Promoter-TSS | -421 |
| DDR2 | chr1 | 162602043 | 162602488 | 232.95 | Promoter-TSS | 46 |
| FGF21 | chr19 | 49276667 | 49277131 | 125.94 | Intergenic | 17575 |

**Table 5.1.- Major ATF4 binding peaks associated with known ATF4 target genes.** Details of the main peaks associated with known ATF4 target genes in the ATF4 ChIP-seq analysis performed in 501mel cells following 4 h glucose deprivation. Annotation was performed using HOMER, which defines promoter-TSS regions as those genomic regions comprising ±1kb from the TSS.

We therefore concluded that the ATF4 ChIP-seq experiment performed worked well and further analysis of the dataset generated will be performed throughout this study.

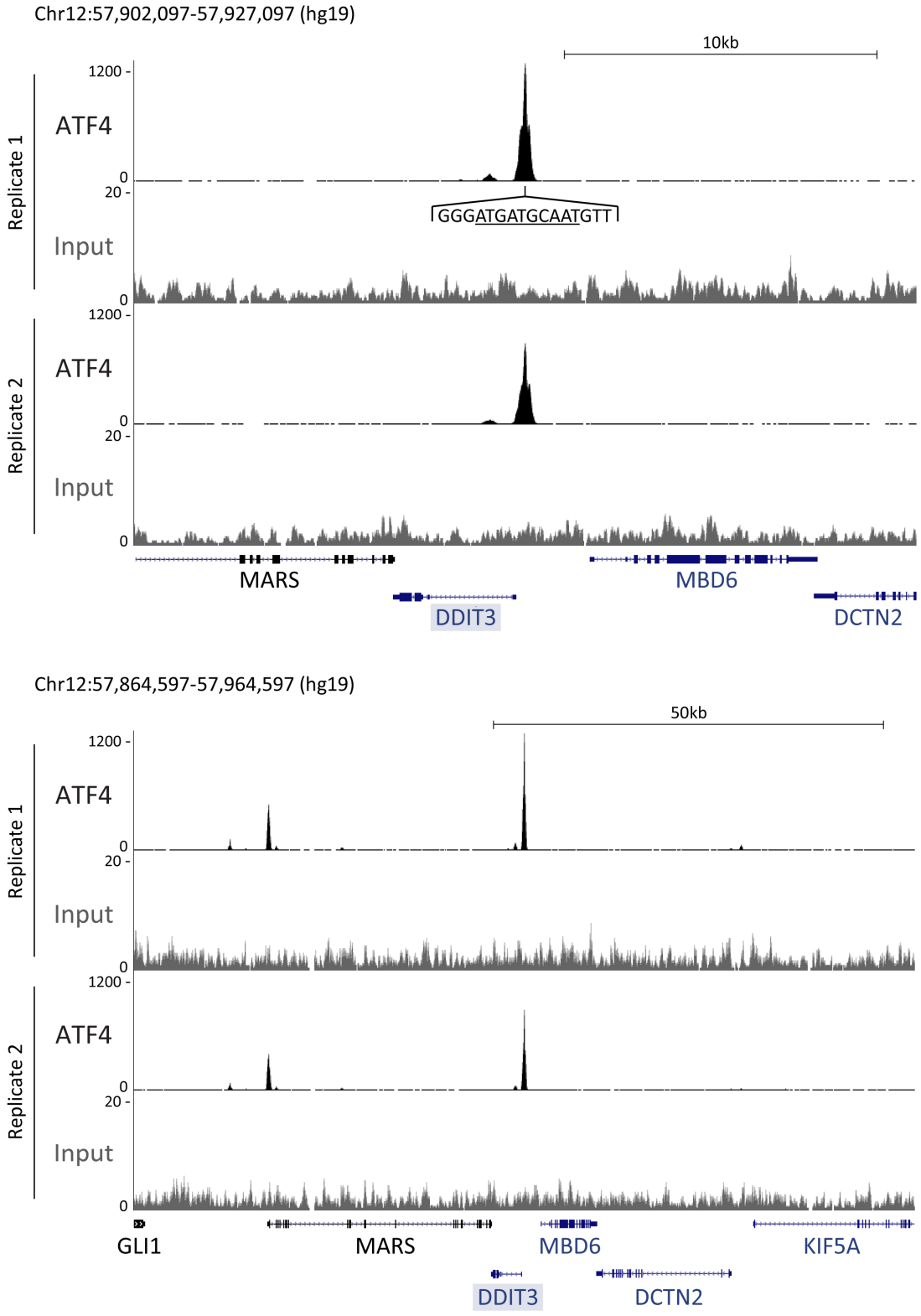


**Figure 5.4.- ATF4 binds the *DDIT3* promoter upon glucose starvation in 501mel cells. (Above)** ATF4 major ChIP-seq peak associated with *DDIT3*, a known ATF4 target gene, following 4 h glucose starvation in 501mel cells. The ATF4 binding motif found in the sequence underlying the peak is represented under the peak corresponding to the first replicate of the experiment. **(Below)** 4-fold zoom out of the genomic region represented above, showing binding in a larger genomic context.

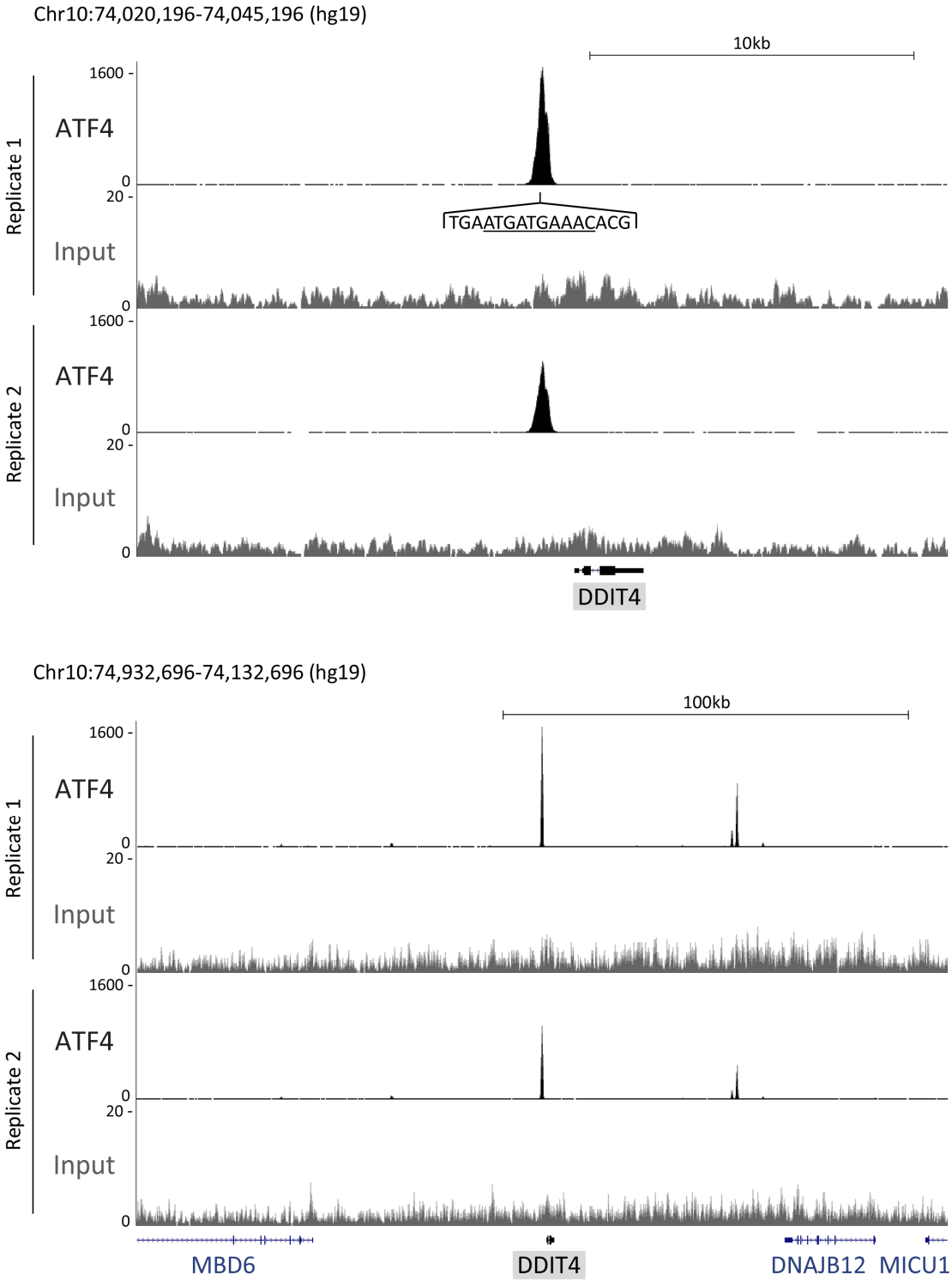


**Figure 5.5.- ATF4 binds upstream of *DDIT4* upon glucose starvation in 501mel cells. (Above)** ATF4 major ChIP-seq peak associated with *DDIT4*, a known ATF4 target gene, following 4 h glucose starvation in 501mel cells. The ATF4 binding motif found in the sequence underlying the peak is represented under the peak corresponding to the first replicate of the experiment. **(Below)** 8-fold zoom out of the genomic region represented above, showing binding in a larger genomic context.

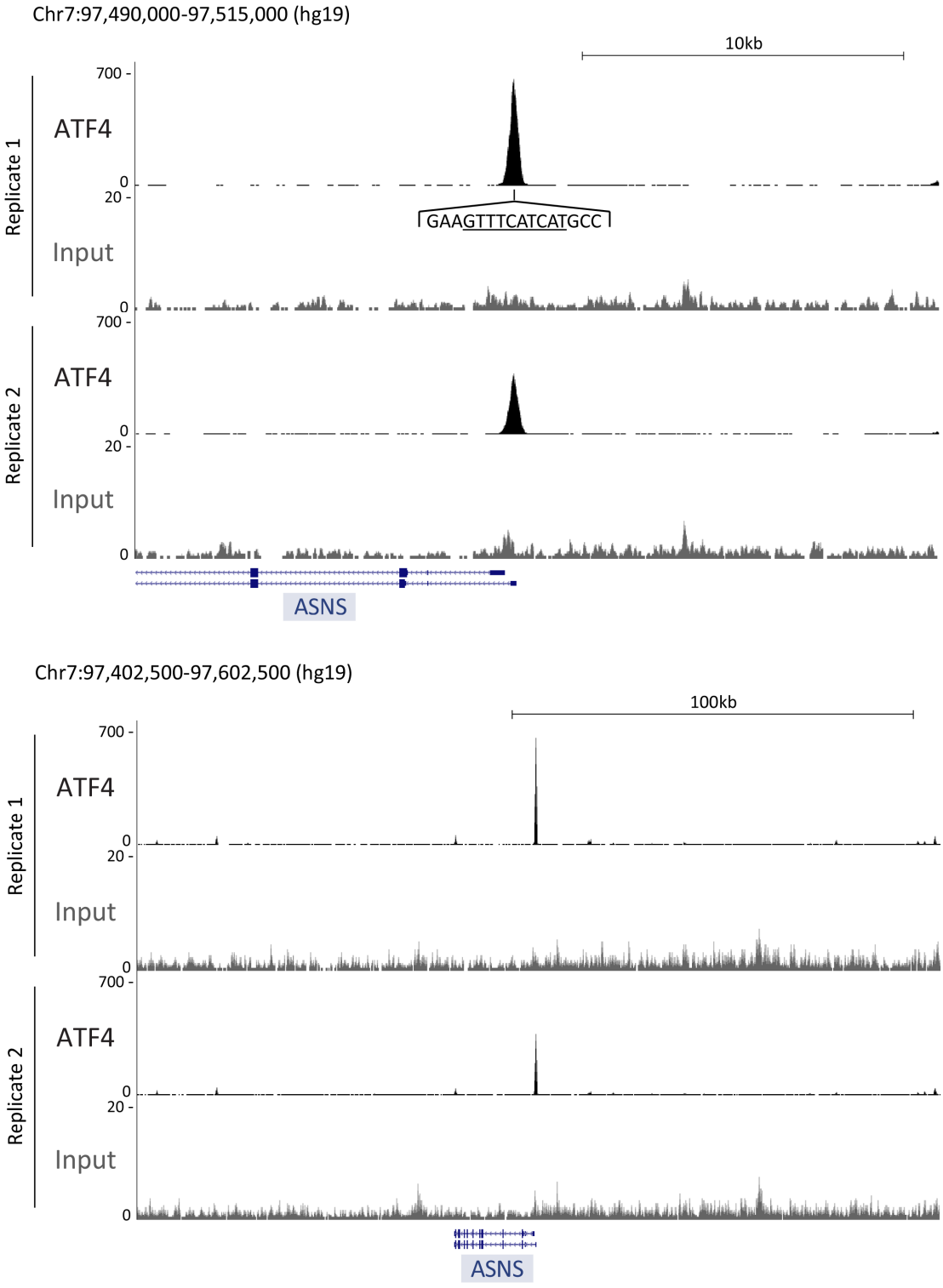


**Figure 5.6.- ATF4 binds the *ASNS* promoter upon glucose starvation in 501mel cells. (Above)** ATF4 major ChIP-seq peak associated with *ASNS*, a known ATF4 target gene, following 4 h glucose starvation in 501mel cells. The ATF4 binding motif found in the sequence underlying the peak is represented under the peak corresponding to the first replicate of the experiment. **(Below)** 8-fold zoom out of the genomic region represented above, showing binding in a larger genomic context.

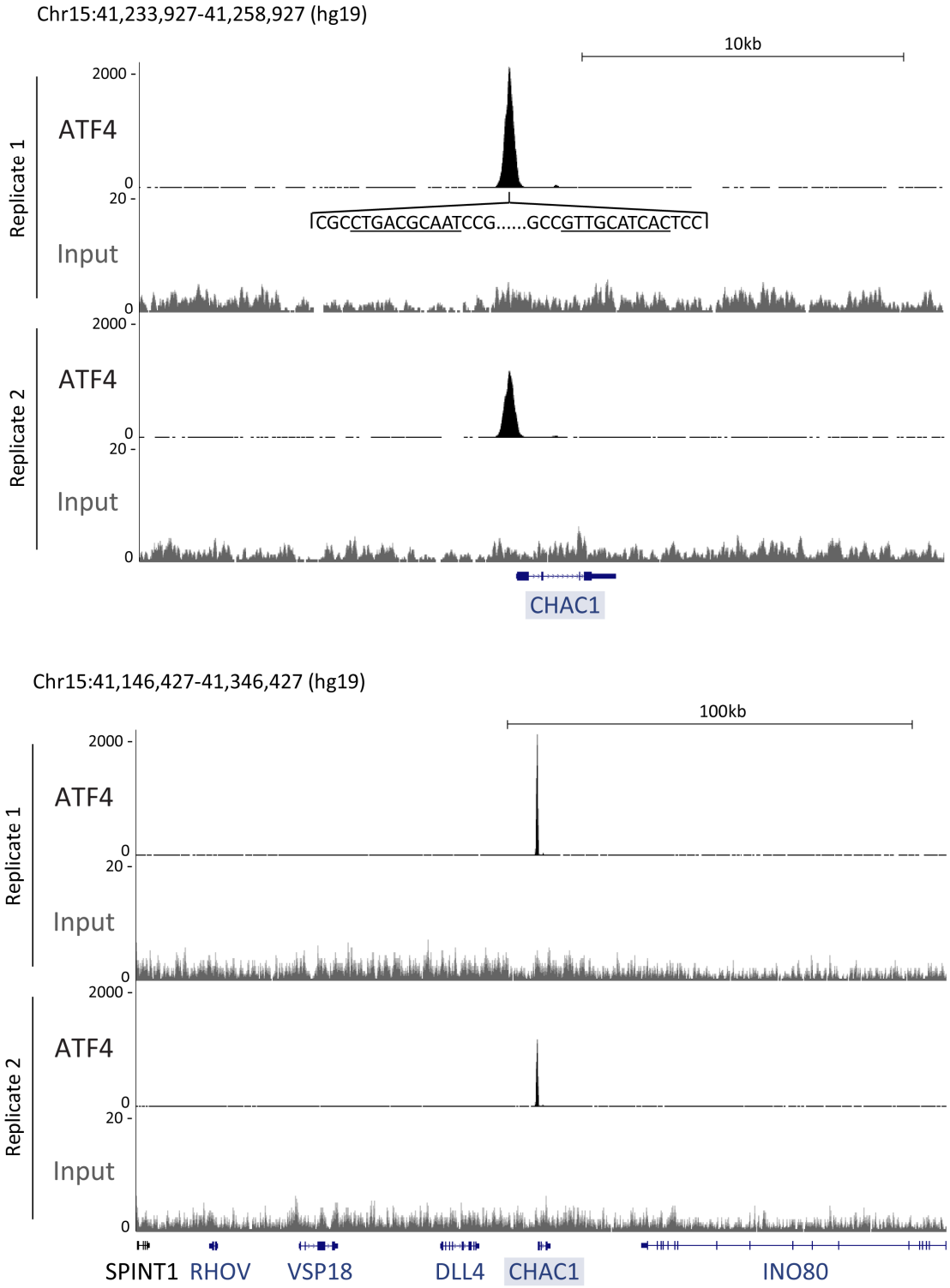


**Figure 5.7.- ATF4 binds upstream of *CHAC1* upon glucose starvation in 501mel cells. (Above)** ATF4 major ChIP-seq peak associated with *CHAC1*, a known ATF4 target gene, following 4 h glucose starvation in 501mel cells. The ATF4 binding motifs found in the sequence underlying the peak are represented under the peak corresponding to the first replicate of the experiment. **(Below)** 8-fold zoom out of the genomic region represented above, showing binding in a larger genomic context.

## 5.3. – Genome-wide analysis of ATF4 gene regulation in melanoma cells

Although ATF4 can be induced by natural stimuli, for example in response to glucose starvation, using a natural inducer we would not be able to distinguish between effects on gene expression mediated by ATF4 versus the effect of low glucose on non-ATF4 regulators. To facilitate identification of ATF4 targets, a human melanoma cell line stably expressing ATF4 under induction with doxycycline was generated, and subsequently a 3' RNA-seq experiment was performed in biological triplicate to measure differential gene expression genome-wide following ATF4 induction.

### 5.3.1. – Generation of a human melanoma cell line with inducible stable expression of HA-tagged ATF4 and the effect of the induction of ectopic ATF4 on MITF levels

To achieve controlled induction of ATF4 expression, a 501mel polyclonal cell line expressing ATF4 HA-tagged at the C-terminus (501mel-i-ATF4-HA) under induction with doxycycline was generated using the PiggyBac (PB) Transposon System described in section 2.3.5. Both an intermediary cell line obtained after the first round of antibiotic selection and the final 501mel-i-ATF4-HA cell line used for the remainder of this study were tested by immunofluorescence. As expected, induction of ATF4 for 48 h in the cell line at the early selection stage led to repression of MITF in those cells expressing the HA-tagged ATF4, as can be appreciated in **Figure 5.8**. Following completion of antibiotic selection, ATF4 expression was detected in the vast majority of cells comprising the final 501mel-i-ATF4-HA cell line (**Supplementary Figure A.8.A**). Examination of ATF4 levels in doxycycline-induced 501mel-i-ATF4-HA cells by western blot further validated the successful expression of the ATF4 construct and confirmed that changing the concentration of doxycycline altered the level of ATF4 expression (**Supplementary Figure A.8.B**).

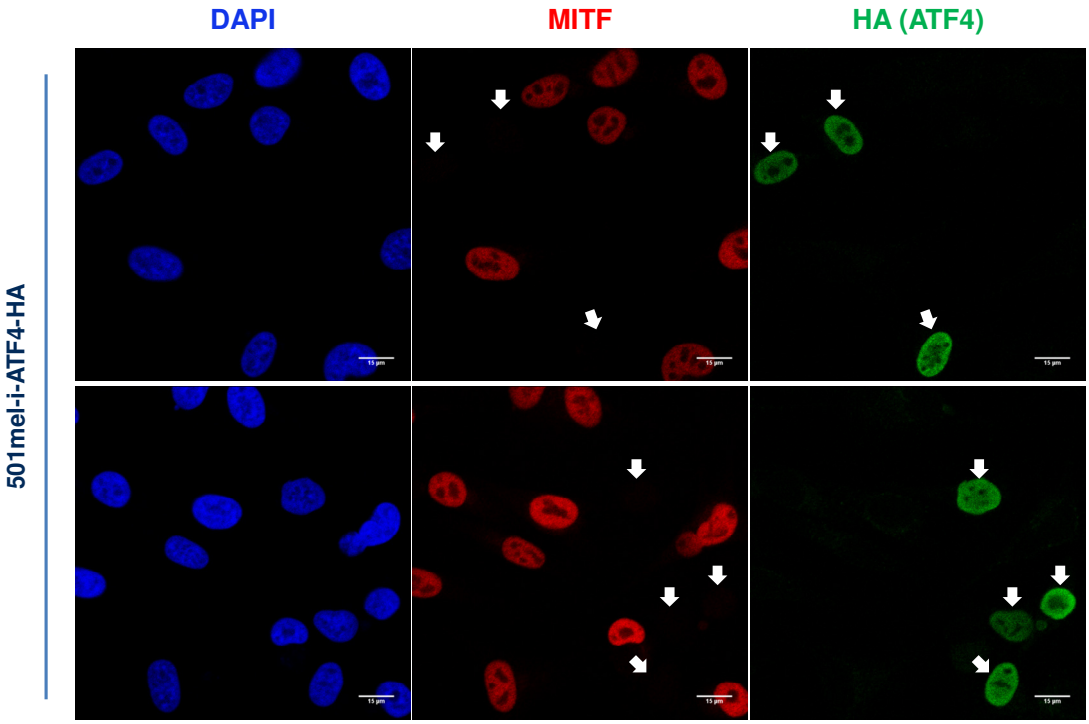


**Figure 5.8.- ATF4 overexpression leads to repression of MITF in 501mel cells.** Immunofluorescence analysis of ATF4 and MITF in 501mel-i-ATF4-HA cells after 48 h induction with 200 ng/ml doxycycline. 97.3 % ± 0.7 (SEM) of the HA-positive cells (marked with white arrows) were negative for MITF. (n=3, 100 HA-positive cells counted per experiment). (Antibodies: α-MITF and α-HA). Scale bars: 15 µm.

Furthermore, qRT-PCR and western blotting were used to further confirm the repression of MITF upon induction of ectopic ATF4 expression in the generated final cell line. For the study of mRNA levels, 501mel-i-ATF4-HA and 501mel control cells were treated with 5 or 20 ng/ml doxycycline for 0, 8 and 24 h. Subsequent qRT-PCR analysis showed a significant decrease in MITF mRNA levels for all concentrations of doxycycline and time points used (**Figure 5.9**). (No significant changes in MITF expression were observed following the equivalent doxycycline treatment in 501mel control cells (**Supplementary Figure A.9**)).

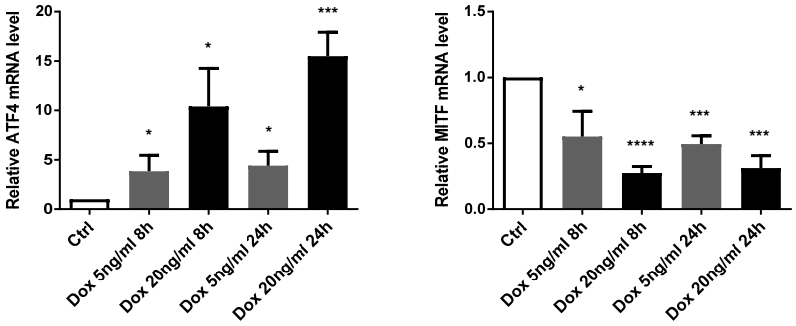


**Figure 5.9.- MITF mRNA levels decrease upon ATF4 overexpression in 501mel cells.** qRT-PCR analysis results for ATF4 and MITF mRNA levels in 501mel-i-ATF4-HA cells induced with 5 or 20 ng/ml doxycycline for 0, 8 and 24 h. (**** $P \leq 0.0001$, *** $P \leq 0.001$, * $P \leq 0.05$, n=3, data represent mean ± SEM).

Finally, western blot analysis of 501mel-i-ATF4-HA cells following treatment with 0, 5 or 20 ng/ml doxycycline for 24 h and 501mel control cells confirmed the downregulation of MITF upon ectopic ATF4 expression also at the protein level (**Figure 5.10**), associated with the expected downregulation of MITF mRNA levels determined by qRT-PCR. Treatment with tunicamycin was used as a positive control for the induction of ATF4 protein (**Figure 5.10.A**).

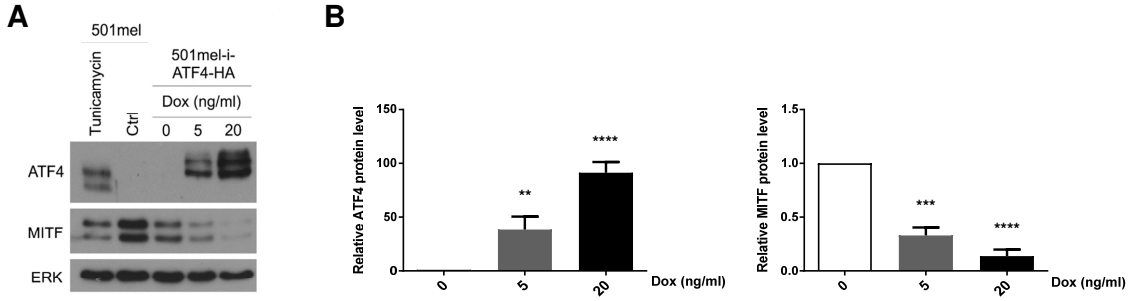


**Figure 5.10.- MITF protein levels decrease upon ATF4 overexpression in 501mel cells. (A)** Western blot analysis of whole cell protein extracts from 501mel control cells, 501mel cells upon 4 h treatment with 2.5 µg/ml tunicamycin (ATF4 positive control) and 501mel-i-ATF4-HA cells induced with 0, 5 or 20 ng/ml doxycycline for 24 h. (Antibodies: α-ATF4, α-MITF and α-ERK). ERK was used as a loading control. **(B)** Quantification of ATF4 and MITF levels detected in doxycycline-induced and non-induced 501mel-i-ATF4-HA cells in the western blot analysis shown in (B). (**** $P \leq 0.0001$, *** $P \leq 0.001$, ** $P \leq 0.01$, n=3, data represent mean ± SEM).

The gradual increase in ATF4 expression following treatment of 501mel-i-ATF4-HA cells with different levels of doxycycline and the resulting repression of MITF at the mRNA and protein levels confirms the validity of the generated cell line and the role of ATF4 as a repressor of MITF.

**5.3.2. – Induction of ATF4 induces extensive changes in genome-wide gene expression**

Having established that induction of ATF4 could repress MITF expression in a doxycycline-dependent fashion, RNA-seq analysis was performed in 501mel-i-ATF4-HA and 501mel cells following treatment with 20 ng/ml doxycycline for 8 and 24 h and the corresponding non-treated 501mel-i-ATF4-HA and 501mel control cells.

For the analysis of differentially expressed genes (DEGs), two comparisons were possible: induced 501mel-i-ATF4-HA cells versus the 501mel parental cell line lacking any ATF4 expression vector, or induced versus non-induced 501mel-i-ATF4-HA cells. Following the analysis of the generated raw data in both ways, some differential gene expression was noted between non-induced 501mel-i-ATF4-HA cells and the 501mel parental cell line, which might either arise as a consequence of some leaky expression of uninduced ATF4, or because of clonal variation, that is, comparison of any clonal derivative with the parental cell line would yield some differential gene expression owing to random variation in the genetic/epigenetic landscape of the derived cells. As ATF4 was not shown to be upregulated in non-induced 501mel-i-ATF4-HA cells versus 501mel control cells (Figure 5.10.A) and most differentially expressed genes did not appear to be ATF4 targets (as for comparison with the parallel analysis of induced versus non-induced 501mel-i-ATF4-HA cells), we considered it unlikely that leaky ATF4 expression was responsible for the differences in gene expression observed. By contrast, a personal communication from Pakavarin Louphraistthiphol, a member of the laboratory, raised the possibility that 501mel cells exhibit chromosome instability, as fluorescent in situ hybridisation of mitotic chromosome spreads in these cells showed a significant degree of chromosome rearrangements and duplications. Consequently, any 501mel derivative cell line might well exhibit a degree of differential gene expression owing to variations in genetic makeup. As such, the analyses presented in this study correspond to the comparison between non-induced 501mel-i-ATF4-HA cells and

501mel-i-ATF4-HA cells induced with 20 ng/ml doxycycline for 8 and 24 h. In order to control for the potential effect of doxycycline on gene expression, an equivalent analysis was also performed in 501mel cells treated with 20 ng/ml doxycycline for 8 and 24 h versus non-treated control 501mel cells.

Analysis of differentially expressed genes between doxycycline-induced and control 501mel-i-ATF4-HA cells showed upregulation of 682 genes and downregulation of 347 genes (FDR < 0.05) following induction of ATF4 expression for 8 h (**Figure 5.11.A** and **Supplementary Table S.5.A** on Data CD), and upregulation of 2,453 genes and downregulation of 1,948 genes (FDR < 0.05) upon induction of ATF4 expression for 24 h (**Figure 5.11.B** and **Supplementary Table S.5.B** on Data CD). Among the differentially expressed genes corresponding to the 8 h time point, the fold change was ≥ 2 for 483 and 164 of the upregulated and downregulated genes, respectively, and for the 24 h time point, the fold change was ≥ 2 for 1,494 and 689 of the upregulated and downregulated genes, respectively.

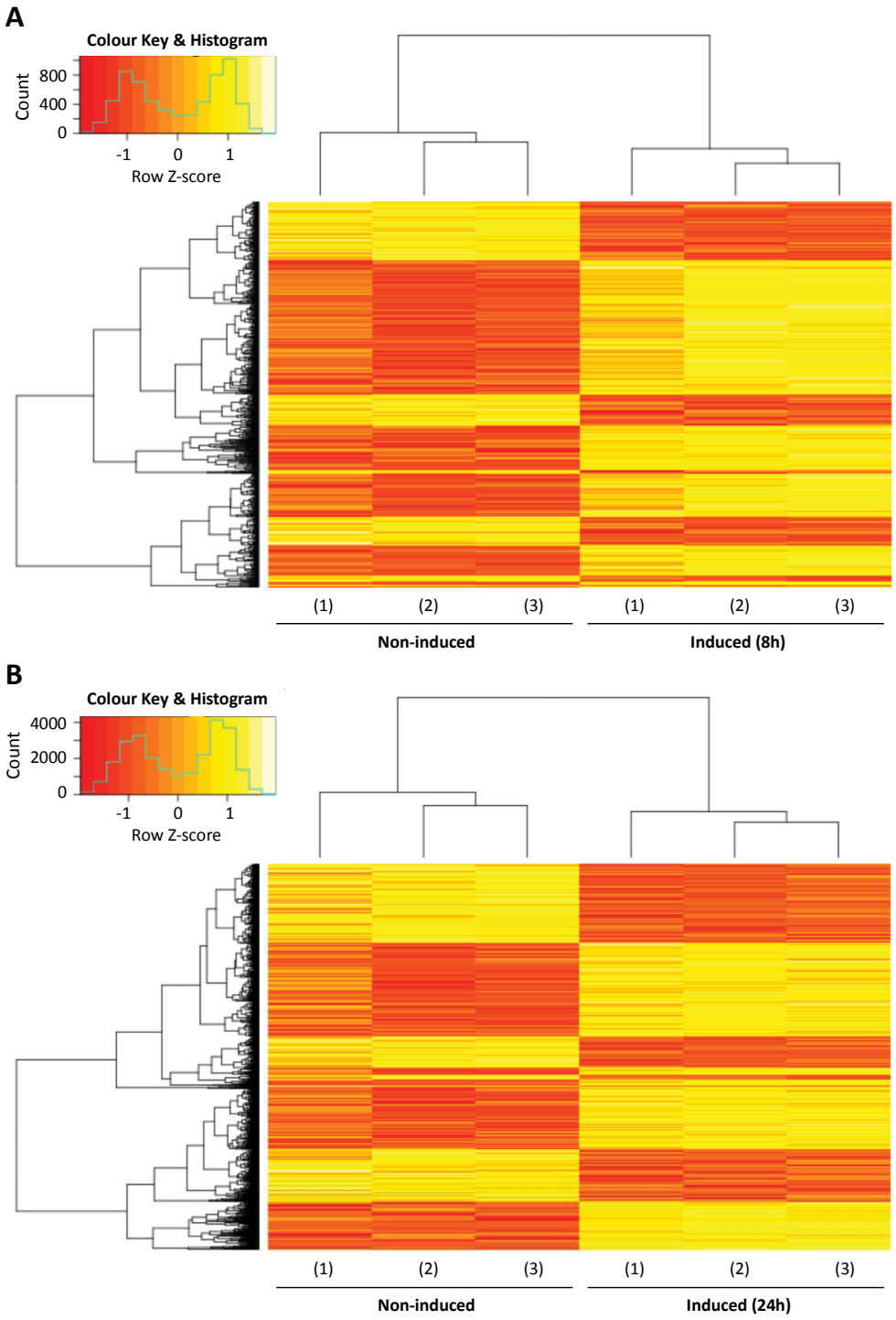


**Figure 5.11.- Heatmaps showing differential gene expression following ATF4 induction in 501mel cells. (A)** Heatmap representing colour-coded expression levels of DEGs (FDR < 0.05) following 8 h induction of ATF4 expression with 20 ng/ml doxycycline in 501mel-i-ATF4-HA cells versus non-induced control 501mel-i-ATF4-HA cells. In total, 1,029 genes were found to be differentially expressed (FDR < 0.05), from which 647 showed a fold change ≥ 2. **(B)** Heatmap representing colour-coded expression levels of DEGs (FDR < 0.05) following 24 h induction of ATF4 expression with 20 ng/ml doxycycline in 501mel-i-ATF4-HA cells versus non-induced control 501mel-i-ATF4-HA cells. In total, 4,401 genes were found to be differentially expressed (FDR < 0.05), from which 2,183 showed a fold change ≥ 2.

Regarding the 501mel control cells, 62 genes were upregulated and 18 genes were downregulated (FDR < 0.05) following 8 h doxycycline treatment (**Supplementary Figure A.10.A** and **Supplementary Table S.5.C** on Data CD), and 265 genes were upregulated and 62 genes were downregulated (FDR < 0.05) following 24 h doxycycline treatment (**Supplementary Figure A.10.B** and **Supplementary Table S.5.D** on Data CD). Among these differentially expressed genes, the fold change was ≥ 2 for 4 of the upregulated genes corresponding to the 8 h time point, and for 86 and 13 of the upregulated and downregulated genes corresponding to the 24 h time point, respectively.

We therefore concluded that ATF4 overexpression induces extensive changes in gene expression genome-wide and that doxycycline treatment exerts some effect on a restricted number of genes that will need to be taken into account.

### 5.3.3. – Induction of ATF4 leads to upregulation of known ATF4 target genes

To confirm that the ATF4 RNA-seq experiment performed worked well, changes in gene expression of known ATF4 target genes and ATF4 itself following induction of its expression were examined. An increase of around 2-fold was observed in ATF4 mRNA levels following doxycycline treatment of 501mel-i-ATF4-HA cells for 8 or 24 h, and consequently, most known ATF4 target genes were also differentially expressed in these cells versus non-induced 501mel-i-ATF4-HA cells (**Table 5.2** and **Supplementary Tables S.5.A** and **B** on Data CD). No significant changes were observed in the expression of any of these ATF4 target genes following doxycycline treatment in 501mel control cells (**Supplementary Tables S.5.C** and **D** on Data CD). However, a few known ATF4 target genes which were associated with binding peaks in the ATF4 ChIP-seq experiment (Table 5.1) were not significantly differentially expressed in this RNA-seq experiment. This might be because these genes are only regulated under specific cellular conditions that were not fulfilled in the experiment

performed, resulting in the absence of binding partners or other factors required for stable ATF4 binding to their genomic regulatory regions and functional regulation of the expression of these genes.

| | 8h Induction ATF4 | | 24h Induction ATF4 | |
|---|---|---|---|---|
| **Gene Name** | **Fold Change** | ***P* value** | **Fold Change** | ***P* value** |
| ATF4 | 1.92 | $2.78 \times 10^{-3}$ | 2.01 | $4.16 \times 10^{-10}$ |
| WARS | 1.91 | $3.30 \times 10^{-6}$ | 4.83 | $1.29 \times 10^{-36}$ |
| DDIT3 | 2.80 | $4.62 \times 10^{-6}$ | 3.54 | $3.73 \times 10^{-14}$ |
| TARS | 1.48 | $2.70 \times 10^{-3}$ | | |
| DDIT4 | 4.64 | $6.44 \times 10^{-9}$ | 6.10 | $5.29 \times 10^{-25}$ |
| ASNS | 4.08 | $1.41 \times 10^{-17}$ | 6.49 | $1.86 \times 10^{-43}$ |
| CHAC1 | 12.9 | $2.21 \times 10^{-15}$ | 23.2 | $1.15 \times 10^{-47}$ |
| SARS | 1.50 | $3.00 \times 10^{-3}$ | 1.70 | $3.05 \times 10^{-6}$ |
| TRIB3 | 4.99 | $3.08 \times 10^{-19}$ | 4.00 | $1.46 \times 10^{-22}$ |
| SESN2 | 22.9 | $6.32 \times 10^{-115}$ | 16.4 | $1.06 \times 10^{-74}$ |
| ATF3 | 8.10 | $1.31 \times 10^{-26}$ | 9.50 | $8.93 \times 10^{-34}$ |
| GARS | 2.61 | $1.26 \times 10^{-13}$ | 2.78 | $6.76 \times 10^{-19}$ |
| PCK2 | 4.86 | $3.72 \times 10^{-28}$ | 9.82 | $3.17 \times 10^{-60}$ |
| CTH | 14.0 | $9.03 \times 10^{-32}$ | 16.0 | $7.74 \times 10^{-56}$ |
| XPOT | 2.05 | $1.10 \times 10^{-4}$ | | |
| PPP1R15A | 2.16 | $2.06 \times 10^{-6}$ | 3.65 | $5.73 \times 10^{-19}$ |
| ATF5 | | | 2.58 | $8.82 \times 10^{-9}$ |
| VEGFA | 2.86 | $3.99 \times 10^{-11}$ | 3.49 | $7.21 \times 10^{-17}$ |
| P4HB | | | 1.46 | $7.60 \times 10^{-4}$ |
| DDR2 | 4.40 | $8.75 \times 10^{-6}$ | 10.1 | $7.24 \times 10^{-17}$ |
| FGF21 | | | 130.3 | $8.18 \times 10^{-12}$ |

**Table 5.2.- Known ATF4 target genes and ATF4 itself are upregulated following induction of ectopic ATF4 in 501mel cells.** Fold changes and associated *P* values corresponding to ATF4 and known ATF4 target genes extracted from the RNA-seq analysis of DEGs in 501mel-i-ATF4-HA cells induced with 20 ng/ml doxycycline for 8 or 24 h versus non-induced control 501mel-i-ATF4-HA cells.

Therefore, following the observation of the significant upregulation of ATF4 mRNA levels and most of its known target genes upon induction of ATF4 expression in 501mel cells, we concluded that the RNA-seq experiment performed worked well and proceeded with further analysis of the generated data.

### 5.3.4. – ATF4 mainly regulates processes involved in the integrated stress response

To investigate which of the differentially expressed genes upon the induction of ATF4 expression could potentially be regulated directly by ATF4, the previously generated glucose

starvation ATF4 ChIP-seq dataset (Supplementary Tables S.4.A and B on Data CD) was examined for the presence of binding peaks associated with these genes. For this analysis, only those differentially expressed genes (FDR < 0.05) with fold change ≥ 2 upon ATF4 expression and not showing any significant changes following doxycycline treatment in 501mel control cells were considered. Among these, a total of 508 and 1,463 genes were found to have associated ATF4 binding peaks in both replicates of the ChIP-seq experiment performed on glucose starvation conditions and were also differentially expressed (FDR < 0.05, fold-change ≥ 2) upon 8 h or 24 h induction of ATF4 expression, respectively (**Supplementary Tables S.6.A** and **B** on Data CD).

To obtain more information regarding the signalling pathways and biological processes regulated by ATF4 through a potentially direct mechanism, ontology analysis of the gene expression data filtered for ATF4-bound genes was performed using Enrichr (Chen et al. 2013a; Kuleshov et al. 2016). To ensure that only meaningful results were obtained, correlations were only considered when resulting from an overlap of five or more differentially expressed genes with the gene set of the correlated TF network, biological process or signalling pathway. Due to the vast majority of correlated processes falling below this threshold for the sets of ATF4-bound downregulated genes (FDR < 0.05, fold-change ≥ 2) upon ATF4 induction, only the results of the analyses of the gene sets corresponding to ATF4-bound upregulated genes (FDR < 0.05, fold-change ≥ 2) following 8 or 24 h induction of ATF4 expression (containing a total of 405 and 1,069 genes, respectively) are presented below.

As expected, analysis of correlations with TF-driven regulatory networks in the Transcriptional Regulatory Relationships Unraveled by Sentence-based Text mining (TRRUST) 2019 database (Han et al. 2018a) revealed the ATF4 network as the most significantly correlated one for the sets of ATF4-bound upregulated genes following both

time points of induction of ATF4 expression (**Table 5.3**). Additionally, the transcriptional regulatory networks of XBP1 and FOXO3, TFs with a key role in the response to ER stress and oxidative stress, respectively (Yoshida et al. 2001; Lee et al. 2003; Marinkovic et al. 2007; Sedding 2008), were also highly correlated (**Table 5.3**) presumably due to the activation of these signalling pathways resulting from the induction of ATF4, a central player in the ISR (section 1.4) (Singleton and Harris 2012; Wortel et al. 2017). Finally, HOXB7 is a homeodomain transcription factor that plays a role in proliferation and differentiation (Carè et al. 1999; De Souza Setubal Destro et al. 2010). However, no reports have to date linked it to ER stress, the UPR or ATF4 and it is unclear why a HOXB7 transcription program might be associated with up-regulation of ATF4 (**Table 5.3**).

| **Gene set: 8h Induction Ectopic ATF4 in 501mel cells – Upregulated genes** | | | | | |
|---|---|---|---|---|---|
| Index | Name | *P* value | Adjusted *P* value | Z-score | Combined score |
| 1 | ATF4 | 2.22E-12 | 6.96E-10 | -1.92 | 51.61 |
| 2 | FOXO3 | 3.48E-08 | 5.47E-06 | -2.38 | 40.90 |
| 3 | XBP1 | 3.06E-05 | 1.29E-03 | -2.73 | 28.42 |
| **Gene set: 24h Induction Ectopic ATF4 in 501mel cells – Upregulated genes** | | | | | |
| Index | Name | P value | Adjusted P value | Z-score | Combined score |
| 1 | ATF4 | 8.92E-11 | 1.83E-08 | -1.92 | 44.34 |
| 2 | FOXO3 | 1.76E-06 | 1.44E-04 | -2.36 | 31.24 |
| 3 | HOXB7 | 8.69E-05 | 3.95E-03 | -3.08 | 28.83 |

**Table 5.3.- Top correlated TF-driven networks for the sets of ATF4-bound genes upregulated following induction of ectopic ATF4 in 501mel cells.** Top three most correlated TF-driven networks from the TRRUST database ranked by EnrichR combined score (Kuleshov et al. 2016) revealed in the analysis of the sets of ATF4-bound genes upregulated upon induction with 20 ng/ml doxycycline for 8 or 24 h in 501mel-i-ATF4-HA cells versus non-induced control 501mel-i-ATF4-HA cells.

Analysis of correlations with biological processes in the Gene Ontology (GO) Biological Process 2018 database (Ashburner et al. 2000; The Gene Ontology Consortium 2019) mainly revealed the activation of processes involved in the ISR, including apoptosis, response to ER stress and PERK-mediated unfolded protein response (**Table 5.4**), in accordance with the central role of ATF4 in this cellular stress response pathway and the ability of ATF4, via

activation of DDIT3 expression, to promote apoptotic cell death (section 1.4) (Harding et al. 2003; Pakos-Zebrucka et al. 2016).

| **Gene set: 8h Induction Ectopic ATF4 in 501mel cells – Upregulated genes** | | | | | |
|---|---|---|---|---|---|
| Index | Name | *P* value | Adjusted *P* value | Z-score | Combined score |
| 1 | Positive regulation of neuron death | 9.37E-07 | 2.15E-03 | -2.05 | 28.43 |
| 2 | Positive regulation of response to endoplasmic reticulum stress | 1.68E-05 | 5.14E-03 | -2.31 | 25.41 |
| 3 | Liver development | 3.85E-05 | 6.22E-03 | -2.50 | 25.38 |
| 4 | Hepaticobiliary system development | 6.58E-05 | 7.19E-03 | -2.29 | 22.09 |
| 5 | Regulation of apoptotic process | 4.41E-06 | 2.53E-03 | -1.79 | 22.03 |
| 6 | Positive regulation of cell death | 2.09E-05 | 5.14E-03 | -2.03 | 21.91 |
| 7 | Apoptotic process | 2.20E-05 | 5.14E-03 | -2.03 | 21.75 |
| 8 | Regulation of transcription, DNA-templated | 1.02E-05 | 3.89E-03 | -1.83 | 21.04 |
| 9 | Regulation of endoplasmic reticulum stress-induced intrinsic apoptotic signalling pathway | 5.17E-04 | 6.59E-03 | -2.08 | 20.52 |
| 10 | PERK-mediated unfolded protein response | 3.74E-06 | 2.53E-03 | -1.63 | 20.35 |
| **Gene set: 24h Induction Ectopic ATF4 in 501mel cells – Upregulated genes** | | | | | |
| Index | Name | *P* value | Adjusted *P* value | Z-score | Combined score |
| 1 | Positive regulation of transcription from RNA polymerase II promoter | 3.60E-09 | 1.25E-05 | -1.90 | 36.91 |
| 2 | Serine family amino acid biosynthetic process | 1.58E-06 | 5.49E-04 | -2.30 | 30.75 |
| 3 | Positive regulation of transcription, DNA-templated | 4.17E-08 | 4.84E-05 | -1.71 | 29.11 |
| 4 | Regulation of apoptotic process | 2.15E-07 | 1.87E-04 | -1.79 | 27.43 |
| 5 | Regulation of transcription from RNA polymerase II promoter | 9.03E-09 | 1.57E-05 | -1.38 | 25.50 |
| 6 | Positive regulation of neuron death | 4.06E-06 | 1.01E-03 | -2.03 | 25.26 |
| 7 | Intrinsic apoptotic signalling pathway in response to endoplasmic reticulum stress | 3.23E-06 | 8.65E-04 | -2.00 | 25.23 |
| 8 | L-serine metabolic process | 7.64E-07 | 4.43E-04 | -1.71 | 24.05 |
| 9 | Negative regulation of transcription, DNA-templated | 1.48E-06 | 5.49E-04 | -1.75 | 23.52 |
| 10 | Regulation of transcription, DNA-templated | 9.01E-06 | 2.07E-03 | -1.81 | 21.07 |

**Table 5.4.- Top biological processes correlated with the sets of ATF4-bound genes upregulated following induction of ectopic ATF4 in 501mel cells.** Top ten most correlated biological processes from the GO Biological Process database ranked by EnrichR combined score (Kuleshov et al. 2016) revealed in the analysis of the sets of ATF4-bound genes upregulated upon induction with 20 ng/ml doxycycline for 8 or 24 h in 501mel-i-ATF4-HA cells versus non-induced control 501mel-i-ATF4-HA cells.

Analysis of correlations with signalling pathways from the Kyoto Encyclopedia of Genes and Genomes (KEGG) database (Kanehisa and Goto 2000; Kanehisa et al. 2017; Kanehisa et al. 2019) revealed the regulation of some amino acid metabolic pathways, in accordance with the role of ATF4 in the regulation of amino acid metabolism (Harding et al. 2003), as

well as the TNF signalling pathway, which can be activated by ATF4 (Chen et al. 2013b) (**Table 5.5**). IL-17 signalling and Th17 cell differentiation were also among the most correlated pathways following 8 h ATF4 induction (**Table 5.5**), which was unexpected considering previous studies suggesting a role of ATF4 and the amino acid starvation response in the suppression of Th17 cell differentiation and IL-17 production (Sundrud et al. 2009; Yang et al. 2013). However, it is possible that the apparent opposite regulation is due to the fact that melanoma cells are not necessarily an appropriate model for the study of mechanisms of Th17 differentiation, but rather some of the genes associated with Th17 differentiation happen to be regulated by ATF4 in melanoma. Additionally, toll-like receptor (TLR) signalling and osteoclast differentiation were among the most correlated processes (**Table 5.5**), in agreement with ATF4 acting as a mediator of the TLR-triggered immune response (Zhang et al. 2013a) and osteoclast differentiation (Cao et al. 2010). Similarly, NF-kappa B and TGF-β signalling were correlated with the gene set analysed (**Table 5.5**), according to the reported cross-talk between ATF4 and these signalling pathways (González-González et al. 2018; Schmitz et al. 2018). Finally, the correlation of the set of upregulated genes following ATF4 induction with some cancer pathways (**Table 5.5**) suggests that stresses leading to activation of ATF4 are associated with cancer progression.

We therefore conclude that ATF4 mainly regulates processes related to the adaptation to cellular stress conditions consistent with its key role in the ISR. The gene expression analysis also provides further evidence supporting the previously reported role of ATF4 in the activation of genes associated with TNF signalling, and suggests a potential role of ATF4 in the induction of a gene expression signature contributing to cancer progression. Note that gene sets associated with various cancers were likely identified since cancer progression is closely linked with stresses that drive ATF4 expression (García-Jiménez and Goding 2019).

| **Gene set: 8h Induction Ectopic ATF4 in 501mel cells – Upregulated genes** | | | | | |
|---|---|---|---|---|---|
| Index | Name | *P* value | Adjusted *P* value | Z-score | Combined score |
| 1 | TNF signalling pathway | 1.45E-05 | 9.66E-04 | -81.45 | 907.40 |
| 2 | RIG-I-like receptor signalling pathway | 1.37E-02 | 1.34E-01 | -91.45 | 392.24 |
| 3 | Small cell lung cancer | 2.82E-03 | 6.49E-02 | -66.80 | 392.14 |
| 4 | Colorectal cancer | 8.02E-03 | 9.36E-02 | -45.91 | 221.57 |
| 5 | IL-17 signalling pathway | 6.00E-04 | 2.42E-02 | -25.23 | 187.16 |
| 6 | Th17 cell differentiation | 2.17E-02 | 1.56E-01 | -47.63 | 182.40 |
| 7 | Toll-like receptor signalling pathway | 1.92E-02 | 1.42E-01 | -37.11 | 146.75 |
| 8 | Osteoclast differentiation | 4.37E-03 | 7.71E-02 | -25.58 | 139.02 |
| 9 | NF-kappa B signalling pathway | 1.28E-02 | 1.32E-01 | -26.41 | 115.21 |
| 10 | Prostate cancer | 7.93E-04 | 2.42E-02 | -15.34 | 109.52 |
| **Gene set: 24h Induction Ectopic ATF4 in 501mel cells – Upregulated genes** | | | | | |
| Index | Name | *P* value | Adjusted *P* value | Z-score | Combined score |
| 1 | Endometrial cancer | 2.17E-04 | 1.21E-02 | -302.24 | 2549.39 |
| 2 | Glycine, serine and threonine metabolism | 1.08E-03 | 1.89E-02 | -298.38 | 2037.91 |
| 3 | TNF signalling pathway | 7.53E-04 | 1.51E-02 | -72.89 | 524.15 |
| 4 | Basal cell carcinoma | 1.76E-03 | 2.60E-02 | -63.68 | 403.85 |
| 5 | Colorectal cancer | 6.22E-04 | 1.35E-02 | -48.57 | 358.58 |
| 6 | Alanine, aspartate and glutamate metabolism | 9.85E-03 | 7.33E-02 | -54.07 | 249.82 |
| 7 | Arginine and proline metabolism | 4.54E-02 | 1.76E-01 | -77.81 | 240.65 |
| 8 | Acute myeloid leukemia | 2.39E-02 | 1.20E-01 | -59.78 | 223.13 |
| 9 | Osteoclast differentiation | 4.30E-04 | 1.25E-02 | -27.22 | 210.98 |
| 10 | TGF-beta signalling pathway | 2.98E-03 | 3.18E-02 | -30.86 | 179.54 |

**Table 5.5.- Top signalling pathways correlated with the sets of ATF4-bound genes upregulated following induction of ectopic ATF4 in 501mel cells.** Top ten most correlated signalling pathways from the KEGG database ranked by EnrichR combined score (Kuleshov et al. 2016) revealed in the analysis of the sets of ATF4-bound genes upregulated upon induction with 20 ng/ml doxycycline for 8 or 24 h in 501mel-i-ATF4-HA cells versus non-induced control 501mel-i-ATF4-HA cells.

### 5.3.5. – ATF4 does not seem to regulate *AXL* at the transcriptional level

As previously mentioned, AXL is induced by glutamine starvation and inducible ATF4 upregulation in melanoma cells can lead to an increase in *AXL* expression (Falletta et al. 2017), which together with the repressive effect on MITF expression results in an *AXL*-high/*MITF*-low cell phenotype, characteristic of melanoma drug resistance (Müller et al. 2014; Falletta et al. 2017). To address the underlying mechanism of ATF4 regulation of AXL, the gene body and flanking genomic regions corresponding to this receptor tyrosine kinase were examined for ATF4 binding. While an ATF4 peak in the 5' region of *AXL* was called and associated with this gene in both replicates of the ChIP-seq experiment performed in

501mel cells following 4 h glucose starvation, and two other peaks located in *AXL* gene body were called in one of the replicates of the experiment, the peak height was very low for all of them (**Figure 5.12** and **Supplementary Tables S.4.A** and **B**), compared for example to those for known ATF4 targets (Figures 5.4-5.7), suggesting they may represent low affinity binding sites. Inspection of the area under these peaks located in the *AXL* gene body and 5' region however did lead to the identification of ATF4 binding sequences derived from the consensus motif represented in Figure 5.3 (**Figure 5.12**), and binding of some ATF4 binding partners including C/EBPβ, Fos, JUN and JUND to the genomic regions underlying these peaks has previously been described (Gerstein et al. 2012; Wang et al. 2012b; Wang et al. 2013b).

Examination of the changes in gene expression detected in the RNA-seq experiment performed following 8 or 24 h induction of ATF4 expression in 501mel-i-ATF4-HA cells, unexpectedly revealed no significant changes in AXL mRNA levels (Supplementary Tables S.5.A and B), suggesting that under the experimental conditions used the low ATF4 peaks detected in the ChIP-seq experiment were likely non-productive for transcription regulation. This was especially surprising due to the fact that the same melanoma cell line used in our RNA-seq experiment was used in the previous studies reporting AXL upregulation both at the mRNA and protein levels following ATF4 overexpression (Falletta et al. 2017). The differences in the results obtained in these experiments might however be the consequence of distinct levels of expression of ATF4 and possibly different timing of induction of ATF4 expression (not specified for previous reported qRT-PCR experiments) (Falletta et al. 2017).

Thus, although a potential direct regulation of *AXL* expression by ATF4 is possible, given the reduced peak heights compared to known ATF4 targets and our failure to reproduce changes in AXL mRNA expression on ATF4 induction we feel it is more likely that regulation of AXL by ATF4 is indirect and may occur at the protein level.

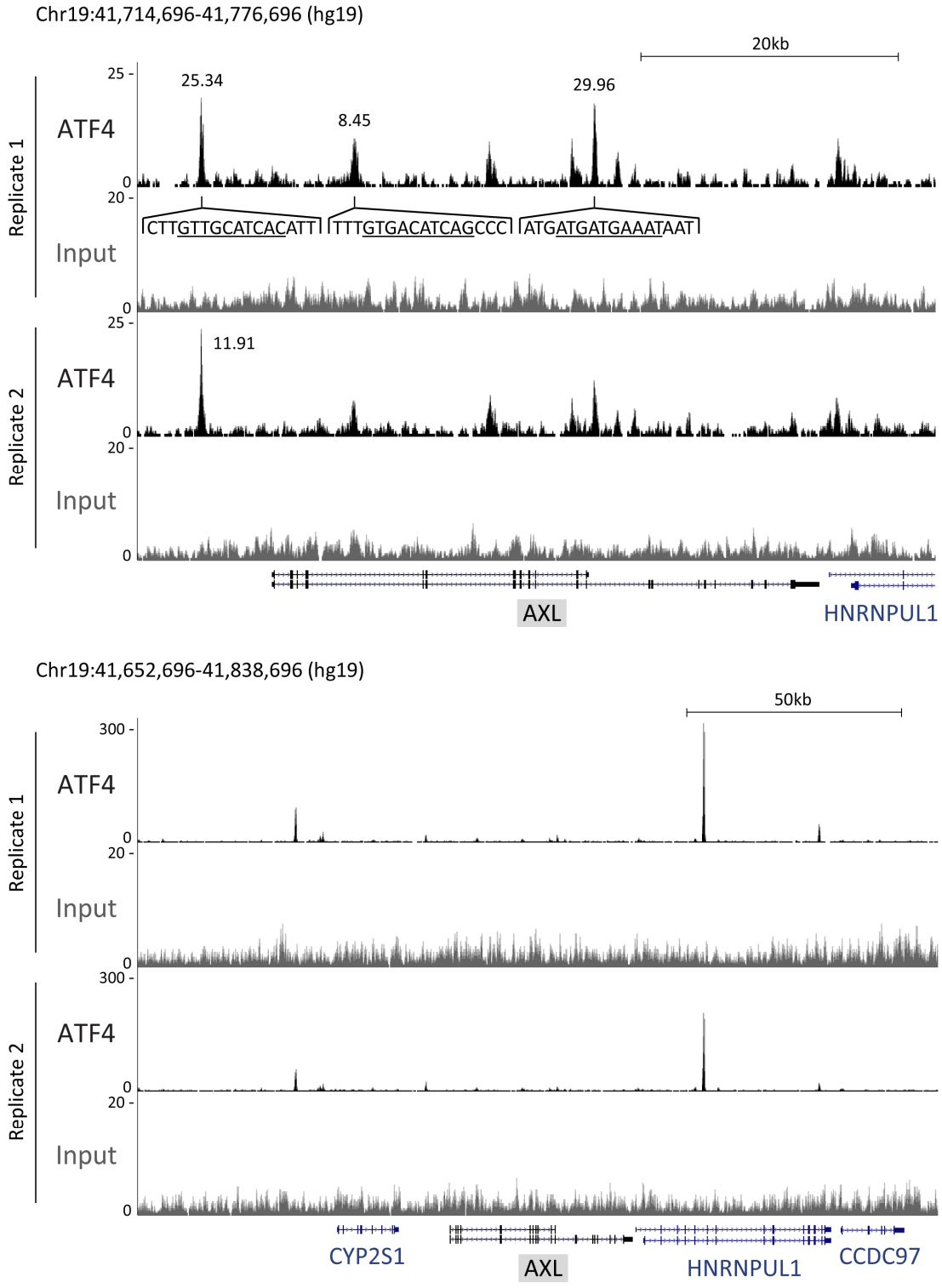


**Figure 5.12.- Only small ATF4 ChIP-seq peaks are associated with *AXL* upon glucose starvation in 501mel cells. (Above)** ATF4 ChIP-seq peaks located in the gene body and 5' region of *AXL* following 4 h glucose starvation in 501mel cells. Called peaks are marked with their associated peak score on top or by the peak. The ATF4 binding motif found in the sequence underlying called peaks is represented under the peaks corresponding to the first replicate of the experiment. **(Below)** 3-fold zoom out of the genomic region represented above, showing binding in a wider genomic context.

## 5.4. – Genome-wide analysis of gene regulation in glucose-starved cells

It has recently been suggested that nutrient starvation may constitute an inducer of cancer invasion (section 1.2.3.4) (Falletta et al. 2017; Rambow et al. 2018; García-Jiménez and Goding 2019). Particularly, glutamine deprivation has been shown to induce an invasive phenotype in melanoma cells with concomitant upregulation and downregulation of ATF4 and MITF expression, respectively (Falletta et al. 2017). Glucose deprivation constitutes another type of cellular stress leading to upregulation and downregulation of ATF4 and MITF expression, respectively, in melanoma cells (Ferguson et al. 2017). To investigate which other genes are regulated under conditions of glucose starvation genome-wide, a 3' RNA-seq experiment was performed in biological triplicate following 8 or 24 h glucose withdrawal from the cell culture medium in 501mel cells.

Analysis of differentially expressed genes in glucose-starved versus control 501mel cells showed upregulation of 1,367 genes and downregulation of 1,189 genes (FDR < 0.05) upon 8 h glucose deprivation (**Figure 5.13.A** and **Supplementary Table S.7.A**), and upregulation of 1,211 genes and downregulation of 1,042 genes (FDR < 0.05) following 24 h glucose deprivation (**Figure 5.13.B** and **Supplementary Table S.7.B**). Among the differentially expressed genes corresponding to the 8 h time point, the fold change was ≥ 2 for 603 and 334 of the upregulated and downregulated genes, respectively, and for the 24 h time point, the fold change was ≥ 2 for 302 and 72 of the upregulated and downregulated genes, respectively.

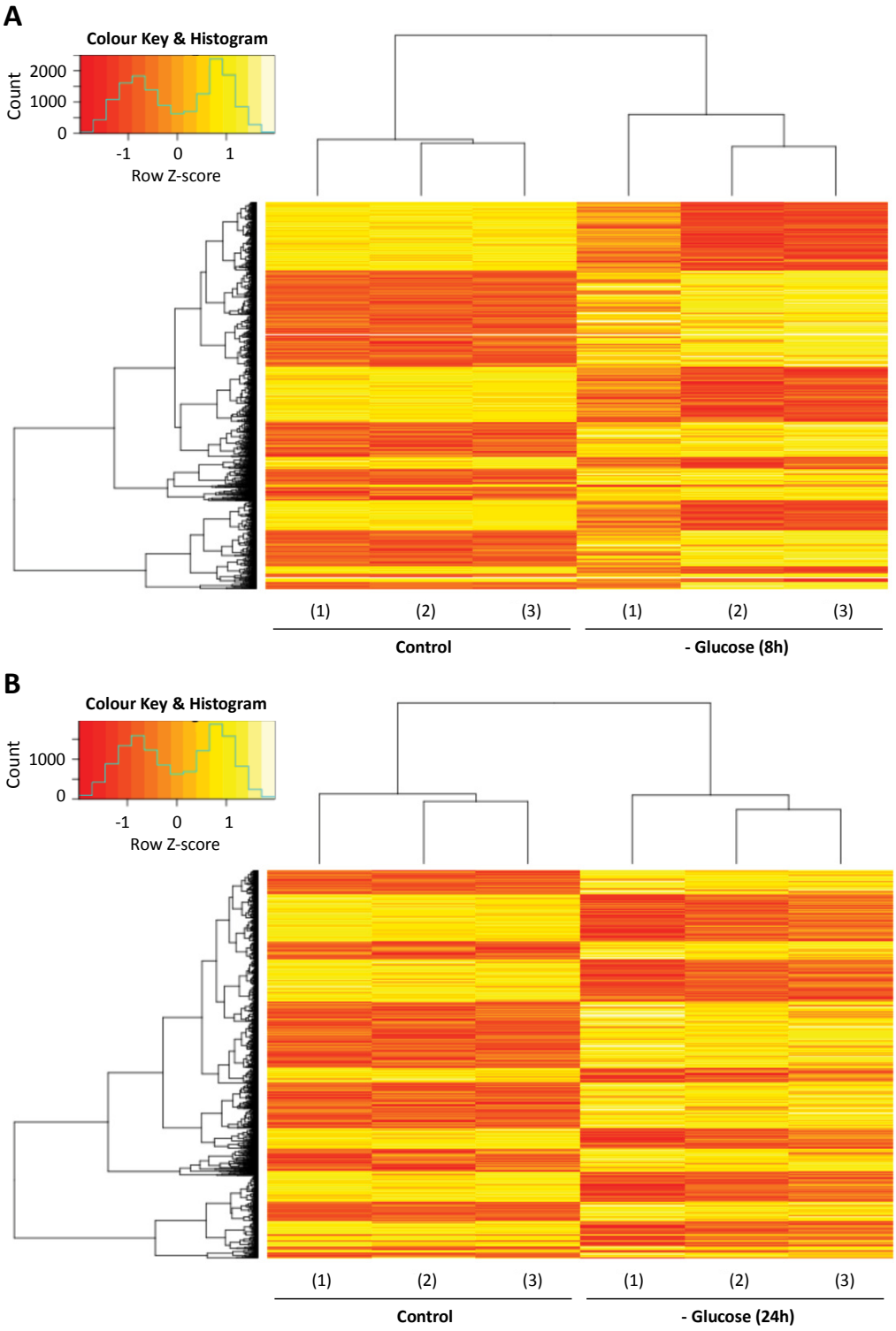


**Figure 5.13.- Heatmaps showing differential gene expression following glucose starvation in 501mel cells. (A)** Heatmap representing colour-coded expression levels of DEGs (FDR < 0.05) following 8 h glucose starvation in 501mel cells relative to control 501mel cells. In total, 2,556 genes were found to be differentially expressed (FDR < 0.05), from which 937 showed a fold change ≥ 2. **(B)** Heatmap representing colour-coded expression levels of DEGs (FDR < 0.05) following 24 h glucose starvation in 501mel cells relative to control 501mel cells. In total, 2,253 genes were found to be differentially expressed (FDR < 0.05), from which 374 showed a fold change ≥ 2.

### 5.4.1. – Glucose starvation leads to upregulation of known ATF4 target genes

To confirm that the glucose starvation RNA-seq experiment performed led to the expected upregulation of ATF4 and its known target genes, information regarding changes in gene expression levels corresponding to these genes was extracted from the DEG analysis presented above, bearing in mind that since translational regulation of ATF4 is a major mechanism of ATF4 induction in response to cellular stresses (Harding et al. 2000; Baird and Wek 2012), more significant changes in the expression of ATF4 will occur at the protein level. ATF4 and most of its known target genes examined were confirmed to be differentially expressed (FDR < 0.05) following 8 or 24 h glucose deprivation (**Table 5.6** and **Supplementary Tables S.7.A** and **B**).

| | 8h Glucose Starvation | | 24h Glucose Starvation | |
|---|---|---|---|---|
| **Gene Name** | **Fold Change** | ***P* value** | **Fold Change** | ***P* value** |
| ATF4 | 2.92 | $4.73 \times 10^{-21}$ | 1.97 | $6.26 \times 10^{-24}$ |
| WARS | 2.20 | $3.06 \times 10^{-10}$ | 2.09 | $1.85 \times 10^{-21}$ |
| DDIT3 | 5.44 | $4.62 \times 10^{-6}$ | 4.01 | $1.48 \times 10^{-34}$ |
| TARS | 1.37 | $5.34 \times 10^{-3}$ | | |
| DDIT4 | 7.21 | $1.37 \times 10^{-21}$ | 3.80 | $1.04 \times 10^{-28}$ |
| ASNS | 12.5 | $5.04 \times 10^{-82}$ | 6.48 | $4.91 \times 10^{-109}$ |
| CHAC1 | 5.12 | $2.49 \times 10^{-19}$ | 7.84 | $3.93 \times 10^{-73}$ |
| MARS | 1.80 | $7.03 \times 10^{-6}$ | 1.44 | $2.35 \times 10^{-8}$ |
| SARS | 3.28 | $1.45 \times 10^{-21}$ | 2.15 | $1.77 \times 10^{-31}$ |
| TRIB3 | 7.05 | $8.71 \times 10^{-37}$ | 2.26 | $1.11 \times 10^{-22}$ |
| ATF6 | 1.59 | $3.60 \times 10^{-4}$ | | |
| IARS | | | 1.41 | $1.23 \times 10^{-4}$ |
| SESN2 | 10.7 | $6.31 \times 10^{-63}$ | 6.34 | $1.48 \times 10^{-77}$ |
| ATF3 | 4.25 | $1.27 \times 10^{-7}$ | 4.37 | $2.16 \times 10^{-9}$ |
| GARS | 1.62 | $3.10 \times 10^{-26}$ | 2.78 | $6.63 \times 10^{-12}$ |
| PCK2 | 8.78 | $1.47 \times 10^{-46}$ | 4.42 | $7.92 \times 10^{-40}$ |
| CTH | 6.63 | $1.00 \times 10^{-33}$ | 2.78 | $3.44 \times 10^{-21}$ |
| XPOT | 1.61 | $5.39 \times 10^{-3}$ | 1.53 | $1.23 \times 10^{-3}$ |
| PPP1R15A | 5.72 | $1.59 \times 10^{-30}$ | 1.93 | $1.60 \times 10^{-8}$ |
| ATF5 | 1.90 | $2.30 \times 10^{-4}$ | | |
| DDR2 | 16.8 | $1.14 \times 10^{-8}$ | | |
| VEGFA | 3.29 | $1.26 \times 10^{-12}$ | 3.04 | $1.80 \times 10^{-15}$ |

**Table 5.6.- Known ATF4 target genes and ATF4 itself are upregulated under glucose starvation conditions in 501mel cells.** Fold changes and associated *P* values corresponding to ATF4 and known ATF4 target genes extracted from the RNA-seq analysis of DEGs in 501mel cells following 8 or 24 h glucose withdrawal from the cell culture medium versus control 501mel cells.

We therefore concluded that the RNA-seq experiment performed worked well and proceeded with further analysis of the generated data.

### 5.4.2. – ATF4 is a major effector in the cellular response to glucose starvation

To investigate which biological processes and signalling pathways are regulated in melanoma cells under glucose starvation conditions, ontology analysis of the sets of differentially expressed genes obtained in the glucose deprivation RNA-seq experiment with fold change ≥ 2 was performed using Enrichr (Chen et al. 2013a; Kuleshov et al. 2016). To ensure that only meaningful results were obtained, correlations were only considered when resulting from an overlap of five or more differentially expressed genes with the gene set of the correlated TF network, biological process or signalling pathway.

First, analysis of the sets of upregulated genes (FDR < 0.05, fold-change ≥ 2) following 8 or 24 h glucose deprivation in search of associated TF-driven regulatory networks revealed the ATF4 network as the most significantly correlated one (**Table 5.7**), meaning that the changes in gene expression characteristic of glucose-starved melanoma cells are to a great extent the result of the induction of ATF4 expression.

| **Gene set: 8h Glucose Starvation in 501mel cells – Upregulated genes** | | | | | |
|---|---|---|---|---|---|
| Index | Name | *P* value | Adjusted *P* value | Z-score | Combined score |
| 1 | ATF4 | 1.20E-11 | 3.44E-09 | -1.92 | 48.36 |
| 2 | SMAD3 | 2.79E-06 | 3.98E-04 | -2.42 | 30.93 |
| 3 | DDIT3 | 1.52E-04 | 8.67E-03 | -2.58 | 22.66 |
| **Gene set: 24h Glucose Starvation in 501mel cells – Upregulated genes** | | | | | |
| Index | Name | *P* value | Adjusted *P* value | Z-score | Combined score |
| 1 | ATF4 | 4.07E-08 | 8.71E-06 | -1.92 | 32.73 |
| 2 | SMAD3 | 9.35E-05 | 5.00E-03 | -2.39 | 22.22 |

**Table 5.7.- Top correlated TF-driven networks for the sets of upregulated genes upon glucose deprivation in 501mel cells.** Top most correlated TF-driven networks from the TRRUST database ranked by EnrichR combined score (Kuleshov et al. 2016) revealed in the analysis of the sets of upregulated genes following glucose deprivation for 8 or 24 h in 501mel cells.

Furthermore, a high correlation was observed with the SMAD3 transcriptional network, likely as a consequence of the cross-talk between ATF4 and SMAD3 signalling (González-

González et al. 2018), and with the transcriptional network of DDIT3, an ATF4 target and binding partner (Wortel et al. 2017).

Consequently, biological processes associated with ATF4 activation and the ISR such as cellular response to oxidative and ER stress and positive regulation of the apoptotic pathway in response to ER stress were among the most correlated in the analysis of these datasets against the GO Biological Process database (**Table 5.8**).

| **Gene set: 8h Glucose Starvation in 501mel cells – Upregulated genes** | | | | | |
|---|---|---|---|---|---|
| Index | Name | *P* value | Adjusted *P* value | Z-score | Combined score |
| 1 | Positive regulation of transcription from RNA polymerase II promoter in response to endoplasmic reticulum stress | 1.63E-05 | 9.78E-03 | -2.41 | 26.57 |
| 2 | Positive regulation of transcription from RNA polymerase II promoter in response to stress | 2.12E-06 | 5.10E-03 | -1.83 | 23.93 |
| 3 | Intrinsic apoptotic signalling pathway in response to endoplasmic reticulum stress | 6.55E-06 | 7.87E-03 | -2.00 | 23.92 |
| 4 | Cellular response to oxidative stress | 4.79E-05 | 1.92E-02 | -2.03 | 20.18 |
| 5 | Positive regulation of apoptotic process | 2.32E-05 | 1.11E-02 | -1.69 | 17.99 |
| **Gene set: 24h Glucose Starvation in 501mel cells – Upregulated genes** | | | | | |
| Index | Name | *P* value | Adjusted *P* value | Z-score | Combined score |
| 1 | Intrinsic apoptotic signalling pathway in response to endoplasmic reticulum stress | 3.15E-05 | 1.88E-02 | -2.00 | 20.78 |
| 2 | Positive regulation of transcription from RNA polymerase II promoter in response to stress | 7.94E-05 | 3.14E-02 | -1.83 | 17.28 |
| 3 | Intrinsic apoptotic signalling pathway | 1.58E-04 | 5.01E-02 | -1.77 | 15.50 |
| 4 | Positive regulation of protein complex assembly | 4.00E-04 | 1.06E-01 | -1.97 | 15.42 |
| 5 | Response to endoplasmic reticulum stress | 3.56E-05 | 1.88E-02 | -1.26 | 12.91 |

**Table 5.8.- Top biological processes correlated with the sets of genes upregulated upon glucose deprivation in 501mel cells.** Top five most correlated biological processes from the GO Biological Process database ranked by EnrichR combined score (Kuleshov et al. 2016) revealed in the analysis of the sets of upregulated genes following glucose deprivation for 8 or 24 h in 501mel cells.

Finally, analysis of the set of downregulated genes following 8 h glucose deprivation against the GO Biological Process database revealed a high correlation with processes related to DNA synthesis and repair and cholesterol biosynthesis (**Table 5.9**), which likely reflects the downregulation of proliferation under glucose starvation conditions or following induction of ATF4 (Falletta et al. 2017; Ferguson et al. 2017) and therefore a reduced need for DNA replication and synthesis of cellular membranes. Additionally, alcohol biosynthetic

processes were among the most correlated (**Table 5.9**), which might result from the lack of resources in glucose starvation conditions.

| Gene set: 8h Glucose Starvation in 501mel cells – Downregulated genes | | | | | |
|---|---|---|---|---|---|
| Index | Name | *P* value | Adjusted *P* value | Z-score | Combined score |
| 1 | Strand displacement | 7.52E-05 | 1.02E-02 | -2.58 | 24.53 |
| 2 | Secondary alcohol biosynthetic process | 3.12E-05 | 6.83E-03 | -2.04 | 21.18 |
| 3 | Regulation of alcohol biosynthetic process | 2.24E-05 | 6.83E-03 | -1.85 | 19.83 |
| 4 | Mismatch repair | 2.04E-04 | 2.10E-02 | -2.15 | 18.30 |
| 5 | Cholesterol biosynthetic process | 2.65E-05 | 6.83E-03 | -1.73 | 18.20 |

**Table 5.9.- Top biological processes correlated with the set of genes downregulated upon glucose deprivation in 501mel cells.** Top five most correlated biological processes from the GO Biological Process database ranked by EnrichR combined score (Kuleshov et al. 2016) revealed in the analysis of the set of downregulated genes following glucose deprivation for 8 h in 501mel cells.

No GO analysis was performed for the set of downregulated genes following 24 h glucose starvation due to the low number of genes contained in this gene set (< 100).

We therefore conclude that ATF4 is a major driver of the response to glucose starvation in melanoma cells and we will continue to investigate further processes and genes regulated in this nutrient limitation conditions that are potentially regulated by ATF4.

### 5.4.3. – ATF4 binds and regulates genes mainly involved in the integrated stress response under glucose starvation conditions

Since glucose starvation is a natural stimulus for the upregulation of ATF4 expression and we have seen that ATF4 is likely a main driver of the cellular response to glucose starvation, we wanted to investigate which genes are regulated by ATF4 through a potential direct mechanism in these cellular conditions.

Examination of the previously generated data on differentially expressed genes (FDR < 0.05, fold-change ≥ 2) following induction of ectopic ATF4 expression with associated ATF4 binding peaks in the glucose starvation ChIP-seq dataset (Supplementary Tables S.6.A and B) for genes that were also differentially expressed (FDR < 0.05, fold-change ≥ 2) following glucose deprivation (Supplementary Tables S.7.A and B), produced a new dataset of genes

directly bound and regulated by ATF4 under glucose starvation conditions (physiological stimulus) and upon induction of ectopic ATF4 expression (which allows for the selection of effects on gene regulation resulting from ATF4 expression) that were also bound in glucose starvation conditions (indicative of a potential direct mechanism of regulation) (**Supplementary Table B.2**). This analysis was performed without differentiating between time points of induction of ectopic ATF4 expression or glucose starvation, since the kinetics of ATF4 induction and regulation of genes are likely to vary between these conditions. As such, an independent intersection of ATF4-bound genes differentially expressed at specific time points following ectopic ATF4 expression or glucose starvation might have resulted in an unjustified loss of information.

In total, 257 ATF4-bound genes were differentially expressed (FDR < 0.05, fold-change ≥ 2) upon 8 h and/or 24 h induction of ectopic ATF4 expression and following 8 h and/or 24 h glucose starvation (Supplementary Table B.2). Among these, 163 and 45 genes were upregulated and downregulated, respectively, both upon induction of ectopic ATF4 expression and following glucose deprivation (highlighted in Supplementary Table B.2), 24 genes were upregulated upon induction of ectopic ATF4 expression and downregulated following glucose deprivation, and 25 genes were downregulated upon induction of ectopic ATF4 expression and upregulated following glucose deprivation.

Ontology analysis of the set of ATF4-bound genes upregulated both upon induction of ectopic ATF4 expression and following glucose deprivation, confirmed the expected correlation between this gene set and the ATF4-driven regulatory network in the TRRUST database (**Table 5.10**). Furthermore, a high correlation with the BRCA1 transcriptional network was revealed (**Table 5.10**), likely resulting from a cross-talk between ATF4 and BRCA1 signalling consequence of their roles in the regulation of oxidative stress (Lange et al. 2008; Yi et al. 2014). Finally, the transcriptional network of CEBPB, an ATF4 binding partner

(Podust et al. 2001; Tominaga et al. 2008; Jin et al. 2009; Cohen et al. 2015), was also among the most correlated TF-driven networks reflecting its cooperation with ATF4 in the transcriptional regulation of genes.

| **Gene set: Intersection Induction Ectopic ATF4 and Glucose Starvation in 501mel cells Upregulated genes** | | | | | |
|---|---|---|---|---|---|
| Index | Name | *P* value | Adjusted *P* value | Z-score | Combined score |
| 1 | ATF4 | 1.51E-13 | 2.70E-11 | -1.92 | 56.78 |
| 2 | BRCA1 | 1.01E-04 | 3.60E-03 | -1.82 | 16.75 |
| 3 | CEBPB | 1.29E-04 | 3.84E-03 | -1.83 | 16.35 |

**Table 5.10.- Top correlated TF-driven networks for the set of ATF4-bound genes upregulated following induction of ectopic ATF4 and upon glucose deprivation in 501mel cells.** Top three most correlated TF-driven networks from the TRRUST database revealed through Enrichr analysis of the set of ATF4-bound upregulated genes both following induction of ectopic ATF4 expression and upon glucose deprivation for 8 and/or 24 h in 501mel cells.

Consequently, many biological processes associated with ATF4 activation were identified in the analysis of this dataset against the GO Biological Process database using Enrichr, including response to endoplasmic reticulum stress, PERK-mediated unfolded stress response, and apoptotic signalling pathway (**Tables 5.11**). Moreover, a high correlation with response to insulin was also observed in this analysis (**Table 5.11**), and insulin resistance was revealed as one of the most correlated signalling pathways in the analysis of the same dataset against the KEGG database (**Table 5.12**), which is in accordance with previous studies suggesting a role of ATF4 in the regulation of insulin sensitivity (Yoshizawa et al. 2009; Zhang et al. 2013b).

The analysis of correlations with signalling pathways in the KEGG database also revealed p53 signalling as highly correlated (**Table 5.12**). While this is likely at least partly due to the cross-talk between ATF4 and p53 signalling, regulating common genes such as *SESN2*, *GADD45A*, *BBC3* and *PMAIP1* (Velasco-Miguel et al. 1999; Han et al. 2001; Zhan 2005; Jiang et al. 2007; Wang et al. 2009; Galehdar et al. 2010; Ebert et al. 2012; Brüning et al. 2013; Garaeva et al. 2016; Bagheri-Yarmand et al. 2019), a role of ATF4 in the stabilisation of p53 protein has also been reported (Horiguchi et al. 2013).

| **Gene set: Intersection Induction Ectopic ATF4 and Glucose Starvation in 501mel cells Upregulated genes** | | | | | |
|---|---|---|---|---|---|
| Index | Name | *P* value | Adjusted *P* value | Z-score | Combined score |
| 1 | Intrinsic apoptotic signalling pathway in response to endoplasmic reticulum stress | 4.16E-08 | 2.82E-05 | -2.00 | 34.06 |
| 2 | PERK-mediated unfolded protein response | 4.12E-08 | 2.82E-05 | -1.63 | 27.72 |
| 3 | Intrinsic apoptotic signalling pathway | 1.88E-06 | 6.36E-04 | -1.77 | 23.37 |
| 4 | Positive regulation of transcription from RNA polymerase II promoter in response to stress | 4.09E-06 | 9.24E-04 | -1.83 | 22.70 |
| 5 | Cellular response to glucose starvation | 7.78E-06 | 1.51E-03 | -1.62 | 19.09 |
| 6 | Regulation of apoptotic process | 3.84E-05 | 4.33E-03 | -1.77 | 18.04 |
| 7 | Response to endoplasmic reticulum stress | 2.70E-06 | 7.31E-04 | -1.26 | 16.15 |
| 8 | Response to insulin | 3.05E-04 | 1.91E-02 | -1.96 | 15.84 |
| 9 | Positive regulation of apoptotic process | 2.24E-04 | 1.69E-02 | -1.67 | 14.02 |
| 10 | Positive regulation of protein complex assembly | 8.09E-04 | 4.04E-02 | -1.94 | 13.83 |

**Table 5.11.- Top biological processes correlated with the set of ATF4-bound genes upregulated following induction of ectopic ATF4 and upon glucose deprivation in 501mel cells.** Top ten most correlated biological processes from the GO Biological Process database ranked by EnrichR combined score (Kuleshov et al. 2016) revealed in the analysis of the set of ATF4-bound upregulated genes both following the induction of ectopic ATF4 and upon glucose deprivation for 8 and/or 24 h in 501mel cells.

Finally, a high correlation with transcriptional misregulation in cancer was revealed (**Table 5.12**), again suggesting a potential association of cancer progression with cellular stress and ATF4 induction.

| **Gene set: Intersection Induction Ectopic ATF4 and Glucose Starvation in 501mel cells Upregulated genes** | | | | | |
|---|---|---|---|---|---|
| Index | Name | *P* value | Adjusted *P* value | Z-score | Combined score |
| 1 | Protein processing in endoplasmic reticulum | 2.36E-03 | 6.54E-02 | -23.90 | 144.60 |
| 2 | p53 signalling pathway | 3.05E-04 | 1.60E-02 | -7.49 | 60.63 |
| 3 | Insulin resistance | 1.92E-03 | 6.54E-02 | -7.17 | 44.88 |
| 4 | Apoptosis | 1.74E-04 | 1.60E-02 | -5.18 | 44.84 |
| 5 | Transcriptional misregulation in cancer | 4.25E-03 | 8.24E-02 | -3.10 | 16.93 |

**Table 5.12.- Top signalling pathways correlated with the set of ATF4-bound genes upregulated following induction of ectopic ATF4 and upon glucose deprivation in 501mel cells.** Top ten most correlated signalling pathways from the KEGG database ranked by EnrichR combined score (Kuleshov et al. 2016) revealed in the analysis of the set of ATF4-bound upregulated genes both following the induction of ectopic ATF4 and upon glucose deprivation for 8 and/or 24 h in 501mel cells.

No GO analysis of the ATF4-bound downregulated genes upon induction of ectopic ATF4 expression and following glucose deprivation was performed due to the small size of the dataset (< 100).

### 5.4.4. – Identification of ATF4 target genes in melanoma

Following further inspection of the new generated set of ATF4-bound genes differentially expressed upon both induction of ectopic ATF4 and glucose starvation (**Supplementary Table B.2**), we highlight a number of specific genes suggesting they may play a role in melanoma biology under the stress conditions leading to ATF4 induction. However, in all cases, binding by ATF4 is only indicative of direct regulation. Confirmation that ATF4 does indeed directly regulate the genes identified will await genome editing to inactivate the ATF4 binding sites identified, combined with assays to assess responsiveness on ATF4 induction.

#### 5.4.4.1. – ATF4 binds and regulates *HOXB9* under glucose starvation conditions

Homeobox B9 (*HOXB9*) is a transcription factor involved in the regulation of developmental processes which has been reported to promote metastasis in breast and colon cancer and associate with poor survival in colon cancer patients (Hayashida et al. 2010; Huang et al. 2014b). A study recently performed in human T cells showed how *HOXB9* expression is induced under amino acid deprivation conditions through a mechanism mediated by ATF4 (Hayashi et al. 2016). This study suggested a potential direct regulation of *HOXB9* by ATF4 following the location of an ATF4 binding motif around 350 kb upstream from *HOXB9* translation start site (Hayashi et al. 2016). Here we show that *HOXB9* is also upregulated upon 8 or 24 h of glucose starvation (fold change 9.78 and 5.63, *P* value 1.78 x $10^{-16}$ and 3.45 x $10^{-17}$, respectively) as well as following 8 h ectopic ATF4 overexpression in melanoma cells (fold change 3.28, *P* value 7.48 x $10^{-4}$) (Supplementary Table B.2), and confirm the binding of ATF4 to the previously identified binding motif in *HOXB9* promoter region (**Figure 5.14**).

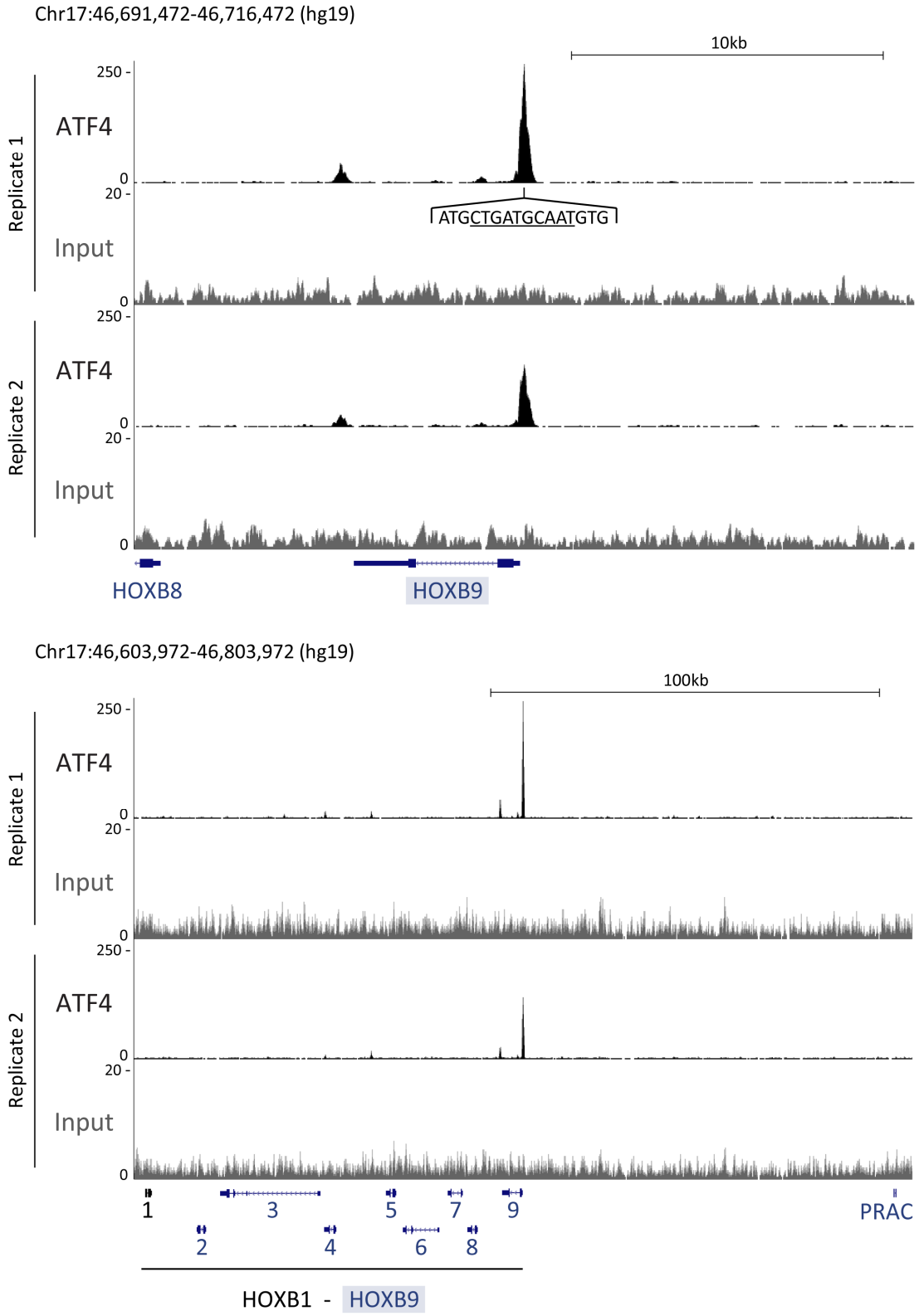


**Figure 5.14.- ATF4 binds the *HOXB9* promoter upon glucose starvation in 501mel cells. (Above)** ATF4 major ChIP-seq peak associated to *HOXB9* following 4 h glucose starvation in 501mel cells. The ATF4 binding motif found in the sequence underlying the peak is represented under the peak corresponding to the first replicate of the experiment. **(Below)** 8-fold zoom out of the genomic region represented above, showing binding in a wider genomic context.

While an increase in *HOXB9* mRNA levels following 24 h induction of ATF4 expression in 501mel-i-ATF4-HA cells was also observed (fold change 3.12, *P* value 8.70 x $10^{-8}$) (Supplementary Table S.5.B on Data CD), the change in *HOXB9* mRNA levels also upon 24 h doxycycline treatment in 501mel control cells (fold change 2.31, *P* value 7.81 x $10^{-4}$) (Supplementary Table S.5.D), prevented us from considering this upregulation as a sole result of ATF4 expression and therefore was not taken into account.

However, the increase in *HOXB9* expression following both time points of glucose starvation and 8 h ectopic ATF4 overexpression, and the confirmed binding to *HOXB9* promoter suggests that a direct mechanism of regulation of HOXB9 by ATF4 is highly likely. Further research will be needed to confirm this mechanism of regulation and whether the likely *HOXB9* regulation by ATF4 plays any role in the process of melanoma metastasis in response to nutrient deprivation.

5.4.4.2. – ATF4 binds and regulates *HERPUD1* under glucose starvation conditions

Homocysteine-inducible ER protein with ubiquitin-like domain 1 (Herpud1) is an ER resident membrane protein involved in the transport of ubiquitinated substrates for proteasomal degradation (Kokame et al. 2000; Okuda-Shimizu and Hendershot 2007; Huang et al. 2014a). Furthermore, Herpud1 has been shown to play a cytoprotective role, with knock-down of *HERPUD1* expression resulting in increased susceptibility to ER stress and oxidative stress induced apoptosis (Chan et al. 2004; Hori et al. 2004; Nogalska et al. 2006; Shinozaki et al. 2013; Paredes et al. 2016).

ATF4 induces the expression of *HERPUD1* under amino acid deprivation or ER stress conditions, and can bind to an C/EBP-ATF composite motif in the *HERPUD1* promoter as previously demonstrated by others through electrophoretic mobility assays (Ma and Hendershot 2004).

Here we show that *HERPUD1* expression is also increased in glucose starvation conditions (fold change 1.93 and 2.53, *P* value 1.41 x $10^{-6}$ and 2.25 x $10^{-36}$, respectively, for the 8 and 24 h time points) as well as following ectopic ATF4 overexpression in melanoma cells (fold change 3.41 and 3.65, *P* value 4.13 x $10^{-16}$ and 9.11 x $10^{-16}$, respectively, for the 8 and 24 h time points) (Supplementary Table S.7.A on Data CD and Supplementary Table B.2), and confirm the binding of ATF4 to the previously identified binding motif in *HERPUD1* promoter region (**Figure 5.15**).

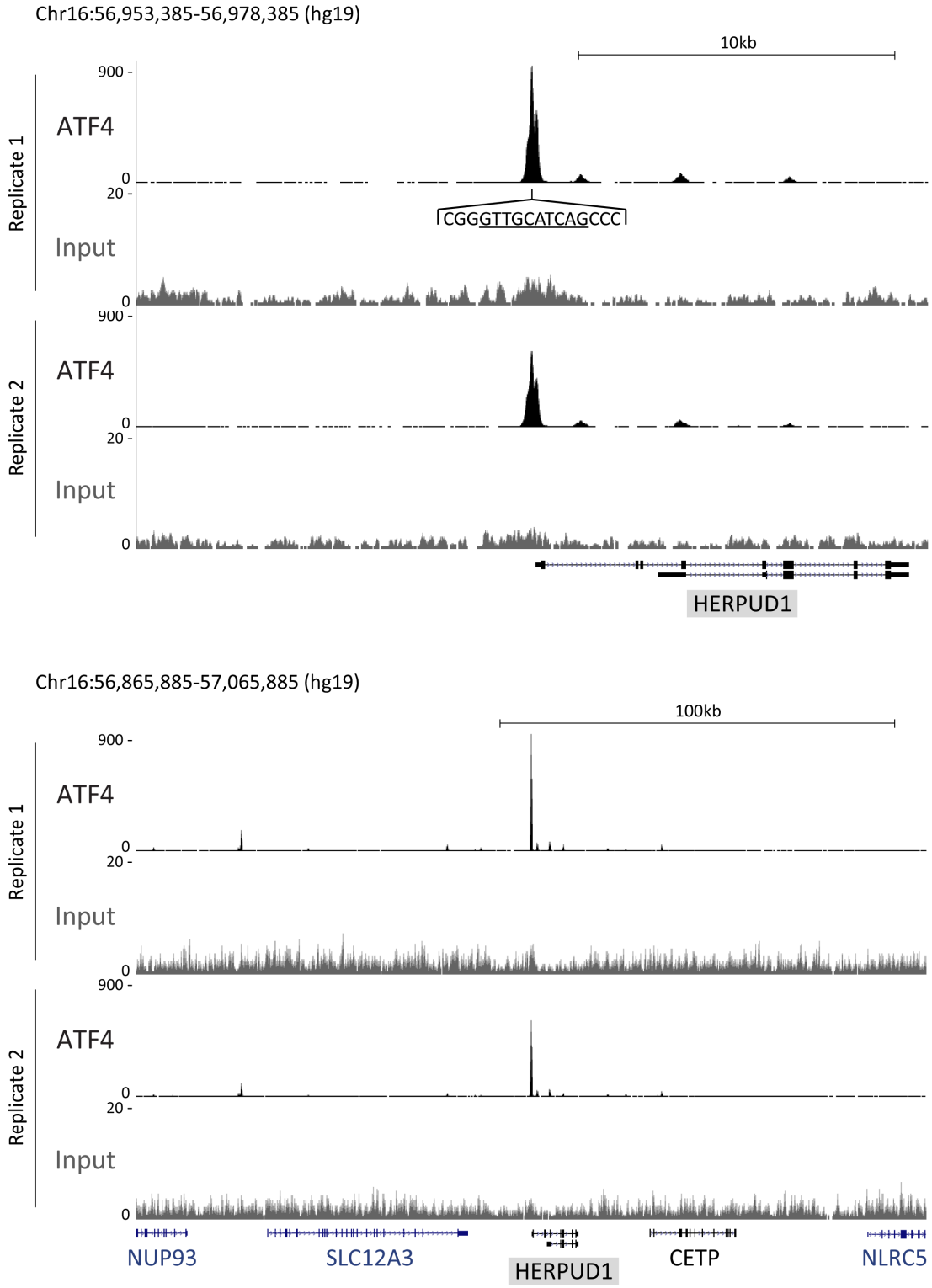


**Figure 5.15.- ATF4 binds the *HERPUD1* promoter upon glucose starvation in 501mel cells. (Above)** ATF4 major ChIP-seq peak associated with *HERPUD1* following 4 h glucose starvation in 501mel cells. The ATF4 binding motif found in the sequence underlying the peak is represented under the peak corresponding to the first replicate of the experiment. **(Below)** 8-fold zoom out of the genomic region represented above, showing ATF4 binding in a wider genomic context.

5.4.4.3. – ATF4 binds and regulates *S100P* under glucose starvation conditions

S100P belongs to the superfamily of $Ca^{2+}$ binding proteins S100, which are mediators of $Ca^{2+}$ dependent signalling and are mainly involved in the modulation of cell differentiation, metabolism, cell cycle and growth (Becker et al. 1992; Donato 2001). S100P promotes growth, cell migration and invasion in a variety of cancers, including pancreatic cancer, lung cancer, nasopharyngeal carcinoma, and endometrial cancer (Arumugam et al. 2005; Whiteman et al. 2007; Hsu et al. 2015; Jiang et al. 2016; Liu et al. 2017). Moreover, knock-down of S100P can inhibit colon cancer growth and metastasis (Jiang et al. 2011).

A role of ATF4 in the positive regulation of S100P has previously been reported, and a direct mechanism of regulation involving binding of ATF4 to a consensus binding site in the *S100P* promoter has been suggested (Namba et al. 2009; Maruyama et al. 2016). Here, we confirm the upregulation of *S100P* expression upon 8 or 24 h ectopic ATF4 expression or 8 h glucose limitation in melanoma cells (fold change 25.1 and 231.7, *P* value $9.66 \times 10^{-79}$ and $1.53 \times 10^{-201}$, respectively, for the 8 and 24 h time points of ectopic ATF4 induction; fold change 3.36, *P* value $7.93 \times 10^{-4}$, for the 8 h time point of glucose deprivation) (Supplementary Table B.2). However, no ATF4 binding to the *S100P* promoter region was observed under glucose limitation conditions (**Figure 5.16**). Instead, ATF4 showed binding to the 3' region of S100P (**Figure 5.16**).

We therefore provide further evidence supporting the regulation of *S100P* expression by ATF4 but suggest a different potential mechanism of transcriptional regulation.

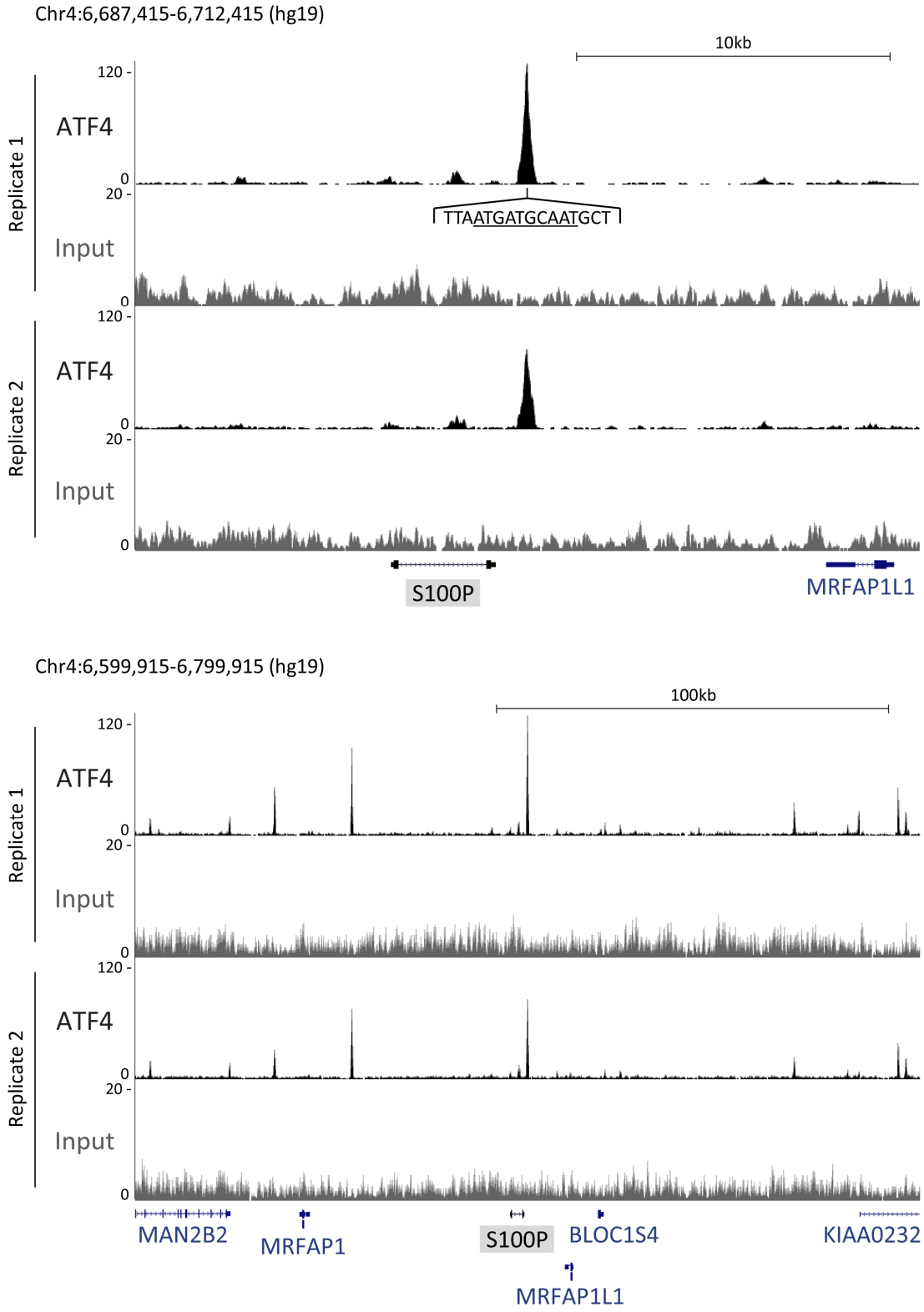


**Figure 5.16.- ATF4 binds the *S100P* 3' region upon glucose starvation in 501mel cells. (Above)** ATF4 major ChIP-seq peak associated with *S100P* following 4 h glucose starvation in 501mel cells. The ATF4 binding motif found in the sequence underlying the peak is represented under the peak corresponding to the first replicate of the experiment. **(Below)** 8-fold zoom out of the genomic region represented above, showing ATF4 binding in a wider genomic context.

5.4.4.4. – ATF4 binds and regulates *CLIC4* under glucose starvation conditions

The redox-regulated chloride intracellular channel 4 (CLIC4) is an integral member of the TGF-β signalling pathway through its function preventing dephosphorylation of nuclear Smad2/3, which is also upregulated by TGF-β (Shukla et al. 2009; Shukla and Yuspa 2010). Likely as a consequence of the dual role of TGF-β as a tumour suppressor and in the promotion of cancer invasion (Massagué 2008; Giampieri et al. 2010), CLIC4 has also been reported as a tumour suppressor in cutaneous squamous cell carcinoma (Suh et al. 2012), and high expression of CLIC4 in cancer stroma has been associated to enhanced tumour invasiveness and progression (Shukla et al. 2014).

Here we show that *CLIC4* expression is also increased in glucose starvation conditions (fold change 3.16 and 2.04, *P* value $5.36 \times 10^{-22}$ and $2.32 \times 10^{-17}$, respectively, for the 8 and 24 h time points) as well as following ectopic ATF4 overexpression (fold change 2.33 and 2.39, *P* value $2.34 \times 10^{-8}$ and $1.54 \times 10^{-8}$) in melanoma cells (Supplementary Table B.2), and provide evidence for the binding of ATF4 to the *CLIC4* gene under glucose starvation conditions (**Figure 5.17**), which suggest a potential direct mechanism of regulation.

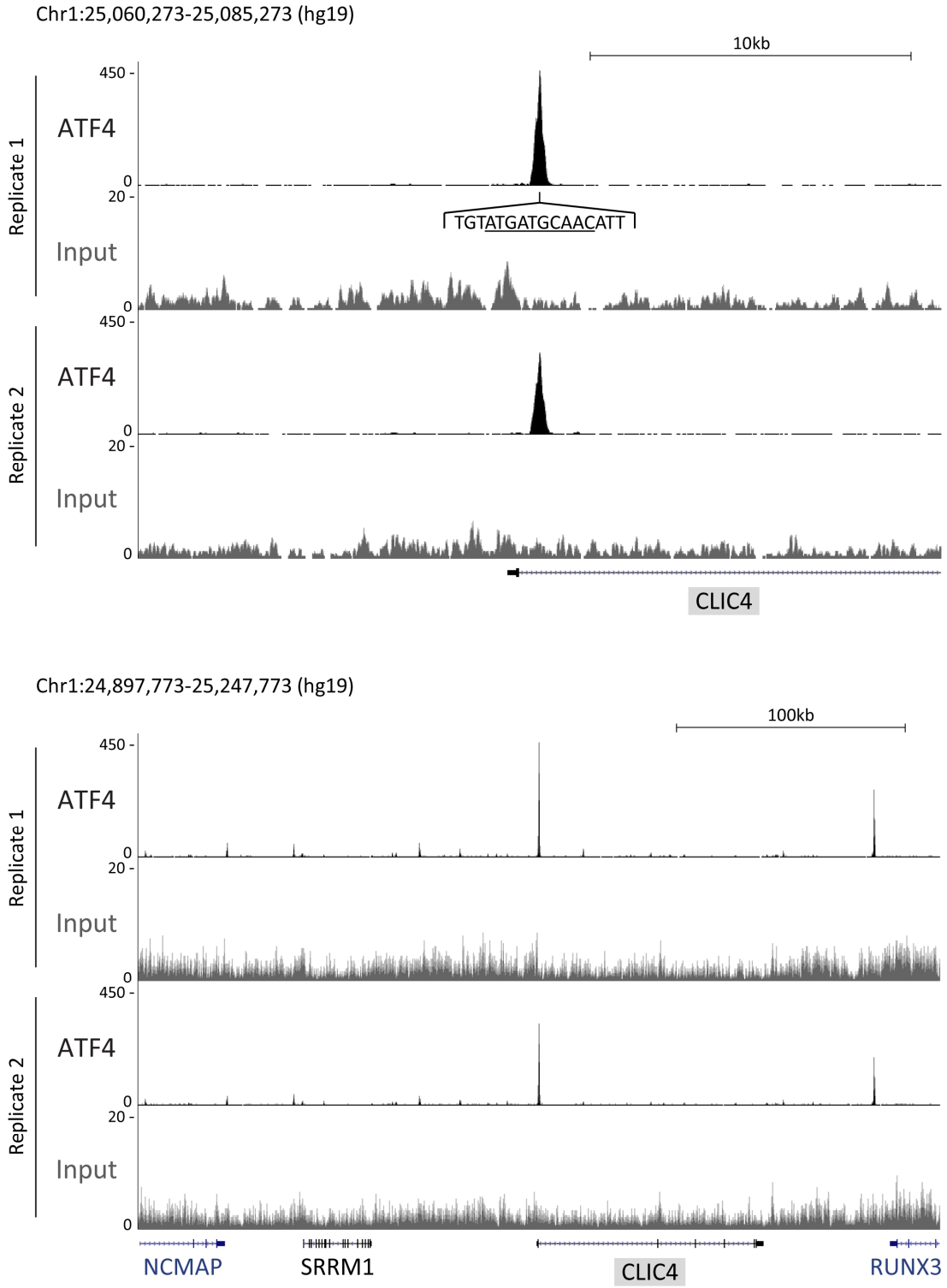


**Figure 5.17.- ATF4 binds *CLIC4* intron 1 upon glucose starvation in 501mel cells. (Above)** ATF4 major ChIP-seq peak associated with *CLIC4* following 4 h glucose starvation in 501mel cells. The ATF4 binding motif found in the sequence underlying the peak is represented under the peak corresponding to the first replicate of the experiment. **(Below)** 14-fold zoom out of the genomic region represented above, showing ATF4 binding in a wider genomic context.

5.4.4.5. – ATF4 binds and regulates *SERPINE2* under glucose starvation conditions

Serpin clade E member 2 (serpinE2) is a serine protease inhibitor with a key role in the regulation of tissue-type and urokinase-type plasminogen activators (Baker and Gronke 1986; Gomez et al. 2013). SerpinE2 has recently been associated with invasiveness in melanoma cells and reported to promote melanoma metastasis through a mechanism involving GSK3β signalling, while knock-down of *SERPINE2* expression inhibits melanoma metastasis *in vivo* (Wu 2016; Perego et al. 2018). Oncogenic activation of Ras, BRAF and MEK1 (frequently occurring in melanoma) results in serpinE2 upregulation in models of colorectal cancer (Bergeron et al. 2010).

Here we show that *SERPINE2* expression is also increased in glucose starvation conditions (fold change 1.84 and 2.14, *P* value $1.07 \times 10^{-3}$ and $1.34 \times 10^{-17}$, respectively, for the 8 and 24 h time points) as well as following 24 h of ectopic ATF4 overexpression (fold change 7.09, *P* value $9.03 \times 10^{-25}$) in melanoma cells (Supplementary Table S.7.A on Data CD and Supplementary Table B.2), and provide evidence for the binding of ATF4 to the 5' region of *SERPINE2* gene under glucose starvation conditions (**Figure 5.18**), which suggests a potential direct mechanism of regulation.

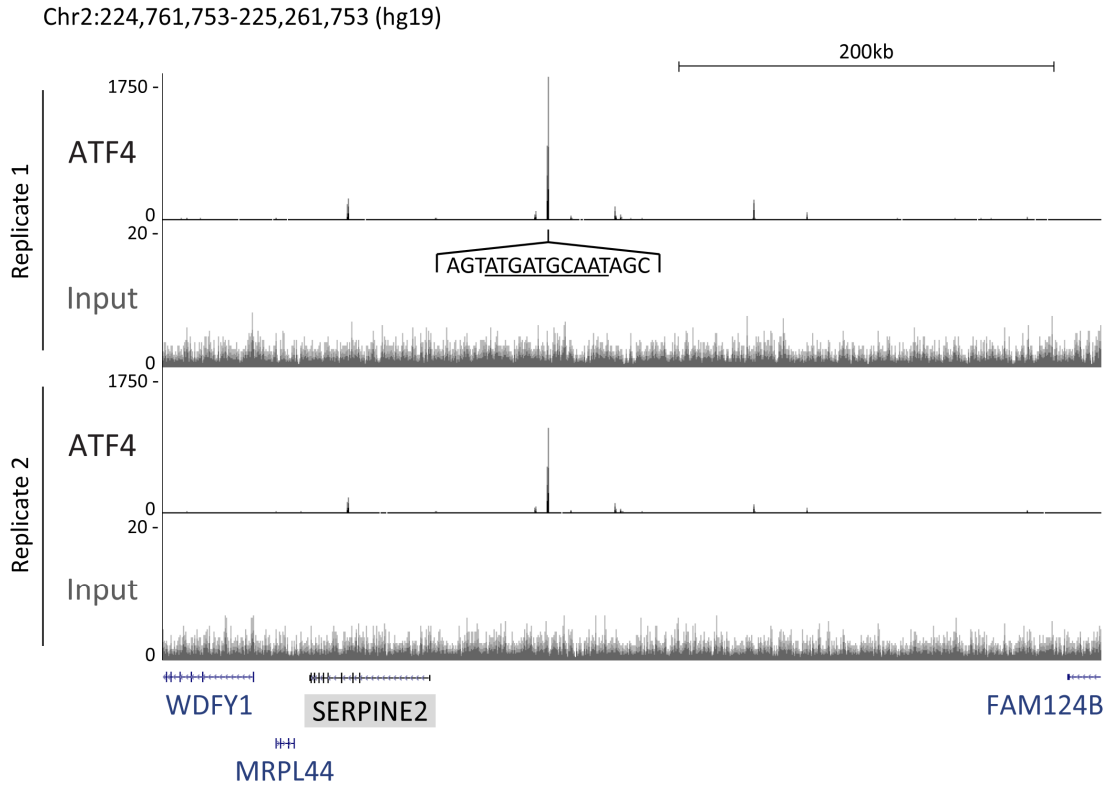


**Figure 5.18.- ATF4 binds *SERPINE2* 5' region upon glucose starvation in 501mel cells.** ATF4 major ChIP-seq peak associated to *SERPINE2* following 4 h glucose starvation in 501mel cells. The ATF4 binding motif found in the sequence underlying the peak is represented under the peak corresponding to the first replicate of the experiment.

5.4.4.6. – ATF4 binds and regulates *MITF* under glucose starvation conditions

Ectopic ATF4 overexpression or ATF4 induction in response to cellular stresses such as glucose or glutamine limitation leads to MITF repression in melanoma cells (Falletta et al. 2017; Ferguson et al. 2017). A potential direct mechanism of regulation involving competition of ATF4 with CREB (an important MITF positive regulator) for binding to a cAMP response element (CRE) site located in the *MITF* promoter has been suggested (Ferguson et al. 2017) based on the following evidence. First, glucose deprivation decreases transcriptional activity of the *MITF* promoter, with this responsiveness to glucose levels being lost upon introduction of a point mutation in the promoter construct inactivating the CRE site (Ferguson et al. 2017). Second, binding of ATF4 to the *MITF* promoter on glucose

starvation conditions has been confirmed through chromatin immunoprecipitation (ChIP) followed by qPCR, which also shows a reduction in CREB binding in glucose limitation conditions, and ectopic expression of ATF4 represses an *MITF* promoter luciferase reporter in melanoma cells (Falletta et al. 2017; Ferguson et al. 2017). Finally, activation of CREB using forskolin, an adenylate cyclase activator that promotes CREB phosphorylation and its interaction with transcription cofactors, almost completely restores *MITF* expression in low glucose conditions in melanoma cells (Ferguson et al. 2017). It is therefore possible that upregulation of ATF4 in response to nutrient limitation or other cellular stresses results in its binding to the *MITF* promoter, displacing CREB and therefore impairing *MITF* expression.

However, the only direct evidence that ATF4 does indeed bind the *MITF* promoter comes from the ChIP-qPCR experiments, where increasing the rounds of PCR can give false positive results in that weak binding can be detected at sites where binding may not be stable enough to regulate gene expression.

Here, we confirm that ectopic ATF4 expression or glucose limitation conditions result in downregulation of *MITF* expression in melanoma cells (fold change 0.35 and 0.43, *P* value $8.22 \times 10^{-13}$ and $2.08 \times 10^{-11}$, respectively, for the 8 and 24 h time points of ectopic ATF4 induction; fold change 0.33 and 0.78, *P* value $9.53 \times 10^{-16}$ and $6.68 \times 10^{-5}$, respectively, for the 8 and 24 h time points of glucose deprivation) (Supplementary Table S.7.B on Data CD, Supplementary Table B.2 and Figures 5.9 and 5.10). However, no ATF4 binding to the *MITF* promoter region was observed under glucose limitation conditions (**Figure 5.19**). Instead, ATF4 showed binding to the *MITF* gene body, specifically to the beginning of exon 4 of *MITF-M* (**Figure 5.19**).

The absence of ATF4 binding to the CRE site of the *MITF* promoter upon glucose limitation is surprising considering the evidence generated in previous studies suggesting this mechanism of regulation. However, it is possible that a higher expression of ATF4 in

response to longer periods of low glucose conditions (not specified in the Ferguson et al study) or resulting from ATF4 ectopic expression might have led to the binding of ATF4 to the CRE binding site which is not observed in our analysis. Consequently, the displacement of CREB is unlikely to mediate the reduction of *MITF* expression in our studies, though it may determine repression of an MITF-promoter-luciferase reporter in co-transfection assays.

Considering the observed binding of ATF4 to known target genes examined under the glucose limitation conditions used in our study, and the significant peak detected in *MITF* gene body, we consider that our ChIP-seq experiment most likely reflects binding of ATF4 in physiological conditions and that the mechanism of *MITF* regulation unexpectedly does not involve binding of ATF4 to the *MITF* promoter. Similarly, the observation of ATF4 binding to exon 4 in *MITF* gene body was unexpected but correlates with an increasing recognition that regulatory elements are present in exon coding sequences (Neznanov et al. 1997; Lang et al. 2005b; Barthel and Liu 2008; Khan et al. 2012; Ritter et al. 2012; Ahituv 2016). The potential relevance of the ATF4 peak found in *MITF* exon 4 was further supported by the presence of two ATF4 binding motifs under the peak and the previous identification of ATF4 binding partners such as C/EBPβ binding in the same region (Gerstein et al. 2012; Wang et al. 2012b; Wang et al. 2013b).

Finally, analysis of the raw ChIP-seq data was independently performed by a bioinformatician to confirm that the alignments corresponding to the analysis presented in this Chapter are correct. UCSC screenshots of the ATF4 major binding peak associated with *MITF* gene from both the analysis performed by the bioinformatician, where the hg38 genome was used as reference, and the analysis presented in this Chapter, where the hg19 genome was used as reference, are shown in **Supplementary Figure A.11**. Comparison of the relative location of the peaks in these analyses confirms the lack of any error in the ChIP-seq bioinformatic analysis performed and presented in this Chapter.

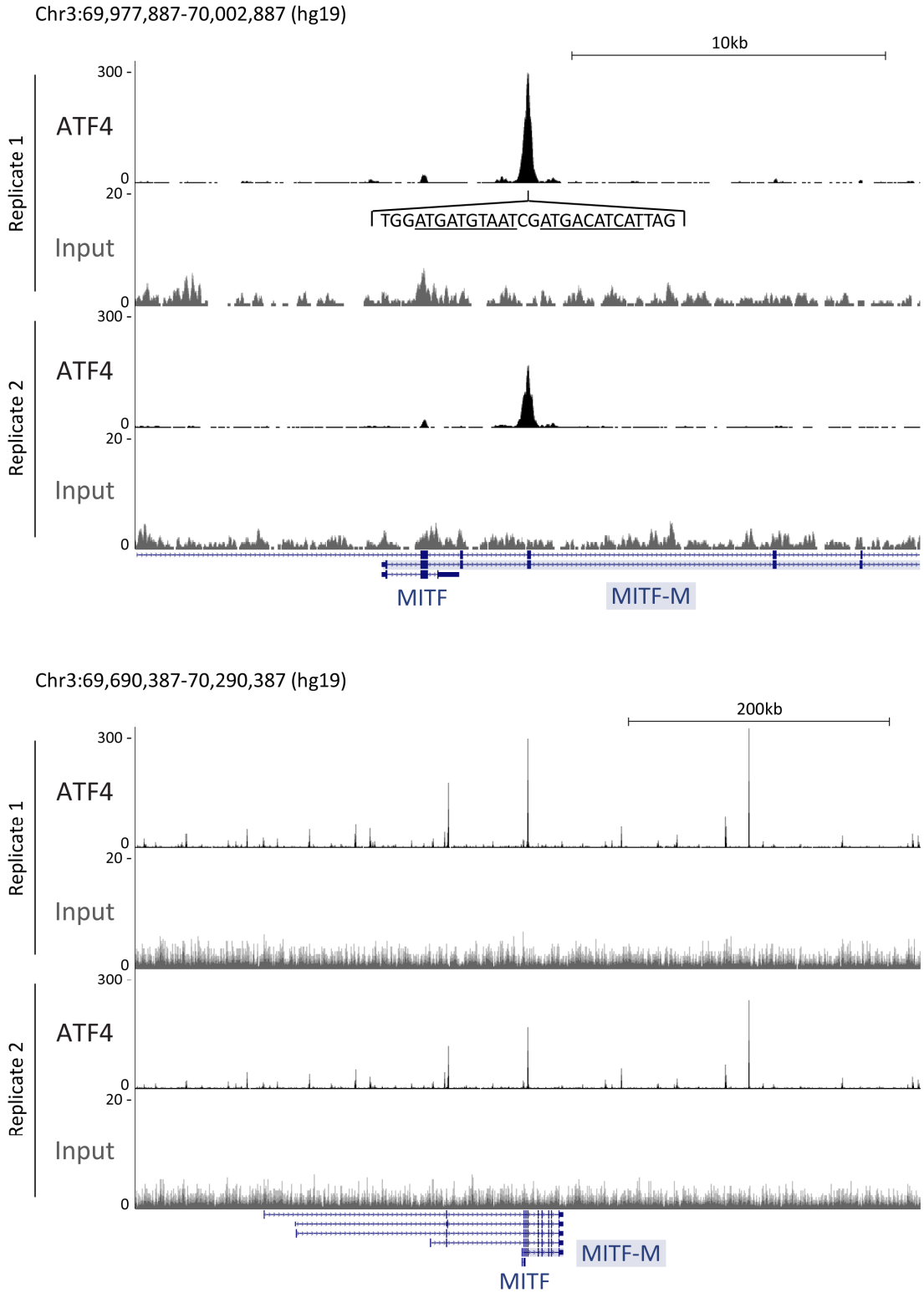


**Figure 5.19.- ATF4 binds *MITF* exon 4 upon glucose starvation in 501mel cells. (Above)** ATF4 major ChIP-seq peak associated to *MITF* following 4 h glucose starvation in 501mel cells. The ATF4 binding motifs found in the sequence underlying the peak are represented under the peak corresponding to the first replicate of the experiment. **(Below)** 24-fold zoom out of the genomic region represented above, showing ATF4 binding in a wider genomic context.

While further research will be required to elucidate the mechanism of ATF4 regulation of *MITF* expression, the identified binding of ATF4 to *MITF* gene body might suggest that binding by ATF4 would interrupt an activating promoter/enhancer gene loop, leading to *MITF* repression. Such a model is currently speculative, but could be confirmed through a combination of genome editing to disrupt the ATF4 binding site combined with chromosome conformation capture (3C) assays to assess the conformation of the *MITF* gene with and without ATF4 occupancy at the regulatory element.

5.4.4.7. – ATF4 binds and regulates *GLI2* under glucose starvation conditions

As previously introduced, GLI2 is an MITF transcriptional repressor and promoter of melanoma invasiveness which is upregulated by the TGF-β pathway (Alexaki et al. 2010; Javelaud et al. 2011; Pierrat et al. 2012).

Here we show that *GLI2* expression is increased upon 8 or 24 h glucose deprivation (fold change 5.45 and 3.02, *P* value $5.18 \times 10^{-5}$ and $4.20 \times 10^{-3}$, respectively) as well as following 24 h ectopic ATF4 overexpression (fold change 5.72, *P* value $2.24 \times 10^{-14}$) in melanoma cells (Supplementary Table B.2), and provide evidence for the binding of ATF4 to the 5' region of *GLI2* gene under glucose starvation conditions (**Figure 5.20**), which suggests a potential direct mechanism of regulation.

While ATF4 binding to *MITF* gene body might reflect a direct mechanism of regulation (section 5.4.3.5), the presence of an ATF4 binding peak associated to *GLI2*, an MITF repressor, adds the possibility of an indirect mechanism of repression of MITF by ATF4 via regulation of *GLI2* expression.

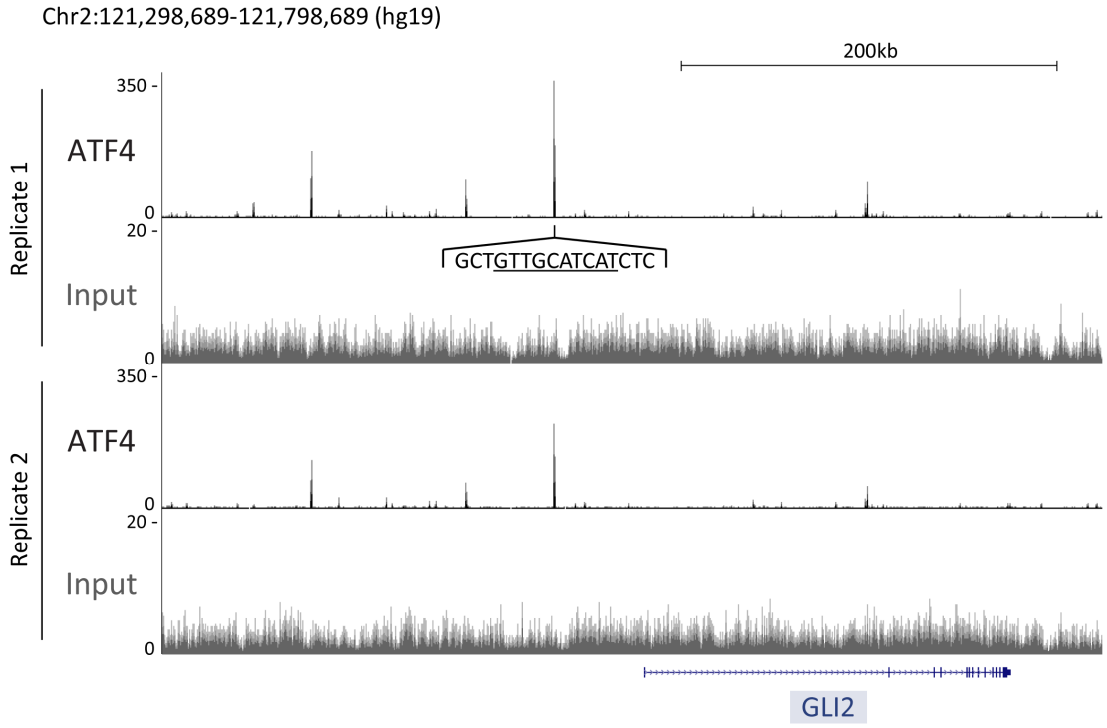


**Figure 5.20.- ATF4 binds *GLI2* 5' region upon glucose starvation in 501mel cells.** ATF4 major ChIP-seq peak associated to *GLI2* following 4 h glucose starvation in 501mel cells. The ATF4 binding motif found in the sequence underlying the peak is represented under the peak corresponding to the first replicate of the experiment.

## 5.5. – Genome-wide analysis of gene regulation by both MITF and ATF4

The inverse correlation between ATF4 and MITF expression, the potential direct mechanism of ATF4 regulation of MITF expression via binding to exon 4, and the association of low MITF expression with an invasive, undifferentiated phenotype, and high MITF levels with a proliferative or differentiated phenotype in melanoma cells, led us to hypothesise that ATF4 and MITF might cooperate to establish mutually exclusive gene expression signatures leading to inverse phenotypes in melanoma cells through the antagonistic regulation of a common subset of genes.

First, the previously generated RNA-seq datasets of differentially expressed genes upon 8 or 24 h ectopic ATF4 expression (Supplementary Tables S.5.A and B on Data CD) were

examined for the presence of well-known MITF target genes (Cheli et al. 2010; Vazquez et al. 2013), among which were found those shown in **Table 5.13**. No significant changes in gene expression were found for any of these genes upon an equivalent doxycycline treatment in 501mel cells (Supplementary Tables S.5.C and D on Data CD).

| | 8h Induction ATF4 | | 24h Induction ATF4 | |
|---|---|---|---|---|
| **Gene Name** | **Fold Change** | ***P* value** | **Fold Change** | ***P* value** |
| MET | | | 0.70 | $1.64 \times 10^{-3}$ |
| PPARGC1A | | | 0.51 | $6.71 \times 10^{-6}$ |
| DIAPH1 | | | 0.67 | $2.95 \times 10^{-3}$ |
| MC1R | 0.41 | $2.78 \times 10^{-7}$ | 0.40 | $6.95 \times 10^{-9}$ |
| RAB27A | | | 0.49 | $7.64 \times 10^{-8}$ |
| CDK2 | | | 0.64 | $8.30 \times 10^{-3}$ |
| DCT | | | 0.40 | $2.58 \times 10^{-14}$ |
| MLANA | | | 0.53 | $3.53 \times 10^{-8}$ |
| KIT | 0.53 | $8.17 \times 10^{-5}$ | | |
| TRPM1 | 0.49 | $1.69 \times 10^{-6}$ | 0.34 | $2.20 \times 10^{-12}$ |

**Table 5.13.- Well-known MITF target genes differentially expressed upon ATF4 overexpression in 501mel cells.** Fold changes and associated *P* values corresponding to known MITF target genes extracted from the RNA-seq analysis of DEGs in 501mel-i-ATF4-HA cells induced with 20 ng/ml doxycycline for 8 or 24 h versus non-induced control 501mel-i-ATF4-HA cells.

However, since ATF4 represses MITF expression, the detection of a very moderate, though statistically significant, decrease in the expression of known MITF target genes following the induction of ectopic ATF4 expression could be a result of direct regulation by both MITF and ATF4 or just the consequence of the repression of MITF expression by ATF4. The fact that most MITF targets were only differentially expressed at the 24 h time point suggests that the regulation could be indirect.

To investigate the possibility of a dual mechanism of regulation of the MITF target genes differentially expressed upon ATF4 overexpression (Table 5.4) by both MITF and ATF4, the ATF4 ChIP-seq dataset previously generated in glucose-starved 501mel cells (Supplementary Tables S.4.A and B on Data CD) was examined for ATF4 binding peaks associated with these genes. The well-characterised MITF target genes *MET, PPARGC1A, RAB27A, DCT, MLANA, KIT* and *TRPM1* (Tsujimura et al. 1996; Bertolotto et al. 1998b; Du et

al. 2003; Miller et al. 2004; McGill et al. 2006; Beuret et al. 2007; Chiaverini et al. 2008; Vazquez et al. 2013) (differentially expressed upon ectopic ATF4 expression, Table 5.4), all had associated ATF4 binding peaks on the examined ATF4 ChIP-seq dataset (**Figures 5.21 - 5.27**).

The presence of ATF4 binding peaks on the gene bodies and flanking genomic regions of known MITF target genes raises the possibility that these MITF target genes may be directly regulated by ATF4. However, further research will be needed to establish whether these binding peaks reflect a functional transcriptional regulation.

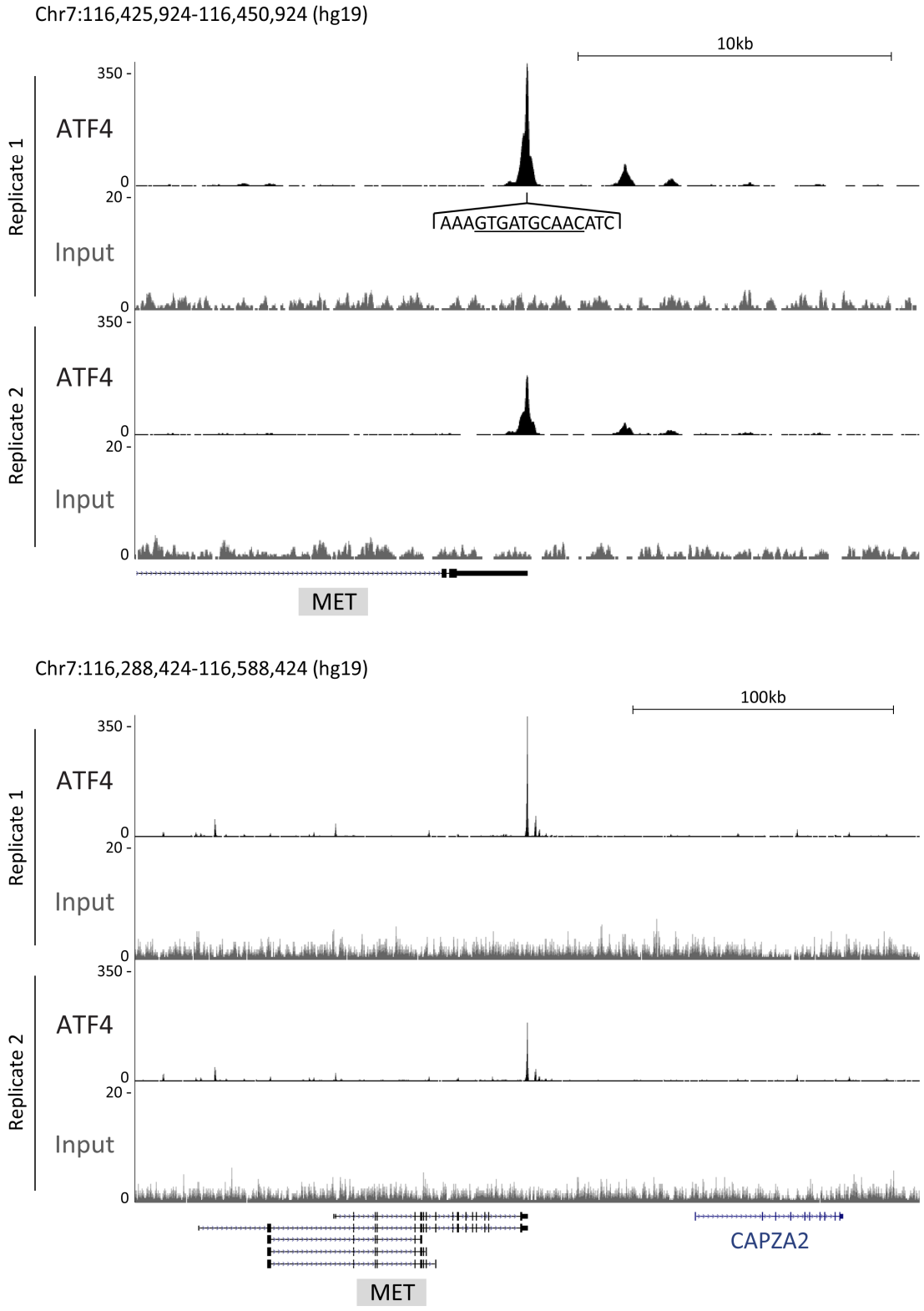


**Figure 5.21.- ATF4 binds *MET* TTS upon glucose starvation in 501mel cells. (Above)** ATF4 major ChIP-seq peak associated with *MET* following 4 h glucose starvation in 501mel cells. The ATF4 binding motif found in the sequence underlying the peak is represented under the peak corresponding to the first replicate of the experiment. **(Below)** 12-fold zoom out of the genomic region represented above, showing ATF4 binding in a wider genomic context.

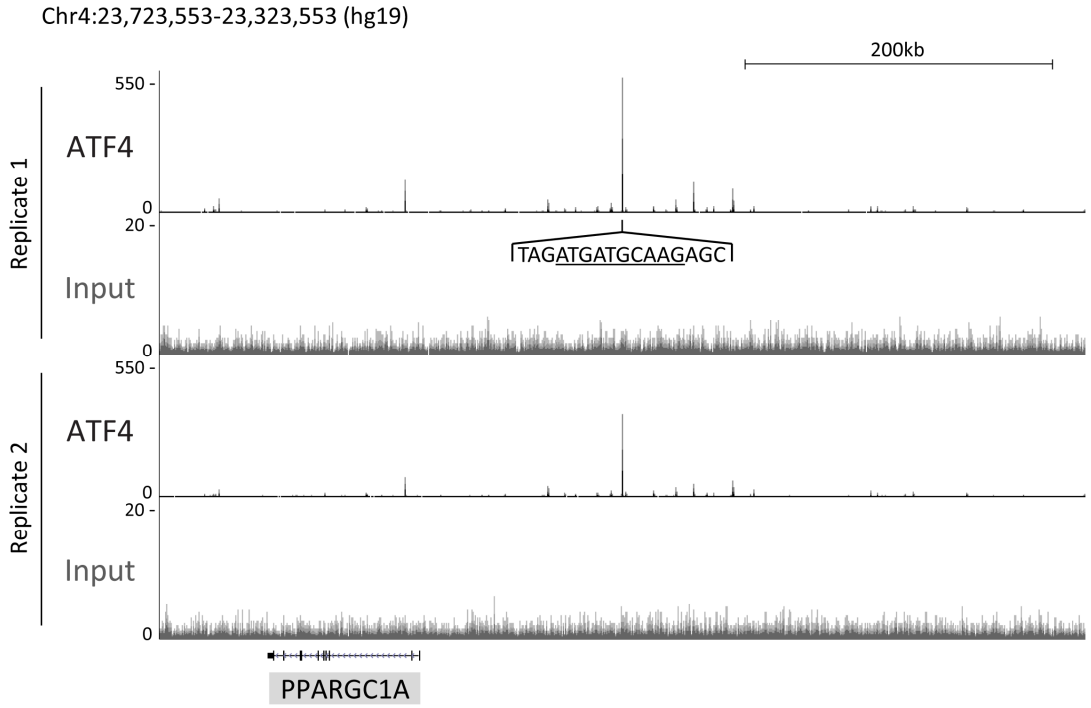


**Figure 5.22.- ATF4 binds *PPARGC1A* 5' region upon glucose starvation in 501mel cells.** ATF4 major ChIP-seq peak associated with *PPARGC1A* following 4 h glucose deprivation in 501mel cells. The ATF4 binding motif found in the sequence underlying the peak is represented under the peak corresponding to the first replicate of the experiment.

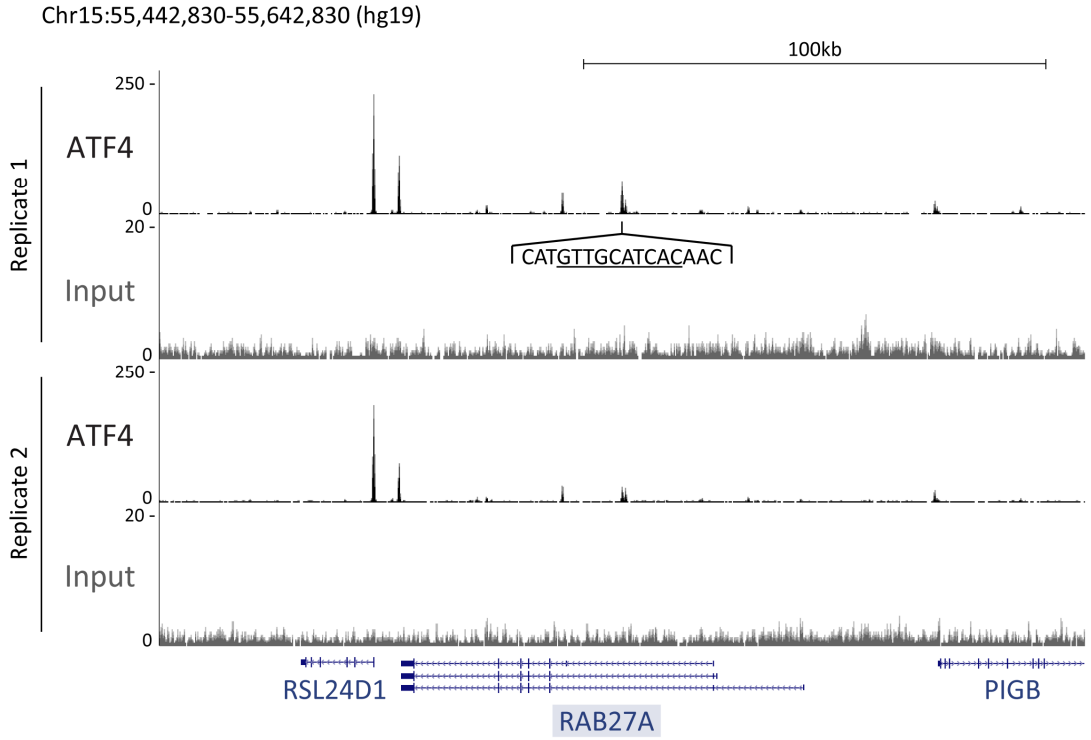


**Figure 5.23.- ATF4 binds *RAB27A* gene body upon glucose starvation in 501mel cells.** ATF4 main ChIP-seq peak associated with *RAB27A* following 4 h glucose deprivation in 501mel cells. The ATF4 binding motif found in the sequence underlying the peak is represented under the peak corresponding to the first replicate of the experiment.

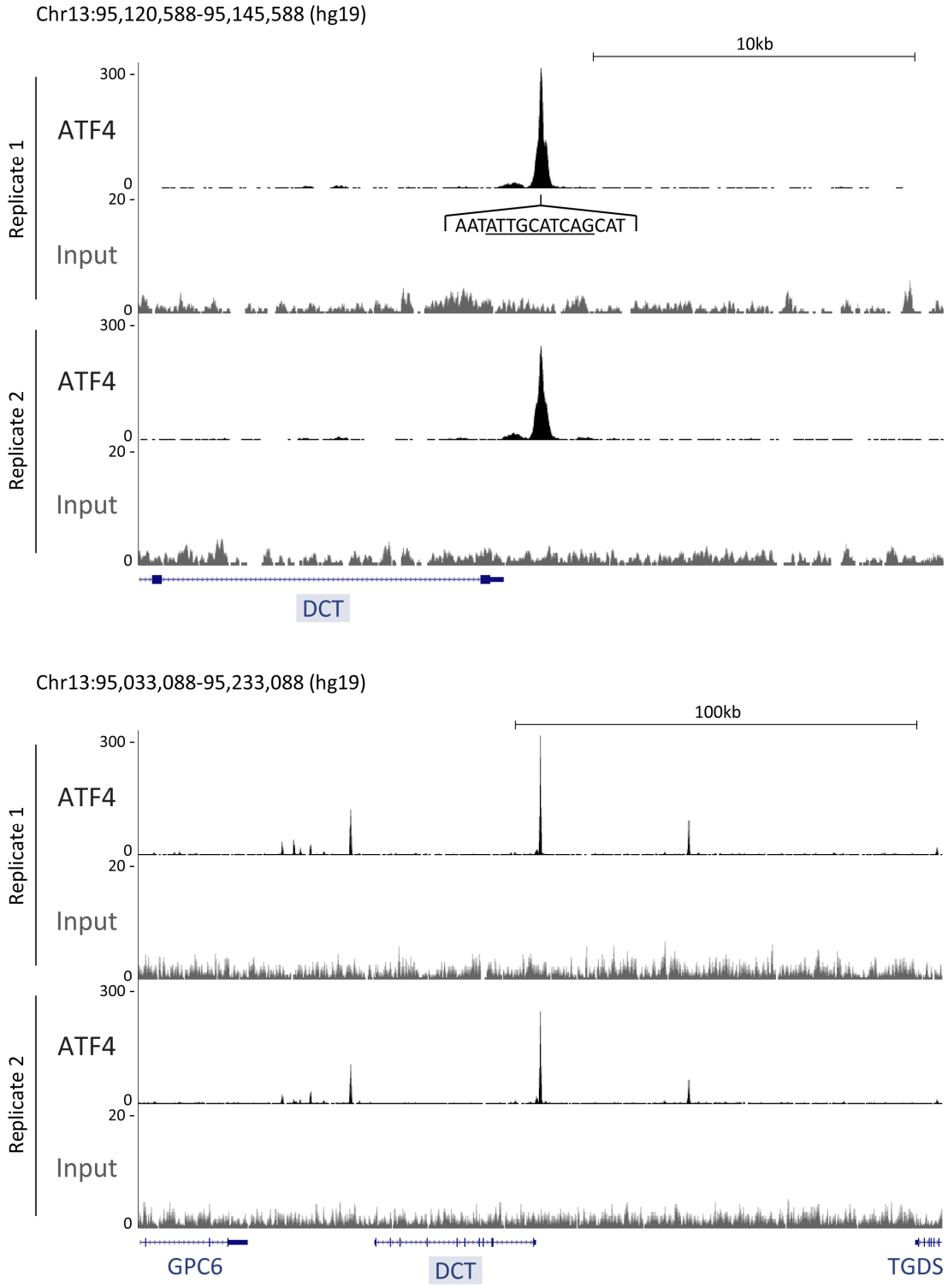


**Figure 5.24.- ATF4 binds *DCT* 5' region upon glucose starvation in 501mel cells. (Above)** ATF4 major ChIP-seq peak associated with *DCT* following 4 h glucose deprivation in 501mel cells. The ATF4 binding motif found in the sequence underlying the peak is represented under the peak corresponding to the first replicate of the experiment. **(Below)** 8-fold zoom out of the genomic region represented above, showing ATF4 binding in a wider genomic context.

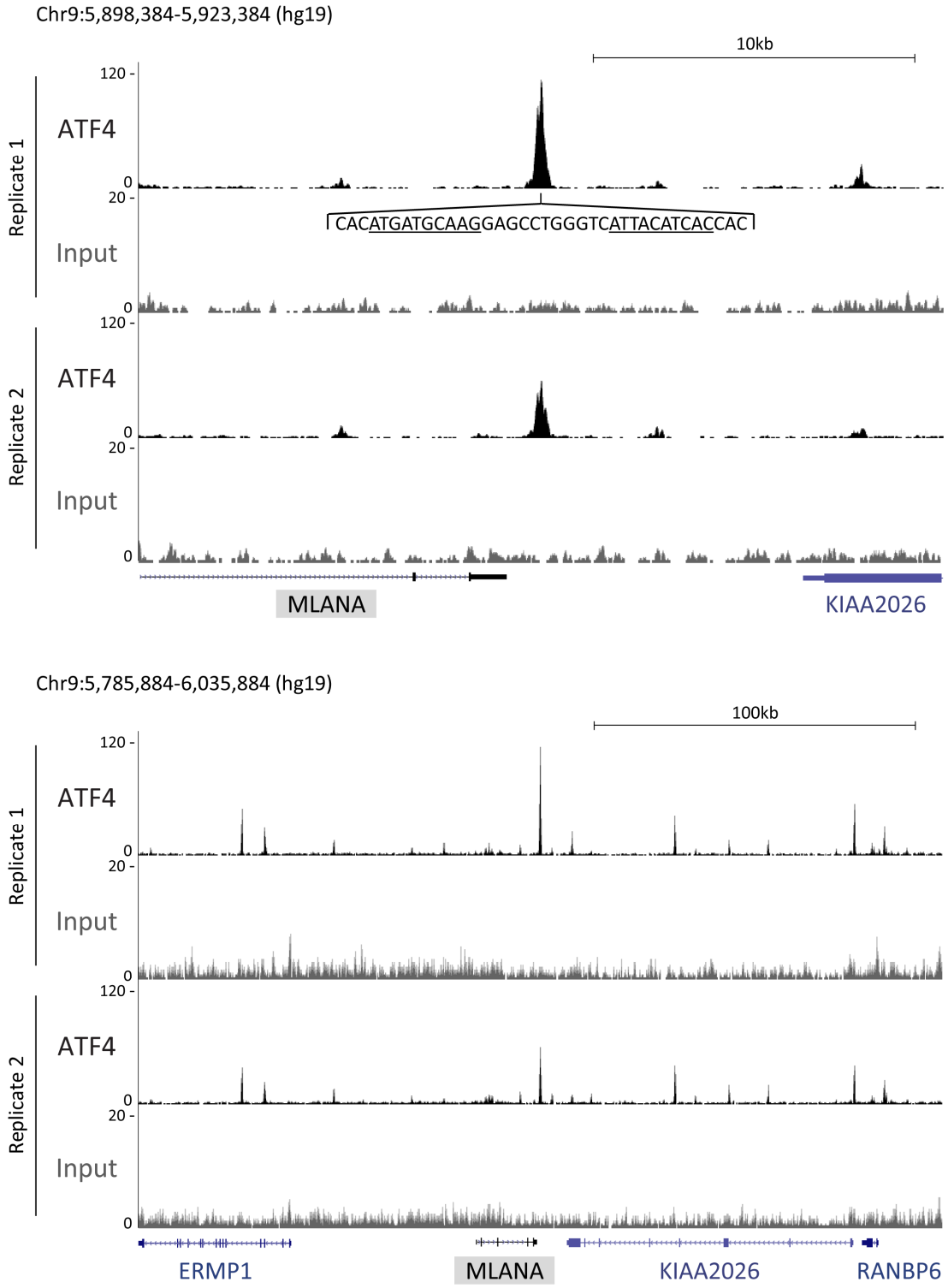


**Figure 5.25.- ATF4 binds *MLANA* 5' region upon glucose starvation in 501mel cells. (Above)** ATF4 major ChIP-seq peak associated with *MLANA* following 4 h glucose deprivation in 501mel cells. The ATF4 binding motif found in the sequence underlying the peak is represented under the peak corresponding to the first replicate of the experiment. **(Below)** 10-fold zoom out of the genomic region represented above, showing ATF4 binding in a wider genomic context.

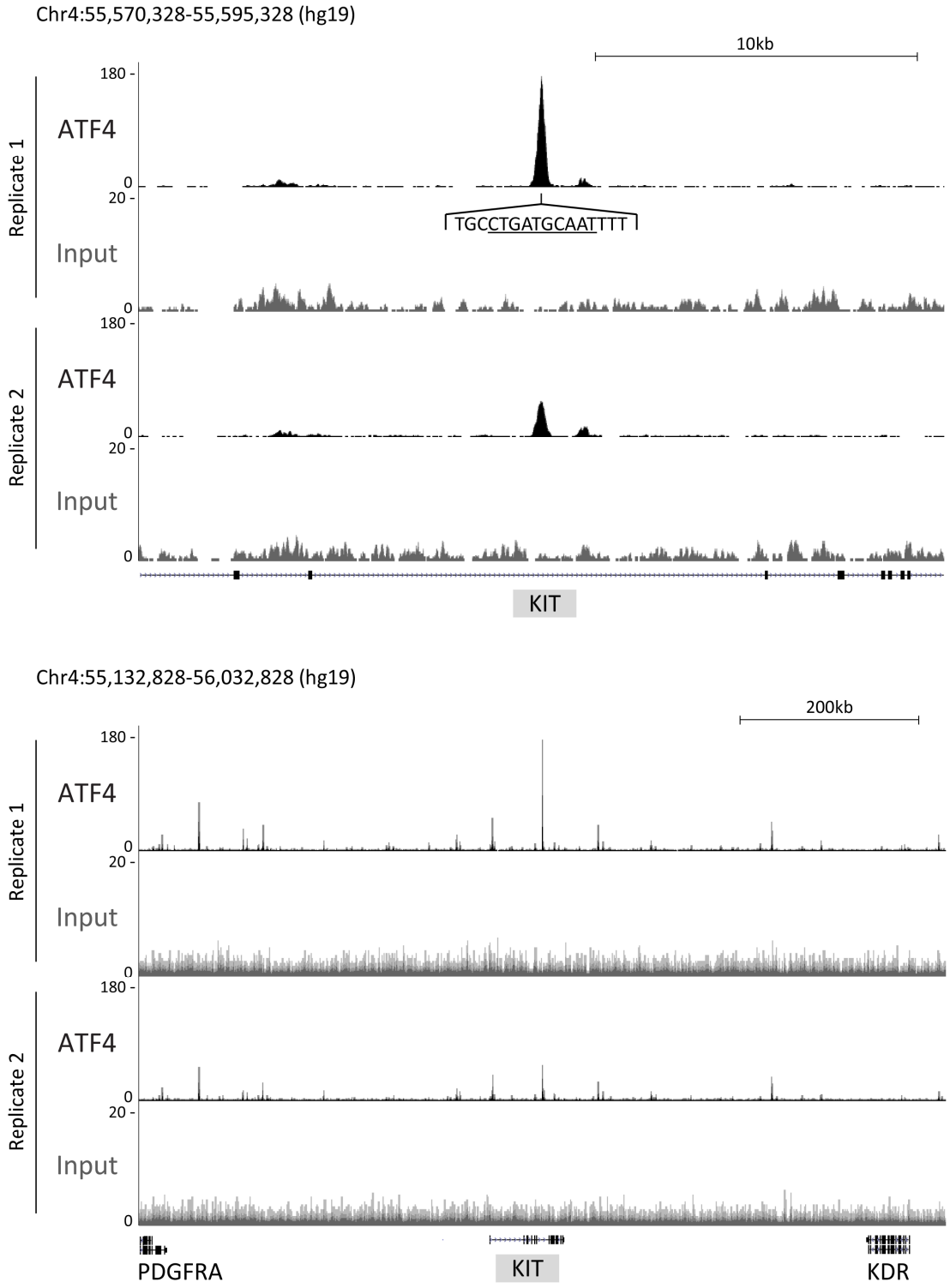


**Figure 5.26.- ATF4 binds *KIT* gene body upon glucose starvation in 501mel cells. (Above)** ATF4 major ChIP-seq peak associated with *KIT* following 4 h glucose deprivation in 501mel cells. The ATF4 binding motif found in the sequence underlying the peak is represented under the peak corresponding to the first replicate of the experiment. **(Below)** 36-fold zoom out of the genomic region represented above, showing ATF4 binding in a wider genomic context.

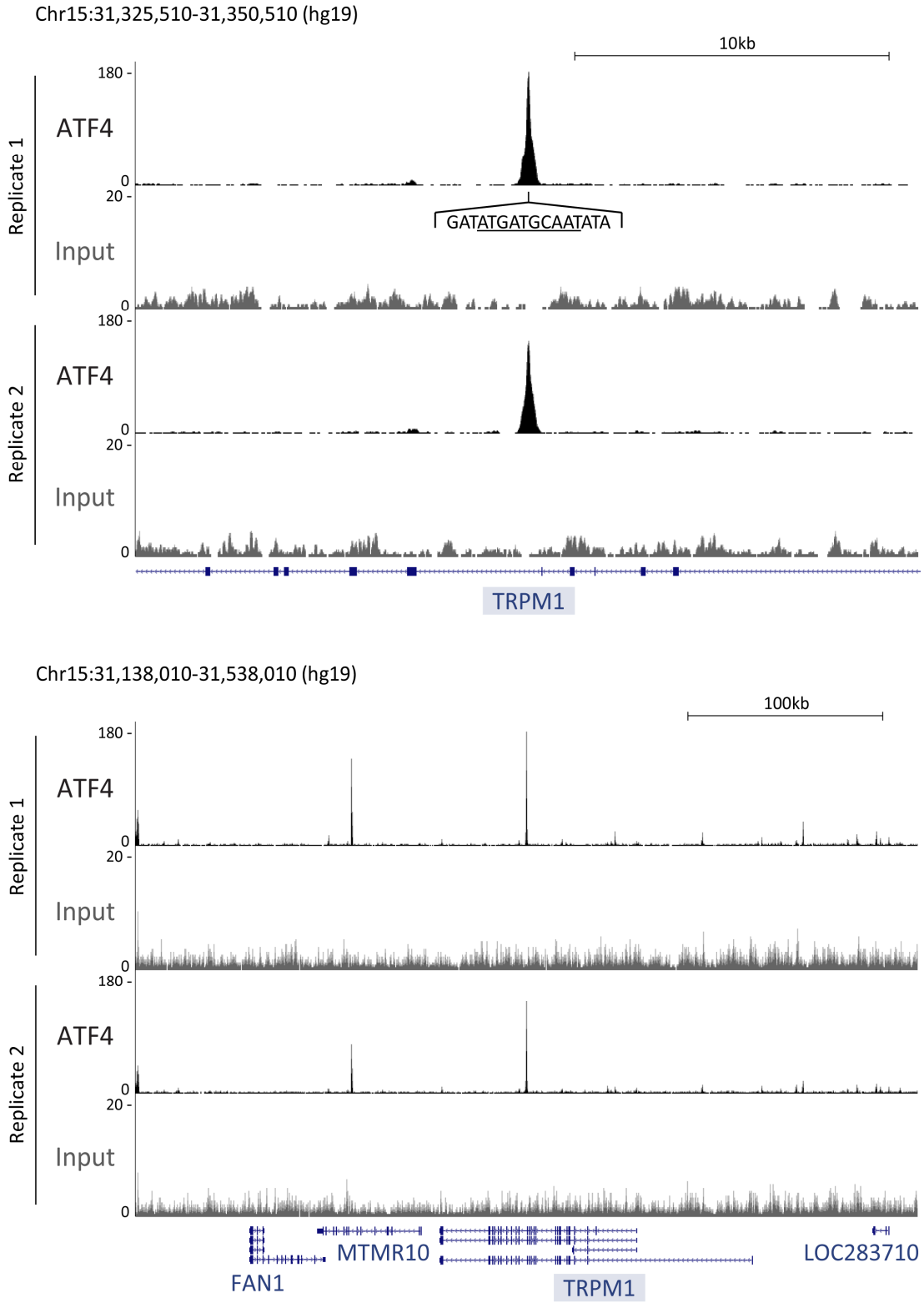


**Figure 5.27.- ATF4 binds *TRPM1* gene body upon glucose starvation in 501mel cells. (Above)** ATF4 major ChIP-seq peak associated with *TRPM1* following 4 h glucose deprivation in 501mel cells. The ATF4 binding motif found in the sequence underlying the peak is represented under the peak corresponding to the first replicate of the experiment. **(Below)** 16-fold zoom out of the genomic region represented above, showing ATF4 binding in a wider genomic context.

Finally, in order to investigate the potential of additional genes to be regulated by both MITF and ATF4, the lists of MITF-bound and ATF4-bound differentially expressed genes (FDR < 0.05, fold-change ≥ 2) identified upon MITF silencing or ATF4 ectopic expression (Supplementary Tables S.3 and S.6.A and B, respectively), were examined for common MITF and ATF4-bound differentially expressed genes upon both MITF silencing and ATF4 ectopic expression. A total of 271 genes were found to be bound by both transcription factors and differentially expressed (FDR < 0.05, fold-change ≥ 2) upon MITF silencing and following 8 and/or 24 h induction of ectopic ATF4 expression (**Supplementary Table B.3**). Among these, 136 and 84 genes were upregulated and downregulated, respectively, upon MITF silencing and following 8 and/or 24 h induction of ectopic ATF4 expression (highlighted in **Supplementary Table B.3**); 16 genes were upregulated upon MITF silencing and downregulated following 8 and/or 24 h induction of ectopic ATF4 expression; and 36 genes were downregulated upon MITF silencing and upregulated following 8 and/or 24 h induction of ectopic ATF4 expression.

Examination of the set of genes upregulated upon MITF silencing and following 8 and/or 24 h induction of ectopic ATF4 expression, and therefore repressed and activated by MITF and ATF4, respectively, identified PTEN and DEPTOR, two potential MITF targets revealed in Chapter 4, which were also differentially expressed following ectopic ATF4 expression (PTEN fold change 2.26 and 2.79, *P* value 6.44 x $10^{-8}$ and 4.34 x $10^{-15}$, respectively, for the 8 and 24 h time points; DEPTOR fold change 6.81, *P* value 5.17 x $10^{-16}$, corresponding to the 24 h time point) (**Supplementary Table B.3**) and had associated ATF4 binding peaks in the performed ChIP-seq experiment in glucose-starved melanoma cells (**Figures 5.28** and **5.29**).

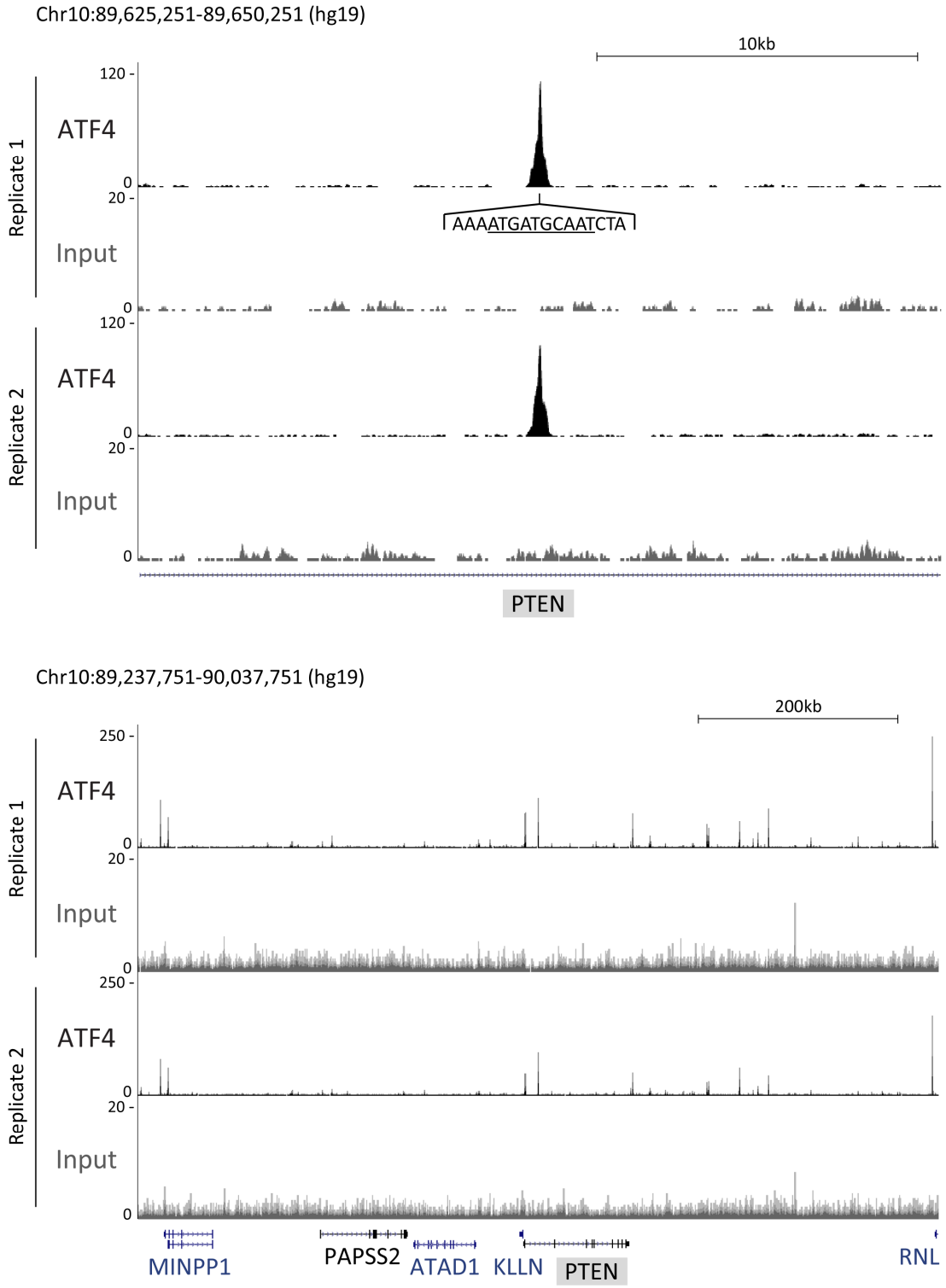


**Figure 5.28.- ATF4 binds *PTEN* gene body upon glucose starvation in 501mel cells. (Above)** ATF4 major ChIP-seq peak associated with *PTEN* following 4 h glucose deprivation in 501mel cells. The ATF4 binding motif found in the sequence underlying the peak is represented under the peak corresponding to the first replicate of the experiment. **(Below)** 32-fold zoom out of the genomic region represented above, showing ATF4 binding in a wider genomic context.

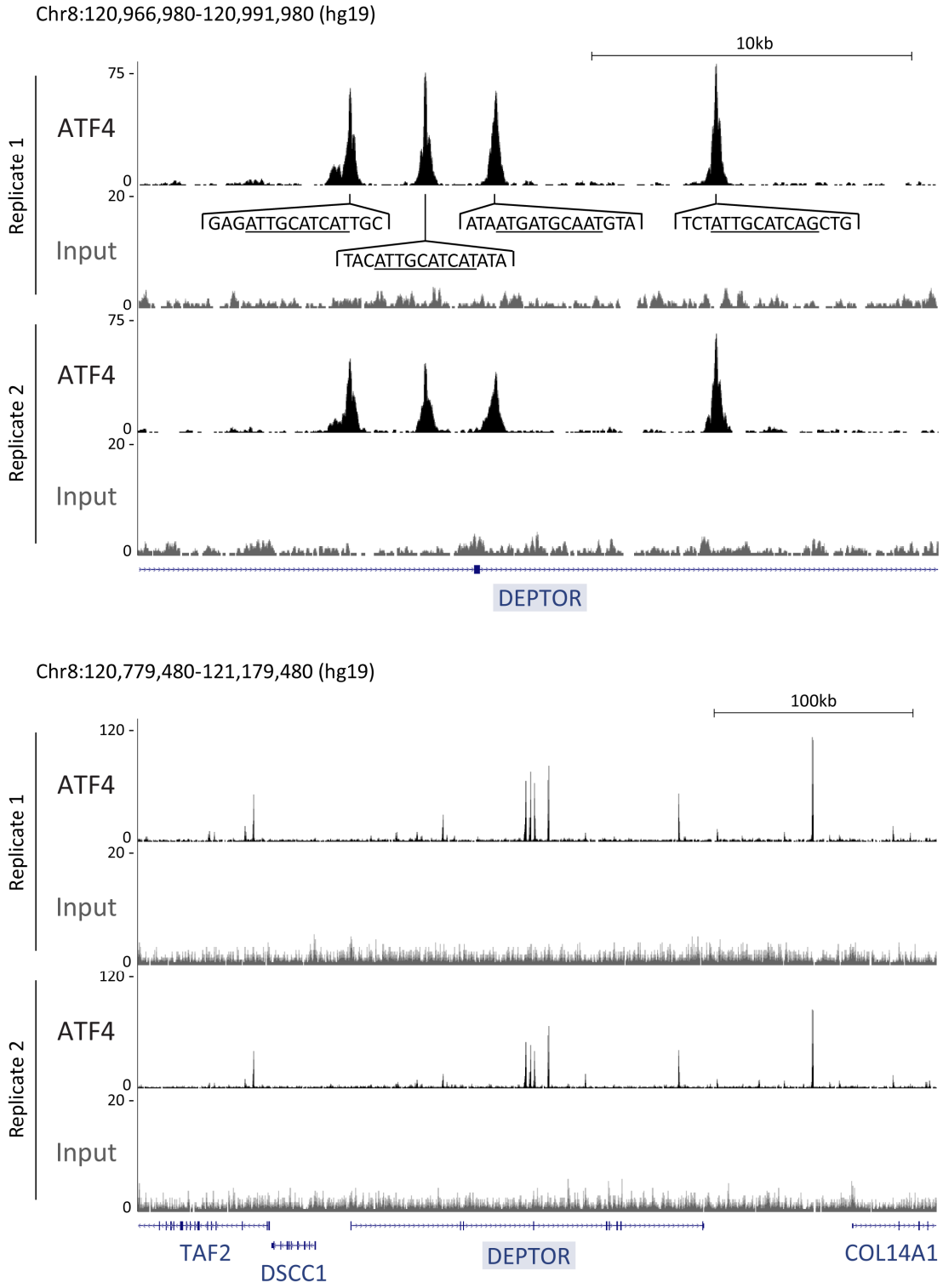


**Figure 5.29.- ATF4 binds *DEPTOR* gene body upon glucose starvation in 501mel cells. (Above)** ATF4 major ChIP-seq peaks associated with *DEPTOR* following 4 h glucose deprivation in 501mel cells. The ATF4 binding motifs found in the sequences underlying the peaks are represented under the peaks corresponding to the first replicate of the experiment. **(Below)** 16-fold zoom out of the genomic region represented above, showing ATF4 binding in a wider genomic context.

The potential direct mechanism of upregulation of *PTEN* and *DEPTOR* by ATF4 might reflect a means to promote survival by reducing protein synthesis in response to cellular stress. While the downregulation of MITF consequence of ATF4 induction would relieve the repression exerted on *PTEN* and *DEPTOR* expression, the additional mechanism of positive regulation by ATF4 might constitute a faster response to cellular stress to further increase *PTEN* and *DEPTOR* levels.

Further examination of the set of genes upregulated upon MITF silencing and induction of ectopic ATF4 expression however did not reveal any further set of genes that could suggest an antagonistic role of MITF and ATF4 in the regulation of additional biological processes.

We therefore conclude that ATF4 might cooperate with MITF for the antagonistic regulation of *PTEN* and *DEPTOR*, as well as several key target genes mainly involved in differentiation (*MLANA*, *DCT*, *RAB27A*, *TRPM1*) but also metabolism (*PPARGC1A*), survival (*KIT*) and motility (*MET*). However, further investigation involving genome editing in combination with ATF4 induction will be required to confirm or rule out the role in ATF4 in the regulation of these genes.

## 5.6. – Discussion

In this chapter, a genome-wide study of the regulation of gene expression by ATF4 in melanoma cells was performed. The results reveal for the first time the repertoire of ATF4 targets in this cell type and highlight some potentially intriguing regulatory events that may affect melanoma progression driven by the stresses leading to ATF4 expression.

First, the role of ATF4 as an *MITF* repressor in melanoma cells (Falletta et al. 2017; Ferguson et al. 2017) was confirmed. The repression of *MITF* by ATF4 allows for the downregulation of *MITF* expression in response to microenvironment conditions causing cellular stress, such as hypoxia, nutrient limitation or inflammation, which lead to the induction of *ATF4* expression (Pakos-Zebrucka et al. 2016; Wortel et al. 2017). This is highly relevant because these microenvironmental conditions are potential inducers of melanoma invasion (Falletta et al. 2017; García-Jiménez and Goding 2019), and low levels of MITF have been associated with an invasive cell phenotype (Carreira et al. 2006; Goding 2011).

Second, evidence was produced supporting a direct mechanism of transcriptional regulation involving binding of ATF4 to *MITF* exon 4, whereas no binding to the MITF promoter was observed as previously suggested (Falletta et al. 2017; Ferguson et al. 2017). While a mechanism of transcriptional regulation via binding to a coding region might be unexpected, and requires validation by a combination of genome-editing and 3C assays as highlighted above, the result would be consistent with ATF4 binding impairing formation of a transcriptionally productive enhancer/promoter gene loop essential for *MITF* expression. Alternatively, ATF4 repression of *MITF* could be exerted through its binding to a silencer region far away from the gene, which would not have been identified in our ChIP-seq analysis but might also be revealed by 3C techniques. Indeed, the ATF4 ChIP-seq does

identify an ATF4 binding event around 150 kb downstream of the main body of the *MITF* gene, though again whether this site might participate in regulation of MITF is unknown.

Third, our study revealed that the changes in the gene expression signature of melanoma cells induced by glucose starvation appear mainly driven by ATF4. Interestingly, a single cell RNA-seq study of melanoma minimal residual disease (MRD) following RAF/MEK inhibition recently identified a drug-resistant subpopulation of cells characterised by a starvation-like transcriptional program, which appeared to be a transition state to other drug-resistant subpopulations, including one with a gene expression signature characteristic of invasiveness (Rambow et al. 2018). It is therefore possible that nutrient limitation conditions such as low glucose, or other microenvironmental stresses that induce ATF4, can contribute to the induction of drug-resistant and invasive cell phenotypes in melanoma cells via ATF4.

Further analysis of the differentially expressed genes in glucose starvation conditions which were also differentially expressed upon ectopic ATF4 expression and had associated binding peaks in the ATF4 ChIP-seq experiment (meaning that they are potential directly regulated ATF4 targets) identified *MITF* and the novel ATF4 targets (for which the regulation by ATF4 had not been previously described or the potential for a direct mechanism of regulation had not been confirmed by ChIP-seq) *HOXB9*, *HERPUD1*, *S100P*, *CLIC4*, *SERPINE2* and *GLI2*, among others.

Among these targets, which were all upregulated in response to ATF4 expression, Herpud1 has a cytoprotective role, which may contribute to prevent apoptosis induced by the cellular stress conditions in melanoma cells. Regarding Homeobox B9, S100P, CLIC4, serpinE2 and GLI2, they have all been associated with the promotion of cancer invasiveness and/or metastasis (Arumugam et al. 2005; Whiteman et al. 2007; Alexaki et al. 2010; Hayashida et al. 2010; Jiang et al. 2011; Huang et al. 2014b; Shukla et al. 2014; Hsu et al.

2015; Jiang et al. 2016; Wu 2016; Liu et al. 2017; Perego et al. 2018). It is therefore possible that at least partly through the regulation of these targets by ATF4, cellular stresses such as nutrient deprivation can induce an invasive phenotype in melanoma cells. This would enable cells to escape a stressful microenvironment and would also fit well with the association of low MITF levels in melanoma cells with invasion, since both ATF4 and GLI2 are negative regulators of *MITF* expression (Javelaud et al. 2011; Pierrat et al. 2012).

The potential role of ATF4 in the downregulation of MITF and upregulation of genes such as *HOXB9*, *S100P*, CLIC4, *SERPINE2* and *GLI2*, and the evidence generated supporting a possible direct mechanism of regulation is indicative of ATF4 as a potential driver of melanoma invasion in response to cellular stress conditions. However, further research will be needed to determine whether the ATF4 binding peaks associated with the novel target genes highlighted are functional and whether the upregulation of these genes by ATF4 indeed results in an increase in melanoma invasiveness.

While studies performed by others have already shown that cellular stress conditions can increase melanoma invasiveness (Rankin and Giaccia 2016; Falletta et al. 2017), ATF4 has so far been reported to be insufficient to induce invasiveness in melanoma models (Falletta et al. 2017). This may be because ectopic expression of ATF4, while inducing changes in gene expression, does not affect the phosphorylation of the eIF2α translation initiation factor. In the absence of translation-reprogramming initiated by eIF2α phosphorylation, it is possible that the alterations in gene expression driven by ATF4 will not be manifested as changes in protein expression required for invasion. Further investigation will therefore be needed to determine the role or contribution of ATF4 to the promotion of invasiveness under cellular stress conditions and the additional mechanisms leading to this cell phenotype in this setting.

Finally, the moderate downregulation of several well-characterised MITF target genes following ATF4 overexpression and the association of ATF4 ChIP-seq binding peaks with most of these genes reflected the functionality of MITF repression by ATF4, but also suggested the potential antagonistic regulation of a subset of genes by ATF4 and MITF, which would likely constitute a strategy for phenotype-switching. Further analysis of genes potentially regulated by both ATF4 and MITF through a direct mechanism identified the novel MITF targets *PTEN* and *DEPTOR*, whose additional regulation by ATF4 could constitute a strategy for a faster further upregulation of their expression in cellular stress conditions, and consequently a reduction in protein synthesis that would facilitate survival by reducing nutrient demand under starvation conditions.

Although further work will be necessary to confirm the direct regulation of specific genes by ATF4 and the downstream consequences of their regulation, the results generated have provided a key resource that will be instrumental in deciphering the impact of microenvironmental stress on melanoma progression.

# Chapter 6 – Concluding discussion and future perspectives

## 6.1. – Potential limitations of the molecular and cell biology techniques used

Over the last 40 years, the emphasis of biomedical research has moved from the study of disease in patients mainly at the systemic and organ level to its definition at the molecular and cellular level. The development of new technology has allowed the isolation and sequencing of genes and the study of their function, leading to key advances in the field of medical research in general and the area of oncology in particular. However, part of the research presented in this study highlights the limitations of the techniques currently used in molecular biology research and emphasises the caution needed to interpret them.

As seen in the "gene regulation" section of the Introduction (section 1.5), an impressively extensive variety of mechanisms fine tune the level of expression of genes in response to specific cellular conditions. Alteration of gene expression levels above (as well as below) a certain threshold can generate phenotypic changes and can lead to the development of disease. For example, overexpression of wild-type MYC, HER2, REL or AKT2 are known to drive progression of several human cancers (Shastry 1995). The fact that overexpression of wild-type proteins can produce altered phenotypes has been exploited by geneticists to study gene function for almost four decades, resulting in the establishment of functional links for many genes and cellular processes in different species (Wright et al. 1988; Sokol et al. 1991; Halder et al. 1995; Palatnik et al. 2003). Overexpression studies offer the advantages of providing insights into the function of even redundant genes, having dominant effects which allows them to be readily used in diploid organisms, and being able to reveal regulatory steps in signalling pathways, among others. However, overexpression studies also have important associated limitations. For example, it is possible that an overexpressed protein may lead to outputs that are not physiologically relevant. For example, an overexpressed transcription factor or epigenetic regulator may target genes or

chromatin domains that are not normally regulated by that factor when expressed at physiological levels. Overexpression of specific proteins may disrupt regulatory processes or overload signalling pathways, cause the aggregation of proteins, titrate endogenous factors leading to their limitation, and/or lead to an imbalance in protein complex composition (Vavouri et al. 2009; Birchler and Veitia 2012; Makanae et al. 2013; Tang and Amon 2013; Bolognesi et al. 2016). Furthermore, long-term or extremely high overexpression of any protein may eventually deplete resources and saturate a cell's capacity for the synthesis, proper folding and transport of proteins (Raden et al. 2005; Stoebel et al. 2008; Moriya 2015).

For example, studies performed in yeast have estimated that the limit of overexpression of proteins is around 15% of the total protein content in the cell, and when the limit of a cell's "protein burden" is reached it may lead to the impairment of cellular growth (Kintaka et al. 2016; Eguchi et al. 2018). However, this limit can be much lower when an overexpressed protein exerts "toxic" effects (Kintaka et al. 2016; Eguchi et al. 2018).

In the work presented here, overexpression of the bromodomain protein ZMYND8 led to the almost complete repression of MITF expression, yet deletion mutations in ZMYND8 failed to reveal any specific domain required for the MITF repression observed, and siRNA-mediated depletion of ZMYND8 failed to affect MITF expression. It is possible that MITF repression arose as a consequence of a non-specific stress response triggered by too high levels of ZMYND8 WT or mutant expression, possibly saturating the protein folding capacity of cells and leading to activation of the integrated stress response. This would lead to repression of MITF mRNA expression via ATF4, and also reduce MITF protein levels via the translation reprogramming that occurs under stress conditions (Falletta et al. 2017; Ferguson et al. 2017). However, unlike in yeast, no studies have been performed to determine in melanoma cells the levels of protein overexpression necessary to trigger a

stress response, and although it is unlikely that melanoma cells will be more sensitive to stress arising from overexpression of proteins than other cell types, without evidence that the overexpression of ZMYND8 does indeed lead to activation of ATF4 translation, this potential interpretation remains speculative.

Alternatively, ZMYND8 overexpression may repress MITF inappropriately through regulation of the chromatin conformation at the MITF gene. This might occur for example if overexpressed ZMYND8 was not fully incorporated into the regulatory complexes that may direct ZMYND8 to specific physiologically relevant targets, or if ZMYND8 was complexed with a repressor such that at physiological levels it is inactivated, but overexpression titrates out the repressor enabling ZMYND8 to regulate its targets. These potential mechanisms underlying the ability of ZMYND8 to regulate *MITF* expression are at this stage also speculative, and further research will therefore be needed to determine precisely how ectopic overexpressed ZMYND8 might exert its effects. Particularly important will be to test whether ZMYND8 does indeed induce cellular stress, or whether depletion or overexpression of ZMYND8 affects any known targets.

While the results regarding ZMYND8 may indicate that overexpression of a protein may drive an unphysiological response, siRNA-mediated knock-down of specific genes, a key tool for the study of gene function which has been widely used for *in vitro* studies during almost two decades, is also associated with major problems of interpretation. The ease of use (including production and delivery of siRNAs into mammalian cells), possibility for genome-wide screens and powerful knock-down of gene expression are among the main reasons for their widespread use. Furthermore, huge efforts have been made to exploit the therapeutic potential of siRNAs (and other RNAi-based techniques), which have led to the recent FDA approval of the first siRNA drug, developed for the treatment of symptoms of peripheral nerve disease caused by hereditary transthyretin-mediated amyloidosis (Adams et al. 2018).

Moreover, 19 other synthetic siRNAs are currently in clinical trials for the treatment of various diseases including cancer (Saw and Song 2019). However, the therapeutic use of siRNAs generally presents major challenges which still require further work to be overcome, including their stability and targeted delivery, and the prevention of the triggering of an immune response and potential off-target effects (Saw and Song 2019).

Our results obtained with siRNA-mediated knock-down of the p66β and p66α subunits of the NuRD complex revealed that depletion experiments, like overexpression studies, may be highly problematic. Using siRNAs against both p66β and p66α encoded by different genes led to suppression of MITF expression. These observations therefore provided a strong validation that the NuRD complex regulates MITF expression. However, the use of additional siRNAs to knock-down p66β and p66α revealed that despite efficient knock-down of the target genes, only the first two (previously used) siRNAs were able to supress MITF. We therefore concluded that the p66 subunits/NuRD are not essential for MITF expression and that the previously observed effect on MITF expression was due to off-target effects associated to the siRNAs used. However, we cannot rule out the possibility that off-target effects of some siRNAs could suppress the loss of MITF. As such, we were unable to draw a robust conclusion as to the potential role of p66 or the NuRD complex in the regulation of MITF expression.

Similarly, our study of the potential role of MITF in the regulation of translation led us to identify dramatic differences in the phenotypes adopted by cells knocked-down for MITF using distinct siRNAs. These cells were in several cases clearly distinguishable just by brightfield microscopy and showed different rates of translation. Given the variability in protein synthesis using different siRNAs targeting MITF to a similar degree, we were unable to attribute an effect of MITF silencing on protein synthesis and concluded that the difference in phenotypes resulting from silencing MITF using different siRNAs was due to the

presence of off-target effects. However, again we cannot determine whether the off-target effects using siRNAs where MITF was suppressed caused a decrease in translation or suppressed a decrease in translation caused by MITF depletion. The latter interpretation would be consistent with the upregulation of PTEN observed using several different siRNAs targeting MITF.

The work presented in this study therefore strongly underscores the limitation to the use of siRNAs in therapy and in the study of gene function associated with the presence of off-target effects. Further investigation will consequently be needed to develop strategies that prevent off-target effects, among which the introduction of some chemical modifications in the siRNAs have already emerged as potential ways to address the problem (Jackson et al. 2006a; Zhang et al. 2018). Note that CRISPR/Cas9-mediated gene silencing can be used to generated gene-specific knock-outs without major off-target effects. However, knock-out of MITF is expected to cause a cell cycle arrest and consequently it would be difficult to establish knock-out cell lines unless they adapt to proliferate in an MITF-independent fashion.

The obstacles encountered over the course of this study in overexpression and silencing experiments are associated with the molecular biology tools used, and therefore emphasise the risk of drawing inaccurate conclusions from experiments performed using them when the appropriate controls are missing or insufficient caution is taken. The observations made therefore highlight the importance of perturbing the system to the minimum possible extent if relevant findings are to be generated.

Antibodies constitute another tool widely used in molecular biology that has been extensively used throughout this study. Antibodies have been the workhorses of experiments for many decades, yet there is currently a growing concern for their specificity and their lot-to-lot variability that is placing them as one of the main sources of problems in

molecular biology laboratories. Studies have estimated that around half of the antibodies commercially available are unreliable, and many scientists have already experienced the major issues arising from the use of antibodies that have been insufficiently validated (Baker 2015). To prevent the generation of false results, the antibodies used in this study have been validated in the laboratory at least through target depletion and when possible also through overexpression of a tagged version of the recognised protein. Moreover, we also made extensive use of expression of epitope-tagged proteins where the issues surrounding antibody specificity are circumvented.

In addition to the molecular biology tools used, the results generated in the experiments performed throughout this study might have been affected by the cell culture conditions used, which do not represent the physiological conditions encountered by tumour cells *in vivo*. Cell culture media are generally designed to optimise cell growth and increase the time before key nutrients are depleted. They consequently contain ultra-high concentrations of nutrients, well above those found in the tumour metabolic environment. For example, RPMI contains 11 mM glucose, compared to 5 mM found in blood. The realisation of the potential impact of these high nutrient conditions on cell metabolism and consequently the results of the experiments performed has promoted the production of new cell culture media better resembling physiological conditions (Schug et al. 2015; Tardito et al. 2015; Davidson et al. 2016; Cantor et al. 2017; Muir et al. 2017; Vande Voorde et al. 2019). Other problems associated with *in vitro* cell culture include the absence of an appropriate mechanical environment (Pampaloni et al. 2007), the excess of oxygen when culturing cells at atmospheric $O_2$ concentration (Ivanovic 2009), the presence in most cases of undefined serum (Arora 2013), and the accumulation of waste products (Halldorsson et al. 2015). These limitations might be important in interpreting the results generated here. For example, while several siRNAs targeting MITF led to upregulation of PTEN, the effects on

AKT activation downstream from PI3K signalling and upstream from the mTORC1 complex that controls protein translation was variable. However, as AKT phosphorylation is also controlled by glucose levels via mTORC2, the high glucose present in culture medium could affect the activation of AKT when PTEN expression is upregulated following MITF depletion. Therefore, it is important that the results generated in this study are confirmed *in vivo* and research would benefit from the use of cell culture conditions closer to those found in the physiological setting.

Additionally, cell confluency in cell culture can affect the results of the experiments performed. Throughout the experimentation undertaken in this study we noted that very high confluency of melanoma cells (a situation leading to cellular stress) results in the induction of ATF4 (not shown), perhaps as a consequence of rapid nutrient depletion. To minimise the risk of irreproducibility due to differences in cell confluency, the experiments presented in this study have all been performed at around 65% confluency, with slight variations depending on the specific conditions of the experiments and their duration.

Moreover, while cell lines remain the most commonly used model for the study of cancer biology, presenting advantages such as low cost, ease of use, consistency, and unlimited supply, it has long been recognised that they do not always adequately represent their counterpart primary cells or recapitulate the disease (Kaur and Dufour 2012; Hynds et al. 2018). The genetic manipulation involved in the process of immortalisation of primary cells may alter their phenotype and modify their response to stimuli, and the repetitive passage of the generated cell lines, including those derived from tumours without additional genetic manipulation, can lead to the accumulation of additional genotypic and phenotypic changes making the cell line progressively less representative and more heterogeneous. Furthermore, when derived from the tumour, only a subpopulation of cells makes it through the process and a uniform cell line is finally generated, with many of the tumour features

being lost. To ensure that the results obtained in this study are not dependent on the characteristics of a specific cell line, most of the experiments presented have been performed in at least two different cell lines and for the few experiments which, for limited time and/or resources, have only been performed in one cell line, it will be a priority in future investigation to be repeated in at least another cell line.

Finally, bioinformatics pipelines can lead to different results depending on the settings and thresholds established using the analysis tools. To ensure the generation of robust conclusions from the experiments performed in this study where bioinformatic analysis was carried out, all the main results were validated in an independent analysis performed by a bioinformatician.

## 6.2. – Potential role of ATF4 in phenotype switching as a regulator of the expression of MITF and other genes

As previously introduced, melanoma is a highly heterogeneous type of cancer where different cell populations have been identified in tumours and have been attributed specific roles in metastasis and drug-resistance, eventually responsible for most deaths in melanoma patients (Somasundaram et al. 2012; Perego et al. 2018). It is therefore crucial to achieve a better understanding of intra-tumoural phenotypic heterogeneity with the main aim of generating therapies targeting those populations responsible for melanoma metastasis and drug-resistance.

The association of different levels of MITF with distinct phenotypes in cells (from a quiescent/invasive to a proliferative and a differentiated cell cycle arrested phenotype) (Hoek and Goding 2010; Goding 2011), led us to further study the regulation of MITF. Previous evidence had already pointed to the repression of MITF expression by ATF4 and

had suggested an underlying direct mechanism of regulation involving binding of ATF4 to the MITF promoter (Falletta et al. 2017; Ferguson et al. 2017). In this study, we confirmed the role of ATF4 as a repressor of MITF but generated evidence indicating that ATF4 binds to exon 4 of *MITF* gene body instead, which might impair the formation of a promoter/enhancer gene loop essential for MITF expression. Disruption of the consensus ATF4 binding sites found under the ATF4 ChIP-seq peak indicating binding of ATF4 to *MITF* exon 4 using CRISPR technology will be required in conjunction with assays for induction of ATF4 expression to confirm this potential direct mechanism underlying ATF4 regulation of MITF.

However, with the binding of TFs to enhancer regions having emerged as a major mechanism of transcriptional regulation, especially in development and differentiation (Ong and Corces 2011; Spitz and Furlong 2012), it is also possible that a direct regulation of *MITF* by ATF4 could imply binding of ATF4 to a regulatory genomic region far away from the *MITF* gene body which we would have not been able to associate to *MITF* regulation through the ChIP-seq experiment performed. Chromosome conformation capture assays (Dekker et al. 2002) will therefore be also required to examine the possibility of an alternative direct mechanism of regulation of *MITF* expression by ATF4.

Additionally, the ATF4 ChIP-seq and RNA-seq analyses performed in this study provided evidence supporting the potential role of ATF4 in the direct regulation of some of the main known MITF targets and further genes that have been associated with invasion and/or metastasis including *HOXB9*, *S100P*, *CLIC4*, *SERPINE2* and *GLI2* (Arumugam et al. 2005; Whiteman et al. 2007; Alexaki et al. 2010; Hayashida et al. 2010; Javelaud et al. 2011; Jiang et al. 2011; Huang et al. 2014b; Shukla et al. 2014; Hsu et al. 2015; Jiang et al. 2016; Wu 2016; Liu et al. 2017; Perego et al. 2018). It is therefore possible that the regulation of ATF4 expression in stress conditions frequently found in tumours, such as nutrient limitation or

hypoxia, leads to the induction of an invasive phenotype in melanoma cells at least partly through the direct regulation of the expression of *MITF* and some of its target genes, as well as the potential direct regulation of *HOXB9*, *S100P*, *CLIC4*, *SERPINE2* and *GLI2*. However, it is important to note that direct effects of eIF2α phosphorylation on translation of specific mRNAs are also likely to play a role, though precisely which proteins contribute will require a detailed analysis of the repertoire of translated proteins under stress versus non-stress conditions.

The association of ATF4 expression with cancer invasiveness and/or metastasis has not only been identified in melanoma (Falletta et al. 2017), but also in other cancer types including breast cancer (González-González et al. 2018) and oesophageal squamous cell carcinoma (Zhu et al. 2014), pointing to a general mechanism of induction of an invasive phenotype by ATF4 not limited to melanoma. Furthermore, induction of ATF4 expression has been associated with drug resistance in several types of cancer (Igarashi et al. 2007; Rzymski et al. 2009; Zhu et al. 2012; Chen et al. 2017; Pathria et al. 2018; Shi et al. 2019).

Interestingly, a single cell RNA-seq study recently showed that a drug-resistant cell population present in minimal residual disease (MRD) following RAF/MEK inhibition in BRAF-mutant melanomas is characterised by a "starvation"-like transcriptional program and low MITF expression, and appears to be a transition state to an invasive (also drug-resistant) population (Rambow et al. 2018). Our study provides a potential mechanism that might underlie the generation of these invasive/drug-resistant subpopulations in starved regions of melanoma tumours. Induction of ATF4 likely drives a key part of the response to the nutrient limitation conditions found in tumours, as identified in our experiments using glucose limitation performed in this study. Through the downregulation of *MITF* and their target genes and the upregulation of different genes associated with invasion, ATF4 may

drive a phenotype-switch allowing the generation of a subpopulation of melanoma cells with an invasive phenotype able to produce metastasis.

Previous studies have suggested the induction of cytoprotective autophagy resulting from the triggering of ER stress induced by RAF/MEK inhibition (Ma et al. 2014). In part this response, leading to drug-resistance, may be mediated by ATF4 according to its role in the induction of autophagy (Rzymski et al. 2009; Rouschop et al. 2010; Rzymski et al. 2010; B'chir et al. 2013) and its upregulation in response to ER stress (Pakos-Zebrucka et al. 2016; Wortel et al. 2017). Furthermore, the well-known role of ATF4 in the adaptation to different types of cellular stress likely contributes to the survival of drug-resistant cells (Wortel et al. 2017). Additionally, the evidence presented in this study suggests a potential direct regulation by ATF4 of *HERPUD1*, which has a cytoprotective role (Chan et al. 2004; Hori et al. 2004; Nogalska et al. 2006; Shinozaki et al. 2013; Paredes et al. 2016), as well as the potentially direct (or MITF-mediated) upregulation of *PTEN* and *DEPTOR* expression, which might also facilitate survival contributing to the adaptation to low nutrient conditions by reducing protein sysnthesis. Finally, different types of cellular stress can confer drug-resistance through a mechanism involving the AP-1 family component c-Jun, an ATF4 binding partner (Emmons et al. 2019), which could cooperate with ATF4 in the transcriptional regulation of specific genes involved in the induction of a drug-resistant phenotype.

In addition to the potential direct effects of ATF4 in the induction of a drug-resistant phenotype, additional mechanisms mediated by the downregulation of *MITF* expression by ATF4 may also contribute, as low MITF has been associated with drug-resistance (Konieczkowski et al. 2014; Müller et al. 2014). While it is currently not fully understood how low MITF levels might confer a drug-resistant phenotype, it has been proposed that an underlying mechanism could involve the derepression of the expression of several receptor

tyrosine kinases, including AXL (Müller et al. 2014). However, we have shown in this study that the potential regulation of *AXL* by MITF is at least unlikely to be direct, since no significant ATF4 ChIP-seq peaks were found around AXL genomic region, although we cannot rule out a mechanism involving binding of ATF4 to a distant enhancer region. Finally, low *MITF* expression confers a dedifferentiated state in melanoma cells, and dedifferentiation has been associated with therapy resistance (Konieczkowski et al. 2014; Müller et al. 2014; Rambow et al. 2018; Tsoi et al. 2018).

Furthermore, additional mechanisms of induction of an invasive/drug-resistant phenotype involving factors upstream of ATF4 in the integrated stress response triggered in nutrient starvation conditions or other cellular stresses may also contribute. Indeed, ectopic expression of ATF4 using a doxycycline-inducible system is insufficient to drive melanoma invasion, while pharmacological inhibition of eIF2α dephosphorylation can induce invasiveness in melanoma cells (Falletta et al. 2017). It is therefore possible that ATF4 contributes to the induction of an invasive phenotype but that phosphorylation of eIF2α (upstream of ATF4 in the integrated stress response) by the kinases sensing different types of cellular stress (see section 1.4) (Pakos-Zebrucka et al. 2016) is the main driver of this process. Since phosphorylation of eIF2α triggers translation reprograming (see sections 1.4 and 1.5.3) (Harding et al. 2000; Sonenberg and Hinnebusch 2009), it is possible that the shutdown of global translation is necessary for the induction of invasiveness or alternatively that the increase in cap-independent translation of another/other specific mRNA/s plays a key role in this process. However, it is also possible that in the nutrient rich conditions used for the experiments of doxycycline-induced ectopic ATF4 expression (Falletta et al. 2017), the potential promotion of invasiveness by ATF4 was suppressed, or that ATF4 binding partners or further activators of its activity were absent.

Finally, while the present study has focused on the regulation of gene expression by ATF4 in conditions of glucose starvation, our results are likely highly applicable to other types of cellular stresses, including amino acid limitation, hypoxia, ER stress, and other types of cellular stress triggering the integrated stress response and the consequent induction of ATF4 expression. While nutrient limitation and hypoxia may be the main external drivers of an invasive/drug-resistant phenotype, in part through the induction of ATF4 expression in core tumour regions, tumour cells at the edge of tumours, have also been shown to be invasive (Christofori 2006). Cells on the periphery of tumours might undergo a phenotype-switch as a consequence of exposure to inflammatory cytokines, such as TNF-α (Balkwill 2009), and TGF-β, a cytokine with an important role in development that has been associated with the induction of EMT (Bierie and Moses 2006; Pickup et al. 2013; Nieto et al. 2016; Pastushenko et al. 2018). Both TNF-α and TGF-β, frequently secreted by tumour associated immune cells, can also induce eIF2α phosphorylation and ATF4 expression (Srivastava et al. 1998; Feng et al. 2014; Falletta et al. 2017). Finally, targeted therapy can also induce cellular stress (Ma et al. 2014), which might contribute to the generation of the invasive and drug-resistant phenotypes that have been shown to originate following RAF/MEK inhibition in melanoma cells (Rambow et al. 2018).

In summary, the results presented in this thesis, reveal for the first time the genome-wide consequences of glucose limitation in melanoma, as well as the role of ATF4 in regulating the global response to glucose (and other stresses). The work also highlights the role of MITF in suppressing PTEN and DEPTOR expression, known regulators of PI3K and mTORC1 signalling (**Figure 6.1**).

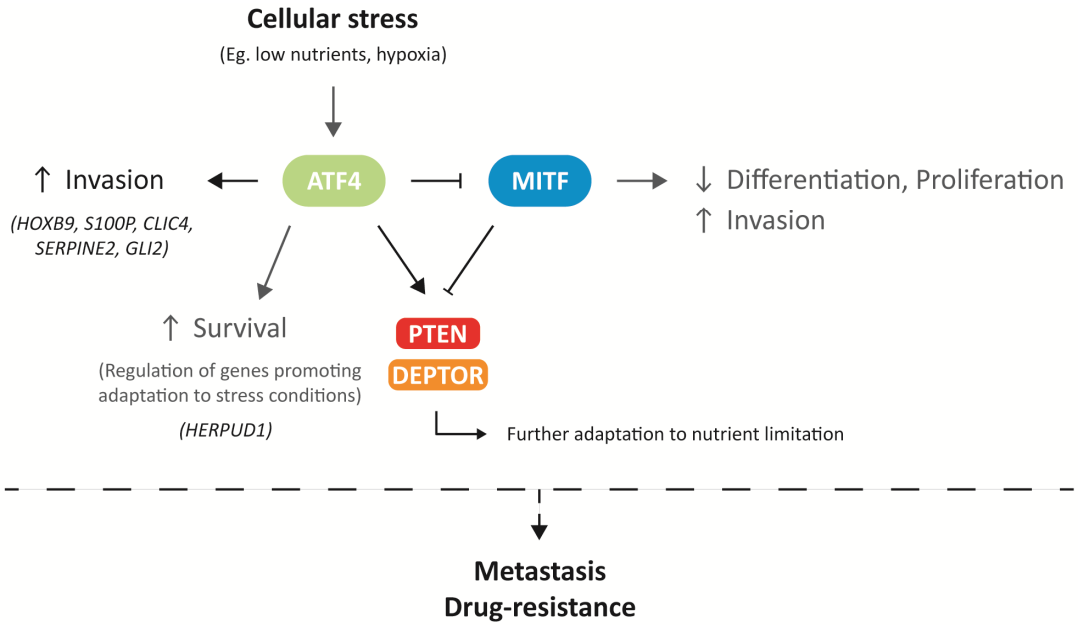


**Figure 6.1.- Proposed model of phenotype-switching under cellular stress conditions in melanoma.** Cellular stress conditions such as low nutrients or hypoxia, frequently found in certain regions of tumours, result in the induction of ATF4 expression, which might promote invasion at least partly through the positive regulation of *HOXB9*, *S100P*, *CLIC4*, *SERPINE2* and *GLI2*, genes that have been associated with invasion and/or metastasis (Arumugam et al. 2005; Whiteman et al. 2007; Alexaki et al. 2010; Hayashida et al. 2010; Javelaud et al. 2011; Jiang et al. 2011; Huang et al. 2014b; Shukla et al. 2014; Hsu et al. 2015; Jiang et al. 2016; Wu 2016; Liu et al. 2017; Perego et al. 2018). Furthermore, ATF4 can promote survival through the regulation of well-known targets driving adaptation to cellular stress conditions (Wortel et al. 2017), and the potential regulation of *HERPUD1*, a gene with a described cytoprotective role (Chan et al. 2004; Hori et al. 2004; Nogalska et al. 2006; Shinozaki et al. 2013; Paredes et al. 2016). ATF4 negatively regulates *MITF* expression and low MITF is associated with invasiveness, dedifferentiation and low proliferation (Carreira et al. 2006; Goding 2011). Finally, ATF4 positively regulates *PTEN* and *DEPTOR* directly and/or through the downregulation of MITF, a potential repressor of *PTEN* and *DEPTOR*, which may contribute to the adaptation to nutrient limitation conditions by reducing protein synthesis. All these mechanisms might lead to a reversible switch to an invasive phenotype with increased survival capacity in melanoma cells driving metastasis and drug-resistance in response to cellular stress triggered by microenvironmental conditions. (Previously known processes marked in grey).

Although further work will be necessary to define definitely the direct regulation of *PTEN* and *DEPTOR* by MITF, as well as the precisely how stress induces invasion via eIF2α phosphorylation (Falletta et al. 2017), defining the repertoire of direct ATF4 targets in melanoma represents a key step in our understanding of the molecular mechanisms underlying the proliferative to invasive phenotype-switch. To take our understanding further, experiments triggering the integrated stress response with simultaneous knock-

down of ATF4 will be needed to confirm the requirement of ATF4 in the induction of an invasive melanoma phenotype in response to stress conditions, or at least determine its contribution. This is expected to be highly significant considering evidence linking ATF4 and invasion in breast cancer and oesophageal squamous cell carcinoma that revealed a decrease in invasion and metastasis when silencing ATF4 (Zhu et al. 2014; González-González et al. 2018).

While the genetic heterogeneity observed within and among tumours in a patient constitutes a big challenge for the generation of targeted therapies, the presence of reversible mechanisms of phenotype-switching driving transitions between different phenotypes likely common to most tumours, presents the possibility of generating therapies targeting specific cell phenotypes or driving cells into a sensitive phenotype independently of the genetic background (Sáez-Ayala et al. 2013). The evidence generated in this study provides a better understanding of the mechanisms of phenotype-switching triggered by cellular stress conditions in melanoma which will hopefully contribute to the development of new therapeutic strategies directed toward the elimination of drug-resistant and invasive cells generated through non-genetic mechanisms.

# References

Abbas T, Dutta A. 2009. p21 in cancer: intricate networks and multiple activities. *Nat Rev Cancer* **9**: 400-414.

Adams D, Gonzalez-Duarte A, O'Riordan WD, Yang CC, Ueda M, Kristen AV, Tournev I, Schmidt HH, Coelho T, Berk JL et al. 2018. Patisiran, an RNAi Therapeutic, for Hereditary Transthyretin Amyloidosis. *N Engl J Med* **379**: 11-21.

Adelman K, Lis JT. 2012. Promoter-proximal pausing of RNA polymerase II: emerging roles in metazoans. *Nat Rev Genet* **13**: 720-731.

Ahituv N. 2016. Exonic enhancers: proceed with caution in exome and genome sequencing studies. *Genome Med* **8**: 14.

Ahmed F, Haass NK. 2018. Microenvironment-Driven Dynamic Heterogeneity and Phenotypic Plasticity as a Mechanism of Melanoma Therapy Resistance. *Front Oncol* **8**: 173.

Aksan I, Goding CR. 1998. Targeting the microphthalmia basic helix-loop-helix-leucine zipper transcription factor to a subset of E-box elements in vitro and in vivo. *Mol Cell Biol* **18**: 6930-6938.

Alexaki VI, Javelaud D, Van Kempen LC, Mohammad KS, Dennler S, Luciani F, Hoek KS, Juàrez P, Goydos JS, Fournier PJ et al. 2010. GLI2-mediated melanoma invasion and metastasis. *J Natl Cancer Inst* **102**: 1148-1159.

Alkhatib SG, Landry JW. 2011. The nucleosome remodeling factor. *FEBS Lett* **585**: 3197-3207.

Alonso SR, Tracey L, Ortiz P, Pérez-Gómez B, Palacios J, Pollán M, Linares J, Serrano S, Sáez-Castillo AI, Sánchez L et al. 2007. A high-throughput study in melanoma identifies epithelial-mesenchymal transition as a major determinant of metastasis. *Cancer Res* **67**: 3450-3460.

Alves CP, Yokoyama S, Goedert L, Pontes CLS, Sousa JF, Fisher DE, Espreafico EM. 2017. MYO5A Gene Is a Target of MITF in Melanocytes. *J Invest Dermatol* **137**: 985-989.

Amae S, Fuse N, Yasumoto K, Sato S, Yajima I, Yamamoto H, Udono T, Durlu YK, Tamai M, Takahashi K et al. 1998. Identification of a novel isoform of microphthalmia-associated transcription factor that is enriched in retinal pigment epithelium. *Biochem Biophys Res Commun* **247**: 710-715.

Ameri K, Lewis CE, Raida M, Sowter H, Hai T, Harris AL. 2004. Anoxic induction of ATF-4 through HIF-1-independent pathways of protein stabilization in human cancer cells. *Blood* **103**: 1876-1882.

American Cancer Society. Melanoma Statistics.

Ampofo E, Sokolowsky T, Götz C, Montenarh M. 2013. Functional interaction of protein kinase CK2 and activating transcription factor 4 (ATF4), a key player in the cellular stress response. *Biochim Biophys Acta* **1833**: 439-451.

Andrey G, Mundlos S. 2017. The three-dimensional genome: regulating gene expression during pluripotency and development. *Development* **144**: 3646-3658.

Ansari SA, Paul E, Sommer S, Lieleg C, He Q, Daly AZ, Rode KA, Barber WT, Ellis LC, LaPorta E et al. 2014. Mediator, TATA-binding protein, and RNA polymerase II contribute to low histone occupancy at active gene promoters in yeast. *J Biol Chem* **289**: 14981-14995.

Aranda-Orgilles B, Saldaña-Meyer R, Wang E, Trompouki E, Fassl A, Lau S, Mullenders J, Rocha PP, Raviram R, Guillamot M et al. 2016. MED12 Regulates HSC-Specific Enhancers Independently of Mediator Kinase Activity to Control Hematopoiesis. *Cell Stem Cell* **19**: 784-799.

Arora M. 2013. Cell Culture Media: A Review. *Materials and Methods* **3**: 175.

Arozarena I, Sanchez-Laorden B, Packer L, Hidalgo-Carcedo C, Hayward R, Viros A, Sahai E, Marais R. 2011. Oncogenic BRAF induces melanoma cell invasion by downregulating the cGMP-specific phosphodiesterase PDE5A. *Cancer Cell* **19**: 45-57.

Arts N, Cané S, Hennequart M, Lamy J, Bommer G, Van den Eynde B, De Plaen E. 2015. microRNA-155, induced by interleukin-1ß, represses the expression of microphthalmia-associated transcription factor (MITF-M) in melanoma cells. *PLoS One* **10**: e0122517.

Arumugam T, Simeone DM, Van Golen K, Logsdon CD. 2005. S100P promotes pancreatic cancer growth, survival, and invasion. *Clin Cancer Res* **11**: 5356-5364.

Ascierto PA, Kirkwood JM, Grob JJ, Simeone E, Grimaldi AM, Maio M, Palmieri G, Testori A, Marincola FM, Mozzillo N. 2012. The role of BRAF V600 mutation in melanoma. *J Transl Med* **10**: 85.

Ashburner M, Ball CA, Blake JA, Botstein D, Butler H, Cherry JM, Davis AP, Dolinski K, Dwight SS, Eppig JT et al. 2000. Gene ontology: tool for the unification of biology. The Gene Ontology Consortium. *Nat Genet* **25**: 25-29.

Aubert C, Rougé F, Galindo JR. 1980. Tumorigenicity of human malignant melanocytes in nude mice in relation to their differentiation in vitro. *J Natl Cancer Inst* **64**: 1029-1040.

Ayer S, Benyajati C. 1990. Conserved enhancer and silencer elements responsible for differential Adh transcription in Drosophila cell lines. *Mol Cell Biol* **10**: 3512-3523.

B'chir W, Maurin AC, Carraro V, Averous J, Jousse C, Muranishi Y, Parry L, Stepien G, Fafournoux P, Bruhat A. 2013. The eIF2α/ATF4 pathway is essential for stress-induced autophagy gene expression. *Nucleic Acids Res* **41**: 7683-7699.

Badenhorst P, Voas M, Rebay I, Wu C. 2002. Biological functions of the ISWI chromatin remodeling complex NURF. *Genes Dev* **16**: 3186-3198.

Bagheri-Yarmand R, Sinha KM, Gururaj AE, Ahmed Z, Rizvi YQ, Huang SC, Ladbury JE, Bogler O, Williams MD, Cote GJ et al. 2015. A novel dual kinase function of the RET proto-oncogene negatively regulates activating transcription factor 4-mediated apoptosis. *J Biol Chem* **290**: 11749-11761.

Bagheri-Yarmand R, Sinha KM, Li L, Lu Y, Cote GJ, Sherman SI, Gagel RF. 2019. Combinations of Tyrosine Kinase Inhibitor and ERAD Inhibitor Promote Oxidative Stress-Induced Apoptosis through ATF4 and KLF9 in Medullary Thyroid Cancer. *Mol Cancer Res* **17**: 751-760.

Bai L, Morozov AV. 2010. Gene regulation by nucleosome positioning. *Trends Genet* **26**: 476-483.

Baird TD, Wek RC. 2012. Eukaryotic initiation factor 2 phosphorylation and translational control in metabolism. *Adv Nutr* **3**: 307-321.

Baker JB, Gronke RS. 1986. Protease nexins and cellular regulation. *Semin Thromb Hemost* **12**: 216-220.

Baker M. 2015. Reproducibility crisis: Blame it on the antibodies. *Nature* **521**: 274-276.

Balkwill F. 2009. Tumour necrosis factor and cancer. *Nat Rev Cancer* **9**: 361-371.

Banerjee T, Chakravarti D. 2011. A peek into the complex realm of histone phosphorylation. *Mol Cell Biol* **31**: 4858-4873.

Bannister AJ, Kouzarides T. 2011. Regulation of chromatin by histone modifications. *Cell Res* **21**: 381-395.

Baptista T, Grünberg S, Minoungou N, Koster MJE, Timmers HTM, Hahn S, Devys D, Tora L. 2017. SAGA Is a General Cofactor for RNA Polymerase II Transcription. *Mol Cell* **68**: 130-143.e135.

Bartel DP. 2009. MicroRNAs: target recognition and regulatory functions. *Cell* **136**: 215-233.

Barthel KK, Liu X. 2008. A transcriptional enhancer from the coding region of ADAMTS5. *PLoS One* **3**: e2184.

Basta J, Rauchman M. 2015. The nucleosome remodeling and deacetylase complex in development and disease. *Transl Res* **165**: 36-47.

Becker PB, Hörz W. 2002. ATP-dependent nucleosome remodeling. *Annu Rev Biochem* **71**: 247-273.

Becker T, Gerke V, Kube E, Weber K. 1992. S100P, a novel Ca(2+)-binding protein from human placenta. cDNA cloning, recombinant protein expression and Ca2+ binding properties. *Eur J Biochem* **207**: 541-547.

Bemis LT, Chen R, Amato CM, Classen EH, Robinson SE, Coffey DG, Erickson PF, Shellman YG, Robinson WA. 2008. MicroRNA-137 targets microphthalmia-associated transcription factor in melanoma cell lines. *Cancer Res* **68**: 1362-1368.

Bennett DC. 2016. Genetics of melanoma progression: the rise and fall of cell senescence. *Pigment Cell Melanoma Res* **29**: 122-140.

Berg OG, Winter RB, von Hippel PH. 1981. Diffusion-driven mechanisms of protein translocation on nucleic acids. 1. Models and theory. *Biochemistry* **20**: 6929-6948.

Bergeron S, Lemieux E, Durand V, Cagnol S, Carrier JC, Lussier JG, Boucher MJ, Rivard N. 2010. The serine protease inhibitor serpinE2 is a novel target of ERK signaling involved in human colorectal tumorigenesis. *Mol Cancer* **9**: 271.

Bernards R, Weinberg RA. 2002. A progression puzzle. *Nature* **418**: 823.

Bertolotto C, Abbe P, Hemesath TJ, Bille K, Fisher DE, Ortonne JP, Ballotti R. 1998a. Microphthalmia gene product as a signal transducer in cAMP-induced differentiation of melanocytes. *J Cell Biol* **142**: 827-835.

Bertolotto C, Buscà R, Abbe P, Bille K, Aberdam E, Ortonne JP, Ballotti R. 1998b. Different cis-acting elements are involved in the regulation of TRP1 and TRP2 promoter activities by cyclic AMP: pivotal role of M boxes (GTCATGTGCT) and of microphthalmia. *Mol Cell Biol* **18**: 694-702.

Bertolotto C, Lesueur F, Giuliano S, Strub T, de Lichy M, Bille K, Dessen P, d'Hayer B, Mohamdi H, Remenieras A et al. 2011. A SUMOylation-defective MITF germline mutation predisposes to melanoma and renal carcinoma. *Nature* **480**: 94-98.

Beuret L, Flori E, Denoyelle C, Bille K, Busca R, Picardo M, Bertolotto C, Ballotti R. 2007. Up-regulation of MET expression by alpha-melanocyte-stimulating hormone and MITF allows hepatocyte growth factor to protect melanocytes and melanoma cells from apoptosis. *J Biol Chem* **282**: 14140-14147.

Beuret L, Ohanna M, Strub T, Allegra M, Davidson I, Bertolotto C, Ballotti R. 2011. BRCA1 is a new MITF target gene. *Pigment Cell Melanoma Res* **24**: 725-727.

Bhattacharyya S, Wei J, Melichian DS, Milbrandt J, Takehara K, Varga J. 2009. The transcriptional cofactor nab2 is induced by tgf-Beta and suppresses fibroblast activation: physiological roles and impaired expression in scleroderma. *PLoS One* **4**: e7620.

Bhinder B, Djaballah H. 2013. Systematic analysis of RNAi reports identifies dismal commonality at gene-level and reveals an unprecedented enrichment in pooled shRNA screens. *Comb Chem High Throughput Screen* **16**: 665-681.

Bi M, Naczki C, Koritzinsky M, Fels D, Blais J, Hu N, Harding H, Novoa I, Varia M, Raleigh J et al. 2005. ER stress-regulated translation increases tolerance to extreme hypoxia and promotes tumor growth. *EMBO J* **24**: 3470-3481.

Bianchi-Smiraglia A, Bagati A, Fink EE, Moparthy S, Wawrzyniak JA, Marvin EK, Battaglia S, Jowdy P, Kolesnikova M, Foley CE et al. 2017. Microphthalmia-associated

transcription factor suppresses invasion by reducing intracellular GTP pools. *Oncogene* **36**: 84-96.

Biddie SC, John S, Sabo PJ, Thurman RE, Johnson TA, Schiltz RL, Miranda TB, Sung MH, Trump S, Lightman SL et al. 2011. Transcription factor AP1 potentiates chromatin accessibility and glucocorticoid receptor binding. *Mol Cell* **43**: 145-155.

Bierie B, Moses HL. 2006. Tumour microenvironment: TGFbeta: the molecular Jekyll and Hyde of cancer. *Nat Rev Cancer* **6**: 506-520.

Birchler JA, Veitia RA. 2012. Gene balance hypothesis: connecting issues of dosage sensitivity across biological disciplines. *Proc Natl Acad Sci U S A* **109**: 14746-14753.

Birmingham A, Anderson EM, Reynolds A, Ilsley-Tyree D, Leake D, Fedorov Y, Baskerville S, Maksimova E, Robinson K, Karpilow J et al. 2006. 3' UTR seed matches, but not overall identity, are associated with RNAi off-targets. *Nat Methods* **3**: 199-204.

Blainey PC, van Oijen AM, Banerjee A, Verdine GL, Xie XS. 2006. A base-excision DNA-repair protein finds intrahelical lesion bases by fast sliding in contact with DNA. *Proc Natl Acad Sci U S A* **103**: 5752-5757.

Bollag G, Hirth P, Tsai J, Zhang J, Ibrahim PN, Cho H, Spevak W, Zhang C, Zhang Y, Habets G et al. 2010. Clinical efficacy of a RAF inhibitor needs broad target blockade in BRAF-mutant melanoma. *Nature* **467**: 596-599.

Bolognesi B, Lorenzo Gotor N, Dhar R, Cirillo D, Baldrighi M, Tartaglia GG, Lehner B. 2016. A Concentration-Dependent Liquid Phase Separation Can Cause Toxicity upon Increased Protein Expression. *Cell Rep* **16**: 222-231.

Bonnet I, Biebricher A, Porté PL, Loverdo C, Bénichou O, Voituriez R, Escudé C, Wende W, Pingoud A, Desbiolles P. 2008. Sliding and jumping of single EcoRV restriction enzymes on non-cognate DNA. *Nucleic Acids Res* **36**: 4118-4127.

Bonnet J, Wang CY, Baptista T, Vincent SD, Hsiao WC, Stierle M, Kao CF, Tora L, Devys D. 2014. The SAGA coactivator complex acts on the whole transcribed genome and is required for RNA polymerase II transcription. *Genes Dev* **28**: 1999-2012.

Bonvin E, Falletta P, Shaw H, Delmas V, Goding CR. 2012. A phosphatidylinositol 3-kinase-Pax3 axis regulates Brn-2 expression in melanoma. *Mol Cell Biol* **32**: 4674-4683.

Bornelöv S, Reynolds N, Xenophontos M, Gharbi S, Johnstone E, Floyd R, Ralser M, Signolet J, Loos R, Dietmann S et al. 2018. The Nucleosome Remodeling and Deacetylation Complex Modulates Chromatin Structure at Sites of Active Transcription to Fine-Tune Gene Expression. *Mol Cell* **71**: 56-72.e54.

Bouazoune K, Mitterweger A, Längst G, Imhof A, Akhtar A, Becker PB, Brehm A. 2002. The dMi-2 chromodomains are DNA binding modules important for ATP-dependent nucleosome mobilization. *EMBO J* **21**: 2430-2440.

Bouillet P, Cory S, Zhang LC, Strasser A, Adams JM. 2001. Degenerative disorders caused by Bcl-2 deficiency prevented by loss of its BH3-only antagonist Bim. *Dev Cell* **1**: 645-653.

Bowen NJ, Fujita N, Kajita M, Wade PA. 2004. Mi-2/NuRD: multiple complexes for many purposes. *Biochim Biophys Acta* **1677**: 52-57.

Brackertz M, Gong Z, Leers J, Renkawitz R. 2006. p66alpha and p66beta of the Mi-2/NuRD complex mediate MBD2 and histone interaction. *Nucleic Acids Res* **34**: 397-406.

Bruhat A, Chérasse Y, Maurin AC, Breitwieser W, Parry L, Deval C, Jones N, Jousse C, Fafournoux P. 2007. ATF2 is required for amino acid-regulated transcription by orchestrating specific histone acetylation. *Nucleic Acids Res* **35**: 1312-1321.

Brüning A, Rahmeh M, Friese K. 2013. Nelfinavir and bortezomib inhibit mTOR activity via ATF4-mediated sestrin-2 regulation. *Mol Oncol* **7**: 1012-1018.

Calhoun VC, Stathopoulos A, Levine M. 2002. Promoter-proximal tethering elements regulate enhancer-promoter specificity in the Drosophila Antennapedia complex. *Proc Natl Acad Sci U S A* **99**: 9243-9247.

Cancer Genome Atlas Network. 2015. Genomic Classification of Cutaneous Melanoma. *Cell* **161**: 1681-1696.

Cancer Research UK. Melanoma Statistics.

Cantor JR, Abu-Remaileh M, Kanarek N, Freinkman E, Gao X, Louissaint A, Lewis CA, Sabatini DM. 2017. Physiologic Medium Rewires Cellular Metabolism and Reveals Uric Acid as an Endogenous Inhibitor of UMP Synthase. *Cell* **169**: 258-272.e217.

Cao H, Yu S, Yao Z, Galson DL, Jiang Y, Zhang X, Fan J, Lu B, Guan Y, Luo M et al. 2010. Activating transcription factor 4 regulates osteoclast differentiation in mice. *J Clin Invest* **120**: 2755-2766.

Caplen NJ, Parrish S, Imani F, Fire A, Morgan RA. 2001. Specific inhibition of gene expression by small double-stranded RNAs in invertebrate and vertebrate systems. *Proc Natl Acad Sci U S A* **98**: 9742-9747.

Caramel J, Papadogeorgakis E, Hill L, Browne GJ, Richard G, Wierinckx A, Saldanha G, Osborne J, Hutchinson P, Tse G et al. 2013. A switch in the expression of embryonic EMT-inducers drives the development of malignant melanoma. *Cancer Cell* **24**: 466-480.

Carey TE, Takahashi T, Resnick LA, Oettgen HF, Old LJ. 1976. Cell surface antigens of human malignant melanoma: mixed hemadsorption assays for humoral immunity to cultured autologous melanoma cells. *Proc Natl Acad Sci U S A* **73**: 3278-3282.

Carreira S, Goodall J, Aksan I, La Rocca SA, Galibert MD, Denat L, Larue L, Goding CR. 2005. Mitf cooperates with Rb1 and activates p21Cip1 expression to regulate cell cycle progression. *Nature* **433**: 764-769.

Carreira S, Goodall J, Denat L, Rodriguez M, Nuciforo P, Hoek KS, Testori A, Larue L, Goding CR. 2006. Mitf regulation of Dia1 controls melanoma proliferation and invasiveness. *Genes Dev* **20**: 3426-3439.

Carthew RW, Sontheimer EJ. 2009. Origins and Mechanisms of miRNAs and siRNAs. *Cell* **136**: 642-655.

Carè A, Valtieri M, Mattia G, Meccia E, Masella B, Luchetti L, Felicetti F, Colombo MP, Peschle C. 1999. Enforced expression of HOXB7 promotes hematopoietic stem cell proliferation and myeloid-restricted progenitor differentiation. *Oncogene* **18**: 1993-2001.

Chae YK, Chang S, Ko T, Anker J, Agte S, Iams W, Choi WM, Lee K, Cruz M. 2018. Epithelial-mesenchymal transition (EMT) signature is inversely associated with T-cell infiltration in non-small cell lung cancer (NSCLC). *Sci Rep* **8**: 2918.

Chalhoub N, Baker SJ. 2009. PTEN and the PI3-kinase pathway in cancer. *Annu Rev Pathol* **4**: 127-150.

Chan HM, La Thangue NB. 2001. p300/CBP proteins: HATs for transcriptional bridges and scaffolds. *J Cell Sci* **114**: 2363-2373.

Chan SL, Fu W, Zhang P, Cheng A, Lee J, Kokame K, Mattson MP. 2004. Herp stabilizes neuronal Ca2+ homeostasis and mitochondrial function during endoplasmic reticulum stress. *J Biol Chem* **279**: 28733-28743.

Chang B, Chen Y, Zhao Y, Bruick RK. 2007. JMJD6 is a histone arginine demethylase. *Science* **318**: 444-447.

Cheli Y, Giuliano S, Fenouille N, Allegra M, Hofman V, Hofman P, Bahadoran P, Lacour JP, Tartare-Deckert S, Bertolotto C et al. 2012. Hypoxia and MITF control metastatic behaviour in mouse and human melanoma cells. *Oncogene* **31**: 2461-2470.

Cheli Y, Ohanna M, Ballotti R, Bertolotto C. 2010. Fifteen-year quest for microphthalmia-associated transcription factor target genes. *Pigment Cell Melanoma Res* **23**: 27-40.

Chen D, Rauh M, Buchfelder M, Eyupoglu IY, Savaskan N. 2017. The oxido-metabolic driver ATF4 enhances temozolamide chemo-resistance in human gliomas. *Oncotarget* **8**: 51164-51176.

Chen EY, Tan CM, Kou Y, Duan Q, Wang Z, Meirelles GV, Clark NR, Ma'ayan A. 2013a. Enrichr: interactive and collaborative HTML5 gene list enrichment analysis tool. *BMC Bioinformatics* **14**: 128.

Chen JJ. 2007. Regulation of protein synthesis by the heme-regulated eIF2alpha kinase: relevance to anemias. *Blood* **109**: 2693-2699.

Chen Y, Gao H, Yin Q, Chen L, Dong P, Zhang X, Kang J. 2013b. ER stress activating ATF4/CHOP-TNF-α signaling pathway contributes to alcohol-induced disruption of osteogenic lineage of multipotential mesenchymal stem cell. *Cell Physiol Biochem* **32**: 743-754.

Chiaverini C, Beuret L, Flori E, Busca R, Abbe P, Bille K, Bahadoran P, Ortonne JP, Bertolotto C, Ballotti R. 2008. Microphthalmia-associated transcription factor regulates RAB27A gene expression and controls melanosome transport. *J Biol Chem* **283**: 12635-12642.

Chin L, Garraway LA, Fisher DE. 2006. Malignant melanoma: genetics and therapeutics in the genomic era. *Genes Dev* **20**: 2149-2182.

Christofori G. 2006. New signals from the invasive front. *Nature* **441**: 444-450.

Chérasse Y, Maurin AC, Chaveroux C, Jousse C, Carraro V, Parry L, Deval C, Chambon C, Fafournoux P, Bruhat A. 2007. The p300/CBP-associated factor (PCAF) is a cofactor of ATF4 for amino acid-regulated transcription of CHOP. *Nucleic Acids Res* **35**: 5954-5965.

Cismasiu VB, Adamo K, Gecewicz J, Duque J, Lin Q, Avram D. 2005. BCL11B functionally associates with the NuRD complex in T lymphocytes to repress targeted promoter. *Oncogene* **24**: 6753-6764.

Clapier CR, Cairns BR. 2009. The biology of chromatin remodeling complexes. *Annu Rev Biochem* **78**: 273-304.

Clapier CR, Cairns BR. 2012. Regulation of ISWI involves inhibitory modules antagonized by nucleosomal epitopes. *Nature* **492**: 280-284.

Clark WH, Elder DE, Guerry D, Epstein MN, Greene MH, Van Horn M. 1984. A study of tumor progression: the precursor lesions of superficial spreading and nodular melanoma. *Hum Pathol* **15**: 1147-1165.

Cohen DM, Won KJ, Nguyen N, Lazar MA, Chen CS, Steger DJ. 2015. ATF4 licenses C/EBPβ activity in human mesenchymal stem cells primed for adipogenesis. *Elife* **4**: e06821.

Colina R, Costa-Mattioli M, Dowling RJ, Jaramillo M, Tai LH, Breitbach CJ, Martineau Y, Larsson O, Rong L, Svitkin YV et al. 2008. Translational control of the innate immune response through IRF-7. *Nature* **452**: 323-328.

Copeland RA, Solomon ME, Richon VM. 2009. Protein methyltransferases as a target class for drug discovery. *Nat Rev Drug Discov* **8**: 724-732.

Coquel F, Silva MJ, Técher H, Zadorozhny K, Sharma S, Nieminuszczy J, Mettling C, Dardillac E, Barthe A, Schmitz AL et al. 2018. SAMHD1 acts at stalled replication forks to prevent interferon induction. *Nature* **557**: 57-61.

Corbett AH. 2018. Post-transcriptional regulation of gene expression and human disease. *Curr Opin Cell Biol* **52**: 96-104.

Corona DF, Längst G, Clapier CR, Bonte EJ, Ferrari S, Tamkun JW, Becker PB. 1999. ISWI is an ATP-dependent nucleosome remodeling factor. *Mol Cell* **3**: 239-245.

Crawford RR, Prescott ET, Sylvester CF, Higdon AN, Shan J, Kilberg MS, Mungrue IN. 2015. Human CHAC1 Protein Degrades Glutathione, and mRNA Induction Is Regulated by the Transcription Factors ATF4 and ATF3 and a Bipartite ATF/CRE Regulatory Element. *J Biol Chem* **290**: 15878-15891.

Cremer T, Cremer M. 2010. Chromosome territories. *Cold Spring Harb Perspect Biol* **2**: a003889.

Cui R, Widlund HR, Feige E, Lin JY, Wilensky DL, Igras VE, D'Orazio J, Fung CY, Schanbacher CF, Granter SR et al. 2007. Central role of p53 in the suntan response and pathologic hyperpigmentation. *Cell* **128**: 853-864.

Curran K, Raible DW, Lister JA. 2009. Foxd3 controls melanophore specification in the zebrafish neural crest by regulation of Mitf. *Dev Biol* **332**: 408-417.

Cuthbert GL, Daujat S, Snowden AW, Erdjument-Bromage H, Hagiwara T, Yamada M, Schneider R, Gregory PD, Tempst P, Bannister AJ et al. 2004. Histone deimination antagonizes arginine methylation. *Cell* **118**: 545-553.

D'Oto A, Tian QW, Davidoff AM, Yang J. 2016. Histone demethylases and their roles in cancer epigenetics. *J Med Oncol Ther* **1**: 34-40.

Dancy BM, Cole PA. 2015. Protein lysine acetylation by p300/CBP. *Chem Rev* **115**: 2419-2452.

Danen EH, de Vries TJ, Morandini R, Ghanem GG, Ruiter DJ, van Muijen GN. 1996. E-cadherin expression in human melanoma. *Melanoma Res* **6**: 127-131.

Dankort D, Curley DP, Cartlidge RA, Nelson B, Karnezis AN, Damsky WE, You MJ, DePinho RA, McMahon M, Bosenberg M. 2009. Braf(V600E) cooperates with Pten loss to induce metastatic melanoma. *Nat Genet* **41**: 544-552.

Davidson SM, Papagiannakopoulos T, Olenchock BA, Heyman JE, Keibler MA, Luengo A, Bauer MR, Jha AK, O'Brien JP, Pierce KA et al. 2016. Environment Impacts the Metabolic Dependencies of Ras-Driven Non-Small Cell Lung Cancer. *Cell Metab* **23**: 517-528.

Davies H, Bignell GR, Cox C, Stephens P, Edkins S, Clegg S, Teague J, Woffendin H, Garnett MJ, Bottomley W et al. 2002. Mutations of the BRAF gene in human cancer. *Nature* **417**: 949-954.

de la Serna IL, Ohkawa Y, Berkes CA, Bergstrom DA, Dacwag CS, Tapscott SJ, Imbalzano AN. 2005. MyoD targets chromatin remodeling complexes to the myogenin locus prior to forming a stable DNA-bound complex. *Mol Cell Biol* **25**: 3997-4009.

de la Serna IL, Ohkawa Y, Higashi C, Dutta C, Osias J, Kommajosyula N, Tachibana T, Imbalzano AN. 2006. The microphthalmia-associated transcription factor requires SWI/SNF enzymes to activate melanocyte-specific genes. *J Biol Chem* **281**: 20233-20241.

De Santa F, Barozzi I, Mietton F, Ghisletti S, Polletti S, Tusi BK, Muller H, Ragoussis J, Wei CL, Natoli G. 2010. A large fraction of extragenic RNA pol II transcription sites overlap enhancers. *PLoS Biol* **8**: e1000384.

De Souza Setubal Destro MF, Bitu CC, Zecchin KG, Graner E, Lopes MA, Kowalski LP, Coletta RD. 2010. Overexpression of HOXB7 homeobox gene in oral cancer induces cellular proliferation and is associated with poor prognosis. *Int J Oncol* **36**: 141-149.

de Wit E, de Laat W. 2012. A decade of 3C technologies: insights into nuclear organization. *Genes Dev* **26**: 11-24.

Dekker J, Rippe K, Dekker M, Kleckner N. 2002. Capturing chromosome conformation. *Science* **295**: 1306-1311.

Denker A, de Laat W. 2016. The second decade of 3C technologies: detailed insights into nuclear organization. *Genes Dev* **30**: 1357-1382.

Desantis A, Bruno T, Catena V, De Nicola F, Goeman F, Iezzi S, Sorino C, Ponzoni M, Bossi G, Federico V et al. 2015. Che-1-induced inhibition of mTOR pathway enables stress-induced autophagy. *EMBO J* **34**: 1214-1230.

Deutsch PJ, Hoeffler JP, Jameson JL, Lin JC, Habener JF. 1988. Structural determinants for transcriptional activation by cAMP-responsive DNA elements. *J Biol Chem* **263**: 18466-18472.

Dhillon AS, Hagan S, Rath O, Kolch W. 2007. MAP kinase signalling pathways in cancer. *Oncogene* **26**: 3279-3290.

Ding N, Zhou H, Esteve PO, Chin HG, Kim S, Xu X, Joseph SM, Friez MJ, Schwartz CE, Pradhan S et al. 2008. Mediator links epigenetic silencing of neuronal gene expression with x-linked mental retardation. *Mol Cell* **31**: 347-359.

Dixon JR, Gorkin DU, Ren B. 2016. Chromatin Domains: The Unit of Chromosome Organization. *Mol Cell* **62**: 668-680.

Dixon JR, Selvaraj S, Yue F, Kim A, Li Y, Shen Y, Hu M, Liu JS, Ren B. 2012. Topological domains in mammalian genomes identified by analysis of chromatin interactions. *Nature* **485**: 376-380.

Dobin A, Davis CA, Schlesinger F, Drenkow J, Zaleski C, Jha S, Batut P, Chaisson M, Gingeras TR. 2013. STAR: ultrafast universal RNA-seq aligner. *Bioinformatics* **29**: 15-21.

Donato R. 2001. S100: a multigenic family of calcium-modulated proteins of the EF-hand type with intracellular and extracellular functional roles. *Int J Biochem Cell Biol* **33**: 637-668.

Dorrello NV, Peschiaroli A, Guardavaccaro D, Colburn NH, Sherman NE, Pagano M. 2006. S6K1- and betaTRCP-mediated degradation of PDCD4 promotes protein translation and cell growth. *Science* **314**: 467-471.

Dorsky RI, Raible DW, Moon RT. 2000. Direct regulation of nacre, a zebrafish MITF homolog required for pigment cell formation, by the Wnt pathway. *Genes Dev* **14**: 158-162.

Dror I, Rohs R, Mandel-Gutfreund Y. 2016. How motif environment influences transcription factor search dynamics: Finding a needle in a haystack. *Bioessays* **38**: 605-612.

Drouin J. 2014. Minireview: pioneer transcription factors in cell fate specification. *Mol Endocrinol* **28**: 989-998.

Du J, Miller AJ, Widlund HR, Horstmann MA, Ramaswamy S, Fisher DE. 2003. MLANA/MART1 and SILV/PMEL17/GP100 are transcriptionally regulated by MITF in melanocytes and melanoma. *Am J Pathol* **163**: 333-343.

Du J, Widlund HR, Horstmann MA, Ramaswamy S, Ross K, Huber WE, Nishimura EK, Golub TR, Fisher DE. 2004. Critical role of CDK2 for melanoma growth linked to its melanocyte-specific transcriptional regulation by MITF. *Cancer Cell* **6**: 565-576.

Duan S, Skaar JR, Kuchay S, Toschi A, Kanarek N, Ben-Neriah Y, Pagano M. 2011. mTOR generates an auto-amplification loop by triggering the βTrCP- and CK1α-dependent degradation of DEPTOR. *Mol Cell* **44**: 317-324.

Dugo M, Nicolini G, Tragni G, Bersani I, Tomassetti A, Colonna V, Del Vecchio M, De Braud F, Canevari S, Anichini A et al. 2015. A melanoma subtype with intrinsic resistance to BRAF inhibition identified by receptor tyrosine kinases gene-driven classification. *Oncotarget* **6**: 5118-5133.

Dynek JN, Chan SM, Liu J, Zha J, Fairbrother WJ, Vucic D. 2008. Microphthalmia-associated transcription factor is a critical transcriptional regulator of melanoma inhibitor of apoptosis in melanomas. *Cancer Res* **68**: 3124-3132.

Dyson NJ. 2016. RB1: a prototype tumor suppressor and an enigma. *Genes Dev* **30**: 1492-1502.

Eberharter A, Ferrari S, Längst G, Straub T, Imhof A, Varga-Weisz P, Wilm M, Becker PB. 2001. Acf1, the largest subunit of CHRAC, regulates ISWI-induced nucleosome remodelling. *EMBO J* **20**: 3781-3788.

Ebert SM, Dyle MC, Kunkel SD, Bullard SA, Bongers KS, Fox DK, Dierdorff JM, Foster ED, Adams CM. 2012. Stress-induced skeletal muscle Gadd45a expression reprograms myonuclei and causes muscle atrophy. *J Biol Chem* **287**: 27290-27301.

Eguchi Y, Makanae K, Hasunuma T, Ishibashi Y, Kito K, Moriya H. 2018. Estimating the protein burden limit of yeast cells by measuring the expression limits of glycolytic proteins. *Elife* **7**.

Elbashir SM, Martinez J, Patkaniowska A, Lendeckel W, Tuschl T. 2001. Functional anatomy of siRNAs for mediating efficient RNAi in Drosophila melanogaster embryo lysate. *EMBO J* **20**: 6877-6888.

Eleuteri B, Aranda S, Ernfors P. 2018. NoRC Recruitment by H2A.X Deposition at rRNA Gene Promoter Limits Embryonic Stem Cell Proliferation. *Cell Rep* **23**: 1853-1866.

Elf J, Li GW, Xie XS. 2007. Probing transcription factor dynamics at the single-molecule level in a living cell. *Science* **316**: 1191-1194.

Emery CM, Vijayendran KG, Zipser MC, Sawyer AM, Niu L, Kim JJ, Hatton C, Chopra R, Oberholzer PA, Karpova MB et al. 2009. MEK1 mutations confer resistance to MEK and B-RAF inhibition. *Proc Natl Acad Sci U S A* **106**: 20411-20416.

Emmons MF, Faião-Flores F, Sharma R, Thapa R, Messina JL, Becker JC, Schadendorf D, Seto E, Sondak VK, Koomen JM et al. 2019. HDAC8 Regulates a Stress Response Pathway in Melanoma to Mediate Escape from BRAF Inhibitor Therapy. *Cancer Res* **79**: 2947-2961.

Erdel F, Schubert T, Marth C, Längst G, Rippe K. 2010. Human ISWI chromatin-remodeling complexes sample nucleosomes via transient binding reactions and become immobilized at active sites. *Proc Natl Acad Sci U S A* **107**: 19873-19878.

Eskiw CH, Fraser P. 2011. Ultrastructural study of transcription factories in mouse erythroblasts. *J Cell Sci* **124**: 3676-3683.

Falletta P, Sanchez-Del-Campo L, Chauhan J, Effern M, Kenyon A, Kershaw CJ, Siddaway R, Lisle R, Freter R, Daniels MJ et al. 2017. Translation reprogramming is an evolutionarily conserved driver of phenotypic plasticity and therapeutic resistance in melanoma. *Genes Dev* **31**: 18-33.

Fane ME, Chhabra Y, Smith AG, Sturm RA. 2019. BRN2, a POUerful driver of melanoma phenotype switching and metastasis. *Pigment Cell Melanoma Res* **32**: 9-24.

Fawcett TW, Martindale JL, Guyton KZ, Hai T, Holbrook NJ. 1999. Complexes containing activating transcription factor (ATF)/cAMP-responsive-element-binding protein (CREB) interact with the CCAAT/enhancer-binding protein (C/EBP)-ATF composite site to regulate Gadd153 expression during the stress response. *Biochem J* **339 ( Pt 1)**: 135-141.

Feige E, Yokoyama S, Levy C, Khaled M, Igras V, Lin RJ, Lee S, Widlund HR, Granter SR, Kung AL et al. 2011. Hypoxia-induced transcriptional repression of the melanoma-associated oncogene MITF. *Proc Natl Acad Sci U S A* **108**: E924-933.

Feng Q, Cao R, Xia L, Erdjument-Bromage H, Tempst P, Zhang Y. 2002. Identification and functional characterization of the p66/p68 components of the MeCP1 complex. *Mol Cell Biol* **22**: 536-546.

Feng YX, Sokol ES, Del Vecchio CA, Sanduja S, Claessen JH, Proia TA, Jin DX, Reinhardt F, Ploegh HL, Wang Q et al. 2014. Epithelial-to-mesenchymal transition activates PERK-eIF2α and sensitizes cells to endoplasmic reticulum stress. *Cancer Discov* **4**: 702-715.

Ferguson J, Smith M, Zudaire I, Wellbrock C, Arozarena I. 2017. Glucose availability controls ATF4-mediated MITF suppression to drive melanoma cell growth. *Oncotarget* **8**: 32946-32959.

Ferlay J, Soerjomataram I, Dikshit R, Eser S, Mathers C, Rebelo M, Parkin DM, Forman D, Bray F. 2015. Cancer incidence and mortality worldwide: sources, methods and major patterns in GLOBOCAN 2012. *Int J Cancer* **136**: E359-386.

Filipowicz W, Bhattacharyya SN, Sonenberg N. 2008. Mechanisms of post-transcriptional regulation by microRNAs: are the answers in sight? *Nat Rev Genet* **9**: 102-114.

Fogh J, Fogh JM, Orfeo T. 1977. One hundred and twenty-seven cultured human tumor cell lines producing tumors in nude mice. *J Natl Cancer Inst* **59**: 221-226.

Fujita N, Jaye DL, Geigerman C, Akyildiz A, Mooney MR, Boss JM, Wade PA. 2004. MTA3 and the Mi-2/NuRD complex regulate cell fate during B lymphocyte differentiation. *Cell* **119**: 75-86.

Fusakio ME, Willy JA, Wang Y, Mirek ET, Al Baghdadi RJ, Adams CM, Anthony TG, Wek RC. 2016. Transcription factor ATF4 directs basal and stress-induced gene expression in the unfolded protein response and cholesterol metabolism in the liver. *Mol Biol Cell* **27**: 1536-1551.

Fuse N, Yasumoto K, Takeda K, Amae S, Yoshizawa M, Udono T, Takahashi K, Tamai M, Tomita Y, Tachibana M et al. 1999. Molecular cloning of cDNA encoding a novel microphthalmia-associated transcription factor isoform with a distinct amino-terminus. *J Biochem* **126**: 1043-1051.

Galehdar Z, Swan P, Fuerth B, Callaghan SM, Park DS, Cregan SP. 2010. Neuronal apoptosis induced by endoplasmic reticulum stress is regulated by ATF4-CHOP-mediated induction of the Bcl-2 homology 3-only member PUMA. *J Neurosci* **30**: 16938-16948.

Gandini S, Sera F, Cattaruzza MS, Pasquini P, Picconi O, Boyle P, Melchi CF. 2005. Meta-analysis of risk factors for cutaneous melanoma: II. Sun exposure. *Eur J Cancer* **41**: 45-60.

Gao D, Inuzuka H, Tan MK, Fukushima H, Locasale JW, Liu P, Wan L, Zhai B, Chin YR, Shaik S et al. 2011. mTOR drives its own activation via SCF(βTrCP)-dependent degradation of the mTOR inhibitor DEPTOR. *Mol Cell* **44**: 290-303.

Gao Z, Lee P, Stafford JM, von Schimmelmann M, Schaefer A, Reinberg D. 2014. An AUTS2-Polycomb complex activates gene expression in the CNS. *Nature* **516**: 349-354.

Garaeva AA, Kovaleva IE, Chumakov PM, Evstafieva AG. 2016. Mitochondrial dysfunction induces SESN2 gene expression through Activating Transcription Factor 4. *Cell Cycle* **15**: 64-71.

García MA, Meurs EF, Esteban M. 2007. The dsRNA protein kinase PKR: virus and cell control. *Biochimie* **89**: 799-811.

García-Jiménez C, Goding CR. 2019. Starvation and Pseudo-Starvation as Drivers of Cancer Metastasis through Translation Reprogramming. *Cell Metab* **29**: 254-267.

Garnatz AS, Gao Z, Broman M, Martens S, Earley JU, Svensson EC. 2014. FOG-2 mediated recruitment of the NuRD complex regulates cardiomyocyte proliferation during heart development. *Dev Biol* **395**: 50-61.

Garneau NL, Wilusz J, Wilusz CJ. 2007. The highways and byways of mRNA decay. *Nat Rev Mol Cell Biol* **8**: 113-126.

Garraway LA, Widlund HR, Rubin MA, Getz G, Berger AJ, Ramaswamy S, Beroukhim R, Milner DA, Granter SR, Du J et al. 2005. Integrative genomic analyses identify MITF as a lineage survival oncogene amplified in malignant melanoma. *Nature* **436**: 117-122.

Gaszner M, Felsenfeld G. 2006. Insulators: exploiting transcriptional and epigenetic mechanisms. *Nat Rev Genet* **7**: 703-713.

Gebert LFR, MacRae IJ. 2019. Regulation of microRNA function in animals. *Nat Rev Mol Cell Biol* **20**: 21-37.

Gerstein MB, Kundaje A, Hariharan M, Landt SG, Yan KK, Cheng C, Mu XJ, Khurana E, Rozowsky J, Alexander R et al. 2012. Architecture of the human regulatory network derived from ENCODE data. *Nature* **489**: 91-100.

Ghisletti S, Barozzi I, Mietton F, Polletti S, De Santa F, Venturini E, Gregory L, Lonie L, Chew A, Wei CL et al. 2010. Identification and characterization of enhancers controlling the inflammatory gene expression program in macrophages. *Immunity* **32**: 317-328.

Ghosh K, Tang M, Kumari N, Nandy A, Basu S, Mall DP, Rai K, Biswas D. 2018. Positive Regulation of Transcription by Human ZMYND8 through Its Association with P-TEFb Complex. *Cell Rep* **24**: 2141-2154.e2146.

Giampieri S, Pinner S, Sahai E. 2010. Intravital imaging illuminates transforming growth factor beta signaling switches during metastasis. *Cancer Res* **70**: 3435-3439.

Girotti MR, Pedersen M, Sanchez-Laorden B, Viros A, Turajlic S, Niculescu-Duvaz D, Zambon A, Sinclair J, Hayes A, Gore M et al. 2013. Inhibiting EGF receptor or SRC family kinase signaling overcomes BRAF inhibitor resistance in melanoma. *Cancer Discov* **3**: 158-167.

Giuliano S, Cheli Y, Ohanna M, Bonet C, Beuret L, Bille K, Loubat A, Hofman V, Hofman P, Ponzio G et al. 2010. Microphthalmia-associated transcription factor controls the DNA damage response and a lineage-specific senescence program in melanomas. *Cancer Res* **70**: 3813-3822.

Gjymishka A, Palii SS, Shan J, Kilberg MS. 2008. Despite increased ATF4 binding at the C/EBP-ATF composite site following activation of the unfolded protein response, system A transporter 2 (SNAT2) transcription activity is repressed in HepG2 cells. *J Biol Chem* **283**: 27736-27747.

Godet AC, David F, Hantelys F, Tatin F, Lacazette E, Garmy-Susini B, Prats AC. 2019. IRES Trans-Acting Factors, Key Actors of the Stress Response. *Int J Mol Sci* **20**.

Goding CR. 2011. Commentary. A picture of Mitf in melanoma immortality. *Oncogene* **30**: 2304-2306.

Gomez D, Kessler K, Borges LF, Richard B, Touat Z, Ollivier V, Mansilla S, Bouton MC, Alkoder S, Nataf P et al. 2013. Smad2-dependent protease nexin-1 overexpression differentiates chronic aneurysms from acute dissections of human ascending aorta. *Arterioscler Thromb Vasc Biol* **33**: 2222-2232.

Gong F, Chiu LY, Cox B, Aymard F, Clouaire T, Leung JW, Cammarata M, Perez M, Agarwal P, Brodbelt JS et al. 2015. Screen identifies bromodomain protein ZMYND8 in chromatin recognition of transcription-associated DNA damage that promotes homologous recombination. *Genes Dev* **29**: 197-211.

González-González A, Muñoz-Muela E, Marchal JA, Cara FE, Molina MP, Cruz-Lozano M, Jiménez G, Verma A, Ramírez A, Qian W et al. 2018. Activating Transcription Factor 4 Modulates TGFβ-Induced Aggressiveness in Triple-Negative Breast Cancer via SMAD2/3/4 and mTORC2 Signaling. *Clin Cancer Res* **24**: 5697-5709.

Goodall J, Carreira S, Denat L, Kobi D, Davidson I, Nuciforo P, Sturm RA, Larue L, Goding CR. 2008. Brn-2 represses microphthalmia-associated transcription factor expression and marks a distinct subpopulation of microphthalmia-associated transcription factor-negative melanoma cells. *Cancer Res* **68**: 7788-7794.

Goodall J, Martinozzi S, Dexter TJ, Champeval D, Carreira S, Larue L, Goding CR. 2004a. Brn-2 expression controls melanoma proliferation and is directly regulated by beta-catenin. *Mol Cell Biol* **24**: 2915-2922.

Goodall J, Wellbrock C, Dexter TJ, Roberts K, Marais R, Goding CR. 2004b. The Brn-2 transcription factor links activated BRAF to melanoma proliferation. *Mol Cell Biol* **24**: 2923-2931.

Greer EL, Shi Y. 2012. Histone methylation: a dynamic mark in health, disease and inheritance. *Nat Rev Genet* **13**: 343-357.

Grill C, Bergsteinsdóttir K, Ogmundsdóttir MH, Pogenberg V, Schepsky A, Wilmanns M, Pingault V, Steingrímsson E. 2013. MITF mutations associated with pigment deficiency syndromes and melanoma have different effects on protein function. *Hum Mol Genet* **22**: 4357-4367.

Grzywa TM, Paskal W, Włodarski PK. 2017. Intratumor and Intertumor Heterogeneity in Melanoma. *Transl Oncol* **10**: 956-975.

Gu S, Jin L, Zhang Y, Huang Y, Zhang F, Valdmanis PN, Kay MA. 2012. The loop position of shRNAs and pre-miRNAs is critical for the accuracy of dicer processing in vivo. *Cell* **151**: 900-911.

Gu S, Zhang Y, Jin L, Huang Y, Zhang F, Bassik MC, Kampmann M, Kay MA. 2014. Weak base pairing in both seed and 3' regions reduces RNAi off-targets and enhances si/shRNA designs. *Nucleic Acids Res* **42**: 12169-12176.

Guertin DA, Sabatini DM. 2007. Defining the role of mTOR in cancer. *Cancer Cell* **12**: 9-22.

Guo J, Zhang JF, Wang WM, Cheung FW, Lu YF, Ng CF, Kung HF, Liu WK. 2014. MicroRNA-218 inhibits melanogenesis by directly suppressing microphthalmia-associated transcription factor expression. *RNA Biol* **11**: 732-741.

Gupta PB, Kuperwasser C, Brunet JP, Ramaswamy S, Kuo WL, Gray JW, Naber SP, Weinberg RA. 2005. The melanocyte differentiation program predisposes to metastasis after neoplastic transformation. *Nat Genet* **37**: 1047-1054.

Gupta S, Schoer RA, Egan JE, Hannon GJ, Mittal V. 2004. Inducible, reversible, and stable RNA interference in mammalian cells. *Proc Natl Acad Sci U S A* **101**: 1927-1932.

Gómez-Cuadrado L, Tracey N, Ma R, Qian B, Brunton VG. 2017. Mouse models of metastasis: progress and prospects. *Dis Model Mech* **10**: 1061-1074.

Haflidadóttir BS, Bergsteinsdóttir K, Praetorius C, Steingrímsson E. 2010. miR-148 regulates Mitf in melanoma cells. *PLoS One* **5**: e11574.

Hah N, Murakami S, Nagari A, Danko CG, Kraus WL. 2013. Enhancer transcripts mark active estrogen receptor binding sites. *Genome Res* **23**: 1210-1223.

Hai T, Curran T. 1991. Cross-family dimerization of transcription factors Fos/Jun and ATF/CREB alters DNA binding specificity. *Proc Natl Acad Sci U S A* **88**: 3720-3724.

Hai T, Hartman MG. 2001. The molecular biology and nomenclature of the activating transcription factor/cAMP responsive element binding family of transcription factors: activating transcription factor proteins and homeostasis. *Gene* **273**: 1-11.

Halder G, Callaerts P, Gehring WJ. 1995. Induction of ectopic eyes by targeted expression of the eyeless gene in Drosophila. *Science* **267**: 1788-1792.

Halldorsson S, Lucumi E, Gómez-Sjöberg R, Fleming RMT. 2015. Advantages and challenges of microfluidic cell culture in polydimethylsiloxane devices. *Biosens Bioelectron* **63**: 218-231.

Halterman MW, De Jesus C, Rempe DA, Schor NF, Federoff HJ. 2008. Loss of c/EBP-beta activity promotes the adaptive to apoptotic switch in hypoxic cortical neurons. *Mol Cell Neurosci* **38**: 125-137.

Hammar P, Leroy P, Mahmutovic A, Marklund EG, Berg OG, Elf J. 2012. The lac repressor displays facilitated diffusion in living cells. *Science* **336**: 1595-1598.

Hammond SM, Bernstein E, Beach D, Hannon GJ. 2000. An RNA-directed nuclease mediates post-transcriptional gene silencing in Drosophila cells. *Nature* **404**: 293-296.

Han H, Cho JW, Lee S, Yun A, Kim H, Bae D, Yang S, Kim CY, Lee M, Kim E et al. 2018a. TRRUST v2: an expanded reference database of human and mouse transcriptional regulatory interactions. *Nucleic Acids Res* **46**: D380-D386.

Han J, Back SH, Hur J, Lin YH, Gildersleeve R, Shan J, Yuan CL, Krokowski D, Wang S, Hatzoglou M et al. 2013. ER-stress-induced transcriptional regulation increases protein synthesis leading to cell death. *Nat Cell Biol* **15**: 481-490.

Han J, Flemington C, Houghton AB, Gu Z, Zambetti GP, Lutz RJ, Zhu L, Chittenden T. 2001. Expression of bbc3, a pro-apoptotic BH3-only gene, is regulated by diverse cell death and survival signals. *Proc Natl Acad Sci U S A* **98**: 11318-11323.

Han S, Ren Y, He W, Liu H, Zhi Z, Zhu X, Yang T, Rong Y, Ma B, Purwin TJ et al. 2018b. ERK-mediated phosphorylation regulates SOX10 sumoylation and targets expression in mutant BRAF melanoma. *Nat Commun* **9**: 28.

Hanahan D, Weinberg RA. 2011. Hallmarks of cancer: the next generation. *Cell* **144**: 646-674.

Hansen AS, Cattoglio C, Darzacq X, Tjian R. 2018. Recent evidence that TADs and chromatin loops are dynamic structures. *Nucleus* **9**: 20-32.

Hao HX, Xie Y, Zhang Y, Charlat O, Oster E, Avello M, Lei H, Mickanin C, Liu D, Ruffner H et al. 2012. ZNRF3 promotes Wnt receptor turnover in an R-spondin-sensitive manner. *Nature* **485**: 195-200.

Harding HP, Novoa I, Zhang Y, Zeng H, Wek R, Schapira M, Ron D. 2000. Regulated translation initiation controls stress-induced gene expression in mammalian cells. *Mol Cell* **6**: 1099-1108.

Harding HP, Zhang Y, Ron D. 1999. Protein translation and folding are coupled by an endoplasmic-reticulum-resident kinase. *Nature* **397**: 271-274.

Harding HP, Zhang Y, Zeng H, Novoa I, Lu PD, Calfon M, Sadri N, Yun C, Popko B, Paules R et al. 2003. An integrated stress response regulates amino acid metabolism and resistance to oxidative stress. *Mol Cell* **11**: 619-633.

Hargreaves DC, Crabtree GR. 2011. ATP-dependent chromatin remodeling: genetics, genomics and mechanisms. *Cell Res* **21**: 396-420.

Hartman ML, Czyz M. 2015. MITF in melanoma: mechanisms behind its expression and activity. *Cell Mol Life Sci* **72**: 1249-1260.

Hassan AH, Prochasson P, Neely KE, Galasinski SC, Chandy M, Carrozza MJ, Workman JL. 2002. Function and selectivity of bromodomains in anchoring chromatin-modifying complexes to promoter nucleosomes. *Cell* **111**: 369-379.

Havas K, Flaus A, Phelan M, Kingston R, Wade PA, Lilley DM, Owen-Hughes T. 2000. Generation of superhelical torsion by ATP-dependent chromatin remodeling activities. *Cell* **103**: 1133-1142.

Hayashi K, Ouchi M, Endou H, Anzai N. 2016. HOXB9 acts as a negative regulator of activated human T cells in response to amino acid deficiency. *Immunol Cell Biol* **94**: 612-617.

Hayashida T, Takahashi F, Chiba N, Brachtel E, Takahashi M, Godin-Heymann N, Gross KW, Vivanco M, Wijendran V, Shioda T et al. 2010. HOXB9, a gene overexpressed in breast cancer, promotes tumorigenicity and lung metastasis. *Proc Natl Acad Sci U S A* **107**: 1100-1105.

Hayward N. 2000. New developments in melanoma genetics. *Curr Oncol Rep* **2**: 300-306.

Heerboth S, Housman G, Leary M, Longacre M, Byler S, Lapinska K, Willbanks A, Sarkar S. 2015. EMT and tumor metastasis. *Clin Transl Med* **4**: 6.

Heinz S, Benner C, Spann N, Bertolino E, Lin YC, Laslo P, Cheng JX, Murre C, Singh H, Glass CK. 2010. Simple combinations of lineage-determining transcription factors prime cis-regulatory elements required for macrophage and B cell identities. *Mol Cell* **38**: 576-589.

Hemesath TJ, Price ER, Takemoto C, Badalian T, Fisher DE. 1998. MAP kinase links the transcription factor Microphthalmia to c-Kit signalling in melanocytes. *Nature* **391**: 298-301.

Hendrich B, Tweedie S. 2003. The methyl-CpG binding domain and the evolving role of DNA methylation in animals. *Trends Genet* **19**: 269-277.

Herbert K, Binet R, Lambert JP, Louphrasitthiphol P, Kalkavan H, Sesma-Sanz L, Robles-Espinoza CD, Sarkar S, Suer E, Andrews S et al. 2019. BRN2 suppresses apoptosis, reprograms DNA damage repair, and is associated with a high somatic mutation burden in melanoma. *Genes Dev* **33**: 310-332.

Hershey CL, Fisher DE. 2005. Genomic analysis of the Microphthalmia locus and identification of the MITF-J/Mitf-J isoform. *Gene* **347**: 73-82.

Hodgkinson CA, Moore KJ, Nakayama A, Steingrímsson E, Copeland NG, Jenkins NA, Arnheiter H. 1993. Mutations at the mouse microphthalmia locus are associated with defects in a gene encoding a novel basic-helix-loop-helix-zipper protein. *Cell* **74**: 395-404.

Hoek KS, Goding CR. 2010. Cancer stem cells versus phenotype-switching in melanoma. *Pigment Cell Melanoma Res* **23**: 746-759.

Holcik M. 2015. Could the eIF2α-Independent Translation Be the Achilles Heel of Cancer? *Front Oncol* **5**: 264.

Hong W, Nakazawa M, Chen YY, Kori R, Vakoc CR, Rakowski C, Blobel GA. 2005. FOG-1 recruits the NuRD repressor complex to mediate transcriptional repression by GATA-1. *EMBO J* **24**: 2367-2378.

Hori O, Ichinoda F, Yamaguchi A, Tamatani T, Taniguchi M, Koyama Y, Katayama T, Tohyama M, Stern DM, Ozawa K et al. 2004. Role of Herp in the endoplasmic reticulum stress response. *Genes Cells* **9**: 457-469.

Horiguchi M, Koyanagi S, Hamdan AM, Kakimoto K, Matsunaga N, Yamashita C, Ohdo S. 2013. Rhythmic control of the ARF-MDM2 pathway by ATF4 underlies circadian accumulation of p53 in malignant cells. *Cancer Res* **73**: 2639-2649.

Hsieh CL, Fei T, Chen Y, Li T, Gao Y, Wang X, Sun T, Sweeney CJ, Lee GS, Chen S et al. 2014. Enhancer RNAs participate in androgen receptor-driven looping that selectively enhances gene activation. *Proc Natl Acad Sci U S A* **111**: 7319-7324.

Hsu YL, Hung JY, Liang YY, Lin YS, Tsai MJ, Chou SH, Lu CY, Kuo PL. 2015. S100P interacts with integrin α7 and increases cancer cell migration and invasion in lung cancer. *Oncotarget* **6**: 29585-29598.

Huang CH, Chu YR, Ye Y, Chen X. 2014a. Role of HERP and a HERP-related protein in HRD1-dependent protein degradation at the endoplasmic reticulum. *J Biol Chem* **289**: 4444-4454.

Huang K, Yuan R, Wang K, Hu J, Huang Z, Yan C, Shen W, Shao J. 2014b. Overexpression of HOXB9 promotes metastasis and indicates poor prognosis in colon cancer. *Chin J Cancer Res* **26**: 72-80.

Huang ZQ, Li J, Sachs LM, Cole PA, Wong J. 2003. A role for cofactor-cofactor and cofactor-histone interactions in targeting p300, SWI/SNF and Mediator for transcription. *EMBO J* **22**: 2146-2155.

Huber WE, Price ER, Widlund HR, Du J, Davis IJ, Wegner M, Fisher DE. 2003. A tissue-restricted cAMP transcriptional response: SOX10 modulates alpha-melanocyte-stimulating hormone-triggered expression of microphthalmia-associated transcription factor in melanocytes. *J Biol Chem* **278**: 45224-45230.

Huggins CJ, Mayekar MK, Martin N, Saylor KL, Gonit M, Jailwala P, Kasoji M, Haines DC, Quiñones OA, Johnson PF. 2015. C/EBPγ Is a Critical Regulator of Cellular Stress

Response Networks through Heterodimerization with ATF4. *Mol Cell Biol* **36**: 693-713.

Hynds RE, Vladimirou E, Janes SM. 2018. The secret lives of cancer cell lines. *Dis Model Mech* **11**.

Igarashi T, Izumi H, Uchiumi T, Nishio K, Arao T, Tanabe M, Uramoto H, Sugio K, Yasumoto K, Sasaguri Y et al. 2007. Clock and ATF4 transcription system regulates drug resistance in human cancer cell lines. *Oncogene* **26**: 4749-4760.

Imbalzano AN, Kwon H, Green MR, Kingston RE. 1994. Facilitated binding of TATA-binding protein to nucleosomal DNA. *Nature* **370**: 481-485.

Intemann J, Saidu NE, Schwind L, Montenarh M. 2014. ER stress signaling in ARPE-19 cells after inhibition of protein kinase CK2 by CX-4945. *Cell Signal* **26**: 1567-1575.

Ito T, Levenstein ME, Fyodorov DV, Kutach AK, Kobayashi R, Kadonaga JT. 1999. ACF consists of two subunits, Acf1 and ISWI, that function cooperatively in the ATP-dependent catalysis of chromatin assembly. *Genes Dev* **13**: 1529-1539.

Ivanovic Z. 2009. Hypoxia or in situ normoxia: The stem cell paradigm. *J Cell Physiol* **219**: 271-275.

Iwabu M, Yamauchi T, Okada-Iwabu M, Sato K, Nakagawa T, Funata M, Yamaguchi M, Namiki S, Nakayama R, Tabata M et al. 2010. Adiponectin and AdipoR1 regulate PGC-1alpha and mitochondria by Ca(2+) and AMPK/SIRT1. *Nature* **464**: 1313-1319.

Iwafuchi-Doi M. 2019. The mechanistic basis for chromatin regulation by pioneer transcription factors. *Wiley Interdiscip Rev Syst Biol Med* **11**: e1427.

Iwafuchi-Doi M, Donahue G, Kakumanu A, Watts JA, Mahony S, Pugh BF, Lee D, Kaestner KH, Zaret KS. 2016. The Pioneer Transcription Factor FoxA Maintains an Accessible Nucleosome Configuration at Enhancers for Tissue-Specific Gene Activation. *Mol Cell* **62**: 79-91.

Iwafuchi-Doi M, Zaret KS. 2014. Pioneer transcription factors in cell reprogramming. *Genes Dev* **28**: 2679-2692.

Jackson AL, Bartz SR, Schelter J, Kobayashi SV, Burchard J, Mao M, Li B, Cavet G, Linsley PS. 2003. Expression profiling reveals off-target gene regulation by RNAi. *Nat Biotechnol* **21**: 635-637.

Jackson AL, Burchard J, Leake D, Reynolds A, Schelter J, Guo J, Johnson JM, Lim L, Karpilow J, Nichols K et al. 2006a. Position-specific chemical modification of siRNAs reduces "off-target" transcript silencing. *RNA* **12**: 1197-1205.

Jackson AL, Burchard J, Schelter J, Chau BN, Cleary M, Lim L, Linsley PS. 2006b. Widespread siRNA "off-target" transcript silencing mediated by seed region sequence complementarity. *RNA* **12**: 1179-1187.

Jackson RJ, Hellen CU, Pestova TV. 2010. The mechanism of eukaryotic translation initiation and principles of its regulation. *Nat Rev Mol Cell Biol* **11**: 113-127.

Jacquemin P, Lannoy VJ, O'Sullivan J, Read A, Lemaigre FP, Rousseau GG. 2001. The transcription factor onecut-2 controls the microphthalmia-associated transcription factor gene. *Biochem Biophys Res Commun* **285**: 1200-1205.

Janku F, Yap TA, Meric-Bernstam F. 2018. Targeting the PI3K pathway in cancer: are we making headway? *Nat Rev Clin Oncol* **15**: 273-291.

Javelaud D, Alexaki VI, Pierrat MJ, Hoek KS, Dennler S, Van Kempen L, Bertolotto C, Ballotti R, Saule S, Delmas V et al. 2011. GLI2 and M-MITF transcription factors control exclusive gene expression programs and inversely regulate invasion in human melanoma cells. *Pigment Cell Melanoma Res* **24**: 932-943.

Jiang H, Hu H, Lin F, Lim YP, Hua Y, Tong X, Zhang S. 2016. S100P is Overexpressed in Squamous Cell and Adenosquamous Carcinoma Subtypes of Endometrial Cancer and Promotes Cancer Cell Proliferation and Invasion. *Cancer Invest* **34**: 477-488.

Jiang HY, Jiang L, Wek RC. 2007. The eukaryotic initiation factor-2 kinase pathway facilitates differential GADD45a expression in response to environmental stress. *J Biol Chem* **282**: 3755-3765.

Jiang L, Lai YK, Zhang J, Wang H, Lin MC, He ML, Kung HF. 2011. Targeting S100P inhibits colon cancer growth and metastasis by Lentivirus-mediated RNA interference and proteomic analysis. *Mol Med* **17**: 709-716.

Jin HO, Seo SK, Woo SH, Kim ES, Lee HC, Yoo DH, An S, Choe TB, Lee SJ, Hong SI et al. 2009. Activating transcription factor 4 and CCAAT/enhancer-binding protein-beta negatively regulate the mammalian target of rapamycin via Redd1 expression in response to oxidative and endoplasmic reticulum stress. *Free Radic Biol Med* **46**: 1158-1167.

Johannessen CM, Boehm JS, Kim SY, Thomas SR, Wardwell L, Johnson LA, Emery CM, Stransky N, Cogdill AP, Barretina J et al. 2010. COT drives resistance to RAF inhibition through MAP kinase pathway reactivation. *Nature* **468**: 968-972.

Johnson KM, Wang J, Smallwood A, Arayata C, Carey M. 2002. TFIID and human mediator coactivator complexes assemble cooperatively on promoter DNA. *Genes Dev* **16**: 1852-1863.

Johnson LF, Levis R, Abelson HT, Green H, Penman S. 1976. Changes in RNA in relation to growth of the fibroblast. IV. Alterations in theproduction and processing of mRNA and rRNA in resting and growing cells. *J Cell Biol* **71**: 933-938.

Jonas S, Izaurralde E. 2015. Towards a molecular understanding of microRNA-mediated gene silencing. *Nat Rev Genet* **16**: 421-433.

Kagey MH, Newman JJ, Bilodeau S, Zhan Y, Orlando DA, van Berkum NL, Ebmeier CC, Goossens J, Rahl PB, Levine SS et al. 2010. Mediator and cohesin connect gene expression and chromatin architecture. *Nature* **467**: 430-435.

Kaidi A, Jackson SP. 2013. KAT5 tyrosine phosphorylation couples chromatin sensing to ATM signalling. *Nature* **498**: 70-74.

Kalkavan H, Green DR. 2018. MOMP, cell suicide as a BCL-2 family business. *Cell Death Differ* **25**: 46-55.

Kamaraju AK, Bertolotto C, Chebath J, Revel M. 2002. Pax3 down-regulation and shut-off of melanogenesis in melanoma B16/F10.9 by interleukin-6 receptor signaling. *J Biol Chem* **277**: 15132-15141.

Kanehisa M, Furumichi M, Tanabe M, Sato Y, Morishima K. 2017. KEGG: new perspectives on genomes, pathways, diseases and drugs. *Nucleic Acids Res* **45**: D353-D361.

Kanehisa M, Goto S. 2000. KEGG: kyoto encyclopedia of genes and genomes. *Nucleic Acids Res* **28**: 27-30.

Kanehisa M, Sato Y, Furumichi M, Morishima K, Tanabe M. 2019. New approach for understanding genome variations in KEGG. *Nucleic Acids Res* **47**: D590-D595.

Kaplan N, Moore I, Fondufe-Mittendorf Y, Gossett AJ, Tillo D, Field Y, Hughes TR, Lieb JD, Widom J, Segal E. 2010. Nucleosome sequence preferences influence in vivo nucleosome organization. *Nat Struct Mol Biol* **17**: 918-920.

Karve TM, Cheema AK. 2011. Small changes huge impact: the role of protein posttranslational modifications in cellular homeostasis and disease. *J Amino Acids* **2011**: 207691.

Kaur G, Dufour JM. 2012. Cell lines: Valuable tools or useless artifacts. *Spermatogenesis* **2**: 1-5.

Kawakami A, Fisher DE. 2017. The master role of microphthalmia-associated transcription factor in melanocyte and melanoma biology. *Lab Invest* **97**: 649-656.

Keenen B, Qi H, Saladi SV, Yeung M, de la Serna IL. 2010. Heterogeneous SWI/SNF chromatin remodeling complexes promote expression of microphthalmia-associated transcription factor target genes in melanoma. *Oncogene* **29**: 81-92.

Keibler MA, Wasylenko TM, Kelleher JK, Iliopoulos O, Vander Heiden MG, Stephanopoulos G. 2016. Metabolic requirements for cancer cell proliferation. *Cancer Metab* **4**: 16.

Kevil CG, De Benedetti A, Payne DK, Coe LL, Laroux FS, Alexander JS. 1996. Translational regulation of vascular permeability factor by eukaryotic initiation factor 4E: implications for tumor angiogenesis. *Int J Cancer* **65**: 785-790.

Khan AH, Lin A, Smith DJ. 2012. Discovery and characterization of human exonic transcriptional regulatory elements. *PLoS One* **7**: e46098.

Kieffer-Kwon KR, Tang Z, Mathe E, Qian J, Sung MH, Li G, Resch W, Baek S, Pruett N, Grøntved L et al. 2013. Interactome maps of mouse gene regulatory domains reveal basic principles of transcriptional regulation. *Cell* **155**: 1507-1520.

Kilberg MS, Shan J, Su N. 2009. ATF4-dependent transcription mediates signaling of amino acid limitation. *Trends Endocrinol Metab* **20**: 436-443.

Kim J, Sif S, Jones B, Jackson A, Koipally J, Heller E, Winandy S, Viel A, Sawyer A, Ikeda T et al. 1999. Ikaros DNA-binding proteins direct formation of chromatin remodeling complexes in lymphocytes. *Immunity* **10**: 345-355.

Kim TK, Hemberg M, Gray JM, Costa AM, Bear DM, Wu J, Harmin DA, Laptewicz M, Barbara-Haley K, Kuersten S et al. 2010. Widespread transcription at neuronal activity-regulated enhancers. *Nature* **465**: 182-187.

Kim YJ, Björklund S, Li Y, Sayre MH, Kornberg RD. 1994. A multiprotein mediator of transcriptional activation and its interaction with the C-terminal repeat domain of RNA polymerase II. *Cell* **77**: 599-608.

Kintaka R, Makanae K, Moriya H. 2016. Cellular growth defects triggered by an overload of protein localization processes. *Sci Rep* **6**: 31774.

Klein CA. 2013. Selection and adaptation during metastatic cancer progression. *Nature* **501**: 365-372.

Kokame K, Agarwala KL, Kato H, Miyata T. 2000. Herp, a new ubiquitin-like membrane protein induced by endoplasmic reticulum stress. *J Biol Chem* **275**: 32846-32853.

Komar AA, Hatzoglou M. 2011. Cellular IRES-mediated translation: the war of ITAFs in pathophysiological states. *Cell Cycle* **10**: 229-240.

Konieczkowski DJ, Johannessen CM, Abudayyeh O, Kim JW, Cooper ZA, Piris A, Frederick DT, Barzily-Rokni M, Straussman R, Haq R et al. 2014. A melanoma cell state distinction influences sensitivity to MAPK pathway inhibitors. *Cancer Discov* **4**: 816-827.

Koumenis C, Naczki C, Koritzinsky M, Rastani S, Diehl A, Sonenberg N, Koromilas A, Wouters BG. 2002. Regulation of protein synthesis by hypoxia via activation of the endoplasmic reticulum kinase PERK and phosphorylation of the translation initiation factor eIF2alpha. *Mol Cell Biol* **22**: 7405-7416.

Koutelou E, Hirsch CL, Dent SY. 2010. Multiple faces of the SAGA complex. *Curr Opin Cell Biol* **22**: 374-382.

Kremer SB, Kim S, Jeon JO, Moustafa YW, Chen A, Zhao J, Gross DS. 2012. Role of Mediator in regulating Pol II elongation and nucleosome displacement in Saccharomyces cerevisiae. *Genetics* **191**: 95-106.

Krivega I, Dean A. 2012. Enhancer and promoter interactions-long distance calls. *Curr Opin Genet Dev* **22**: 79-85.

Krivega I, Dean A. 2017. LDB1-mediated enhancer looping can be established independent of mediator and cohesin. *Nucleic Acids Res* **45**: 8255-8268.

Kuleshov MV, Jones MR, Rouillard AD, Fernandez NF, Duan Q, Wang Z, Koplev S, Jenkins SL, Jagodnik KM, Lachmann A et al. 2016. Enrichr: a comprehensive gene set enrichment analysis web server 2016 update. *Nucleic Acids Res* **44**: W90-97.

Kunz M. 2013. MicroRNAs in melanoma biology. *Adv Exp Med Biol* **774**: 103-120.

Kuroyanagi J, Shimada Y, Zhang B, Ariyoshi M, Umemoto N, Nishimura Y, Tanaka T. 2014. Zinc finger MYND-type containing 8 promotes tumour angiogenesis via induction of vascular endothelial growth factor-A expression. *FEBS Lett* **588**: 3409-3416.

Lai AY, Wade PA. 2011. Cancer biology and NuRD: a multifaceted chromatin remodelling complex. *Nat Rev Cancer* **11**: 588-596.

Lambert AW, Pattabiraman DR, Weinberg RA. 2017. Emerging Biological Principles of Metastasis. *Cell* **168**: 670-691.

Lambert SA, Jolma A, Campitelli LF, Das PK, Yin Y, Albu M, Chen X, Taipale J, Hughes TR, Weirauch MT. 2018. The Human Transcription Factors. *Cell* **175**: 598-599.

Lang D, Lu MM, Huang L, Engleka KA, Zhang M, Chu EY, Lipner S, Skoultchi A, Millar SE, Epstein JA. 2005a. Pax3 functions at a nodal point in melanocyte stem cell differentiation. *Nature* **433**: 884-887.

Lang G, Gombert WM, Gould HJ. 2005b. A transcriptional regulatory element in the coding sequence of the human Bcl-2 gene. *Immunology* **114**: 25-36.

Lange PS, Chavez JC, Pinto JT, Coppola G, Sun CW, Townes TM, Geschwind DH, Ratan RR. 2008. ATF4 is an oxidative stress-inducible, prodeath transcription factor in neurons in vitro and in vivo. *J Exp Med* **205**: 1227-1242.

Langmead B, Salzberg SL. 2012. Fast gapped-read alignment with Bowtie 2. *Nat Methods* **9**: 357-U354.

Larsson O, Li S, Issaenko OA, Avdulov S, Peterson M, Smith K, Bitterman PB, Polunovsky VA. 2007. Eukaryotic translation initiation factor 4E induced progression of primary human mammary epithelial cells along the cancer pathway is associated with targeted translational deregulation of oncogenic drivers and inhibitors. *Cancer Res* **67**: 6814-6824.

Larsson O, Perlman DM, Fan D, Reilly CS, Peterson M, Dahlgren C, Liang Z, Li S, Polunovsky VA, Wahlestedt C et al. 2006. Apoptosis resistance downstream of eIF4E: posttranscriptional activation of an anti-apoptotic transcript carrying a consensus hairpin structure. *Nucleic Acids Res* **34**: 4375-4386.

Le Guezennec X, Vermeulen M, Brinkman AB, Hoeijmakers WA, Cohen A, Lasonder E, Stunnenberg HG. 2006. MBD2/NuRD and MBD3/NuRD, two distinct complexes with different biochemical and functional properties. *Mol Cell Biol* **26**: 843-851.

Lee AH, Iwakoshi NN, Glimcher LH. 2003. XBP-1 regulates a subset of endoplasmic reticulum resident chaperone genes in the unfolded protein response. *Mol Cell Biol* **23**: 7448-7459.

Leith JS, Tafvizi A, Huang F, Uspal WE, Doyle PS, Fersht AR, Mirny LA, van Oijen AM. 2012. Sequence-dependent sliding kinetics of p53. *Proc Natl Acad Sci U S A* **109**: 16552-16557.

Leonardi GC, Falzone L, Salemi R, Zanghì A, Spandidos DA, Mccubrey JA, Candido S, Libra M. 2018. Cutaneous melanoma: From pathogenesis to therapy (Review). *Int J Oncol* **52**: 1071-1080.

Leppä S, Bohmann D. 1999. Diverse functions of JNK signaling and c-Jun in stress response and apoptosis. *Oncogene* **18**: 6158-6162.

Levy C, Khaled M, Robinson KC, Veguilla RA, Chen PH, Yokoyama S, Makino E, Lu J, Larue L, Beermann F et al. 2010. Lineage-specific transcriptional regulation of DICER by MITF in melanocytes. *Cell* **141**: 994-1005.

Levy C, Lee YN, Nechushtan H, Schueler-Furman O, Sonnenblick A, Hacohen S, Razin E. 2006. Identifying a common molecular mechanism for inhibition of MITF and STAT3 by PIAS3. *Blood* **107**: 2839-2845.

Levy C, Sonnenblick A, Razin E. 2003. Role played by microphthalmia transcription factor phosphorylation and its Zip domain in its transcriptional inhibition by PIAS3. *Mol Cell Biol* **23**: 9073-9080.

Li FZ, Dhillon AS, Anderson RL, McArthur G, Ferrao PT. 2015. Phenotype switching in melanoma: implications for progression and therapy. *Front Oncol* **5**: 31.

Li N, Li Y, Lv J, Zheng X, Wen H, Shen H, Zhu G, Chen TY, Dhar SS, Kan PY et al. 2016. ZMYND8 Reads the Dual Histone Mark H3K4me1-H3K14ac to Antagonize the Expression of Metastasis-Linked Genes. *Mol Cell* **63**: 470-484.

Li W, Notani D, Ma Q, Tanasa B, Nunez E, Chen AY, Merkurjev D, Zhang J, Ohgi K, Song X et al. 2013. Functional roles of enhancer RNAs for oestrogen-dependent transcriptional activation. *Nature* **498**: 516-520.

Li X. 2013. SIRT1 and energy metabolism. *Acta Biochim Biophys Sin (Shanghai)* **45**: 51-60.

Liao Y, Smyth GK, Shi W. 2014. featureCounts: an efficient general purpose program for assigning sequence reads to genomic features. *Bioinformatics* **30**: 923-930.

Lickwar CR, Mueller F, Hanlon SE, McNally JG, Lieb JD. 2012. Genome-wide protein-DNA binding dynamics suggest a molecular clutch for transcription factor function. *Nature* **484**: 251-255.

Lim SY, Menzies AM, Rizos H. 2017. Mechanisms and strategies to overcome resistance to molecularly targeted therapy for melanoma. *Cancer* **123**: 2118-2129.

Lin KL, Chou CH, Hsieh SC, Hwa SY, Lee MT, Wang FF. 2010. Transcriptional upregulation of DDR2 by ATF4 facilitates osteoblastic differentiation through p38 MAPK-mediated Runx2 activation. *J Bone Miner Res* **25**: 2489-2503.

Liu Y, Wang C, Shan X, Wu J, Liu H, Zhang J, Xu W, Sha Z, He J, Fan J. 2017. S100P is associated with proliferation and migration in nasopharyngeal carcinoma. *Oncol Lett* **14**: 525-532.

Liu Z, Lam N, Thiele CJ. 2015. Zinc finger transcription factor CASZ1 interacts with histones, DNA repair proteins and recruits NuRD complex to regulate gene transcription. *Oncotarget* **6**: 27628-27640.

Liu Z, Myers LC. 2012. Med5(Nut1) and Med17(Srb4) are direct targets of mediator histone H4 tail interactions. *PLoS One* **7**: e38416.

Liu Z, Tjian R. 2018. Visualizing transcription factor dynamics in living cells. *J Cell Biol* **217**: 1181-1191.

Livak KJ, Schmittgen TD. 2001. Analysis of relative gene expression data using real-time quantitative PCR and the 2(T)(-Delta Delta C) method. *Methods* **25**: 402-408.

Loercher AE, Tank EM, Delston RB, Harbour JW. 2005. MITF links differentiation with cell cycle arrest in melanocytes by transcriptional activation of INK4A. *J Cell Biol* **168**: 35-40.

Loffreda A, Jacchetti E, Antunes S, Rainone P, Daniele T, Morisaki T, Bianchi ME, Tacchetti C, Mazza D. 2017. Live-cell p53 single-molecule binding is modulated by C-terminal acetylation and correlates with transcriptional activity. *Nat Commun* **8**: 313.

Loftus SK, Baxter LL, Cronin JC, Fufa TD, Pavan WJ, Program NCS. 2017. Hypoxia-induced HIF1α targets in melanocytes reveal a molecular profile associated with poor melanoma prognosis. *Pigment Cell Melanoma Res* **30**: 339-352.

Lorch Y, Beve J, Gustafsson CM, Myers LC, Kornberg RD. 2000. Mediator-nucleosome interaction. *Mol Cell* **6**: 197-201.

Loyola A, Almouzni G. 2004. Histone chaperones, a supporting role in the limelight. *Biochim Biophys Acta* **1677**: 3-11.

Lu C, Allis CD. 2017. SWI/SNF complex in cancer. *Nat Genet* **49**: 178-179.

Lu X, Zhu X, Li Y, Liu M, Yu B, Wang Y, Rao M, Yang H, Zhou K, Chen Y et al. 2016. Multiple P-TEFbs cooperatively regulate the release of promoter-proximally paused RNA polymerase II. *Nucleic Acids Res* **44**: 6853-6867.

Luo C, Merz PR, Chen Y, Dickes E, Pscherer A, Schadendorf D, Eichmüller SB. 2013. MiR-101 inhibits melanoma cell invasion and proliferation by targeting MITF and EZH2. *Cancer Lett* **341**: 240-247.

Längst G, Becker PB. 2001. ISWI induces nucleosome sliding on nicked DNA. *Mol Cell* **8**: 1085-1092.

Ma XH, Piao SF, Dey S, McAfee Q, Karakousis G, Villanueva J, Hart LS, Levi S, Hu J, Zhang G et al. 2014. Targeting ER stress-induced autophagy overcomes BRAF inhibitor resistance in melanoma. *J Clin Invest* **124**: 1406-1417.

Ma Y, Hendershot LM. 2004. Herp is dually regulated by both the endoplasmic reticulum stress-specific branch of the unfolded protein response and a branch that is shared with other cellular stress pathways. *J Biol Chem* **279**: 13792-13799.

Machanick P, Bailey TL. 2011. MEME-ChIP: motif analysis of large DNA datasets. *Bioinformatics* **27**: 1696-1697.

Magnani L, Eeckhoute J, Lupien M. 2011. Pioneer factors: directing transcriptional regulators within the chromatin environment. *Trends Genet* **27**: 465-474.

Makanae K, Kintaka R, Makino T, Kitano H, Moriya H. 2013. Identification of dosage-sensitive genes in Saccharomyces cerevisiae using the genetic tug-of-war method. *Genome Res* **23**: 300-311.

Mamane Y, Petroulakis E, Rong L, Yoshida K, Ler LW, Sonenberg N. 2004. eIF4E--from translation to transformation. *Oncogene* **23**: 3172-3179.

Mandal SS, Chu C, Wada T, Handa H, Shatkin AJ, Reinberg D. 2004. Functional interactions of RNA-capping enzyme with factors that positively and negatively regulate promoter escape by RNA polymerase II. *Proc Natl Acad Sci U S A* **101**: 7572-7577.

Manderfield LJ, Engleka KA, Aghajanian H, Gupta M, Yang S, Li L, Baggs JE, Hogenesch JB, Olson EN, Epstein JA. 2014. Pax3 and hippo signaling coordinate melanocyte gene expression in neural crest. *Cell Rep* **9**: 1885-1895.

Mann IK, Chatterjee R, Zhao J, He X, Weirauch MT, Hughes TR, Vinson C. 2013. CG methylated microarrays identify a novel methylated sequence bound by the CEBPB|ATF4 heterodimer that is active in vivo. *Genome Res* **23**: 988-997.

Mansky KC, Sankar U, Han J, Ostrowski MC. 2002. Microphthalmia transcription factor is a target of the p38 MAPK pathway in response to receptor activator of NF-kappa B ligand signaling. *J Biol Chem* **277**: 11077-11083.

Marinkovic D, Zhang X, Yalcin S, Luciano JP, Brugnara C, Huber T, Ghaffari S. 2007. Foxo3 is required for the regulation of oxidative stress in erythropoiesis. *J Clin Invest* **117**: 2133-2144.

Martina JA, Diab HI, Li H, Puertollano R. 2014. Novel roles for the MiTF/TFE family of transcription factors in organelle biogenesis, nutrient sensing, and energy homeostasis. *Cell Mol Life Sci* **71**: 2483-2497.

Maruyama R, Shimizu M, Ishijima T, Nakai Y, Inoue J, Sato R. 2016. Searching for novel ATF4 target genes in human hepatoma cells by microarray analysis. *Biosci Biotechnol Biochem* **80**: 1149-1154.

Massagué J. 2008. TGFbeta in Cancer. *Cell* **134**: 215-230.

Matsumoto H, Miyazaki S, Matsuyama S, Takeda M, Kawano M, Nakagawa H, Nishimura K, Matsuo S. 2013. Selection of autophagy or apoptosis in cells exposed to ER-stress depends on ATF4 expression pattern with or without CHOP expression. *Biol Open* **2**: 1084-1090.

Mayes K, Qiu Z, Alhazmi A, Landry JW. 2014. ATP-dependent chromatin remodeling complexes as novel targets for cancer therapy. *Adv Cancer Res* **121**: 183-233.

McCullough KD, Martindale JL, Klotz LO, Aw TY, Holbrook NJ. 2001. Gadd153 sensitizes cells to endoplasmic reticulum stress by down-regulating Bcl2 and perturbing the cellular redox state. *Mol Cell Biol* **21**: 1249-1259.

McGill GG, Haq R, Nishimura EK, Fisher DE. 2006. c-Met expression is regulated by Mitf in the melanocyte lineage. *J Biol Chem* **281**: 10365-10373.

McGill GG, Horstmann M, Widlund HR, Du J, Motyckova G, Nishimura EK, Lin YL, Ramaswamy S, Avery W, Ding HF et al. 2002. Bcl2 regulation by the melanocyte master regulator Mitf modulates lineage survival and melanoma cell viability. *Cell* **109**: 707-718.

Medic S, Rizos H, Ziman M. 2011. Differential PAX3 functions in normal skin melanocytes and melanoma cells. *Biochem Biophys Res Commun* **411**: 832-837.

Meijer HA, Kong YW, Lu WT, Wilczynska A, Spriggs RV, Robinson SW, Godfrey JD, Willis AE, Bushell M. 2013. Translational repression and eIF4A2 activity are critical for microRNA-mediated gene regulation. *Science* **340**: 82-85.

Melgar MF, Collins FS, Sethupathy P. 2011. Discovery of active enhancers through bidirectional expression of short transcripts. *Genome Biol* **12**: R113.

Mellor J, Morillon A. 2004. ISWI complexes in Saccharomyces cerevisiae. *Biochim Biophys Acta* **1677**: 100-112.

Mendoza MC, Er EE, Blenis J. 2011. The Ras-ERK and PI3K-mTOR pathways: cross-talk and compensation. *Trends Biochem Sci* **36**: 320-328.

Meng Z, Moroishi T, Guan KL. 2016. Mechanisms of Hippo pathway regulation. *Genes Dev* **30**: 1-17.

Menzies AM, Long GV, Murali R. 2012. Dabrafenib and its potential for the treatment of metastatic melanoma. *Drug Des Devel Ther* **6**: 391-405.

Miccio A, Blobel GA. 2010. Role of the GATA-1/FOG-1/NuRD pathway in the expression of human beta-like globin genes. *Mol Cell Biol* **30**: 3460-3470.

Miller AJ, Du J, Rowan S, Hershey CL, Widlund HR, Fisher DE. 2004. Transcriptional regulation of the melanoma prognostic marker melastatin (TRPM1) by MITF in melanocytes and melanoma. *Cancer Res* **64**: 509-516.

Miller AJ, Levy C, Davis IJ, Razin E, Fisher DE. 2005. Sumoylation of MITF and its related family members TFE3 and TFEB. *J Biol Chem* **280**: 146-155.

Miller AJ, Mihm MC. 2006. Melanoma. *N Engl J Med* **355**: 51-65.

Mockenhaupt S, Grosse S, Rupp D, Bartenschlager R, Grimm D. 2015. Alleviation of off-target effects from vector-encoded shRNAs via codelivered RNA decoys. *Proc Natl Acad Sci U S A* **112**: E4007-4016.

Moore CE, Omikorede O, Gomez E, Willars GB, Herbert TP. 2011. PERK activation at low glucose concentration is mediated by SERCA pump inhibition and confers preemptive cytoprotection to pancreatic β-cells. *Mol Endocrinol* **25**: 315-326.

Moore KJ. 1995. Insight into the microphthalmia gene. *Trends Genet* **11**: 442-448.

Moore MJ, Proudfoot NJ. 2009. Pre-mRNA processing reaches back to transcription and ahead to translation. *Cell* **136**: 688-700.

Moriya H. 2015. Quantitative nature of overexpression experiments. *Mol Biol Cell* **26**: 3932-3939.

Muir A, Danai LV, Gui DY, Waingarten CY, Lewis CA, Vander Heiden MG. 2017. Environmental cystine drives glutamine anaplerosis and sensitizes cancer cells to glutaminase inhibition. *Elife* **6**.

Murakami H, Arnheiter H. 2005. Sumoylation modulates transcriptional activity of MITF in a promoter-specific manner. *Pigment Cell Res* **18**: 265-277.

Murthy A, Li Y, Peng I, Reichelt M, Katakam AK, Noubade R, Roose-Girma M, DeVoss J, Diehl L, Graham RR et al. 2014. A Crohn's disease variant in Atg16l1 enhances its degradation by caspase 3. *Nature* **506**: 456-462.

Müller J, Krijgsman O, Tsoi J, Robert L, Hugo W, Song C, Kong X, Possik PA, Cornelissen-Steijger PD, Geukes Foppen MH et al. 2014. Low MITF/AXL ratio predicts early resistance to multiple targeted drugs in melanoma. *Nat Commun* **5**: 5712.

Nakayama A, Nguyen MT, Chen CC, Opdecamp K, Hodgkinson CA, Arnheiter H. 1998. Mutations in microphthalmia, the mouse homolog of the human deafness gene MITF, affect neuroepithelial and neural crest-derived melanocytes differently. *Mech Dev* **70**: 155-166.

Namba T, Homan T, Nishimura T, Mima S, Hoshino T, Mizushima T. 2009. Up-regulation of S100P expression by non-steroidal anti-inflammatory drugs and its role in anti-tumorigenic effects. *J Biol Chem* **284**: 4158-4167.

Nasr Z, Robert F, Porco JA, Muller WJ, Pelletier J. 2013. eIF4F suppression in breast cancer affects maintenance and progression. *Oncogene* **32**: 861-871.

National Cancer Institute. CellMiner™ Database, https://discover.nci.nih.gov/cellminer/.

Nazarian R, Shi H, Wang Q, Kong X, Koya RC, Lee H, Chen Z, Lee MK, Attar N, Sazegar H et al. 2010. Melanomas acquire resistance to B-RAF(V600E) inhibition by RTK or N-RAS upregulation. *Nature* **468**: 973-977.

Neve J, Patel R, Wang Z, Louey A, Furger AM. 2017. Cleavage and polyadenylation: Ending the message expands gene regulation. *RNA Biol* **14**: 865-890.

Neznanov N, Umezawa A, Oshima RG. 1997. A regulatory element within a coding exon modulates keratin 18 gene expression in transgenic mice. *J Biol Chem* **272**: 27549-27557.

Ngeow KC, Friedrichsen HJ, Li L, Zeng Z, Andrews S, Volpon L, Brunsdon H, Berridge G, Picaud S, Fischer R et al. 2018. BRAF/MAPK and GSK3 signaling converges to control MITF nuclear export. *Proc Natl Acad Sci U S A* **115**: E8668-E8677.

Nieto MA, Huang RY, Jackson RA, Thiery JP. 2016. EMT: 2016. *Cell* **166**: 21-45.

Nock A, Ascano JM, Barrero MJ, Malik S. 2012. Mediator-regulated transcription through the +1 nucleosome. *Mol Cell* **48**: 837-848.

Nogalska A, Engel WK, McFerrin J, Kokame K, Komano H, Askanas V. 2006. Homocysteine-induced endoplasmic reticulum protein (Herp) is up-regulated in sporadic inclusion-body myositis and in endoplasmic reticulum stress-induced cultured human muscle fibers. *J Neurochem* **96**: 1491-1499.

Nora EP, Goloborodko A, Valton AL, Gibcus JH, Uebersohn A, Abdennur N, Dekker J, Mirny LA, Bruneau BG. 2017. Targeted Degradation of CTCF Decouples Local Insulation of Chromosome Domains from Genomic Compartmentalization. *Cell* **169**: 930-944.e922.

Nora EP, Lajoie BR, Schulz EG, Giorgetti L, Okamoto I, Servant N, Piolot T, van Berkum NL, Meisig J, Sedat J et al. 2012. Spatial partitioning of the regulatory landscape of the X-inactivation centre. *Nature* **485**: 381-385.

Nozawa K, Schneider TR, Cramer P. 2017. Core Mediator structure at 3.4 Å extends model of transcription initiation complex. *Nature* **545**: 248-251.

O'Connor L, Strasser A, O'Reilly LA, Hausmann G, Adams JM, Cory S, Huang DC. 1998. Bim: a novel member of the Bcl-2 family that promotes apoptosis. *EMBO J* **17**: 384-395.

Oboki K, Morii E, Kataoka TR, Jippo T, Kitamura Y. 2002. Isoforms of mi transcription factor preferentially expressed in cultured mast cells of mice. *Biochem Biophys Res Commun* **290**: 1250-1254.

Ohanna M, Bonet C, Bille K, Allegra M, Davidson I, Bahadoran P, Lacour JP, Ballotti R, Bertolotto C. 2014. SIRT1 promotes proliferation and inhibits the senescence-like phenotype in human melanoma cells. *Oncotarget* **5**: 2085-2095.

Oikonomou E, Koustas E, Goulielmaki M, Pintzas A. 2014. BRAF vs RAS oncogenes: are mutations of the same pathway equal? Differential signalling and therapeutic implications. *Oncotarget* **5**: 11752-11777.

Oki M, Aihara H, Ito T. 2007. Role of histone phosphorylation in chromatin dynamics and its implications in diseases. *Subcell Biochem* **41**: 319-336.

Okuda-Shimizu Y, Hendershot LM. 2007. Characterization of an ERAD pathway for nonglycosylated BiP substrates, which require Herp. *Mol Cell* **28**: 544-554.

Ong CT, Corces VG. 2011. Enhancer function: new insights into the regulation of tissue-specific gene expression. *Nat Rev Genet* **12**: 283-293.

Opdecamp K, Nakayama A, Nguyen MT, Hodgkinson CA, Pavan WJ, Arnheiter H. 1997. Melanocyte development in vivo and in neural crest cell cultures: crucial dependence on the Mitf basic-helix-loop-helix-zipper transcription factor. *Development* **124**: 2377-2386.

Osborne CS, Chakalova L, Brown KE, Carter D, Horton A, Debrand E, Goyenechea B, Mitchell JA, Lopes S, Reik W et al. 2004. Active genes dynamically colocalize to shared sites of ongoing transcription. *Nat Genet* **36**: 1065-1071.

Pakos-Zebrucka K, Koryga I, Mnich K, Ljujic M, Samali A, Gorman AM. 2016. The integrated stress response. *EMBO Rep* **17**: 1374-1395.

Palatnik JF, Allen E, Wu X, Schommer C, Schwab R, Carrington JC, Weigel D. 2003. Control of leaf morphogenesis by microRNAs. *Nature* **425**: 257-263.

Pampaloni F, Reynaud EG, Stelzer EH. 2007. The third dimension bridges the gap between cell culture and live tissue. *Nat Rev Mol Cell Biol* **8**: 839-845.

Paredes F, Parra V, Torrealba N, Navarro-Marquez M, Gatica D, Bravo-Sagua R, Troncoso R, Pennanen C, Quiroga C, Chiong M et al. 2016. HERPUD1 protects against oxidative stress-induced apoptosis through downregulation of the inositol 1,4,5-trisphosphate receptor. *Free Radic Biol Med* **90**: 206-218.

Pastushenko I, Brisebarre A, Sifrim A, Fioramonti M, Revenco T, Boumahdi S, Van Keymeulen A, Brown D, Moers V, Lemaire S et al. 2018. Identification of the tumour transition states occurring during EMT. *Nature* **556**: 463-468.

Pathria G, Scott DA, Feng Y, Sang Lee J, Fujita Y, Zhang G, Sahu AD, Ruppin E, Herlyn M, Osterman AL et al. 2018. Targeting the Warburg effect via LDHA inhibition engages ATF4 signaling for cancer cell survival. *EMBO J* **37**.

Patton EE, Widlund HR, Kutok JL, Kopani KR, Amatruda JF, Murphey RD, Berghmans S, Mayhall EA, Traver D, Fletcher CD et al. 2005. BRAF mutations are sufficient to promote nevi formation and cooperate with p53 in the genesis of melanoma. *Curr Biol* **15**: 249-254.

Pedraza-Fariña LG. 2006. Mechanisms of oncogenic cooperation in cancer initiation and metastasis. *Yale J Biol Med* **79**: 95-103.

Perego M, Maurer M, Wang JX, Shaffer S, Müller AC, Parapatics K, Li L, Hristova D, Shin S, Keeney F et al. 2018. A slow-cycling subpopulation of melanoma cells with highly invasive properties. *Oncogene* **37**: 302-312.

Peterlin BM, Price DH. 2006. Controlling the elongation phase of transcription with P-TEFb. *Mol Cell* **23**: 297-305.

Peterson TR, Laplante M, Thoreen CC, Sancak Y, Kang SA, Kuehl WM, Gray NS, Sabatini DM. 2009. DEPTOR is an mTOR inhibitor frequently overexpressed in multiple myeloma cells and required for their survival. *Cell* **137**: 873-886.

Petrykowska HM, Vockley CM, Elnitski L. 2008. Detection and characterization of silencers and enhancer-blockers in the greater CFTR locus. *Genome Res* **18**: 1238-1246.

Pickup M, Novitskiy S, Moses HL. 2013. The roles of TGFβ in the tumour microenvironment. *Nat Rev Cancer* **13**: 788-799.

Pierrat MJ, Marsaud V, Mauviel A, Javelaud D. 2012. Expression of microphthalmia-associated transcription factor (MITF), which is critical for melanoma progression, is inhibited by both transcription factor GLI2 and transforming growth factor-β. *J Biol Chem* **287**: 17996-18004.

Pindel A, Sadler A. 2011. The role of protein kinase R in the interferon response. *J Interferon Cytokine Res* **31**: 59-70.

Pingault V, Bondurand N, Kuhlbrodt K, Goerich DE, Préhu MO, Puliti A, Herbarth B, Hermans-Borgmeyer I, Legius E, Matthijs G et al. 1998. SOX10 mutations in patients with Waardenburg-Hirschsprung disease. *Nat Genet* **18**: 171-173.

Pinner S, Jordan P, Sharrock K, Bazley L, Collinson L, Marais R, Bonvin E, Goding C, Sahai E. 2009. Intravital imaging reveals transient changes in pigment production and Brn2 expression during metastatic melanoma dissemination. *Cancer Res* **69**: 7969-7977.

Plaschka C, Larivière L, Wenzeck L, Seizl M, Hemann M, Tegunov D, Petrotchenko EV, Borchers CH, Baumeister W, Herzog F et al. 2015. Architecture of the RNA polymerase II-Mediator core initiation complex. *Nature* **518**: 376-380.

Ploper D, Taelman VF, Robert L, Perez BS, Titz B, Chen HW, Graeber TG, von Euw E, Ribas A, De Robertis EM. 2015. MITF drives endolysosomal biogenesis and potentiates Wnt signaling in melanoma cells. *Proc Natl Acad Sci U S A* **112**: E420-429.

Podust LM, Krezel AM, Kim Y. 2001. Crystal structure of the CCAAT box/enhancer-binding protein beta activating transcription factor-4 basic leucine zipper heterodimer in the absence of DNA. *J Biol Chem* **276**: 505-513.

Polunovsky VA, Rosenwald IB, Tan AT, White J, Chiang L, Sonenberg N, Bitterman PB. 1996. Translational control of programmed cell death: eukaryotic translation initiation factor 4E blocks apoptosis in growth-factor-restricted fibroblasts with physiologically expressed or deregulated Myc. *Mol Cell Biol* **16**: 6573-6581.

Porta C, Paglino C, Mosca A. 2014. Targeting PI3K/Akt/mTOR Signaling in Cancer. *Front Oncol* **4**: 64.

Potrony M, Badenas C, Aguilera P, Puig-Butille JA, Carrera C, Malvehy J, Puig S. 2015. Update in genetic susceptibility in melanoma. *Ann Transl Med* **3**: 210.

Potterf SB, Furumura M, Dunn KJ, Arnheiter H, Pavan WJ. 2000. Transcription factor hierarchy in Waardenburg syndrome: regulation of MITF expression by SOX10 and PAX3. *Hum Genet* **107**: 1-6.

Poulikakos PI, Persaud Y, Janakiraman M, Kong X, Ng C, Moriceau G, Shi H, Atefi M, Titz B, Gabay MT et al. 2011. RAF inhibitor resistance is mediated by dimerization of aberrantly spliced BRAF(V600E). *Nature* **480**: 387-390.

Price ER, Ding HF, Badalian T, Bhattacharya S, Takemoto C, Yao TP, Hemesath TJ, Fisher DE. 1998a. Lineage-specific signaling in melanocytes. C-kit stimulation recruits p300/CBP to microphthalmia. *J Biol Chem* **273**: 17983-17986.

Price ER, Horstmann MA, Wells AG, Weilbaecher KN, Takemoto CM, Landis MW, Fisher DE. 1998b. alpha-Melanocyte-stimulating hormone signaling regulates expression of microphthalmia, a gene deficient in Waardenburg syndrome. *J Biol Chem* **273**: 33042-33047.

Puighermanal E, Biever A, Pascoli V, Melser S, Pratlong M, Cutando L, Rialle S, Severac D, Boubaker-Vitre J, Meyuhas O et al. 2017. Ribosomal Protein S6 Phosphorylation Is Involved in Novelty-Induced Locomotion, Synaptic Plasticity and mRNA Translation. *Front Mol Neurosci* **10**: 419.

Puthalakath H, O'Reilly LA, Gunn P, Lee L, Kelly PN, Huntington ND, Hughes PD, Michalak EM, McKimm-Breschkin J, Motoyama N et al. 2007. ER stress triggers apoptosis by activating BH3-only protein Bim. *Cell* **129**: 1337-1349.

Qian H, Yang C, Yang Y. 2017. MicroRNA-26a inhibits the growth and invasiveness of malignant melanoma and directly targets on. *Cell Death Discov* **3**: 17028.

Quirós PM, Prado MA, Zamboni N, D'Amico D, Williams RW, Finley D, Gygi SP, Auwerx J. 2017. Multi-omics analysis identifies ATF4 as a key regulator of the mitochondrial stress response in mammals. *J Cell Biol* **216**: 2027-2045.

Raben N, Puertollano R. 2016. TFEB and TFE3: Linking Lysosomes to Cellular Adaptation to Stress. *Annu Rev Cell Dev Biol* **32**: 255-278.

Raden D, Hildebrandt S, Xu P, Bell E, Doyle FJ, Robinson AS. 2005. Analysis of cellular response to protein overexpression. *Syst Biol (Stevenage)* **152**: 285-289.

Ramanathan A, Robb GB, Chan SH. 2016. mRNA capping: biological functions and applications. *Nucleic Acids Res* **44**: 7511-7526.

Rambow F, Rogiers A, Marin-Bejar O, Aibar S, Femel J, Dewaele M, Karras P, Brown D, Chang YH, Debiec-Rychter M et al. 2018. Toward Minimal Residual Disease-Directed Therapy in Melanoma. *Cell* **174**: 843-855.e819.

Rankin EB, Giaccia AJ. 2016. Hypoxic control of metastasis. *Science* **352**: 175-180.

Rao DD, Senzer N, Cleary MA, Nemunaitis J. 2009. Comparative assessment of siRNA and shRNA off target effects: what is slowing clinical development. *Cancer Gene Ther* **16**: 807-809.

Raught B, Peiretti F, Gingras AC, Livingstone M, Shahbazian D, Mayeur GL, Polakiewicz RD, Sonenberg N, Hershey JW. 2004. Phosphorylation of eucaryotic translation initiation factor 4B Ser422 is modulated by S6 kinases. *EMBO J* **23**: 1761-1769.

Razin SV, Gavrilov AA, Pichugin A, Lipinski M, Iarovaia OV, Vassetzky YS. 2011. Transcription factories in the context of the nuclear and genome organization. *Nucleic Acids Res* **39**: 9085-9092.

Reiter JG, Makohon-Moore AP, Gerold JM, Heyde A, Attiyeh MA, Kohutek ZA, Tokheim CJ, Brown A, DeBlasio RM, Niyazov J et al. 2018. Minimal functional driver gene heterogeneity among untreated metastases. *Science* **361**: 1033-1037.

Rheault TR, Stellwagen JC, Adjabeng GM, Hornberger KR, Petrov KG, Waterson AG, Dickerson SH, Mook RA, Laquerre SG, King AJ et al. 2013. Discovery of Dabrafenib: A Selective Inhibitor of Raf Kinases with Antitumor Activity against B-Raf-Driven Tumors. *ACS Med Chem Lett* **4**: 358-362.

Riesenberg S, Groetchen A, Siddaway R, Bald T, Reinhardt J, Smorra D, Kohlmeyer J, Renn M, Phung B, Aymans P et al. 2015. MITF and c-Jun antagonism interconnects melanoma dedifferentiation with pro-inflammatory cytokine responsiveness and myeloid cell recruitment. *Nat Commun* **6**: 8755.

Ritter DI, Dong Z, Guo S, Chuang JH. 2012. Transcriptional enhancers in protein-coding exons of vertebrate developmental genes. *PLoS One* **7**: e35202.

Robichaud N, del Rincon SV, Huor B, Alain T, Petruccelli LA, Hearnden J, Goncalves C, Grotegut S, Spruck CH, Furic L et al. 2015. Phosphorylation of eIF4E promotes EMT and metastasis via translational control of SNAIL and MMP-3. *Oncogene* **34**: 2032-2042.

Robichaud N, Sonenberg N. 2017. Translational control and the cancer cell response to stress. *Curr Opin Cell Biol* **45**: 102-109.

Robinson MD, McCarthy DJ, Smyth GK. 2010. edgeR: a Bioconductor package for differential expression analysis of digital gene expression data. *Bioinformatics* **26**: 139-140.

Robinson PJ, Trnka MJ, Bushnell DA, Davis RE, Mattei PJ, Burlingame AL, Kornberg RD. 2016. Structure of a Complete Mediator-RNA Polymerase II Pre-Initiation Complex. *Cell* **166**: 1411-1422.e1416.

Rossetto D, Avvakumov N, Côté J. 2012. Histone phosphorylation: a chromatin modification involved in diverse nuclear events. *Epigenetics* **7**: 1098-1108.

Rouschop KM, van den Beucken T, Dubois L, Niessen H, Bussink J, Savelkouls K, Keulers T, Mujcic H, Landuyt W, Voncken JW et al. 2010. The unfolded protein response protects human tumor cells during hypoxia through regulation of the autophagy genes MAP1LC3B and ATG5. *J Clin Invest* **120**: 127-141.

Roux PP, Shahbazian D, Vu H, Holz MK, Cohen MS, Taunton J, Sonenberg N, Blenis J. 2007. RAS/ERK signaling promotes site-specific ribosomal protein S6 phosphorylation via RSK and stimulates cap-dependent translation. *J Biol Chem* **282**: 14056-14064.

Roux PP, Topisirovic I. 2012. Regulation of mRNA translation by signaling pathways. *Cold Spring Harb Perspect Biol* **4**.

Rozpedek W, Pytel D, Mucha B, Leszczynska H, Diehl JA, Majsterek I. 2016. The Role of the PERK/eIF2α/ATF4/CHOP Signaling Pathway in Tumor Progression During Endoplasmic Reticulum Stress. *Curr Mol Med* **16**: 533-544.

Ruvinsky I, Meyuhas O. 2006. Ribosomal protein S6 phosphorylation: from protein synthesis to cell size. *Trends Biochem Sci* **31**: 342-348.

Ruvinsky I, Sharon N, Lerer T, Cohen H, Stolovich-Rain M, Nir T, Dor Y, Zisman P, Meyuhas O. 2005. Ribosomal protein S6 phosphorylation is a determinant of cell size and glucose homeostasis. *Genes Dev* **19**: 2199-2211.

Rzymski T, Milani M, Pike L, Buffa F, Mellor HR, Winchester L, Pires I, Hammond E, Ragoussis I, Harris AL. 2010. Regulation of autophagy by ATF4 in response to severe hypoxia. *Oncogene* **29**: 4424-4435.

Rzymski T, Milani M, Singleton DC, Harris AL. 2009. Role of ATF4 in regulation of autophagy and resistance to drugs and hypoxia. *Cell Cycle* **8**: 3838-3847.

Saito M, Ishikawa F. 2002. The mCpG-binding domain of human MBD3 does not bind to mCpG but interacts with NuRD/Mi2 components HDAC1 and MTA2. *J Biol Chem* **277**: 35434-35439.

Sancak Y, Thoreen CC, Peterson TR, Lindquist RA, Kang SA, Spooner E, Carr SA, Sabatini DM. 2007. PRAS40 is an insulin-regulated inhibitor of the mTORC1 protein kinase. *Mol Cell* **25**: 903-915.

Sanyal A, Lajoie BR, Jain G, Dekker J. 2012. The long-range interaction landscape of gene promoters. *Nature* **489**: 109-113.

Sato S, Roberts K, Gambino G, Cook A, Kouzarides T, Goding CR. 1997. CBP/p300 as a co-factor for the Microphthalmia transcription factor. *Oncogene* **14**: 3083-3092.

Saw PE, Song EW. 2019. siRNA therapeutics: a clinical reality. *Sci China Life Sci*.

Sawicka A, Seiser C. 2014. Sensing core histone phosphorylation - a matter of perfect timing. *Biochim Biophys Acta* **1839**: 711-718.

Saxton RA, Sabatini DM. 2017. mTOR Signaling in Growth, Metabolism, and Disease. *Cell* **169**: 361-371.

Schaukowitch K, Joo JY, Liu X, Watts JK, Martinez C, Kim TK. 2014. Enhancer RNA facilitates NELF release from immediate early genes. *Mol Cell* **56**: 29-42.

Schepsky A, Bruser K, Gunnarsson GJ, Goodall J, Hallsson JH, Goding CR, Steingrimsson E, Hecht A. 2006. The microphthalmia-associated transcription factor Mitf interacts with beta-catenin to determine target gene expression. *Mol Cell Biol* **26**: 8914-8927.

Schmitz ML, Shaban MS, Albert BV, Gökçen A, Kracht M. 2018. The Crosstalk of Endoplasmic Reticulum (ER) Stress Pathways with NF-κB: Complex Mechanisms Relevant for Cancer, Inflammation and Infection. *Biomedicines* **6**.

Schoenberg DR, Maquat LE. 2012. Regulation of cytoplasmic mRNA decay. *Nat Rev Genet* **13**: 246-259.

Schug ZT, Peck B, Jones DT, Zhang Q, Grosskurth S, Alam IS, Goodwin LM, Smethurst E, Mason S, Blyth K et al. 2015. Acetyl-CoA synthetase 2 promotes acetate utilization and maintains cancer cell growth under metabolic stress. *Cancer Cell* **27**: 57-71.

Schwind L, Zimmer AD, Götz C, Montenarh M. 2015. CK2 phosphorylation of C/EBPδ regulates its transcription factor activity. *Int J Biochem Cell Biol* **61**: 81-89.

Sedding DG. 2008. FoxO transcription factors in oxidative stress response and ageing--a new fork on the way to longevity? *Biol Chem* **389**: 279-283.

Seftor EA, Brown KM, Chin L, Kirschmann DA, Wheaton WW, Protopopov A, Feng B, Balagurunathan Y, Trent JM, Nickoloff BJ et al. 2005. Epigenetic transdifferentiation of normal melanocytes by a metastatic melanoma microenvironment. *Cancer Res* **65**: 10164-10169.

Segal E, Widom J. 2009a. From DNA sequence to transcriptional behaviour: a quantitative approach. *Nat Rev Genet* **10**: 443-456.

Segal E, Widom J. 2009b. What controls nucleosome positions? *Trends Genet* **25**: 335-343.

Segura MF, Hanniford D, Menendez S, Reavie L, Zou X, Alvarez-Diaz S, Zakrzewski J, Blochin E, Rose A, Bogunovic D et al. 2009. Aberrant miR-182 expression promotes melanoma metastasis by repressing FOXO3 and microphthalmia-associated transcription factor. *Proc Natl Acad Sci U S A* **106**: 1814-1819.

Sengupta S, Peterson TR, Sabatini DM. 2010. Regulation of the mTOR complex 1 pathway by nutrients, growth factors, and stress. *Mol Cell* **40**: 310-322.

Serra DO, Hengge R. 2014. Stress responses go three dimensional - the spatial order of physiological differentiation in bacterial macrocolony biofilms. *Environ Microbiol* **16**: 1455-1471.

Shain AH, Joseph NM, Yu R, Benhamida J, Liu S, Prow T, Ruben B, North J, Pincus L, Yeh I et al. 2018. Genomic and Transcriptomic Analysis Reveals Incremental Disruption of Key Signaling Pathways during Melanoma Evolution. *Cancer Cell* **34**: 45-55.e44.

Shain AH, Yeh I, Kovalyshyn I, Sriharan A, Talevich E, Gagnon A, Dummer R, North J, Pincus L, Ruben B et al. 2015. The Genetic Evolution of Melanoma from Precursor Lesions. *N Engl J Med* **373**: 1926-1936.

Sharpless NE. 2005. INK4a/ARF: a multifunctional tumor suppressor locus. *Mutat Res* **576**: 22-38.

Shastry BS. 1995. Overexpression of genes in health and sickness. A bird's eye view. *Comp Biochem Physiol B Biochem Mol Biol* **112**: 1-13.

Shaw G, Morse S, Ararat M, Graham FL. 2002. Preferential transformation of human neuronal cells by human adenoviruses and the origin of HEK 293 cells. *FASEB J* **16**: 869-871.

Shen Y, Yue F, McCleary DF, Ye Z, Edsall L, Kuan S, Wagner U, Dixon J, Lee L, Lobanenkov VV et al. 2012. A map of the cis-regulatory sequences in the mouse genome. *Nature* **488**: 116-120.

Shi H, Moriceau G, Kong X, Lee MK, Lee H, Koya RC, Ng C, Chodon T, Scolyer RA, Dahlman KB et al. 2012. Melanoma whole-exome sequencing identifies (V600E)B-RAF amplification-mediated acquired B-RAF inhibitor resistance. *Nat Commun* **3**: 724.

Shi Y. 2017. Mechanistic insights into precursor messenger RNA splicing by the spliceosome. *Nat Rev Mol Cell Biol* **18**: 655-670.

Shi Z, Yu X, Yuan M, Lv W, Feng T, Bai R, Zhong H. 2019. Activation of the PERK-ATF4 pathway promotes chemo-resistance in colon cancer cells. *Sci Rep* **9**: 3210.

Shinozaki S, Chiba T, Kokame K, Miyata T, Kaneko E, Shimokado K. 2013. A deficiency of Herp, an endoplasmic reticulum stress protein, suppresses atherosclerosis in ApoE knockout mice by attenuating inflammatory responses. *PLoS One* **8**: e75249.

Shukla A, Edwards R, Yang Y, Hahn A, Folkers K, Ding J, Padmakumar VC, Cataisson C, Suh KS, Yuspa SH. 2014. CLIC4 regulates TGF-β-dependent myofibroblast differentiation to produce a cancer stroma. *Oncogene* **33**: 842-850.

Shukla A, Malik M, Cataisson C, Ho Y, Friesen T, Suh KS, Yuspa SH. 2009. TGF-beta signalling is regulated by Schnurri-2-dependent nuclear translocation of CLIC4 and consequent stabilization of phospho-Smad2 and 3. *Nat Cell Biol* **11**: 777-784.

Shukla A, Yuspa SH. 2010. CLIC4 and Schnurri-2: a dynamic duo in TGF-beta signaling with broader implications in cellular homeostasis and disease. *Nucleus* **1**: 144-149.

Shukla GC, Singh J, Barik S. 2011. MicroRNAs: Processing, Maturation, Target Recognition and Regulatory Functions. *Mol Cell Pharmacol* **3**: 83-92.

Siersbæk R, Nielsen R, John S, Sung MH, Baek S, Loft A, Hager GL, Mandrup S. 2011. Extensive chromatin remodelling and establishment of transcription factor 'hotspots' during early adipogenesis. *EMBO J* **30**: 1459-1472.

Sigal A, Rotter V. 2000. Oncogenic mutations of the p53 tumor suppressor: the demons of the guardian of the genome. *Cancer Res* **60**: 6788-6793.

Singleton DC, Harris AL. 2012. Targeting the ATF4 pathway in cancer therapy. *Expert Opin Ther Targets* **16**: 1189-1202.

Siolas D, Lerner C, Burchard J, Ge W, Linsley PS, Paddison PJ, Hannon GJ, Cleary MA. 2005. Synthetic shRNAs as potent RNAi triggers. *Nat Biotechnol* **23**: 227-231.

Sokol S, Christian JL, Moon RT, Melton DA. 1991. Injected Wnt RNA induces a complete body axis in Xenopus embryos. *Cell* **67**: 741-752.

Solomon H, Brosh R, Buganim Y, Rotter V. 2010. Inactivation of the p53 tumor suppressor gene and activation of the Ras oncogene: cooperative events in tumorigenesis. *Discov Med* **9**: 448-454.

Somasundaram R, Villanueva J, Herlyn M. 2012. Intratumoral heterogeneity as a therapy resistance mechanism: role of melanoma subpopulations. *Adv Pharmacol* **65**: 335-359.

Sonenberg N, Hinnebusch AG. 2009. Regulation of translation initiation in eukaryotes: mechanisms and biological targets. *Cell* **136**: 731-745.

Soufir N, Avril MF, Chompret A, Demenais F, Bombled J, Spatz A, Stoppa-Lyonnet D, Bénard J, Bressac-de Paillerets B. 1998. Prevalence of p16 and CDK4 germline mutations in 48 melanoma-prone families in France. The French Familial Melanoma Study Group. *Hum Mol Genet* **7**: 209-216.

Soutourina J. 2018. Transcription regulation by the Mediator complex. *Nat Rev Mol Cell Biol* **19**: 262-274.

Spitz F, Furlong EE. 2012. Transcription factors: from enhancer binding to developmental control. *Nat Rev Genet* **13**: 613-626.

Spriggs KA, Bushell M, Willis AE. 2010. Translational regulation of gene expression during conditions of cell stress. *Mol Cell* **40**: 228-237.

Spruijt CG, Luijsterburg MS, Menafra R, Lindeboom RG, Jansen PW, Edupuganti RR, Baltissen MP, Wiegant WW, Voelker-Albert MC, Matarese F et al. 2016. ZMYND8 Co-localizes with NuRD on Target Genes and Regulates Poly(ADP-Ribose)-Dependent Recruitment of GATAD2A/NuRD to Sites of DNA Damage. *Cell Rep* **17**: 783-798.

Srivastava SP, Kumar KU, Kaufman RJ. 1998. Phosphorylation of eukaryotic translation initiation factor 2 mediates apoptosis in response to activation of the double-stranded RNA-dependent protein kinase. *J Biol Chem* **273**: 2416-2423.

Steingrímsson E, Moore KJ, Lamoreux ML, Ferré-D'Amaré AR, Burley SK, Zimring DC, Skow LC, Hodgkinson CA, Arnheiter H, Copeland NG. 1994. Molecular basis of mouse microphthalmia (mi) mutations helps explain their developmental and phenotypic consequences. *Nat Genet* **8**: 256-263.

Stoebel DM, Dean AM, Dykhuizen DE. 2008. The cost of expression of Escherichia coli lac operon proteins is in the process, not in the products. *Genetics* **178**: 1653-1660.

Stolovich M, Tang H, Hornstein E, Levy G, Cohen R, Bae SS, Birnbaum MJ, Meyuhas O. 2002. Transduction of growth or mitogenic signals into translational activation of TOP mRNAs is fully reliant on the phosphatidylinositol 3-kinase-mediated pathway but requires neither S6K1 nor rpS6 phosphorylation. *Mol Cell Biol* **22**: 8101-8113.

Strohner R, Németh A, Nightingale KP, Grummt I, Becker PB, Längst G. 2004. Recruitment of the nucleolar remodeling complex NoRC establishes ribosomal DNA silencing in chromatin. *Mol Cell Biol* **24**: 1791-1798.

Strub T, Giuliano S, Ye T, Bonet C, Keime C, Kobi D, Le Gras S, Cormont M, Ballotti R, Bertolotto C et al. 2011. Essential role of microphthalmia transcription factor for DNA replication, mitosis and genomic stability in melanoma. *Oncogene* **30**: 2319-2332.

Suh KS, Malik M, Shukla A, Ryscavage A, Wright L, Jividen K, Crutchley JM, Dumont RA, Fernandez-Salas E, Webster JD et al. 2012. CLIC4 is a tumor suppressor for cutaneous squamous cell cancer. *Carcinogenesis* **33**: 986-995.

Sun C, Wang L, Huang S, Heynen GJ, Prahallad A, Robert C, Haanen J, Blank C, Wesseling J, Willems SM et al. 2014. Reversible and adaptive resistance to BRAF(V600E) inhibition in melanoma. *Nature* **508**: 118-122.

Sundrud MS, Koralov SB, Feuerer M, Calado DP, Kozhaya AE, Rhule-Smith A, Lefebvre RE, Unutmaz D, Mazitschek R, Waldner H et al. 2009. Halofuginone inhibits TH17 cell differentiation by activating the amino acid starvation response. *Science* **324**: 1334-1338.

Sutherland H, Bickmore WA. 2009. Transcription factories: gene expression in unions? *Nat Rev Genet* **10**: 457-466.

Suzuki C, Garces RG, Edmonds KA, Hiller S, Hyberts SG, Marintchev A, Wagner G. 2008. PDCD4 inhibits translation initiation by binding to eIF4A using both its MA3 domains. *Proc Natl Acad Sci U S A* **105**: 3274-3279.

Suzuki T, Osumi N, Wakamatsu Y. 2010. Stabilization of ATF4 protein is required for the regulation of epithelial-mesenchymal transition of the avian neural crest. *Dev Biol* **344**: 658-668.

Swygert SG, Peterson CL. 2014. Chromatin dynamics: interplay between remodeling enzymes and histone modifications. *Biochim Biophys Acta* **1839**: 728-736.

Sáez-Ayala M, Montenegro MF, Sánchez-Del-Campo L, Fernández-Pérez MP, Chazarra S, Freter R, Middleton M, Piñero-Madrona A, Cabezas-Herrera J, Goding CR et al. 2013. Directed phenotype switching as an effective antimelanoma strategy. *Cancer Cell* **24**: 105-119.

Takeda K, Takemoto C, Kobayashi I, Watanabe A, Nobukuni Y, Fisher DE, Tachibana M. 2000a. Ser298 of MITF, a mutation site in Waardenburg syndrome type 2, is a phosphorylation site with functional significance. *Hum Mol Genet* **9**: 125-132.

Takeda K, Yasumoto K, Kawaguchi N, Udono T, Watanabe K, Saito H, Takahashi K, Noda M, Shibahara S. 2002. Mitf-D, a newly identified isoform, expressed in the retinal pigment epithelium and monocyte-lineage cells affected by Mitf mutations. *Biochim Biophys Acta* **1574**: 15-23.

Takeda K, Yasumoto K, Takada R, Takada S, Watanabe K, Udono T, Saito H, Takahashi K, Shibahara S. 2000b. Induction of melanocyte-specific microphthalmia-associated transcription factor by Wnt-3a. *J Biol Chem* **275**: 14013-14016.

Takemoto CM, Yoon YJ, Fisher DE. 2002. The identification and functional characterization of a novel mast cell isoform of the microphthalmia-associated transcription factor. *J Biol Chem* **277**: 30244-30252.

Tang H, Hornstein E, Stolovich M, Levy G, Livingstone M, Templeton D, Avruch J, Meyuhas O. 2001. Amino acid-induced translation of TOP mRNAs is fully dependent on phosphatidylinositol 3-kinase-mediated signaling, is partially inhibited by rapamycin, and is independent of S6K1 and rpS6 phosphorylation. *Mol Cell Biol* **21**: 8671-8683.

Tang L, Nogales E, Ciferri C. 2010. Structure and function of SWI/SNF chromatin remodeling complexes and mechanistic implications for transcription. *Prog Biophys Mol Biol* **102**: 122-128.

Tang YC, Amon A. 2013. Gene copy-number alterations: a cost-benefit analysis. *Cell* **152**: 394-405.

Tardito S, Oudin A, Ahmed SU, Fack F, Keunen O, Zheng L, Miletic H, Sakariassen P, Weinstock A, Wagner A et al. 2015. Glutamine synthetase activity fuels nucleotide biosynthesis and supports growth of glutamine-restricted glioblastoma. *Nat Cell Biol* **17**: 1556-1568.

Tassabehji M, Newton VE, Read AP. 1994. Waardenburg syndrome type 2 caused by mutations in the human microphthalmia (MITF) gene. *Nat Genet* **8**: 251-255.

Teske BF, Wek SA, Bunpo P, Cundiff JK, McClintick JN, Anthony TG, Wek RC. 2011. The eIF2 kinase PERK and the integrated stress response facilitate activation of ATF6 during endoplasmic reticulum stress. *Mol Biol Cell* **22**: 4390-4405.

Thakor N, Holcik M. 2012. IRES-mediated translation of cellular messenger RNA operates in eIF2α- independent manner during stress. *Nucleic Acids Res* **40**: 541-552.

The Gene Ontology Consortium. 2019. The Gene Ontology Resource: 20 years and still GOing strong. *Nucleic Acids Res* **47**: D330-D338.

Thiagalingam S, Cheng KH, Lee HJ, Mineva N, Thiagalingam A, Ponte JF. 2003. Histone deacetylases: unique players in shaping the epigenetic histone code. *Ann N Y Acad Sci* **983**: 84-100.

Thiery JP, Acloque H, Huang RY, Nieto MA. 2009. Epithelial-mesenchymal transitions in development and disease. *Cell* **139**: 871-890.

Thomas AJ, Erickson CA. 2008. The making of a melanocyte: the specification of melanoblasts from the neural crest. *Pigment Cell Melanoma Res* **21**: 598-610.

Thomas AJ, Erickson CA. 2009. FOXD3 regulates the lineage switch between neural crest-derived glial cells and pigment cells by repressing MITF through a non-canonical mechanism. *Development* **136**: 1849-1858.

Thompson PR, Fast W. 2006. Histone citrullination by protein arginine deiminase: is arginine methylation a green light or a roadblock? *ACS Chem Biol* **1**: 433-441.

Thurber AE, Douglas G, Sturm EC, Zabierowski SE, Smit DJ, Ramakrishnan SN, Hacker E, Leonard JH, Herlyn M, Sturm RA. 2011. Inverse expression states of the BRN2 and MITF transcription factors in melanoma spheres and tumour xenografts regulate the NOTCH pathway. *Oncogene* **30**: 3036-3048.

Tominaga H, Maeda S, Hayashi M, Takeda S, Akira S, Komiya S, Nakamura T, Akiyama H, Imamura T. 2008. CCAAT/enhancer-binding protein beta promotes osteoblast differentiation by enhancing Runx2 activity with ATF4. *Mol Biol Cell* **19**: 5373-5386.

Topisirovic I, Sonenberg N. 2011. mRNA translation and energy metabolism in cancer: the role of the MAPK and mTORC1 pathways. *Cold Spring Harb Symp Quant Biol* **76**: 355-367.

Tsai J, Lee JT, Wang W, Zhang J, Cho H, Mamo S, Bremer R, Gillette S, Kong J, Haass NK et al. 2008. Discovery of a selective inhibitor of oncogenic B-Raf kinase with potent antimelanoma activity. *Proc Natl Acad Sci U S A* **105**: 3041-3046.

Tsai KL, Yu X, Gopalan S, Chao TC, Zhang Y, Florens L, Washburn MP, Murakami K, Conaway RC, Conaway JW et al. 2017. Mediator structure and rearrangements required for holoenzyme formation. *Nature* **544**: 196-201.

Tsoi J, Robert L, Paraiso K, Galvan C, Sheu KM, Lay J, Wong DJL, Atefi M, Shirazi R, Wang X et al. 2018. Multi-stage Differentiation Defines Melanoma Subtypes with Differential Vulnerability to Drug-Induced Iron-Dependent Oxidative Stress. *Cancer Cell* **33**: 890-904.e895.

Tsujimura T, Morii E, Nozaki M, Hashimoto K, Moriyama Y, Takebayashi K, Kondo T, Kanakura Y, Kitamura Y. 1996. Involvement of transcription factor encoded by the mi locus in the expression of c-kit receptor tyrosine kinase in cultured mast cells of mice. *Blood* **88**: 1225-1233.

Turajlic S, Furney SJ, Lambros MB, Mitsopoulos C, Kozarewa I, Geyer FC, Mackay A, Hakas J, Zvelebil M, Lord CJ et al. 2012. Whole genome sequencing of matched primary and metastatic acral melanomas. *Genome Res* **22**: 196-207.

Turner N, Ware O, Bosenberg M. 2018. Genetics of metastasis: melanoma and other cancers. *Clin Exp Metastasis* **35**: 379-391.

Tuschl T, Zamore PD, Lehmann R, Bartel DP, Sharp PA. 1999. Targeted mRNA degradation by double-stranded RNA in vitro. *Genes Dev* **13**: 3191-3197.

Ubeda M, Habener JF. 2003. CHOP transcription factor phosphorylation by casein kinase 2 inhibits transcriptional activation. *J Biol Chem* **278**: 40514-40520.

Udono T, Yasumoto K, Takeda K, Amae S, Watanabe K, Saito H, Fuse N, Tachibana M, Takahashi K, Tamai M et al. 2000. Structural organization of the human microphthalmia-associated transcription factor gene containing four alternative promoters. *Biochim Biophys Acta* **1491**: 205-219.

Ullrich N, Löffek S, Horn S, Ennen M, Sánchez-Del-Campo L, Zhao F, Breitenbuecher F, Davidson I, Singer BB, Schadendorf D et al. 2015. MITF is a critical regulator of the carcinoembryonic antigen-related cell adhesion molecule 1 (CEACAM1) in malignant melanoma. *Pigment Cell Melanoma Res* **28**: 736-740.

Vachtenheim J, Ondrusová L, Borovanský J. 2010. SWI/SNF chromatin remodeling complex is critical for the expression of microphthalmia-associated transcription factor in melanoma cells. *Biochem Biophys Res Commun* **392**: 454-459.

Vallejo M, Ron D, Miller CP, Habener JF. 1993. C/ATF, a member of the activating transcription factor family of DNA-binding proteins, dimerizes with CAAT/enhancer-binding proteins and directs their binding to cAMP response elements. *Proc Natl Acad Sci U S A* **90**: 4679-4683.

van den Beucken T, Magagnin MG, Jutten B, Seigneuric R, Lambin P, Koritzinsky M, Wouters BG. 2011. Translational control is a major contributor to hypoxia induced gene expression. *Radiother Oncol* **99**: 379-384.

van den Broek B, Lomholt MA, Kalisch SM, Metzler R, Wuite GJ. 2008. How DNA coiling enhances target localization by proteins. *Proc Natl Acad Sci U S A* **105**: 15738-15742.

Vande Voorde J, Ackermann T, Pfetzer N, Sumpton D, Mackay G, Kalna G, Nixon C, Blyth K, Gottlieb E, Tardito S. 2019. Improving the metabolic fidelity of cancer models with a physiological cell culture medium. *Sci Adv* **5**: eaau7314.

Vander Haar E, Lee SI, Bandhakavi S, Griffin TJ, Kim DH. 2007. Insulin signalling to mTOR mediated by the Akt/PKB substrate PRAS40. *Nat Cell Biol* **9**: 316-323.

Vavouri T, Semple JI, Garcia-Verdugo R, Lehner B. 2009. Intrinsic protein disorder and interaction promiscuity are widely associated with dosage sensitivity. *Cell* **138**: 198-208.

Vazquez F, Lim JH, Chim H, Bhalla K, Girnun G, Pierce K, Clish CB, Granter SR, Widlund HR, Spiegelman BM et al. 2013. PGC1α expression defines a subset of human melanoma tumors with increased mitochondrial capacity and resistance to oxidative stress. *Cancer Cell* **23**: 287-301.

Velasco-Miguel S, Buckbinder L, Jean P, Gelbert L, Talbott R, Laidlaw J, Seizinger B, Kley N. 1999. PA26, a novel target of the p53 tumor suppressor and member of the GADD family of DNA damage and growth arrest inducible genes. *Oncogene* **18**: 127-137.

Verastegui C, Bille K, Ortonne JP, Ballotti R. 2000. Regulation of the microphthalmia-associated transcription factor gene by the Waardenburg syndrome type 4 gene, SOX10. *J Biol Chem* **275**: 30757-30760.

Vinson CR, Hai T, Boyd SM. 1993. Dimerization specificity of the leucine zipper-containing bZIP motif on DNA binding: prediction and rational design. *Genes Dev* **7**: 1047-1058.

Vlčková K, Vachtenheim J, Réda J, Horák P, Ondrušová L. 2018. Inducibly decreased MITF levels do not affect proliferation and phenotype switching but reduce differentiation of melanoma cells. *J Cell Mol Med* **22**: 2240-2251.

Vogelstein B, Papadopoulos N, Velculescu VE, Zhou S, Diaz LA, Kinzler KW. 2013. Cancer genome landscapes. *Science* **339**: 1546-1558.

Vokes SA, Ji H, Wong WH, McMahon AP. 2008. A genome-scale analysis of the cis-regulatory circuitry underlying sonic hedgehog-mediated patterning of the mammalian limb. *Genes Dev* **22**: 2651-2663.

von Hippel PH, Berg OG. 1989. Facilitated target location in biological systems. *J Biol Chem* **264**: 675-678.

Wagle N, Emery C, Berger MF, Davis MJ, Sawyer A, Pochanard P, Kehoe SM, Johannessen CM, Macconaill LE, Hahn WC et al. 2011. Dissecting therapeutic resistance to RAF inhibition in melanoma by tumor genomic profiling. *J Clin Oncol* **29**: 3085-3096.

Waldron L, Steimle JD, Greco TM, Gomez NC, Dorr KM, Kweon J, Temple B, Yang XH, Wilczewski CM, Davis IJ et al. 2016. The Cardiac TBX5 Interactome Reveals a Chromatin Remodeling Network Essential for Cardiac Septation. *Dev Cell* **36**: 262-275.

Walport LJ, Hopkinson RJ, Chowdhury R, Schiller R, Ge W, Kawamura A, Schofield CJ. 2016. Arginine demethylation is catalysed by a subset of JmjC histone lysine demethylases. *Nat Commun* **7**: 11974.

Wang F, Marshall CB, Ikura M. 2013a. Transcriptional/epigenetic regulator CBP/p300 in tumorigenesis: structural and functional versatility in target recognition. *Cell Mol Life Sci* **70**: 3989-4008.

Wang G, Yang ZQ, Zhang K. 2010. Endoplasmic reticulum stress response in cancer: molecular mechanism and therapeutic potential. *Am J Transl Res* **2**: 65-74.

Wang H, Zhang Q, Wen Q, Zheng Y, Lazarovici P, Philip L, Jiang H, Lin J, Zheng W. 2012a. Proline-rich Akt substrate of 40kDa (PRAS40): a novel downstream target of PI3k/Akt signaling pathway. *Cell Signal* **24**: 17-24.

Wang J, Zhuang J, Iyer S, Lin X, Whitfield TW, Greven MC, Pierce BG, Dong X, Kundaje A, Cheng Y et al. 2012b. Sequence features and chromatin structure around the genomic regions bound by 119 human transcription factors. *Genome Res* **22**: 1798-1812.

Wang J, Zhuang J, Iyer S, Lin XY, Greven MC, Kim BH, Moore J, Pierce BG, Dong X, Virgil D et al. 2013b. Factorbook.org: a Wiki-based database for transcription factor-binding data generated by the ENCODE consortium. *Nucleic Acids Res* **41**: D171-176.

Wang Q, Mora-Jensen H, Weniger MA, Perez-Galan P, Wolford C, Hai T, Ron D, Chen W, Trenkle W, Wiestner A et al. 2009. ERAD inhibitors integrate ER stress with an epigenetic mechanism to activate BH3-only protein NOXA in cancer cells. *Proc Natl Acad Sci U S A* **106**: 2200-2205.

Wang Y, Wysocka J, Sayegh J, Lee YH, Perlin JR, Leonelli L, Sonbuchner LS, McDonald CH, Cook RG, Dou Y et al. 2004. Human PAD4 regulates histone arginine methylation levels via demethylimination. *Science* **306**: 279-283.

Wang YM, Austin RH, Cox EC. 2006. Single molecule measurements of repressor protein 1D diffusion on DNA. *Phys Rev Lett* **97**: 048302.

Watanabe A, Takeda K, Ploplis B, Tachibana M. 1998. Epistatic relationship between Waardenburg syndrome genes MITF and PAX3. *Nat Genet* **18**: 283-286.

Webby CJ, Wolf A, Gromak N, Dreger M, Kramer H, Kessler B, Nielsen ML, Schmitz C, Butler DS, Yates JR et al. 2009. Jmjd6 catalyses lysyl-hydroxylation of U2AF65, a protein associated with RNA splicing. *Science* **325**: 90-93.

Wellbrock C, Rana S, Paterson H, Pickersgill H, Brummelkamp T, Marais R. 2008. Oncogenic BRAF regulates melanoma proliferation through the lineage specific factor MITF. *PLoS One* **3**: e2734.

Wendt KS, Yoshida K, Itoh T, Bando M, Koch B, Schirghuber E, Tsutsumi S, Nagae G, Ishihara K, Mishiro T et al. 2008. Cohesin mediates transcriptional insulation by CCCTC-binding factor. *Nature* **451**: 796-801.

Whiteman HJ, Weeks ME, Dowen SE, Barry S, Timms JF, Lemoine NR, Crnogorac-Jurcevic T. 2007. The role of S100P in the invasion of pancreatic cancer cells is mediated through cytoskeletal changes and regulation of cathepsin D. *Cancer Res* **67**: 8633-8642.

Wickramasinghe VO, Laskey RA. 2015. Control of mammalian gene expression by selective mRNA export. *Nat Rev Mol Cell Biol* **16**: 431-442.

Widlund HR, Horstmann MA, Price ER, Cui J, Lessnick SL, Wu M, He X, Fisher DE. 2002. Beta-catenin-induced melanoma growth requires the downstream target Microphthalmia-associated transcription factor. *J Cell Biol* **158**: 1079-1087.

Widmer DS, Hoek KS, Cheng PF, Eichhoff OM, Biedermann T, Raaijmakers MIG, Hemmi S, Dummer R, Levesque MP. 2013. Hypoxia contributes to melanoma heterogeneity by triggering HIF1α-dependent phenotype switching. *J Invest Dermatol* **133**: 2436-2443.

Wortel IMN, van der Meer LT, Kilberg MS, van Leeuwen FN. 2017. Surviving Stress: Modulation of ATF4-Mediated Stress Responses in Normal and Malignant Cells. *Trends Endocrinol Metab* **28**: 794-806.

Wright R, Basson M, D'Ari L, Rine J. 1988. Increased amounts of HMG-CoA reductase induce "karmellae": a proliferation of stacked membrane pairs surrounding the yeast nucleus. *J Cell Biol* **107**: 101-114.

Wu QW. 2016. Serpine2, a potential novel target for combating melanoma metastasis. *Am J Transl Res* **8**: 1985-1997.

Wysocka J, Swigut T, Xiao H, Milne TA, Kwon SY, Landry J, Kauer M, Tackett AJ, Chait BT, Badenhorst P et al. 2006. A PHD finger of NURF couples histone H3 lysine 4 trimethylation with chromatin remodelling. *Nature* **442**: 86-90.

Xia M, Chen K, Yao X, Xu Y, Yao J, Yan J, Shao Z, Wang G. 2017. Mediator MED23 Links Pigmentation and DNA Repair through the Transcription Factor MITF. *Cell Rep* **20**: 1794-1804.

Xu Y, Poggio M, Jin HY, Shi Z, Forester CM, Wang Y, Stumpf CR, Xue L, Devericks E, So L et al. 2019. Translation control of the immune checkpoint in cancer and its therapeutic targeting. *Nat Med* **25**: 301-311.

Xue Y, Wong J, Moreno GT, Young MK, Côté J, Wang W. 1998. NURD, a novel complex with both ATP-dependent chromatin-remodeling and histone deacetylase activities. *Mol Cell* **2**: 851-861.

Yajima I, Sato S, Kimura T, Yasumoto K, Shibahara S, Goding CR, Yamamoto H. 1999. An L1 element intronic insertion in the black-eyed white (Mitf[mi-bw]) gene: the loss of a single Mitf isoform responsible for the pigmentary defect and inner ear deafness. *Hum Mol Genet* **8**: 1431-1441.

Yang E, van Nimwegen E, Zavolan M, Rajewsky N, Schroeder M, Magnasco M, Darnell JE. 2003. Decay rates of human mRNAs: correlation with functional characteristics and sequence attributes. *Genome Res* **13**: 1863-1872.

Yang G, Li Y, Nishimura EK, Xin H, Zhou A, Guo Y, Dong L, Denning MF, Nickoloff BJ, Cui R. 2008. Inhibition of PAX3 by TGF-beta modulates melanocyte viability. *Mol Cell* **32**: 554-563.

Yang X, Gao X, Zhu Y, Li G, Zhang X, Xiao G, Cao H, Chen X, Yang Q, Lu B. 2013. ATF4 is induced by ROS and regulates Th1 and Th17 cells (P6219). *The Journal of Immunology* **190**: 115.115-115.115.

Ye J, Kumanova M, Hart LS, Sloane K, Zhang H, De Panis DN, Bobrovnikova-Marjon E, Diehl JA, Ron D, Koumenis C. 2010. The GCN2-ATF4 pathway is critical for tumour cell survival and proliferation in response to nutrient deprivation. *EMBO J* **29**: 2082-2096.

Yi YW, Kang HJ, Bae I. 2014. BRCA1 and Oxidative Stress. *Cancers (Basel)* **6**: 771-795.

Yokoyama S, Woods SL, Boyle GM, Aoude LG, MacGregor S, Zismann V, Gartside M, Cust AE, Haq R, Harland M et al. 2011. A novel recurrent mutation in MITF predisposes to familial and sporadic melanoma. *Nature* **480**: 99-103.

Yoshida H, Matsui T, Yamamoto A, Okada T, Mori K. 2001. XBP1 mRNA is induced by ATF6 and spliced by IRE1 in response to ER stress to produce a highly active transcription factor. *Cell* **107**: 881-891.

Yoshizawa T, Hinoi E, Jung DY, Kajimura D, Ferron M, Seo J, Graff JM, Kim JK, Karsenty G. 2009. The transcription factor ATF4 regulates glucose metabolism in mice through its expression in osteoblasts. *J Clin Invest* **119**: 2807-2817.

Young SK, Wek RC. 2016. Upstream Open Reading Frames Differentially Regulate Gene-specific Translation in the Integrated Stress Response. *J Biol Chem* **291**: 16927-16935.

Yuniati L, van der Meer LT, Tijchon E, van Ingen Schenau D, van Emst L, Levers M, Palit SA, Rodenbach C, Poelmans G, Hoogerbrugge PM et al. 2016. Tumor suppressor BTG1 promotes PRMT1-mediated ATF4 function in response to cellular stress. *Oncotarget* **7**: 3128-3143.

Zakut R, Perlis R, Eliyahu S, Yarden Y, Givol D, Lyman SD, Halaban R. 1993. KIT ligand (mast cell growth factor) inhibits the growth of KIT-expressing melanoma cells. *Oncogene* **8**: 2221-2229.

Zandi R, Larsen AB, Andersen P, Stockhausen MT, Poulsen HS. 2007. Mechanisms for oncogenic activation of the epidermal growth factor receptor. *Cell Signal* **19**: 2013-2023.

Zaret KS, Carroll JS. 2011. Pioneer transcription factors: establishing competence for gene expression. *Genes Dev* **25**: 2227-2241.

Zeng H, Jorapur A, Shain AH, Lang UE, Torres R, Zhang Y, McNeal AS, Botton T, Lin J, Donne M et al. 2018. Bi-allelic Loss of CDKN2A Initiates Melanoma Invasion via BRN2 Activation. *Cancer Cell* **34**: 56-68.e59.

Zeng W, Kong Q, Li C, Mao B. 2010. Xenopus RCOR2 (REST corepressor 2) interacts with ZMYND8, which is involved in neural differentiation. *Biochem Biophys Res Commun* **394**: 1024-1029.

Zhan Q. 2005. Gadd45a, a p53- and BRCA1-regulated stress protein, in cellular response to DNA damage. *Mutat Res* **569**: 133-143.

Zhang C, Bai N, Chang A, Zhang Z, Yin J, Shen W, Tian Y, Xiang R, Liu C. 2013a. ATF4 is directly recruited by TLR4 signaling and positively regulates TLR4-trigged cytokine production in human monocytes. *Cell Mol Immunol* **10**: 84-94.

Zhang J, Jackson AF, Naito T, Dose M, Seavitt J, Liu F, Heller EJ, Kashiwagi M, Yoshida T, Gounari F et al. 2011. Harnessing of the nucleosome-remodeling-deacetylase complex controls lymphocyte development and prevents leukemogenesis. *Nat Immunol* **13**: 86-94.

Zhang L, Liang D, Chen C, Wang Y, Amu G, Yang J, Yu L, Dmochowski IJ, Tang X. 2018. Circular siRNAs for Reducing Off-Target Effects and Enhancing Long-Term Gene Silencing in Cells and Mice. *Mol Ther Nucleic Acids* **10**: 237-244.

Zhang Q, Yu J, Liu B, Lv Z, Xia T, Xiao F, Chen S, Guo F. 2013b. Central activating transcription factor 4 (ATF4) regulates hepatic insulin resistance in mice via S6K1 signaling and the vagus nerve. *Diabetes* **62**: 2230-2239.

Zhang Y, Liu T, Meyer CA, Eeckhoute J, Johnson DS, Bernstein BE, Nussbaum C, Myers RM, Brown M, Li W et al. 2008. Model-based Analysis of ChIP-Seq (MACS). *Genome Biol* **9**.

Zhang Y, Moqtaderi Z, Rattner BP, Euskirchen G, Snyder M, Kadonaga JT, Liu XS, Struhl K. 2010. Evidence against a genomic code for nucleosome positioning. Reply to "Nucleosome sequence preferences influence in vivo nucleosome organization.". *Nat Struct Mol Biol* **17**: 920-923.

Zhao X, Fiske B, Kawakami A, Li J, Fisher DE. 2011a. Regulation of MITF stability by the USP13 deubiquitinase. *Nat Commun* **2**: 414.

Zhao Y, Xiong X, Sun Y. 2011b. DEPTOR, an mTOR inhibitor, is a physiological substrate of SCF(βTrCP) E3 ubiquitin ligase and regulates survival and autophagy. *Mol Cell* **44**: 304-316.

Zhu H, Chen X, Chen B, Song W, Sun D, Zhao Y. 2014. Activating transcription factor 4 promotes esophageal squamous cell carcinoma invasion and metastasis in mice and is associated with poor prognosis in human patients. *PLoS One* **9**: e103882.

Zhu H, Xia L, Zhang Y, Wang H, Xu W, Hu H, Wang J, Xin J, Gang Y, Sha S et al. 2012. Activating transcription factor 4 confers a multidrug resistance phenotype to gastric cancer cells through transactivation of SIRT1 expression. *PLoS One* **7**: e31431.

Zhu X, Zhang Y, Bjornsdottir G, Liu Z, Quan A, Costanzo M, Dávila López M, Westholm JO, Ronne H, Boone C et al. 2011. Histone modifications influence mediator interactions with chromatin. *Nucleic Acids Res* **39**: 8342-8354.

Zuleger N, Robson MI, Schirmer EC. 2011. The nuclear envelope as a chromatin organizer. *Nucleus* **2**: 339-349.

Zuo L, Weger J, Yang Q, Goldstein AM, Tucker MA, Walker GJ, Hayward N, Dracopoli NC. 1996. Germline mutations in the p16INK4a binding domain of CDK4 in familial melanoma. *Nat Genet* **12**: 97-99.

# Appendix A – Supplementary Figures

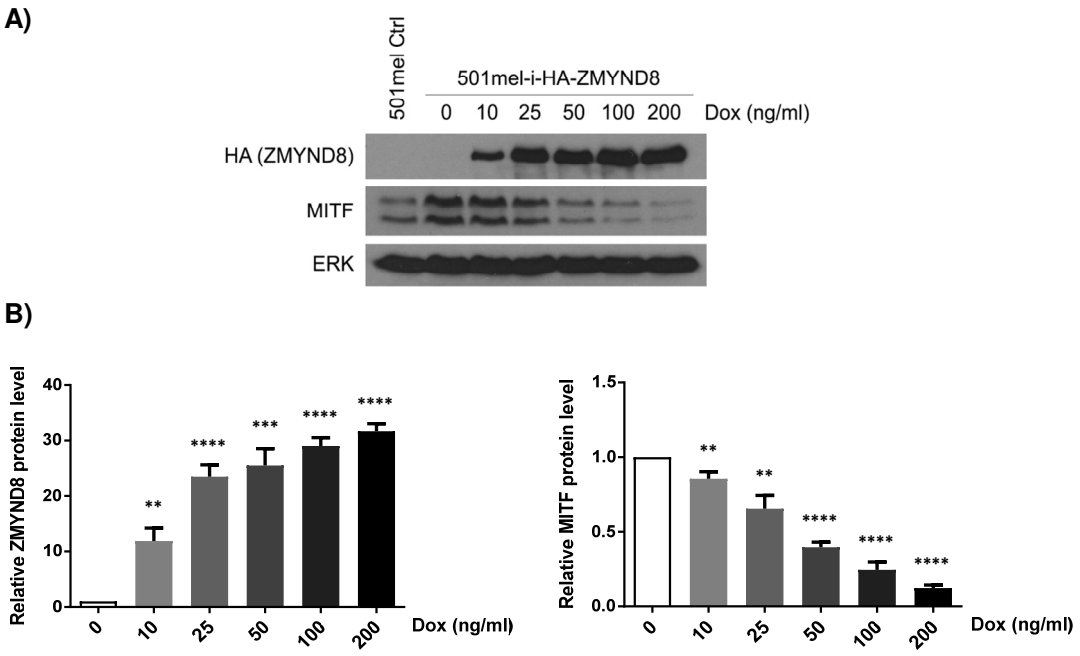


**Supplementary Figure A.1- ZMYND8 overexpression leads to repression of MITF in 501mel cells. (A)** Western blot analysis of whole cell protein extracts from 501mel control and 501mel-i-HA-ZMYND8 (m) cells induced with 0, 10, 25, 50, 100 and 200 ng/ml doxycycline for 72 h. (Antibodies: α-HA, α-MITF and α-ERK). ERK was used as a loading control. **(B)** Quantification of ZMYND8 and MITF levels detected in doxycycline-induced 501mel-i-HA-ZMYND8 cells in the western blot analysis shown in (A). (**** $P \leq 0.0001$, *** $P \leq 0.001$, ** $P \leq 0.01$, n=3, data represent mean ± SEM).

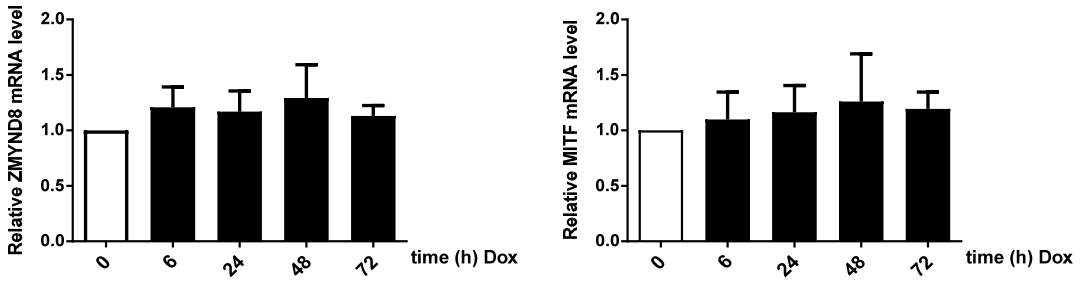


**Supplementary Figure A.2.- Doxycycline treatment does not affect ZMYND8 and MITF mRNA levels in 501mel cells.** qRT-PCR analysis results for ZMYND8 and MITF mRNA levels in 501mel cells following treatment with 100 ng/ml doxycycline for 0, 6, 12, 24, 48 and 72 h. (No statistically significant differences detected ($P > 0.05$), n=3, data represent mean ± SEM).

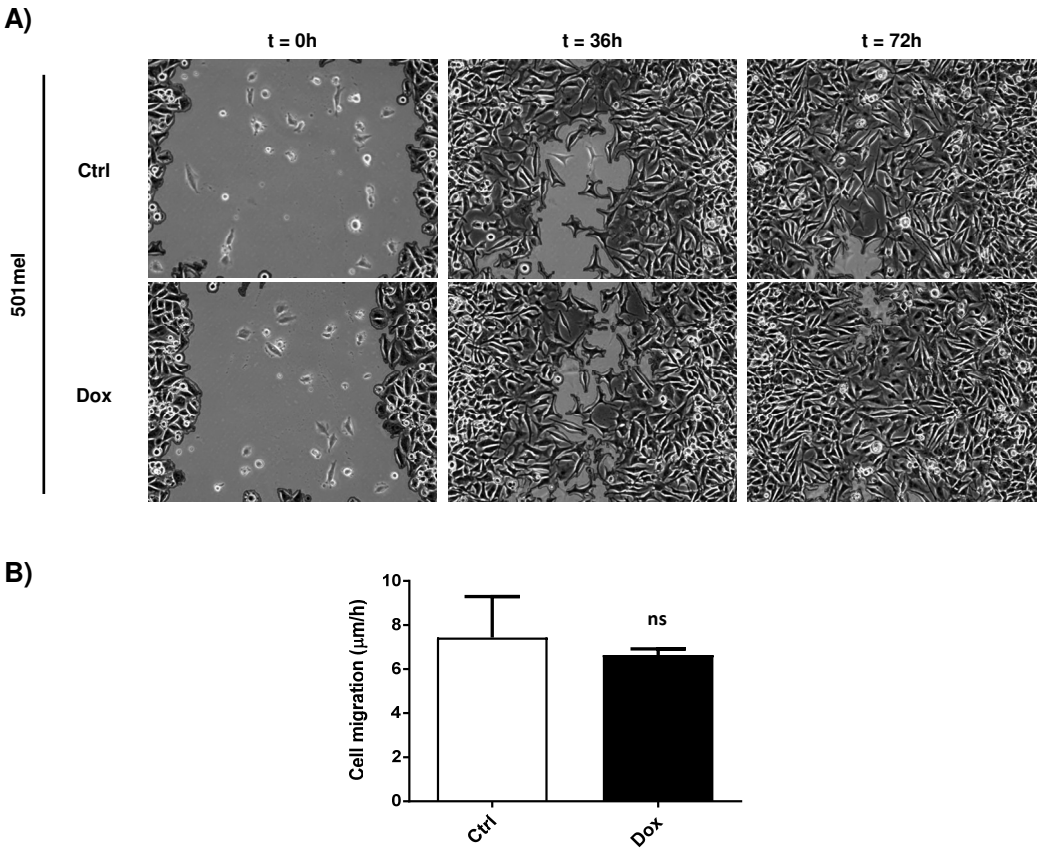


**Supplementary Figure A.3.- Doxycycline treatment does not change cell migration in 501mel cells. (A)** Brightfield microscopy images showing the 0, 36 and 72 h time points of a scratch-wound healing assay performed in 501mel control cells and 501mel cells treated with 100 ng/ml doxycycline. **(B)** Quantification of cell migration corresponding to the experiment showed in (A). (ns $P > 0.05$, n=3, data represent mean ± SEM).

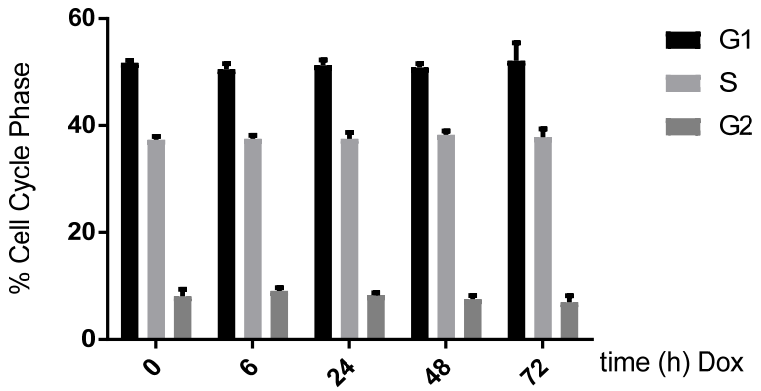


**Supplementary Figure A.4.- Doxycycline treatment does not change the cell cycle profile of 501mel cells.** Cell cycle profiles of 501mel control cells and 501mel cells treated with 100 ng/ml doxycycline for 0, 6, 24, 48 and 72 h. (No statistically significant differences detected ($P > 0.05$), n=3, data represent mean ± SEM).

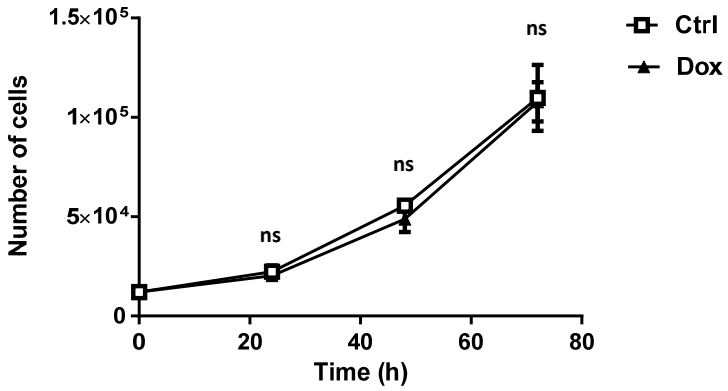


**Supplementary Figure A.5.- Doxycycline treatment does not change proliferation rates in 501mel cells.** Proliferation curves for 501mel control cells and 501mel cells treated with 100 ng/ml doxycycline. (ns $P > 0.05$, n=3, data represent mean ± SEM).

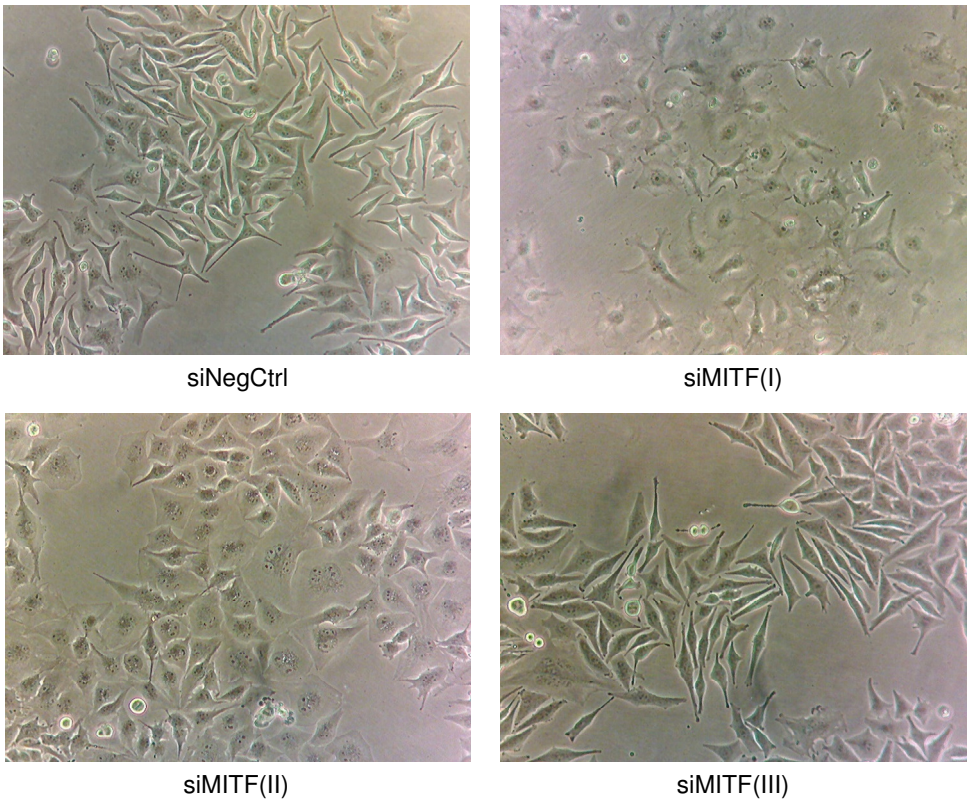


**Supplementary Figure A.6.- MITF knock down using different siRNAs against MITF leads to distinct cell morphologies.** Brightfield microscopy images of SKmel30 cells 72 h after transfection with siMITF(I), siMITF(II), siMITF(III) or siRNA negative control.

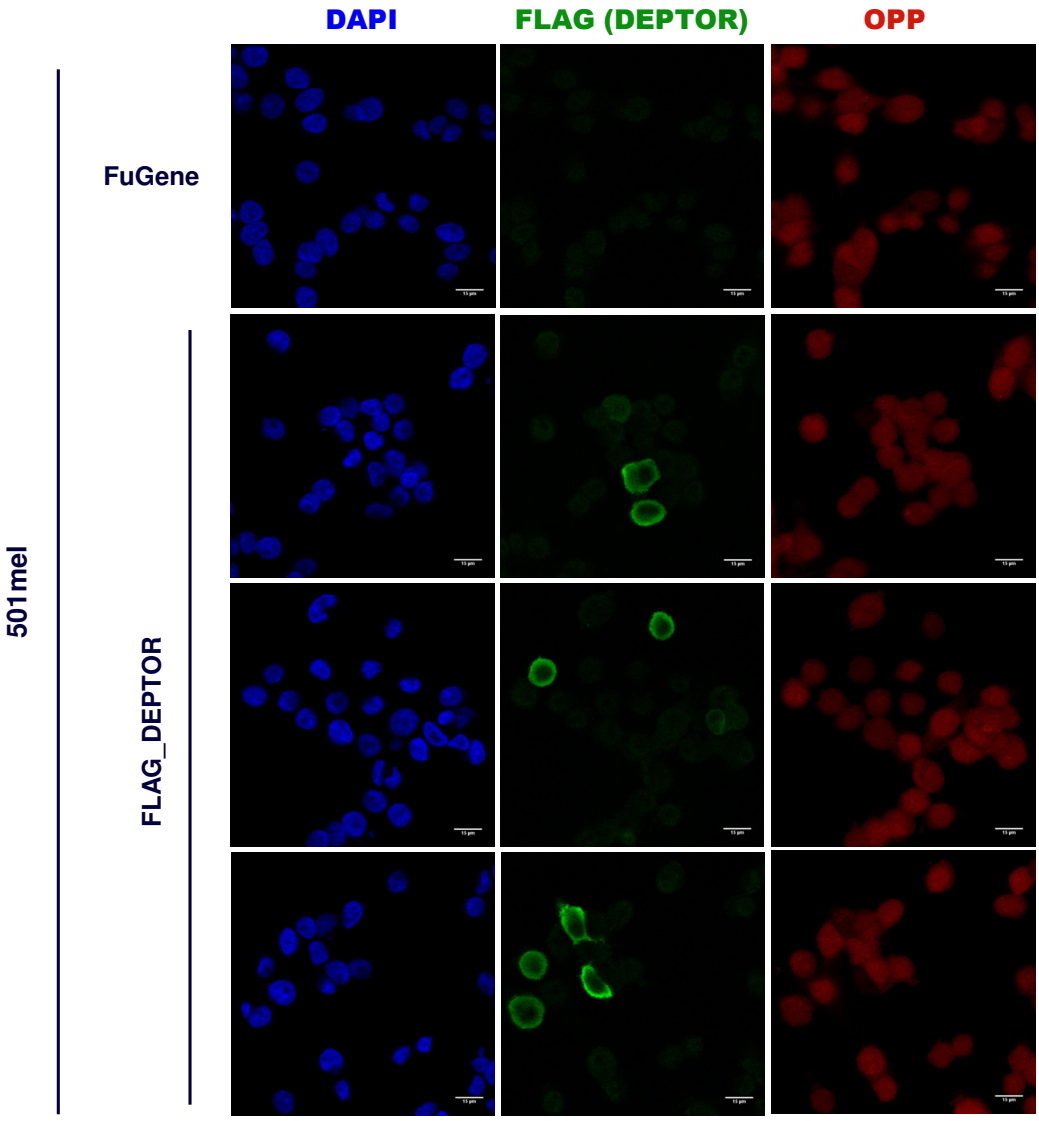


**Supplementary Figure A.7.- OPP incorporation (indicative of protein synthesis) does not change upon DEPTOR overexpression in 501mel cells.** Immunofluorescence analysis of DEPTOR and fluorescently labelled O-propargyl-puromycin in 501mel cells 48 h after transfection with a mammalian expression vector encoding FLAG-tagged DEPTOR or an empty vector (Fugene control). (Antibody: α-FLAG). Scale bars: 15 μm.

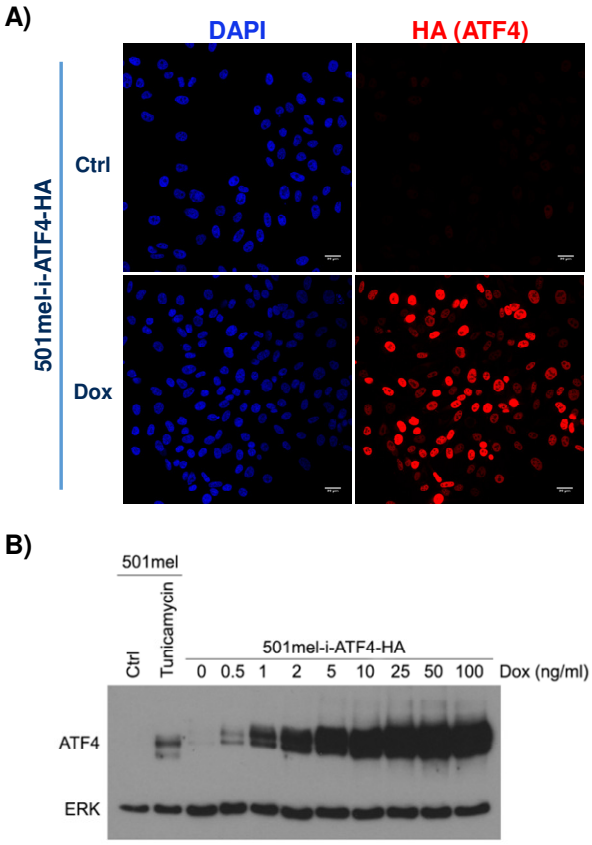


**Supplementary Figure A.8.- Expression of ATF4 following induction with doxycycline in 501mel-i-ATF4-HA cells. (A)** Immunofluorescence analysis of ATF4 levels in 501mel-i-ATF4-HA cells after 24 h induction with 20 ng/ml doxycycline. (Antibody: α-HA). Scale bars: 30 µm. **(B)** Western blot analysis of whole cell protein extracts from 501mel control and 501mel-i-ATF4-HA cells induced with 0, 0.5, 1, 2, 5, 10, 25, 50 and 100 ng/ml doxycycline for 4 h. (Antibodies: α-HA and α-ERK). ERK was used as a loading control.

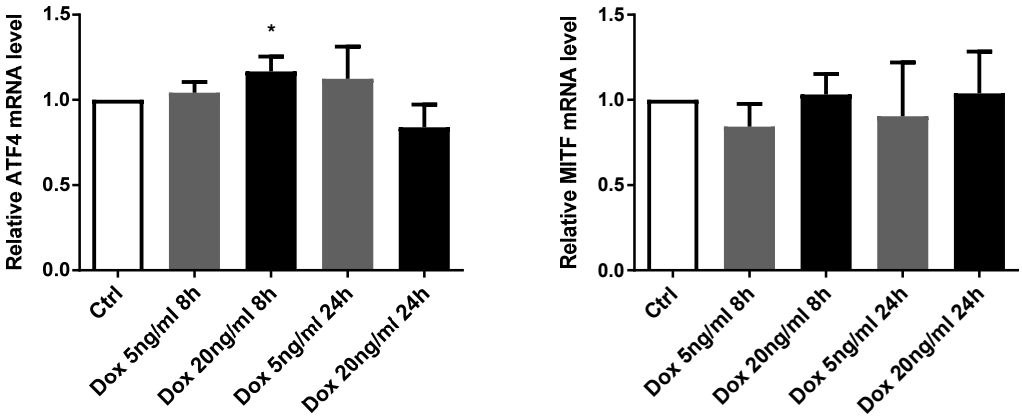


**Supplementary Figure A.9.- Doxycycline treatment does generally not affect ATF4 and MITF mRNA levels in 501mel cells.** qRT-PCR analysis results for ATF4 and MITF mRNA levels in 501mel cells following treatment with 5 or 20 ng/ml doxycycline for 0, 8 and 24 h. (* $P \leq 0.05$, no statistically significant differences detected for all remaining cases ($P > 0.05$), n=3, data represent mean ± SEM).

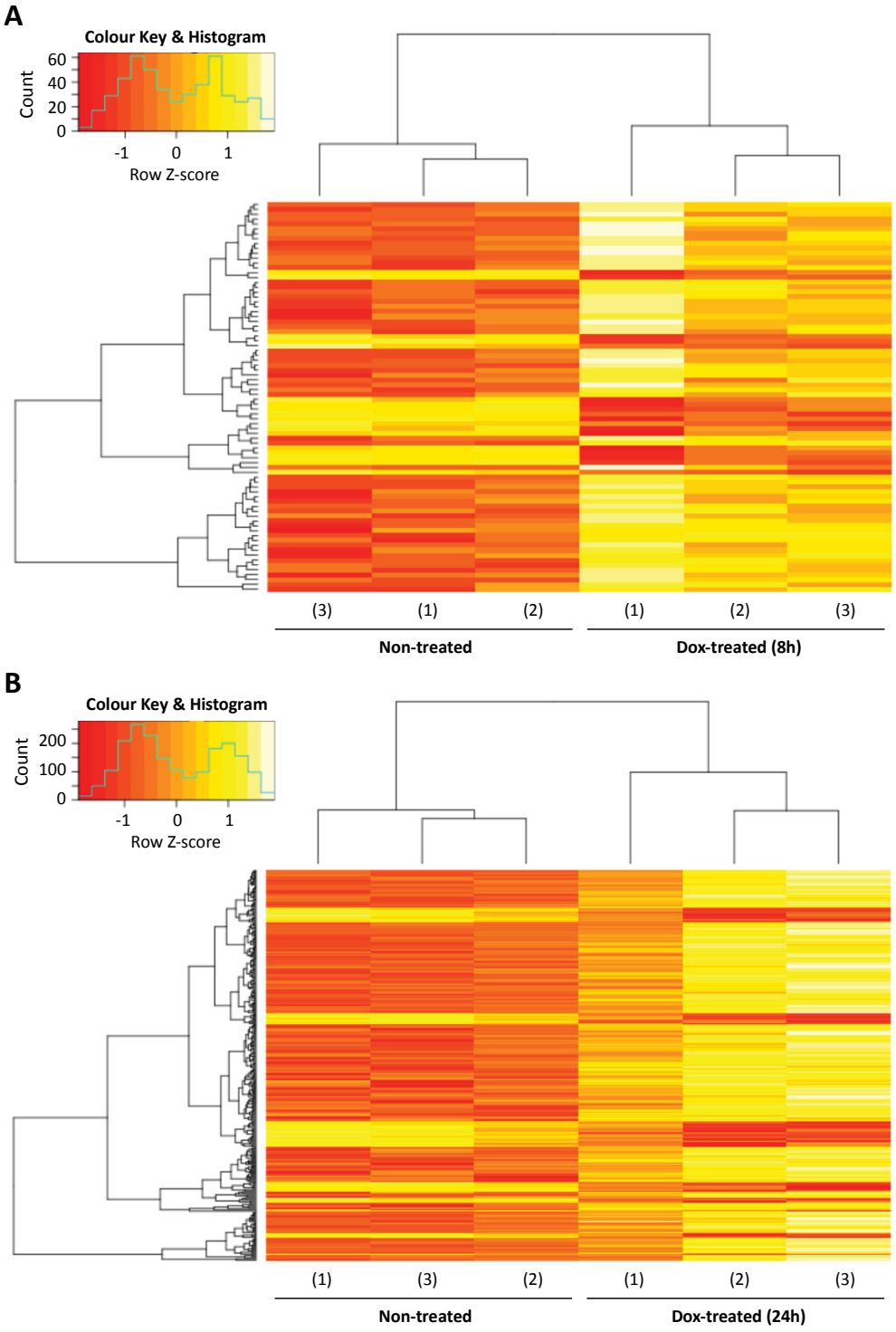


**Supplementary Figure A.10.- Heatmaps showing differential gene expression following doxycycline treatment in 501mel cells. (A)** Heatmap representing colour-coded expression levels of differentially expressed genes (FDR < 0.05) following 8 h treatment with 20 ng/ml doxycycline in 501mel cells. In total, 80 genes were found to be differentially expressed (FDR < 0.05), from which 4 showed a fold change ≥ 2. **(B)** Heatmap representing colour-coded expression levels of differentially expressed genes (FDR < 0.05) following 24 h treatment with 20 ng/ml doxycycline in 501mel cells. In total, 327 genes were found to be differentially expressed (FDR < 0.05), from which 99 showed a fold change ≥ 2.

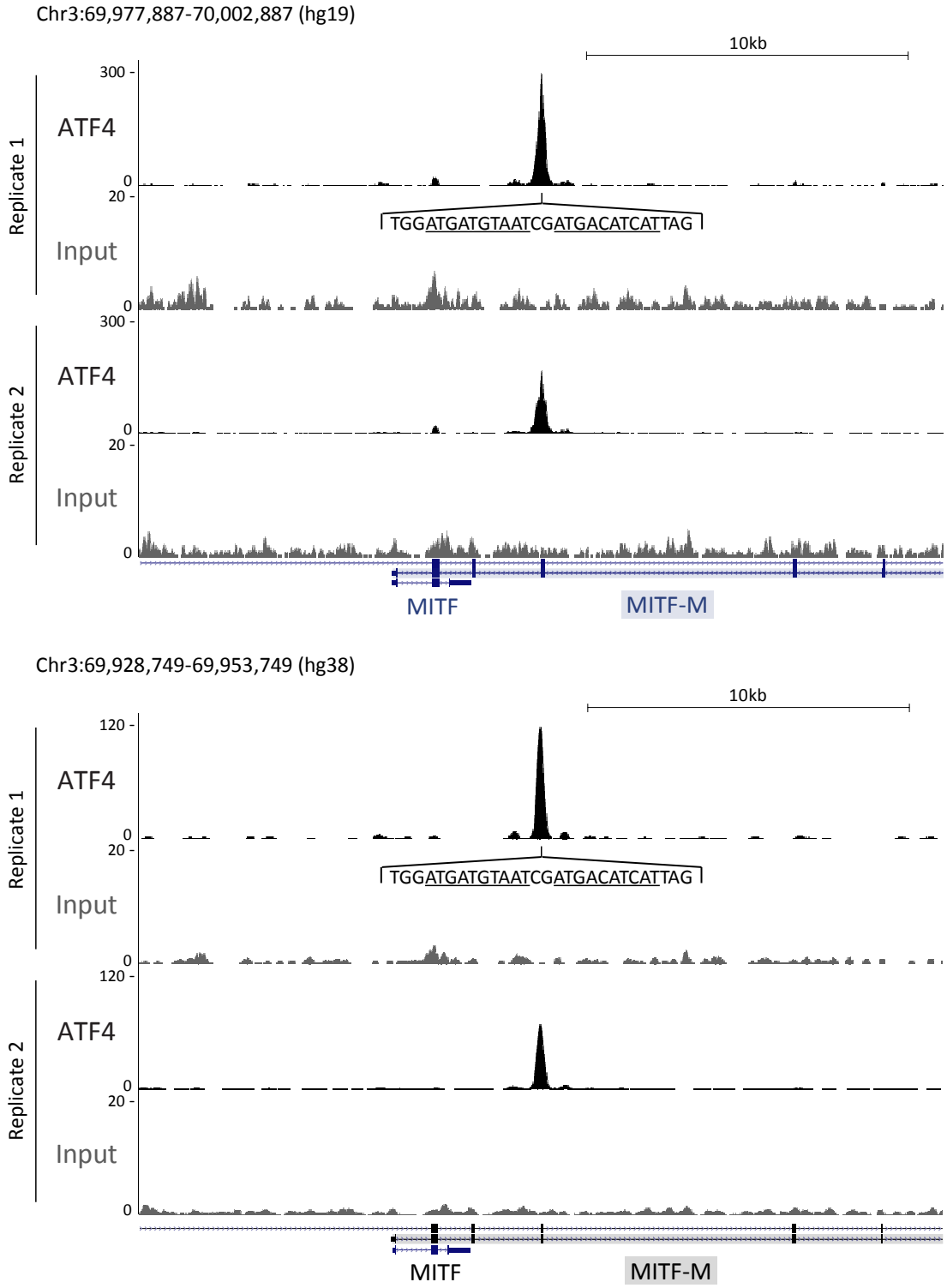


**Supplementary Figure A.11.- Confirmation of ATF4 binding to *MITF* exon 4 upon glucose starvation in 501mel cells.** ATF4 major ChIP-seq peak associated to *MITF* following 4 h glucose starvation in 501mel cells resulting from the analysis of the ATF4 ChIP-seq experiment raw data performed by the thesis author (**above**) and by a bioinformatician (**below**). The ATF4 binding motifs found in the sequence underlying the peak are represented under the peak corresponding to the first replicate of the experiment.

# Appendix B – Supplementary Tables

| | Gene Name | Fold Change | *P* value |
|---|---|---|---|
| 1 | GPR155 | 39.4 | 2.97E-24 |
| 2 | ZMIZ1-AS1 | 33.9 | 4.24E-04 |
| 3 | SLITRK6 | 30.3 | 1.21E-05 |
| 4 | SAMD5 | 26.7 | 2.27E-13 |
| 5 | NOMO2 | 25.6 | 5.05E-03 |
| 6 | OMG | 23.9 | 2.19E-05 |
| 7 | LOC101929427 | 20.8 | 1.99E-05 |
| 8 | PDE4C | 20.2 | 2.09E-02 |
| 9 | SPHK1 | 20.2 | 8.02E-03 |
| 10 | LSMEM1 | 17.5 | 1.14E-02 |
| 11 | C1orf220 | 17.4 | 1.66E-02 |
| 12 | SCART1 | 17.4 | 1.97E-02 |
| 13 | RAB3B | 16.5 | 3.18E-14 |
| 14 | HAO2 | 14.9 | 2.49E-04 |
| 15 | KCNJ13 | 14.8 | 6.79E-10 |
| 16 | SH2D1A | 14.7 | 2.36E-02 |
| 17 | FREM1 | 14.6 | 1.52E-02 |
| 18 | KCNA2 | 14.6 | 1.23E-02 |
| 19 | EPHB1 | 14.2 | 6.48E-04 |
| 20 | ANGPTL7 | 13.9 | 1.23E-04 |
| 21 | PCAT7 | 13.2 | 1.20E-04 |
| 22 | DNAJC6 | 13.1 | 3.20E-08 |
| 23 | AMOTL2 | 12.5 | 2.14E-16 |
| 24 | B3GALT2 | 12.5 | 1.90E-03 |
| 25 | CTNNA2 | 12.4 | 7.86E-19 |
| 26 | LOC728392 | 12.2 | 2.49E-04 |
| 27 | DGKA | 11.8 | 2.65E-03 |
| 28 | NOV | 10.4 | 1.74E-12 |
| 29 | AZGP1 | 10.4 | 7.98E-10 |
| 30 | TMEM59L | 10.3 | 4.61E-04 |
| 31 | SCN1A | 10.1 | 5.10E-04 |
| 32 | CCDC176 | 9.64 | 7.06E-05 |
| 33 | ABAT | 9.57 | 2.05E-06 |
| 34 | ATP1B2 | 9.38 | 3.74E-09 |
| 35 | CRYM | 9.37 | 2.30E-08 |
| 36 | LINC00327 | 8.86 | 4.05E-04 |
| 37 | MXD4 | 8.41 | 2.67E-16 |
| 38 | PTX3 | 8.38 | 3.13E-07 |
| 39 | SORBS2 | 8.33 | 5.98E-19 |
| 40 | PPFIA2 | 8.32 | 2.59E-03 |
| 41 | CD24 | 8.30 | 3.63E-03 |
| 42 | BAIAP3 | 7.87 | 3.01E-03 |
| 43 | SRGAP3 | 7.87 | 2.94E-03 |
| 44 | MAL2 | 7.75 | 2.16E-08 |
| 45 | SLITRK2 | 7.73 | 7.23E-08 |
| 46 | PTCH1 | 7.67 | 1.28E-07 |
| 47 | DENND6B | 7.65 | 1.51E-02 |
| 48 | GBGT1 | 7.63 | 1.30E-02 |
| 49 | VPS37D | 7.22 | 4.04E-04 |
| 50 | FGF7 | 7.21 | 4.10E-04 |
| 51 | DEPTOR | 7.11 | 3.23E-10 |
| 52 | SOSTDC1 | 7.04 | 2.50E-08 |
| 53 | TMEM74B | 6.93 | 1.63E-04 |
| 54 | MYO1F | 6.93 | 1.87E-03 |
| 55 | UNC80 | 6.78 | 2.11E-06 |
| 56 | BMF | 6.74 | 6.90E-10 |
| 57 | PCDH17 | 6.59 | 1.54E-05 |
| 58 | ENPP2 | 6.53 | 2.88E-09 |
| 59 | FAM198B | 6.50 | 1.67E-22 |
| 60 | ARRDC3 | 6.37 | 2.97E-15 |
| 61 | MATN2 | 6.33 | 1.85E-02 |
| 62 | FREM2 | 6.25 | 5.70E-04 |
| 63 | MLIP | 6.19 | 3.30E-08 |
| 64 | NPAS3 | 6.16 | 5.45E-09 |
| 65 | AIF1L | 6.11 | 2.90E-03 |
| 66 | COL25A1 | 6.08 | 5.07E-05 |
| 67 | DACT1 | 6.00 | 4.84E-08 |
| 68 | LSAMP | 6.00 | 4.18E-19 |
| 69 | FLRT3 | 5.99 | 1.98E-06 |
| 70 | IFI44L | 5.92 | 3.06E-03 |
| 71 | COL9A1 | 5.90 | 2.84E-11 |
| 72 | BCAS1 | 5.88 | 3.66E-04 |
| 73 | RFTN2 | 5.86 | 3.67E-05 |
| 74 | LIMCH1 | 5.73 | 8.05E-21 |
| 75 | CDH19 | 5.65 | 2.10E-18 |
| 76 | SEPP1 | 5.58 | 1.66E-04 |
| 77 | ZNF365 | 5.53 | 2.68E-03 |
| 78 | DGAT2 | 5.48 | 1.14E-02 |
| 79 | RBMS3 | 5.43 | 6.15E-14 |
| 80 | CEBPD | 5.43 | 4.86E-15 |
| 81 | SNTB1 | 5.42 | 4.82E-13 |
| 82 | LOC653513 | 5.42 | 2.77E-03 |
| 83 | HOXB3 | 5.41 | 1.11E-02 |
| 84 | MACROD2 | 5.39 | 2.07E-13 |
| 85 | FAT4 | 5.37 | 1.28E-04 |
| 86 | C1orf53 | 5.33 | 3.38E-03 |
| 87 | ID2 | 5.33 | 1.64E-13 |
| 88 | WDR78 | 5.32 | 2.31E-03 |
| 89 | ABCA9 | 5.31 | 1.14E-04 |
| 90 | CYR61 | 5.27 | 5.60E-19 |
| 91 | KCNMA1 | 5.22 | 3.27E-03 |
| 92 | SLC16A9 | 5.18 | 8.04E-03 |
| 93 | TLE4 | 5.15 | 8.55E-08 |
| 94 | TRIM48 | 5.09 | 1.03E-10 |
| 95 | LRIG1 | 5.03 | 1.26E-11 |
| 96 | JPX | 5.00 | 1.07E-03 |
| 97 | TCP11L2 | 4.99 | 1.75E-03 |
| 98 | CDHR3 | 4.99 | 7.32E-05 |
| 99 | RARB | 4.98 | 2.03E-05 |
| 100 | LURAP1L | 4.95 | 9.98E-07 |

(Table continues in following page)

| | Gene Name | Fold Change | *P* value |
|---|---|---|---|
| 101 | FOXP2 | 4.90 | 5.19E-05 |
| 102 | SYNPR | 4.86 | 2.02E-02 |
| 103 | PLD2 | 4.85 | 2.02E-03 |
| 104 | CTGF | 4.81 | 7.89E-16 |
| 105 | BTD | 4.78 | 8.82E-08 |
| 106 | AHNAK | 4.73 | 3.27E-12 |
| 107 | YPEL2 | 4.72 | 1.90E-14 |
| 108 | BFSP1 | 4.71 | 7.67E-07 |
| 109 | SYNPO2 | 4.68 | 3.31E-09 |
| 110 | LRRC27 | 4.65 | 3.61E-04 |
| 111 | STK32A | 4.63 | 1.14E-16 |
| 112 | TMEM2 | 4.57 | 1.06E-21 |
| 113 | CERS4 | 4.55 | 2.03E-03 |
| 114 | LINC00462 | 4.55 | 4.89E-03 |
| 115 | PNRC1 | 4.53 | 1.78E-17 |
| 116 | APOD | 4.53 | 2.68E-09 |
| 117 | S100B | 4.53 | 1.81E-17 |
| 118 | VASN | 4.50 | 1.62E-05 |
| 119 | LRFN5 | 4.48 | 8.10E-10 |
| 120 | C6orf165 | 4.47 | 4.66E-04 |
| 121 | MPZ | 4.45 | 4.41E-07 |
| 122 | PTEN | 4.43 | 7.07E-16 |
| 123 | KIF26B | 4.33 | 9.54E-04 |
| 124 | NAV3 | 4.32 | 3.38E-12 |
| 125 | UGT8 | 4.31 | 1.85E-02 |

**Supplementary Table B.1.- Top 125 MITF-bound upregulated genes following MITF silencing in 501mel cells.** Fold changes and associated *P* values for the 125 most upregulated MITF-bound genes (see Supplementary Tables S.2.A and B for MITF ChIP-seq data) following 48 h MITF silencing (using siMITF(I)) in 501mel cells relative to siRNA negative control-transfected 501mel cells. Data obtained from RNA-seq experiment performed in biological triplicate. Genes of interest for the presented study are highlighted in blue.

| | | 8h Induction Ectopic ATF4 | | 24h Induction Ectopic ATF4 | | 8h Glucose Starvation | | 24h Glucose Starvation | |
|---|---|---|---|---|---|---|---|---|---|
| | Gene Name | Fold Change | *P* value | Fold Change | *P* value | Fold Change | *P* value | Fold Change | *P* value |
| 1 | ABHD5 | | | 2.80 | 1.62E-05 | 0.46 | 4.08E-05 | | |
| 2 | ABL2 | | | 2.11 | 7.08E-11 | 2.18 | 3.16E-10 | | |
| 3 | ADAM12 | | | 0.26 | 1.59E-03 | 2.71 | 3.92E-03 | | |
| 4 | AHNAK | | | 3.84 | 8.36E-16 | 4.51 | 8.22E-13 | 3.16 | 1.05E-08 |
| 5 | AHSA2 | | | 2.58 | 2.11E-06 | | | 2.42 | 8.15E-07 |
| 6 | AJUBA | 4.70 | 2.58E-18 | 4.63 | 2.55E-18 | 2.59 | 1.90E-09 | | |
| 7 | AKNA | 8.14 | 3.37E-24 | 7.25 | 2.37E-25 | 28.88 | 1.33E-66 | 7.05 | 4.14E-20 |
| 8 | ANKRD1 | 0.36 | 4.00E-03 | | | 46.43 | 1.22E-52 | | |
| 9 | ANXA1 | 3.44 | 2.52E-06 | 4.94 | 1.03E-15 | 3.22 | 1.04E-04 | 2.43 | 4.00E-04 |
| 10 | ARHGEF2 | | | 2.20 | 1.15E-07 | 2.68 | 2.82E-13 | | |
| 11 | ARHGEF3 | 3.05 | 2.36E-03 | 2.58 | 1.82E-03 | 2.97 | 8.88E-06 | | |
| 12 | ARMC9 | | | 2.58 | 2.70E-12 | 3.90 | 1.48E-12 | 2.52 | 1.68E-17 |
| 13 | ARNTL | | | 4.07 | 4.49E-10 | | | 0.29 | 1.26E-08 |
| 14 | ASNS | 4.08 | 1.41E-17 | 6.49 | 1.86E-43 | 12.50 | 5.04E-82 | 6.48 | 4.91E-109 |
| 15 | ATF3 | 8.10 | 1.31E-26 | 9.50 | 8.93E-34 | 4.25 | 1.27E-07 | 4.37 | 2.16E-09 |
| 16 | ATF4 | | | 2.01 | 4.16E-10 | 2.92 | 4.73E-21 | | |
| 17 | ATP1A1 | | | 0.47 | 2.77E-05 | 2.26 | 3.90E-05 | | |
| 18 | BBC3 | | | 2.01 | 8.17E-08 | 5.16 | 3.62E-25 | 2.23 | 9.46E-13 |
| 19 | CARS | | | 2.06 | 1.26E-08 | 2.66 | 1.67E-19 | | |
| 20 | CBS | | | 2.92 | 2.12E-18 | 2.28 | 2.31E-11 | | |
| 21 | CBX7 | 2.50 | 7.18E-04 | 4.26 | 6.95E-11 | 2.73 | 2.24E-04 | 2.30 | 2.26E-03 |
| 22 | CCL18 | 9.58 | 3.79E-12 | 13.3 | 1.59E-26 | | | 2.97 | 3.99E-05 |
| 23 | CCNE2 | | | 0.32 | 1.28E-05 | 0.42 | 2.68E-03 | | |
| 24 | CCPG1 | 3.36 | 1.04E-07 | 5.98 | 1.08E-25 | 2.98 | 5.00E-06 | | |
| 25 | CD22 | | | 0.36 | 2.24E-03 | 3.02 | 3.32E-05 | | |
| 26 | CDH19 | 2.94 | 4.47E-14 | 2.96 | 2.48E-11 | 2.26 | 8.23E-07 | | |
| 27 | CEACAM1 | | | 0.37 | 2.53E-09 | 0.40 | 1.17E-10 | 0.35 | 3.61E-32 |
| 28 | CEBPG | 2.29 | 4.66E-05 | | | 2.59 | 1.64E-10 | | |
| 29 | CECR6 | | | 8.95 | 1.96E-13 | 2.93 | 2.78E-03 | | |
| 30 | CEP170 | 2.21 | 1.77E-03 | 3.07 | 5.07E-09 | 0.47 | 4.66E-05 | | |
| 31 | CHAC1 | 12.9 | 2.21E-15 | 23.2 | 1.15E-47 | 5.12 | 2.49E-19 | 7.84 | 3.93E-73 |
| 32 | CHST9 | 0.42 | 6.01E-04 | 0.20 | 5.37E-08 | 0.42 | 2.87E-04 | | |
| 33 | CLIC4 | 2.33 | 2.34E-08 | 2.39 | 1.54E-08 | 3.16 | 5.36E-22 | 2.04 | 2.32E-17 |
| 34 | CNPY1 | 2.74 | 1.38E-07 | 2.76 | 3.14E-08 | 2.87 | 9.84E-08 | | |
| 35 | CNTRL | | | 0.49 | 8.35E-04 | 2.04 | 1.54E-03 | | |
| 36 | COL12A1 | | | 0.21 | 5.85E-03 | 3.63 | 6.52E-03 | | |
| 37 | COL9A1 | | | 0.45 | 3.20E-03 | | | 0.45 | 4.39E-03 |
| 38 | CPOX | | | 0.48 | 9.52E-08 | 0.46 | 1.46E-08 | | |
| 39 | CPS1 | 3.50 | 1.57E-04 | | | | | 2.19 | 5.13E-03 |
| 40 | CREB5 | 5.95 | 1.13E-22 | 5.92 | 1.09E-19 | 4.55 | 6.49E-16 | | |
| 41 | CRIM1 | | | 2.41 | 9.36E-05 | 13.82 | 8.22E-13 | 8.92 | 5.18E-08 |
| 42 | CSAD | | | 4.53 | 5.57E-05 | | | 3.15 | 9.01E-03 |
| 43 | CSTA | 51.4 | 7.47E-29 | 398.1 | 2.89E-114 | 10.06 | 5.19E-05 | 9.87 | 1.93E-05 |
| 44 | CTGF | 2.34 | 1.90E-07 | 3.96 | 6.18E-20 | 5.46 | 1.54E-29 | 2.01 | 1.32E-09 |
| 45 | CTH | 14.0 | 9.03E-32 | 16.03 | 7.74E-56 | 6.63 | 1.00E-33 | 2.78 | 3.44E-21 |
| 46 | CTLA4 | | | 0.38 | 2.37E-07 | 0.21 | 4.30E-14 | 0.26 | 2.51E-18 |
| 47 | CXXC1 | | | 3.71 | 4.14E-09 | 0.34 | 4.08E-06 | | |

(Table continues in following page)

| | | 8h Induction Ectopic ATF4 | | 24h Induction Ectopic ATF4 | | 8h Glucose Starvation | | 24h Glucose Starvation | |
|---|---|---|---|---|---|---|---|---|---|
| | Gene Name | Fold Change | *P* value | Fold Change | *P* value | Fold Change | *P* value | Fold Change | *P* value |
| 48 | CYP1A1 | | | 4.23 | 4.18E-20 | 3.58 | 1.50E-10 | | |
| 49 | DCPS | | | 0.39 | 1.31E-06 | 2.15 | 1.58E-05 | | |
| 50 | DDIT3 | 2.80 | 4.62E-06 | 3.54 | 3.73E-14 | 5.44 | 1.02E-17 | 4.01 | 1.48E-34 |
| 51 | DDIT4 | 4.64 | 6.44E-09 | 6.10 | 5.29E-25 | 7.21 | 1.37E-21 | 3.80 | 1.04E-28 |
| 52 | DDR2 | 4.01 | 8.75E-06 | 10.1 | 7.24E-17 | 16.82 | 1.14E-08 | | |
| 53 | DFNA5 | | | 2.87 | 1.19E-07 | | | 2.28 | 9.08E-07 |
| 54 | DKK1 | | | 0.28 | 8.82E-03 | | | 3.12 | 7.91E-03 |
| 55 | DNA2 | | | 0.46 | 7.69E-03 | 0.40 | 6.23E-05 | | |
| 56 | DOCK6 | | | 2.70 | 4.30E-07 | | | 2.30 | 2.16E-05 |
| 57 | DOK6 | | | 10.1 | 3.53E-10 | | | 7.29 | 3.16E-03 |
| 58 | DSCR4 | | | 2.60 | 2.82E-03 | 0.30 | 1.05E-02 | | |
| 59 | DUSP7 | | | 0.47 | 1.39E-04 | 0.43 | 2.13E-07 | | |
| 60 | E2F7 | | | 0.34 | 1.83E-03 | 0.43 | 7.76E-04 | | |
| 61 | EGR1 | 7.79 | 1.50E-28 | 7.16 | 1.84E-40 | 2.68 | 9.75E-09 | | |
| 62 | ESCO2 | | | 0.40 | 2.40E-05 | 0.43 | 2.05E-05 | | |
| 63 | EVA1A | 0.32 | 2.54E-03 | | | | | 0.32 | 9.14E-03 |
| 64 | EVA1C | | | 2.81 | 7.56E-04 | 3.50 | 4.35E-04 | | |
| 65 | EXO1 | | | 0.44 | 1.05E-07 | 0.47 | 3.77E-07 | | |
| 66 | FAM180B | | | 0.32 | 1.26E-05 | 4.32 | 7.90E-10 | 2.28 | 3.70E-04 |
| 67 | FAM46C | | | 2.15 | 3.65E-03 | 0.43 | 7.74E-03 | 0.32 | 2.17E-03 |
| 68 | FAM84B | | | 2.59 | 1.02E-07 | 0.43 | 2.40E-06 | 0.43 | 3.77E-08 |
| 69 | FBXL13 | | | 3.65 | 3.38E-04 | 7.29 | 1.87E-08 | | |
| 70 | FERMT2 | | | 2.83 | 2.59E-14 | 2.01 | 4.00E-09 | | |
| 71 | FGGY | | | 2.65 | 4.57E-03 | | | 2.48 | 5.70E-04 |
| 72 | FMNL3 | | | 2.72 | 2.88E-06 | 0.34 | 2.18E-05 | | |
| 73 | FRMD4B | 0.43 | 1.72E-03 | 0.49 | 1.76E-03 | 0.42 | 4.90E-04 | | |
| 74 | FUT3 | 101.1 | 1.49E-07 | | | 5.38 | 1.15E-05 | | |
| 75 | GAA | | | 2.36 | 7.05E-05 | 2.67 | 4.41E-05 | 2.07 | 6.78E-04 |
| 76 | GADD45A | 3.80 | 6.40E-16 | 3.36 | 9.84E-09 | 4.20 | 3.45E-20 | | |
| 77 | GADD45B | | | 2.87 | 1.78E-07 | 11.35 | 2.84E-29 | 4.16 | 3.41E-12 |
| 78 | GALNT3 | | | 0.38 | 7.08E-03 | 0.47 | 1.03E-02 | | |
| 79 | GARS | 2.61 | 1.26E-13 | 2.78 | 6.76E-19 | 3.18 | 3.10E-26 | | |
| 80 | GCA | | | 2.32 | 1.55E-02 | 0.43 | 3.21E-03 | | |
| 81 | GDF15 | 2.82 | 8.37E-08 | 3.18 | 1.66E-15 | 5.37 | 6.21E-32 | 2.17 | 9.13E-25 |
| 82 | GLI2 | | | 5.72 | 2.24E-14 | 5.45 | 5.18E-05 | 3.02 | 4.20E-03 |
| 83 | GMCL1 | | | 2.85 | 6.36E-03 | 0.27 | 2.08E-04 | | |
| 84 | GPCPD1 | 2.06 | 4.85E-07 | 2.10 | 2.74E-07 | 2.55 | 2.52E-12 | | |
| 85 | GPRIN1 | | | 0.45 | 4.07E-06 | 0.50 | 7.07E-05 | | |
| 86 | GPT2 | 2.62 | 3.30E-09 | 4.02 | 1.46E-29 | 2.72 | 3.68E-14 | | |
| 87 | GRB10 | 3.09 | 1.00E-17 | 3.73 | 8.15E-29 | 2.49 | 7.76E-15 | | |
| 88 | H6PD | | | 2.92 | 1.45E-10 | 2.04 | 1.48E-05 | 2.14 | 1.71E-08 |
| 89 | HAGHL | 0.49 | 1.29E-04 | | | | | 2.53 | 5.14E-07 |
| 90 | HAS2 | | | 0.39 | 4.55E-04 | 0.28 | 6.92E-08 | | |
| 91 | HDAC9 | | | 4.44 | 2.92E-07 | 3.00 | 9.79E-04 | | |
| 92 | HERPUD1 | 3.41 | 4.13E-16 | 3.65 | 9.11E-16 | | | 2.53 | 2.25E-36 |
| 93 | HGSNAT | | | 2.79 | 1.20E-08 | 0.42 | 1.34E-07 | | |
| 94 | HKDC1 | 2.98 | 7.11E-04 | 3.77 | 2.46E-06 | 5.06 | 1.14E-06 | | |

(Table continues in following page)

| | | 8h Induction Ectopic ATF4 | | 24h Induction Ectopic ATF4 | | 8h Glucose Starvation | | 24h Glucose Starvation | |
|---|---|---|---|---|---|---|---|---|---|
| | Gene Name | Fold Change | *P* value | Fold Change | *P* value | Fold Change | *P* value | Fold Change | *P* value |
| 95 | HOMER3 | | | 2.68 | 1.33E-11 | | | 3.15 | 1.05E-16 |
| 96 | HOXB9 | 3.28 | 7.48E-04 | | | 9.78 | 1.78E-16 | 5.63 | 3.45E-17 |
| 97 | ICOS | 0.24 | 3.86E-06 | 0.30 | 1.26E-04 | | | 0.11 | 7.15E-07 |
| 98 | IDI1 | | | 0.50 | 3.85E-05 | 0.48 | 3.64E-07 | | |
| 99 | IDNK | | | 3.03 | 3.75E-05 | 4.24 | 1.58E-06 | | |
| 100 | IL20RB | | | 27.7 | 4.05E-28 | 3.41 | 5.20E-04 | | |
| 101 | IL23A | | | 5.69 | 4.79E-08 | 4.13 | 1.72E-05 | | |
| 102 | INHBA | 24.1 | 6.88E-37 | 142.6 | 6.67E-122 | 7.32 | 3.97E-04 | | |
| 103 | INHBE | 11.7 | 2.72E-47 | 73.3 | 3.87E-137 | 33.47 | 2.64E-25 | 11.19 | 1.84E-08 |
| 104 | IQSEC2 | | | 3.06 | 4.59E-06 | | | 2.75 | 3.29E-03 |
| 105 | JDP2 | 2.59 | 2.42E-05 | 2.85 | 1.11E-08 | 15.17 | 1.44E-31 | 10.13 | 2.63E-39 |
| 106 | JMY | 2.19 | 9.35E-04 | 5.74 | 4.97E-18 | 2.30 | 2.83E-05 | | |
| 107 | JUP | | | 2.85 | 2.27E-10 | 2.56 | 3.75E-05 | 2.06 | 1.38E-04 |
| 108 | KBTBD8 | 3.50 | 4.11E-04 | 5.41 | 6.37E-09 | | | 0.22 | 5.75E-04 |
| 109 | KDM4A | 3.39 | 1.42E-17 | 4.31 | 1.42E-30 | 2.17 | 2.37E-09 | | |
| 110 | KIAA0226L | 0.40 | 4.05E-07 | | | 0.24 | 1.33E-23 | 0.40 | 3.49E-18 |
| 111 | KIAA0754 | 0.37 | 2.54E-03 | | | 3.33 | 3.04E-06 | | |
| 112 | KIAA1522 | | | 0.30 | 3.10E-03 | 0.27 | 1.59E-05 | | |
| 113 | KIF1A | | | 0.46 | 6.27E-03 | 2.35 | 2.69E-04 | 2.12 | 3.74E-04 |
| 114 | KIF6 | 0.48 | 1.76E-03 | | | | | 2.46 | 7.64E-04 |
| 115 | KLC2 | | | 0.37 | 4.45E-03 | 4.69 | 1.32E-05 | | |
| 116 | KLF5 | 2.38 | 2.18E-04 | 3.77 | 2.05E-14 | 3.82 | 5.76E-15 | | |
| 117 | KLF7 | 4.84 | 1.06E-14 | 5.27 | 6.30E-25 | 2.59 | 5.99E-08 | | |
| 118 | KLHDC7B | 42.6 | 1.11E-04 | 104.6 | 1.19E-08 | 61.83 | 1.71E-06 | | |
| 119 | KLHL15 | 3.70 | 3.12E-05 | 4.47 | 3.26E-11 | 0.38 | 1.08E-03 | | |
| 120 | LDLR | | | 0.47 | 5.87E-08 | 0.34 | 2.59E-12 | | |
| 121 | LHFPL3-AS1 | 0.46 | 8.80E-05 | 0.40 | 3.80E-07 | | | 0.45 | 6.92E-16 |
| 122 | LIMCH1 | 2.23 | 2.20E-09 | 2.38 | 9.30E-13 | 4.48 | 2.44E-35 | 2.16 | 8.13E-15 |
| 123 | LIMK2 | 2.53 | 7.58E-11 | 3.75 | 3.70E-24 | 2.70 | 1.57E-12 | | |
| 124 | LINC00052 | | | 0.23 | 4.49E-03 | 2.51 | 4.22E-04 | | |
| 125 | LINC00326 | 48.3 | 5.76E-37 | 60.5 | 3.78E-42 | 5.69 | 1.35E-03 | | |
| 126 | LINC00520 | | | 0.46 | 4.49E-08 | 0.45 | 3.38E-10 | | |
| 127 | LINC00645 | 0.36 | 1.13E-07 | 0.47 | 3.85E-05 | 0.42 | 9.01E-08 | 0.37 | 9.83E-14 |
| 128 | LINC00662 | 6.11 | 3.09E-09 | 8.76 | 1.13E-21 | 3.37 | 4.44E-04 | | |
| 129 | LOC100131564 | | | 2.93 | 2.13E-04 | | | 3.63 | 1.11E-07 |
| 130 | LOC100270746 | | | 2.81 | 3.17E-04 | | | 2.21 | 9.68E-04 |
| 131 | LOC285000 | | | 0.37 | 8.21E-04 | 0.44 | 7.05E-03 | | |
| 132 | LOC344887 | 2.24 | 1.52E-03 | | | 3.03 | 1.91E-06 | | |
| 133 | LOC440028 | | | 3.95 | 5.32E-07 | 3.19 | 2.47E-03 | | |
| 134 | LOC642852 | | | 2.73 | 1.73E-09 | | | 2.16 | 3.03E-10 |
| 135 | LOC653160 | | | 3.25 | 1.50E-02 | | | 12.41 | 7.63E-04 |
| 136 | LOC728730 | | | 4.47 | 7.98E-07 | 4.00 | 1.00E-04 | 3.94 | 7.81E-05 |
| 137 | LRAT | 0.33 | 5.77E-04 | 0.15 | 2.50E-06 | 2.46 | 1.25E-06 | | |
| 138 | LRP1 | | | 5.14 | 7.88E-09 | 3.19 | 2.58E-03 | 2.59 | 4.93E-03 |
| 139 | LRRC20 | 0.42 | 9.54E-04 | | | 0.34 | 3.23E-05 | | |
| 140 | LZTFL1 | 2.27 | 3.42E-06 | | | 2.80 | 4.72E-12 | | |
| 141 | MAGEA1 | | | 0.47 | 1.43E-04 | 0.47 | 1.59E-05 | | |

(Table continues in following page)

| | | 8h Induction Ectopic ATF4 | | 24h Induction Ectopic ATF4 | | 8h Glucose Starvation | | 24h Glucose Starvation | |
|---|---|---|---|---|---|---|---|---|---|
| | Gene Name | Fold Change | *P* value | Fold Change | *P* value | Fold Change | *P* value | Fold Change | *P* value |
| 142 | MAP1B | 7.14 | 1.71E-33 | 13.7 | 5.46E-64 | 9.69 | 4.05E-32 | 3.18 | 1.08E-09 |
| 143 | MATN4 | | | 2.65 | 5.16E-03 | 6.97 | 3.99E-05 | | |
| 144 | MBNL2 | 2.35 | 4.49E-04 | 2.98 | 2.15E-08 | 2.30 | 2.82E-04 | | |
| 145 | MCM10 | | | 0.32 | 4.57E-14 | 0.49 | 1.40E-07 | | |
| 146 | MCOLN2 | | | 0.42 | 1.28E-07 | 0.48 | 2.64E-06 | | |
| 147 | MGC16025 | | | 0.45 | 6.52E-04 | 2.64 | 2.34E-04 | | |
| 148 | MITF | 0.35 | 8.22E-13 | 0.43 | 2.08E-11 | 0.33 | 9.53E-16 | | |
| 149 | MORN4 | 2.06 | 5.56E-04 | 3.14 | 8.83E-09 | 2.42 | 1.20E-06 | | |
| 150 | MRAS | | | 2.07 | 9.73E-03 | 8.28 | 2.68E-05 | 5.17 | 9.48E-03 |
| 151 | MREG | 0.48 | 2.32E-03 | 0.37 | 8.81E-05 | 0.44 | 2.45E-04 | | |
| 152 | MTHFD2 | 4.43 | 6.47E-10 | 4.30 | 1.83E-17 | 2.15 | 2.93E-05 | | |
| 153 | MUC7 | | | 0.27 | 4.56E-03 | | | 0.25 | 1.71E-05 |
| 154 | MXD1 | 6.56 | 1.80E-16 | 18.3 | 4.91E-64 | 2.01 | 4.97E-03 | | |
| 155 | MXD4 | | | 2.90 | 2.21E-06 | 2.43 | 1.45E-03 | 3.06 | 1.03E-05 |
| 156 | MYOM1 | 4.33 | 1.64E-10 | 4.24 | 4.68E-07 | 3.75 | 1.72E-04 | | |
| 157 | NAT16 | 2.58 | 8.77E-06 | 5.33 | 4.47E-18 | 7.87 | 3.49E-24 | 3.11 | 4.20E-07 |
| 158 | NAV3 | | | 3.69 | 3.00E-08 | 3.96 | 9.67E-05 | 3.78 | 1.08E-05 |
| 159 | NBEA | | | 2.20 | 1.10E-04 | | | 2.35 | 5.04E-05 |
| 160 | NDRG1 | | | 6.37 | 9.33E-27 | 3.84 | 3.61E-12 | | |
| 161 | NMRK2 | | | 0.22 | 3.46E-03 | | | 3.34 | 2.37E-04 |
| 162 | NOX4 | | | 3.20 | 3.60E-04 | 5.04 | 3.65E-06 | | |
| 163 | NPAS3 | | | 4.67 | 2.45E-07 | 3.38 | 6.17E-03 | 3.72 | 1.52E-03 |
| 164 | NR4A3 | 0.48 | 3.73E-07 | 0.50 | 2.24E-06 | 0.50 | 2.60E-07 | | |
| 165 | NUAK1 | | | 4.17 | 1.66E-09 | 3.65 | 6.86E-03 | | |
| 166 | NUPR1 | | | 2.04 | 3.89E-05 | 16.67 | 1.29E-31 | 6.13 | 3.13E-68 |
| 167 | NXF1 | | | 2.47 | 7.00E-07 | 0.39 | 6.24E-06 | | |
| 168 | OGT | 2.59 | 9.49E-11 | 3.78 | 6.92E-21 | 2.60 | 2.92E-14 | | |
| 169 | OPLAH | | | 2.77 | 3.76E-03 | 10.96 | 1.01E-06 | 6.60 | 3.22E-04 |
| 170 | P2RX7 | 0.32 | 3.08E-04 | 0.28 | 2.09E-07 | 2.35 | 1.10E-05 | | |
| 171 | PCK2 | 4.86 | 3.72E-28 | 9.82 | 3.17E-60 | 8.78 | 1.47E-46 | 4.42 | 7.92E-40 |
| 172 | PCMTD1 | | | 2.93 | 8.24E-05 | 2.83 | 2.04E-03 | | |
| 173 | PDCD4 | 2.90 | 1.98E-15 | 2.68 | 2.97E-14 | 2.25 | 7.16E-09 | | |
| 174 | PDGFA | | | 2.20 | 6.51E-03 | 3.51 | 4.99E-03 | | |
| 175 | PELI3 | 0.41 | 1.87E-03 | | | 0.49 | 4.17E-03 | | |
| 176 | PEX5L | 19.8 | 1.40E-22 | 17.1 | 5.26E-21 | 4.73 | 3.42E-03 | | |
| 177 | PI15 | 2.72 | 3.57E-03 | 3.77 | 7.79E-09 | | | 0.43 | 1.58E-15 |
| 178 | PIEZO1 | | | 2.04 | 2.45E-05 | | | 2.41 | 1.24E-09 |
| 179 | PM20D2 | | | 0.48 | 1.76E-05 | 0.44 | 1.55E-06 | | |
| 180 | PMAIP1 | 4.96 | 6.17E-20 | 5.34 | 8.05E-24 | 2.90 | 6.52E-06 | 2.80 | 1.32E-06 |
| 181 | PPARGC1B | | | 0.40 | 9.72E-04 | 0.49 | 3.95E-04 | | |
| 182 | PPM1E | | | 2.85 | 4.93E-03 | 3.07 | 6.34E-03 | | |
| 183 | PPP1R15A | 2.16 | 2.06E-06 | 3.65 | 5.73E-19 | 5.72 | 1.59E-30 | | |
| 184 | PPP4R1L | 2.97 | 6.64E-05 | 27.2 | 5.85E-52 | | | 0.32 | 5.05E-03 |
| 185 | PQLC3 | | | 2.62 | 3.96E-03 | | | 2.33 | 8.87E-07 |
| 186 | PRICKLE1 | | | 6.49 | 2.49E-10 | 2.37 | 4.84E-03 | | |
| 187 | PROM1 | | | 0.29 | 1.89E-03 | | | 0.27 | 4.21E-05 |
| 188 | PRR5L | 0.32 | 8.82E-04 | | | 0.45 | 2.24E-03 | | |

(Table continues in following page)

| | | 8h Induction Ectopic ATF4 | | 24h Induction Ectopic ATF4 | | 8h Glucose Starvation | | 24h Glucose Starvation | |
|---|---|---|---|---|---|---|---|---|---|
| | Gene Name | Fold Change | *P* value | Fold Change | *P* value | Fold Change | *P* value | Fold Change | *P* value |
| 189 | PSPH | 4.90 | 6.02E-26 | 4.22 | 3.81E-30 | 2.53 | 1.21E-13 | | |
| 190 | PTCRA | | | 0.25 | 4.38E-03 | 2.65 | 7.60E-03 | | |
| 191 | PYGL | | | 0.34 | 2.64E-10 | 2.30 | 1.88E-09 | | |
| 192 | RAB39B | 14.2 | 1.18E-23 | 21.4 | 2.99E-35 | 14.48 | 2.46E-15 | 4.47 | 5.16E-04 |
| 193 | RCAN1 | 2.98 | 1.44E-16 | 3.18 | 1.54E-21 | 2.48 | 5.44E-15 | | |
| 194 | RGS2 | 2.24 | 6.03E-05 | 2.45 | 1.32E-08 | 2.73 | 1.96E-09 | | |
| 195 | RIMS3 | 5.59 | 3.20E-15 | 16.4 | 8.60E-56 | 4.32 | 1.51E-06 | 2.34 | 9.33E-03 |
| 196 | RIPK4 | 0.47 | 3.83E-05 | | | 0.46 | 7.98E-09 | | |
| 197 | RNF24 | | | 3.91 | 5.78E-16 | 0.47 | 8.17E-05 | | |
| 198 | ROPN1 | | | 0.30 | 2.28E-05 | | | 0.41 | 5.01E-05 |
| 199 | RPS6KA2 | 3.57 | 2.62E-18 | 6.84 | 3.71E-46 | 3.86 | 9.36E-14 | 3.15 | 6.22E-12 |
| 200 | S100P | 25.1 | 9.66E-79 | 231.7 | 1.53E-201 | 3.36 | 7.93E-04 | | |
| 201 | SAMD1 | 0.09 | 5.37E-05 | | | | | 4.74 | 4.29E-04 |
| 202 | SCG3 | | | 4.39 | 1.15E-04 | | | 4.15 | 4.88E-04 |
| 203 | SCRG1 | 8.06 | 6.77E-18 | 22.8 | 5.57E-52 | 55.88 | 6.60E-06 | 72.21 | 7.37E-08 |
| 204 | SDSL | | | 3.02 | 2.26E-04 | 7.19 | 4.37E-06 | 6.57 | 2.06E-05 |
| 205 | SEC24D | 3.46 | 3.01E-05 | 8.15 | 1.14E-21 | | | 2.01 | 5.00E-04 |
| 206 | SEL1L3 | 2.75 | 1.56E-07 | 9.28 | 1.83E-40 | | | 2.66 | 4.04E-09 |
| 207 | SEMA6A | 0.43 | 7.49E-10 | 0.47 | 6.34E-08 | 0.47 | 6.22E-10 | | |
| 208 | SERPINB8 | 8.92 | 5.61E-09 | 15.6 | 4.86E-27 | 3.20 | 9.58E-05 | | |
| 209 | SERPINE2 | | | 7.09 | 9.03E-25 | | | 2.14 | 1.34E-17 |
| 210 | SERTAD4 | 0.27 | 2.88E-09 | 0.29 | 7.04E-08 | 2.72 | 1.02E-09 | | |
| 211 | SESN2 | 16.4 | 1.06E-74 | 22.9 | 6.32E-115 | 10.67 | 6.31E-63 | 6.34 | 1.48E-77 |
| 212 | SH3TC1 | | | 2.36 | 7.83E-06 | 3.59 | 4.09E-07 | | |
| 213 | SH3TC2 | | | 0.49 | 1.26E-03 | 2.33 | 2.77E-06 | | |
| 214 | SHISA2 | 0.49 | 5.23E-04 | | | 0.36 | 1.62E-06 | 0.23 | 2.66E-12 |
| 215 | SIN3A | | | 2.55 | 4.46E-07 | 0.49 | 4.71E-04 | | |
| 216 | SLC22A15 | 3.90 | 4.40E-06 | 4.29 | 3.50E-07 | 3.49 | 1.03E-02 | | |
| 217 | SLC24A1 | | | 2.09 | 6.69E-05 | 3.39 | 4.45E-08 | | |
| 218 | SLC7A11 | 2.45 | 9.52E-12 | 2.30 | 5.13E-11 | 3.04 | 6.74E-21 | 2.47 | 1.10E-36 |
| 219 | SLFN5 | 2.32 | 1.73E-07 | 2.93 | 1.60E-15 | 3.64 | 6.73E-21 | | |
| 220 | SMIM14 | 2.67 | 2.67E-04 | 9.29 | 3.51E-25 | 2.39 | 4.46E-05 | | |
| 221 | SNAPC5 | | | 0.45 | 9.48E-03 | 3.29 | 4.20E-03 | | |
| 222 | SPG11 | | | 2.11 | 1.23E-02 | 2.12 | 3.48E-03 | 2.67 | 1.34E-05 |
| 223 | SPIN3 | 2.17 | 3.97E-03 | 2.89 | 4.51E-05 | 2.27 | 3.86E-03 | | |
| 224 | SPTA1 | 3.12 | 3.59E-04 | | | 3.04 | 2.18E-03 | | |
| 225 | SQLE | | | 0.48 | 3.30E-07 | 0.41 | 9.31E-09 | | |
| 226 | SREBF1 | | | 2.13 | 2.43E-07 | | | 0.42 | 2.16E-10 |
| 227 | SSBP2 | | | 10.9 | 5.50E-22 | | | 3.03 | 7.40E-03 |
| 228 | STK17A | 3.90 | 2.93E-22 | 3.41 | 1.54E-22 | | | 0.42 | 4.46E-14 |
| 229 | STRADA | | | 2.15 | 1.68E-04 | 0.41 | 1.31E-04 | | |
| 230 | SYNE1 | | | 17.5 | 1.52E-24 | 4.75 | 1.12E-03 | | |
| 231 | TBC1D8 | 3.21 | 2.81E-07 | 4.46 | 2.94E-10 | 3.03 | 1.33E-07 | 2.08 | 1.22E-03 |
| 232 | TLCD2 | | | 5.49 | 1.64E-22 | 2.13 | 1.79E-04 | | |
| 233 | TMEM140 | 3.90 | 2.97E-04 | 5.73 | 8.46E-10 | 3.99 | 1.43E-03 | | |
| 234 | TMEM143 | | | 2.23 | 2.55E-03 | | | 2.04 | 6.44E-04 |
| 235 | TMEM8B | | | 2.33 | 1.63E-03 | | | 3.05 | 4.44E-05 |

(Table continues in following page)

| | | 8h Induction Ectopic ATF4 | | 24h Induction Ectopic ATF4 | | 8h Glucose Starvation | | 24h Glucose Starvation | |
|---|---|---|---|---|---|---|---|---|---|
| | Gene Name | Fold Change | *P* value | Fold Change | *P* value | Fold Change | *P* value | Fold Change | *P* value |
| 236 | TMTC2 | | | 2.48 | 6.90E-03 | 3.71 | 3.55E-05 | | |
| 237 | TNRC18 | 2.15 | 7.67E-04 | | | 3.20 | 2.80E-03 | | |
| 238 | TRIB3 | 4.99 | 3.08E-19 | 4.00 | 1.46E-22 | 7.05 | 8.71E-37 | 2.26 | 1.11E-22 |
| 239 | TRIM48 | | | 2.15 | 3.54E-03 | 0.15 | 1.64E-08 | 0.34 | 7.43E-05 |
| 240 | TRPM4 | | | 3.59 | 2.86E-04 | | | 5.17 | 2.98E-03 |
| 241 | TTC25 | 5.46 | 3.30E-07 | 16.1 | 3.12E-27 | 3.71 | 2.09E-04 | | |
| 242 | TUBE1 | 3.23 | 3.75E-09 | 3.29 | 1.22E-12 | 3.42 | 3.85E-13 | 2.03 | 4.27E-05 |
| 243 | UBALD2 | 2.14 | 7.62E-04 | | | 3.83 | 2.92E-18 | | |
| 244 | UGDH | | | 2.09 | 3.67E-06 | 0.33 | 3.47E-08 | | |
| 245 | VAMP4 | | | 2.18 | 4.39E-05 | 2.05 | 3.69E-05 | | |
| 246 | VEGFA | 2.86 | 3.99E-11 | 3.49 | 7.21E-17 | 3.29 | 1.26E-12 | 3.04 | 1.80E-15 |
| 247 | WARS | | | 4.83 | 1.29E-36 | 2.20 | 3.06E-10 | 2.09 | 1.85E-21 |
| 248 | WBSCR16 | | | 2.01 | 4.31E-03 | 0.41 | 1.29E-03 | | |
| 249 | WDR45 | | | 3.71 | 5.00E-22 | 2.04 | 6.27E-06 | | |
| 250 | WIPI1 | 2.47 | 2.24E-07 | | | 2.02 | 3.73E-07 | | |
| 251 | XBP1 | 3.49 | 9.57E-12 | 2.98 | 5.58E-16 | 2.53 | 2.15E-13 | | |
| 252 | ZCCHC2 | 0.44 | 1.58E-03 | | | 0.41 | 4.55E-05 | | |
| 253 | ZDBF2 | 2.03 | 1.65E-03 | 2.18 | 8.90E-05 | 2.83 | 3.25E-05 | | |
| 254 | ZDHHC14 | 0.47 | 1.81E-03 | | | 0.23 | 5.29E-10 | | |
| 255 | ZNF333 | 4.36 | 2.68E-03 | 4.98 | 6.77E-04 | 2.30 | 8.72E-03 | | |
| 256 | ZNF804A | | | 2.34 | 3.55E-03 | | | 3.14 | 6.98E-04 |
| 257 | ZSWIM3 | | | 2.43 | 4.49E-04 | 2.06 | 2.85E-03 | | |

**Supplementary Table B.2.- ATF4-bound differentially expressed genes following induction of ectopic ATF4 and upon glucose starvation in 501mel cells.** Fold changes and associated *P* values for the DEGs (FDR < 0.05, fold change ≥ 2) identified in the RNA-seq experiments performed upon 8 and/or 24 h induction of ectopic ATF4 with 20 ng/ml doxycycline in 501mel-i-ATF4-HA cells and following 8 and/or 24 h glucose starvation in 501mel cells presenting associated binding peaks in the ATF4 ChIP-seq experiment performed upon 4 h glucose starvation in 501mel cells (see Supplementary Tables 4.A and B on Data CD for ATF4 ChIP-seq data). Genes upregulated and downregulated upon both ectopic ATF4 expression and glucose deprivation are highlighted in yellow and green, respectively.

| | | 48 MITF silencing | | 8h Induction Ectopic ATF4 | | 24h Induction Ectopic ATF4 | |
|---|---|---|---|---|---|---|---|
| | **Gene Name** | **Fold Change** | ***P* value** | **Fold Change** | ***P* value** | **Fold Change** | ***P* value** |
| 1 | ABTB1 | 3.12 | 7.78E-04 | | | 5.39 | 6.17E-08 |
| 2 | ABTB2 | 3.73 | 2.88E-08 | 5.49 | 1.53E-12 | 14.3 | 5.27E-32 |
| 3 | ACOT12 | 3.74 | 2.80E-04 | 6.21 | 1.12E-04 | 17.6 | 2.29E-16 |
| 4 | ADAMTS17 | 0.49 | 2.64E-03 | | | 0.44 | 1.05E-02 |
| 5 | ADCY3 | 0.48 | 3.67E-09 | | | 0.40 | 3.63E-06 |
| 6 | AHNAK | 4.73 | 3.27E-12 | | | 3.84 | 8.36E-16 |
| 7 | AIF1L | 6.11 | 2.90E-03 | | | 2.86 | 1.20E-04 |
| 8 | AK4 | 0.45 | 3.74E-10 | | | 0.47 | 5.98E-04 |
| 9 | AKNA | 0.47 | 8.37E-03 | 8.14 | 3.37E-24 | 7.25 | 2.37E-25 |
| 10 | AKR1B1 | 0.50 | 3.11E-09 | | | 2.03 | 7.64E-07 |
| 11 | AMOT | 2.01 | 2.96E-06 | 3.72 | 2.93E-16 | | |
| 12 | APOD | 4.53 | 2.68E-09 | 3.01 | 1.30E-05 | 2.70 | 1.83E-06 |
| 13 | APPBP2 | 2.25 | 5.08E-11 | 2.11 | 1.09E-06 | | |
| 14 | ARHGAP23 | 3.88 | 1.44E-02 | | | 4.23 | 5.16E-08 |
| 15 | ARHGEF10L | 2.12 | 3.57E-05 | | | 2.54 | 4.81E-05 |
| 16 | ARHGEF3 | 2.86 | 4.16E-04 | 3.05 | 2.36E-03 | 2.58 | 1.82E-03 |
| 17 | ARRDC3 | 6.37 | 2.97E-15 | | | 5.38 | 7.70E-09 |
| 18 | ASTN2 | 0.40 | 5.72E-05 | 0.48 | 4.30E-04 | | |
| 19 | ATAD2 | 0.33 | 7.75E-15 | | | 0.45 | 1.51E-09 |
| 20 | ATP6V0A4 | 0.44 | 1.76E-06 | | | 0.42 | 2.49E-06 |
| 21 | AZGP1 | 10.4 | 7.98E-10 | | | 8.81 | 2.35E-06 |
| 22 | BASP1 | 2.42 | 1.44E-07 | | | 13.2 | 1.20E-38 |
| 23 | BBS10 | 2.40 | 3.58E-04 | 2.52 | 3.65E-03 | 2.81 | 1.47E-03 |
| 24 | BCHE | 2.77 | 1.82E-11 | | | 2.42 | 2.14E-06 |
| 25 | BRE-AS1 | 0.32 | 1.46E-02 | 14.7 | 6.50E-31 | 8.09 | 1.13E-17 |
| 26 | C15orf41 | 0.21 | 1.69E-04 | | | 0.47 | 1.13E-02 |
| 27 | C1orf112 | 0.29 | 1.88E-09 | | | 0.48 | 1.78E-06 |
| 28 | C20orf194 | 2.83 | 1.16E-09 | | | 2.15 | 1.09E-04 |
| 29 | C2orf72 | 0.26 | 3.35E-09 | | | 0.48 | 1.24E-04 |
| 30 | C2orf88 | 0.20 | 3.14E-04 | | | 0.21 | 1.29E-03 |
| 31 | C4orf19 | 0.17 | 5.30E-03 | | | 0.33 | 3.65E-03 |
| 32 | C6orf165 | 4.47 | 4.66E-04 | | | 66.4 | 5.78E-06 |
| 33 | C8orf46 | 0.38 | 1.28E-04 | | | 0.35 | 1.77E-04 |
| 34 | CALCOCO1 | 2.73 | 1.07E-07 | | | 3.27 | 7.72E-06 |
| 35 | CASZ1 | 0.23 | 3.73E-05 | 3.59 | 3.71E-07 | 6.57 | 1.98E-13 |
| 36 | CBLB | 2.56 | 5.73E-09 | | | 3.37 | 2.77E-13 |
| 37 | CCDC71L | 2.55 | 2.95E-09 | 3.23 | 2.56E-10 | 3.32 | 1.18E-12 |
| 38 | CCDC92 | 2.01 | 3.10E-03 | | | 3.21 | 2.63E-07 |
| 39 | CCM2 | 0.35 | 1.76E-05 | | | 0.47 | 4.44E-05 |
| 40 | CCND1 | 0.46 | 1.68E-14 | 0.47 | 1.87E-03 | 0.37 | 7.17E-11 |
| 41 | CD82 | 3.51 | 6.04E-03 | | | 7.93 | 1.38E-05 |
| 42 | CDCA7 | 0.41 | 5.64E-11 | | | 0.39 | 2.54E-09 |
| 43 | CDH19 | 5.65 | 2.10E-18 | 2.94 | 4.47E-14 | 2.96 | 2.48E-11 |
| 44 | CDON | 0.32 | 1.50E-05 | 2.65 | 1.68E-05 | | |
| 45 | CDS1 | 0.28 | 2.68E-08 | 2.30 | 1.90E-03 | 4.09 | 1.30E-07 |
| 46 | CEP128 | 0.40 | 5.36E-07 | | | 0.35 | 1.40E-03 |
| 47 | CEP170 | 2.70 | 8.58E-13 | 2.21 | 1.77E-03 | 3.07 | 5.07E-09 |
| 48 | CEP19 | 3.48 | 2.91E-07 | 2.21 | 3.61E-04 | 3.59 | 3.73E-10 |
| 49 | CGN | 2.26 | 2.08E-05 | | | 0.41 | 1.68E-02 |

(Table continues in following page)

| | | 48 MITF silencing | | 8h Induction Ectopic ATF4 | | 24h Induction Ectopic ATF4 | |
|---|---|---|---|---|---|---|---|
| | Gene Name | Fold Change | *P* value | Fold Change | *P* value | Fold Change | *P* value |
| 50 | CHAF1A | 0.29 | 1.28E-13 | | | 0.45 | 4.96E-09 |
| 51 | CHAF1B | 0.31 | 4.58E-10 | | | 0.42 | 2.53E-09 |
| 52 | CHST11 | 0.33 | 2.22E-15 | | | 0.41 | 3.69E-08 |
| 53 | CHST9 | 0.46 | 4.65E-07 | 0.42 | 6.01E-04 | 0.20 | 5.37E-08 |
| 54 | CITED2 | 2.58 | 6.93E-06 | 4.06 | 1.07E-13 | 5.65 | 1.21E-16 |
| 55 | CLN6 | 0.38 | 1.37E-07 | | | 0.43 | 2.49E-07 |
| 56 | COL19A1 | 2.84 | 4.96E-06 | 3.28 | 1.32E-06 | 2.87 | 2.91E-05 |
| 57 | COL9A1 | 5.90 | 2.84E-11 | | | 0.45 | 3.20E-03 |
| 58 | CPED1 | 4.11 | 1.14E-06 | 2.17 | 3.90E-03 | 4.96 | 2.13E-14 |
| 59 | CPNE5 | 0.24 | 1.24E-05 | | | 0.34 | 8.21E-03 |
| 60 | CREBRF | 2.94 | 3.86E-10 | 2.54 | 1.65E-04 | 3.17 | 8.95E-09 |
| 61 | CTDSP2 | 2.01 | 6.47E-11 | | | 2.46 | 4.83E-12 |
| 62 | CTGF | 4.81 | 7.89E-16 | 2.34 | 1.90E-07 | 3.96 | 6.18E-20 |
| 63 | CTLA4 | 2.32 | 3.60E-10 | | | 0.38 | 2.37E-07 |
| 64 | CTNNA2 | 12.4 | 7.86E-19 | | | 2.44 | 1.66E-02 |
| 65 | CXorf57 | 0.33 | 9.42E-04 | 2.41 | 2.62E-03 | 3.77 | 7.76E-06 |
| 66 | DENND2A | 0.32 | 2.69E-13 | | | 0.25 | 3.66E-16 |
| 67 | DEPTOR | 7.11 | 3.23E-10 | | | 6.81 | 5.17E-16 |
| 68 | DFNA5 | 3.26 | 3.29E-07 | | | 2.87 | 1.19E-07 |
| 69 | DGAT2 | 5.48 | 1.14E-02 | 5.21 | 3.97E-08 | 18.0 | 1.87E-30 |
| 70 | DGKA | 11.8 | 2.65E-03 | | | 6.01 | 4.32E-06 |
| 71 | DIRC2 | 0.45 | 2.12E-06 | | | 3.70 | 9.03E-19 |
| 72 | DLC1 | 2.63 | 6.25E-13 | | | 2.62 | 2.02E-15 |
| 73 | DLX2 | 2.10 | 1.10E-02 | 25.0 | 2.27E-30 | 31.6 | 7.77E-61 |
| 74 | DNAJC6 | 13.1 | 3.20E-08 | | | 4.43 | 3.58E-05 |
| 75 | DOK6 | 2.84 | 6.11E-03 | | | 10.1 | 3.53E-10 |
| 76 | DUSP10 | 0.43 | 2.85E-03 | 0.37 | 1.34E-03 | 0.41 | 7.88E-03 |
| 77 | DUSP5 | 0.42 | 8.86E-04 | | | 3.32 | 5.59E-11 |
| 78 | E2F7 | 0.29 | 7.61E-10 | | | 0.34 | 1.83E-03 |
| 79 | E2F8 | 0.21 | 1.49E-09 | | | 0.15 | 2.25E-05 |
| 80 | EEPD1 | 0.26 | 3.00E-03 | | | 0.30 | 3.00E-04 |
| 81 | EFNA1 | 2.60 | 7.14E-07 | | | 2.15 | 8.73E-05 |
| 82 | ENPP2 | 6.53 | 2.88E-09 | 4.86 | 3.63E-06 | 2.88 | 4.10E-03 |
| 83 | EPS15 | 2.15 | 7.65E-14 | | | 2.19 | 4.07E-09 |
| 84 | ESCO2 | 0.34 | 1.47E-07 | | | 0.40 | 2.40E-05 |
| 85 | EXO1 | 0.32 | 9.55E-10 | | | 0.44 | 1.05E-07 |
| 86 | FAM134B | 2.09 | 8.43E-08 | | | 3.49 | 7.19E-09 |
| 87 | FAM167A | 0.09 | 3.30E-05 | 4.75 | 3.23E-06 | 8.16 | 4.55E-18 |
| 88 | FAM171A1 | 0.27 | 1.34E-03 | | | 5.67 | 5.74E-04 |
| 89 | FAXC | 0.43 | 2.18E-07 | 0.40 | 3.11E-08 | 0.45 | 2.11E-06 |
| 90 | FCRLA | 2.12 | 1.46E-04 | | | 2.15 | 5.66E-04 |
| 91 | FGFBP3 | 0.41 | 3.15E-06 | 0.43 | 1.68E-03 | 0.39 | 1.82E-05 |
| 92 | FLRT3 | 5.99 | 1.98E-06 | 3.75 | 3.41E-04 | | |
| 93 | FMNL3 | 0.40 | 1.50E-03 | | | 2.72 | 2.88E-06 |
| 94 | FNIP2 | 0.39 | 1.47E-11 | 0.47 | 7.11E-08 | | |
| 95 | FRMD6 | 3.94 | 1.85E-14 | | | 2.08 | 8.46E-06 |
| 96 | GAA | 2.21 | 4.66E-05 | | | 2.36 | 7.05E-05 |
| 97 | GAB2 | 0.33 | 5.94E-16 | | | 2.02 | 2.12E-08 |
| 98 | GALNT3 | 0.37 | 4.75E-08 | | | 0.38 | 7.08E-03 |

(Table continues in following page)

| | | 48 MITF silencing | | 8h Induction Ectopic ATF4 | | 24h Induction Ectopic ATF4 | |
|---|---|---|---|---|---|---|---|
| | **Gene Name** | **Fold Change** | ***P* value** | **Fold Change** | ***P* value** | **Fold Change** | ***P* value** |
| 99 | GCC2 | 2.02 | 9.01E-09 | | | 2.15 | 6.18E-09 |
| 100 | GFOD1 | 0.47 | 5.50E-06 | 4.06 | 4.47E-20 | 4.49 | 2.59E-20 |
| 101 | GFPT2 | 2.91 | 5.84E-04 | | | 4.98 | 9.24E-09 |
| 102 | GNG2 | 2.16 | 2.51E-03 | | | 0.29 | 1.56E-03 |
| 103 | GPT2 | 0.41 | 1.56E-09 | 2.62 | 3.30E-09 | 4.02 | 1.46E-29 |
| 104 | GUCY1A2 | 2.20 | 1.09E-07 | | | 3.20 | 1.83E-12 |
| 105 | HAS2 | 0.49 | 2.12E-06 | | | 0.39 | 4.55E-04 |
| 106 | HECTD2 | 0.44 | 9.12E-03 | | | 4.24 | 2.28E-03 |
| 107 | HHEX | 0.10 | 3.87E-04 | | | 0.35 | 1.19E-03 |
| 108 | HLA-L | 0.31 | 1.75E-02 | | | 12.6 | 1.45E-06 |
| 109 | HPGD | 2.01 | 1.40E-14 | | | 0.44 | 4.37E-08 |
| 110 | ID2 | 5.33 | 1.64E-13 | 0.49 | 1.19E-04 | | |
| 111 | IL6R | 0.35 | 3.49E-17 | 0.31 | 1.27E-10 | 0.24 | 3.56E-19 |
| 112 | IL6ST | 2.10 | 1.34E-05 | 2.41 | 2.12E-05 | 3.59 | 1.61E-13 |
| 113 | INSIG2 | 3.20 | 2.26E-10 | | | 2.79 | 5.83E-05 |
| 114 | IQSEC2 | 2.35 | 1.48E-02 | | | 3.06 | 4.59E-06 |
| 115 | ITGAV | 2.16 | 1.77E-11 | | | 3.00 | 5.85E-18 |
| 116 | KBTBD11 | 0.27 | 1.80E-03 | | | 2.60 | 2.29E-03 |
| 117 | KCNMB4 | 2.78 | 1.62E-02 | | | 2.62 | 2.41E-03 |
| 118 | KCNN2 | 2.73 | 1.19E-07 | 0.47 | 2.42E-03 | 0.14 | 1.05E-10 |
| 119 | KCTD12 | 3.02 | 6.01E-03 | | | 2.05 | 6.53E-04 |
| 120 | KIAA1522 | 0.36 | 5.60E-06 | | | 0.30 | 3.10E-03 |
| 121 | KIF1A | 0.35 | 7.28E-07 | | | 0.46 | 6.27E-03 |
| 122 | KIF26B | 4.33 | 9.54E-04 | | | 0.08 | 3.50E-04 |
| 123 | KLF9 | 2.51 | 3.38E-09 | | | 2.02 | 3.24E-04 |
| 124 | LDLR | 0.39 | 1.38E-11 | | | 0.47 | 5.87E-08 |
| 125 | LGALS3 | 0.42 | 2.25E-11 | | | 0.34 | 6.11E-12 |
| 126 | LIG1 | 0.26 | 6.18E-14 | | | 0.47 | 2.74E-08 |
| 127 | LIMCH1 | 5.73 | 8.05E-21 | 2.23 | 2.20E-09 | 2.38 | 9.30E-13 |
| 128 | LINC00520 | 0.42 | 4.17E-12 | | | 0.46 | 4.49E-08 |
| 129 | LMNB1 | 0.35 | 2.41E-14 | | | 0.35 | 3.07E-16 |
| 130 | LOC100131564 | 3.94 | 4.14E-08 | | | 2.93 | 2.13E-04 |
| 131 | LOC100505715 | 2.41 | 1.40E-04 | | | 2.25 | 4.90E-04 |
| 132 | LPL | 0.39 | 4.92E-03 | | | 0.47 | 3.16E-03 |
| 133 | LRIG1 | 5.03 | 1.26E-11 | 2.52 | 6.28E-07 | 6.29 | 8.23E-29 |
| 134 | LRP1 | 3.60 | 1.79E-07 | | | 5.14 | 7.88E-09 |
| 135 | LRRC20 | 0.44 | 9.78E-04 | 0.42 | 9.54E-04 | | |
| 136 | LSR | 0.43 | 1.17E-02 | | | 0.26 | 7.34E-04 |
| 137 | LTBP1 | 2.50 | 2.44E-07 | 2.34 | 7.23E-07 | 8.83 | 5.41E-50 |
| 138 | LURAP1L | 4.95 | 9.98E-07 | | | 4.52 | 2.55E-04 |
| 139 | MAL2 | 7.75 | 2.16E-08 | | | 3.75 | 3.20E-04 |
| 140 | MAML3 | 2.90 | 2.95E-07 | | | 2.55 | 4.81E-04 |
| 141 | MAP7 | 0.39 | 4.75E-04 | | | 3.88 | 7.08E-05 |
| 142 | MBNL2 | 3.24 | 3.18E-09 | 2.35 | 4.49E-04 | 2.98 | 2.15E-08 |
| 143 | MCM10 | 0.36 | 1.82E-09 | | | 0.32 | 4.57E-14 |
| 144 | MDGA1 | 0.30 | 2.03E-02 | | | 2.44 | 1.85E-02 |
| 145 | MELK | 0.42 | 4.33E-11 | | | 0.49 | 3.81E-04 |
| 146 | METRNL | 0.47 | 5.93E-07 | | | 2.43 | 2.78E-07 |
| 147 | MGC16025 | 3.02 | 1.76E-03 | | | 0.45 | 6.52E-04 |

(Table continues in following page)

| | | 48 MITF silencing | | 8h Induction Ectopic ATF4 | | 24h Induction Ectopic ATF4 | |
|---|---|---|---|---|---|---|---|
| | Gene Name | Fold Change | *P* value | Fold Change | *P* value | Fold Change | *P* value |
| 148 | MIER2 | 0.46 | 2.58E-03 | | | 2.43 | 2.93E-04 |
| 149 | MROH1 | 0.35 | 8.36E-03 | | | 2.53 | 3.84E-03 |
| 150 | MRPS25 | 0.49 | 9.27E-12 | | | 0.41 | 1.92E-08 |
| 151 | MTM1 | 3.50 | 3.32E-03 | | | 2.85 | 1.79E-03 |
| 152 | MURC | 0.45 | 6.26E-03 | | | 0.33 | 1.06E-02 |
| 153 | MXD4 | 8.41 | 2.67E-16 | | | 2.90 | 2.21E-06 |
| 154 | MYOM1 | 2.72 | 1.75E-02 | 4.33 | 1.64E-10 | 4.24 | 4.68E-07 |
| 155 | NANOS1 | 2.12 | 1.35E-08 | | | 4.01 | 2.29E-21 |
| 156 | NAV3 | 4.32 | 3.38E-12 | | | 3.69 | 3.00E-08 |
| 157 | NBEA | 3.30 | 6.23E-15 | | | 2.20 | 1.10E-04 |
| 158 | NCAPG2 | 0.40 | 7.35E-11 | | | 0.37 | 3.13E-06 |
| 159 | NCAPH | 0.37 | 2.49E-10 | | | 0.26 | 8.36E-14 |
| 160 | NCS1 | 0.37 | 2.12E-09 | | | 0.50 | 1.74E-07 |
| 161 | NDRG1 | 2.04 | 5.08E-06 | | | 6.37 | 9.33E-27 |
| 162 | NMRK2 | 0.22 | 4.52E-05 | | | 0.22 | 3.46E-03 |
| 163 | NOV | 10.4 | 1.74E-12 | | | 0.39 | 2.40E-03 |
| 164 | NPAS3 | 6.16 | 5.45E-09 | | | 4.67 | 2.45E-07 |
| 165 | NRP2 | 2.38 | 2.73E-16 | | | 0.47 | 1.83E-10 |
| 166 | NT5M | 0.26 | 2.41E-03 | | | 0.40 | 9.06E-03 |
| 167 | NUAK1 | 0.40 | 1.80E-03 | | | 4.17 | 1.66E-09 |
| 168 | NXN | 2.36 | 4.97E-07 | | | 2.33 | 1.93E-10 |
| 169 | OS9 | 2.07 | 1.97E-08 | | | 2.26 | 1.16E-09 |
| 170 | OSBPL10 | 0.35 | 3.31E-09 | | | 0.40 | 3.68E-05 |
| 171 | PAG1 | 2.68 | 5.98E-15 | | | 3.43 | 1.49E-20 |
| 172 | PAPSS1 | 2.13 | 7.16E-11 | | | 2.03 | 2.01E-04 |
| 173 | PARD3B | 3.21 | 3.24E-03 | | | 4.61 | 1.14E-02 |
| 174 | PCDH1 | 2.83 | 3.22E-03 | | | 4.32 | 2.08E-08 |
| 175 | PCDH17 | 6.59 | 1.54E-05 | 3.41 | 7.09E-05 | 11.7 | 6.12E-23 |
| 176 | PCMTD1 | 2.53 | 6.00E-08 | | | 2.93 | 8.24E-05 |
| 177 | PDE4D | 2.47 | 1.20E-08 | 2.51 | 3.96E-06 | 3.59 | 2.38E-13 |
| 178 | PDE7B | 2.44 | 9.35E-05 | | | 2.01 | 2.90E-03 |
| 179 | PDXDC1 | 0.44 | 1.99E-15 | | | 0.35 | 1.19E-06 |
| 180 | PER3 | 0.45 | 1.87E-07 | 0.49 | 1.56E-05 | 0.26 | 1.14E-13 |
| 181 | PEX5L | 3.97 | 4.02E-03 | 19.8 | 1.40E-22 | 17.1 | 5.26E-21 |
| 182 | PHGDH | 0.43 | 9.80E-13 | | | 2.50 | 2.91E-14 |
| 183 | PI15 | 0.44 | 2.30E-11 | 2.72 | 3.57E-03 | 3.77 | 7.79E-09 |
| 184 | PKD2 | 2.15 | 4.35E-06 | | | 2.18 | 1.50E-04 |
| 185 | PNRC1 | 4.53 | 1.78E-17 | | | 4.11 | 5.30E-10 |
| 186 | POLA2 | 0.32 | 2.07E-08 | | | 0.43 | 2.96E-08 |
| 187 | PPM1E | 0.44 | 1.48E-02 | | | 2.85 | 4.93E-03 |
| 188 | PRICKLE1 | 3.83 | 1.52E-04 | | | 6.49 | 2.49E-10 |
| 189 | PRR5 | 0.37 | 6.55E-03 | | | 0.44 | 3.24E-03 |
| 190 | PTCH1 | 7.67 | 1.28E-07 | | | 2.17 | 1.13E-02 |
| 191 | PTEN | 4.43 | 7.07E-16 | 2.26 | 6.44E-08 | 2.79 | 4.34E-15 |
| 192 | PTGS2 | 3.71 | 1.16E-02 | 14.2 | 1.22E-30 | 37.9 | 3.50E-89 |
| 193 | PTX3 | 8.38 | 3.13E-07 | 27.6 | 3.74E-23 | 39.1 | 9.90E-38 |
| 194 | RAB27A | 0.45 | 1.94E-13 | | | 0.49 | 7.64E-08 |
| 195 | RAB3B | 16.5 | 3.18E-14 | | | 3.25 | 4.78E-03 |
| 196 | RABAC1 | 2.12 | 1.35E-06 | | | 2.31 | 2.54E-08 |

(Table continues in following page)

| | | 48 MITF silencing | | 8h Induction Ectopic ATF4 | | 24h Induction Ectopic ATF4 | |
|---|---|---|---|---|---|---|---|
| | Gene Name | Fold Change | *P* value | Fold Change | *P* value | Fold Change | *P* value |
| 197 | RAP1GAP | 0.33 | 4.92E-04 | | | 0.40 | 1.25E-02 |
| 198 | RASSF3 | 0.45 | 3.07E-13 | 0.43 | 1.47E-07 | 0.25 | 2.11E-10 |
| 199 | RBM48 | 2.32 | 1.23E-03 | | | 2.02 | 5.20E-03 |
| 200 | RBMS3 | 5.43 | 6.15E-14 | | | 2.33 | 7.39E-06 |
| 201 | REEP4 | 0.43 | 7.32E-08 | 2.63 | 7.64E-14 | 2.20 | 4.99E-11 |
| 202 | RFTN2 | 5.86 | 3.67E-05 | | | 7.64 | 1.44E-02 |
| 203 | RGS12 | 0.48 | 3.64E-07 | 0.50 | 1.54E-04 | | |
| 204 | RUNX2 | 3.60 | 2.44E-03 | 6.62 | 1.09E-05 | 17.1 | 8.01E-17 |
| 205 | SATB1 | 3.51 | 3.44E-08 | | | 4.15 | 4.88E-09 |
| 206 | SETD7 | 2.28 | 7.22E-11 | 2.76 | 4.52E-15 | 3.64 | 2.72E-27 |
| 207 | SGMS1 | 2.41 | 4.32E-07 | | | 2.04 | 7.50E-03 |
| 208 | SGPP1 | 0.30 | 1.02E-07 | 3.07 | 4.99E-10 | 3.40 | 7.00E-13 |
| 209 | SH3BGRL2 | 2.57 | 4.65E-07 | 3.14 | 3.46E-05 | 3.82 | 1.12E-11 |
| 210 | SH3PXD2B | 0.29 | 3.09E-14 | | | 0.49 | 4.47E-05 |
| 211 | SHISA2 | 0.47 | 1.42E-06 | 0.49 | 5.23E-04 | | |
| 212 | SLC1A3 | 3.26 | 4.14E-03 | 2.55 | 1.15E-03 | 2.92 | 5.10E-05 |
| 213 | SLC1A4 | 2.10 | 1.85E-14 | | | 2.22 | 8.07E-07 |
| 214 | SLC20A1 | 0.40 | 1.32E-11 | | | 0.48 | 2.67E-08 |
| 215 | SLC24A4 | 3.72 | 1.76E-09 | | | 0.17 | 7.80E-04 |
| 216 | SLC39A10 | 0.41 | 1.27E-12 | | | 0.42 | 3.23E-06 |
| 217 | SLC47A1 | 0.14 | 2.63E-04 | | | 2.38 | 9.48E-04 |
| 218 | SLIT2 | 2.62 | 3.31E-04 | | | 24.6 | 4.30E-09 |
| 219 | SLITRK2 | 7.73 | 7.23E-08 | | | 3.47 | 3.24E-05 |
| 220 | SLITRK6 | 30.3 | 1.21E-05 | | | 6.90 | 1.36E-10 |
| 221 | SLX4 | 0.47 | 8.37E-03 | 0.48 | 4.30E-03 | | |
| 222 | SNAP25 | 0.29 | 1.86E-09 | | | 2.31 | 1.24E-02 |
| 223 | SNX29 | 2.00 | 2.78E-05 | | | 4.61 | 2.52E-18 |
| 224 | SOBP | 3.90 | 1.06E-12 | 0.34 | 5.25E-07 | | |
| 225 | SOX5 | 2.64 | 3.43E-06 | 0.26 | 1.24E-03 | 0.42 | 1.69E-02 |
| 226 | SP8 | 0.13 | 7.08E-05 | | | 4.37 | 3.93E-05 |
| 227 | SPATA2 | 0.40 | 1.76E-08 | | | 2.62 | 2.17E-08 |
| 228 | SPATA6 | 2.68 | 3.73E-05 | | | 2.01 | 9.12E-03 |
| 229 | SPDL1 | 0.48 | 2.81E-09 | | | 0.42 | 4.01E-08 |
| 230 | SPEG | 2.16 | 4.20E-03 | | | 13.5 | 7.59E-21 |
| 231 | SPRED1 | 2.35 | 3.18E-11 | 2.11 | 1.35E-03 | | |
| 232 | SPRY1 | 0.50 | 4.26E-03 | | | 0.39 | 8.06E-03 |
| 233 | SPTAN1 | 2.01 | 5.06E-07 | | | 3.07 | 1.96E-11 |
| 234 | SSBP2 | 2.82 | 1.58E-03 | | | 10.9 | 5.50E-22 |
| 235 | ST3GAL6 | 0.29 | 3.28E-19 | | | 0.45 | 9.58E-09 |
| 236 | STARD13 | 2.52 | 3.39E-09 | 0.50 | 1.10E-03 | | |
| 237 | STEAP1 | 0.43 | 1.04E-03 | | | 0.30 | 2.22E-05 |
| 238 | STK17A | 0.35 | 1.72E-09 | 3.90 | 2.93E-22 | 3.41 | 1.54E-22 |
| 239 | STK32A | 4.63 | 1.14E-16 | | | 0.42 | 5.70E-03 |
| 240 | SULT1A1 | 2.21 | 3.75E-04 | | | 2.18 | 4.17E-03 |
| 241 | SYNE1 | 2.16 | 1.91E-02 | | | 17.5 | 1.52E-24 |
| 242 | TBPL1 | 2.03 | 2.38E-04 | | | 2.29 | 9.29E-06 |
| 243 | TCN1 | 3.21 | 1.13E-03 | | | 13.3 | 1.70E-13 |
| 244 | TCP10L | 4.26 | 4.11E-04 | | | 3.35 | 1.57E-03 |
| 245 | TCP11L2 | 4.99 | 1.75E-03 | | | 17.1 | 3.09E-05 |

(Table continues in following page)

| | | 48 MITF silencing | | 8h Induction Ectopic ATF4 | | 24h Induction Ectopic ATF4 | |
|---|---|---|---|---|---|---|---|
| | **Gene Name** | **Fold Change** | ***P* value** | **Fold Change** | ***P* value** | **Fold Change** | ***P* value** |
| 246 | TGIF1 | 2.07 | 5.80E-04 | | | 2.17 | 3.54E-04 |
| 247 | TLE4 | 5.15 | 8.55E-08 | | | 11.1 | 1.77E-18 |
| 248 | TMCC3 | 0.47 | 4.00E-07 | 0.38 | 3.30E-06 | 0.32 | 7.10E-08 |
| 249 | TMEM201 | 0.48 | 3.75E-06 | | | 0.44 | 2.01E-09 |
| 250 | TMEM38B | 0.48 | 1.17E-07 | | | 0.36 | 1.19E-08 |
| 251 | TMEM44-AS1 | 3.09 | 1.90E-02 | | | 3.44 | 6.61E-03 |
| 252 | TMTC2 | 2.06 | 4.92E-03 | | | 2.48 | 6.90E-03 |
| 253 | TOP2A | 0.44 | 3.02E-15 | | | 0.45 | 4.32E-09 |
| 254 | TRIB3 | 0.39 | 3.48E-11 | 4.99 | 3.08E-19 | 4.00 | 1.46E-22 |
| 255 | TRIM48 | 5.09 | 1.03E-10 | | | 2.15 | 3.54E-03 |
| 256 | TRO | 2.32 | 4.50E-07 | | | 2.04 | 3.71E-05 |
| 257 | TSC22D1 | 3.49 | 2.39E-17 | 2.21 | 6.39E-06 | 5.96 | 2.98E-38 |
| 258 | TSC22D3 | 3.05 | 4.79E-04 | 8.09 | 4.17E-06 | 23.9 | 7.40E-20 |
| 259 | TTC39A | 0.36 | 1.40E-14 | | | 0.26 | 1.38E-16 |
| 260 | TUB | 0.32 | 6.47E-07 | | | 0.46 | 2.52E-04 |
| 261 | TUBB4A | 0.43 | 1.61E-06 | | | 0.39 | 8.94E-10 |
| 262 | TUBGCP5 | 0.41 | 1.14E-06 | | | 0.48 | 6.67E-05 |
| 263 | WDR19 | 2.72 | 2.52E-06 | 2.63 | 3.02E-03 | 3.02 | 1.93E-05 |
| 264 | WNT5A | 0.49 | 1.63E-02 | 7.34 | 1.07E-11 | 16.6 | 1.85E-30 |
| 265 | YPEL2 | 4.72 | 1.90E-14 | 2.67 | 8.67E-05 | 3.10 | 2.16E-05 |
| 266 | ZBED6 | 2.09 | 1.48E-06 | | | 2.22 | 2.33E-03 |
| 267 | ZBTB34 | 2.02 | 2.84E-04 | 4.30 | 1.11E-06 | 4.95 | 4.86E-17 |
| 268 | ZMIZ1-AS1 | 33.9 | 4.24E-04 | | | 68.0 | 7.03E-07 |
| 269 | ZNF114 | 0.18 | 3.78E-04 | | | 0.19 | 4.47E-04 |
| 270 | ZNF367 | 0.32 | 1.36E-06 | | | 0.43 | 1.88E-04 |
| 271 | ZNF714 | 0.33 | 2.09E-04 | | | 0.37 | 2.57E-05 |

**Supplementary Table B.3.- MITF and ATF4-bound genes differentially expressed upon both MITF silencing and induction of ectopic ATF4 expression in 501mel cells.** Fold changes and associated *P* values for the DEGs (FDR < 0.05, fold-change ≥ 2) identified in the RNA-seq experiments performed following 48 h MITF silencing and upon 8 or 24 h induction of ectopic ATF4 in 501mel cells, presenting associated binding peaks in the MITF ChIP-seq experiment performed following induction of expression of ectopic MITF and the ATF4 ChIP-seq experiment performed on glucose starvation conditions in 501mel cells (see Supplementary Tables 2.A and B and 4.A and B on Data CD for MITF and ATF4 ChIP-seq data, respectively). Genes upregulated and downregulated upon both MITF silencing and induction of ectopic ATF4 are highlighted in yellow and green, respectively.